United States
Environmental Protection
Agency

Industrial Environmental Research
Laboratory
Research Triangle Park NC 27711

EPA-600/9-82-005d
July 1982

Research and Development

EPA

# Third Symposium on the Transfer and Utilization of Particulate Control Technology:

## Volume IV. Atypical Applications

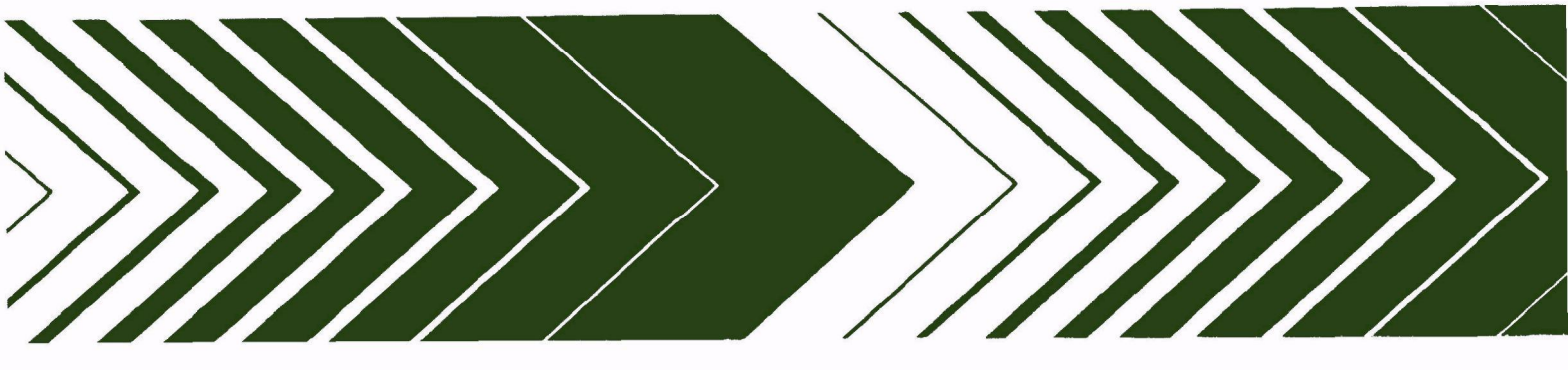

EPA-600/9-82-005d

# THIRD SYMPOSIUM ON THE TRANSFER AND UTILIZATION OF PARTICULATE CONTROL TECHNOLOGY VOLUME IV. ATYPICAL APPLICATIONS

Compiled by:

F.P. Venditti, J.A. Armstrong, and M. Durham

Denver Research Institute
P.O. Box 10127
Denver, Colorado 80208

Grant Number: R805725

Project Officer

Dale L. Harmon
Office of Environmental Engineering and Technology
Industrial Environmental Research Laboratory
Research Triangle Park, NC 27711

Prepared for:

INDUSTRIAL ENVIRONMENTAL RESEARCH LABORATORY
OFFICE OF RESEARCH AND DEVELOPMENT
U.S. ENVIRONMENTAL PROTECTION AGENCY
RESEARCH TRIANGLE PARK, NC 27711

## DISCLAIMER

This report has been reviewed by the Industrial Environmental Research Laboratory-Research Triangle Park, North Carolina, Office of Research and Development, U.S. Environmental Protection Agency, and approved for publication. Approval does not signify that the contents necessarily reflect the views and policies of the U.S. Environmental Protection Agency, nor does mention of trade names or commercial products constitute endorsement or recommendation for use.

ABSTRACT

The papers in these four volumes of Proceedings were presented at the Third Symposium on the Transfer and Utilization of Particulate Control Technology held in Orlando, Florida during 9 March through 13 March 1981, sponsored by the Particulate Technology Branch of the Industrial Environmental Research Laboratory of the Environmental Protection Agency and coordinated by the Denver Research Institute of the University of Denver.

The purpose of the symposium was to bring together researchers, manufacturers, users, government agencies, educators and students to discuss new technology and to provide an effective means for the transfer of this technology out of the laboratories and into the hands of the users.

The three major categories of control technologies -- electrostatic precipitators, scrubbers, and fabric filters -- were the major concern of the symposium. These technologies were discussed from the perspectives of economics; new technical advancements in science and engineering; and applications. Several papers dealt with combinations of devices and technologies, leading to a concept of using a systems approach to particulate control rather than device control. Additional topic areas included novel control devices, high temperature/high pressure applications, fugitive emissions, and measurement techniques.

These proceedings are divided into four volumes, each volume containing a set of related session topics to provide easy access to a unified technology area.

VOLUME IV

Page

VOLUME I. COAL FIRED BOILERS--CONTENTS . . . . . x
VOLUME II. ELECTROSTATIC PRECIPITATORS--CONTENTS . . . xiv
VOLUME III. PARTICULATE CONTROL DEVICES--CONTENTS . . . xviii

Section A - Advanced Energy Applications

HIGH TEMPERATURE PARTICLE COLLECTION WITH A.P.T. EPxP DRY SCRUBBER . . . . . 1
S. Yung, T. Lee, R.C. Patterson, S. Calvert and D.C. Drehmel

PARTICLE COLLECTION IN CYCLONES AT HIGH TEMPERATURE AND HIGH PRESSURE . . . . . 2
R. Parker, R. Jain, S. Calvert, D.C. Drehmel and J. Abbott

OPERATING RESULTS OF ELECTROSTATIC PRECIPITATORS AT HIGH TEMPERATURE AND HIGH PRESSURES . . . . . 3
P.L. Feldman and K.S. Kumar

CONTROL OF PARTICULATES IN PROCESS AREA 12, SOLVENT REFINED COAL PROCESS . . . . . 15
W.H. Wilks, P.D. Wilkinson and J.A. Schlosberg

NON-PLUGGING RETAINING STRUCTURE FOR GRANULAR BED FILTER FOR HTHP APPLICATION . . . . . 26
A.M. Presser and J.C. Alexander

PARTICULATE EMISSIONS CONTROL FROM A COAL-FIRED OPEN-CYCLE MAGNETOHYDRODYNAMICS/STEAM POWER PLANT . . . 36
H.H. Wang and T.E. Dowdy

REAL TIME COARSE PARTICLE MASS MEASUREMENTS IN A HIGH TEMPERATURE AND PRESSURE COAL GASIFIER PROCESS TREATMENT . . . . . 46
J. Wegrzyn, J. Saunders and W. Marlow

THE DESIGN, ENGINEERING, AND STARTUP OF A VENTURI SCRUBBER SYSTEM ON AN OIL SHALE OFF-GAS INCINERATOR . . . 55
P.A. Czuchra and J.S. Sterrett

FLUIDIZED-BED COMBUSTION HOT FLUE GAS CLEANUP PERSPECTIVE ON CYCLONES AND OTHER DEVICES . . . . . 63
R.F. Henry and W.F. Podolski

VOLUME IV CONTENTS (cont.)

Page

PRESSURIZED AND NON-PRESSURIZED ACOUSTIC AGGLOMERATORS FOR HOT-GAS CLEANUP APPLICATIONS . . . . . 73
K.H. Chou and D.T. Shaw

ALKALIS AND THEIR CONTRIBUTIONS TO CORONA CURRENT AT HIGH TEMPERATURE AND HIGH PRESSURE . . . . . 74
R.W.L. Snaddon

HOT GAS CLEANUP IN PRESSURIZED FLUIDIZED BED COMBUSTION . . . . . 83
L.N. Rubow and M.G. Klett

VENTURI SCRUBBING FOR CONTROL OF PARTICULATE EMISSIONS FROM OIL SHALE RETORTING . . . . . 95
G.M. Rinaldi and R.C. Thurnau

OVERVIEW OF THE DEPARTMENT OF ENERGY'S PRESSURIZED FLUIDIZED-BED COMBUSTOR CLEANUP TECHNOLOGY PROGRAM . . . 105
W.E. Moore

THE CYCLOCENTRIFUGE$^{TM}$--AN ADVANCED GAS/SOLIDS SEPARATOR FOR COAL CONVERSION PROCESSES . . . . . 116
P.R. Albrecht, J.T. McCabe and W. Fedarko

Section B - Fugitive Emissions

DEMONSTRATION OF THE USE OF CHARGED FOG IN CONTROLLING FUGITIVE DUST FROM LARGE-SCALE INDUSTRIAL SOURCES . . . . . 125
E.T. Brookman, R.C. McCrillis and D.C. Drehmel

THE CONTROL OF FUGITIVE EMISSIONS USING WINDSCREENS . . . 135
D. Carnes and D.C. Drehmel

THE INFLUENCE OF AGGREGATE PILE SHAPE AND ORIENTATION ON PARTICULATE FUGITIVE EMISSIONS . . . . . 145
D. Martin

SPRAY CHARGING AND TRAPPING SCRUBBER FOR FUGITIVE PARTICLE EMISSION CONTROL . . . . . 155
S. Yung, S. Calvert and D.C. Drehmel

IMPROVED STREET SWEEPER FOR CONTROLLING URBAN INHALABLE PARTICULATE MATTER . . . . . 156
S. Calvert, H. Brattin, S. Bhutra, R. Parker and D.C. Drehmel

VOLUME IV CONTENTS (cont.)

Page

A WIND TUNNEL FOR DUST ENTRAINMENT STUDIES . . . . . 168
A.S. Viner, M.B. Ranade, E.J. Shaughnessy, D.C. Drehmel and B.E. Daniels

TECHNIQUES AND EQUIPMENT FOR MEASURING INHALABLE PARTICULATE FUGITIVE EMISSIONS . . . . . 179
H.J. Kolnsberg

BALLOON SAMPLING TO CHARACTERIZE PARTICLE EMISSIONS FROM FUGITIVE SOURCES. . . . . 188
J.A. Armstrong and D.C. Drehmel

AN ELECTROSTATICALLY CHARGED FOG GENERATOR FOR THE CONTROL OF INHALABLE PARTICLES . . . . . 200
C.V. Mathai, L.A. Rathbun and D.C. Drehmel

RELATIVE EFFECTIVENESS OF CHEMICAL ADDITIVES AND WIND SCREENS FOR FUGITIVE DUST CONTROL. . . . . 210
D.C. Drehmel and B.E. Daniel

PARTICULATE IMPACT COMPARISON BETWEEN CONTROLLED STACK EMISSIONS FOR A 2000 MW ELECTRICAL GENERATING STATION . . . . . 222
H.E. Hesketh and F.L. Cross

OPERATING EXPERIENCE AND THE TECHNIQUES IN THE CONTROL OF COAL DUST EMISSIONS FROM LARGE STORAGE PILE AT NANTICOKE TGS . . . . . 232
N. Krishnamurthy, W. Whitman and Y.V. Nguyen

Section C - Opacity

MODELING SMOKE PLUME OPACITY FROM PARTICULATE CONTROL EQUIPMENT . . . . . 242
D.S. Ensor, P.A. Lawless, S.J. Cowen

TETHERED BALLOON PLUME SAMPLING OF A PORTLAND CEMENT PLANT . . . . . 252
J.A. Armstrong, P.A. Russell, M.N. Plooster

THE RELATIONSHIP OF FLY ASH LIGHT ABSORPTION TO SMOKE PLUME OPACITY . . . . . 264
S.J. Cowen, D.S. Ensor

VOLUME IV CONTENTS (cont.)

Page

Section D - Measurements

A SPECIAL METHOD FOR THE ANALYSIS OF SULFURIC ACID MISTS . . . . . 275
P. Urone, R.B. Mitchell, J.E. Rusnak, R.A. Lucas and J.F. Griffiths

A MICROCOMPUTER-BASED CASCADE-IMPACTOR DATA-REDUCTION SYSTEM . . . . . 285
M. Durham, S. Tegtmeyer, K. Wasmundt and L.E. Sparks

DEVELOPMENT OF A SAMPLING TRAIN FOR STACK MEASUREMENT OF INHALABLE PARTICULATE . . . . . 297
A.D. Williamson, W.B. Smith

INHALABLE PARTICULATE MATTER SAMPLING PROGRAM FOR IRON AND STEEL: AN OVERVIEW PROGRESS REPORT . . . . . 306
R.C. McCrillis

DEVELOPMENT OF IP EMISSION FACTORS . . . . . 317
D.L. Harmon

INHALABLE PARTICULATE EMISSION FACTOR PROGRAM PURPOSE AND DEVELOPMENT . . . . . 326
F.M. Noonan and J.H. Southerland

INHALABLE PARTICULATE EMISSION FACTORS FOR BLAST FURNACE CASTHOUSES IN THE IRON AND STEEL INDUSTRY . . . . 335
P.D. Spawn, S. Piper and S. Gronberg

INHALABLE PARTICULATE EMISSIONS FROM VEHICLES TRAVELING ON PAVED ROADS . . . . . 344
R. Bohn

QUALITY ASSURANCE FOR PARTICLE-SIZING MEASUREMENTS . . . 353
C.E. Tatsch

PARTICULATE EMISSIONS CHARACTERIZATION FOR OIL-FIRED BOILERS . . . . . 363
D. Mormile, S. Hersh, B.F. Piper and M. McElroy

A CONTINUOUS REAL-TIME PARTICULATE MASS MONITOR FOR STACK EMISSION APPLICATIONS . . . . . 373
J.C.F. Wang, H. Patashnick and G. Rupprecht

VOLUME IV CONTENTS (cont.)

Page

Section E - Mobile Sources

STUDIES OF PARTICULATE REMOVAL FROM DIESEL EXHAUSTS WITH ELECTROSTATIC AND ELECTROSTATICALLY-AUGMENTED TECHNIQUES . . . . . 383
J.L. DuBard, M.G. Faulkner, J.R. McDonald, D.C. Drehmel and J.H. Abbott

STUDIES OF PARTICULATE REMOVAL FROM DIESEL EXHAUSTS WITH MECHANICAL TECHNIQUES . . . . . 395
M.G. Faulkner, J.L. DuBard, J.R. McDonald, D.C. Drehmel and J.H. Abbott

UPDATE ON STATUS OF CONNECTICUT'S CONTROL PROGRAM FOR TRANSPORTATION-RELATED PARTICULATE EMISSIONS . . . . 406
H.L. Chamberlain and J.H. Gastler

AUTHOR INDEX . . . . . 413

VOLUME I

COAL FIRED BOILERS

Section A - Fabric Filters


Page

COAL PROPERTIES AND FLY ASH FILTERABILITY . . . . . 1
R. Dennis, J.A. Dirgo and L.S. Hovis

PULSE-JET FILTRATION WITH ELECTRICALLY CHARGED FLYASH . . . . . 11
R.P. Donovan, L.S. Hovis, G.H. Ramsey and J.H. Abbott

ELECTRICALLY CHARGED FLYASH EXPERIMENTS IN A LABORATORY SHAKER BAGHOUSE . . . . . 23
L.S. Hovis, J.H. Abbott, R.P. Donovan and C.A. Pareja

ELECTROSTATIC AUGMENTATION OF FABRIC FILTRATION . . . . 35
D.W. VanOsdell, G.P. Greiner, G.E.R. Lamb and L.S. Hovis

FABRIC WEAR STUDIES AT HARRINGTON STATION . . . . . 45
R. Chambers, K. Ladd, S. Kunka and D. Harmon

SPS PILOT BAGHOUSE OPERATION . . . . . 55
K. Ladd, W. Hooks, S. Kunka and D. Harmon

REVIEW OF SPS INVESTIGATION OF HARRINGTON STATION UNIT 2 FABRIC FILTER SYSTEM . . . . . 65
K. Ladd, S. Kunka

A SUMMARY OF PERFORMANCE TESTING OF THE APITRON ELECTROSTATICALLY AUGMENTED FABRIC FILTER . . . . . 75
D. Helfritch and L. Kirsten

FABRIC FILTER OPERATING EXPERIENCE FROM SEVERAL MAJOR UTILITY UNITS . . . . . 82
O.F. Fortune, R.L. Miller and E.A. Samuel

EVALUATION OF THE 25 MW KRAMER STATION BAGHOUSE: TRACE ELEMENT EMISSION CONTROL. . . . . 94
M.W. McElroy and R.C. Carr

CHARACTERIZATION OF A 10 MW FABRIC FILTER PILOT PLANT . . . . . 96
W.B. Smith, K.M. Cushing and R.C. Carr

SPECIFYING A FABRIC FILTER SYSTEM . . . . . 107
R.L. Ostop and D.A. Single

Page

EVALUATION OF THE 25 MW KRAMER STATION BAGHOUSE: OPERATIONAL FACTORS IN PARTICULATE MATTER EMISSION CONTROL . . . . . 118
R.C. Carr and M.W. McElroy

PULSE-JET TYPE FABRIC FILTER EXPERIENCE AT AIR TO CLOTH RATIOS OF 5 TO 1 ON A BOILER FIRING PULVERIZED COAL . . . . . 120
G.L. Pearson

SELECTION AND OPERATION OF BAGHOUSES AT R.D. NIXON STATION, UNIT #1 . . . . . 129
R.C. Hyde, J. Arello and D.J. Huber

POTENTIAL FOR IMPROVEMENT IN BAGHOUSE DESIGN . . . . . 138
R.M. Jensen

REVIEW OF OPERATING AND MAINTENANCE EXPERIENCES WITH HIGH TEMPERATURE FILTER MEDIA ON COAL-FIRED BOILERS . . . 148
L.K. Crippen

Section B - Electrostatic Precipitators

PILOT DEMONSTRATION OF THE PRECHARGER-COLLECTOR SYSTEM. . . . . 157
P. Vann Bush, Duane H. Pontius

REMEDIAL TREATMENTS FOR DETERIORATED HOT SIDE PRECIPITATOR PERFORMANCE . . . . . 165
R.E. Bickelhaupt

EVALUATION OF THE UNITED McGILL ELECTROSTATIC PRECIPITATOR . . . . . 176
D.S. Ensor, P.A. Lawless, A.S. Damle

PREDICTING THE EFFECT OF PROPRIETARY CONDITIONING AGENTS ON FLY ASH RESISTIVITY. . . . . 185
R.J. Jaworowski and J.J. Lavin

$SO_3$ CONDITIONING TO ENABLE ELECTROSTATIC PRECIPITATORS TO MEET DESIGN EFFICIENCIES . . . . . 197
J.J. Ferrigan, III

ENHANCED PRECIPITATOR COLLECTION EFFICIENCIES THROUGH RESISTIVITY MODIFICATION . . . . . 206
D.F. Mahoney

VOLUME I CONTENTS (cont.)

Page

DEVELOPMENT OF A NEW SULFUR TYPE ASH CONDITIONING . . . . 216
R.H. Gaunt

OPERATING EXPERIENCE WITH FLUE GAS CONDITIONING SYSTEMS AT COMMONWEALTH EDISON COMPANY . . . . . 226
L.L. Weyers and R.E. Cook

THE APPLICATION OF A TUBULAR WET ELECTROSTATIC PRECIPITATOR FOR FINE PARTICULATE CONTROL AND DEMISTING IN AN INTEGRATED FLY ASH AND $SO_2$ REMOVAL SYSTEM ON COAL-FIRED BOILERS . . . . . 236
E. Bakke and H.P. Willett

FIELD EVALUATIONS OF AMMONIUM SULFATE CONDITIONING FOR IMPROVEMENT OF COLD SIDE ELECTROSTATIC PRECIPITATOR PERFORMANCE . . . . . 237
E.C. Landham, Jr., G.H. Marchant, Jr., J.P. Gooch and R.F. Altman

EVALUATION OF PERFORMANCE ENHANCEMENT OBTAINED WITH PULSE ENERGIZATION SYSTEMS ON A HOT SIDE ELECTROSTATIC PRECIPITATOR . . . . . 253
W. Piulle, L.E. Sparks, G.H. Marchant, Jr. and J.P. Gooch

A NEW MICROCOMPUTER AND STRATEGY FOR THE CONTROL OF ELECTROSTATIC PRECIPITATORS . . . . . 265
K.J. McLean, T.S. Ng, Z. Herceg and Z. Rana

ASSESSMENT OF THE COMMERCIAL POTENTIAL FOR THE HIGH INTENSITY IONIZER IN THE ELECTRIC UTILITY INDUSTRY . . . . 272
J.S. Lagarias, J.R. McDonald and D.V. Giovanni

APPLICATION OF ENERGY CONSERVING PULSE ENERGIZATION FOR PRECIPITATORS--PRACTICAL AND ECONOMIC ASPECTS . . . . 291
H. H. Petersen and P. Lausen

Section C - Dry $SO_2$ Scrubbers

$SO_2$ REMOVAL BY DRY INJECTION AND SPRAY ABSORPTION TECHNIQUES . . . . . 303
E.L. Parsons, Jr., V. Boscak, T.G. Brna and R.L. Ostop

DRY SCRUBBING $SO_2$ AND PARTICULATE CONTROL . . . . . 313
N.J. Stevens, G.B. Manavizadeh, G.W. Taylor and M.J. Widico

FIBER AND FABRIC ASPECTS FOR $SO_2$ DRY SCRUBBING BAGHOUSE SYSTEMS . . . . . 323
L. Bergmann

VOLUME I CONTENTS (cont.)

Page

TWO-STAGE DRY FLUE GAS CLEANING USING CALCIUM ALKALIS . . . . . 333
D.C. Gehri, D.F. Dustin and S.J. Stachura

CONTROL OF SULFUR DIOXIDE, CHLORINE, AND TRACE ELEMENT EMISSIONS FROM COAL-FIRED BOILERS BY FABRIC FILTRATION . . . . . 341
R.J. Demski, J.T. Yeh and J.I. Joubert

Section D - Scrubbers

FLYASH COLLECTION USING A VENTURI SCRUBBER--MINNESOTA POWER'S COMMERCIAL OPERATING EXPERIENCE . . . . . 352
C.A. Johnson

AUTHOR INDEX . . . . . 361

VOLUME II

ELECTROSTATIC PRECIPITATORS

Section A - Fundamentals


Page

MATHEMATICAL MODELING OF IONIC CONDUCTION IN FLY ASH LAYERS . . . . . 1
R.B. Mosley, J.R. McDonald and L.E. Sparks

MEASUREMENTS OF ELECTRICAL PROPERTIES OF FLY ASH LAYERS . . . . . 13
R.B. Mosley, P.R. Cavanaugh, J.R. McDonald and L.E. Sparks

LASER DOPPLER ANEMOMETER MEASUREMENTS OF PARTICLE VELOCITY IN A LABORATORY PRECIPITATOR . . . . . 25
P.A. Lawless, A.S. Damle, A.S. Viner, E.J. Shaughnessy and L.E. Sparks

PROGRESS IN MODELING BACK CORONA. . . . . 35
P.A. Lawless

A COMPUTER MODEL FOR ESP PERFORMANCE . . . . . 44
P.A. Lawless, J.W. Dunn and L.E. Sparks

MEASUREMENT AND INTERPRETATION OF CURRENT DENSITY DISTRIBUTION AND CHARGE/MASS DATA . . . . . 54
M. Durham, G. Rinard, D. Rugg and L.E. Sparks

THE RELATIONSHIP BETWEEN GAS STREAM TURBULENCE AND COLLECTION EFFICIENCY IN A LAB-SCALED ELECTROSTATIC PRECIPITATOR . . . . . 66
B.E. Pyle, J.R. McDonald, W.B. Smith

PARTICLE DEPOSITION PROFILES AND REENTRAINMENT IN A WIRE-PLATE ELECTROSTATIC PRECIPITATOR . . . . . 76
E. Arce-Medina and R.M. Felder

PARTICLE TRANSPORT IN THE EHD FIELD . . . . . 87
T. Yamamoto

SURFACE REENTRAINMENT OF COLLECTED FLY ASH IN ELECTROSTATIC PRECIPITATORS . . . . . 97
M. Mitchner, M.J. Fisher, D.S. Gere, R.N. Leach and S.A. Self

ELECTROMECHANICS OF PRECIPITATED ASH LAYERS . . . . . 109
G.B. Moslehi and S.A. Self

VOLUME II CONTENTS (cont.)

Page

EXPERIMENTAL MEASUREMENTS OF THE EFFECT OF TURBULENT DIFFUSION ON PRECIPITATOR EFFICIENCY . . . . . 120
G.L. Leonard, M. Mitchner and S.A. Self

CAN REENTRAINMENT BE EXPLAINED USING A NEW PRECIPITATOR FORMULA? . . . . . 130
S. Maartmann

A LABORATORY FURNACE FOR THE PRODUCTION OF SYNTHETIC FLY ASH FROM SMALL COAL SAMPLES . . . . . 141
K.M. Sullivan

COMPUTER SIMULATION OF THE WIDE PLATE SPACING EFFECT . . . . . 149
E.A. Samuel

SIMULTANEOUS MEASUREMENTS OF AERODYNAMIC SIZE AND ELECTRIC CHARGE OF AEROSOL PARTICLES IN REAL TIME ON A SINGLE PARTICLE BASIS . . . . . 160
M.K. Mazumder, R.G. Renninger, T.H. Chang, R.W. Raible, W.G. Hood, R.E. Ware and R.A. Sims

APPLICATION OF LASER DOPPLER INSTRUMENTATION TO PARTICLE TRANSPORT MEASUREMENTS IN AN ELECTROSTATIC PRECIPITATOR . . . . . 169
M.K. Mazumder, W.T. Clark III, R.E. Ware, P.C. McLeod, W.G. Hood, J.E. Straub and S. Wanchoo

THE APPLICATION OF MEASUREMENTS OF AEROSOL CHARGE ACQUISITION BY BIPOLAR IONS TO THE PROBLEM OF BACK CORONA . . . . . 179
R.A. Fjeld, R.O. Gauntt, G.J. Laughlin and A.R. McFarland

IDENTIFICATION OF BACK DISCHARGE SEVERITY . . . . . 189
S. Masuda and Y. Nonogaki

Section B - Operations and Maintenance

MODELING OF ELECTROSTATIC PRECIPITATORS WITH RESPECT TO RAPPING REENTRAINMENT AND OUTLET OPACITY . . . . . 199
M.G. Faulkner, W.E. Farthing, J.R. McDonald and L.E. Sparks

NEW PRECIPITATOR TECHNOLOGY FOR PARTICULATE CONTROL . . . . . 208
J.R. Zarfoss

VOLUME II CONTENTS (cont.)

Page

AN APPLICATION SUMMARY OF HIGH ENERGY SONIC CLEANING APPLIED TO ELECTROSTATIC PRECIPITATORS . . . . . 218
M.J. Berlant

THE IMPACT OF INTELLIGENT PRECIPITATOR CONTROLS . . . . . 230
N.Z. Shilling, R.O. Reese and J.A. Fackler

AN ENERGY MANAGEMENT SYSTEM FOR ELECTROSTATIC PRECIPITATORS . . . . . 242
R.R. Crynack and M.P. Downey

RELATIONSHIP BETWEEN ELECTROSTATIC PRECIPITATOR PERFORMANCE AND RECORDKEEPING PRACTICES . . . . . 252
S.P. Schliesser

AN OPERATION AND MAINTENANCE PROGRAM FOR A PHOSPHATE ROCK ELECTROSTATIC PRECIPITATOR . . . . . 262
D.B. Rimberg

Section C - Advanced Design

ELECTROSTATIC PRECIPITATOR PERFORMANCE WITH PULSE EXCITATION. . . . . 273
D. Rugg, M. Durham, G. Rinard and L.E. Sparks

DEVELOPMENT OF A CHARGING DEVICE FOR HIGH-RESISTIVITY DUST USING HEATED AND COOLED ELECTRODES. . . . . 283
G. Rinard, M. Durham, D. Rugg and L.E. Sparks

THE EVALUATION OF NOVEL ELECTROSTATIC PRECIPITATOR SYSTEMS USING A TRANSPORTABLE PROTOTYPE . . . . . 295
G. Rinard, M. Durham, D. Rugg, J. Armstrong, L.E. Sparks and J.H. Abbott

ANALYSIS OF THE ELECTRICAL AND CHARGING CHARACTERISTICS OF A THREE ELECTRODE PRECHARGER . . . . 304
K.J. McLean

PARTICLE CHARGING IN AN ELECTROSTATIC PRECIPITATOR BY PULSE AND DC VOLTAGES . . . . . 314
L.E. Sparks, G.H. Ramsey, R.E. Valentine and J.H. Abbott

PARTICLE COLLECTION IN A TWO STAGE ELECTROSTATIC PRECIPITATOR WITH VARIOUS COLLECTOR STAGES. . . . . 326
L.E. Sparks, G.H. Ramsey, R.E. Valentine and J.H. Abbott

HIGH INTENSITY IONIZER DEVELOPMENT . . . . . 334
M.H. Anderson, J.R. McDonald, J.P. Gooch and D.V. Giovanni

VOLUME III

PARTICULATE CONTROL DEVICES

Section A - Scrubbers


Page

THE CALVERT SCRUBBER . . . . . 1
S. Calvert, R.G. Patterson and S. Yung

FLUX FORCE/CONDENSATION SCRUBBER SYSTEM FOR COLLECTION OF FINE PARTICULATE EMISSIONS FROM AN IRON MELTING CUPOLA . . . . . 10
S. Calvert and D.L. Harmon

DEMONSTRATION OF HIGH-INTENSITY-IONIZER-ENHANCED VENTURI SCRUBBER ON A MAGNESIUM RECOVERY FURNACE FUME EMISSIONS . . . . . 21
A. Prem, M.T. Kearns and D.L. Harmon

A NEW ENTRY IN THE HIGH EFFICIENCY SCRUBBER FIELD . . . . 33
L.C. Hardison and F. Ekman

PERFORMANCE OF PARTICULATE SCRUBBERS AS INFLUENCED BY GAS-LIQUID CONTACTOR DESIGN AND BY DUST FLOCCULATION . . . . . 43
K.T. Semrau and R.J. Lunn

INVESTIGATION OF VENTURI SCRUBBER EFFICIENCY AND PRESSURE DROP . . . . . 51
R. Parker, T. Le and S. Calvert

SCRUBBER TECHNOLOGY AND THE INTERACTION OF A UNIQUE STRUCTURE AS MIST ELIMINATOR . . . . . 60
G.C. Pedersen

NOVEL ANNULAR VENTURI SCRUBBER DESIGN REDUCES WASTE DISCHARGE PROBLEMS . . . . . 71
H.P. Beutner

CONSIDERATION OF THE PERTINENT DESIGN AND OPERATING CHARACTERISTICS ESSENTIAL FOR OPTIMIZATION OF VENTURI SCRUBBER PERFORMANCE . . . . . 80
H.S. Oglesby

APPLICATION OF SCRUBBERS FOR PARTICULATE CONTROL OF INDUSTRIAL BOILERS . . . . . 90
M. Borenstein

VOLUME II CONTENTS (cont.)

Page

DEMONSTRATION OF AIR POLLUTION SYSTEMS HIGH INTENSITY IONIZER/ELECTROSTATIC PRECIPITATOR ON AN OIL-FIRED BOILER . . . . . 349
G.A. Raemhild, A. Prem and F. Weisz

PRIMARY AND SECONDARY IONIZATION IN AN ELECTRON BEAM PRECIPITATOR SYSTEM . . . . . 358
W.C. Finney, L.C. Thanh, J.S. Clements and R.H. Davis

INFLUENCE ON PARTICLE CHARGING OF ELECTRICAL PARAMETERS AT DC AND PULSE VOLTAGES . . . . . 370
H.J. Joergensen, J.T. Kristiansen and P. Lausen

BOXER-CHARGER MARK III AND ITS APPLICATION IN ESP'S . . . . . 380
S. Masuda, H. Nakatani and A. Mizuno

THE PERFORMANCE OF AN EXPERIMENTAL PRECIPITATOR WITH AN ALL-PLATE ZONE . . . . . 390
J. Dalmon

THE PHYSICS OF PULSE ENERGIZATION OF ELECTROSTATIC PRECIPITATORS . . . . . 404
L. Menegozzi and P.L. Feldman

ADVANCED ELECTRODE DESIGN FOR ELECTROSTATIC PRECIPITATORS . . . . . 405
S. Bernstein, K. Ushimaru and E.W. Geller

Section D - Industrial Applications

PROBLEMS IN APPLYING AN ELECTROSTATIC PRECIPITATOR TO A SALVAGE FUEL-FIRED BOILER. . . . . 415
C.R. Thompson

THE APPLICATION OF ELECTROSTATIC PRECIPITATORS TO BOILERS FIRING MULTIPLE FUELS . . . . . 425
R.L. Bump

AUTHOR INDEX . . . . . 435

VOLUME III CONTENTS (cont.)

Page

APPLICATION OF HIGH ENERGY VENTURI SCRUBBERS TO SEWAGE INCINERATION . . . . . 102
F.X. Reardon

AN INCINERATOR SCRUBBER THAT WORKS: A CASE STUDY . . . . . 111
C. Menoher

EVALUATION OF ENTRAINED LIQUOR CONTRIBUTION TO TOTAL MASS EMISSIONS DOWNSTREAM OF A WET SCRUBBER . . . 119
W. David Balfour, L.O. Edwards and H.J. Williamson

Section B - Fabric Filters

A DUAL-BEAM BACKSCATTER BETA-PARTICLE GAUGE FOR MEASURING THE DUST CAKE THICKNESS ON OPERATING BAG FILTERS INDEPENDENT OF POSITION . . . . . 128
R.P. Gardner, R.P. Donovan and L.S. Hovis

DIAGNOSING FILTER FABRIC CAPABILITIES WITH LIGHT SCATTERING AND NUCLEI DETECTING INSTRUMENTATION . . . . 140
R. Dennis, D.V. Bubenick and L.S. Hovis

ACID DEWPOINT CORROSION IN PARTICULATE CONTROL EQUIPMENT . . . . . 150
T.E. Mappes, R.D. Tems and K.E. Foster

SECOND GENERATION OF EMISSIONS CONTROL SYSTEM FOR COKE OVENS . . . . . 160
J.D. Patton

EFFECTS OF FLYASH SIZE DISTRIBUTION ON THE PERFORMANCE OF A FIBERGLASS FILTER . . . . . 171
W.F. Frazier and W.T. Davis

FUNDAMENTAL STUDY OF A FABRIC FILTER WITH A CORONA PRECHARGER . . . . . 181
K. Iinoya and Y. Mori

ECONOMIC EVALUATION FACTORS IN BID EVALUATIONS--A SENSITIVITY ANALYSIS . . . . . 193
J.G. Musgrove and J.E. Shellabarger

FLY ASH RE-ENTRAINMENT IN A BAGHOUSE-- WHAT DOES IT COST? . . . . . 201
J.G. Musgrove

VOLUME III CONTENTS (cont.)

Page

WHY PERFORM MODEL STUDY OF FABRIC FILTER COLLECTOR? . . . . . 211
W.T. Langan, N.Z. Shilling, W.A. Van Kleunen and O.F. Fortune

EXPERIENCES OF A SMALL INSULATION MANUFACTURER IN MAINTAINING COMPLIANCE WITH AIR POLLUTION CONTROL REGULATIONS . . . . . 221
R.L. Hawks

ADVANCED FABRIC FILTER TECHNOLOGY FOR DIFFICULT PARTICULATE EMISSIONS . . . . . 228
H.P. Beutner

DEVELOPMENT OF GUIDELINES FOR OPTIMUM BAGHOUSE FLUID DYNAMIC SYSTEM DESIGN . . . . . 238
D. Eskinazi, G.B. Gilbert and R.C. Carr

THEORETICAL ASPECTS OF PRESSURE DROP REDUCTION IN A FABRIC FILTER WITH CHARGED PARTICLES . . . . . 250
T. Chiang, E.A. Samuel and K.E. Wolpert

EXPERIMENTAL CORRELATION OF DUST CAKE POROSITY, AIR-TO-CLOTH RATIO AND PARTICLE-SIZE DISTRIBUTIONS . . . . 261
T. Chiang and R.L. Ostop

MODEL FOR DUST PENETRATION THROUGH A PULSE-JET FABRIC FILTER . . . . . 270
D. Leith and M.J. Ellenbecker

PERFORMANCES OF DUST LOADED AIR FILTERS . . . . . 280
C. Kanaoka, H. Emi and M. Ohta

ELECTROSTATICALLY ENHANCED FABRIC FILTRATION OF PARTICULATES . . . . . 290
T. Ariman and S.T. McComas

A STAGGERED ARRAY MODEL OF A FIBROUS FILTER WITH ELECTRICAL ENHANCEMENT . . . . . 301
F. Henry and T. Ariman

Section C - Granular Beds

AEROSOL FILTRATION BY A COCURRENT MOVING GRANULAR BED: PENETRATION THEORY . . . . . 311
T.W. Kalinowski and D. Leith

FUNDAMENTAL EXPERIMENTS ON A GRANULAR BED FILTER . . . . . 321
K. Iinoya and Y. Mori

VOLUME III CONTENTS (cont.)

Page

DRY DUST COLLECTION OF BLAST FURNACE EXHAUST GAS BY MOVING GRANULAR BED FILTER . . . . . 332
A. Wakabayashi, T. Sugawara and S. Watanabe

Section D - Novel Devices

IRON AND STEEL AIR POLLUTION CONTROL USING MAGNETIC SEPARATION . . . . . 341
D.C. Drehmel, C.E. Ball and C.H. Gooding

TECHNICAL AND ECONOMIC EVALUATION OF TWO NOVEL PARTICULATE CONTROL DEVICES . . . . . 353
R.R. Boericke, J.T. Kuo and K.R. Murphy

THE ELECTROSCRUBBER™ FILTER--APPLICATIONS AND PARTICULATE COLLECTION PERFORMANCE . . . . . 363
D. Parquet

HIGH EFFICIENCY PARTICULATE REMOVAL WITH SINTERED METAL FILTERS . . . . . 373
B.E. Kirstein, W.J. Paplawsky, D.T. Pence and T.G. Hedahl

APPLICATION OF ELECTROSTATIC TECHNIQUES TO THE REMOVAL OF DUST AND FUME FROM THE INDUSTRIAL ENVIRONMENT . . . . . 382
S.A. Hoenig

THE DRY VENTURI . . . . . 393
A.J. Teller and D.R.J. Roy

FIBER BED FILTER SYSTEM CONTROL OF WELDING PARTICULATES . . . . . 398
J.A. Bamberger and W.K. Winegardner

THE USE OF GLASS CAPILLARY FILTERS TO CLASSIFY ACTINOLITE FIBERS . . . . . 406
J.W. Gentry, T.C. Chen, S.W. Lin and P.Y. Yu

ULTRA-HIGH EFFICIENCY FILTRATION SYSTEMS (AIR RECIRCULATION) . . . . . 417
R.W. Potokar

THE WET WALL ELECTROSTATIC PRECIPITATOR . . . . . 428
J. Starke, J. Kautz and K-R. Hegemann

VOLUME III CONTENTS (cont.)

Page

Section E - Mechanical Collectors

TROUBLESHOOTING MULTIPLE CYCLONES ON FUEL-OIL-FIRED BOILERS . . . . . 438
F. Crowson and R.L. Gibbs

COLLECTION EFFICIENCIES OF CYCLONE SEPARATORS. . . . . 449
P.W. Dietz

ELECTROSTATICALLY AUGMENTED COLLECTION IN VORTICAL FLOWS . . . . . 459
P.W. Dietz

HIGH PERFORMANCE CYCLONE DEVELOPMENT . . . . . 468
W.G. Giles

AUTHOR INDEX . . . . . 481

# HIGH TEMPERATURE PARTICLE COLLECTION WITH A. P. T. EPxP DRY SCRUBBER

By: S. Yung, T. Lee, R.C. Patterson and S. Calvert
Air Pollution Technology, Inc.
4901 Morena Blvd., Suite 402
San Diego, CA 92117

D.C. Drehmel
Particulate Technology Branch
Industrial Environmental Research Branch
U.S. Environmental Protection Agency
Research Triangle Park, NC 27711

## ABSTRACT

The A. P. T. EPxP dry Scrubber is a novel device for controlling fine particle emissions at high temperatures and pressures. It uses relatively large particles as collection centers for the fine particles in the gas stream. Fine particles and collector granules are contacted in a venturi type contactor and fine particles are collected by the granules through the mechanisms of inertial impaction, diffusion and electrostatic deposition. For maximum efficiency the particles are pre-charged and the collectors are polarized.

Bench scale (0.5 $Am^3/min$) and pilot scale (4.8 $Am^3/min$) experiments have been run at temperatures from $20^oC$ to $820^oC$ to determine the performance characteristics of the system. This paper presents the system design and experimental results for the bench scale and pilot scale tests.

NOTE: Please contact the authors for further information regarding this paper.

# PARTICLE COLLECTION IN CYCLONES AT HIGH TEMPERATURE AND HIGH PRESSURE

By: R. Parker, R. Jain, and S. Calvert
Air Pollution Technology, Incorporated
4901 Morena Boulevard, Suite 402
San Diego, CA 92117

D. Drehmel and J. Abbott
Particulate Technology Branch
Industrial Environmental Research Laboratory
U.S. Environmental Protection Agency
Research Triangle Park, NC 27711

## ABSTRACT

An experimental study of cyclone efficiency and pressure drop was conducted at temperatures up to 700°C and pressures up to 25 atm. The cyclone efficiency was found to decrease at high temperature and increase at high pressure for a constant inlet velocity. Available theoretical models could not predict the observed effects of high temperature and high pressure on collection efficiency. Pressure-drop models predict the effects of temperature and pressure fairly well. Collection-efficiency data correlated well against Reynolds number and the square root of Stokes' number. This correlation accurately accounted for the effects of both temperature and pressure. These data are for a 2-in. diameter cyclone at relatively low velocities ($<5$ m/s). Data for a 6-in. cyclone of similar configuration and operating at 635°C, 700 kPa, and 36 m/s also agreed well with this correlation.

NOTE: Published in Environmental Science & Technology, 15:451-58, April 1981.

# OPERATING RESULTS OF ELECTROSTATIC PRECIPITATORS AT HIGH TEMPERATURE AND HIGH PRESSURES

By: Paul L. Feldman and K. Sampath Kumar
Research-Cottrell, Inc.
P. O. Box 1500
Somerville, New Jersey 08876

## ABSTRACT

This paper presents Research-Cottrell's experience with pilot electrostatic precipitators (ESPs) under extreme conditions of temperature and pressure. Case studies of five pilot systems are provided which describe operations at temperatures upto 1700°F and pressures upto 850 psig. This discussion brings out the lessons learned from these pilot ESP's and points out the future development needs in selection of materials, mechanical design and process understanding. Some case studies have a direct bearing on the design and operation of ESP's for hot gas cleanup in pressurized fluidized bed combustion systems.

## INTRODUCTION

The investigation of electrostatic precipitator for applications in unusual temperature and pressure environment has been underway for several decades. During mid 1920's research began on the application of high pressure ESP's for high pressure coal gas pipelines to collect oil and tar impurities from the gases. Elaborate research work was later pursued by Wintermute[1] in the 30's, Cooperman[2] in the 50's, Shale[3], Brown[4], and Robinson[5] in the 60's. Bush, Feldman and Robinson[6] continued the research work on corona stability in the 70's covering a wide range of temperature and pressure.

Because of the strong foundation of research established by workers during earlier decades, opportunities surfaced during the 60's for pilot scale experiments on the performance characteristics of the high pressure and high temperature(HTHP) precipitators.

## CASE STUDIES

First of the five pilot programs to be discussed is the Union Carbide pilot plant. Table 1 is a concise compilation of all the important aspects of these five pilot plants.

TABLE 1. PILOT HTHP ELECTROSTATIC PRECIPITATOR EXPERIENCE

| Item | Union Carbide Olefins | Bureau of Mines | Combustion Power Co. | Texaco Co. | Texas Gas Transmission Co. |
|---|---|---|---|---|---|
| Dates Tested | 1962-1964 | 1963-1968 | 1966-1968 | 1961-1963 | 1965-1967 |
| Location | Institute, W. VA | Morgantown, W. VA | Montebello, CA | Montebello, CA | Lake Cormorant, MI |
| Fuel | Coal | Natural Gas | Methanol | Heavy Oil (#840 12° API) | Pipeline |
| System | PFB Burner | H.P. Gas Burner (lab) | S.U.E. Burner | Gasifier | Pipeline |
| Dust: Type | Ash | Flyash - Reinjected | Alumina/Flyash Injected | Carbon | Lube - Oil |
| Mean ϕ (μ) | 2.6 | 30 | 6-10 | 0.007 to 0.01 | 0.7 |
| T (°K) | 870-1000 | 1000-1100 | 1150-1200 | 400-465 | 310-316 |
| P (ATM) | 3-8 | 4.5-6.5 | 4.5-11 | 21-25 | 53-56 |
| # Pipes Tested | 19 | 16 | 1 | 5, 3, 1 | Plates: 7 Ducts |
| Pipe Diameter (cm) | 15.2 | 15.2 | 20.3 | 10.2, 15.2, 20.3 | 7.6 (Plate spacing) |
| Pipe Length (m) | 1.83 | 1.83 | 4.57 | 1.83 | 3.05 x .6 high |
| Gas Velocity (m/s) | .2-1.2 | .3-1.1 | 2.9 | .61-1.1 | 3-9 |
| Gas Flow (kG/hr) | 570-820 | 2600 | 980 | 490 | 163,000 |
| SCA ($ft^2$/1000 acfm) | 200-1200 | ~230 | 157 | 180-300 | 96 |
| Discharge Electrode: Type | Wires | Wires | Twisted Wires | Twisted Wires, Rigid Electrodes | Wires |
| Discharge Electrode: Diameter (mm) | 2.1, 3.4 | 2.1 | 3 x 2.8 | One 3 x 1.8 Twisted, Five 3 x 1.8 Twisted, 6 Vane Paddlewheel | .25 |
| Typical Collection Efficiency (%) | 98.8 | 91-96 | 80-82 | 98.8 | 99 |
| Cleaning System: | | | | | |
| HT | Rapper | Rapper | Rapper | Water Flush | Spray Systems |
| LT | Rapper | Rapper | Rapper | | |

Union Carbide Olefins Co.

Union Carbide, in 1961, operated a pilot pressurized fluidized bed combustor (PFBC) in Institute, W. Virginia. A HTHP precipitator was supplied in early 1963 with the purpose of removing particulates at 1300°F and 100 psig, prior to the gas turbine cycle.

The test program consisted of over one hundred tests in a six month period. Current-voltage characteristics were obtained for various temperature and pressure conditions, which are described in Figure 1. It could be seen from this illustration that operating pressure had an very important bearing on the ESP operation at Union Carbide. Even though the temperature was about 1300°F, the operating pressure of 70 psig shifted the i-v curve to the right, making possible the application high electric field strengths, often exceeding 20 kV/in. Figure 2 illustrates the effect of operating field strengths on collection efficiency of ESP. Higher operating field strengths resulted in higher collection efficiency, conforming to the dust collection phenomena of ESP's in high sulfur coal applications.

The ESP consistently achieved collection efficiencies of 98-99%. Flyash particulates were rather fine with a mass median diameter of 2.6 microns. Precipitator gas velocities were generally above 4 ft/second. No difference in particulate collection efficiency was reported for two wire diameters that were tested. There were no operating problems encountered with this unit. Both the collecting tubes and discharge electrodes were kept clean by the cleaning system arrangement.

Texaco

In early 1960 Texaco operated a pilot synthesis gas generator at Montebello, California. Oxidation of heavy fuel oil had geneated fine carbon material which was limiting the life of shift converter catalysts downstream. Research-Cottrell was asked to design a system that would reduce the concentration of these submicron (0.007 to 0.01 μm) carbon particles from 400 ppm down to 5 ppm or less. Operating temperatures were typically 350°F but the operating pressure was high, about 350 psig.

Research-Cottrell designed a wet wall precipitator to prevent both carbon reentrainment and build up on electrodes. Two rigid discharge electrode designs are reported here, one with a six vane "paddlewheel" structure and another with a rigid central mast with five twisted wires mounted around it.

Seventy short runs and one extended test run of one hundred hours were examined. The eight inch collecting pipe had maximum electrical stability with the wet wall opeation. Current-voltage

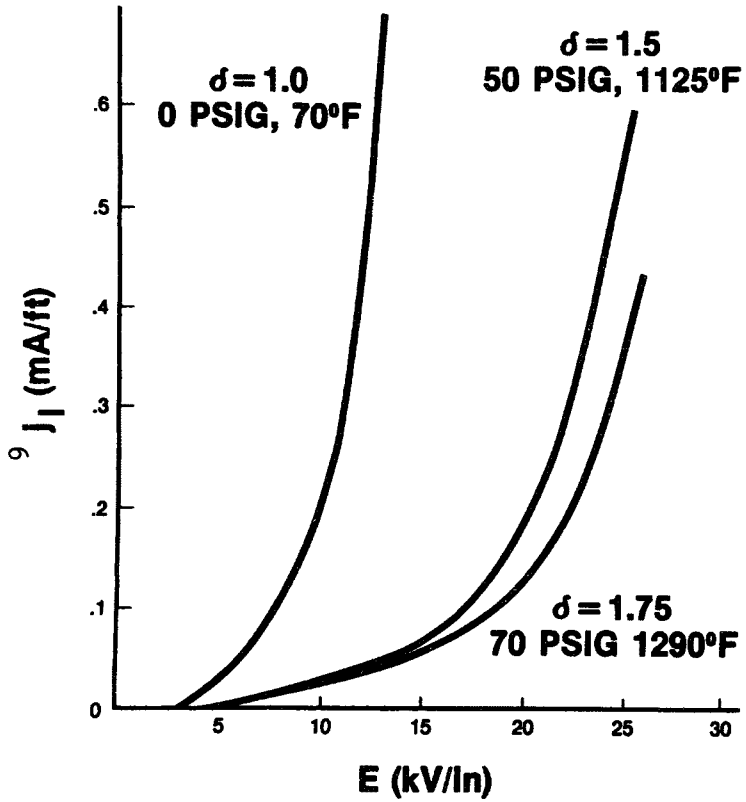


Figure 1 **CURRENT-VOLTAGE CURVES TAKEN IN PROTOTYPE HTHP PPTR PILOT**
(Union Carbide Olefins Co.)

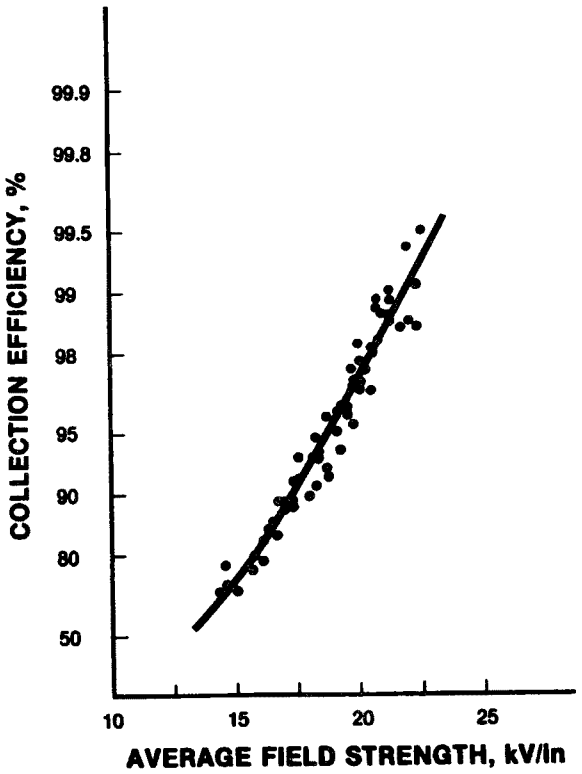


Figure 2 **PERFORMANCE of a HTHP WIRE-PIPE PPTR FOLLOWING an OPERATING PFBC at 1300°F**
(Union Carbide Olefins Co.)

characteristics with the eight inch tube are shown with 5-wire stiff discharge electrode on Figure 3, while those with the paddlewheel design are shown in Figure 4. It can be seem from these figures that good electrical stability could be maintained by these electrodes, resulting in high operating voltages (and hence field strengths).

Both the short test runs and the extended operation showed that particulate loading after the ESP could be consistently maintained below the 5 ppm level, resulting in particulate collection efficiency near 99%. Above results were possible only with negative polarity of the applied voltage. When positive polarity runs were attempted, particulate loading increased to 19 ppm.

Bureau of Mines

During the mid 1960's C. C. Shale extended his HTHP precipitator investigations to pilot scale. Flue gas was generated by burning natural gas and flyash particle were reinjected to simulate the dust burden. Research-Cottrell supplied the precipitator to operate upto 1500°F and 80 psig. Precipitator consisted of sixteen six inch diameter pipes with 0.083" discharge electrodes. Both pipes and wires were cleaned by pneumatic rapping systems similar to the Union Carbide system.

Shale encountered several opeating problems with this pilot unit. Tube sheet, which held all the collecting tubes, was distorted due to thermal expansion problems, and the horizontal rapping system added to the tubes' further dislocation from the vertical axis. Misalignment had reduced the clearance between discharge and collector electrode by an inch, resulting in reduced applied voltages. The high voltage support insulator had overheating problems, which further limited the application of high voltage. In spite of these adverse conditions, the ESP performed reasonably well when the polarity of applied voltage was negative.

Collection efficiency under the operating condition of 1470°F and 80 psig was 95% with negative polarity. Operating voltage was 38 kV at a precipitator current of 180 mA. However, the collection efficiency with positive polarity was 75%. Though the operating voltage was high, at 55 kV, the precipitator current was only about a fifth of that with negative polarity at 40 mA.

It is felt that the high current densities in the precipitator can introduce sufficient adhesive forces on collecting electrodes overcoming the reentrainment problems associated with high conductivity of particulates at the high operating temperatures. Positive polarity inspite of higher voltage, may be

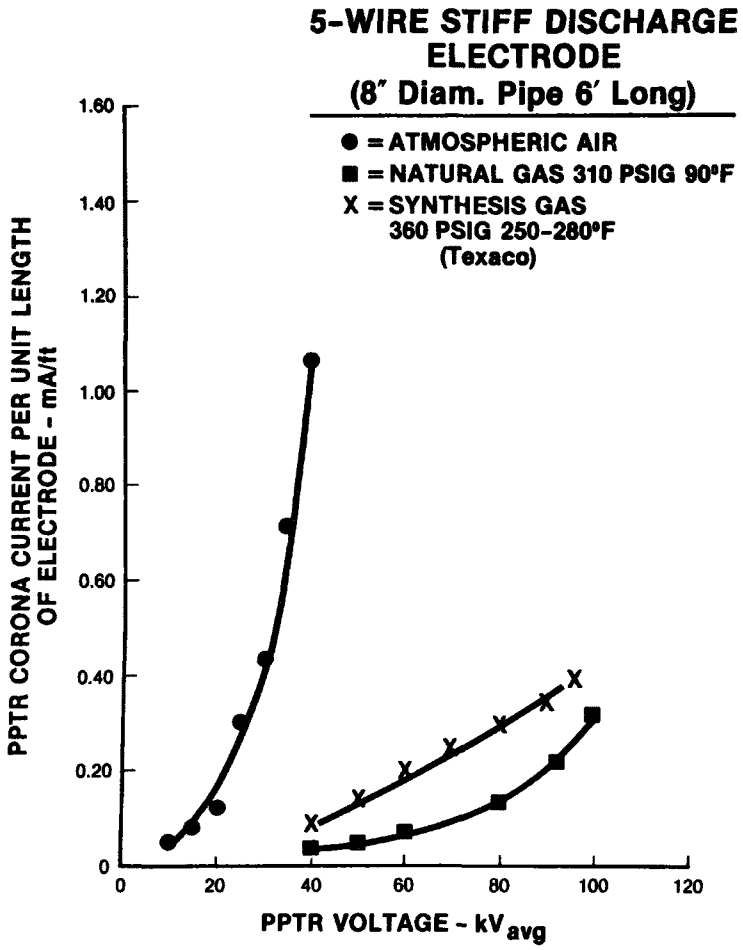


Figure 3 CURRENT-VOLTAGE CHARACTERISTICS

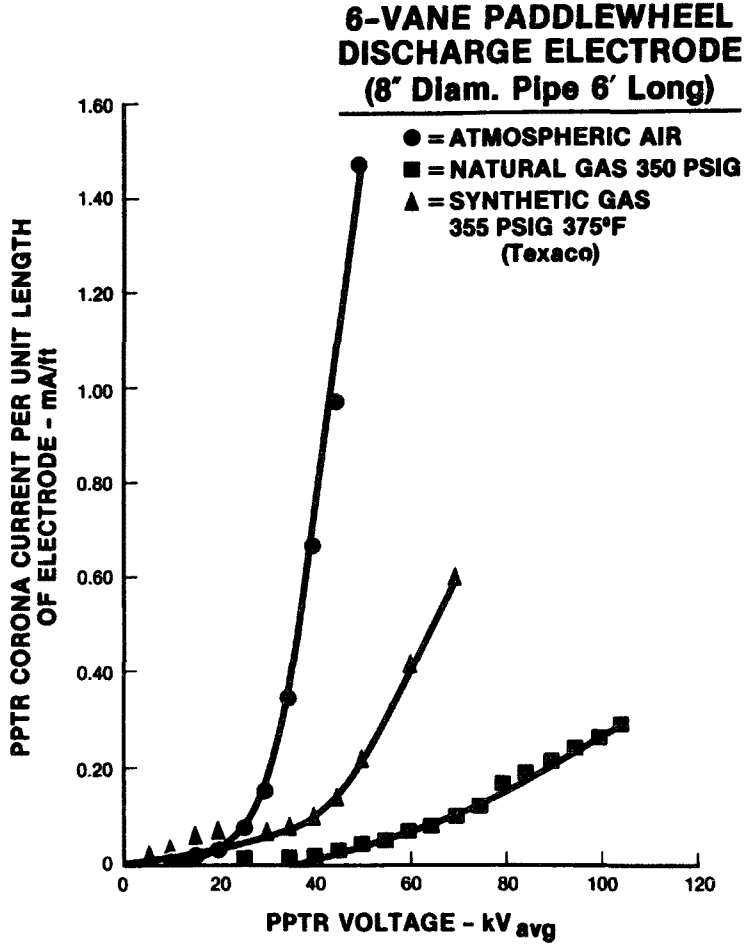


Figure 4 CURRENT-VOLTAGE CHARACTERISTICS

suffering from particulate reentrainment problems associated with low current densities.

Figure 5 shows the current voltage relationship with negative polarity at various relative densities, at a temperature of 1470°F. Again, we see the shift in these curves to the right as the relative density (or pressure) goes up. Runaway currents are possible at high temperatures if the operating relative density is too low. Shale noted in his work that negative field required a relative density of at least 1.25 for corona stability.

Combustion Power Company

In the mid 60's Combustion Power Company was investigating pressurized incineration of municipal solid waste for U.S. Department of H.E.W. Particulate collection was to be accomplished by an electrostatic precipitator at 1600-1700°F and 50-150 psig.

Figure 6 shows the typical i-v data at two levels of gas density for positive and negative polarity. Testing showed that both negative and positive polarity were stable at 1700°F as long as pressure was greater than 3.5 atmospheres. Also, the positive polarity showed higher sparkover voltage than negative.

However,as noted in the earlier work, negative corona resulted in much higher collection efficiencies than positive. Figure 7 correlates electric field strength (E) to collection efficiency ($\eta$) for both negative and positive polarity. Good correlation with $E^2$ and ln $(1-\eta)$ is seen, which is typical of conventional precipitators.

Alkali (KCl) addition to flue gas was tested to determine if high alkali levels would result in excessive unstable currents at the high temperatures. Figure 8 describes the effect of KCl addition at 0, 40 and 400 ppm at 1700°F. The addition of alklai increased the current between 60 to 90% at 40 ppm and several times at 400 ppm. Corona instability is indicated at the high ppm levels of alkalis. The real effect of alkali pressure in PFBC effluents on the ESP remains to be seen during the ensuing pilot plant work with DOE.

One of the problems noted in this work was the discharge electrode oscillation at high temperatures. Oscillation spans of 2-4" had limited the electrical operation to 12 kV/in. Much higher field strengths would have been possible in the absence of this phenomenon. This adverse phenomenon may partially explain the low efficiency of 87% attained during the tests. In addition to low field strengths (and hence low precipitator current), high gas velocities of 9.5 ft/sec during the tests

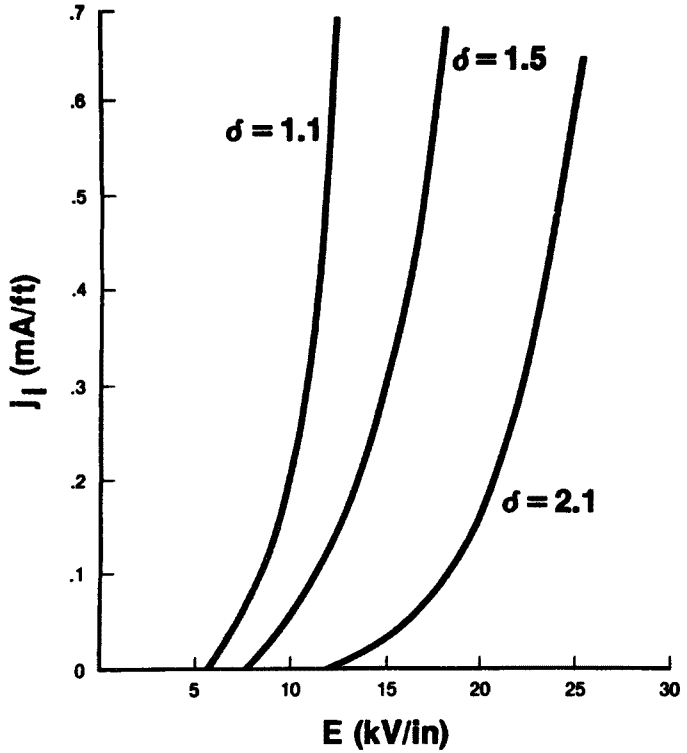


Figure 5

**HTHP PILOT PPTR CURRENT-VOLTAGE DATA TAKEN by C. SHALE at MORGANTOWN COAL RESEARCH CENTER, US BUREAU of MINES**

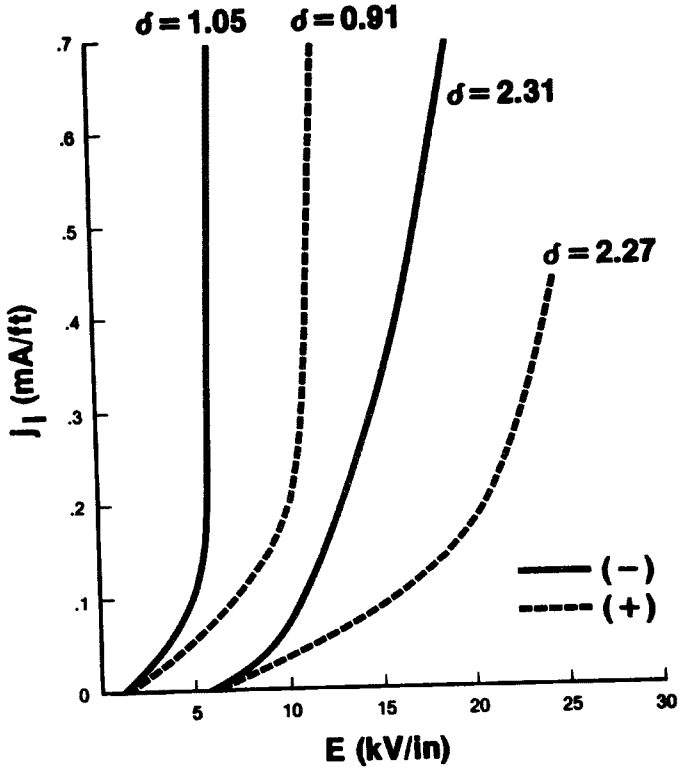


Figure 6

**CURRENT-VOLTAGE DATA FOR T = 1650-1720 °F, P = 50-140 PSIA**
(Combustion Power Co.)

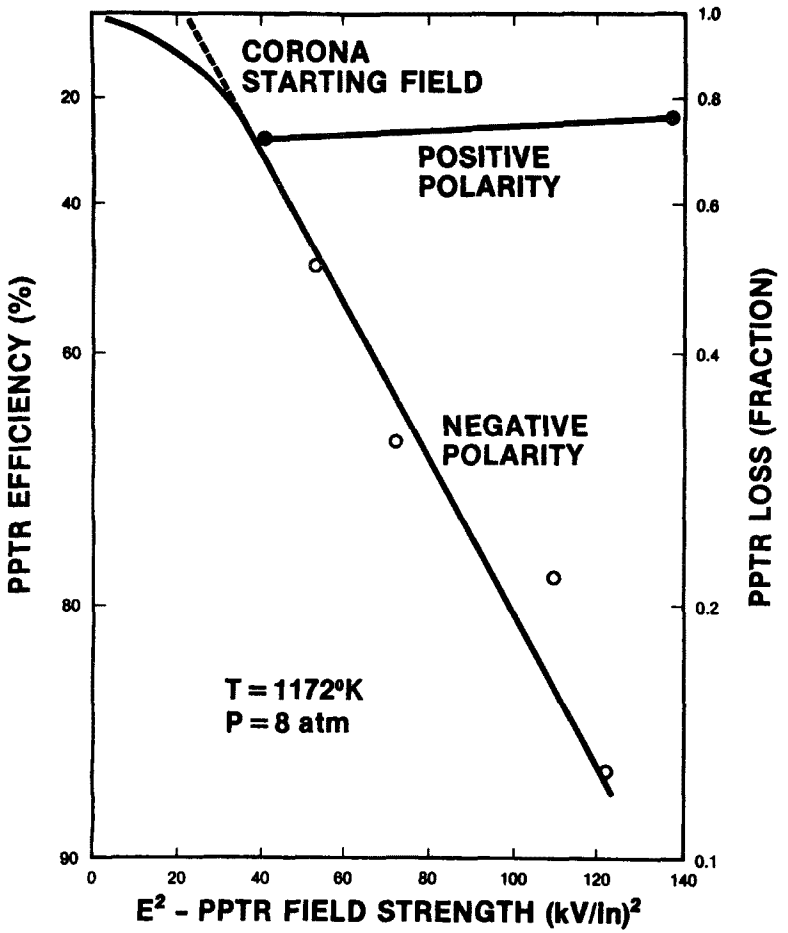


Figure 7 **PPTR COLLECTION EFFICIENCY ON ALUMINA TEST DUST AS A FUNCTION OF FIELD STRENGTH**
(Combustion Power Co.)

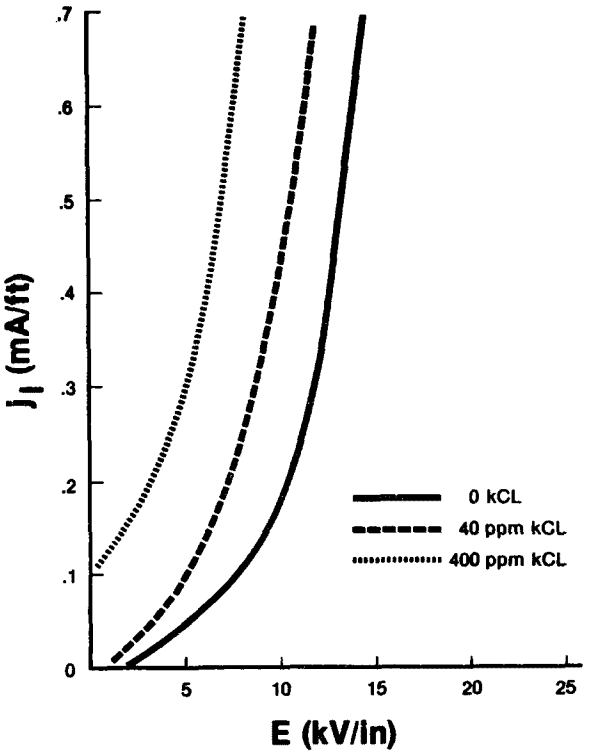


Figure 8 **EFFECTS of ALKALI ADDITION AT 1700°F, 115 PSIA**
(Combustion Power Co.)

could also have contributed to a reentrainment problem.

Texas Gas Transmission Co.

Natural gas pipelines had faced the problem of submicron oil mist from oil lubricated compressors, thereby limiting the pipeline transmission efficiency. In 1965 Research-Cottrell worked with Texas Gas Transmission Co. to develop a precipitator for removing the oil mist and increasing pipeline efficiency.

The precipitator operated for one year in steady state operation and was a successful demonstration. Collection efficiencies were above 99%. Inlet grain loadings were 0.03 grains/acf with a particle size of 0.7 micron. The pipeline efficiency improved from 93.6% to 99% with the use of ESP's.

## FUTURE DEVELOPMENT NEEDS

Although the case studies of five pilot precipitators provide data base for design with more confidence, there is a definite need for further extended testing on the demonstration scale to resolve several key issues.

### Ash Characteristics

Ash characteristics such as stickiness, ease of dislodgement are important issues affecting precipitator performance and these can only be evaluated under actual operation conditions.

### Reentrainment

It is important to characterize the parameters that can exacerbate the reentrainment of ash back into the gas stream, thus lowering the overall collection efficiency. Factors such as gas velocity, applied electric field strengths and rapping characteristics need to be evaluated to ensure high efficiency operation.

### Electrode Alignment

Good alignment between discharge electrodes and collecting tubes is of paramount importance to maintain high precipitator efficiency. Mechanical designs should account for thermal expansion effects and rapping stress effects to overcome the misalignment potential. Further, only an on-site demonstration can confirm the efficacy of such designs.

### Discharge Electrode and Collector Tube Cleaning

Though rappers have been used in the past work, there is a

necessity to minimize impacting requirements on component members at high temperature to improve hardware reliability. Use of sonic energy to dislodge collected particulates has been successfully demonstrated in several applications. Sonic energy systems do not impose severe stresses on structural members. Therefore, optional combination of cleaning systems is essential to improve component reliability.

Tube Shape

Collector tubes using cylindrical pipes have inherent deficiency in packing more collector area for a given volume. This leeds to larger pressure vessels and hence are less cost effective. Designs should consider "hexagonal" type collector tubes with a honeycomb arrangement. If this design proves out to be successful, significant cost savings can be achieved by improving packaging efficiency of precipitator components.

Power Supply and Bushings

Optimum operation may require use of high voltage power supplies that are at present beyond the state-of-the-art technology. Data for such applications depend on the temperature, pressure condition of the process. Further, temperature controlled insulators are necessary to overcome heating problems at high temperature.

Materials of Construction

High temperature applications beyond 1500$^{o}$F need careful choice of materials that have both oxidation resistance and high yeild strengths under typical ESP operation.

Economics

Cost analysis performed by Bush, et al[7] have shown that high temperature high pressure precipitators can be cost effective for PFBC conditions, assuming reasonable sizing and design parameters. Demonstration scale tests are needed to generate data for commercial offerings.

## CONCLUSIONS

Though the past pilot plants at extremes of temperature and pressure have provided a data base for design and sizing of ESP's, several development questions need to be answered. Extended testing on "demonstrator" pilot plants are needed prior to reliable product offerings. Research-Cottrell's ongoing contract with DOE to demonstrate HTHP precipitator performance on a 2 MW PFBC system for hot gas cleanup is a step in the right direction. It is felt that emerging energy technologies

will revive the interest in ESP use for extreme temperature and pressure applications.

## ENDNOTES


1. H. Wintermute, "Report on Voltage and Current Tests at High Pressures", Research Corporation, April (1931).

2. P. Cooperman, "The Effects of Gas Temperature, Pressure and Composition on the Electrical Characteristics of the Corona Discharge", Research-Cottrell, September (1953).

3. C. C. Shale, "High Temperature, High Pressure Electrostatic Precipitation", APCA Paper No. 66-125, 1966.

4. R. F. Brown, "An Experimental High Temperature High Pressure Electrostatic Precipitator Module Design and Evaluation", Research-Cottrell, (1969).

5. M. Robinson, R. F. Brown, F. W. Schmitz, "Pilot Plant Tests of an Electrostatic Precipitator on High Pressure Synthesis Gas (Texaco Process)", Research-Cottrell, Inc., April (1963).

6. J. R. Bush, P. L. Feldman, M. Robinson, "Development of a High Temperature, High Pressure Electrostatic Precipitator", EPA-600/7-77-132, November (1977).

7. J. R. Bush, F. L. Blum, P. L. Feldman, "Comparative Economic Analyses of Selected Particulate Control Systems for Advanced Combined Cycle Power Plants", Second EPA Symposium on Transfer and Utilization Control Technology, July, 1979.

# CONTROL OF PARTICULATES IN PROCESS AREA 12, SOLVENT REFINED COAL PROCESS

By: W. H. Wilks, P.D. Wilkinson
Catalytic, Inc.
1500 Market Street
Philadelphia, Pa. 19102

J.A. Schlosberg
International Coal Refining Company
P.O. Box 2752
Allentown, Pa. 18001

## ABSTRACT

The Solvent Refined Coal Process is one of the major undertakings in the Synthetic Fuels Program of the U.S. Department of Energy (DOE). International Coal Refining Company (ICRC), a partnership of Air Products and Chemicals and Wheelabrator-Frye, is now in the design stage of a 6000 TPD demonstration plant. There are many facets of the process where proven technology is not yet available, which is part of the reason for a relativly large demonstration plant. The environmental atmospheric emission problems on the other hand, were investigated and solved with established control technology.

Catalytic, Inc. has the responsibility for the design, engineering and special equipment procurement in one process area. This paper describes the environmental approach used by Catalytic, Inc. to control particulate emissions in that area. The contents include: a description of the SRC-1 process, identification of the emission sources, definition of the problem area, application of basic control principles, and equipment selection and design based on accepted and proven approaches.

## INTRODUCTION

The Solvent Refined Coal (SRC-1) Process, one of the most advanced direct coal-liquefaction processes available, has attracted considerable national attention as a partial answer to the continuing energy crisis. The SRC-1 Process will utilize America's abundant supply of high-sulfur bituminous coal to produce a varied selection of reliable and environmentally acceptable products. These include low-sulfur ash-free boiler fuels, metallurgical and anode grade coke; and with further refinement distillate fuels as well as petrochemical and gasoline feed stocks. Air Products and Chemicals, Inc. and Wheelabrator-Frye Inc. both bring much research, development, and engineering experience in coal-liquefaction technology to the Demonstration Plant Program. Catalytic, Inc. (a subsidiary of Air Products) has engineered, built, and now operates a six ton-per-day SRC Pilot Plant at Wilsonville, Ala., while Rust Engineering (A subsidiary of Wheelabrator-Frye) designed built and operates the DOE Pilot Plant at Fort Lewis, WA. During the initial phase of the current project (referred to as Phase 0), Catalytic has used this experience in the conceptual design and environmental appraisal in its assigned process area. In addition, Catalytic has evaluated process options and identified critical technology areas requiring additional

data. Alternatives and refinements are being evaluated in Phase 1 to improve overall process and environmental systems. The ultimate purposes of the 6000 TPD Demonstration Plant are to establish the feasibility of large-scale production economics, to prove the applicability and reliability of commercial mechanical equipment, and to define environmental problems and evaluate the applied control technology. Ultimately, this will serve as the basis for expanding to a 30,000 TPD commercial plant.

## DESCRIPTION OF THE SRC-1 PROCESS

The SRC-1 process begins with mixing of dry pulverized coal with a process-derived solvent in the Coal Slurry Drums. (See Figure 1.) The resulting slurry is pumped to reaction pressure, a hot hydrogen-rich recycle gas is added before the mixture is heated to reaction temperatures in the Coal Slurry Heaters. Additional hot hydrogen-rich recycle gas is added at the exit of these fired heaters, and the mixture flows through the first coal dissolver. Cold hydrogen-rich recycle gas is added as a quench at the exit of the first dissolver before entry into the second dissolver for further hydrogenation and desulfurization, producing a slurry of low-sulfur SRC (Solvent Refined Coal) and mineral ash, plus liquid and gaseous by-products.

Vapors are separated from the liquids and the SRC/mineral ash slurry in a High-Pressure (HP) Separator (operating at reaction conditions) and in the Medium-Pressure (MP) and Low-Pressure (LP) Flash Drums, in which the pressure is progressively lowered resulting in further vapor/liquid separation. Vapors containing excess unreacted hydrogen are partially condensed in the Hydrogen Recovery Section, medium-pressure hydrogen-rich sour gas is separated, compressed, and combined with high pressure sour gas and forwarded to a gas-treatment unit for acid-gas removal before being recycled to the coal dissolvers. Hydrocarbon liquids recovered from the Hydrogen Recovery Section and vapors from the LP Flash Drum are sent to the Solvent Column for fractionation into medium and heavy oils. Over-head distillates from this column are partially condensed, yielding a medium oil product and a low-pressure noncondensable off gas which is compressed and forwarded to gas treatment for use as process fuel gas. The bottoms product is the process solvent or heavy oil; part is sent to the Process Solvent Drum for recycle to the Coal Slurry Drums, and the rest removed as heavy oil product.

The SRC/Mineral ash slurry exiting the LP Flash Drum is charged to a Vacuum Column for further recovery of process solvent. Non-condensable overhead vapors are collected in a vent system and incinerated in the Coal Slurry Heaters. The bottoms product (SRC, mineral ash, and unconverted carbon) is sent to the Kerr-McGee Critical Solvent Deashing Unit (CSDU) where solid mineral ash and unconverted carbon are separated from the SRC using a proprietary process. Ash concentrate from the CSDU is conveyed to a gasifier for hydrogen production and to convert the ash to an environmentally acceptable slag. Molten ash-free SRC from the CSDU is then divided into three approximately equal streams. One-third is delivered to an Expanded-Bed Hydrocracker for further hydrogenation to liquid distillates, one-third is sent to a Coker-Calciner for coke production, and the remainder

is cooled and solidified on the SRC Solidifiers (sufficient capacity is provided to solidify 100 percent of the Molten SRC produced). The low-sulfur, ash-free solid SRC product is then conveyed to storage.

## BASIS FOR SELECTION OF CONTROL SYSTEMS

### Government Requirements

The entire facility is considered a "major source" that will be constructed in an environmental area designated as attainment. It is therefore subject to EPA's PSD (Prevention of Significant Deterioration of Air Quality) regulations, which have been promulgated in 40 CFR 52.21. This requires the application of BACT (Best Available Control Technology).

This requirement for the application of BACT means that the emissions limitations (including a visible-emissions standard) must be based on the maximum degree of reduction achievable for each pollutant subject to control under the Clean Air Act. The maximum degree of reduction achievable for each pollutant emitted is determined by the Administrator on a case-by case basis. This determination takes into account energy, environmental, and economic impacts and costs. Beside the conventional air-pollution-control approaches, this effort involves application of in-plant pollution-abatement measures in the production processes and of other control methods, including fuel cleaning or treatment, and innovative combustion techniques.

The application of BACT cannot result in emissions of any pollutant that would violate any applicable standard under the New Source Performance Standards (40 CFR 60), National Emission Standards for Hazardous Air Pollutants (40 CFR 61), or an approved State Implementation Plan.

### Process Restrictions

Some information required for the Kentucky Air Permit applications was not available, either because of process decisions that were yet to be made, detailed engineering that was not yet completed, or data to be supplied by a vendor who had yet to be selected. If permit application preparation were delayed until all such needed information was available, construction could be delayed a year or more. We therefore addressed all relevant air pollution control and air quality concerns in the most thorough manner possible. Kentucky had agreed to accept preliminary information based on best engineering judgement as to the outcome of process option studies and detailed design. This was contingent upon the willingness to make conservative judgements with respect to potential air quality impacts and to update the preliminary information as necessary. This approach is typical of environmental input at the onset of a project, where the environmental engineer works closely with process engineers and other disciplines. It has resulted in a mutual understanding of each other's responsibilities and problems and has established a consensus for selecting the best solutions, whether through process change and/or control-equipment application.

## IDENTIFICATION OF PROBLEMS AND DEVELOPMENT OF SELECTED CONTROL SYSTEMS

### Process Heaters

The process area (Refer to Figure 1) will have four indirect-fired types of heat exchangers, which are governed by Kentucky Air Pollution Control Regulation 401 KAR 59:015, Section 4:

1. The coal-slurry heaters - to heat the coal slurry to the reaction temperature required in the dissolvers.

2. The CSD heater - to heat the proprietary solvent and the SRC mixture.

3. The vacuum heater - used only on startup, to heat the SRC solvent and ash slurry and to raise the vacuum column to designated normal operating temperature.

4. The hot-oil heater - to raise heat-transfer fluid to operating temperatures.

The total heat level for all heaters is 522 MM BTU/Hr. During normal operation the heaters will be fired with process-derived fuel gas, which is equivalent to natural gas. During startup the heater will be fired with process-derived fuel oil, equivalent to No. 6 fuel oil. Regular operating schedule will be 24 hours per day, 330 days per year, based on one scheduled 35-day shutdown.

### Proposed Controls

The control of particulate emissions is a function of the design and operation of the combustor, which will be designed for low excess air combustion with commercially-proven burners. No attempt will be made to operate at off-stoichiometric combustion conditions; thus any unburned hydrocarbons due to incomplete combustion will be insignificant.

The residence time in the heaters will be 1-2 seconds at 2200$^{o}$F, plus an additional second at 1500$^{o}$F. This time/temperature combination will achieve 100 percent combustion of hydrocarbons, with a corresponding reduction in particulates approaching zero emission. A continuous monitoring instrument will be used to measure unburned hydrocarbon in each stack. If the emission levels approach design limitations, excess air rates will be changed to insure complete combustion.

The opacity regulation for individual indirect heat exchangers with heat input capacity less than 250 MM/BTU/Hr is that a maximum of forty (40) percent opacity shall be permissible for not more than six (6) consecutive minutes in any sixty (60) consecutive minutes during cleaning of the fire box or blowing soot. This regulation will be met by determining the frequency of soot blowing during actual operation of each heater.

Expected Control Efficiency

The design and operation of the heaters, as confirmed by the monitoring, will result in emissions levels for particulate well below the value stated in the Kentucky regulation, which is 0.10 lb/MM BTU for a source (all heaters) having a total heat input greater than 250 mm BTU/Hr. The values submitted on the Kentucky Air Pollution Control Permits Applications were from EPA AP-42 "Compilation of Air Pollutant Emission Factors", which are 0.0095 lb/MM BTU for gas-fired and 0.056 lb/MM BTU for oil-fired heaters. Based on vendor information, the actual emissions should be less than these factors. The schedule of soot blowing will insure compliance with the opacity regulation.

BACT Rationale

The operational controls adopted for these heaters will reduce the emissions of particulate (including opacity) well below the allowable for applicable State regulations and also meet the BACT control requirements. Additional end-of-pipe controls for further reduction are not warranted.

Emissions from Process Operations

The following two vent streams emitting particulate are governed by Kentucky Air Pollution Control Regulation 401 KAR 59:010 for New Process Operations:

1. The emissions produced when pulverized coal and process solvent are charged to the coal slurry drums

2. The emissions produced from exhausting the solidifier hoods during the solidification of SRC in the SRC solidifiers.

Proposed Control System

Proposed Control System 1 is shown schematically in Figure 2 and described in the following paragraphs.

Emissions from the Coal Slurry Drums (water vapor, nitrogen, argon, process solvent vapors, and coal particles) will be treated for particulate removal in a venturi scrubbing system consisting of coal slurry vent ejectors, vent separators, and vent condensers.

Recovered solvent/water will be reprocessed and the solvent reused. Coal Slurry Vent Condenser emissions, which will consist of small amounts of particulate and solvent vapor in nitrogen and argon, will be sent through Coal-Slurry Vent Blowers to the SRC H.C. Vent Vapor Seal Pot.

Emissions from the SRC Solidifier hoods through the Solidifier Fume Blowers (SRC particulate and hydrocarbon vapors) will be sent to the Solidification Vent Vapor Seal Pot. The emissions from points 1 & 2 (see Figure 2) will be combined and ultimately incinerated in the Coal Slurry Heaters, along with fuel gas normally used to fire these heaters.

When the Coal-Slurry Heaters are shut down, the vapor stream from the Solidification Vent Vapor Seal Pot will be diverted to the Vent Waste Incinerator because the SRC solidifier has to operate after the rest of the process is down in order to process residual molten SRC material in the process vessels and in the Molten SRC Tank. The solidifier will operate at a reduced rate under these conditions to keep the incinerator size to a minimum. The incinerator is expected to operate approximately 1-2 days per shutdown, and fired with process fuel oil.

When the entire process is shut down, the stream from the SRC Vent Vapor Seal Pot will be diverted to the Flare Header. The vapor stream at this time will contain only small quantities of emissions, resulting from the breathing of several vessels.

The residence time in the coal slurry heaters will be 1-2 seconds at 2200$^{o}$F, plus an additional second at 1500$^{o}$F.

The residence time in the Vent Waste Incinerator will be 2 seconds at 1000$^{0}$C (1832$^{o}$F), which are the operating criteria proposed by EPA in Section 250.45-1 of Hazardous Waste Guidelines and Regulations dated December 1978. These criteria were suggested by the Kentucky Division of Air Pollution Control as acceptable without further qualification. Other operating conditions can be submitted when updating the permits, as long as there is sufficient technical backup and documentation.

Expected Control Efficiency

The vent-ejector type of scrubber, operating with liquid at the appropriate pressure (minimum of 100 psig) and liquid/gas ratio (40 gpm/1000 acfm), will remove a minimum of 94 weight percent of particles larger than 2 microns. In the condenser/accumulator, the coolant temperature will be such that 96.8 percent of the total vapors will be condensed and reprocessed. Also, during the condensing unit operation, the remaining particulate will act as a nucleus for formation of condensed droplets. This will result in removal of at least 80 percent of the remaining particulate.

In the heater operation, there will be more than enough time and temperature for 100 percent combustion of process solvent, waste vapors, and combustible particulate (coal), and also for 100 percent conversion of the $H_2S$ to $SO_x$.

The time and temperature conditions selected for the Vent Waste Incinerator will assure 100 percent combustion of process solvent, waste vapor, and combustible particulate.

BACT Rationale

The vapors from the Coal-Slurry Drums will contain a considerable amount of water, resulting in high humidity; the particulates will be sticky and tend to agglomerate in a solid mass. A wet scrubber, therefore, appears to be the most appropriate device for removal of the particulates in this

gas stream. Solvent will be used as the scrubbing liquid because it has a natural affinity for the coal dust (aiding in the removal of particulate). The slurry blowdown is returned directly to the Coal Slurry Drums.

No control system that provides a greater degree of particulate removal is applicable to this process. The physical characteristics of the particulate and of the vapors emitted by the Coal Slurry Drums preclude the use of fabric filters and electrostatic precipitators. The hydrocarbon boiling point range is such that the condenser/accumulator is highly efficient (96.84%) in removing total vapors. Incineration of the remaining solvent vapors and coal dust (along with waste vapors) in a process heater that operates continually will provide for emission control with a high degree of efficiency and reliability. Other feasible alternatives such as a separate thermal combustor or carbon-bed adsorber would not provide any greater degree of control or reliability; neither would be cost effective, as each would require additional capital expenditures, additional energy usage, and manpower for operation and maintenance.

Use of an incinerator as a standby thermal combustor on process heater shutdown will provide a safe, efficient and reliable means of combusting the exhaust from the solidifier hoods, which will consist primarily of air. The use of process fuel will make this unit energy self-sufficient.

A wet scrubber system is not feasible for removing hydrocarbon vapors. The solubility of the organic vapors in water is very low, thereby resulting in poor removal efficiencies and creating a water pollution problem.

A carbon bed adsorber although it is highly efficient may present problems in the disposal of the spent carbon in a sacrificial bed or the condensed vapors from a regenerative bed.

Decoking Operation

The emissions produced during tube decoking of process heaters are also governed by Kentucky Air Pollution Control Regulation 401 KAR 59:010 for New Process Operations.

The process heaters will require tube decoking at periodic intervals, at least once per year. This operation will consist of introducing steam and air into the tubes while operating the heaters at approximately 10 percent of normal heat capacity. The mechanics of decoking are as follows:

1. Shrinking and cracking coke loose by heating the tubes from the outside while steam is introduced from the inside. This dislodges the coke, and the steam flow carries the particles through the tubes. This is called spalling.

2. Reaction of hot coke with steam, to produce CO, $CO_2$, and $H_2$.

3. Reaction of coke and oxygen in air, to produce CO and $CO_2$.

Each decoking operation will require approximately 48 hours per pass. Some heaters will have multiple passes, and in order to reduce the total decoking time, several passes can be done in parallel.

Emissions of "coke" particles, CO, and $CO_2$ from the decoking operation will vary from a maximum at the initial stages and taper off to zero at the end of the cycle. The end of the cycle will be determined by measuring the CO and $CO_2$ levels; a zero reading will indicate completion.

Proposed Control System

The control system for the decoking operation (System 2) is shown schematically in Figure 3 and described below.

The emissions from the tube decoking of the Coal-Slurry Heaters will be sent to the Slurry-Heater Decoking Drum, those from the Hot-Oil Heater to the Hot-Oil-Heater Decoking Drum, and those from the CSD Heater and Vacuum Column Heater to the CSD/Vacuum-Heater Decoking Drum. The drums will be cyclonic separators capable of removing more than 90 percent of the particulate (designated as "Coke"); water will be fed to the top of the drum to enhance collection of the particulate. The resulting vapor streams from the decoking drums (essentially water vapor, air, CO, $CO_2$, $H_2$ and "Coke" particles) will be sent to the Vent Waste Incinerator for combustion of the CO and "Coke" to $CO_2$. The operating criteria for the Vent Waste Incinerator for this application will tentatively be the same as those for Proposed Control System 1.

Expected Control Efficiency

The particulate from the decoking operation will be generated mostly during the spalling part of the cycle. The particle size can vary from a fraction of an inch to the sub-micron range. The fines will be produced by the abrasion of the coke particles along the inside of the tubes due to the high velocity gas flow. Because there is no documented information on the expected size distribution of particulate emission from decoking operations, the efficiency of the decoking drums has to be stated in terms of typical theoretical efficiencies. Estimated grade efficiencies for Cyclone separators are 65 percent at 20 microns, 83 percent at 60 microns, and 96 percent at 60 microns. Since less than 1 percent by weight of the coke particles will be less than 20 microns, an average efficiency of greater than 90 percent is estimated. Since this is not acceptable by Kentucky as BACT, the discharge of the decoking drums will be sent to the Vent Waste Incinerator. The operation of the incinerator in terms of residence time and temperature will assure 100 percent conversion of CO and "coke" to $CO_2$.

BACT Rationale

The vapors from the decoking drums will contain CO and particulate plus a high percentage of water vapor. A cyclonic separator is the most suitable

device for this application, because of the high humidity and the size of the particles more that 99 percent of which will be larger than 20 microns in diameter. Overall efficiency will be greater than 90 percent.

A bag filter would not be appropriate because the high humidity would cause condensation on the bags and result in plugging of the unit. A wet-type scrubber, which may be slightly better in collection efficiency, would require more equipment (ejector venturi, separator, tanks, liquid-recirculation system, instrumentation, etc.), resulting in higher capital costs, energy usage and operating labor; and would create a water-pollution problem. Neither device would remove any of the CO.

The Vent Waste Incinerator is the logical backup control unit for disposing of the CO and the particulate carryover from the decoking drums. The equipment has already been justified for use in the previously described Control System 1, thereby making it even more cost effective. It would be 100 percent efficient in converting the contaminants. (The use of process fuel will produce negligible amounts of criteria pollutants.)

Fugitive Particulate Emission

Any areas in the process where there is a possibility of fugitive particulate emissions will be equipped with a hood or similar device to capture the fugitive particulates, which will then be exhausted to a control system. Therefore, no additional "Fugitive" control measures for particulate are required.

Summary

This paper is an example of what can be accomplished in a complex source (requiring a PSD Permit Application) when there is cooperation and understanding between industry and the regulatory agencies.

Ground rules were initially set by the agencies to allow for a lack of well-defined process design information and final equipment selection by accepting good engineering judgement with the option to make necessary revisions when more data becomes available. This paper demonstrates what can be accomplished when the environmental discipline is actively involved in the initial stages of a project in an integrated effort with other engineering disciplines to mutually define and solve environmental problems.

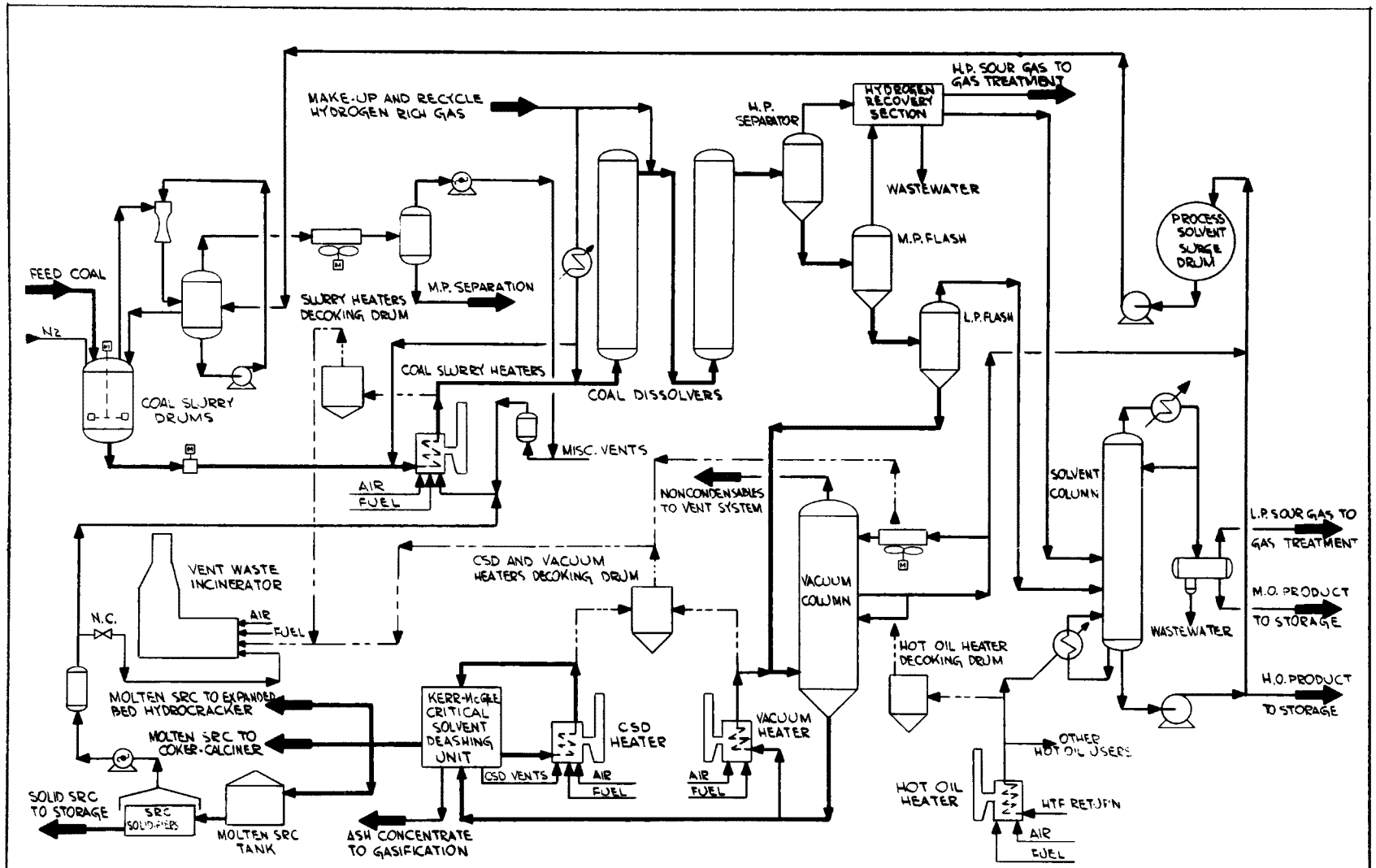


FIGURE 1

SIMPLIFIED SRC-I PROCESS FLOW DIAGRAM

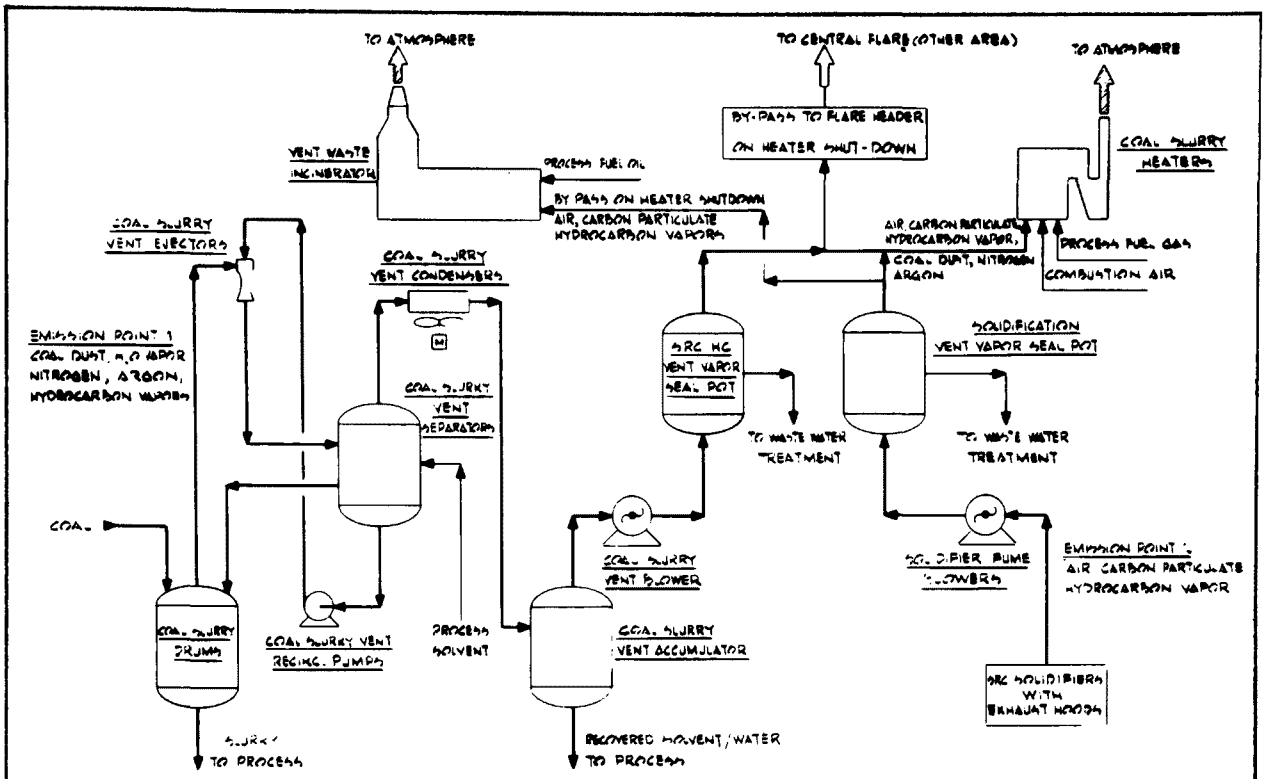


FIGURE 2— PROPOSED CONTROL SYSTEM 1 FOR COAL SLURRY DRUMS & SOLIDIFIER HOOD EMISSIONS

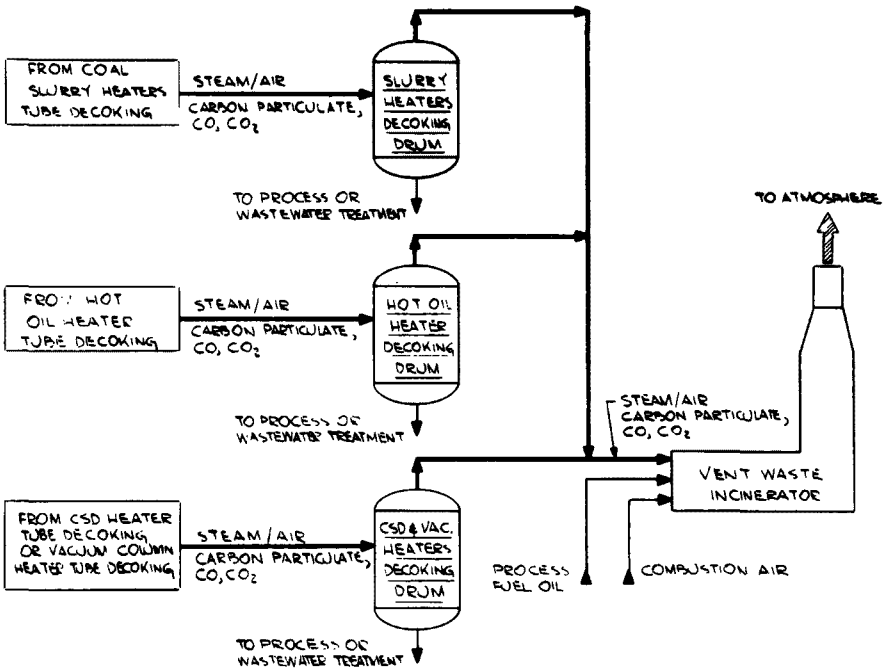


FIGURE 3

PROPOSED CONTROL SYSTEM 2 FOR PROCESS HEATERS DECOKING EMISSIONS

# NON-PLUGGING RETAINING STRUCTURE FOR GRANULAR BED FILTER FOR HTHP APPLICATION

By: A. M. Presser, J. C. Alexander
EFB, Inc.
Woburn, MA 01801

## ABSTRACT

Electrically augmented granular bed filters, modeled after commercial Electrified Filter Bed (EFB) technology, are being considered as HTHP particulate control devices. High efficiency filtration in a moving granular bed is achieved through the combined action of inertial impaction and electrical image forces. Plugging of granule-retaining structures by buildups of sticky dust, a fundamental problem encountered in HTHP gas cleanup is prevented by employing large inlet louvers backed by a shallow "fast face" region. In this region, granules are moved at a significantly faster rate than in the remaining bulk of the bed, sweeping away dust accumulations.

An 84-hour test of an EFB collecting Burgess #10 pigment dispersed in 0.38 $Nm^3/sec$ (800 scfm) of room temperature air at concentrations up to 4 $gm/Nm^3$ showed no filter plugging. Dust buildups on superfluous metal structures, which might lead to problems in longer duration tests, were shown to be eliminated in another set of similar tests

## INTRODUCTION

The success of power generation systems utilizing direct fired turbines with fluidized bed coal combustors may ride on the ability to prevent erosion of gas turbine elements by hot particulate matter in the combustion gas stream. Granular bed filters have been the focus of much investigation because of their inherent resistance to degradation in hostile environments. However, filter plugging problems caused by the sticky nature of flyash at HTHP conditions have slowed development of these filters. The tests reported here demonstrate a non-plugging granular bed filter design.

The plugging problems which must be surmounted can be illustrated by previous work. The DUCON filter is a granular bed in which filtration is effected by a cake of particulate which is allowed to build on the front face of the granule bed. Periodically, the bed must be blown back to remove the cake and keep the pressure drop within reasonable limits. In tests by Exxon (1), the front cake built to a level where it could not be blown back or, in other tests, removed by fluidizing the bed. This is an example of front face plugging, where dust actually blinds the incident face of the granular ged filter.

Combustion Power Co. (2) has tested a moving granular bed where, by utilizing relatively large granules, filtration occurs in the interstices of the bed. Here, however, the dust loaded the bed void regions to such an extent that bed motion was inhibited, leading to unacceptable buildups. This is termed bed freezing.

## Problem Approach

General Electric Company and EFB, Inc. are currently investigating a novel approach to the HTHP cleaning problem. In the Electro-granular Bed (EGB) the combined action of inertial impaction and electrical image force provide for dust filtration in the interstices of a bed composed of large granules. The EGB is a direct extension of commercially available Electrified Filter Bed (EFB) air pollution control eqiupment developed and marketed by EFB, Inc. Several patented features of this technology are directly applicable to the prevention of plugging problems. These features are described now with reference to Figure 1, a schematic of an EFB pilot system also used for part of the current tests. The schematic represents a cross-sectional view of a circular cylindrical unit in which two filter stages are vertically arranged. Inlet dust laden gas passes first through the lower stage. It is on this incident filter face, the outside of the lower tube, that the severest problems are expected because much of the filtration occurs in this first filter. The partially cleaned gas then travels upward in the hollow center where a corona discharge emitted from the centrally hung high voltage electrode electrically charges the dust. Finally, the gas exits through the upper filter stage in which the granules are electrically polarized by an applied electric field in order to collect the charged dust effeciently. In the EGB, the collection force due to the applied field is replaced with the force due to the electrical image of the charged particles.

On a continuous basis, the granules move downward through the beds with granule speed being controlled by the screw feeder at the bottom. The granule-dust mixture is separated, and the cleaned granules are transported to the top of the unit by an exterior pneumatic conveying system.

In order to achieve long term, non-plugging performance, a retaining structure for the granules has been developed which incorporates large inclined slats of metal which hold granules in the bed by action of their angle of repose, while providing a large open area where the dust laden gas essentially impinges on a free surface of gravel. The continuous motion of the gravel breaks up bridges of dust between granules and carries away any dust buildups. This feature prevents the so-called front face plugging.

As dust deposits in the bulk of the bed, it accumulates most heavily in the front regions of the bed. Excessive dust buildup in any region can cause bed freezing. The EFB system incorporates a "fast face" region defined by the inlet side louvers and a coarse mesh screen located about 1/4 of the bed overall depth away from the front louvers. Granules in this region are moved downward at a faster rate than in the remaining bed, thus removing the greater accumulations of dust faster.

The standard EFB design needed to be modified to prevent accumulation of dust on exposed portions of the bed inlet side louvers. This problem was identified in the course of these tests and is illustrated in Figure 2. The proposed solution, reducing louver area to the minimum necessary to retain the granules, proved effective in a second set of tests performed in a specially prepared model unit.

## Test Program Description

As part of the research program at EFB, Inc., cold flow experiments were performed to provide data that could be used to project HTHP performance of the EGB. The desired objectives of the test program were to demonstrate the non-plugging design during a relatively long duration at nominal dust loading, and to simulate an operational upset in which gravel motion is slowed and observe the recovery capabilities of the design.

The 800 cfm pilot unit was run at room temperature and pressure and Burgess #10 dust was dispersed as the sticky dust simulating HTHP flyash. Details of the pilot unit design are shown in Table 1. Pressure drop across each of the beds was monitored as a means of detecting plugging problems which might develop. Also, visual observations were useful in spotting areas of particulate buildup on support structures in the EGB.

The 84-hour ($3\frac{1}{2}$ day) test was preceded by one and ten hour duration tests to shake down the test equipment and procedures and to indicate problems which might occur. Table 2 shows the relevant parameters for the 84-hour test. During the run, the pressure drop across each bed was continuously monitored, and inlet and outlet dust loadings were periodically monitored. To simulate the image force that is expected to be present at HTHP conditions, an electric field of $2 \times 10^5$ v/m was imposed in the second stage. A field on the outlet bed has no effect on the performance of the anti-plugging features. At the end of 100 hours, the unit was visually inspected.

For the first 30 hours, the dust source was freshly dispersed Burgess #10 pigment. From 30 hours on, the dust source was a combination of freshly dispersed pigment and pigment cleaned from the gravel and carried by the exhaust pneumatic transport air.

A smaller filter with "reduced area louvers" was employed in another test to demonstrate the resistence of this louver design to buildups on exposed louver surfaces. This test was run at very high inlet dust loadings to accentuate the problem. Only visual observation was necessary to verify performance. Table 2 shows the test parameters.

## Test Results

Test results from the 84-hour test are shown as the evolution of pressure drop with time (Figure 3) and photographs of the louver regions after the test (Figure 4-7). Initially, pressure drop was relatively constant, with small variations caused by changes in the dust feed rate and air volume flow through the bed. After 42 hours, the granule downward motion was slowed, simulating an operational upset. Pressure drop rose in the inlet bed due to the increased loading of dust in that bed. At 52 hours, full bed motion was restored and by 60 hours the inlet bed pressure drop had recovered to its former level.

Figures 4 and 5 illustrate the state of the inlet face at the end of the test. Both are views of the louvers from above, but Figure 4 is a tangential view while Figure 5 is looking straight on. One observes that there is a heavy

growth of dust on the louvers, but open regions are visible and individual granules are discernable with no bridges between granules. That is, the fast face motion apparently destroys any bridges before they can act to freeze the bed.

Figure 7 shows a level view of the louvers. The growth of dust structures, as described in Figure 2, is evident. To confirm the theory that this growth would only occur on louver area that was not swept by granules, the Reduced Area Louver Test was run.

The test filter of Figure 2d had shortened louvers so that there were no extraneous metal surfaces where dust could accumulate. This filter was subjected to a loading of dust of roughly 13 times the loading used in the 84-hour test. Table 3 shows the parameters used in this test. The increased dust loading accentuated deposition and as a result the test time was considerably shortened. To carry off the large amount of dust, the bed granules were also removed at an increased rate over normal.

Figure 8 shows the modified louvers before and after the test. During the first two hours, dust accumulated on the louvers and built up a rounded edge on the head of the louvers. After that, a steady state buildup appeared to be reached so the test was terminated at the end of the third hour. Figure 8b shows the louvers with some deposition, but none of the vertical dust structures which were observed in the 84 hour test. Deposition appeared limited to the 1/8" of metal at the top of the louver which was unswept by granules. This provided too small a base for large dust structures to grow.

## Conclusions

The EGB design, with large inlet louvers backed by a fast face region, modified by eliminating exposed louver surfaces has proven effective in eliminating all types of plugging problems. Long term tests with Burgess #10 pigment to simulate a "sticky" dust typical of HTHP flyash were successful in maintenance of low filter pressure drop and in avoiding dust buildups on metal structures. As a result of these tests, work is progressing to demonstrate this non-plugging design for filtration of flyash from high temperature (1550°F) fluidized bed coal combustor effluent gas.

## Acknowledgement

This work was supported by the Department of Energy under Contract DE-SC21-79ET15490 to General Electric Company. The work was performed by EFB, Inc. under subsontract to General Electric.

## End Notes

1. Hoke, R. C. and Gregory, M. W. Evaluation of a Granular Bed Filter for Particulate Control in Fluidized Bed Combustion. (Presented at EPA/DOE Symposium on High Temperature, High Pressure Particulate Control, Washington, D.C. Sept. 20-21, 1977.

2. Wade, G. L. Performance and Modeling of Moving Granular Bed Filters.

(Presented at EPA/DOE Symposium on High Temperature, High Pressure Particulate Control, Washington, D.C. Sept. 20-21, 1977).

TABLE 1. EGB DESIGN AND OPERATING PARAMETERS

| | |
|---|---|
| Bed Depth | 10 cm (4 in.) |
| Bed Outer Diameter | 60 cm (24 in.) |
| Bed Inner Diameter | 40 cm (24 in.) |
| Active Bed Face Area | 1.1 $m^2$(12.6 $ft^2$) |
| Fast Face Depth | 2.5 cm (1 in.) |
| Media Diameter | 2 mm |
| Gas Face Velocity | 0.3 m/s (60 ft/min) |
| Lift Pipe Air Velocity | 40 m/s (120 ft/s) |
| Charger | Sharpened square rod ($\frac{1}{4}$ in.) |
| Louver Vertical Spacing | 10 cm (4 in.) |
| Louver Angle | 60° from horizontal |
| Ratio Fast Face Velocity: Bulk Velocity | 3 |
| Media Feed Rate | 300 pounds/hour |

TABLE 2. 84 HOUR TEST PARAMETERS

| | |
|---|---|
| Injected Dust | Burgess No.10 pigment |
| Granular Bed Media | NJ #2 Sand (2-3 mm. diameter) |
| Inlet Gas Flow | 800 acfm |
| Fast Face Media Velocity | 5.8 ft/hr |
| Charger Voltage | 45 KV |
| Bed Applied Field | $2x10^5$ v/m |
| Media Feed Rate | 300 pounds/hr |

| Time into test | Inlet dust loading |
|---|---|
| 18 hours | 4.0 grams/$m^3$ |
| 38 | 2.6 |
| 72 | 1.8 |

TABLE 3. MODIFIED LOUVER TEST PARAMETERS

| | |
|---|---|
| Bed Depth | 10 cm (4 in.) |
| Active Bed Face Area | 0.14 $m^2$ (1.5 $ft^2$) |
| Fast Face Depth | 2.5 cm (1 in.) |
| Media Diameter | 4 mm |
| Face Velocity | 0.3 m/s (60 ft/min) |
| Louver Spacing | 10 cm (4 in.) |
| Louver Angle | 60° from horizontal |
| Average Dust Loading | 20 g/$m^3$ |
| Test Duration | 3 hours |

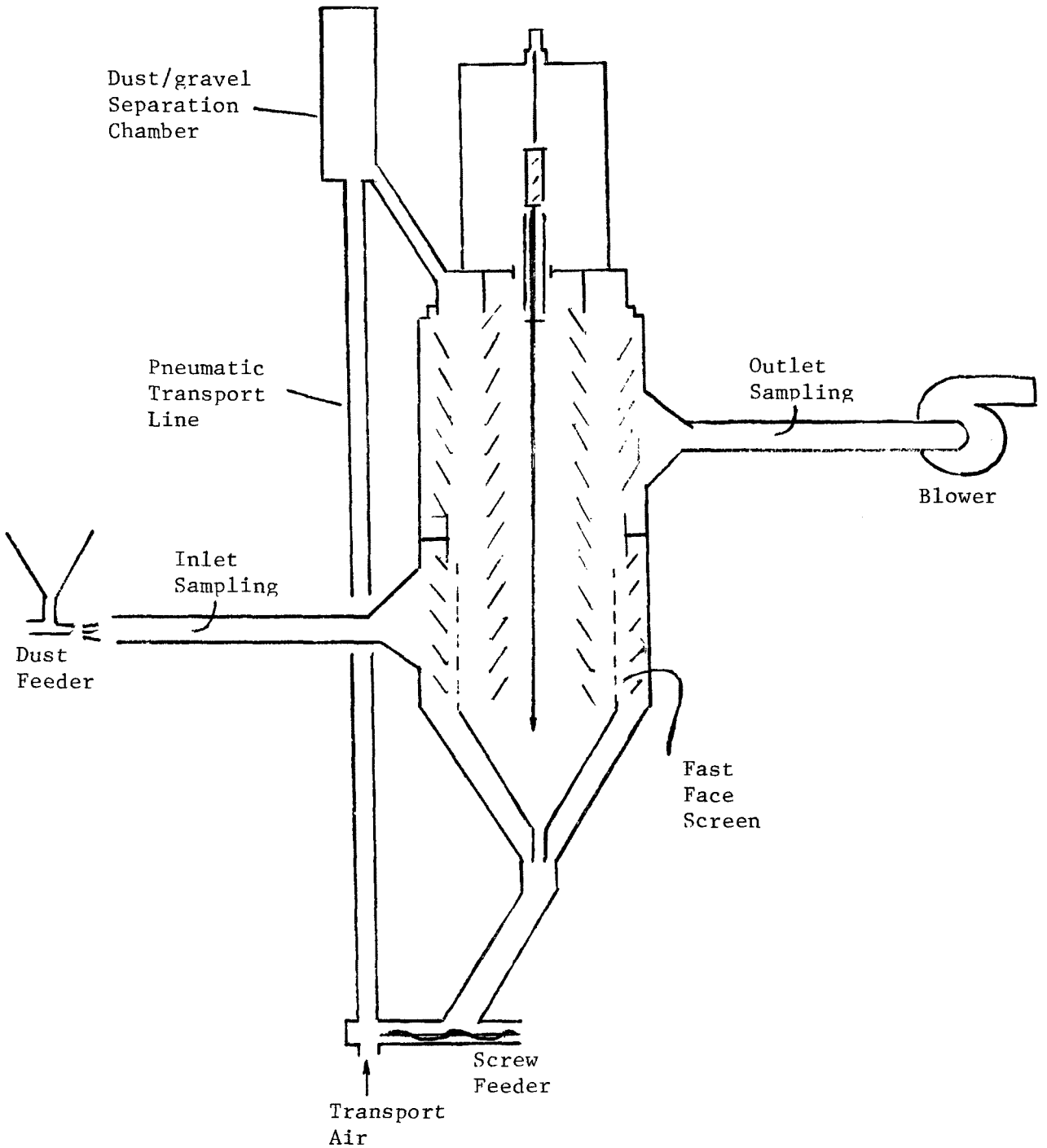


Figure 1. 800 cfm Pilot Unit Schematic

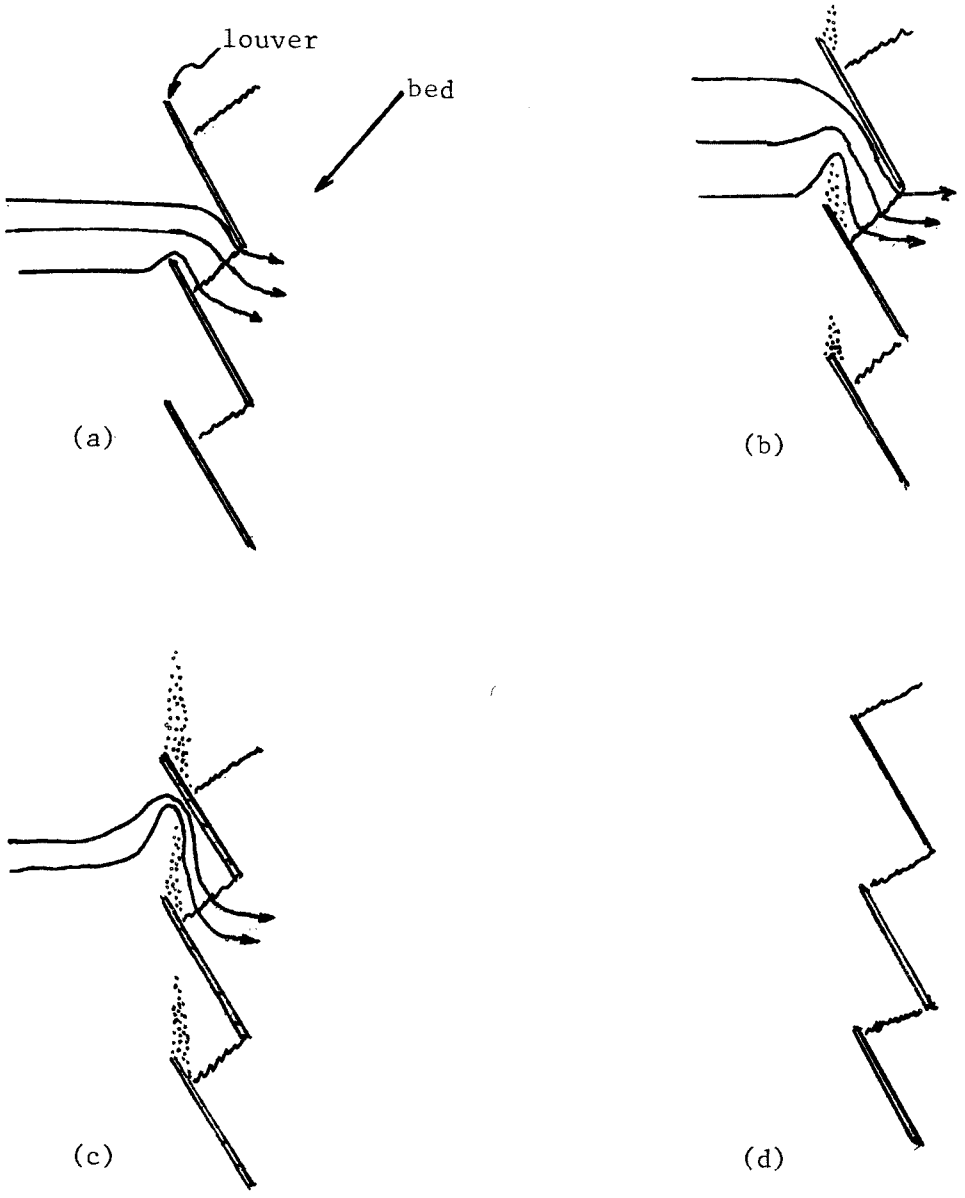


Figure 2. Deposition Problem and Solution

(a) Impaction on louver tips creates small blockages which accentuate impaction and dropout.

(b) Dropout behind blockage build a thick base for dust growths.

(c) The thick base provides support for more growth of these blockages.

(d) Proposed solution to this problem is staggered louvers so there is little bare metal for structures to build on.

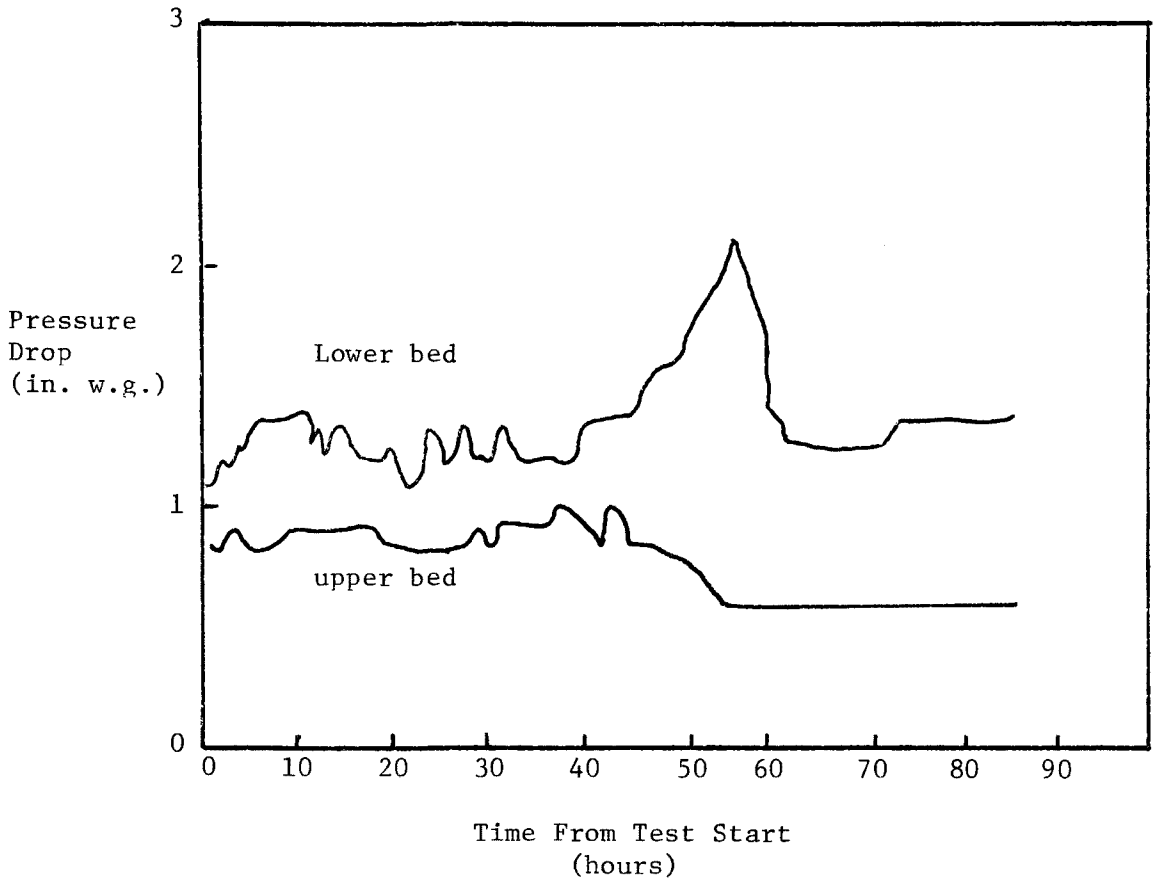


Figure 3. Bed Pressure Drop During The 84-hour Test.

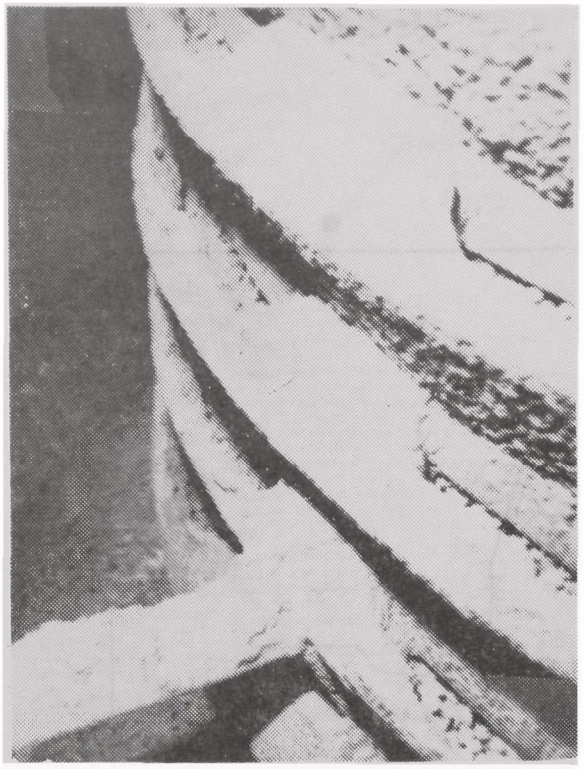

Figure 4

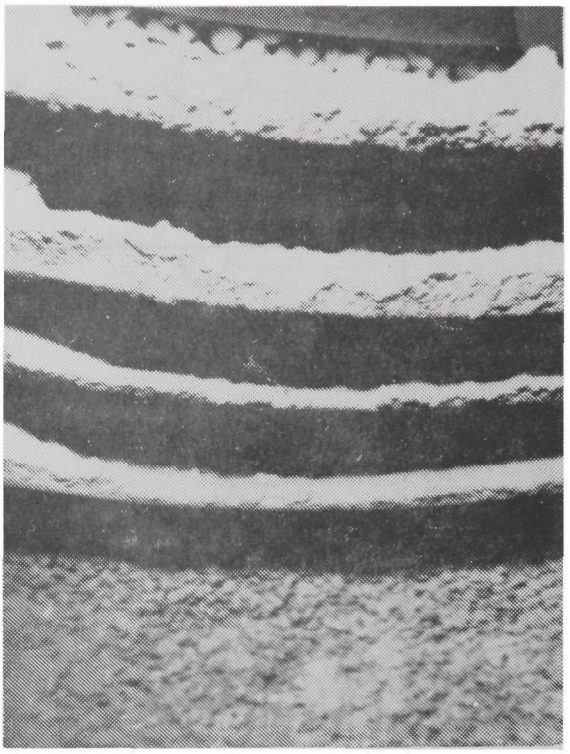

Figure 5

Figure 6

Figure 7

Figures 4-7. Photographs of the Inlet Louvers of 800 cfm pilot unit after 84-hour test.

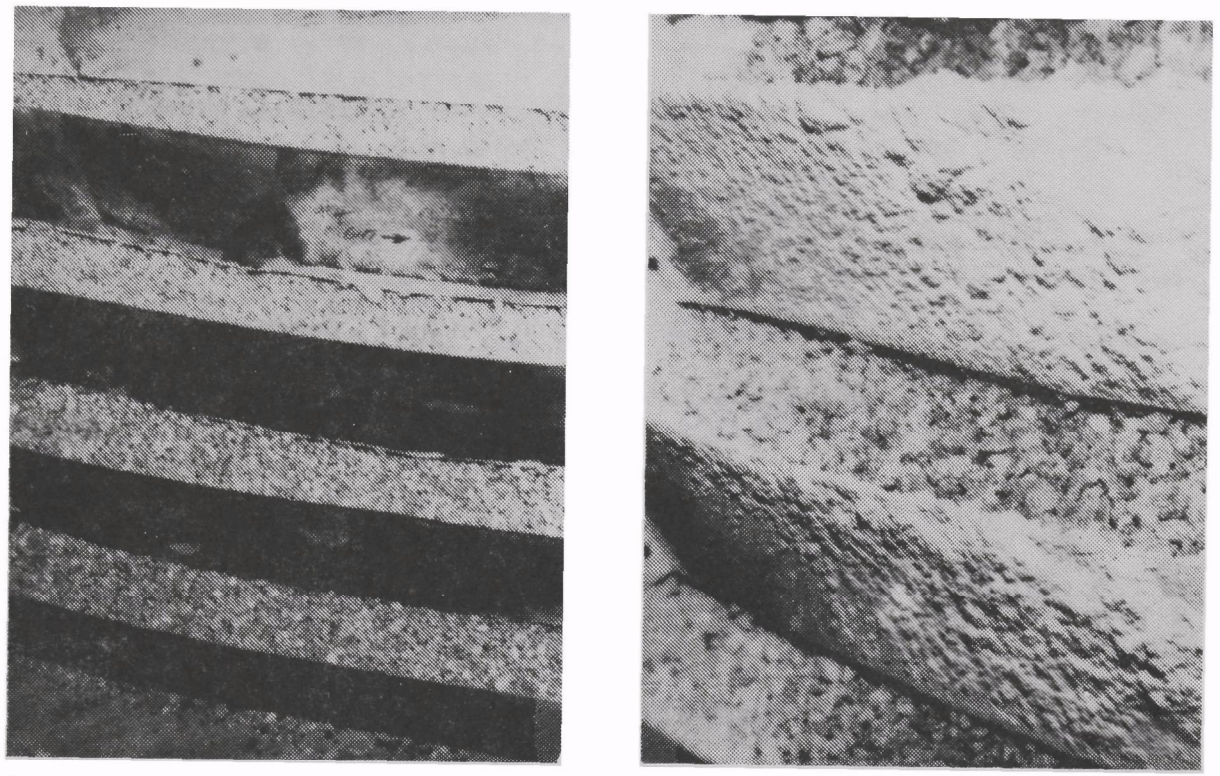

(a) (b)

Figure 8. Photographs of 14" x 18" Reduced Area Louvers Model

(a) Before Test.
(b) After 3-Hour Test.

# PARTICULATE EMISSIONS CONTROL FROM A COAL-FIRED OPEN-CYCLE MAGNETOHYDRODYNAMICS/STEAM POWER PLANT*

By: Hsuan-Hsien Wang and Thomas E. Dowdy

The University of Tennessee Space Institute
Energy Conversion Division
Tullahoma, TN 37388

## ABSTRACT

A coal-fired open-cycle magnetohydrodynamics (MHD)/steam power plant will generate particulates that differ significantly from those produced in conventional coal combustion. Potassium carbonate is added to the extremely hot combustion gases (approximately 3000K) to increase gas electrical conductivity and to capture the sulfur as potassium sulfate. This material, along with coal ash constituents that have been melted and/or vaporized and recondensed, form the particulates that must be collected. The size distribution of these particles, along with chemical composition and dust loading must be experimentally verified. A test facility designed to fire 0.9 Kg/s of coal is under construction at the University of Tennessee Space Institute (UTSI) near Tullahoma, Tennessee. In order to specify and design the most appropriate particulate collection system for the Coal Fired Flow Facility (CFFF), a review has been made of available information concerning MHD process particulates and high efficiency particle collection devices. High energy wet scrubbers, electrostatic precipitators and fabric filters, with and without agglomerating pretreatment, were considered.

## INTRODUCTION

Magnetohydrodynamics (MHD) electric power generation is based on the direct conversion of thermal energy to electric energy by passing a high temperature (approximately 3000K), high velocity (approximately 1000 m/s) combustion gas through a magnetic field. The gas is made electrically conducting by adding a seed, typically potassium. The principle is similar to that of a conventional turbine generator system, the difference being that the rotating conductors of a turbo generator are replaced by a partially ionized combustion gas which interacts with the magnetic field. The interaction of the high velocity conducting fluid with the intense trans-

*This work was sponsored by the Department of Energy under Contract No. DE-AC02-79ET10815.

verse magnetic field induces an electric field within the fluid. Electrodes convey the electricity to an inverter where the direct current power produced is transformed to alternating current which can be transmitted directly through an electric power grid. The gases leaving the MHD channel pass through a steam bottoming plant which produces additional power by means of a conventional steam turbine generator.

The University of Tennessee Space Institute under Department of Energy (DOE) sponsorship is currently developing and constructing a Coal-Fired Flow Facility as part of the overall DOE effort to advance coal-fired MHD electric power generation. The conceptual arrangement of the CFFF is shown in Figure 1. The CFFF flow train consists of twelve components including vitiation heater, coal-fired combustor, nozzle, diagnostic channel or MHD generator channel, power conditioner, diffuser, radiant slagging furnace, secondary combustor, superheater, air heater and particulate collector. The design goal for all components in the CFFF, is the demonstration of predicted system characteristics required of an MHD system (e.g. life, performance, reliability, failure mode, etc.) so that the data obtained can be used as the technological data base for future scale-up of a coal-fired open-cycle MHD/steam power plant.

The vitiation heater reacts mixtures of oxygen and nitrogen with No. 2 fuel oil to produce a gas at an elevated temperature having the required N/O ratio for the coal-fired combustor. In the coal-fired combustor vitiated oxidizer reacts with pulverized coal and its carrier gas. The coal is mixed with a seed material, potassium carbonate and/or potassium sulfate, and burned substoichiometrically at high temperatures to produce an ionized gas suitable for MHD power generation. The nozzle accelerates the gas from the combustor and serves as a geometric transition between the coal-fired combustor and the channels. The diagnostic channel is a Hall device which measures plasma average electrical conductivity. The generator channel converts some of the thermal energy released from the coal to electrical energy. The power conditioner is designed to be compatible with the generator/diagnostic channel operating characteristics so as to operate during both steady state and transient periods. The diffuser recovers the static pressure from the generator/diagnostic channel(s) to a value near atmospheric pressure and reduces the velocity of the plasma to values acceptable for the downstream components. These seven components make up the MHD topping cycle.(1)

The radiant slagging furnace rejects the major amount of entering slag from the gas stream and removes the slag to a transfer point while retaining the seed in a gaseous state. The radiant slagging furnace absorbs heat from the gas stream, flashes heated water to steam, vents the steam to atmosphere, and further reduces the velocity of the gas stream. The radiant slagging furnace has sufficient gas residence time which, along with proper temperature reduction, promotes the decomposition of $NO_x$. The secondary combustor mixes air, either at ambient temperature or preheated by the air heater, with the gas stream to complete combustion of the gases. Excess air is provided to complete combustion while maintaining $NO_x$ levels below Environmental Protection Agency (EPA) utility limits. The superheater simu-

lates the operating conditions in a large scale superheater by duplicating temperatures of the bulk gas and metal temperature of the tubes. The air heater provides heated air to the secondary combustor. The particulate collector ensures that particulate emissions do not exceed EPA limits and demonstrates adequate particulate collection performance under MHD operating conditions. The above five components belong to the steam bottoming cycle.(1)

The design for the air heater and superheater, which are components upstream of the particulate collector in the CFFF, have not been completed. In addition, there is limited prior experience with the seed/slag chemistry, slag/seed separation, slag/gas separation, strong magnetic field (approximately 3 Tesla), high combustion temperature (approximately 3000K), flow pattern and heat transfer characteristics of the MHD process. Thus, information about the inlet particle-laden gas stream of the particulate collection system of the CFFF is incomplete. This information must be experimentally verified. This is a major objective of the CFFF Low Mass Flow (LMF) test train in the future.

The MHD particulates are significantly different from particulates generated from the conventional coal-fired power plant. These particulates must be collected efficiently so that the coal-fired open-cycle MHD/steam power plant will be environmentally as well as economically acceptable. The purpose of this paper is to discuss available information concerning MHD particulates and to evaluate the feasibility of applying commercially available fine particulate collection technology to the CFFF.

## MHD PARTICULATES

Several factors unique to a coal-fired open-cycle MHD/steam power plant influence the generation of particulates. The coal-fired combustor operates at temperatures sufficiently high (approximately 3000K) that a major portion of the mineral content of the coal will be vaporized. This slag will begin to condense and solidify in the cooler downstream components to form small particulates. The greatest fraction of these particles will be removed in the radiant slagging furnace. These slag particulates will have a different chemical composition as compared with the slag generated in conventional coal-fired power plants because of different gas characteristics and slag condensation as well as solidification environments.

The seed material, potassium carbonate ($K_2CO_3$), is added to the coal-fired combustor to increase the gas electrical conductivity and to capture the sulfur present in the coal as potassium sulfate ($K_2SO_4$). This material solidifies at temperatures around 1342K in the cooler downstream components primarily in the air heater and superheater to form predominately submicron particulates.

There is some experimental evidence obtained in small-scale facilities which indicates that the strong magnetic field (approximately 2 Tesla) in MHD generators may influence the formation of particulates. Apparently this results in the formation of a larger number concentration of submicron

particulates than is obtained without the field.(2) The magnetic field may suppress turbulence and prevent nucleation of new particulates until high supersaturation ratios are reached. In addition, when thermal energy is extracted from the MHD channel, the gas cools more rapidly as it travels through the channel, which directly alters the particulate size distribution.(2) Consequently, both of these factors will contribute to decrease the time available for agglomerating smaller particulates into larger ones.

The entrained coal slag particulates may serve as condensation nuclei for the seed material when the combustion gas is cooled below the dew point of $K_2SO_4$ of approximately 1943K. Tempelmeyer, et al compared Scanning Electron Microscope (SEM) micrographs of fly ash from a conventional power plant with that obtained from an MHD system.(3) They observed a coating of $K_2SO_4$ on the surface of the MHD particulates, illustrating that the entrained coal slag particulates serve as nuclei upon which $K_2SO_4$ vapor condenses.

The condensation of seed will cause the particulates to grow into the size range of 0.3 to 1.0 microns, depending on the number of coal slag particulates and the amount of $K_2SO_4$.(4) The MHD particulate size is projected in the submicron range. Im, et al estimated that the mean size of MHD particulates is in the range of 0.2 to 0.5 microns.(4) Some USSR data from the U-02 facility shows a mass mean diameter of 0.2 microns.(5) It should be noted that this facility fires clean fuel and injects ash. Researchers at UTSI have measured and counted the particulate matter taken from the bag filter of their Energy Conversion Facility (ECF) which has no magnet on the test leg. The result of this mesured MHD particulate size distribution is shown in Figure 2. In this figure, the estimated particulate size distribution of MHD particulates and the measured particulate size distribution typical of fly ash from a conventional coal-fired power plant(6) is also presented.

The MHD particulates size is projected to be one to two orders of magnitude smaller than fly ash particulates generated from conventional coal-fired power plants. In addition, the chemical composition of MHD particulates is quite different from the conventional fly ash particulates. Furthermore, the electrical resistivity of particulates is strongly dependent on their chemical composition and the characteristics of their carrier gas stream. At present, it is not known how the high concentration of $K_2SO_4$ will affect the MHD particulate electrical resistivity. Researchers at UTSI have measured the electrical resistivity of the MHD particulate taken from their ECF. It is ranged from 3.8 to 4.3 x $10^{10}$ ohm-cm. Based on this information, the inlet gas stream characteristics to the particulate collector of the CFFF has been estimated so that evaluation of commercially available fine particulate collectors is possible. The estimated characteristics of the gas stream are shown as follows:

| | |
|---|---|
| Pressure: | 0.88 atm |
| Temperature: | 411K |
| Total mass flow rate: | 5.88 Kg/s |

Volumetric flow rate of gas: 7.13 $m^3/s$
Dust loading: 5.75 $g/m^3$ (average)
41.63 $g/m^3$ (maximum)

Gas composition:

| | Volume Fraction |
|---|---|
| $O_2$ | 0.04530 |
| $N_2$ | 0.52179 |
| $CO_2$ | 0.29026 |
| $H_2O$ | 0.14186 |
| $NO_x$ | 0.00069 |
| $SO_x$ | 0.00010 |
| | 1.00000 |

Particulate electrical resistivity: 3.8 to 4.3 x $10^{10}$ ohm-cm
Particulate density: 2.66 $g/cm^3$
Particulate size distribution: See Figure 2
Particulate chemical composition:

| | Weight Fraction |
|---|---|
| $K_2SO_4$ | 0.939 |
| $K_2SO_3$ | 0.004 |
| $K_2S$ | 0.001 |
| $K_2CO_3$ | 0.050 |
| Fly ash | 0.006 |
| | 1.000 |

## PARTICULATE COLLECTORS

High-energy wet scrubbers, electrostatic precipitators and fabric filters are commercially available fine particulate collectors. There are also many agglomerating methods which can be used as a gas preconditioner to alter the size distribution of particulates so that it is easier to collect them in the major collector. At present, sonic agglomeration seems the most appropriate compared with space-charge agglomeration, magnetic agglomeration, turbulent agglomeration, thermal agglomeration, and radiation agglomeration based on the theoretical and experimental background, although there is much uncertainty in sonic field generation with respect to wave form, power consumption and the coagulation rate.(7)

Typical features of fabric filters (FF), electrostatic precipitators (ESP), wet scrubbers (WS) and sonic agglomerators (SA) are shown in Table 1. Wet scrubbers are considered because of the high water solubility of $K_2SO_4$. However, high energy consumption, insufficient grade mass collection efficiency over the submicron range, scaling and fouling, and low operational reliability ruled them out as a major particulate collector for the CFFF. Electrostatic precipitators are considered due to their wide use in industry. However, insufficient grade mass collection efficiency over the submicron range and the considerable difficulties achieving a 10 percent opacity may force them to connect with a preconditioner to meet the particulate emission standards. Fabric filters are of interest because of their high grade mass collection efficiency over the submicron range. In addition, they are the only type of particulate collector that can perform

adequately under cyclic loading. Furthermore, the expected promulgation of a fine particulate emission standard of 0.02 lb/$10^6$ Btu during the 1980's and the uncertainties as well as variabilities of coal source which the utility industry may face in the future, make fabric filters more attractive for collecting MHD particulates.

Researchers in Electric Power Research Institute (EPRI) have conducted research on the economics of fabric filters versus electrostatic precipitators for particulate collection.(8) They concluded that the trend toward increasingly stricter particulate emission standards has raised the cost for electrostatic precipitators such that fabric filters have become cost competitive.(8) The relative economic feasibility of a well designed fabric filter and sonic/electrostatic precipitator for the CFFF have not been done. At present, we believe the fabric filter approach may be the less expensive.

Although we presently favor the fabric filter, it is not without problems. The MHD particulates are fine, hygroscopic and sticky. They have the potential to blind a fabric filter. The performance of the fabric filter in collecting MHD particulates must be experimentally verified.

The performance requirements of the particulate collection system for the CFFF is shown as follows:

Durability: $10^4$ hours
Particulate mass collection efficiency: 99 percent
Exit temperature of gas: 411K
Exit mass flow rate of gas from the collector: 5.88 Kg/s
Particulate emission standard: 0.03 lb/$10^6$ Btu (i.e. 13 ng/J)
Maximum allowable exit mass flow rate of particulates: 0.36 g/s
Maximum allowable particulate concentration: 0.038 grains/SCF

Most of the MHD particulates are removed in the radiant slagging furnace. Only a small mass fraction of particulates entrained in the gas stream go to the particulate collection system of the CFFF. In order to meet the seed recovery and particulate emission goal of the CFFF, the choice of particulate collection system is strongly dependent on the performance of slag rejection of the radiant slagging furnace.

Babcock and Wilcox under DOE contract will provide a heat recovery/seed recovery (HRSR) system to the CFFF to be tested by UTSI. The particulate collector of the B&W HRSR is an electrostatic precipitator. We currently plan to test both the B&W's ESP and a slip stream fabric filter.

## SUMMARY

The fabric filter approach for the seed recovery and particulate emissions control from MHD systems may be the system of choice. However, there is uncertainty about the slag rejection capability which may force us a change in the performance requirements of the particulate collection system of the CFFF. Furthermore, there is potential of blinding the fabric

filter by the fine, hygroscopic and sticky MHD particulates. Since a recommendation has been made to utilize the electrostatic precipitator from Babcock & Wilcox heat recovery/seed recovery contract for the CFFF, we have also elected to test a slip stream fabric filter.

## ACKNOWLEDGEMENTS

The efforts of many individuals in the Energy Conversion Division of the University of Tennessee Space Institute were required to perform the work which is described in this paper.

## ENDNOTES

1. Strom, S. S., M. H. Scott, and R. C. Attig. Overall Test Plan for the Low Mass Flow Test Train at the Coal-Fired Flow Facility. The University of Tennessee Space Institute, Tullahoma, Tennessee, September 1980.

2. Tempelmeyer, K. E., et al. Investigation of Factors Influencing Potassium Seed Recovery in Direct Coal-Fired Generator Systems. Proceedings of the 16th Symposium on Engineering Aspects of MHD, University of Pittsburgh, April 1977.

3. Tempelmeyer, K. E., et al. Recent Experimental Studies of the Interaction of Potassium Seed with Coal Slag in a Direct Coal-Fired MHD Generator. Proceedings of the 15th Symposium on Engineering Aspects of MHD, University of Pennsylvania, May 1976.

4. Im, K. H., J. Patten, T. Johnson, and K. Tempelmeyer. Condensation and Deposition of Seed in the MHD Bottoming Plant. Proceedings of the 18th Symposium on Engineering Aspects of MHD, Butte, Montana, June 1979.

5. Selby, R. C. Department of Energy, Chicago Operations and Regional Office to J. Epstein. Letter communication, March 28, 1980.

6. Cheng, R. J. Characteristics of Particulates from Power Plants. Journal of the Air Pollution Control Association, Vol. 26, No. 8, August 1976. p. 787.

7. Wang, H. H. An Evaluation of Various Particle Agglomeration Methods for Fine Particle Control in Low Mass Flow Coal-Fired Flow Facility System, Internal Report. The University of Tennessee Space Institute, Tullahoma, Tennessee, August 1980.

8. Severson, S. D., R. W. Scheck, K. S. Campbell, and F. A. Horney. The Economics of Fabric Filters and Precipitators. Chemical Engineering Progress, January 1980. p. 68.

TABLE 1. FEATURES OF FINE PARTICULATE COLLECTORS

| Features | Fabric Filters (FF) | Electrostatic Precipitators (ESP) | Wet Scrubbers (WS) | Sonic Agglomerators (SA) |
|---|---|---|---|---|
| Specific Energy Consumption | 1 to 3 hp/$10^3$ acfm | 1 to 1.5 hp/$10^3$ acfm | 10 to 20 hp/$10^3$ acfm | 1.5 to 46 hp/$10^3$ acfm for traveling wave SA<br>0.5 to 2 hp/$10^3$ acfm for standing-wave SA |
| Pressure Drop | 0.5 to 10 in. w.g. | 0.5 to 1.5 in. w.g. | 60 to 100 in. w.g. | |
| Grade Mass Efficiency for Submicron Particulate | > 99% | 95% to 99% for hot-side ESP<br>90% to 95% for cold-side ESP | 90% to 99% | (only used as a precollector) |
| Maximum Operating Temperature | 560K | 700K | | |
| Effluent Opacity | 0% | 10% to 20% | 10% to 20% | |
| Effluent Particulate Loading | < 0.02 gr/SCF | < 0.04 gr/SCF | < 0.07 gr/SCF | |

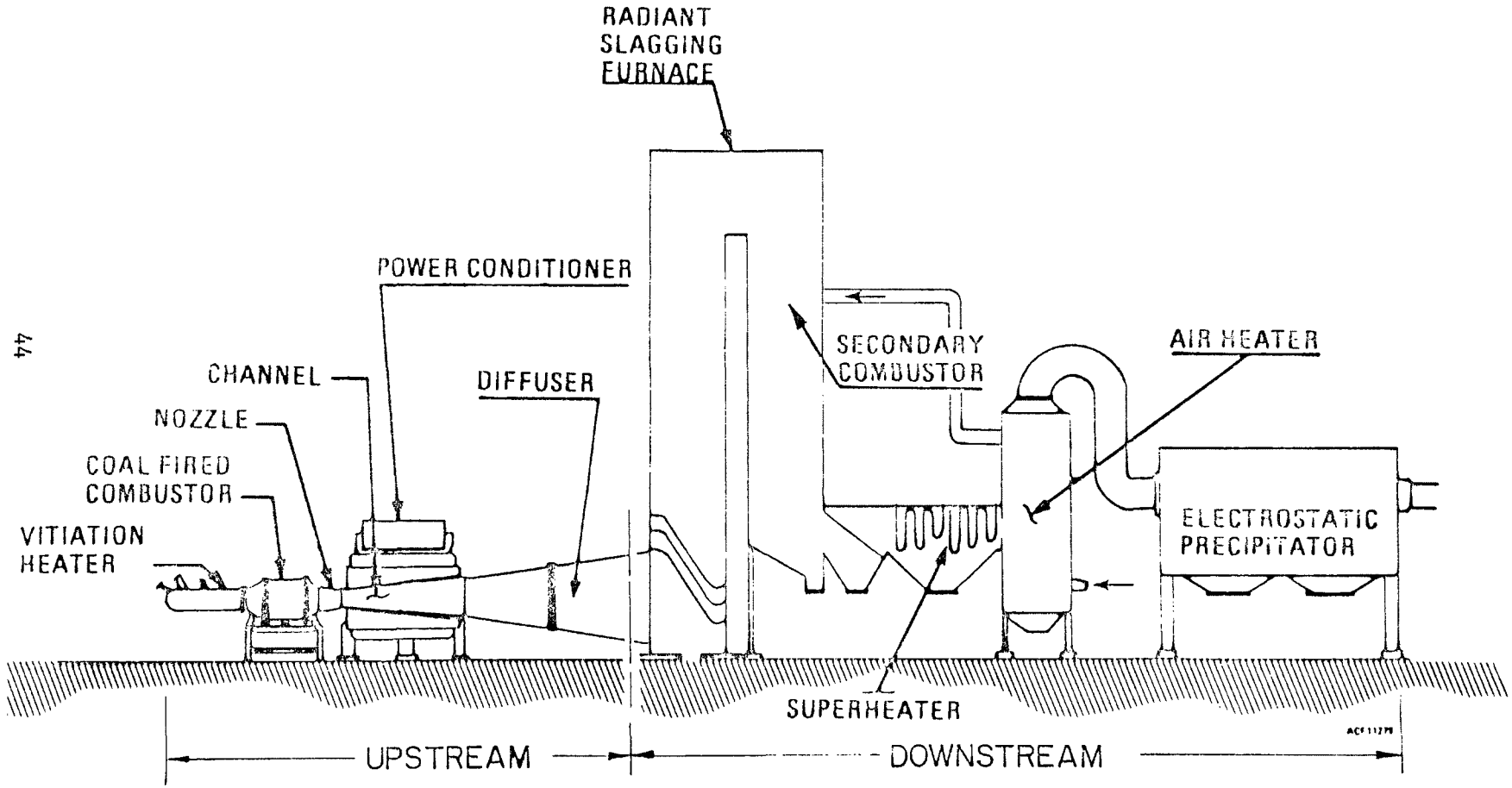


FIGURE 1
Conceptual Arrangement of MHD System Including Steam Bottoming Plant

FIGURE 2. Particulate Size Distribution of the MHD Particulates and the Particulates Generated from the Conventional Coal-Fired Power Plant.

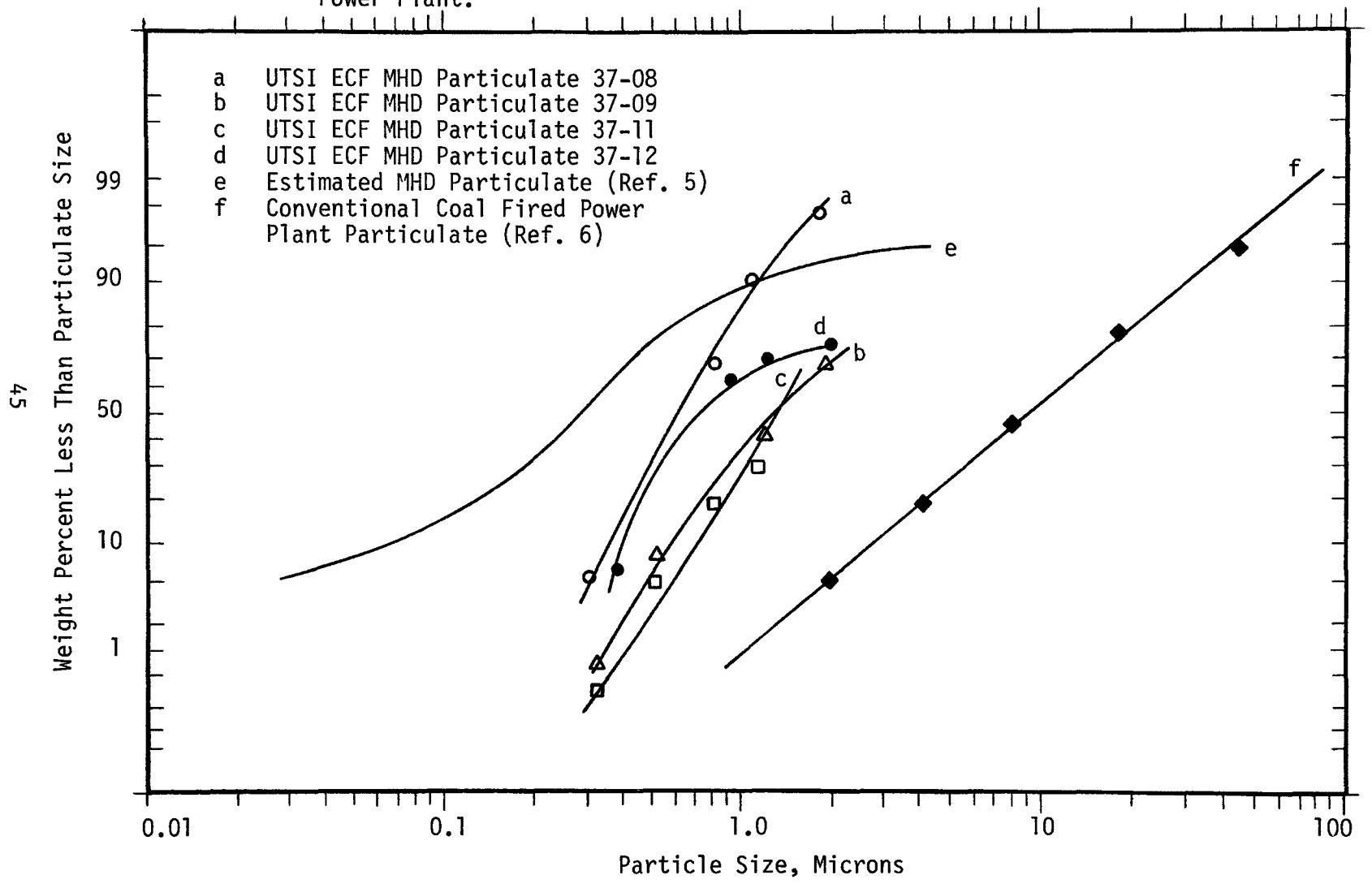

# REAL TIME COARSE PARTICLE MASS MEASUREMENTS IN A HIGH TEMPERATURE AND PRESSURE COAL GASIFIER PROCESS TREATMENT

By: J. Wegrzyn, J. Saunders, and W. Marlow

Brookhaven National Laboratory
Department of Energy & Environment
Upton, New York 11973

## ABSTRACT

A sampling system has been designed and is under construction at Brookhaven National Laboratory that employs a probe appropriate for direct extracted sampling of erosive range particulate matter from a coal gasifier outlet or a high pressure fluidized bed combustor. The sampling train is scheduled to be tested at the Morgantown Energy Technology Center on their 42 inch coal gasifier unit. This sampling system consists of four modules: 1) a null balance extractive probe with injection through a porous lined tube to minimize wall loss, 2) a stem type virtual impactor to separate coarse from fine particles, 3) a filter tape collector, and 4) a Beta gauge total mass detector. The key design feature of this system is a stem type virtual impactor which separates at ambient gas stream conditions the coarse particles from the sampling stream so that at upon filtration no condensible vapors, fine particles or reactive gases pass through the filter tape. This system should provide coarse particle mass flux data with a time resolution of thirty seconds or better.

## INTRODUCTION

Erosion by particles greater than 2 microns of turbines located in post combustion gas streams from coal fired combustors is currently one of the major obstacles to the increased utilization of coal for direct power generation either with or without gasification. Various sampling methods exist and others are under development for the measurement of these erosive particles, but there is currently no accepted approach for the measurement of post combustion stream, particulate mass content to assert the effectiveness of the cleanup devices. Measurement of the particulate mass flux in the erosive size range, as it exists under the appropriate high temperature pressure conditions and in the presence of high partial pressures of condensible vapors, is needed to provide the necessary information on the effectiveness of the cleanup devices. The effort at Brookhaven National Laboratory is towards the construction of a general purpose sampling train to determine the effectiveness of the various air cleaning devices in either a coal combustor or gasifier. The validity of aspiration sampling is well established for both laboratory[1] and stack applications (EPA Method-5). However, care must be taken when employing these techniques to the problems of sampling a high temperature and pressure environment where there is a presence of large amounts of condensible vapors. Since condensation, evaporation, and additional chemical reactions within the sampling train can alter the

particulate size, density, and composition. The objectives of this work are to 1) maintain sample integrity by perserving the representativeness of the particulate sample 2) produce readily interpretable data by measuring mass directly 3) minimize and measure any errors associated with extractive sampling.

The following sections of this paper details some of the critical design features of the Brookhaven National Laboratory sampling train and further discusses some of the major problems associated with aspiration sampling. A brief theoretical discussion is also being presented to facilitate in discussing some of the inherent problems in aspiration sampling.

Figure 1 illustrates the distortion in measurement from sampling at a higher then free stream velocity. Particles whose stopping distance $\lambda_p$ are larger than the length of the disturbance of stream L will penetrate past the probe, while these with $\lambda_p < L$ will enter the probe resulting in a higher mass flux measurement of particulate matter. Mathematically this can be modelled by the following equation.

$$M_s = C_s V_s a = C_o V_o a + (1 - \alpha_d)\, C_o V_o (A-a) \tag{1}$$

where $_d$ is the fraction the particles of diameter d that were not collected, and so that the complement of $(1-\alpha_d)$ is the fraction of particles within the area (A-a) collected. This equation can be recast in the form for mass flux by substituting the following equation.

$$A = \frac{aV_s}{V_o} \tag{2}$$

into equation 1 and rewriting as the following equation.

$$\frac{M_s}{M_o} = (1 - \alpha_d)\frac{V_s}{V_o} + \alpha_d \tag{3}$$

The expression for $\alpha_d$ has generally been given as a function of the Stokes number[2] where the Stokes number is defined as

$$Stk = \frac{\lambda p}{L} \tag{4}$$

Corrections are needed with this type of model when, the flow is not streamlined, the mass loading of the aerosol is high, and the particle's size distribution is polydisperse. Particulate sampling in a turbulent duct flow has recently been treated by R. A. Bajura[3] and work is underway at Brookhaven National Laboratory to investigate sampling high mass loading polydisperse aerosols to establish their effects on the stopping distance $\lambda_p$. The mass loading of the process stream is a problem only upstream of the cleanup devices but in order to determine a cleanup device efficiency both upstream and downstream measurements need to be taken. Typically numbers larger than 10 grams per cubic meter would qualify an aerosol as having a high mass loading.

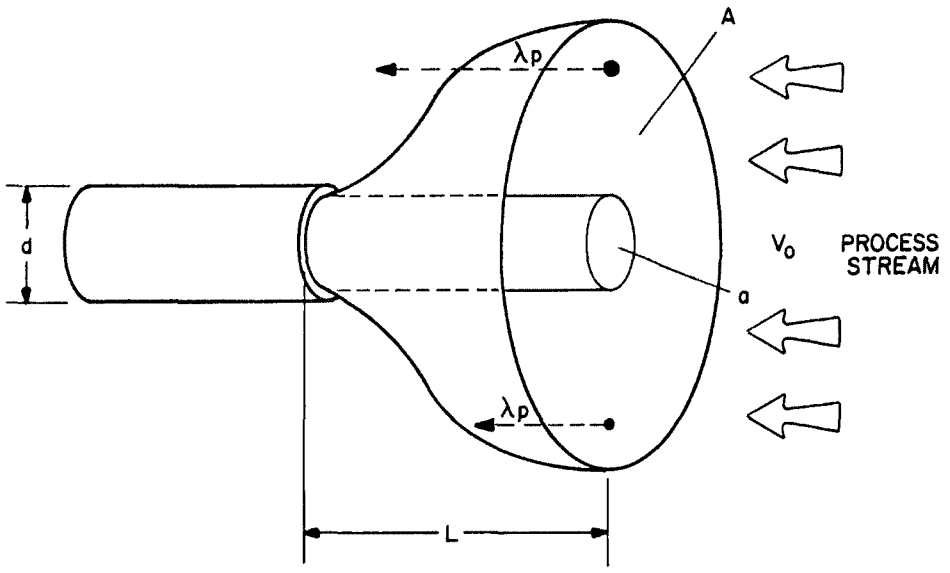


Figure 1 - Particle Trajectories for Sampling ($V_s > V_o$)

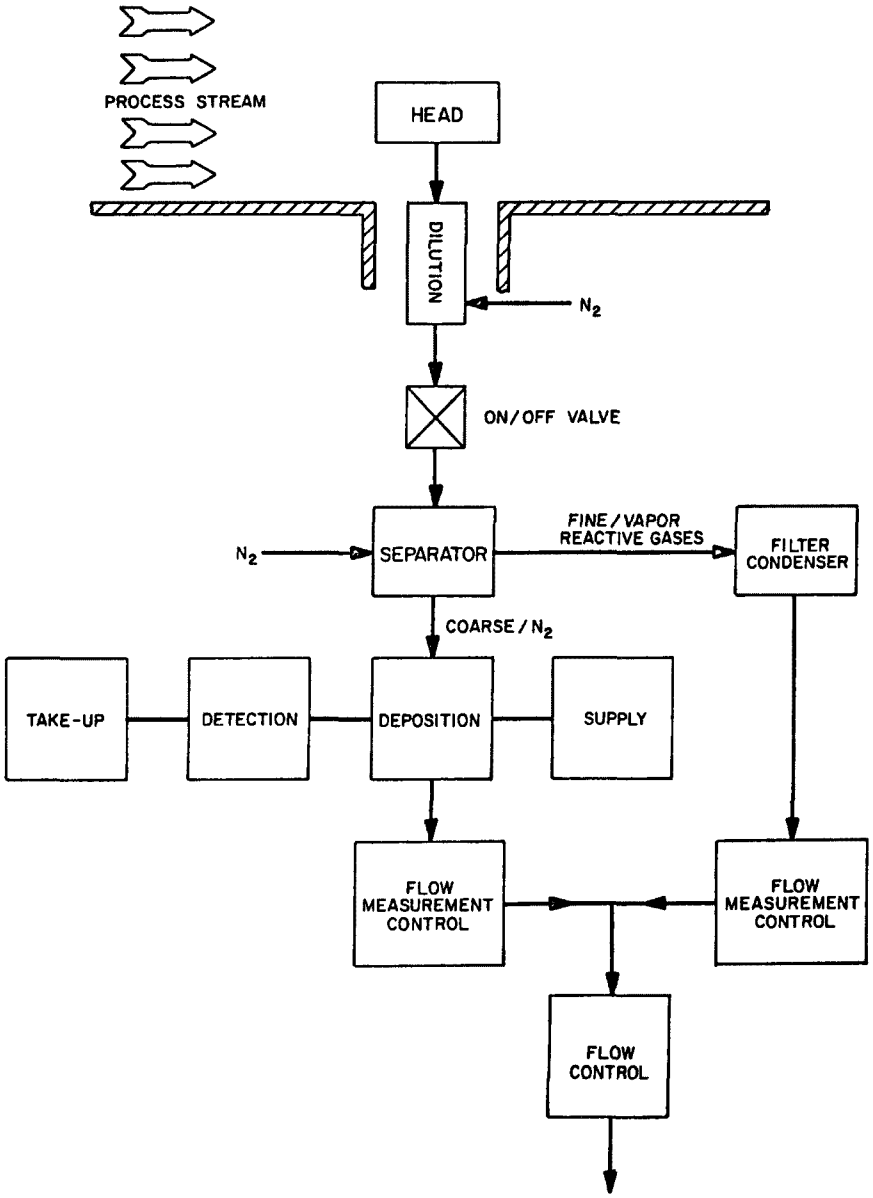


Figure 2 - Sampling Train Module Components

## DESCRIPTION

Sampling requirements of particle integrity, artifacts of measurements, and validity of signal for high temperature, high pressure aerosols have to be addressed if meaningful particulate measurements are to be made on a combustion or gasifier process stream. These problems as applicable to the Brookhaven National Laboratory probe have been addressed by W. Marlow[4] and will not be reviewed here.

The sampling train as it is being built at Brookhaven National Laboratory is constructed of sections of schedule 40 304 stainless steel pipe, that are connected by either 1 inch or 2 inch ASME rated 300 psi flanges. The hinge cap closures on the tape reels and particle deposition chamber also have a 300 psi rating. Thermocouples and pressure transducers are placed along the sampling train and cooling coils to monitor the system. If any of these signals exceeds the safety limit the probe is programmed to go to a safety mode by closing the main valves and purging the system with dry nitrogen. The hinge cap closures are also equiped with safety locks which prohibit opening if that part of the train is under high pressure. The electronics, flow meters, secondary valves, and data logger are all included in a heated cabinet, not shown in this drawing, which protects them from the environment.

Figure 2 is a box diagram of the sampling train. The train has been designed in module form for two reasons. First, a module design permits tailoring the train for the problems that may exist at the specific sampling site. Secondly, any deficient module can be easily replaced without major redesigning of the whole probe.

An ideal sampling head consists of a flow sensor mounted near the entrance of thin wall knife edge gas skimmer. The hostile environment of the process stream eliminates the use of most flow sensors to set the isokinetic condition and only null balance static pressure taps have been employed successfully. This system balances the static pressure inside and outside of the sampling head. However, the thick walls required to mount the static taps result in a flow disturbance that causes a pressure difference between the two taps even under isokinetic condition. Brookhaven National Laboratory is currently studying this error as well as exploring alternative isokinetic sensors.

More than 75% of the particulate matter can be lost in the walls of a poorly designed sampling train.[3] To overcome this problem, work is being done at Brookhaven National Laboratory on the use of a porous lined sampling tube. Initial cold tests of preventing wall deposition in a porous tube by the injection through the porous tube of a secondary gas stream have been encouraging. These tests however were performed on the straight section of tubing and further tests are planned to assert whether this technique will also prevent particle deposition in a right angle bend. The major disadvantages of using porous lined sampling trains are flow control and flow measurement.

Figure 3 shows a stem type virtual impactor. The scaling of this device follows the theoritical restraints as put forth by V. A. Marple[5] for the overall design of a virtual impactor, and its concentric flow pattern is similiar to a virtual impactor built and tested by the H. Masuda[6]. The separator as seen in Figure 3 is built within a 300 psia s.s. orifice flange. This unique design has the capability of separating at high temperatures and pressures the coarse particles from the process stream, as nitrogen gas is leaked through the conical tip of the stem. This secondary flow of gas helps to divide the process stream into concentric flows, and this flow is accelerated to about a third of a Mach by the converging nozzle which is directed at a knife edge skimmer. The inner most part of this flow, that is the nitrogen which came from the stem tip and the coarse particles whose inertia carried them into this region, is then separated off into the lower section while the remaining stream consisting of condensible vapors, reactive gases, and fine particles, is forced to reverse its direction and is removed by the tee connection located above the separator. Once the coarse particles are removed from the process stream they can be cooled down and collected for analysis.

The coarse particles are filtered from the gas in the deposition chamber by a continuously fed filter tape. This tape runs from the supply reel to the take up reel and consists of a one inch wide filter material of glass microfibers supported by a glass cloth. The length of the tape is 250 feet and it has a temperature limitation of 1200°F. The hinge pipe cap closure permits easy access and maintenance of the filtering region. Non-metallic seals are used, however, which necessitates selectively cooling the seals to temperatures below 500°F.

Figure 4 shows construction of the beta gauge. Beta gauges have long been recognized as a preferred solution to the problem of automated mass measurement of particulate matter in flue gases.[7] The theory and operation of Beta gauges for particulate mass measurement is given in a paper by P. Lilienfeld.[8] The BNL gauge consists of a New England Nuclear carbon-14 beta source, a Nuclear Enterprize NE-102 plastic scintillator which converts the beta particles into a light pulse and a EMI model 9824B photo multiplier tube which detects the light pulses. An analysis of the response data for the NE-102 scintillator for .1 to 1 MeV Beta particles has been given by R. L. Craun.[9] The attenuation of the light pulses is directly proportional to the amount of mass that is present between the source and the scintillator. A reading of the particulate mass on the tape is achieved by recording the attenuation of the beta particles and subtracting out the attenuation due to the mass of the filter tape and the surrounding gases. The combination of a beta sensitive scintillator and a PM tube is used instead of the conventional Geiger counter because of its superior frequency response. This permits higher counting rates which results in lower statistical counting error.

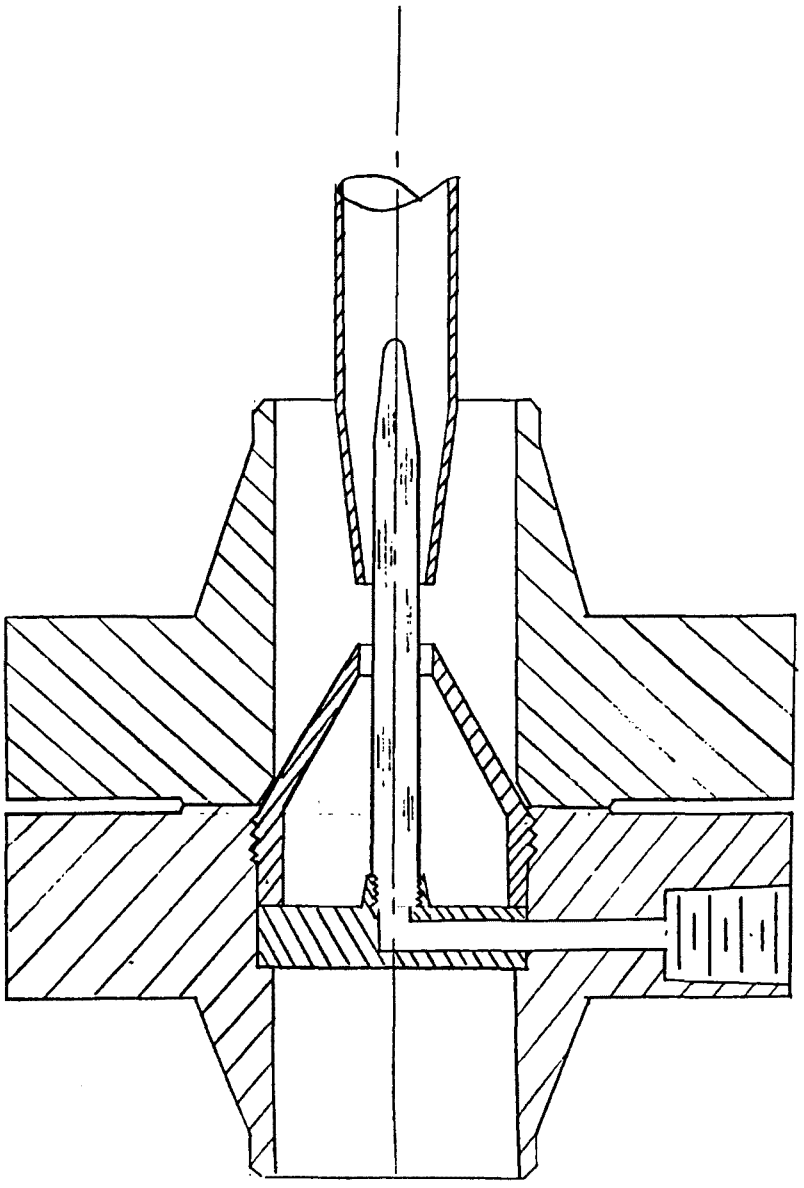

Figure 3 - Virtual Stem Type Impactor

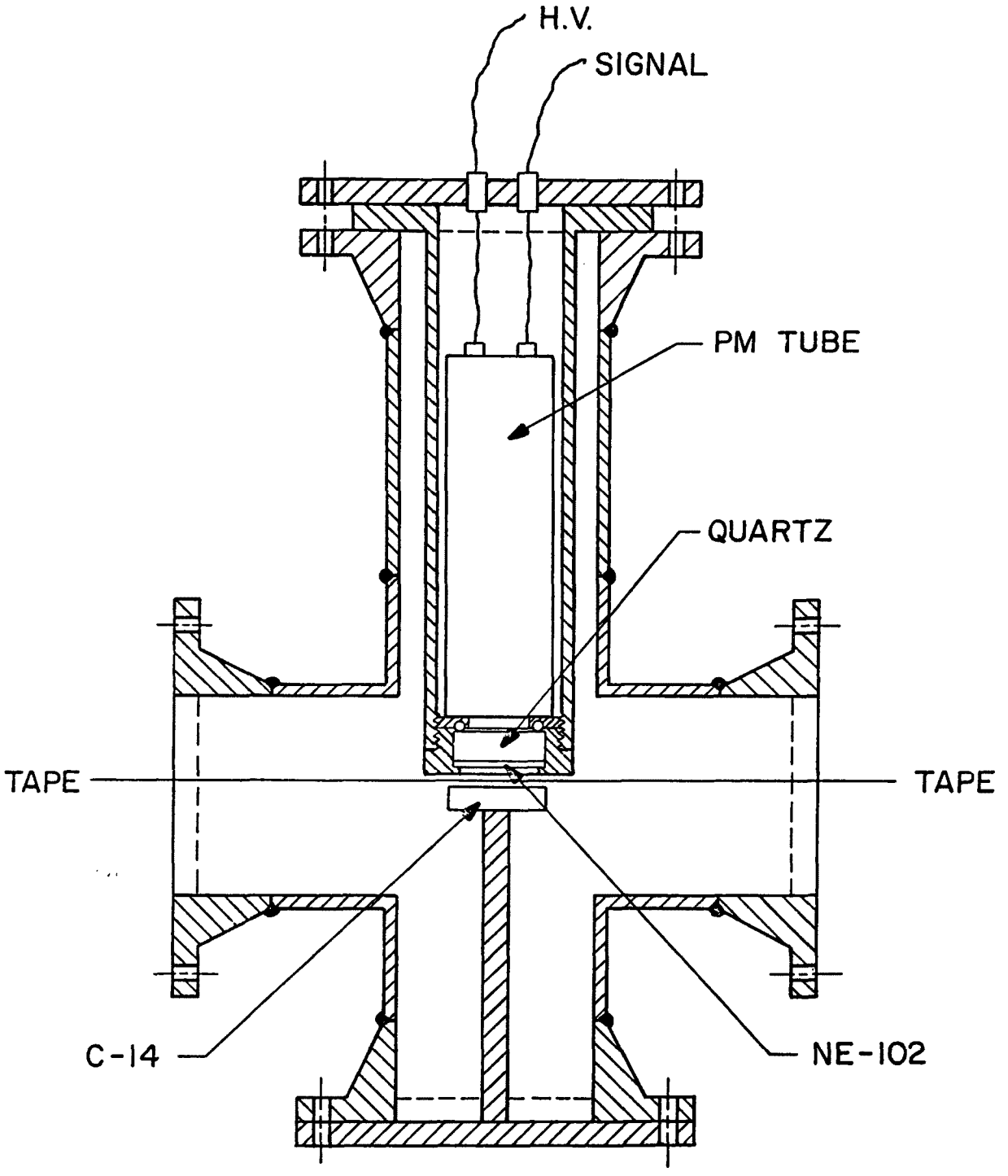


Figure 4 - Beta Gauge Mass Detector

## CONCLUSION

Brookhaven National Laboratory is constructing a sampling train for the measurement of the total particulate mass in a high temperature and pressure coal stream. The probe attemps to maintain integrity of the sample and has high mass loading applications. The train is designed in module form so that it can be tailored to the particular needs of the process stream. The accuracy of the system and its components, including sampling, transport, and detection have to be determined. Accurate measurement of the aspiration velocity and setting of the isokinetic conditions appears to be a problem.

## REFERENCES


1. Balyaev, S. P. and L. M. Levin. J. Aerosol Sci., Vol. 5, p.325 (1974).

2. Hawksley, P. G. W., S. Badzioch, and J. H. Blackett. Measurement of Solids in FLue Gases. The Institute of Fuel London, (1977).

3. Bajura, R. A., et al. Morgantown Energy Technology Cneter, Project DE-AT21-78MC07087/T0-36.

4. Marlow, W. H. and N. Abuaf. The Proceedings of the 1978 Symposium on Instrumentatin and Control for Fossil Demonstration Plants, Newport Beach, CA, June 19-20, 1978. ANL-78-62

5. Marple, V. A. and C. M. Chien. Env. Sci. Tech. Vol.14, No. 8, p. 976, August 1980.

6. Masuda, H. D. Hoehrainer, and W. Stober. J. Aerosol Sci., Vol 10, p.275 (1979).

7. Sem, G. J., et al. "State of the Art: 1971 Instrumentation for Measurement of Particulate Emissions from Combustion Sources", EPA Contract No. CPA-70-23 (1971).

8. Lilienfeld, P. Staub-Reinhalt Luft, Vol. 35, No. 12, p.458 (1975).

9. Craun, R. L. and D. L. Smith. Nuclear Instruments and Methods, Vol. 80, p. 239 (1970).


## ACKNOWLEDGEMENT


The authors are pleased to acknowledge the support of this work by the Department of Energy under Contract No. DE-AC02-76CH00016.

# THE DESIGN, ENGINEERING, AND STARTUP OF A VENTURI SCRUBBER SYSTEM ON AN OIL SHALE OFF-GAS INCINERATOR

By: P. A. Czuchra
FMC Corporation
Air Quality Control Operation
1800 FMC Drive West
Itasca, Illinois 60143

J. S. Sterrett
Rio Blanco Oil Shale Company
Rio Blanco, Colorado

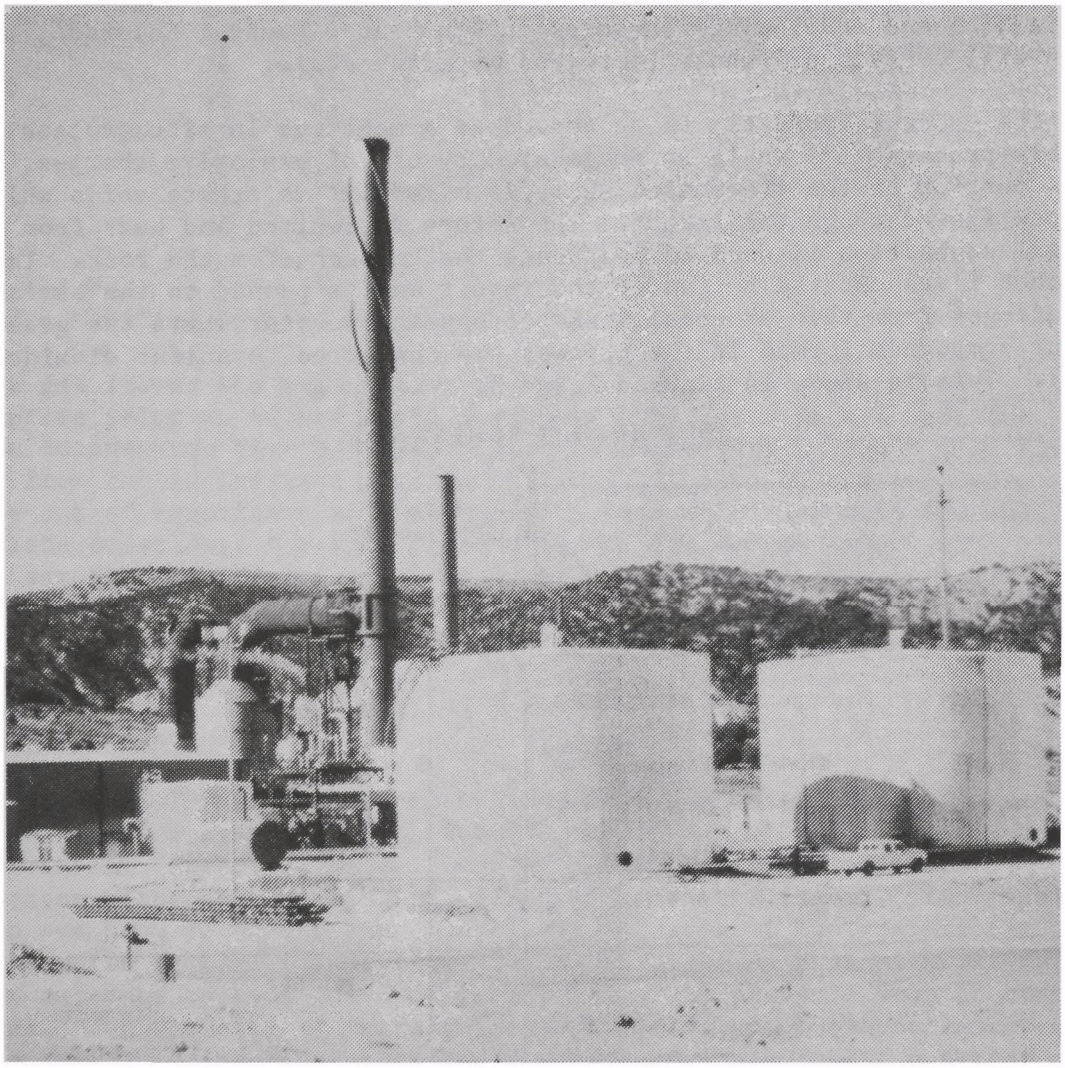

Figure 1 - Rio Blanco Job Site

ABSTRACT

This paper describes the design, engineering and startup of a venturi scrubber removing particulate matter and sulfur dioxide from an oil shale retort off-gas incinerator. Since oil shale recovery is a new technology, a scarcity of data exists concerning conditions to be expected going to the scrubber. Therefore, certain assumptions concerning design conditions had to be made. The assumptions made to develop the design criteria for the scrubber system will be discussed along with the preliminary results concerning the accuracy of these assumptions.

TEXT

Background Information

Rio Blanco Oil Shale Company is a general partnership consisting of Standard Oil Company of Indiana and Gulf Oil Corporation. Together they are testing and developing a process in Rio Blanco County, Colorado, which will extract oil shale (kerogen) from the shale.

The process currently being tested is a modified in-situ process. In this process, the shale is fragmented by use of explosive charges, and a portion of the fragmented shale is mined out to create voids which enhance flow through the retort. The retort is ignited and heat from partial combustion is used to evaporate the kerogen from the rock. The oil then flows out the bottom of the retort and is pumped to the surface. The off-gas from this process is sent to an incinerator where the gaseous sulfur compounds formed in the process are converted to sulfur dioxide ($SO_2$). This is shown in figures 2 and 3.

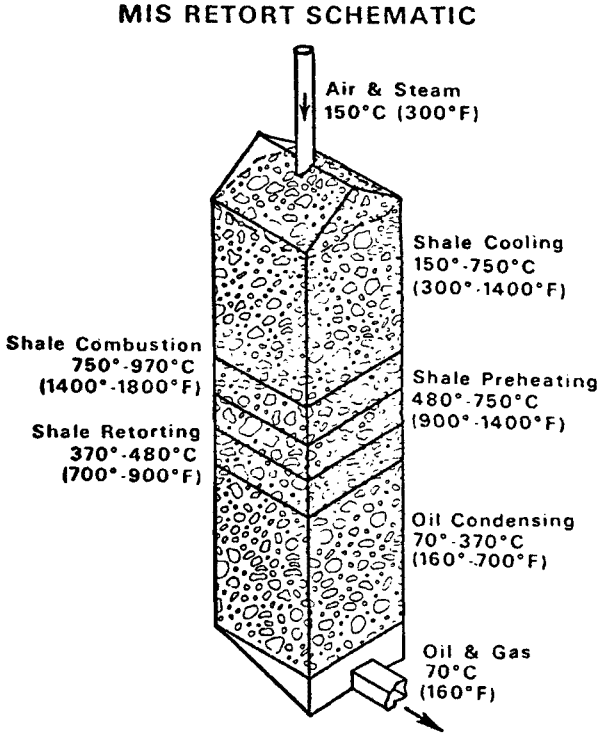


Figure 2

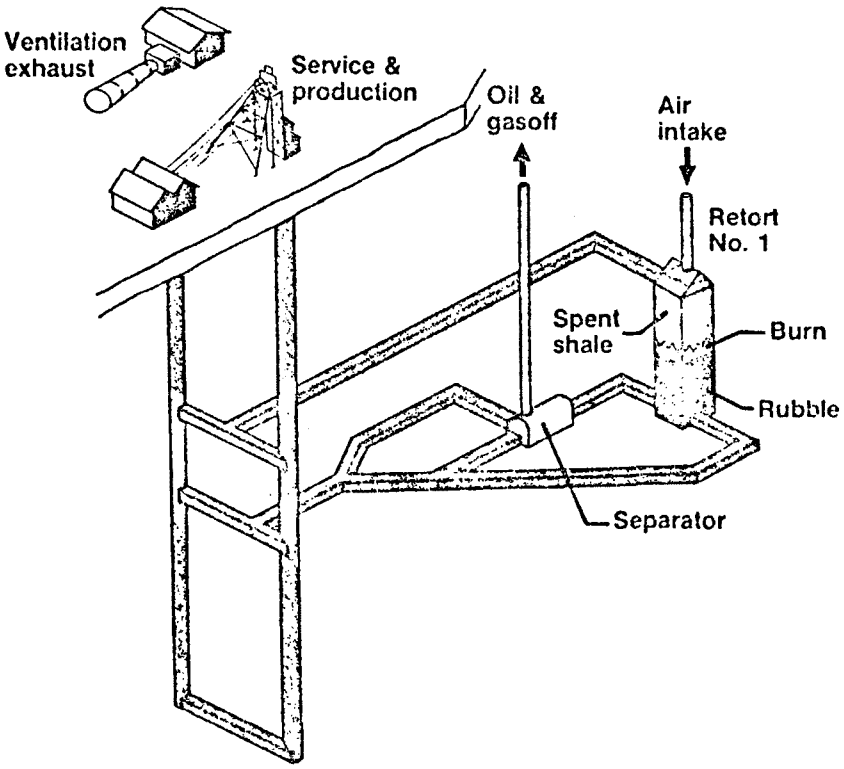


Figure 3 - Modified In-Situ Process Pictorial

The gas leaves the incinerator and is subjected to a series of water sprays prior to entering the scrubber. The water sprays cool the gas from incinerator fire box temperature to approximately 260°C (500°F). The gas from the incinerator also contains particulate matter and hence would be out of compliance with air quality regulations on both $SO_2$ and particulate emissions. For this reason, it was decided to select a venturi scrubber to simultaneously collect the $SO_2$ and particulate matter which is generated. A venturi scrubber is a flexible device. It can yield higher particulate removal efficiencies by simply increasing the pressure drop.

Equipment Description

In March of 1978, FMC Corporation received a contract to design and furnish a scrubber system for Rio Blanco. The heart of the system is an FMC Dual Throat Venturi Scrubber. The scrubber, as shown in figure 4, incorporates a rectangular housing with a wedge-shaped insert. The insert moves up and down to change the cross-sectional area of the venturi throat. This allows the venturi to maintain a constant pressure drop with varying gas flow rates or to have the ability to change the pressure drop at constant gas flows. The geometry of rectangular housing and wedge-shaped insert allows a true venturi configuration of a constant angle inlet, a throat of constant cross-sectional area, and a constant angle of divergence in the expander section to be maintained throughout the turndown range of the scrubber.

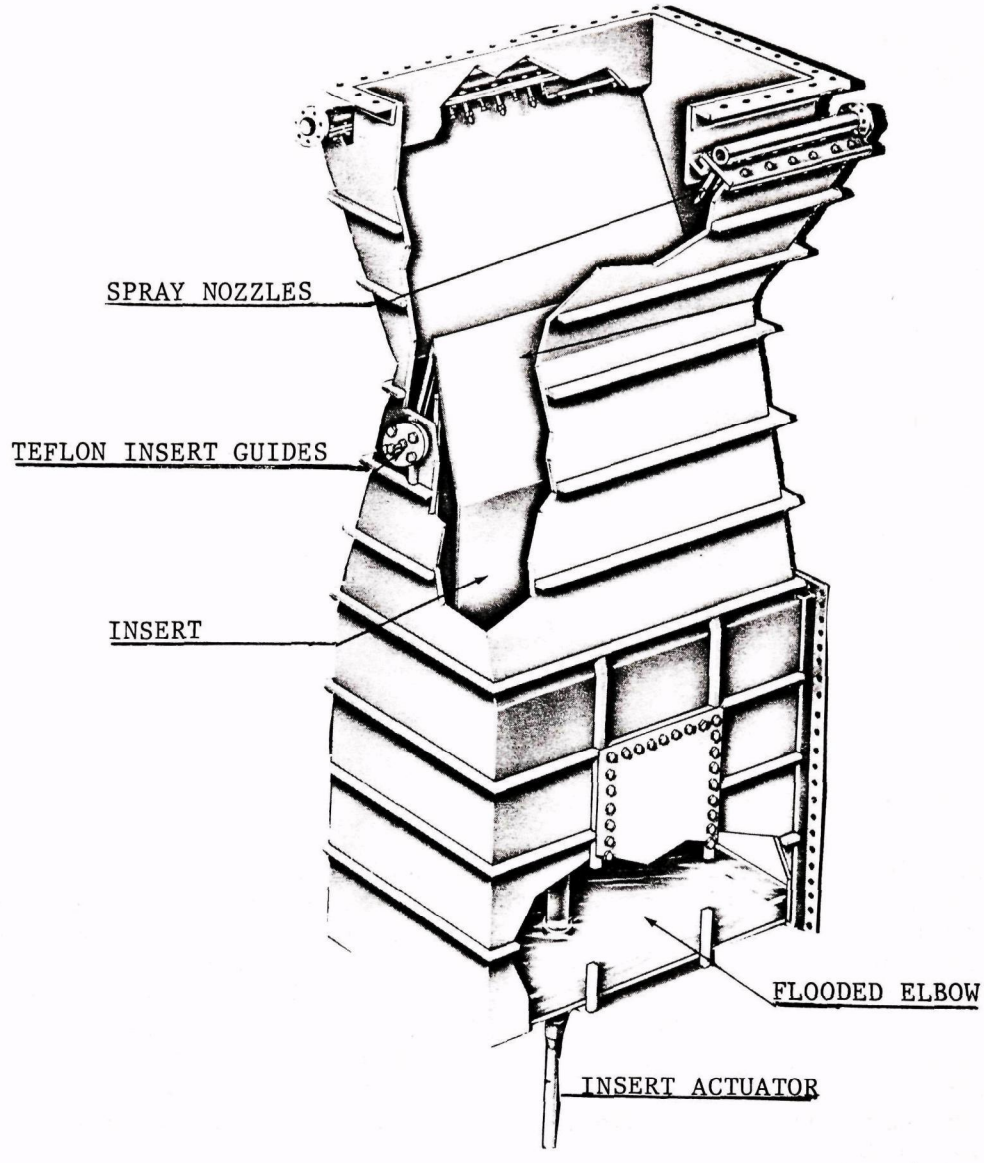


Figure 4 - FMC Dual Throat Venturi

The insert is raised or lowered by a hydraulic cylinder at the bottom of the unit. Teflon guides mounted on the sides of the housing prevent the insert from fluttering in the gas stream while providing a smooth surface for easy movement of the insert.

Liquid is introduced to the scrubber by large-diameter, low-pressure-drop spray nozzles. The nozzles provide good water coverage to the throat while minimizing the chances of pluggage. The nozzles are recessed out of direct contact with the gas stream, thus diminishing the possibility of material buildup from a wet/dry interface. The venturi is approximately 6.7 meters (22 feet) high. The coarse separation of the water droplets from the gas stream is accomplished by a cyclonic entrainment separator. Gas

from the venturi is directed into the separator tangentially. The water droplets impact into the side of the separator and drain down into an integral recirculation tank. Additional gas/liquid separation is accomplished by a chevron mist eliminator located near the top of the separator. The separator is approximately 14.6 meters (48 feet) high and 6.7 meters (22 feet) in diameter. The venturi is constructed of Incoloy 825 and the separator and mist eliminator of 316L stainless steel. The venturi and separator are shown together in figure 5.

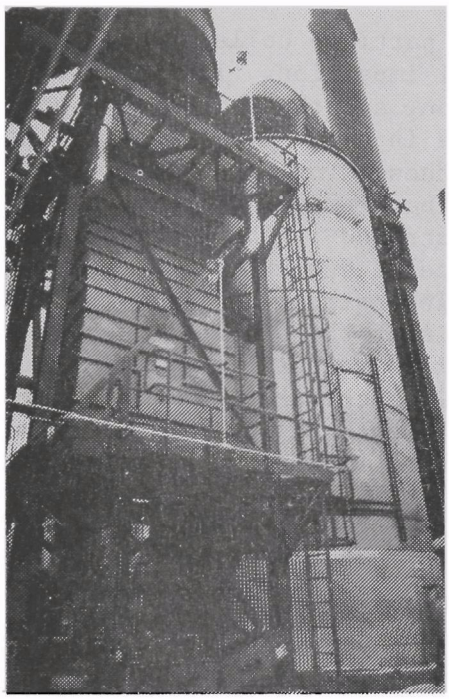

Figure 5 - FMC Dual Throat Venturi and Separator at Rio Blanco

Due to the potential abrasiveness of the particulate being collected and the corrosive nature of the recirculation liquor, rubber-lined recirculation pumps were chosen for the system. Also due to the conditions described above, FMC recommended the use of either abrasion resistant FRP or rubber-lined cast iron for the recirculation piping. It was decided to install the rubber-lined pipe. The neutralization tank was constructed of corrosion-resistant FRP. All piping and tanks associated with the recirculation system are well insulated to prevent any possibility of freezing the scrubber and soda ash solutions. This was necessary due to local weather conditions.

The soda ash storage tank is a unique feature of the system. Soda ash is pneumatically conveyed into the tank through a device called a Slur-O-Lyzer®. The device contains a series of spray nozzles which wet the soda ash as it is blown in. Some of the wetted soda ash forms a monohydrate crystal bed at the bottom of the tank while the rest goes into a saturated solution. Solution is circulated through this bed and maintains a constant concentration of approximately 30% dissolved solids. As the solution is withdrawn from the tank, it is replaced with fresh water. More soda ash

then dissolves from the crystal bed to maintain the 30 percent dissolved solids concentration. When the bed is reduced to a certain depth, more dry soda ash is added to the tank. The monohydrate crystals can exist only at temperatures above 110°F; otherwise a different, less soluble crystal forms. Therefore, it is important that the tank be kept above this temperature. The tank has steam plate coils to maintain the temperature above 110°F. The Slur-O-Lyzer® and tank stand approximately 9.2 meters (30 feet) high and 6.1 meters (20 feet) in diameter.

Process Description

The main mechanism for particle collection in the FMC Dual Throat Venturi Scrubber is inertial impaction. In this phenomenon gas is accelerated in the venturi section, and the particulate matter accelerates along with it. Water droplets are injected from the spray nozzles, and the particulate matter impacts into these droplets. The water droplets containing the particulate matter are then removed from the gas stream in the separator in the manner previously described . The water collected in the integral recirculation tank is recirculated back up into the liquid introduction system of the venturi. A bleed stream is taken from the recirculation system at a rate which maintains either the suspended solids concentration at approximately 0.5% or the dissolved salt concentration at about 10%, whichever is closest to its limit. Since the abrasion characteristics of the particulate being collected were unknown, the 0.5% limit was considered to be a conservative compromise between water conservation and equipment life. This bleed stream is then neutralized and sent to a series of ponds where the solids are expected to settle out. Fresh water is added to the integral recirculation tank to replenish the water lost from the bleed stream and evaporation in the venturi. It is also intended that some water from the ponds will be used as make-up water.

Sulfur dioxide absorption is accomplished in the venturi throat using a sodium based alkaline solution. A schematic of this process is shown in Figure 6. Sulfur dioxide is absorbed in a solution containing sodium sulfite ($Na_2SO_3$), sodium bisulfite ($NaHSO_3$), and sodium sulfate ($Na_2SO_4$). As $SO_2$ is absorbed, the sodium sulfite is converted to sodium bisulfite and a percentage is oxidized to sodium sulfate. These reactions are shown below:

$$SO_2 + Na_2SO_3 + H_2O \rightarrow 2NaHSO_3 \quad (1)$$

$$2Na_2SO_3 + O_2 \rightarrow 2Na_2SO_4 \quad (2)$$

The bleed stream taken from the recirculation system for the particulate removal also prevents the solution from becoming saturated with dissolved solids. To replenish the sodium lost in this bleed stream, soda ash is added from the soda ash storage tank at a rate which maintains the solution at the design pH of about 6.5. The $Na_2CO_3$ reacts with $NaHSO_3$ forming $Na_2SO_3$ as shown below:

$$Na_2CO_3 + 2NaHSO_3 \rightarrow 2Na_2SO_3 + CO_2\uparrow + H_2O \quad (3)$$

The bleed stream is sent to a neutralization tank where soda ash is added to convert any remaining $NaHSO_3$ to $Na_2SO_3$.

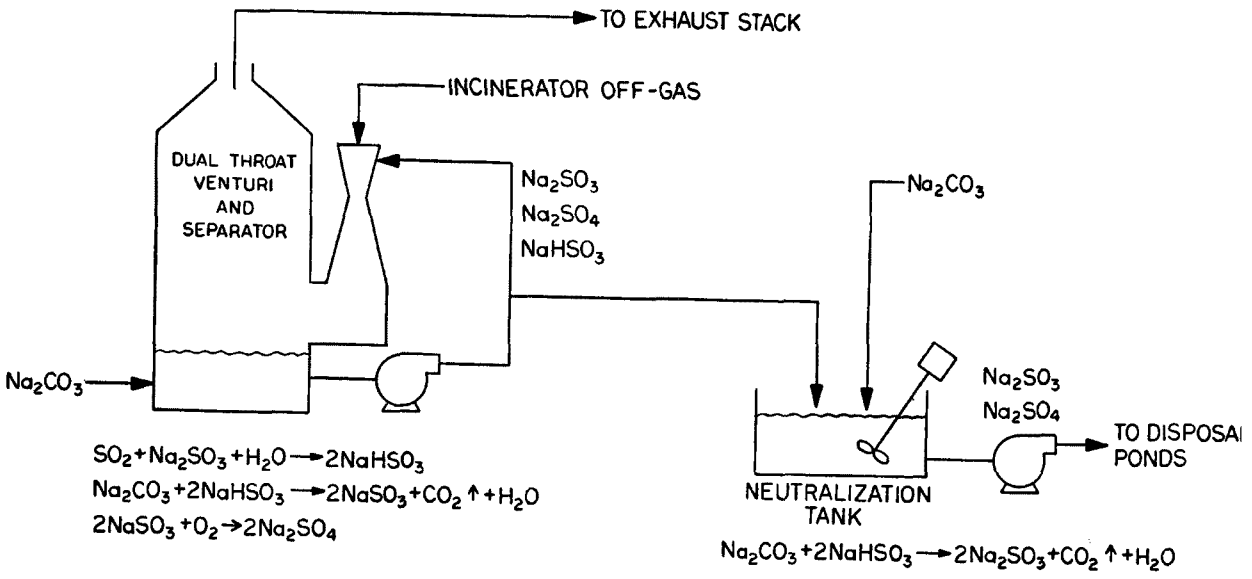


Figure 6 - Sodium Based $SO_2$ Absorption Process

Design of the System

There was a significant challange in predicting the design conditions for this application, since this particular oil shale extraction process had never been done before. Lab studies had indicated subsequent to the design and construction of the unit that $SO_2$ inlet concentrations might be about 10 times the original design concentration. Immediate plans by Rio Blanco, however, are to run the scrubber at only about 25% of original flow design. It is our belief that the scrubber will still remove sulfur under these conditions within compliance of Rio Blanco's PSD permit (90% removal, 250 ppm $SO_2$ in the outlet, and 63 kilograms per hour (138 pounds per hour) $SO_2$ emission).

If Rio Blanco were to operate additional test retorts with this equipment at higher flow rates and at high inlet concentrations of $SO_2$, modifications would probably have to be made to the equipment. A preliminary study by FMC recommended additional spray nozzles and revisions to the soda ash feed system, as minimum requirements to incrementally increase the capacity of the scrubber. Addition of spray nozzles to the separator would increase the $SO_2$ collection efficiency of the system. Also, addition of a dry soda ash storage silo was recommended to increase the storage capacity of the soda ash system. The soda ash from these silos would be pneumatically

transferred into the Slur-O-Lyzer® as required. Lastly, the scrubber blowdown ponds would also have to be expanded if higher flow rates are planned.

Determining the proper scrubber pressure drop for particulate collection also posed a design problem. It was believed that the bench scale testing would not be effective for determining the particle size distribution coming into the scrubber. Therefore, FMC decided to use a particle size distribution from previous analogous applications to determine the proper operating pressure drop. This pressure drop was found to be 114 centimeters (45 inches) water gauge for an efficiency of 97.8%.

## System Construction and Startup

The fabrication and construction of the system went smoothly. Rio Blanco was able to erect the system with no need for construction supervision from FMC. A three day training session was conducted by FMC to familiarize Rio Blanco personnel with the operation of the system.

The system was started up on October 13, 1980, and after some initial fine tuning was ready to be placed on line later that same day. The FMC startup engineer was on the job site for approximately one week during the startup period.

## Initial Operation and Test Results

During Retort "0", the scrubber was operated in a manner to minimize operability problems, i.e. dilute soda ash feed and dilute scrubber/blowdown liquor. Once the monohydrate crystal bed is formed in the Slur-O-Lyzer® it must be continuously heated to maintain the monohydrate structure. Because of the short amount of time the system would be operated for burn "0", the soda ash storage tank was operated without the monohydrate bed. Retort 1, on the other hand, will need to be operated at design conditions with a monohydrate crystal bed soda ash feed system and a concentrated scrubber/blowdown liquor. Retort 1 is currently scheduled to begin in April 1981.

During Retort "0", the scrubber was operated at only about 15% of its rated capacity of 6,160 $m^3$/minute (220,000 acfm). Temperature into the scrubber has been approximately 230°C (450°F). The scrubber was initially operated at a 102 centimeter (40inches) water gauge pressure drop across the throat, but was later reduced after it was found that particulates in the blowdown were well under 0.1 wt%. Cursory results also showed that changing the pressure drop produced no measurable effect on outlet $SO_2$ emission or perceived opacity. Outlet $SO_2$ concentrations have averaged approximately 100 parts per million based on an in-stack $SO_2$ analyzer.

Scrubber efficiency has been approximated at well over 90%. Although no particulate testing was done during the short retort operation, the FMC start-up engineer (who is an untrained stack observer) reported that the stack was clear after dissipation of the steam plume.

# FLUIDIZED-BED COMBUSTION HOT FLUE GAS CLEANUP PERSPECTIVE ON CYCLONES AND OTHER DEVICES

By: R.F. Henry, W.F. Podolski
Chemical Engineering Division
Argonne National Laboratory
9700 South Cass Avenue
Argonne, IL 60439

## ABSTRACT

Pressurized fluidized-bed combustion combined cycle generation of electricity promises appreciably higher efficiencies and less impact upon the environment than conventional boilers with flue gas desulfurization. Implementation of the "combined cycle" requires that flue gas to be expanded in the gas turbine be cleaned of particulates to tolerable levels. This cleanup problem is currently the focus of research and development into several types of improved hot gas cleaning equipment, but to date the best performance has been obtained with the more conventional type cyclones. These performance data have been compared to theory, and predictions for performance for several cyclones in series show that required turbine tolerance levels should be attainable with reasonably sized equipment. Gas cleanup downstream from the turbine might still be required with some coal/sorbent combinations to comply with EPA-NSPS.

## INTRODUCTION

Increased utilization of coal as an alternative to hydrocarbon fuels would reduce the United States dependance on foreign oil. However, use of higher-sulfur-content coals requires provisions for control of potential emissions. This may be accomplished by adding a flue-gas scrubbing system to a conventional coal boiler, by processing of the coal (cleaning), by converting to a synthetic fuel and removing pollutants from the intermediate fuel before burning, or by burning in a bed of sulfur sorbent. Of these alternatives, the latter is of interest in this paper.

Fluidized bed combustion (FBC), at either atmospheric or elevated pressure has potential for meeting environmental regulations concerning sulfur and nitrogen oxides, and it has the potential for generating electricity at increased efficiency, particularly if carried out in the pressurized mode with combined gas and steam turbine generators.

Implementation of the combined cycle concept depends on interfacing of the gas turbine with the pressurized, fluidized-bed combustor. Even though the PFBC has low $NO_x$ and $SO_2$ emissions, the "dirty" nature of coal (ash and alkali), coupled with the highly turbulent nature of contact in the PFBC and the characteristics of sulfur sorbents leads to an effluent with a considerable loading of particles as well as alkali metal concentrations in excess of current limits for oil- and gas-fired turbines. Removal of these particles hot and at elevated pressure is necessary for best efficiency of

the gas turbine. Adsorption of the alkali from the hot flue gas and development of resistant cladding or coatings for turbine blades are being considered as alternatives for corrosion protection.

## BACKGROUND

Allowable levels of particulate matter and alkali compounds for economically-long gas turbine lifetimes are not well defined for PFBC service, but estimates for particulate limitations have been made based on calculations, burner-rig tests and several 1000-hour tests of turbine parts in PFBC system effluent. Extrapolation to reasonable lifetimes has yielded relations as shown in Figure 1. The Westinghouse curves (1) represent a calculation corresponding to an allowable loading and size distribution based on gas turbine inlet specifications and an alternate allowable loading with finer size distribution which would have equivalent erosive properties. The General Electric curves represent extrapolation of some early data (2) obtained at Morgantown and G.E. from coal-fired turbine experiments (the nearly vertical curve) and more recent estimates of allowable particulate matter based on results (3) obtained in PFBC experiments at Exxon and CURL.

Next we look at combustor effluents. Loading and particle size distribution curves are shown in Figure 2 for a typical effluent from the CURL combustor during the 1000-hour test (4) and from data analyzed by G.E. in characterizing the efflux for the PFB/CFCC development program.(5)

If these two groups of data, the PFB effluent and the estimate of the allowable particulate concentration at the turbine inlet are placed on the same plot as in Figure 3, the degree of performance required for the hot gas cleanup system is placed in perspective. Removal of greater than 90 per cent of the total particulate matter loading will surely be required--in fact, removal of greater than 99 per cent may well be required for all particles larger than 10 micrometers (perhaps even for particles larger than 5 micrometers).

Particulate control is of importance in the PFBC concept for another reason--compliance with the EPA-NSPS.(6) As shown in Figure 3, turbines may well tolerate a higher total loading - as long as it consists mainly of finer particles - than will be permissible. This leads to the following "trade-off" which must be made: Hot gas cleanup, at pressure, may be carried out for turbine protection only, with post-turbine, lower temperature and pressure cleanup to meet emission requirements; or the cleanup required to meet NSPS may be carried out before the turbine. In either case, high removal efficiencies of fine particles will be required, but in the former case, at lower temperature and pressure. Cleanup at the lower temperature and pressure is considered to be possible with existing equipment--electrostatic precipitator (ESP) or baghouse technology, for example.

Investigations in PFBC pilot-scale facilities have routinely employed cyclones for at least one or more stages of particulate removal while occasionally testing other devices with potential for performance improvements. To date, no test of a device other than a cyclone has been completely

satisfactory at HTHP conditions experienced in the PFBC pilot-scale facilities.

Three different PFBC development units have completed extensive testing of turbine parts: Exxon in the Miniplant (7), CURL in the PFBC unit at Leatherhead, U.K. (8), and Curtiss-Wright in the PFB/Small Gas Turbine rig (9). At each of these locations, 1000-hour tests have been completed for the specific purpose of exposure of turbine components (stationary cascade of turbine blades in the former two tests and a rotating turbine in the latter) to actual PFBC effluent after some degree of cleaning. Concurrent evaluations of the hot gas cleanup systems used were also made during these tests.

A brief summary of these tests is shown in Table 1. Note first that there are several significant differences: The Exxon and CURL PFBC's are steam-cooled, while Curtiss-Wright's is air-cooled; Exxon and Curtiss-Wright have first-stage cyclones which recycle material to the fluidized bed while CURL does not; the Exxon cleanup system has 2 units (in addition to the recycle cyclone), while CURL and Curtiss-Wright have 3 (in addition to the recycle cyclone at Curtiss-Wright); temperatures at CURL were somewhat lower than at Exxon and Curtiss-Wright. Conclusions from these tests are:

Exxon - Some damage to turbine parts (higher temperature, large particles)

CURL - Essentially no damage

Curtiss-Wright - Essentially no damage

In each test there were turbine parts of several different alloys and in each case one or more materials tolerated the exposure with minimal damage.

These results are encouraging and do justify the prediction that a large facility could be operated, but probably at less than 1600°F turbine inlet temperature (perhaps less than 1500°F) with hot gas cleanup comparable to that demonstrated. Improved performance from the hot gas cleanup system would allow higher turbine inlet temperatures and increased cycle efficiency.

There is also concern that scale-up of hot gas cleanup equipment will cause degradation of performance, since in these three tests, cyclone-type units were used, and the effect of size on separation has been decumented. Calculations were made to estimate performance of a cleanup system comprising three cyclones in series, based on existing theory and results from the recent PFBC tests described above.

## PERFORMANCE CALCULATIONS

Choice of a predictive relation for these calculations was made after review of the literature, including earlier reviews of cyclone and hot gas cleanup work by Stern (10) in 1955, Jackson (11) in 1963, the American Petroleum Institute (12) in 1975, Razgaitis (13) in 1977, and many others. Many approaches to characterization of cyclone performance have been

suggested - with various levels of empiricism. In general, agreement exists on the use of operating conditions as part of a performance prediction model - usually as an impaction number grouping. There is some agreement on use of a geometric factor, ranging from a simple trend based on the ratio of a single dimension to a geometric number to account for all dimensional parameters which is used as part of the overall equation for prediction.

The approach selected for use in this analysis was developed by Leith and Licht.(14) This approach employs the concepts of backmixing, residence time, the tangential velocity profile and natural length phenomenon exhibited by vortex flows. It does not account for any effects of agglomeration or loading--both of which contribute to some conservatism as the general effects of both are to cause higher collection efficiencies than predicted. Probably most importantly, the Leith and Licht model does not depend on scaling of results from a similar unit with the same dust, but allows for prediction of performance a priori.

Comparison of calculated $d_{50}$'s using the method developed by Leith and Licht was made for Exxon tertiary cyclone performance data (7) and CURL primary and secondary cyclone performance data.(8) As shown in Table 2 good agreement was obtained. Performance estimates for a larger hot gas cleanup system comprising three cyclones in series were calculated.

Operating conditions were assumed to be 1600°F and 10 atmospheres pressure. All cyclones were assumed to have the geometry of the Exxon tertiary unit.(7) Primary and secondary units would have 100 feet per second inlet velocity and be 6 feet in diameter, while the tertiary units would have 150 feet per second inlet velocity and be 3 feet in diameter. This information allows calculation of fractional efficiencies with the equations of Leith and Licht, and when used with a typical loading and particle size distribution for combustor effluent from a test period during the 1000-hour series at CURL (8), stage-wise calculation of cyclone outlet loadings is possible.

Results of these calculations, the cyclone outlet loadings and particle sizes, are shown in Figure 4, along with the combustor effluent and turbine tolerance estimates. This hypothetical hot gas cleanup system is seen to be capable of resulting in a turbine inlet (3° cyclone outlet) loading and size distribution very close to those estimated as tolerable for gas turbines.

This cleanup system (of 6-foot and 3-foot diameter cyclones) would provide overall removal efficiency of about 98 per cent, with a pressure drop of about 6 pounds per square inch--based on the correlation of Shepherd and Lapple.(14) The system, as envisioned for cleanup of the hot gas in a PFBC module of 100 MW capacity (25 MW gas turbine in a steam-cooled cycle), would comprise 3 parallel units each in the primary and secondary stages and 8 parallel units in the tertiary cleanup stage.

These calculations indicate a PFBC system could be built and operated with a cyclone type hot gas cleanup system for gas turbine protection. Demonstration of this technology for a long-term and at a large-scale is the aim of PFBC development being conducted by the International Energy Agency at

Grimethorpe (16), Curtiss-Wright in their DOE-sponsored pilot plant program (9), and the team of American Electric Power Service Corporation/STAL-Laval Turbin AB/Deutsche Babcock at their component test facility in Sweden.(17)

Results from turbine materials testing indicate that at higher temperatures, which are desired for better gas turbine efficiency, lower particulate levels and/or smaller sizes will be required for acceptable turbine lifetime.(18) This is due to the complex nature of the corrosion, erosion and fouling mechanisms and their dependance on temperature.

Hot gas cleanup by means of cyclones appears capable of providing adequate turbine protection in first generation PFBC plants, but incentives are clear for operation at higher temperatures. Considerable value accrues to alternative, more efficient hot gas cleanup which would allow higher turbine inlet temperatures and increased cycle efficiency.

There are several classes of devices which have inherently higher particulate capture capabilities (19) - such as electrostatic precipitators (ESP's), scrubbers and several types of filters, but each of them is much more complex than a simple cyclone and has yet to be demonstrated in PFBC service. Some development work and testing has been carried out on ceramic fabric and granular bed filters, as well as preliminary testing of HTHP ESP and an electrostatically enhanced cyclone. Further development of these and several other types of possible "second generation" equipment has been supported by USDOE and USEPA. Some of the current projects are shown in Table 3.(20) Germany and England have active programs for the development of PFBC and Germany has several HTHP gas cleaning processes under development.(21)

Ultimately, development of PFBC systems will be directed by economic decisions. PFBC's are known to be capable of meeting current emission requirements for $SO_2$ and $NO_x$, and for given coal feed, PFBC's are smaller than conventional boilers. Hot gas cleanup cost and performance versus turbine lifetime and various other trade-offs must be made as firm design, performance and cost data are generated in development, demonstration and first-generation units. Table 4 lists some areas of concern which might well govern these economic decisions.

In conclusion, PFBC appears to be a viable alternative for generation of electricity from high-sulfur coal in an environmentally acceptable manner. Hot gas cleanup and its impact on turbine lifetime is the area of most technical and economic uncertainty. At conditions envisioned for first-generation plants, cyclones should provide adequate turbine protection. Future plants will probably be designed for higher turbine inlet temperatures and lower particulate loadings which may be satisfied by the new generation of hot gas cleanup equipment now being developed.

ENDNOTES

1. Keairns, D.L. et al. Fluidized Bed Combustion Process Evaluation. EPA-650/2-75-027-c, September 1975.

2. General Electric, CFCC Development Program. Advanced Clean-up Hardware Performance Guidelines for Commercial Plant. FE-2357-37, September 1977 .

3. Boericke, R.R. et al. Assessment of Gas Turbine Erosion by PFB Combustion Products. The Proceedings of the Sixth International Conference on Fluidized Bed Combustion, April 1980, CONF-800428 Vol. 2, p. 724.

4. Roberts, A.G. et al. Fluidised Bed Combustion. 1000 Hour Test Programme in a Pressurised Fluidised Bed Combustion Facility. Quarterly Report January - March 1980. FE-3121-14, May 1980.

5. General Electric, PFB/CFCC Development Program. Gas Cleanup Performance Requirement Report. FE-2357-66, May 1980.

6. U.S. EPA, New Stationary Sources Performance Standards. Federal Register 44(113) 33580, 1979.

7. Hoke, R.C. et al. Miniplant and Bench Studies of Pressurized Fluidized-Bed Coal Combustion: Final Report EPA-600/7-80-013, January 1980.

8. Roberts, A.G. et al. Fluidised Bed Combustion. 1000 Hour Test Programme in a Pressurised Fluidised Bed Combustion Facility. Vol. I - IV. FE-3121-15 (a - d), June 1980.

9. Curtiss-Wright, Engineer, Design, Construct, Test and Evaluate a Pressurized Fluidized Bed Pilot Plant Using High Sulfur Coal for Production of Electric Power. PFB/SGT Technology Unit Extended Test Report. FE-1726-51A, April 1980.

10. Stern, A.C. et al. Cyclone Dust Collectors. American Petroleum Institute, February 1955.

11. Jackson, R. Mechanical Equipment for Removing Grit and Dust from Gases. Published by BCURA, Leatherhead, England, 1963.

12. American Petroleum Institute, Cyclone Separators. API Publication 931 Ch. 11, May 1975.

13. Razgaitis, R. An Analysis of the High-Temperature Particulate Collection Problem. Argonne National Laboratory Report, ANL-77-14, October 1977.

14. Leith, D. and Licht, W. The Collection Efficiency of Cyclone Type Particle Collectors - A New Theoretical Approach. AIChE Symposium Series 68(126) 196, 1972.

15. Shepherd, C.B. and Lapple, C.E. Flow Patterns and Pressure Drop in Cyclone Dust Collectors. IEC 32(9) 1246, 1940.

16. Carls, E.L. et al. The IEA Grimethorpe Pressurized Fluidized Bed Combustion Experimental Facility. The Proceedings of the Sixth International Conference on Fluidized Bed Combustion, CONF 800428 Vol. 2, p. 225, August 1980.

17. American Electric Power, Pressurized Fluidized Bed Combustion Program, Summer 1980.

18. McCarron, R.L. and Grey, D.A., Materials Problems in Fluidized-Bed Combustion Systems. EPRI CS-1469, August 1980.

19. Spaite, P.W. and Burckle, J.O. Selection, Evaluation and Application of Control Devices. Air Pollution 3rd Ed., Vol. IV, Ch. 2, Academic Press, New York, 1977.

20. U.S. DOE High Temperature, High Pressure Particulate and Alkali Control in Coal Combustion Process Streams--Contractors' Meeting, Morgantown, West Virginia, February 1981.

21. Proceedings of International Conference on Gas Cleaning at High Temperatures and High Pressures. Julich, Federal Republic of Germany (VDI-Berichte 363), May 1980.

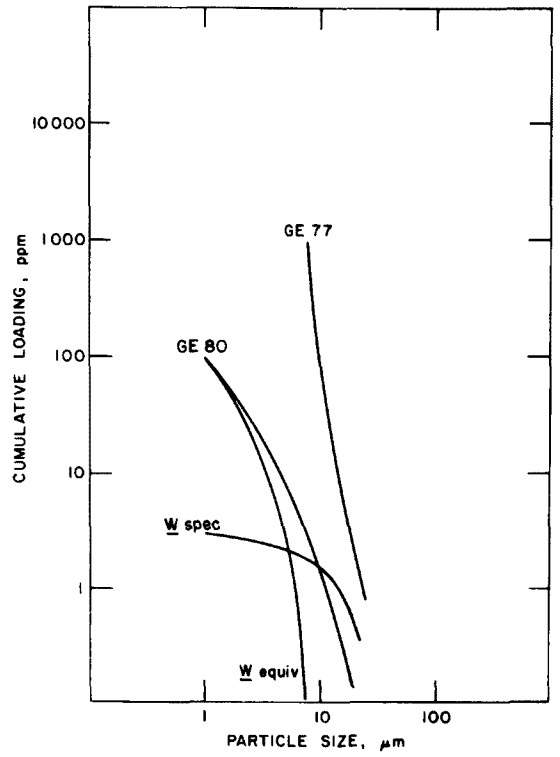


Figure 1
Estimated Turbine Tolerances

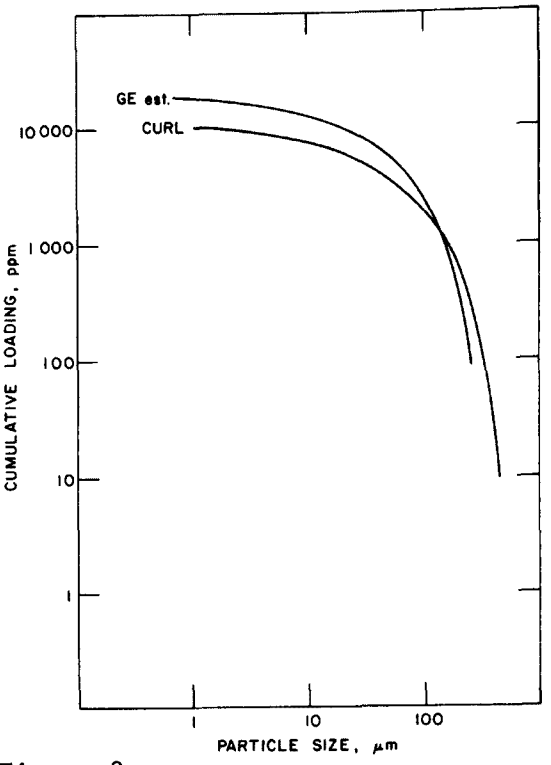


Figure 2
PFBC Effluent Data

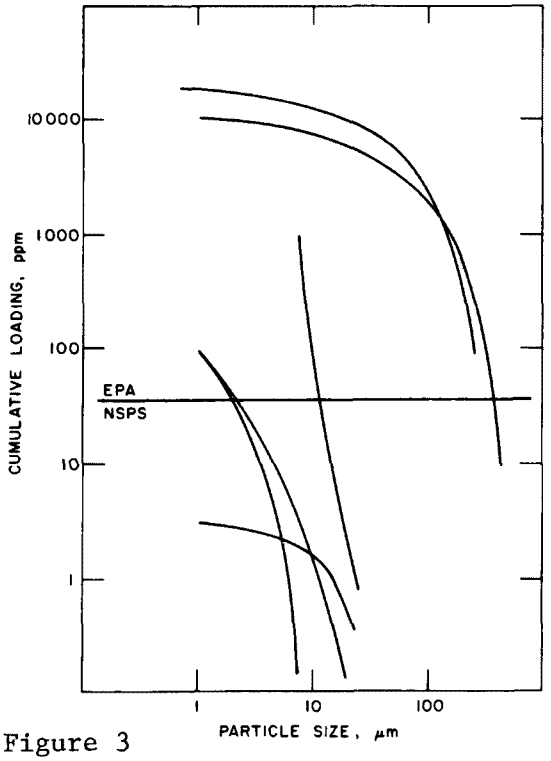


Figure 3
Effluent, Turbine Tolerance, EPA NSPS

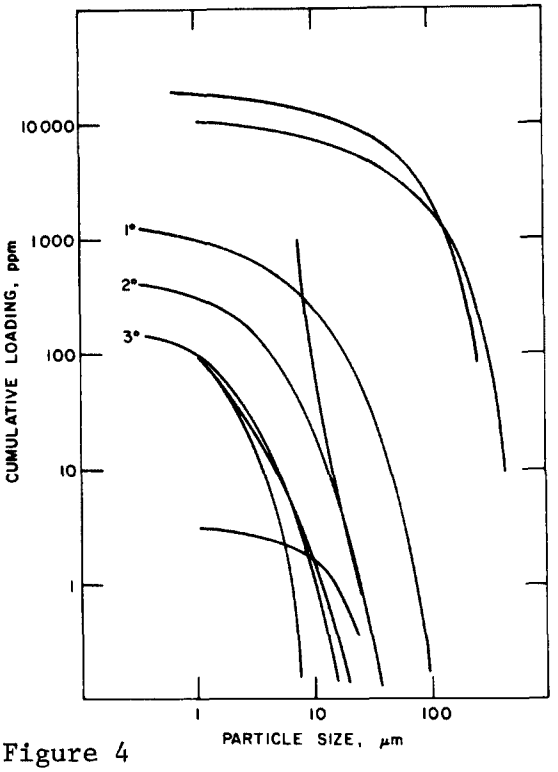


Figure 4
Calculated Cyclone Capabilities

TABLE 1

TEST FACILITY SUMMARIES

Exxon Miniplant - Steam Cycle Simulation

Recycle and 2 Cleanup Cyclones

20-110 ppm with $d_{50}$ = 1-3 μm

but 3-5%>10 μm

1500-1590°F at Cascades

Slight Effects

CURL - Steam Cycle - 2 Streams

| 1 - 3 cyclones | 2 - 3 cyclones |
|---|---|
| 1° van Tongeren | 1° chamber |
| 2° van Tongeren | 2° hybrid volute entry |
| 3° Stairmand | 3° Stairmand |
| 105 ± 35 ppm | 235 ± 40 ppm |
| (155 ± 40) 2 cyclones | |
| 1425°F | 1350 - 1475°F |

$d_{50}$ both 1 - 2 μm

cascades - no damage

Curtiss-Wright - Air Cycle

Recycle, Dyna-therm, Ducon, Aerodyne Cyclones

250 ppm -- Dilution to 80 ppm

1600°F - $d_{50}$ = 1-2 μm

Rover IS/60 Turbine OK

TABLE 2

PREDICTED AND ACTUAL CYCLONE PERFORMANCE

| Cyclone Test | Predicted $d_{50}$ μm | Actual $d_{50}$ μm |
|---|---|---|
| CURL 1° van Tongeren | 2.5 | 2.7 |
| CURL 2° van Tongeren | 1.93 | 1.0 |
| CURL 3° Simple | 1.12 | 0.88 |
| Exxon 3° of Scaled CURL 1° | 1.26 | 1.1 |
| Exxon 3° of Scaled CURL 2° | 1.36 | 1.5 |

TABLE 3

HTHP GAS CLEANUP PROJECTS

US DOE PRDA

I General Electric - Electrostatic Granular
Westinghouse - Ceramic Crossflow Filter
Exxon - Magnetic Granular Bed
Air Pollution Technology - Dry Plate Scrubber
SUNY Buffalo - Accoustic Agglomeration

II General Electric - Electro Cyclone
Westinghouse - "Ducon" Granular Bed
Acurex - Ceramic Bag Filter
Research Cottrell - HTHP ESP

US DOE Non-PRDA

General Electric - Glass Slag Scrubber
M.I.T. - Electro Fluid Bed Filter
Combustion Power - Granular Bed Filter
Penn. State - Accoustic Agglomeration
Denver Res. Inst. - HTHP ESP Test Facility
Linhardt Assoc. - Wedge Separator
Mechanical Technology - Cyclone Centrifuge
Argonne - Alkali Adsorption

Foreign

German, England, Sweden, Canada
South Africa, Australia, Japan

TABLE 4

TRADE-OFF'S, INTERACTIONS, ECONOMIC CONCERNS

Turbine Tolerance - Particulate

VS

EPA NSPS Limits

(Final Stage Cleanup HTHP or Post-Turbine)

Turbine Lifetime/Tolerance Relations

| | | |
|---|---|---|
| Erosion | | Temperature |
| Corrosion | VS | Loading |
| Deposition | | Alkali |

Erosion/Corrosion Interaction

Fluxing Protective Oxides
Exposing Grain Boundaries
Metal Attack (Sulfidation)

Economic Implications of Each (All) of Above:

Conventional Cleanup - Post-Turbine - Turbine
Loadings Higher/Lifetime Shorter (Temperature Lower)

VS

Advanced Method of Cleanup HTHP -- Turbine
Loadings Lower/Lifetime Longer (Temperature Higher)

# PRESSURIZED AND NON-PRESSURIZED ACOUSTIC AGGLOMERATORS FOR HOT-GAS CLEANUP APPLICATIONS

By: K.H. Chou and D.T. Shaw
Laboratory for Power and Environmental Studies
State University of New York at Buffalo
4232 Ridge Lea Road
Amherat, NY 14226

## ABSTRACT

The application of an acoustic agglomerator (AA) as a dust-particle preconditioner has been recently investigated in our laboratory. Several experiments have been conducted with the following AA parameter values: AA tube diameter: 1" to 18"; flow rate: up to 200 SCFM; pressure: 1 to 7 atm; temperature: room to 500°C; sound pressure level: up to 170 db; sound frequency: 0.4 to 20 kHz; acoustic generator types: siren, whistles and EM speakers.

The major advances may be summarized as follows: 1) AA works effectively when acoustic-induced turbulence is initiated at about 160 db. This threshold value is experimentally determined and is shown to be independent of the tube size. 2) The acoustic turbulent agglomeration rate is relatively independent of the sonic frequency. To avoid the mechanical vibration and the intensive sonic attenuation loss along the AA tube, the optium frequency is in the range of 0.8 to 1.2 kHz. 3) The immediate application of AA technology is limited by the lack of experience in large-scale sound generator design and operation. Our preliminary results show that large air-jet choppers driven by dusty air and pneumatically controlled oscillation metallic-diaphragm generators are two possibilities with the least R&D cost.

NOTE: Please contact the authors for further information regarding this paper.

# ALKALIS AND THEIR CONTRIBUTIONS TO CORONA CURRENT AT HIGH TEMPERATURE AND HIGH PRESSURE

By: Robert W.L. Snaddon
General Electric Company
Corporate Research & Development
Schenectady, New York

ABSTRACT

**The corona discharge is being investigated as a means of providing the charging necessary for the electrostatic augmentation of particle removal from high temperature, high pressure (HTHP) gas streams. In coal fired, combined cycle power generation, the HTHP gases contain alkali in the vapor phase. Because of their low ionization potentials, it is feared that alkali metals could have a detrimental effect on the operation of corona chargers in these gases. In this paper the effects of adding alkali to a HTHP gas stream are compared with a chemical analysis of the test gases. It is proposed that examination of the gas phase chemistry offers a useful way of assessing the potential alkali problem. For the limited results reported here, tentative conclusions are put forward regarding the nature and origins of the observed increases in current.**

## Introduction

With the current emphasis on the utilization of coal as a primary energy source, considerable effort is now being delpoyed to develop effective devices for controlling particle concentrations in the high temperature, high pressure (HTHP) gas streams encountered in the combined cycle, Pressurized Fluidized Bed Combustor (PFBC) method of energy conversion. In addition to Electrostatic Precipitators, the Electrocyclone (1) and the Electrostatic Granular Bed Filter (2) are two new electrostatically augmented collection devices presently under investigation. Like the precipitator, these devices rely on a corona discharge to produce the particle charging necessary for the enhanced performance. Since it is understood that the charge acquired by a particle in a corona charger is inherently limited by the intensity of the electric field (3), a good understanding of corona discharges in the PFBC environment is required if a proper appreciation and optimization of the above techniques is to be realized.

The early work by Shale (4) and more recent studies by Feldman et al. (5) have demonstrated that, on their own, the combined operating temperatures and pressures envisaged for the PFBC (i.e., 900 to 1000 °C and 7 to 10 atm) do not preclude the generation of stable corona discharges. However, in the real PFBC environment a further potential problem is posed by the presence of alkalis, where the vapor phase concentrations are expected to amount to a few ppm. Cooperman (6) has pointed out that the low ionization energies of alkali metals could mean that corona currents and operating voltages in PFBC type environments might be dictated by small concentrations of these species. Nevertheless, little attention has been paid to these effects since the work reported by Brown and Walker (7); presumably, because these authors observed only small changes in current when alkali was added to their system.

In recent studies of the PFBC gas chemistry (8), it has been shown that the alkalis in the vapor phase constitute a variety of compounds. The equilibrium concentrations of these compounds as well as the concentrations of atomic sodium and potassium and their ions are controlled by multiple reactions related to the composition of the coal and the conditions under which it is combusted. Even though tests have demonstrated that high fields can be established in a real PFBC environment (9), a wide variety of coals and combustion conditions are to be expected in PFBCs and one must anticipate different effects arising from different levels of thermally ionized species. Also, some caution should

be exercised when drawing conclusions from tests conducted in simulated environments. All the relevant chemical species are not usually present and added alkalis might form stable compounds rather than thermally ionized species.

For the above reasons it is suggested that a proper evaluation of the alkali problem cannot be made without consideration of the gas phase chemistry. In this paper preliminary equilibrium calculations are presented for a simple set of experimental conditions where alkali salt has been added to a simulated HTHP gas stream. An attempt is made to identify the nature of the observed increase in current and the mechanisms controlling its magnitude. The relevance of extrapolating these findings to real PFBC conditions is also discussed.

## Experimental Equipment

The HTHP test facility used in this study is shown schematically in Figure 1. In this system it was possible to carry out experiments at temperatures and pressures up to 950 °C and 10 atm. The high temperature gas stream was obtained by combusting carbon monoxide and air in a swirl-cup burner. The system pressure was controlled by a back-pressure regulator located downstream of the burner and test section.

The burner and test section were located in a vertically mounted stainless steel pressure vessel. The 50.8 mm diameter gas flow channel was formed with a 12.7 mm thick castable ceramic and a further 12.7 mm of ceramic fibre thermal insulation was employed between this and the pressure vessel wall.

Temperatures and pressures were measured with thermocouples and simple Bourdon gauges. The fuel and air flowrates were measured using Fischer and Porter flowmeters and the quantity of water in the test gas was determined by measuring the relative humidity of the air leaving the dryer.

The alkali salt used in this study was sodium chloride. This was injected into the burner air line in the form of a fine powder (3.9 $\mu$m mean diameter) using a small fluidized bed. For reasons described later in the text, the NaCl was introduced to the system in pulses. This was achieved with a solenoid valve located upstream of the fluidized bed.

The details of the electrode system are shown in Figure 2. Observations at ambient conditions indicated that the curvature on the supporting body and the spherical termination were sufficient to ensure that, at high voltages, the corona discharge was confined almost entirely to the 76.2 mm long, 3.18 mm diameter wire electrode. These components as well as the high voltage lead-through were manufactured from stainless steel.

At the test temperatures even high quality ceramic insulators tend to become electrically conducting. Therefore, to minimize the leakage current it was necessary to cool the beryllium oxide and Macor® insulators with air.

The high voltage was delivered by a Hipotronics 875-13, 0- $\pm$ 75 kV, stabilized DC unit. The voltage was monitored with the power supply meter. At the test temperatures the entire inner lining of the pressure vessel was electrically conducting. Consequently, it was not possible to employ the usual technique of measuring the corona current between the collecting electrode and ground. Rather, the currents had to be measured on the delivery side of the system. This was done with a Kiethley 616 digital electrometer.

## Experimental Procedure

The procedures adopted during testing were simple. Before and after HTHP testing the electrode alignment was checked by measuring the current voltage characteristics at ambient conditions. Sufficient time (usually four hours) was allowed for the system to reach thermal equilibrium prior to making measurements at any given HTHP condition. Current voltage characteristics were recorded at regular intervals to monitor drift in background or leakage conduction and to ensure that there were no major changes in the corona threshold and breakdown voltages.

Because the leakage current was found to change significantly over the duration of a test, it was necessary to inject the alkali in pulses. Observation of the current transients during these pulses then

allowed the real changes due to the presence of the alkali to be identified. The output of fluidized bed injector was calibrated in independent tests using absolute filters and gravimetric analysis.

## Experimental Results

The experimental results reported in this paper were all obtained at the same test conditions; i.e., 900 °C and 7 atm. The fuel, air and water vapor flows to the system under these conditions are listed in Table 1.

**TABLE 1. GAS FLOWS TO THE SYSTEM AT 900 °C AND 7 ATM**

| Gas | Flowrate ($gs^{-1}$) |
|---|---|
| CO Fuel | 0.798 |
| Burner Air | 3.641 |
| Cooling Air | 0.493 |
| $H_2O$ | $10.3 \times 10^{-3}$ |

Measurements were made at four different alkali injection rates. The concentrations, the injection rates and the transport air and water vapor flowrates through the fluidized bed are listed in Table 2.

**TABLE 2. ALKALI, TRANSPORT AIR AND WATER VAPOR FLOWRATES AT 4 TEST CONCENTRATIONS**

| NaCl Conc. (ppm) | NaCl Flowrate ($\mu gs^{-1}$) | Air Flowrate ($gs^{-1}$) | $H_2O$ Flowrate ($mgs^{-1}$) |
|---|---|---|---|
| 53 | 275 | 0.261 | 0.65 |
| 169 | 900 | 0.386 | 0.96 |
| 367 | 2000 | 0.510 | 1.28 |
| 717 | 4000 | 0.640 | 1.60 |

The corona threshold and the breakdown voltages without alkali present were found to lie around 7 kV and 12 kV for positive corona and 13 kV and 17 kV for negative corona. With the present equipment it was difficult to establish exact breakdown or sparkover voltages. As breakdown was approached the currents increased rapidly, often activating the current limiting trip on the power supply before any sign of the sparkover could be detected.

Figure 3 shows typical negative current voltage characteristics recorded at the test conditions. The two curves exemplify the changes in leakage current which occurred during the duration of a test; the two curves recorded approximately an hour apart.

Figure 4 shows a typical current transient recorded when alkali was injected into the system. The initial spike resulted from very high alkali concentrations which were caused by the accumulation of NaCl in the transport line between pulses. Once this was carried away the current dropped to a steady level corresponding to steady injection from the bed.

The measured increases in current at added alkali concentrations up to 700 ppm were small, Figure 5 showing these increases for a given constant applied voltage. Tests were also performed at constant alkali concentrations and different applied voltages. Figure 6 gives the results of one such test.

## Gas Phase Chemistry

In order to examine the composition of the test gas and to ascertain the numbers of thermally ionized species which could be expected under these conditions, gas phase equilibrium calculations were performed for the test conditions listed in Tables 1 and 2. A proprietary computer program which performs a system free energy minimization using fundamental thermodynamic properties of the elements in the system was employed in these calculations. The computed equilibria considered 27 species resulting from the known elements in the system and the most likely combinations of these.

Examination of the chemical activities of potential liquid phase species indicated that at the three highest concentrations (i.e., 169, 367 and 717 ppm NaCl) sodium carbonate ($Na_2CO_3$) fume would be formed. Since only gas phase reactions were considered, these observations imply that the calculated equilibrium concentrations are only valid for the 53 ppm NaCl case. The calculated equilibrium concentrations of the four major uncharged and the four major charged species in this case are listed in Table 3.

**TABLE 3. CALCULATED EQUILIBRIUM CONCENTRATIONS OF MAJOR SPECIES AT 53 ppm ADDED NaCl**

| Uncharged Species | Concentration (Part. Press. at 7 atm) | Charged Species | Concentration (Part. Press. at 7 atm) |
|---|---|---|---|
| $N_2$ | 4.954 | $Na^+$ | $4.906 \times 10^{-13}$ |
| $CO_2$ | 1.328 | $Cl^-$ | $4.786 \times 10^{-13}$ |
| $O_2$ | $6.891 \times 10^{-1}$ | $NO_2^-$ | $1.201 \times 10^{-14}$ |
| $H_2O$ | $2.848 \times 10^{-2}$ | $CO_2^-$ | $4.646 \times 10^{-17}$ |

## Discussion and Conclusions

For the reasons stated in the previous section, comparison of the experimental measurements with information deduced from the chemical analysis must be confined to the 53 ppm added NaCl case. Although this restricts the relevant data available for analysis, certain tentative conclusions are possible and these are discussed below.

In terms of the charging capability of a corona, it is of interest to establish (i) whether the increased current is unipolar or bipolar and (ii) what mechanism controls the production of this current. In a corona device the current which performs the charging originates in the ionization zone and is unipolar. If the increased current results from equal numbers of positive and negative ions in the charging zone it is bipolar. Bipolar current does not aid the charging process and in the limit of high concentrations of these bipolar ions, effective charging can be inhibited.

The above two issues are in essence related. To explore these, four limiting cases of the rate of production of thermal (bipolar) ions and the rate of their removal by the field are considered. These are:

a. No rate controlling processes; i.e., both the reaction kinetics and the ion removal by the field are very fast and the reactions giving rise to the thermal ions are driven to completion within the residence time of the gas in the charging field.

b. Reaction kinetics very slow and rate of removal of ions by the field very fast. In this case the measured increases in current would correspond to the rate at which the equilibrium concentration of ions is delivered to the charger by the gas flow.

c. Reaction kinetics very fast and the current controlled by the rate at which ions can be removed by the field. Provided the total concentrations of the elemental constituents of the gas are not altered significantly by the removal of ions, the increased current in this case would be given by

$$\Delta I = neb \int E_w dA_w \qquad A \tag{1}$$

where $n$ is the concentration ($m^{-3}$) of positive and negative ions, $e$ is the electronic charge ($1.6 \times 10^{-19}$ C), b is the mobility ($m^2V^{-1}s^{-1}$) of the ions, $E_w$ is the electric field ($Vm^{-1}$) at the electrode surface and $A_w$ is the area ($m^2$) of the electrode surface.

d. The rate of ion removal by the field is fast and the increased current is controlled by the reaction kinetics and the production of thermal ions.

From simple calculations it is clear that Cases a and b are not tenable. In Case a all the sodium would be ionized and for 53 ppm NaCl this would result in a current of approximately 1 A. For Case b the equilibrium concentrations of ions would only yield a current of some $10^{-9}$ A and this current would not depend on the strength of the applied field.

Since the measured increase in current is very small compared with 1 A, it is feasible to consider Case c. For the given electrode system, evaluation of the integral in equation 1 is difficult. Instead, this was deduced by invoking Gauss' law

$$\epsilon_o \oint \underline{E} \cdot d\underline{A} = q \qquad C \tag{2}$$

and measuring the capacitance of the electrode arrangement (without the HV lead-through). The capacitance was found to be 6 pF. For the ion concentrations in Table 3 and a mobility $\approx 10^{-4}m^2V^{-1}s^{-1}$ this yields

$$\Delta I = \beta \times V \qquad A \tag{3}$$

where

$$\beta \approx 10^{-10}AV^{-1}$$

and V is the applied voltage.

Comparing this with the data in Figure 6, it is apparent that although the linear dependence on voltage is evident, the predicted increase in current is somewhat lower than the measured values. However, given the relative crudity of the experiment and some uncertainty in the value of ion mobility, better agreement would perhaps have been fortuitous. Good values for the ion mobilities at these conditions are not readily available and extrapolation from ambient measurements using the $T^{½}p^{-1}$ temperature pressure dependence (10) was used. Since the interaction of large ions with surrounding gas molecules is expected to be smaller at the HTHP conditions, the estimated value of b might be low. Also, field distortions resulting from the high voltage lead through aren't included in the estimated $\Delta I$ and it is difficult to assess what effect these might have.

Since the predicted increases in current for Case d would lie between those for Cases b and c, the above analysis and arguments strongly suggest that the observed increases in current were due to bipolar ions and that the current was field limited. This conclusion is enhanced by the fact that if the current was unipolar the observed increases would likely have been non-linear with voltage and would likely have only appeared above the corona threshold.

Although the alkali concentrations in the PFBC environment are expected to be much lower than those considered here, it might well be premature to assume that the increased current due to alkali will be small or bipolar. The gas chemistry in the PFBC is entirely different and one must expect varying concentrations of thermal ions depending on coal composition and combustion conditions. Also, one can not ignore the possibility of the presence of low ionization energy or low work function materials in sufficient concentrations which could significantly alter corona ionization or electrode processes. Chemical analysis of the sort presented here appears to offer a cheap expedient means of assessing these possibilities.

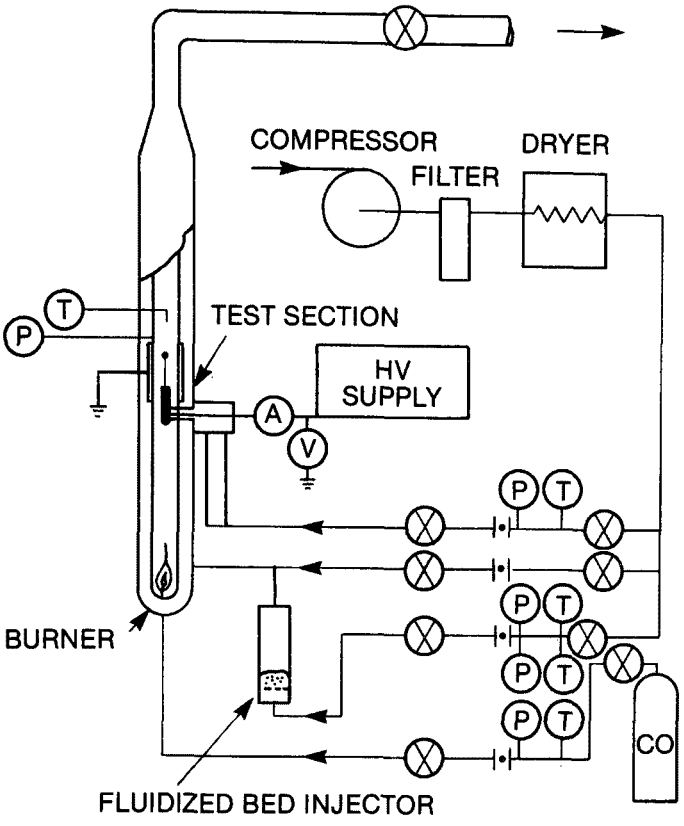


Figure 1. SCHEMATIC LAYOUT OF HTHP TEST FACILITY

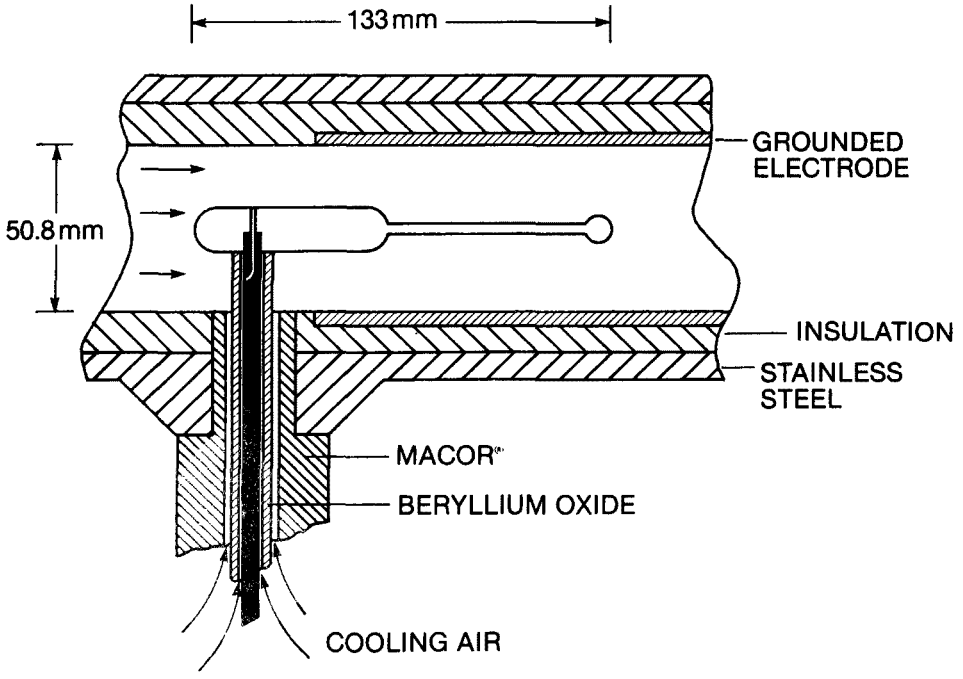


Figure 2. HIGH VOLTAGE ELECTRODE ASSEMBLY

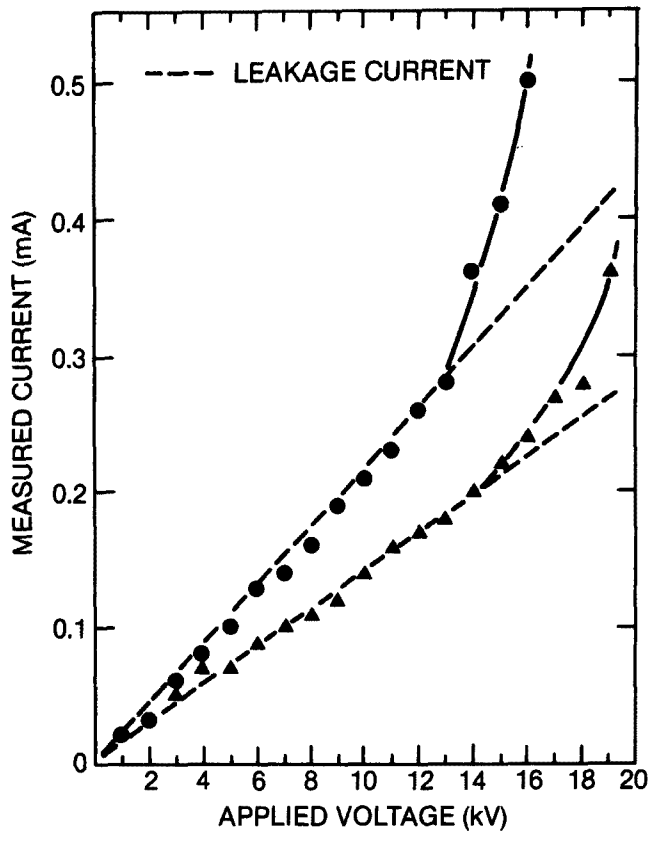


Figure 3. NEGATIVE CORONA CHARACTERISTICS AT 900°C AND 7 ATM

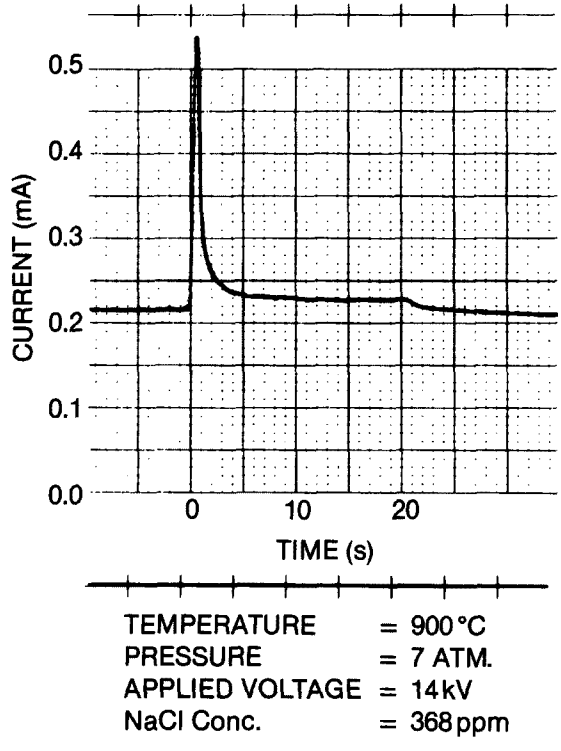


Figure 4. CURRENT TRANSIENT FOR 20s INJECTION PULSE

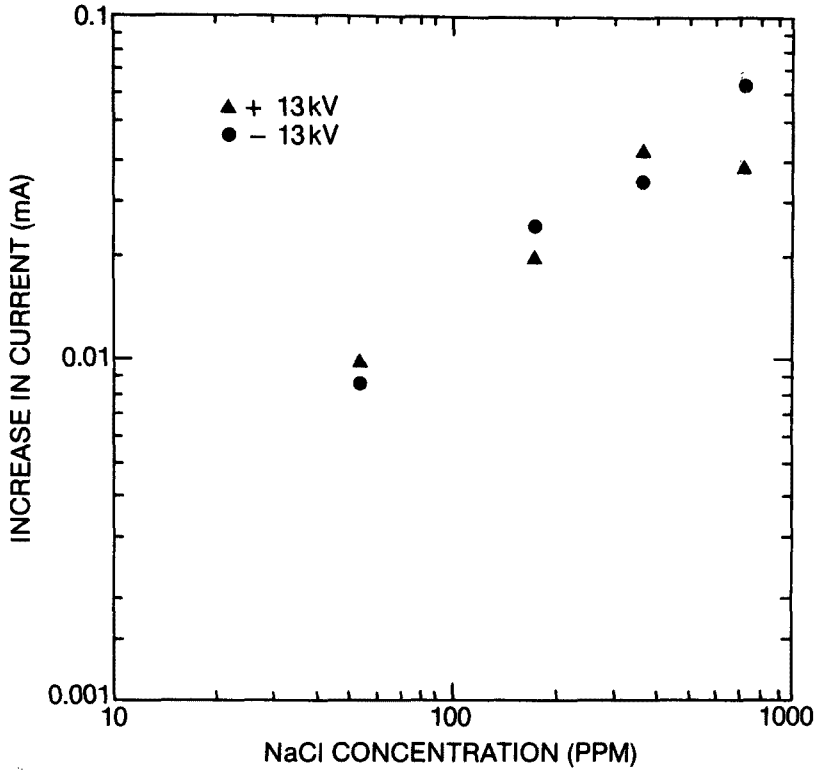


Figure 5. INCREASE IN CURRENT AT CONSTANT APPLIED VOLTAGE

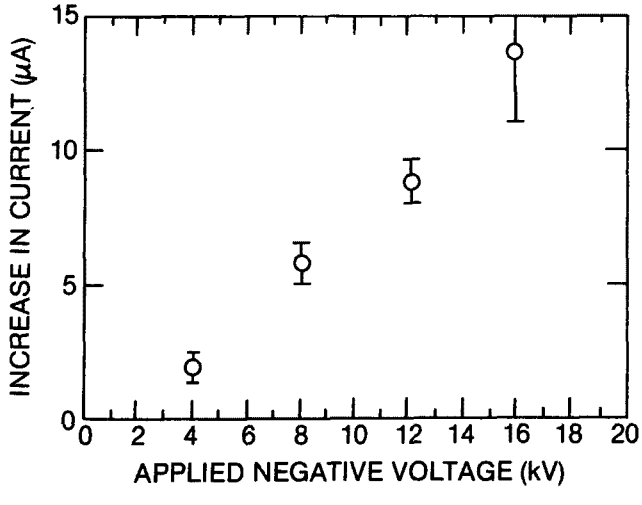


Figure 6. INCREASE IN CURRENT AT 53PPM NaCl

## Acknowledgements

The author would like to thank Dr. K.L. Luthra of General Electric Corporate Research and Development for performing the equilibrium calculations presented in this paper and for the many helpful discussions regarding this work.

This work was performed by Corporate Research and Development under NYS ERDA contract No. 237-ET/FUC-80 and DOE contract No. DE-AC01-80ET17091 to the General Electric Energy Systems Programs Department.

## References

1. Boericke, R.R., Kuo, J.T., Dietz, P.W. and Giles, W.B., "Electrocyclone for High Temperature High Pressure Dust Removal," Presented at A1AA 19th Aerospace Sciences Meeting, St. Louis, MO., January 1981.
2. Kallio, G. and Dietz, P.W., "Image Charge Collection of Fine Particles in Granular Beds," To be presented at the 7th TDFM Convention, Oxford, England, June 1981.
3. Melcher, J.R. and Sachar, K.S., "Charged Droplet Scrubbing of Submicron Particulate," Environmental Protection Technology Series, EPA-650/2-74-075, 1974.
4. Shale, C.C., "The Physical Phenomena Underlying the Negative and Positive Coronas in Air at High Temperatures and Pressures," IEEE National Convention Record, Pt. 7, 1965.
5. Feldman, P., Bush, J. and Robinson, M. "High Temperature, High Pressure Electrostatic Precipitation" Presented at EPA Symposium on the Transfer and Utilization of Particulate Control Technology, Denver, CO., 1977.
6. Cooperman, P. "Spontaneous Ionization of Gases at High Temperature," IEEE Transactions on Industrial Applications, vol. IA-10, No. 4, p. 520, 1974.
7. Brown, R.F. and Walker, A.B. "Feasibility Demonstration of Electrostatic Precipitation at 1700°F," JAPCA, vol. 21, no. 10, p. 617, 1971.
8. Spacil, H.S. and Luthra, K.L., "Thermochemistry of PFB Coal Combustion/Gas Turbine Combined Cycle," General Electric Corporate Research and Development Report no. 80-CRD-238, 1980.
9. Dietz, P.W. and Kallio, G., "Experiments on Electrostatic Charging of Dust in the PFB Combustor Environment," Presented at 6th International Fluidized Bed Conference, Atlanta, GA, 1980.
10. Nasser, E., "Fundamentals of Gaseous Ionization and Plasma Electronics," John Wiley and Sons Inc., 1971.

# HOT GAS CLEANUP IN PRESSURIZED FLUIDIZED BED COMBUSTION

L.N. Rubow
M.G. Klett
Gilbert Associates, Inc.
P.O. Box 1498
Reading, PA 19603

## ABSTRACT

Pressurized fluidized-bed (PFB) combustion for electric power generation provides a direct combustion process for coal and low-grade fuels with the potential for improved thermal conversion efficiency, reduced costs and acceptable environmental impacts. For the successful operation of combined cycle PFB power plants, particulate removal from the combustion off-gases at operating temperatures and pressures is critical. The gas clean-up system must be capable of reducing the particulate loading and alkali metal concentration in the combustion off-gas to levels compatible with gas turbine operating conditions and environmental standards. With the rapid development of PFB combustors, hot gas clean-up threatens to become a bottleneck in the development of a combined cycle power generation system.

This paper summarizes the status of hot gas clean-up development for PFBC. Included is information on approaches taken for hot gas clean-up, an outline of present development programs, and a review of other special problems associated with high temperature and pressure gas clean-up. Special attention is given to recent PFBC tests with cyclones in series, with encouraging results. Projections of performance have been made for commercial sized equipment which demonstrate that cyclones may not provide sufficient clean-up. The effect of clean-up system requirements on the PFBC cycle have also been analyzed and are considered.

## INTRODUCTION

The U.S. Department of Energy is sponsoring development of fluidized-bed combustion (FBC) technology as a promising alternative for utilization of our abundant domestic coal resources in an environmentally acceptable manner.

Fluidized beds as utility boilers have several advantages over conventional pulverized coal fired boilers, including an increase in heat transfer rate, low combustion temperatures and $NO_x$ levels, toleration of a wide range of coal properties, and $SO_2$ removal. By pressurizing the combustor, additional advantages are realized, including higher heat transfer and volumetric heat release rates, (resulting in a smaller volume), fewer coal feed points, lower $NO_x$ emissions, and improved $SO_2$ capture. A pressurized combustor can be applied to a combined cycle plant to take advantage of its inherent high efficiencies.

In 1969, testing began in Leatherhead, England to pressurize the fluidized bed in hopes of realizing these greater potential advantages over conventional coal fired boilers. These tests were successful, and, as a result, programs aimed at developing this technology were initiated in the United States by DOE, EPA, and others.

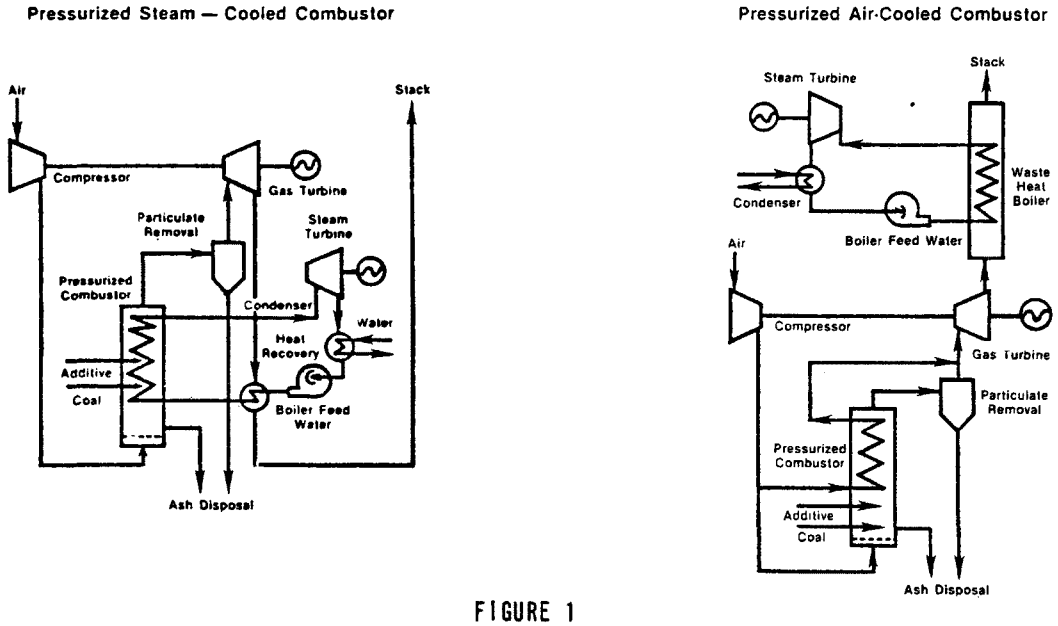


FIGURE 1
PFBC CONCEPTS UNDER DEVELOPMENT

Figure 1 shows the two primary PFBC concepts being developed. The fluidized bed effluent in both concepts contains a high concentration of particulates which must be removed prior to expansion in the turbine. Since no device is available commercially which will remove these particulates at the required temperature, hot gas particulate removal is a key technical issue which may be an obstacle to near term commercialization.

Another potential problem pertaining to hot gas cleanup is that of alkali metal removal, since measured alkali metal emissions are one to two orders of magnitude greater than those produced by the combustion of residual oils in large industrial turbines. Suppressing or filtering the alkalis and/or developing turbine materials which will resist corrosion and sulfidation are under development. Deposition of particulate matter on turbine parts affects the performance of the turbine and may also contribute to the corrosion process.

## EMISSION CHARACTERISTICS

The hot gas cleanup system in PFBC should be capable of reducing the particulate loading in the hot (1500-1700F) combustion off gas to levels compatible with gas turbine operating conditions and environmental

standards. Alkali metal species in the combustion gas may also be too high for adequate turbine life and a filtering device may be necessary.

## Particulate Loadings and Size Distribution

Although cyclones have not been successful in reducing particulate levels to the EPA New Source Performance Standard (NSPS) requirement (equivalent to about 0.02 gr/scf at 20% excess air), they will still play an important part in PFBC cleanup since an advanced cleanup device (i.e., baghouse, precipitator) will likely be preceded by two or three cyclones. Table 1 presents a summary of the data from various technology rigs after cleaning the combustion gases with two or three cyclones. As indicated by this data, the best that has been achieved using "small diameter" cyclones is a particulate carryover of 0.04-0.07 gr/scf with a median particle size of about 1.3 microns. Since this performance level is expected to degrade significantly when large commercial scale cyclones are used, conventional cyclone separators alone appear inadequate for reducing exhaust loadings sufficiently to meet NSPS. They may also be unable to permit long term gas turbine operation, and a tertiary device will be needed in order to produce a viable system to meet turbine requirements.

TABLE 1. PARTICULATE LOADINGS FROM PFB CYCLONES

| Technology Rig | Average Loadings gr/scf | Median Particle Size μm |
|---|---|---|
| CURL | 0.04 | 1.3 |
| ANL | 0.52 | - |
| CPC | 0.42 | 3 - 4 |
| Exxon (Miniplant) | 0.04 | 2 |
| C-W | 0.07 | 1.3 |

## Chemical Characteristics

PFBC particulates from the primary and secondary cyclones and exhaust gas captures have been chemically analyzed by various investigators to determine carbon, sulfur, and calcium contents and, in some cases, ash constituents. Preliminary experiments on the fate of 19 trace elements in a pressurized fluidized-bed combustor have been reported by Argonne National Laboratory[1,2] and Exxon[3]. The alkali content of the effluent stream (primarily Na and K) is a matter of concern because of the potential for fouling and hot corrosion of the gas turbine blading. The alkali present in the form of solids is subject to removal by the various hot gas particulate cleanup devices. However, alkali present in the vapor phase will not be significantly reduced by particulate filtration devices. The experimental data on alkali metal emissions in the vapor phase from tests conducted at NCB/CURL (Leatherhead, England) indicate that about 0.1 to 5 ppm sodium and potassium are liberated into the gas phase from a FBC at about 6 atm pressure and temperatures of 1450°F-1750°F.[4,5,6]

## Cleanup Requirements

The particulate removal system should be capable of reducing the particulate loadings in the combustion off-gas to levels compatible with environmental standards and with gas turbine requirements. Specific potential problems related to the gas turbine include blade erosion, hot alkali corrosion of turbine parts, and gas turbine fouling.

### Environmental

The EPA particulate emission standard for new coal-fired steam generators is presently 0.03 pounds of particulates per million Btu of fuel. For a PFBC operating in the 20-30% excess air range (steam-cooled and air-cooled respectively), this is equivalent to an exhaust emission of less than 0.02 gr/scf. To date, there is no specific restraint on particle size distribution.

### Erosion

Particulate tolerance for gas turbines has been estimated by turbine manufacturers to be as low as 0.0002 gr/scf, based on liquid fuel data.[7] Manufacturers of expander turbines (low temperature) specify a 0.07 gr/scf loading for their large cat-cracker installations. Consideration of recent data by General Electric has resulted in their proposed requirement of not more than 0.001 gr/scf greater than 10 μm and not more than 0.005 gr/scf greater than 5 μm.[8]

### Corrosion and Fouling

Gas turbine components exposed to the hot combustion gases are made of materials that form oxide scales to protect themselves from oxidation. In the presence of alkali metal compounds, which react with the sulfur oxides and chlorides in the combustion gas, liquid films of sulfate and sulfate-chloride mixtures can be deposited on the turbine hardware. These melts must be prevented because they can initiate hot corrosion and can lead to substantial deposit formation (fouling). Actual experimental results to date indicate that gas temperature in terms of both level and consistency, has a critical bearing on the extent of hot gas corrosion.

Fouling is the accumulation of unwanted deposits on the hot turbine components due to ash constituents in the fuel. In tests conducted by the Solar Division of International Harvester Co.,[10] the fouling characteristics of particulate from the CPC combustor were investigated. Solar concluded that the CPC flyash had a marked tendency to form dense deposits on impaction with hot turbomachinery surfaces.

## HOT GAS CLEANUP DEVELOPMENT STATUS

Several approaches have been proposed and are being developed for particulate cleanup of high temperature and high pressure gases. The

processes which have been most actively investigated include inertial devices, granular bed filters of various designs, electrostatic precipitators, fabric filters, metal or ceramic filters, and various hybrid designs. Except for conventional cyclones, these methods must be classified as developmental hot gas cleanup techniques and require considerable developmental effort before they can be reliably used. While some methods and processes are more advanced than others, questions of ultimate efficiency, reliability and equipment life are still unanswered and must be confirmed by both rig and pilot scale experiments.

Technology Rig Results

Technology rigs at Leatherhead England (CURL), Combustion Power Co. (CPC), Argonne National Labs (ANL), Exxon Research Labs (ERE) NASA-Lewis, and more recently, Curtiss-Wright (C-W) Corporation have employed various hot gas cleanup devices.

Cyclones, granular bed filters and baghouse devices have been tested at these technology rigs. Of these devices, only cyclones have proven operable in the system;[6] however, outlet particulate loadings are above the NSPS limit of 0.03 lb/$10^6$ BTU (0.015 gr/scf at 20% excess air). Recent results have shown cyclone "trains" to reduce particulate emissions to 0.04-0.07 gr/scf, with mean and maximum particle sizes of 1.3 and 8 μm respectively. Although granular bed filters and baghouses have produced encouraging results, their operability has not been proven. Following is a brief summary of three recent rig programs.

Work at the Coal Utilization Research Labs CURL, Leatherhead, England has provided the basis for many PFBC designs, but until recently has not been involved in HTHP cleanup programs. The majority of the testing at CURL has been done with two 10 inch diameter cyclones. An Aerodyne cyclone, modified by GE was then tested. As part of the 10 x 100 hour test sequence sponsored by DOE, Van Tongeren and Stairmand cyclones were tested, producing an outlet loading of 0.04 gr/scf.[10]

From 1976 to 1979, Exxon Research Engineering operated a 12 inch diameter PFBC, conducting a number of investigations of combustion, sorbent regeneration, and hot gas cleanup. The initial cleanup configuration consisted of two cyclones. Some modification to the cyclones resulted in an outlet loading of 1 gr/scf, 4 μm mean particle size, considerably above EPA limits. Subsequent testing with a Ducon granular bed filter showed promising results of 0.05 gr/scf, but never achieved "steady state" operation due to cleaning cycle difficulties. The addition of a third cyclone, in addition to a recycle and second stage cyclone, resulted in loadings of 0.02 - 0.05 gr/scf with approximately 2 μm mean particle size. Slipstream testing on a bag filter was encouraging, but an "integrated" cleaning cycle was not demonstrated. This program is currently inactive.[11]

C-W has operated their rig for over 2000 hours, but have tested only cyclone configurations. Testing began with a recycle cyclone followed by an Aerodyne 2-stage cyclone with dirty secondary flow. Subsequent

modifications included the change to secondary flow followed by the addition of two cyclones between the primary cyclone and the Aerodyne. The Ducon cyclone which was installed has performed satisfactorily but the Dynatherm, a somewhat unconventional swirl design, has failed to perform. After modifications to the cyclones, an outlet loading of 0.07 gr/scf with a 1.3 μm mean particle size was achieved. The present configuration has succeeded in supporting a 1000 hour turbine run with minimal erosion damage.

Developmental Programs

DOE and EPA have sponsored most of the development work in hot gas cleanup for PFB combustion. The Office of Energy, Minerals and Industry of the EPA has sponsored fluidized bed combustion for several years. The objectives of EPA were to identify potential environmental problem areas and to develop environmental controls, while the fluidized bed combustion technology is still under development. As part of this program, EPA has sponsored several projects in particulate control at high temperature and pressure.[12] However, present EPA programs in PFBC are primarily in the area of environmental assessment and not in the development of control equipment.

In the past, DOE's work in hot gas cleanup has been in support of specific technology rig and pilot plant programs. There was not a single unified program to develop gas cleaning equipment. In addition to their developmental work for specific technologies DOE has now begun a unified hot gas cleanup developmental program through a multi-contract PRDA (Program Research and Development Announcement). The DOE programs now comprise most of the on going work in hot gas cleanup for PFB combustion.

Research work to date has been primarily concerned with determining process feasibility and in developing lab scale equipment. Correlations of performance to cleanup has received little attention. High temperature and pressure sampling equipment is now becoming available which may allow better correllation of results with data. More effort is needed to develop a basic understanding of high temperature and pressure collection mechanisms.

DOE Sponsored Projects

o Program Research and Development Announcement

DOE issued a Program Research and Development Announcement (PRDA) to initiate the development of new concepts and also to test rig scale equipment. The program participants will address not only particulate removal, but also the removal of alkali and other trace metals.[13]

The solicitation is divided into two categories:

- Category I -- Concept Definition, Laboratory and Bench Scale Testing, and Evaluation (estimated duration - two and one-half years)

- Category II -- Process Design Testing and Verification (estimated duration - three and one-half years)

Five contracts were awarded in Category I. Firms selected by DOE to develop hot gas cleanup techniques include:

1. Exxon Research and Engineering Co. - Magnetic stabilized-bed filter.

2. General Electric Co. - Electrostatic granular bed filter.

3. Westinghouse Electric Corp. - Ceramic cross flow filters.

4. University of Buffalo - Acoustic agglomeration of particles.

5. Air Pollution Tech. - Dry plate scrubber.

Four firms are contracted to produce rig scale devices in Category II. These devices are scheduled to be tested at either the C-W Technology Rig or the Westinghouse Waltz Mill facility. Firms/concepts selected by DOE are the following:

1. Acurex Corporation - Ceramic Bag Filter
2. General Electric - Electrocyclone
3. Cottrell Environmental Sciences - Electrostatic Precipitator
4. Westinghouse - Granular Bed Filter

o Granular Bed Filter (Combustion Power Company). - The Combustion Power Company, under EPA and ERDA sponsorship, designed a moving bed granular filter for use with their CPU-400 pilot plant. A moving bed filter was constructed in November 1975 but during the first system heat up to 1300°F, the inner panel of the filter buckled due to excessive stress. After an ERDA review, a more gradual and lower risk development program was initiated. A series of performance evaluations were carried out under low pressure conditions on hot and cold models. A 1000 hour hot flow performance test was completed in 1979.

Electric Power Research Institute

EPRI sponsored work at Westinghouse has been centered on baghouse development, and recent rig tests have been encouraging.

## EFFECT OF CLEANUP SYSTEM DESIGN ON PLANT PERFORMANCE

Minimization of temperature and pressure losses in hot gas cleanup systems is desirable and is also an important consideration in the design and selection of equipment. Cyclones are typically low $\Delta P$ devices in the 10-30 inch of water range. In the PFBC application, with inlet pressures of 100 to 150 psia, cyclone system $\Delta P$'s have risen to the 4 to 6 psi range.

This is due to the direct relationship of $\Delta P$ to velocity, thus relating to a $\Delta P/P$ ratio, and also to the high design velocities chosen for high efficiency PFBC cyclones.

Figure 2 illustrates the effect of particulate cleanup system $\Delta P$ on plant efficiency for both an air cooled and steam cooled PFBC cycle. Also shown is the approximate range of $\Delta P$s expected for various advanced cleanup devices. The advanced cleanup systems under development are being designed not only for collection performance superior to cyclones but also for relatively low $\Delta P$, thus improving plant performance. Figure 3 shows the effect of particulate cleanup system temperature loss on plant efficiency for the air cooled and steam cooled PFBC cycles. Since the temperature loss occurs only with the combustion gas, the air and steam cooled PFBC concepts experience nearly the same effect. The trend with cyclones will be to improve the performance with smaller diameter units which will increase surface heat losses. Advanced devices will be enclosed in large vessels, thus minimizing heat losses.

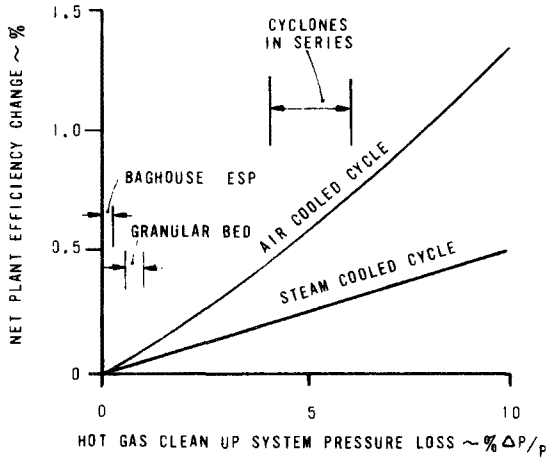


FIGURE 2
EFFECT OF HOT-GAS CLEANUP SYSTEM
PRESSURE LOSS ON PLANT EFFICIENCY

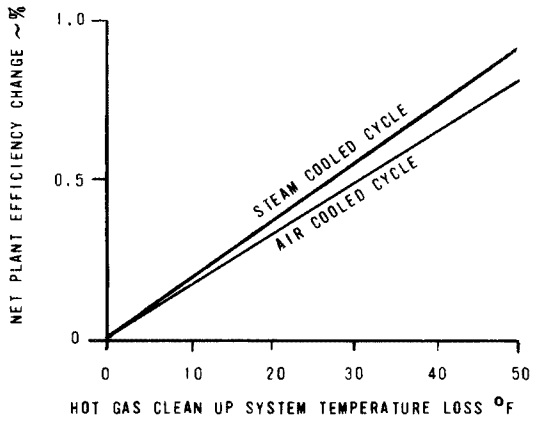


FIGURE 3
EFFECT OF HOT-GAS CLEANUP SYSTEM
TEMPERATURE LOSS ON PLANT EFFICIENCY

With these relationships established, the designer of PFBC systems must choose a device which will not only provide acceptable collection efficiency, but will result in the minimum $\Delta P$ and heat loss penalty to the system.

## ALTERNATIVES TO HOT GAS CLEANUP

As an alternative to the present PFBC concepts, two additional approaches were investigated (PFBC Expander Cycle and a Recuperative Heat

Exchanger Cycle) which, while reducing the cycle efficiency somewhat provide a viable means of gas cleanup.

PFBC Expander Cycle

Increased awareness of the necessity for energy conservation has provided incentive for the development of rugged turbines to recover energy from many processes requiring pressurization. Among these process are fluid catalytic cracking, nitric acid and ethylene oxide production, and recently, steel production. While many of these processes impose severe conditions on the expander none duplicate those anticipated in PFBC operation. However, it has been demonstrated that particulate loadings much heavier than those specified by leading industrial turbine manufacturers can be tolerated in "heavy duty" expanders designed for several years of continuous operation. Particulate limits have been set by many turbine manufacturers to 0.0002 gr/scf.[7] Expanders, however, can withstand loadings of .07 gr/scf at a lower temperature. High temperature turbines are limited to less than 0.01 gr/scf to achieve 50,000 hours lifetime.[14] Whatever the ultimate requirement, a turbine built to withstand a relatively heavy particulate loading is an attractive option for PFBC.

A study to examine the cycle efficiencies of PFBC systems employing an expander has recently been conducted by Gilbert Associates. Two basic systems were investigated: 1) An air-heater PFBC cycle and 2) a steam generating PFBC. The air heater cycle was derived from an EPRI study conducted by Curtiss-Wright.[15] A compressor driven by a low temperature "expander" turbine (1150°F) supplies combustion air to the PFBC (1650°F). The combustion air temperature is reduced by an economizer, which is part of the waste heat steam system. This is a modification of the reference system which increases the cycle efficiency from 31.7 to 35.2%.

The steam cycle was based on the GE CFCC (Coal Fired Combined Cycle) design.[16] As in the air heater cycles, combustion air is supplied by an expander driven compressor and clean-up is provided by a cyclone train. Supercritical steam (3500/1000/1000) is produced within bed heat exchanger tubes and from turbine exhaust heat. The power produced by the turbine is small relative to the steam turbine power production, and therefore, the system is not sensitive to the low temperature required by the expander. The resulting cycle efficiency is 38.3%, very close to the 40% with a "high" temperature turbine. A change to more conservative subcritical steam cycle results in an efficiency of 37.4%, still an attractive system.

It appears that utilization of an expander in PFBC is a viable option and will result in a system which is both cost and performance competitive with conventional technology.

Cold Gas Cleanup With a Recuperative Heat Exchanger

The use of low temperature conventional cleanup in a pressurized fluidized bed combustor system requires the use of recuperative heat exchanger in the gas cycle to maintain a reasonable turbine inlet

temperature. The high pressure combustion gases are cooled by a recuperative heat exchanger, cleaned of particulates, and then reheated by the recuperator before exhausting to the turbine (Figure 4). A high efficiency venturi scrubber was selected as the particulate cleaning device.

The hot gas from the pressurized fluidized bed combustor passes through two stages of cyclone type air cleaners where the entrained medium and coarse dust is separated and removed from the gas stream. The gas then enters the recuperative heat exchangers. In the counterflow heat exchanger, the hot gas in the tubes is cooled as it transfers heat to the clean gas which is flowing on the shell side. The clean gas from the venturi scrubber flows back to the shell side of the recuperative heat exchanger where it is reheated and flows to the gas turbine inlet.

The basic recuperative heat exchanger is presently restricted to about 1000°F due to the limiting factors of materials, thermal expansion and welding procedures. This study was based on a split or two unit heat exchanger which permits approximately two thirds of the required heat transfer area to be fabricated in lower priced material, while the remaining third must be Haynes 25, 310SS, or equivalent.

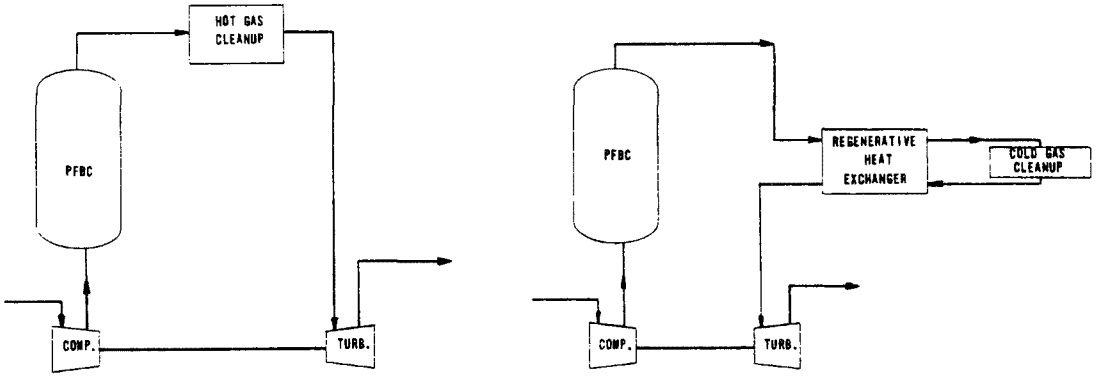


FIGURE 4
COMPARISON OF PFBC HOT AND COLD GAS CLEANUP SYSTEMS

A study was carried out to determine the performance penalty which accompanies reduced temperature particulate cleanup. The hot and cold gas cleanup alternatives were compared for both the air cooled and steam cooled combustor concepts. Two hot gas cleanup cycles were evaluated for the air cooled system, one with a granular bed filter and the second using only cyclones. Cold gas cleanup results in an efficiency loss of 4 to 4.5

percentage points. The reduced performance combined with the added cost of the heat exchanger makes this PFBC option relatively less attractive.

## CONCLUSIONS

Pressurized fluidized bed combustors will require high temperature particulate cleanup for turbine protection. While significant work has been accomplished in the area of hot gas cleanup, progress generally has been slow and encouraged mainly by Government funding. This has been true for the most part because these systems present difficult technical problems which are costly to solve. Manufacturers have not seen assurance of a potential market that would justify development of these systems. With the rapid development of fluidized bed combustion and gasification, hot gas cleanup has threatened to become a bottleneck in the development of a competitive, coal-fired combined cycle power generation system.

The DOE hot gas cleanup program is very important since output from that program may be requisite to PFBC commercialization. Several promising devices are being developed and these devices appear to improve PFBC cycle performance. PFBC cycles using an expander or a recuperative heat exchanger were assessed as an alternative approach. The expander cycle looked very promising whereas the recuperative heat exchanger cycle was less attractive. Questions of expander availability, development and costs must be answered to determine if this option is practical.

## REFERENCES


1. Vogel, G.J., et al. Reduction of Atmospheric Pollution by the Application of Fluidized-Bed Combustion and Regeneration of Sulfur-Containing Additives. EPA-650/2-74-104. September 1974.

2. Vogel, G.J., et al. Annual Report on a Development Program on Pressurized Fluidized-Bed Combustion. ANL/ES-CEN-1011. July 1975.

3. Hoke, R.C., et al. Studies of the Pressurized Fluidized-Bed Coal Combustion Process. EPA-600/7-76-011. September 1976.

4. National Research and Development Corporation. Pressurized Fluidized-Bed Combustion. Office of Coal Research. R&D Report No. 85 Interim #1. July 1974.

5. National Research Development Corporation. Pressurized Fluidized-Bed Combustion, Complete Report of Test Run No. 5. BCURA Ltd. US ERDA. September 1975.

6. National Research Development Corporation. Pressurized Fluidized-Bed Combustion, Report No. 43, Annual Report - July 1976 to June 1977. US ERDA. September 1977.

7. J. P. Meger and M. J. Edwards, "Survey of Industrial Coal Combustion Equipment Capabilities: High Temperaure High Pressure Gas Purification," Oak Ridge National Laboratories, TM-6072, June 1978.

8. General Electric Energy Systems Programs Development. CFCC Development Program, Cleanup Equipment Performance Specification of Commercial Plant, Task 4.1.2. ERDA Contract No. EX-76-C-01-2357. August 1977.

9. Corrosion and Erosion Evaluation of Turbine Materials in an Environment Simulating the CPU-400 Combustor Operating On Coal, Final Report. US ERDA FE/1536-3. April 1977.

10. Roberts, A. G., et. al, Fluidized Bed Combustion - 1000 Hour Test Program in a PFBC Facility, Final Report, (FE-3121-15), December 1980.

11. Exxon Research and Engineering, "Miniplant Studies of Pressurized Fluidized Bed Coal Combustion: Third Annual Report", April 1978, EPA-600/7-78-069.

12. Henschel, D.B. "The EPA Fluidized Bed Combustion Program - An Update." Proceedings of the Fifth International Conference on FBC. December 12-14, 1977. Mitre Corp. for U.S. DOE, December 1978.

13. "Exploratory Research Development, Testing and Evaluation of System or Devices for Hot Gas Cleanup." Program Research and Development Announcement No. (PRDA RA01-79ET15055), Issuance Date April 4, 1979.

14. General Electric, CFCC Development Program, Taks 4.1.2 Report, March 1978, U.S. DOE FE-2357-37.

15. R. Schaeffer, "Cost Estimate of Fluidized Bed Combuster Air Heater for Gas Turbine," EPRI Report FP-995, Technical Planning Study TPS 76-664, February 1979.

16. General Electric, CFCC Development Program, Commercial Plant Design Definition, (FE-2357-28), March 1978.

# VENTURI SCRUBBING FOR CONTROL OF PARTICULATE EMISSIONS FROM OIL SHALE RETORTING

By: Gerald M. Rinaldi
Monsanto Research Corporation
1515 Nicholas Road
Dayton, Ohio 45407

Robert C. Thurnau
U.S. Environmental Protection Agency
5555 Ridge Avenue
Cincinnati, Ohio 45213

## ABSTRACT

During a week-long field study in September 1980, a mobile pilot-scale venturi scrubber was tested for control of particulate emissions from Laramie Energy Technology Center's 150-ton simulated *in-situ* oil shale retort. The retort off-gas flow of 545 acfm, discharged from a heat exchanger at a temperature of 136°F and saturated with water, was scrubbed at liquid-to-gas ratios of 11 to 18 gpm/$10^3$ acfm. Sampling and analysis of the scrubber inlet and outlet gases were conducted to determine particulate removal. Outlet particulate concentrations were consistently reduced to 35 mg/$m^3$, even though inlet loadings varied from 125 to 387 mg/$m^3$ and 50 weight percent of the particles were less than four microns in diameter. Particulate control efficiencies up to 94 percent were achieved, although no correlation to liquid-to-gas ratio was apparent. Simultaneous control of ammonia emissions, at efficiencies up to 75 percent, was also observed.

## INTRODUCTION

Oil shale has been recognized as a potentially substantial energy resource in the United States for more than 100 years. Recently, increasing dependence on foreign oil supplies and rapidly escalating oil prices have provided new incentive for shale oil recovery from deposits in Colorado, Utah, and Wyoming. At least four domestic firms (Colony Development Operation, Paraho Development Corporation, Superior Oil Company, and Union Oil Company) have developed surface retorting processes, in which oil shale is mined and crushed prior to thermal processing in aboveground facilities. *In-situ* or modified *in-situ* processes, in which the shale bed is hydraulically or explosively fractured and retorting is carried out underground, are now being developed by Equity Oil Company, Geokinetics, Inc., Occidental Oil Shale, Inc., and Rio Blanco Oil Shale Company.

Despite the benefits of oil shale retorting as an alternative energy source, byproduct gases containing a complex mixture of criteria pollutants (particulate matter, hydrocarbons, carbon monoxide, and oxides of nitrogen and sulfur) and non-criteria pollutants (e.g., ammonia and hydrogen sulfide) could have an adverse impact on the pristine air quality of the Rocky Mountain region if released uncontrolled. Therefore, pollution control methods capable of adequately reducing environmentally harmful discharges must be available to assure

the emerging oil shale industry's compliance with future standards. Toward this end, the U.S. Environmental Protection Agency (EPA) has contracted with Monsanto Research Corporation (MRC) to characterize point-source air pollution due to surface and *in-situ* oil shale retorting, focusing on particulate emissions, and to evaluate available particulate control methods. This paper presents results of a field test in which a mobile venturi scrubber was used to control particulate emissions from a simulated *in-situ* oil shale retort operated by the Department of Energy's Laramie Energy Technology Center (LETC) in southeastern Wyoming.

## DESCRIPTION OF LETC RETORTING FACILITY

In 1969, a batch-type retort with the capacity to process 150 tons of shale was constructed by the U.S. Bureau of Mines at a site north of the Laramie Energy Technology Center in Laramie, Wyoming (1). Figure 1 is a flow diagram of LETC's 150-ton retort and its auxiliary equipment (1). Combustion of oil shale is initiated via a natural gas burner mounted on the retort lid. Air is forced downward through the shale bed, simulating the vertical modified *in-situ* technologies being developed by Occidental Oil Shale, Inc., and Rio Blanco Oil Shale Company. Shale oil and byproduct water drain to a collection tank located below the retort. The retort off-gas, containing residual oil mist and water, passes through four packed towers (not two as originally designed and indicated in Figure 1) and then through a water-cooled heat exchanger in an attempt to remove this entrained material. After line pressure is increased by a positive-displacement blower, the gas stream is split to allow for recycle. The excess is vented to a waste-gas stack equipped with a natural gas burner to oxidize combustible components before release to the atmosphere. Retorting continues until the bottom grate temperature increases to approximately 500°F, by which time shale oil production has already stopped and the oxygen content of the off-gases has begun to rise.

Relevant details of the operation of LETC's 150-ton oil shale retort during Run 19, when the pilot scrubber test was conducted, are as follows. The shale retorted was medium-grade material, containing about 28 gallons of oil per ton of rock, taken from the DOE mine at Anvil Points, Colorado. A mixture of air and steam was injected to the retort at feed rates of 13,250 dry standard cubic feet per hour and 121.5 pounds per hour, respectively. Ignition and air input began at approximately 10:45 AM MDT, 8 September 1980; retorting continued until 12:30 AM MDT, 15 September 1980. Total oil recovery for the 5.5-day burn was 1,990 gallons, equivalent to a production rate of 360 gallons, or 8.6 barrels, per day. For comparison, commercial oil shale processing facilities will produce as much as 50,000 barrels per day, continuously, for 20 years or longer (2).

## CONTROL DEVICE SELECTION AND OPERATION

### Choice of Wet Scrubbing

During the first phase of EPA Contract No. 68-03-2784, MRC evaluated electrostatic precipitation, fabric filtration, and wet scrubbing relative to their potential ability to control particulate emissions from *in-situ* and surface

retorting (2). The utility of electrostatic precipitation in the application of interest is questionable because of the lack of information on particle resistivity and because of the presence of flammable or explosive gases that represent a potential safety hazard. The formation of a porous dust cake necessary for high particulate removal efficiencies in fabric filtration equipment may be precluded by shale oil mist and possibly by condensed moisture in retorting off-gases. Unlike electrostatic precipitation, there is much less fire or explosion hazard associated with wet scrubbing of retort off-gases containing combustible species. Scrubbers also are preferable to baghouses because the former are not only effective for control of liquid or solid particles in high-temperature, moisture-laden gas streams, but also suitable for treatment of gas streams with fluctuating characteristics, for example, flow rate, temperature, and composition. Wet scrubbing also has the advantage that simultaneous particulate removal and absorption of gaseous pollutants can be accomplished using an appropriate liquid medium. Primarily based on these considerations, MRC recommended wet scrubbers for pilot-scale testing to study the control of particulate emissions from *in-situ* and surface oil shale retorting (2).

Operation of EPA's Mobile Scrubber at LETC

For the pilot-scale particulate control test at Laramie, MRC used a venturi-cyclone scrubber housed in a standard freight trailer and developed by EPA as a mobile research unit. A schematic diagram of the mobile scrubber is given in Figure 2. Prior testing of the mobile wet scrubber, first by MRC and then by Acurex Corporation, led to some design and hardware modifications not indicated in the figure. A single Roots blower replaced the original two Paxton blowers because of the latter's inability to handle residual particulate matter and entrained water droplets passing the demister. The original demister was replaced by an epoxy-coated, reinforced plywood compartment containing a series of zigzag baffles to collected entrained droplets.

Of the three interchangeable venturi throats provided with the mobile scrubbers, the "medium" throat was used at Laramie. This throat has a diameter of 2.36 inches, a length of 12 inches, and two radially opposed liquid feed nozzles two inches below the throat entrance. Piping throughout the scrubber trailer, and that used for external hookup to the retort off-gas line, was six-inch-diameter stainless steel. Because the gas stream treated at Laramie was saturated with moisture and its temperature relatively low, neither the presaturator shown in Figure 2 nor four banks of band heaters along the scrubber inlet line were needed.

LETC's existing ductwork was breached just upstream of the inlet to the thermal incinerator (see Figure 1), venting the entire gas flow to the mobile scrubber. In order to reduce any hazards of environmental contamination or worker exposure associated with emissions of hydrocarbons and other gaseous pollutants, the scrubber outlet gases were piped to the incinerator. The retort off-gases treated had an average temperature of 136°F, an average moisture content of 21 percent by volume, and an average flow rate of 545 acfm, or 314 dscfm.

During the field testing at LETC's 150-ton retort, MRC varied the scrubbing liquid feed flow, and thus the liquid-to-gas (L/G) ratio, over a range typical of commercial installations in order to observe the effect of this parameter. Table 1 describes the various operating conditions employed, in chronological order, specifying the volumetric feed rate and origin of scrubbing liquid, L/G ratios, and durations. The relationship between liquid feed rate, or L/G ratio, and the pressure drop across the venturi scrubber and cyclone is quantified in Table 2. Up to 5 gpm of well water was supplied by LETC, and the recycle consisted of scrubber discharge treated in a mobile stream stripping unit operated by Denver Research Institute. Steam stripping was intended to remove dissolved gases, such as ammonia, carbon dioxide, and hydrogen sulfide, from the recycle stream. Suspended solids were removed by a traveling-grate deep-bed filter mounted in the scrubber trailer. The temperature of the combined scrubber feed varied from 55° to 110°F and the pH from 6 to 9, the higher values reflecting the effect of heating during steam stripping and the uptake of basic dissolved gases, respectively.

TABLE 1. SCRUBBER OPERATING CONDITIONS

| Operation code[a] | Scrubbing liquid feed rates, gpm | | L/G ratio,[b] gpm/$10^3$ acfm | Duration, hr:min |
|---|---|---|---|---|
| | Well water | Recycle | | |
| 8A | 3 | 5 | 15 | 2:25 |
| 10A | 5 | 5 | 18 | 14:10 |
| 10B | 0 | 10 | 18 | 2:00 |
| 6A | 0 | 6 | 11 | 24:50 |
| 6A | 0 | 6 | 11 | 6:50 |
| 10C | 5 | 5 | 18 | 24:00 |
| 8B | 4 | 4 | 15 | 5:45 |

[a]Numerals in codes indicate total scrubbing liquid feed rates, and letters indicate different well water/recycle ratios.

[b]Calculated using average gas flow rate of 545 acfm.

TABLE 2. EFFECT OF LIQUID-TO-GAS RATIO ON PRESSURE DROP

| Total scrubbing liquid feed rate, gpm | Liquid-to-gas ratio, gpm/$10^3$ acfm[a] | Pressure drop, in. $H_2O$[b] |
|---|---|---|
| 5 | 9 | 22 |
| 6 | 11 | 26 |
| 7 | 13 | 28 |
| 8 | 15 | 32 |
| 9 | 17 | 35 |
| 10 | 18 | 38 |

[a]Calculated using average gas flow rate of 545 acfm.

[b]Measured from venturi inlet to cyclone outlet.

## SAMPLING AND ANALYSIS METHODS

The principal objective of gas and liquid sampling and analysis during the venturi scrubbing test at LETC's 150-ton oil shale retort was to determine the particulate control efficiencies achievable. Points sampled included, for the gas phase, the scrubber inlet and outlet and, for the liquid phase, the scrubber feed and discharge water. Equipment and procedures used to determine particulate loading were essentially those described in EPA Method 5 as outlined in the Federal Register (3). The back half of the Method 5 sampling train was modified by including an XAD-2 resin trap (to collect organic vapors) between the filter and the impingers and by using an oxidative reagent solution in the impingers (to collect volatile compounds of trace elements).

Because of the small duct diameter (6"), single-point sampling was used to determine the particulate emission rate, with the probe tip placed at the point of average gas velocity, as determined by a detailed preliminary velocity traverse (EPA Method 1). Particulate mass, as specified by the Federal Register method, is reported as the sum of that collected on the filter and that rinsed from the probe and connecting glassware upstream of the filter. In addition, MRC measured the amount of "back half" residue rinsed from the downstream half of the filter holder and the glassware down to the XAD-2 resin trap.

Particle size distribution was measured using Andersen Mark III cascade impactors, including the preimpactor for separation of coarse particles (4). Glass fiber collection substrates were used because the oily nature of the particulate might otherwise cause problems of carryover from stage to stage. The isokinetic impactor sampling rate with a 1/8-inch-diameter nozzle was approximately 0.2 acfm, and sampling durations were 10 and 20 minutes for the scrubber inlet and outlet, respectively. Due to the control efficiency of the pilot scrubber, the outlet sampling time was too brief to collect a measurable amount of sample; therefore, only the inlet particle size distribution is reported.

## RESULTS AND DISCUSSION

### Particle Size Distribution

MRC's measurements of the size distribution of particles emitted by LETC's 150-ton retort represent the first such determination for that specific facility and one of only very few for the oil shale industry in general. An average distribution, based on three measurements, of particle size in the retort off-gases, that is, the scrubber inlet, is listed in Table 3. Two significant conclusions can be drawn from this data. First, more than half the particulates, by weight, have a diameter less than five microns, with approximately 10 percent less than one micron in diameter. Also, the size distribution appears to be bi-modal, with the fractions larger than 20 microns (~35 percent) and between one and two microns (~30 percent) predominating. Visual inspection of the impactor collection substrates indicated the presence of both straw-colored oily material and a black, possibly inorganic dust, perhaps due to attrition of the shale in the retort.

TABLE 3. SIZE DISTRIBUTION OF PARTICLES IN RETORT OFF-GAS[a]

| Stage | Size range, microns | Weight percent: In size range | Weight percent: Cumulative less than size range |
|---|---|---|---|
| Preimpactor + Stage 0 | >19.5 | 36.8 | 63.2 |
| 1 | 13.6 - 19.5 | 0.6 | 62.6 |
| 2 | 9.1 - 13.6 | 4.4 | 58.2 |
| 3 | 6.3 - 9.1 | 1.3 | 56.9 |
| 4 | 4.0 - 6.3 | 7.0 | 49.9 |
| 5 | 2.0 - 4.0 | 11.0 | 38.9 |
| 6 | 1.3 - 2.0 | 28.4 | 10.5 |
| 7 | 0.9 - 1.3 | 5.0 | 5.5 |
| Backup filter | <0.9 | 5.5 | 0 |

[a]Averages calculated from results of three separate samples.

Particulate Loading and Control Efficiency

Table 4 presents the results of seven Method 5 measurements of particulate loading in LETC's retort off-gases and in the venturi scrubber outlet for three different scrubber operating conditions. These calculated values are based only on the mass collected from the filter and washes of the front-half glassware in the sampling train, thus making this data equivalent to others taken according to the Federal Register method. By comparison, the mass of condensible organic "particulate" matter rinsed from the glassware between the filter and the resin trap (back half) ranged from 2.7 to 5.5 times the amounts in Table 4 for the scrubber inlet and 4.8 to 21 times as much for the scrubber outlet. Therefore, LETC's *in-situ* oil shale retorting off-gases contained a very substantial quantity of potential "particulate" emissions that condense between 250°F and about 70°F, the approximate temperature of the resin trap. The larger ratios of back-half to front-half "particulate" in the scrubber outlet merely indicate, as expected, that venturi scrubbing is not suitable for removal of condensible organic compounds.

Several qualitative conclusions can be derived from the particulate emissions data in Table 4. The overall average concentration of 214 mg/dncm in LETC's retort off-gases falls within the range of 20 to 750 established from available estimates and data MRC gathered during Phase I of this EPA contract (2). The inlet particulate concentration was however highly variable, ranging from 125 to 387 mg/dncm, with no apparent correlation to the progress of the retort burn. By extrapolating the overall average particulate emission rate of 113 grams per hour for LETC's 8.6-barrel-per-day facility, the predicted uncontrolled emissions from a 50,000-barrel-per-day commercial oil shale plant are approximately 5,200 metric tons per year, assuming a 90 percent stream factor.

TABLE 4. CONTROL OF PARTICULATE EMISSIONS FROM OIL SHALE RETORTING[a]

| Operation code[b] | Concentration, mg/dncm[c] | | Mass flow rate, g/hr | | Percent control[d] |
|---|---|---|---|---|---|
| | Inlet | Outlet | Inlet | Outlet | |
| | 245 | 37 | 128 | 17 | 87 |
| 6A | 275 | 32 | 145 | 14 | 90 |
| | 152 | 32 | 80 | 14 | 82 |
| -Averages- | 224 | 34 | 118 | 15 | 87 |
| 8B | 144 | 38 | 78 | 20 | 74 |
| | 125 | 46 | 69 | 23 | 67 |
| 10C | 173 | 35 | 96 | 18 | 82 |
| | 387 | 24 | 198 | 11 | 94 |
| -Averages- | 228 | 35 | 121 | 17 | 86 |

[a]Based on mass collected from front-half train wash and filter.

[b]See Table 1 for explanation.

[c]Milligrams per dry normal cubic meter (20°C, 760 mm Hg).

[d]100 x (inlet flow rate - outlet flow rate) ÷ inlet flow rate.

Regarding the efficiency of venturi scrubbing for control of particulate emissions from oil shale retorting, the most significant conclusion from Table 4 is the ability to consistently achieve an average outlet concentration of 35 mg/dncm despite the three-fold variation of inlet concentrations. An unexpected result is that increasing the liquid-to-gas ratio from 11 gpm/$10^3$ acfm to 18 gpm/$10^3$ acfm did not improve the particulate removal efficiency, as would be predicted by theory, despite the increased pressure drop. Future experiments should consider determining the minimum liquid-to-gas ratio that yields similar particulate control in order to reduce water consumption. Alternatively, determination of the extent to which the liquid-to-gas ratio must be increased beyond 18 gpm/$10^3$ acfm in order to achieve control efficiencies greater than 90 percent would also be of interest, particularly in light of the following. Hesketh (5) has developed an empirical relationship, based on data from a variety of venturi scrubbers, to predict control efficiency for particles less than five microns in diameter. Using this model under the conditions of the mobile scrubber test at Laramie, the liquid-to-gas ratios used - 11, 15, and 18 gpm/$10^3$ acfm - should have given control efficiencies of 93.8, 95.5, and 96.5 percent, respectively. The corresponding actual removals achieved were only 87, 74, and 86 percent, considerably less than predicted. One possible explanation for this performance as applied to particulate emissions from oil shale retorting may be the inability to control the relatively large fraction of sub-micron particles.

Additional characterization of the emissions from LETC's 150-ton *in-situ* oil shale retort indicated the effect that venturi scrubbing had on air pollutants other than particulate matter. As is typical of this source type, retort

off-gas concentrations of ammonia, carbon monoxide, hydrocarbons, and hydrogen sulfide were all substantial. The average concentration of ammonia in the scrubber inlet was 3,000 mg/dncm. On a mass flow basis, 50 to 75 percent control of ammonia emissions was achieved, probably due simply to its high solubility in water because no special measures were taken to obtain such performance.

## ACKNOWLEDGMENTS

This research was funded by the U.S. Environmental Protection Agency (EPA) under Contract No. 68-03-2784. The contents of this publication do not necessarily reflect the views or policies of the EPA, nor does mention of organizations imply endorsement by the U.S. Government. Both MRC and EPA would like to thank Andy Long and Jas Lotwala of the Department of Energy's Laramie Energy Technology Center for their invaluable assistance during preparation for and implementation of this program. The quantity and quality of data generated during the brief field test are due in large part to the efforts of MRC's Chuck Duncan, sampling team leader.

## ENDNOTES

1. Harak, A. E., L. Docktor, A. Long, and H. W. Johns. Oil Shale Retorting in a 150-Ton Batch-Type Pilot Plant. U.S. Bureau of Mines, Laramie, Wyoming, 1974. 35 pp.

2. Rinaldi, G. M., D. L. Zanders, and G. D. Rawlings. Air Pollution Investigations of Oil Shale Retorting: *In-situ* and Surface; Phase I: Review of Retorting Processes and Selection of Technology for Control of Particulate Emissions. Contract No. 68-03-2784, U.S. Environmental Protection Agency, Cincinnati, Ohio, 1980. 63 pp.

3. Determination of Particulate Emissions from Stationary Sources. Federal Register, 42:41776-41782, August 1977.

4. Operating Manual for Andersen 2000 Inc. Mark II and Mark III Particle Sizing Stack Samplers, Revision A. Andersen 2000 Inc., Atlanta, Georgia, 1977. 50 pp.

5. Hesketh, H. E. Fine Particle Collection Efficiency Related to Pressure Drop, Scrubbant and Particle Properties, and Contact Mechanism. Journal of the Air Pollution Control Association, 24:939-942, October 1974.

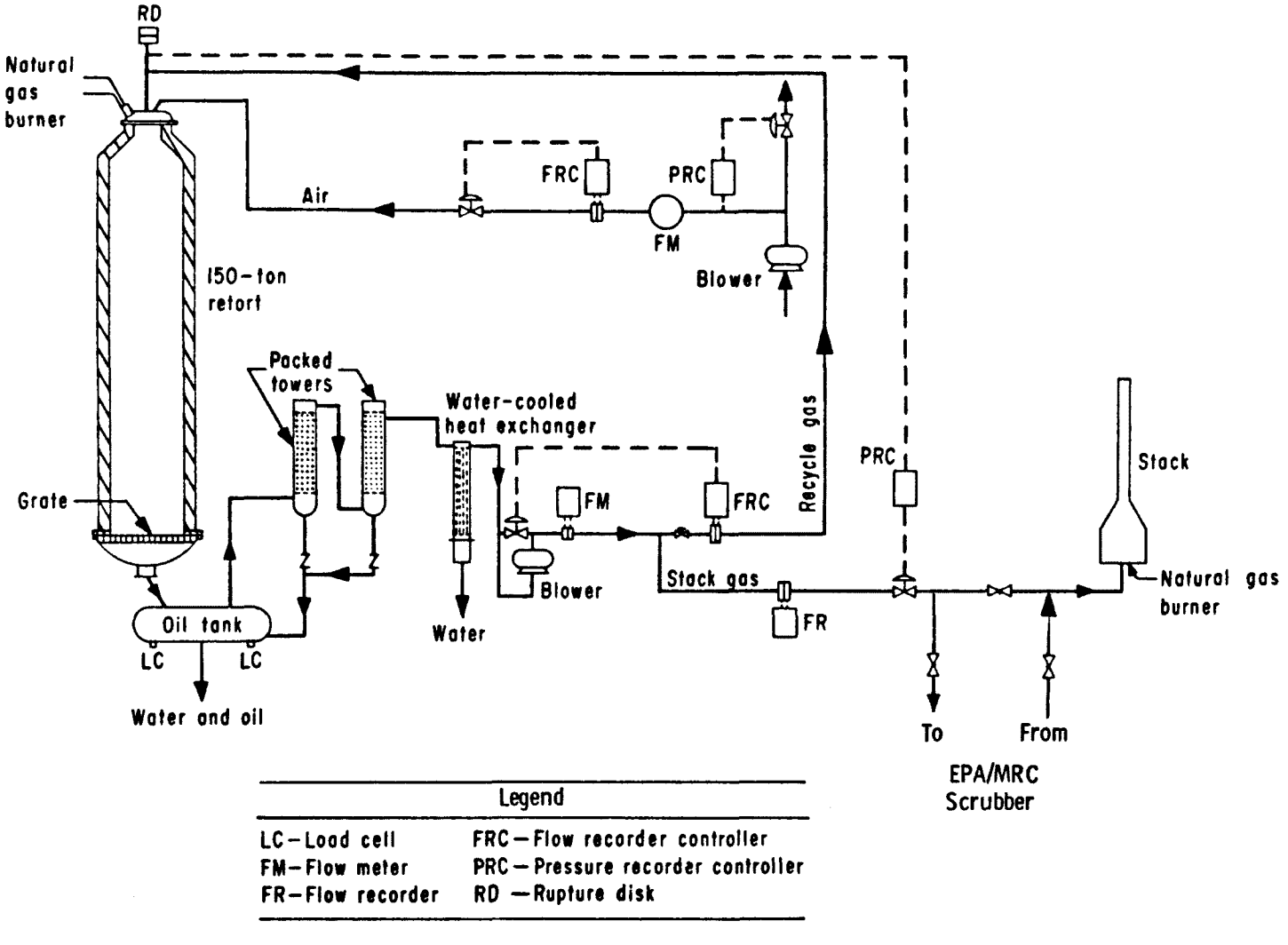


Figure 1. Gas and liquid flows in LETC's 150-ton retorting equipment (1).

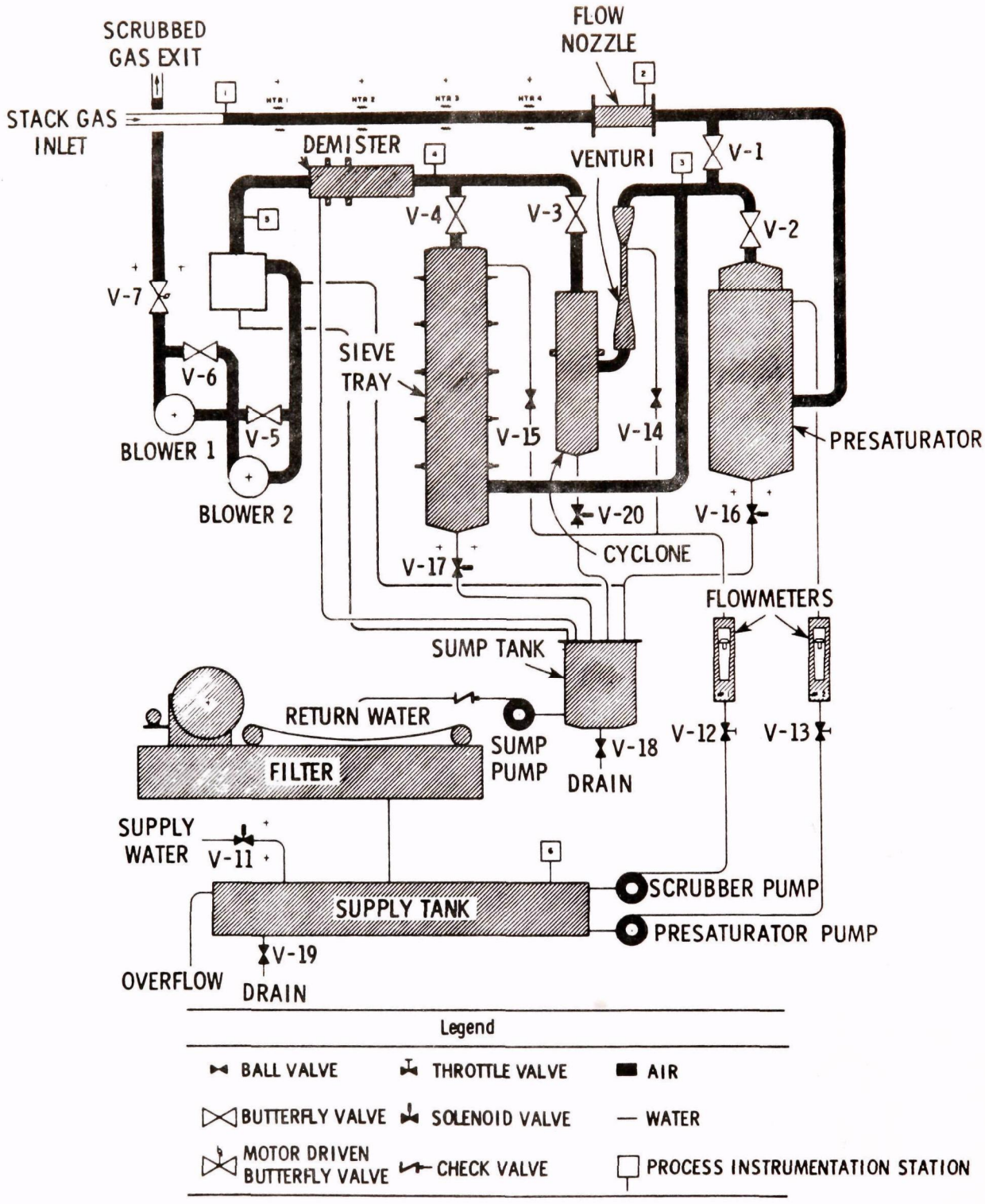


Figure 2 - Schematic diagram of EPA mobile scrubber.

# OVERVIEW OF THE DEPARTMENT OF ENERGY'S PRESSURIZED FLUIDIZED-BED COMBUSTOR CLEANUP TECHNOLOGY PROGRAM

By: William E. Moore
Office of Coal Utilization
Fossil Energy
U. S. Department of Energy
Washington, D. C. 20545

## ABSTRACT

This paper provides a review of the Department of Energy's (DOE) Fossil Energy, Office of Coal Utilization's Pressurized Fluidized-Bed Combustor (PFBC) Cleanup Technology Program. The PFBC cleanup program has two goals:

- Removing contaminants from the gas stream to meet turbine tolerance for erosion/corrosion and deposition.
- Removing pollutants from the gas stream to meet the New Source Performance Standards (NSPS).

The program involves three development areas: particulate control, alkali control and particulate-alkali measurement. The overall program schedule is presented along with a summary status. Finally, the key technical issues are outlined which must be solved for the cleanup equipment to meet contaminant removal goals. To achieve overall program goals will require the coordinated effort of both the public and private sector. This paper seeks to promote this coordination by presenting DOE's PFBC cleanup program, and it is hoped that this program description will improve communication and the end result will be a well coordinated program leading to development of an acceptable cleanup train for ensuring early commercialization of PFBC combined cycle power systems.

## INTRODUCTION

The Department of Energy's (DOE) coal-fired pressurized fluidized-bed combustor (PFBC) cleanup technology development activities are conducted as a part of Fossil Energy's Advanced Environmental Control Technology Program. This PFBC cleanup work is part of the overall gas stream turbine (Figure 1) cleanup effort which also includes cleanup of fuel gas from gasifiers for combined cycle power systems.

This PFBC gas stream cleanup program includes projects that were transferred from the prior Energy Research and Development Administration as well as new projects that were awarded under DOE through a competitive procurement with a Program Research and Development Announcement (PRDA). This PRDA pursued two stages of development: Category I - "Laboratory Bench Scale Testing and Evaluation" and Category II - "Subpilot Scale Design, Testing and Verification." These projects are to develop and demonstrate hardware-oriented prototype systems or devices for cleanup of the PFBC gas stream at system temperature and pressure for use with open cycle turbines in the utility or industrial sector.

The PFBC cleanup program has two goals:

- Removing contaminants from the gas stream to meet turbine tolerance for erosion/corrosion and deposition.

- Removing pollutants from the gas stream to meet New Source Performance Standards (NSPS).

PFBC systems have demonstrated their capability to meet NSPS with respect to $NO_x$ and $SO_x$ emissions leaving particulates as the remaining contaminant of concern. To meet NSPS, particulates have to be removed to levels equal to or less than 0.03 lbs/$10^6$ BTU. Hopefully, the selected cleanup system will meet both the NSPS goal as well as the turbine tolerance goal thereby improving the economics by eliminating the requirement for a downstream particulate removal device.

To meet the NSPS, the particulate removal system must effectively remove particles down to one micron in average diameter. (Reference is made to Figure III -- Depiction of Difficulty with NSPS.) The barrier filtration projects presently underway such as the ceramic felt bag and the granular bed filters are expected to filter the sub-micron particles as well as the particles over two microns sufficiently to meet the NSPS. The electrostatic precipitators removal efficiency under PFBC conditions has to be demonstrated while the enhanced inertial devices such as the electrocyclone are not expected to meet the required mass loading level for NSPS. However, it is exepcted that future commercial selection will depend upon cost, maintainability and pressure drop which have to be determined and verified under high temperature, high pressure PFB conditions.

The greatest obstacle to PFB combustor-power conversion system development is cleaning the gas stream contaminants to levels that are acceptable for commercial utility turbine operation. The off-gas causes erosion, corrosion and deposition problems in the open cycle gas turbine. Corrosion in PFBC turbine operation is primarily caused by the presence of alkali sulfate compounds in the liquid and vaporous state which deposit as liquids on the blade causing sodium/potassium sulfate corrosion. Erosion results from the impact of the high velocity particulate matter while deposition occurs through a buildup of fine particles on the turbine surfaces. Gas turbines have historically

been primarily operated with relatively clean petroleum based fuels and there is only a very limited data base for durability predictions with coal-derived contaminant laden gases. There is no concensus within the turbine industry as to what erosion tolerance the PFB combustor turbines should have other than the safety of adopting the clean fuel specification. There are considerable differences between the design philosophies for aircraft derivative turbines and gas expanders as used in petroleum refineries. The cleanliness goals DOE's program is working toward are 0.02 PPM for alkali (adopted from the clean fuel turbine specifications) and 0.001 grains per standard cubic foot for particles greater than five microns. Since the PFB gas turbine operates solely on sensible heat from the gas stream, it is essential that cleanup processes be operated at or near bed temperature to achieve acceptable efficiency.

DOE's PFBC cleanup program is concerned with three development areas:

- Particulate Removal
- Alakli Removal
- Instrumentation

Particulate Removal

For particulate removal, the only state-of-the-art device available for commercial application with the PFB combustor system is the cyclone. Based on both 1000 hour tests on the subpilot plants located at CURL Leatherhead, England and Curtiss-Wright, Woodridge, New Jersey, it is very doubtful as to whether the conventional cyclone when scaled-up for commercial PFB use can meet acceptable turbine particulate limits (See Figure IV) due to the reduced performance of large size cyclones as predicted by cyclone performance scaling laws. The cyclone train utilized in both these tests consisted of small, under 20-inch diameter cyclones, and achieved an overall particulate removal efficiency of approximately 97 percent for the Curtiss-Wright cyclone train and over 98 percent for the CURL train. The average total dust loading that passed through both cyclone trains was 0.04 to 0.06 grains/scf with a mean particle size of one and one-half to two microns. The emission levels achieved were approximately 0.2 lbs/$10^6$ BTU thus necessitating the use of downstream particulate removal to meet the 0.03 lbs/$10^6$ BTU NSPS level. (For the PFB combustor approximately 99.9 percent removal efficiency is required to meet NSPS.) Cyclone efficiency suffers considerably when scaled to commercial sizes and the use of multi-clones to circumvent scaleup problems has proven difficult since these multi-clones are very prone to plugging.

In view of the aforementioned conventional cyclone problems, DOE is investigating a number of advanced particulate removal concepts including enhanced inertial devices, electrostatic precipitators, fabric filter, dry plate scrubber, acoustic device, granular bed filters, molten glass scrubber and ceramic cross-flow filter.

The following projects that are being pursued are listed below by principle of operation and by contractor.

- Inertial Devices
  - General Electric - Electrocyclone (Subpilot Tests at Curtiss-Wright S.G.T.)
  - Mechanical Technology, Inc. - Cyclocentrifuge
  - General Electric - Glass Slag Particle Separator
- Filters
  - Granular Bed Filters
    - Westinghouse - Fixed Granular Multi-Bed Filter (Subpilot Tests on Simulated PFBC)
    - Combustion Power Company - Moving Granular Bed Filter
    - Exxon - Magnetically Stabilized Granular Bed
    - General Electric - Electrostatic Granular Bed
    - Air Pollution Technology - Dry Plate Scrubber
  - Ceramic Filter
    - Westinghouse - Ceramic Cross-Flow Filter
  - Bag Filter
    - Accurex - Ceramic Felt Bag (Subpilot Tests at Curtiss-Wright S.G.T.)
- Electrostatic Precipitator
  - Research-Cottrell - Tubular ESP (Subpilot Tests at Curtiss-Wright S.G.T.)
  - Denver Research Institute - ESP Test Facility
- Acoustically Enhanced
  - University of Buffalo - Acoustic Agglomerator as Preconditioner Coupled to Cyclone

The above particulate removal projects include both laboratory scale and subpilot scale projects. The laboratory project work is to define and verify the concept in sufficient detail to determine overall system feasibility. The subpilot scale projects are to establish and verify the cleanup process feasibility including scale-up parameters at the subpilot scale level.

The laboratory scale projects are at various stages of completion and some of the accomplishments to date are:

- The operation of an acoustic agglomerator contrary to previous theory is independent of acoustic frequency.
- A two stage electrostatically enhanced GBF has proven feasible at laboratory scale atmospheric conditions and has illustrated the significant collection efficiency through electrostatics for PFB applications.

- Electrostatically charging a dry plate scrubber at atmospheric conditions has demonstrated a substantial increase in collection efficiency.
- Through an interagency agreement with the Environmental Protection Agency, DOE has completed and now has available a flexible HTHP electrostatic precipitator test facility.

These laboratory scale projects are presently preparing for hot pressurized testing from which the overall feasibility of specific particulate removal concepts for future PFB applications can be determined.

The subpilot scale projects involving the electrocyclone, the fixed GBF, ESP and ceramic felt bag have progressed to the stage of final design with PFBC testing scheduled to start the latter part of 1981. Thus, there are no results to discuss at this time. Three of the four devices as indicated will be tested in the small gas turbine facility located at Curtiss-Wright in Woodridge, New Jersey, which is being supplied as Government Furnished Equipment by DOE (Figure V). The fixed granular bed filter pursued by Westinghouse is scheduled for testing at their Waltz Mills PFBC simulator.

The future work for PFBC particulate removal will focus on the completion of bench scale and subpilot testing (See Figure VI). The most promising system will be scaled-up to pilot size (10 to 20 MWe) for pilot plant test verification in the 1984-1985 time period. A possible pilot plant test site is the Curtiss-Wright pilot plant presently under construction at Woodridge, New Jersey (See Figure II).

Alkali Removal

Alkali vapor removal to the partial PPM levels required for reliable turbine operation is extremely difficult. One of the basic problems is that the presence of chlorine and other contaminants limit the alkali vapor pressure in equilibrium with the alumino - silicates. Thus, the alkali vapor level still remaining with in-bed gettering at 1700°F appears to be an order of magnitude above the desired 0.02 PPM turbine tolerance level. Measurements downstream with positive filters indicate that the gas leaving the PFB combustor contains 10 to 20 PPM of alkali vapor consisting of both sodium and potassium compounds. The combustor gas also contains sulfates, chlorine, vanadium and lead presenting a somewhat different gas chemistry problem than that with petroleum based fuel containing alkali. Our present program goal of 0.02 PPM of alkali has been adopted from experience with petroleum fuel.

Due to the complexity of alkali vapor removal to the desired low concentration levels for reliable turbine operation, the following process options for alkali removal are being pursued.

- Fixed sorbent beds utilizing activated bauxite or diatomaceous earth for alkali absorption on solid surfaces.
- Addition of alumino-silicates to the combustion bed as chemical gettering agents for equilibration of the gas phase alkali with the alumino-silicate to form solid compounds.

- Absorbent smoke (submicron sized sorbents) to increase the effective sorbent surface to alkali gas ratio for increased reaction rates.

- Surface ionization wherein alkali vapors are ionized by a platinum catalyst surface and then the alkali ions are directed to an electric field from which they are focused for collection on a collector electrode surface.

Along with these alkali control options, modeling and experimental studies are being conducted to improve the understanding of the PFB combustion stream gas composition. The characterization of the alkali formation processes are being studied through the application of chemiluminescent and laser flourescent techniques.

The following projects are underway in the alkali removal area:

Alkali Removal Concepts

- Combustion Power Company - In-bed Chemical Gettering with Alumino-Silicate

- General Electric - Sorbent Smoke and Surface Ionization

- Argonne National Laboratory - Fixed Sorbent Bed

- Westinghouse - Fixed Sorbent Bed

- APT - Fixed Sorbent Bed

The following alkali characterization/formation and modeling projects are underway:

- National Bureau of Standards

  - Data Base and Experimental Studies of Gas Phase $SO_2$ Interactions

  - Alkali Release from Fly Ash, Slag and Glass

- Georgia Institute of Technology

  - Spectroscopy to determine alkali gas species.

- Aerodyne

  - Alkali Release from Model Organic Materials and Computer Modeling of Gas Stream Chemistry

- MIT

  - Thermodynamic Measurements of Slag Properties

- University of California

- Laser Studies of Alkali Species in Flames

- Morgantown Energy Technology Center

  - Alkali Surface Enrichment and Release from Minerals

The primary results to date from these ongoing alkali projects are:

- Laboratory tests using sorbent beds at high temperature, high pressure conditions using a simulated gas stream have measured removal of up to 99.9 percent of the alkali metal compounds present. (It should be noted that the gas stream used was in the absence of sulfur, chlorine, vanadium and particulate dust contaminants.)

- Preliminary assessment of the alumino-silicate smoke approach has demonstrated that a monolayer coverage can be obtained on the smoke absorbent surface at alkali concentrations low enough to prevent turbine corrosion. Therefore, there is optimism that this increased surface area approach can economically achieve the desired low levels of alkali vapor.

- Combustion stream modeling to determine the condensed alkali species has indicated through calculations that the major percentage of the alkali content in the stream would exist in the solid form as alkali alumino-silicate compounds.

In conjunction with the alkali removal tasks, the following options are being considered:

- Blade replacement as periodic maintenance.

- Operation with cooled blades.

- Operation at lower turbine inlet temperatures.

- The development of improved corrosion resistant blade coatings or a combination of these approaches in order that practical utility operation is achieved.

Instrumentation Efforts

To date an unresolved key bottleneck in the development of particulate and alkali control devices is the lack of reliable accurate instruments for measurement of the subject contaminants at the concentrations of interest. Instruments are needed that can accurately measure and determine in-situ particulate loadings and size distributions as well as alkali concentrations to the desired concentration levels. State-of-the-art impactor devices are not calibrated to the desired temperatures for accurate measurement. Considering these instrument problems, several programs are underway to develop equipment to isokinetically sample PFB effluent to determine the particle loading and distributions. In addition, the direct readout instruments such as laser interferometer analyzers are being developed. Such noncontact

instrument projects have been pursued under the PFB combustion program with Leeds and Northrup and Spectron but a significant amount of baseline calibration testing has to be completed to establish instrument confidence.

On the recent 1000 hour CURL test, the "standard" particulate measuring technique was the isokinetic fixed sampler probe followed by a small high efficiency cyclone with a total backup filter. Size distributions were determined with a coulter counter. DOE for the forthcoming subpilot tests of the prototype scale particulate cleanup devices at Curtiss-Wright is developing an improved version of this high efficiency cyclone collection concept which will provide real-time particle-mass measurements. Real-time measurements will be possible with tapered element oscillating microbalances (TEOM) (one per cyclone) coupled with a multistaged cyclone train of progressively smaller diameter. The multi-cyclone portion of the instrument was tested on the 1000 hour CURL test. For the first time, the sampling/sizing classification will be done at PFB temperature and pressure with real-time mass measurements per each size classification.

For alkali measurement, the atomic emission spectrometer appears to be a promising alkali detector and will be used for the PRDA tests. This instrument was recently tested on DOE's Morgantown Energy Technology Center's gasifier and performed satisfactorily. Due to the difficulty of obtaining accurate alkali particulate measurements, the PFB combustor cleanup program is pursuing the following instrument related programs. A significant amount of PFB combustor testing will be required before these instruments can be reliably used for future demonstrations and commercial applications.

Instrumentation Projects

- Ames Laboratory - Development of alkali monitor (Atomic Emission Spectrometer)
- Brookhaven National Laboratory - Direct Sampling of Particulate Mass Loadings
- Sandia Laboratories - Multi-staged Cyclone Train Coupled to a Tapered Element Oscillating Microbalance
- Spectron - In-Situ Determination of Particle Sizing (laser Interferometer)
- Inhalation Toxicology Research Institute - High Temperature, High Pressure Impactor Measurement

Key Technical Issues

DOE's PFBC cleanup program has a substantial challenge to meet in achieving its contaminant removal goals for alkali and particulates. To achieve these removal goals accurate instruments have to be developed in parallel to verify the results. Some of the key technical issues that have to be confronted and resolved include:

- Measurement of alkali vapors and particulates (particle-mass concentrations) accurately to very low concentrations is necessary for adequate contaminant control. Obtaining meaningful measurements will require instruments that provide real-time in-situ measurements.

- Instruments have to provide for uniform baseline measurements in order to make direct efficiency comparisons of one cleanup concept versus another.

- The PFB combustor gas stream presents a sticky environment which may prevent the barrier devices that will meet NSPS from operating without plugging. Also, the electrostatics may be detrimentally effected.

- Particulate control devices that are capable of meeting NSPS must be extremely efficient while maintaining an acceptable overall system pressure drop.

- The amount of alkali metal compounds that appear in the vapor state versus the percent that is tied up in a solid compound is to some degree still unknown. System tradeoffs regarding alkali metal compound removal versus improved turbine materials remain to be performed.

- Can turbine cladding and coating materials be developed that are resistant to alkali corrosion at the full ($1700^{o}F$) temperature capability of the PFB system?

- Tolerance to erosion/corrosion of gas turbine alloys and coatings in a PFBC gas environment have not been obtained for exposure durations of interest to utility operators.

- Can aluminio-silicate gettering tie up a sufficient amount of the alkali to be considered as a means for alkali control?

- Can cyclones be realistically scaled up to meet the turbine erosion limits or can banks of appropriate sized cyclones especially for the first generation PFBC power system (considering valve and lock hopper problems) be developed with acceptable performance and economics on large commercial PFB utility systems?

- The use of actual PFB combustors for the basic and applied research associated with cleanup development is very expensive. Therefore, a better understanding of the overall PFB combustor gas stream chemistry is needed to allow for closer simulation of the gas stream so that less expensive testing of prototype devices is possible. The importance of realistic simulation is especially true for understanding the alkali problem and developing an effective absorbent since chlorine, sulfur, lead, and vanadium will drastically effect the physical as well as the chemical adsorption/absorption rates.

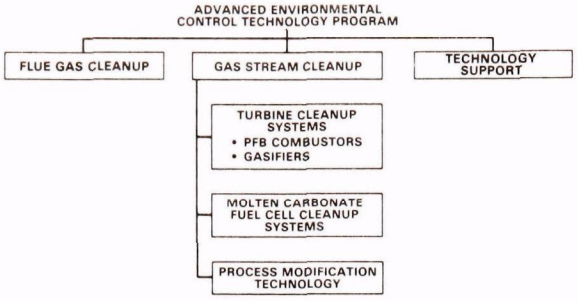


Fig. 1 Advanced Environmental Control Technology Program Structure

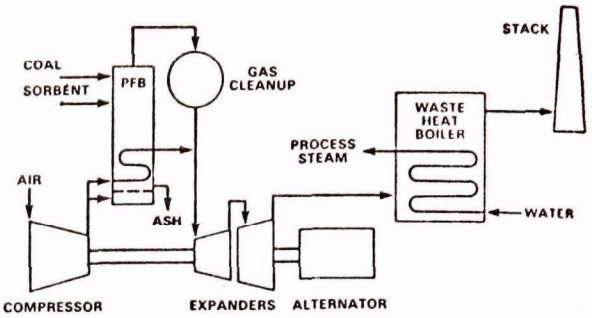


Fig. 2 Simplified Flow Diagram of C.W. Pilot Plant

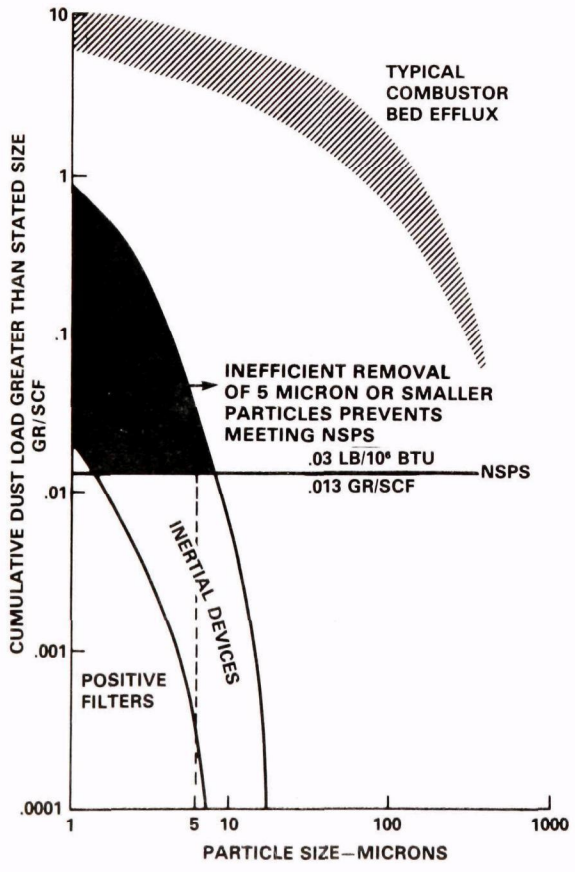


Fig. 3 PFBC Challenge to Meet NSPS

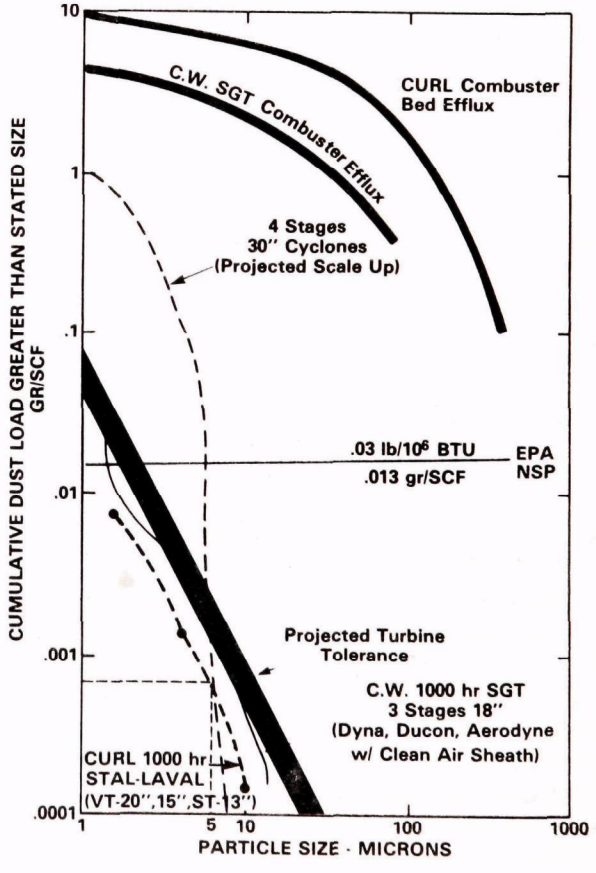


Fig. 4 "State of Art" Cleanup W/Cyclones

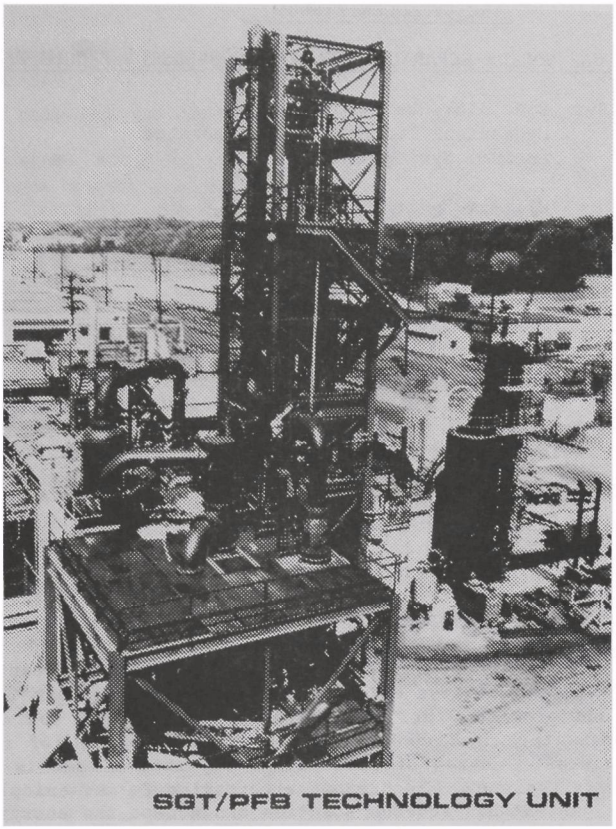


Fig. 5

## DOE'S PFB CLEANUP TECHNOLOGY PROGRAM

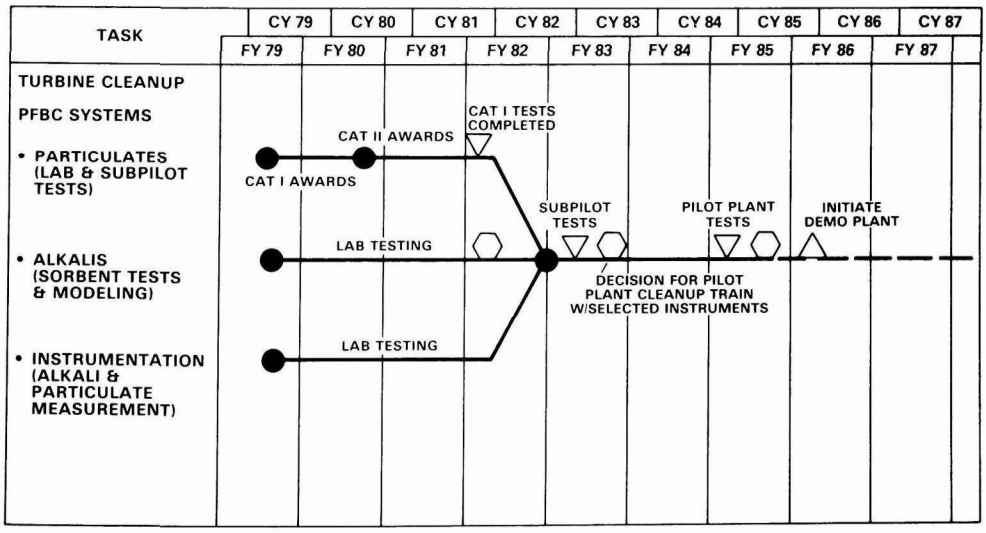


Fig. 6

# THE CYCLOCENTRIFUGE™

## AN ADVANCED GAS/SOLIDS SEPARATOR FOR COAL CONVERSION PROCESSES

By: P.R. Albrecht, J.T. McCabe
Mechanical Technology Incorporated
Latham, New York

William Fedarko
U.S. Deparment of Energy

## ABSTRACT

Various coal conversion processes under development for the emerging United States Energy Program have focused renewed attention on the need for efficient gas cleanup systems. One approach being funded by the U.S. Department of Energy (DOE) is the development of a high-velocity particulate separator called a Cyclocentrifuge. The separation principle is based on centrifugal force generated by a bladed rotor located in a cyclone-shaped vessel. A 1000-acfm laboratory model tested at one atmosphere and 100°F is described. Test results include velocity profiles and particulate separation efficiency measurements. The design of a high-temperature unit is also discussed and plans to test this unit using 1000°F, 250-psi synthesis gas from a coal gasifier are outlined.

## INTRODUCTION

This paper describes the continuing development of a centrifugal device for separating fine particulate matter from a gas. As the United States coal program gains momentum, the status of particulate control technology will become increasingly more important, not just because maintaining air quality is generally desired, but also because particulate control is essential to the economic viability of certain coal conversion processes. In one process, for example, hot, pressurized, coal-produced, fuel gas is used to fire the gas turbine combustor in a combined-cycle power system. For reasonable gas turbine blade life, this application requires a degree of particulate separation that is substantially greater than can be achieved by an ordinary cyclone. The present alternative to mechanical separation for coal-derived fuel gas is to scrub the gas with an aqueous solution and accept the energy loss associated with cooling the gas.

Although there are other areas where high-efficiency separation of fine particulate matter can make a beneficial contribution towards accelerating the commercial viability of some coal conversion processes, the cleanup of low-Btu fuel gas for a gas turbine application was designated as the immediate target for this program.

The work described herein follows a feasibility study [1] in which the role of gas centrifuge technology in coal conversion processes was examined. This study concluded that particulate separation was an area in which some of the concepts from centrifuge technology could be applied to improve the performance of existing equipment. As part of the study, a design approach following centrifuge concepts was established and, to show feasibility, preliminary design calculations and drawings were made for a separation device based on a combined-cycle electric power application. The selected application required stringent particulate removal from 125,000 scfm of coal-produced, low-Btu gas at 1000°F and 250 psia. In this study, the projected separation efficiency was estimated to be about 85% for a 1-micron ash particle. This percentage was a significant improvement over existing cyclones. The separation device was named a Cyclocentrifuge because it consisted of a cyclone containing a centrifuge. Basically, the concept was founded upon the following critical assumptions:

- The normal vortex in a cyclone could be accelerated by appropriate aerodynamic design of a bladed rotor to produce a stable, high-strength vortex.
- The separation potential of the high-strength vortex would not be nullified by secondary mixing effects.
- The high-strength vortex flow would provide high efficient separation of particles in the 1-micron range.
- The rotating assembly could be designed and manufactured to provide high on-line availability while operating in a hot, pressurized coal-produced gas stream.
- The required rotor power would be acceptably low and could be extracted from the cleaned process gas efficiently, using a reaction turbine fitted to the rotor.

Phase II of the program, which is the subject of this paper, provided engineering data on all of the above items, except those relating to hot, pressurized testing. The data were based on a program scope that included:

- The design and construction of 1100-scfm engineering prototype Cyclocentrifuge for cold-flow testing
- The design and construction of a laboratory test loop including a measurement system for performance evaluation
- A test program focusing on measurements of velocity distribution and separation efficiency.

Phase III of the program, which is now in progress, will provide further information on Cyclocentrifuge efficiency at ambient conditions as well as on a unit to be tested at the DOE Morgantown Energy Technology Center (METC) facility. The ongoing Phase III program is intended to expand the data produced to date to include manufacturing considerations for high-temperature service, on-line particulate monitoring, parametric cold-flow laboratory tests, and tests using the full output stream from the METC gasifier.

## GENERAL DESCRIPTION

Figure 1 shows the cross section of the Cyclocentrifuge. The particulate-laden gas enters a cyclone-shaped vessel containing a hollow, high-speed, bladed rotor. The rotor acts to uniformly accelerate the vortex flow causing the centrifugal force on the particles to be increased significantly compared to a conventional cyclone. The centrifugal force drives the particles to the outside wall where they flow downward with the boundary layer into a collection hopper. A small percentage of the process gas is used as continuous blowdown flow to help prevent dust retainment in the hopper. The remainder of the cleaned process gas passes through a reaction turbine mounted in the hollow rotor. This turbine serves a twofold purpose; it drives the bladed rotor and it removes the swirl from the gas. Swirl removal recovers energy and helps minimize particle deposition on the inside of the rotor. The cleaned gas passes through the hollow rotor, then exits the Cyclocentrifuge.

## LABORATORY MODEL DESIGN

The laboratory model was designed to the following specifications:

| | |
|---|---|
| • Inlet Flow | 500 - 1300 acfm (14.2 - 36.8 $m^3$/min) |
| • Air Temperature | 45 - 100°F (7.2 - 37.7°C) |
| • Rotor Speed | 5,000 - 15,000 rpm (523.6 - 1570.8 rad/sec) |
| • Pressure | 9 - 14 psia (3136.1 - 4878.4 $N/m^2$) |

As shown in Figure 1, the rotor is an assembly consisting of the swirl augmentation rotor, drive turbine, and bearings.

The swirl augmentation rotor is a subassembly consisting of the bladed centrifuge shell, upper and lower shell support struts, and three nose cones. The bladed centrifuge shell has eleven blade rows with 16 blades in each row. Each blade has a double circular arc profile and is 0.923 in. (2.39 cm) high with a maximum thickness of 0.1 in. (0.25 cm) and a chord length of 0.577 in. (1.47 cm). Each blade row is oriented with respect to the rotor axis to achieve a smooth, uniform increase in the gas tangential velocity. The cord of each blade in the first blade row makes an angle of 70° with respect to the rotor axis. The angle in each successive blade row decreases by 7° making the cords of the blades in the last row parallel to the rotor axis.

The centrifuge shell has an outer diameter of 6 in. (15.24 cm), a shell thickness of 0.15 in. (0.38 cm), and is 15.375 in. (39.05 cm) long.

The total stress in the shell at 15,000 rpm is about 25,000 psi ($8.7 \times 10 \times 10$ $N/m^2$) which comes from two principle sources. Hoop stress contributes about 65% of the total stress while the remainder is bending stress caused by the blades. The maximum stress occurs at the outer surface where the blade is attached to the shell.

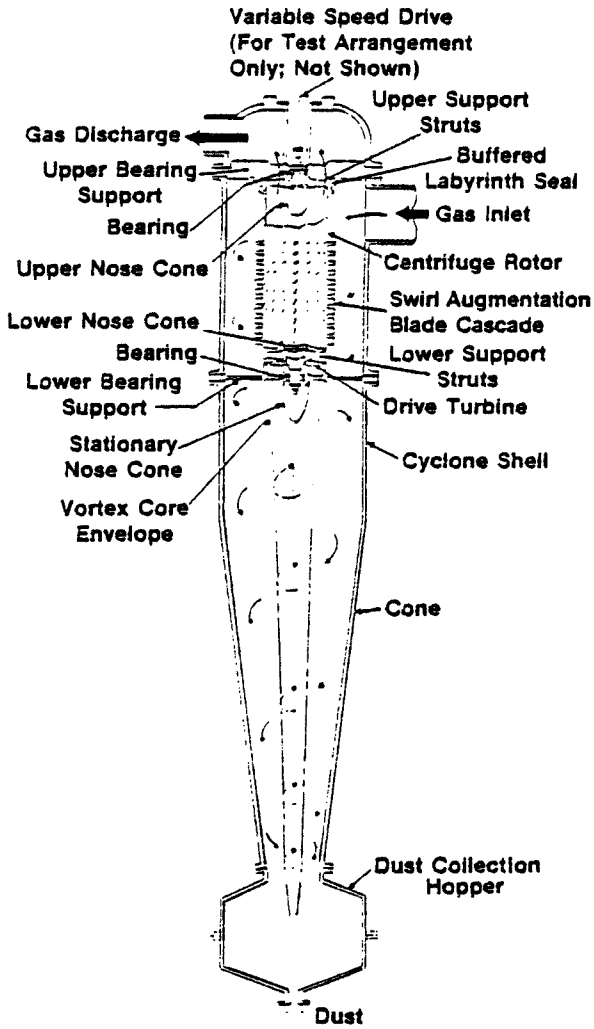


Fig. 1 Cross Section of Laboratory Cyclocentrifuge

The upper and lower support struts connect the stub shafts to the bladed shell via eight spokes. The spokes are designed for high axial and radial stiffness and are shaped to minimize flow disturbance. The lower support strut is electron beam welded to the rotor shell. The upper support strut is bolted to permit access to the rotor interior. This strut also contains a buffered labyrinth seal to prevent the dirty inlet gas from leaking into the cleaned gas discharge plenum.

The bearings are 25-mm, grease-packed, shielded, deep-grooved ball bearings axially preloaded to give a radial stiffness of between 2 x $10^5$ and 5 x $10^5$ lb/in. (1.8 to 4.4 x $10^6$ N/m). This bearing stiffness coupled with the structural stiffness of the bearing support places the first critical speed 20% above the design speed. Figure 2 shows the critical speed map for this design.

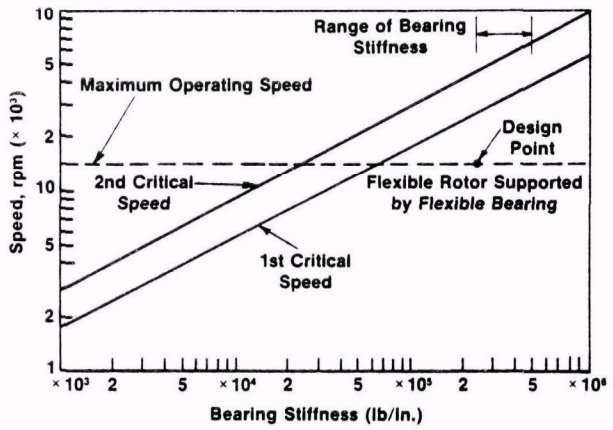


Fig. 2 Critical Speed Map - Flexible Rotor Assumed

Rotor drive power is provided primarily by a reaction turbine that extracts power from the process gas. Thus, the Cyclocentrifuge rotor does not require an external drive which would involve additional bearings and pressure seals.

For speed control during testing a variable speed drive motor is connected to the rotor through a quill shaft.

The stationary assembly of the Cyclocentrifuge is composed of the cyclone vessel, dust collection hopper, discharge gas plenum, and bearing supports. The overall height of the cyclone shell is 7 ft 9 in. (236.2 cm) with a maximum diameter of 16.25 in. (41.3 cm).

The cyclone vessel consists of two parts: a cylindrical upper part referred to as the inlet casing and a lower part which has a cylindrical and conical section, known as the cyclone. The inlet casing houses the rotating assembly and includes the tangentially arranged inlet gas duct.

The bearing supports are located on both ends of the inlet casing. The support struts are aerodynamically designed to minimize flow restriction while maintaining the high structural rigidity necessary for meeting the rotor critical speed criteria. The bottom support includes two types of struts. The outboard struts are angled to achieve zero lift for the average downward velocity outside the stiffening ring while the inboard struts are angled to achieve the same condition for the upward velocity inside the stiffening ring.

The upper support serves to separate the discharge plenum from the inlet casing. The struts in the center of the upper support are not angled because the discharge flow vector from the rotor is parallel to the rotor axis.

The dust collection hopper is located at the bottom of the cyclone and is continuously purged with 2 to 3% of the inlet flow.

## HIGH-TEMPERATURE, HIGH-PRESSURE DESIGN

The design shown schematically in Figure 3 is for the maximum operating conditions of the METC gasifier. These conditions are as follows:

- Volume Flow 450 acfm (12.74 $m^3$/min.)
- Pressure 350 psig (1.2 x 10 $N/m^2$)
- Gas Temperature 1000°F (537.7°C)
- Rotor Speed 9,000 to 13,000 rpm (942.5 to 1,361.4 rad/sec)

The basic design principles are the same as the laboratory model, so only the differences between the two designs will be discussed here.

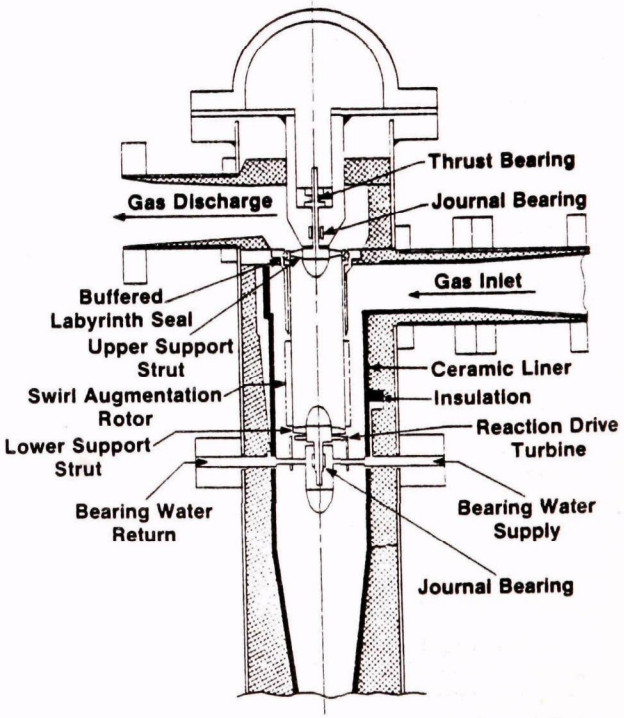


Fig. 3 Schematic of Cyclocentrifuge Designed for the METC Gasifier

The bearings have been changed from grease-packed ball bearings to water-lubricated hydrostatic bearings. The rotor is still supported between two journal bearings to maintain a critical speed that is greater than the design speed. The thrust bearing has been located at the top of the rotor to promote rotor stability. The number of blades rows has been reduced to compensate for a longer bearing span. The blades have been coated with a wear-resistant coating.

A ceramic liner has been added to the cyclone shell to reduce wear, and insulation has been added to maintain the gas temperature above the condensation point of the tars contained in the gas stream.

The high-temperature Cyclocentrifuge is currently being manufactured, and testing is scheduled to begin in late 1981.

## LABORATORY TESTS

### Aerodynamic Test Method

The aerodynamic tests were made by measuring velocity profiles at the axial stations located along the Cyclocentrifuge shell, as shown in Figure 4. Each station was fitted with a traversing mechanism, carrying a pitot tube. A two-degree-of-freedom traversing mechanism was used and carried a three-hole, wedge-shaped, two-dimensional pitot probe. This probe permitted measurements of the total and static pressures as well as yaw angle.

### Aerodynamic Test Results

Although the aerodynamic tests were conducted to map the general velocity profiles within the Cyclocentrifuge, the effects of flow and rotor speed on tangential velocity were of particular interest because this velocity component is a measure of the separation force. To measure this relationship, the inlet flow was varied between 500 and 1,000 acfm, and the rotor speed between 5,000 and 15,000 rpm for a range of flows. During the testing, the breaking characteristics of the motor drive did not allow for testing of all combinations. Most notably, the low rotor speed, high-flow combinations could not be achieved.

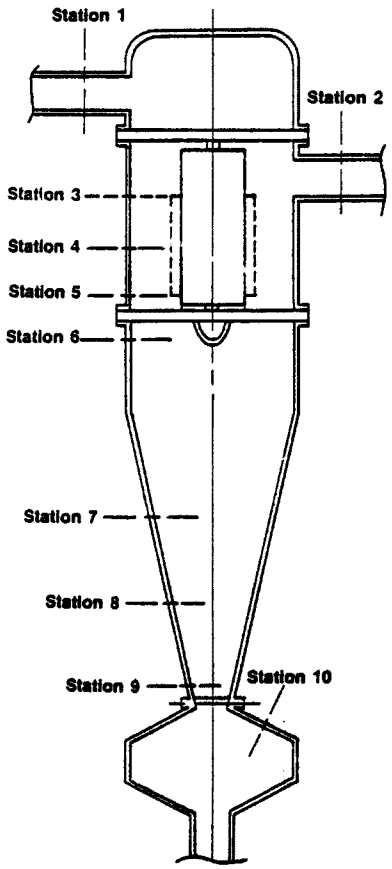


Fig. 4 Schematic of Measurement Station Locations

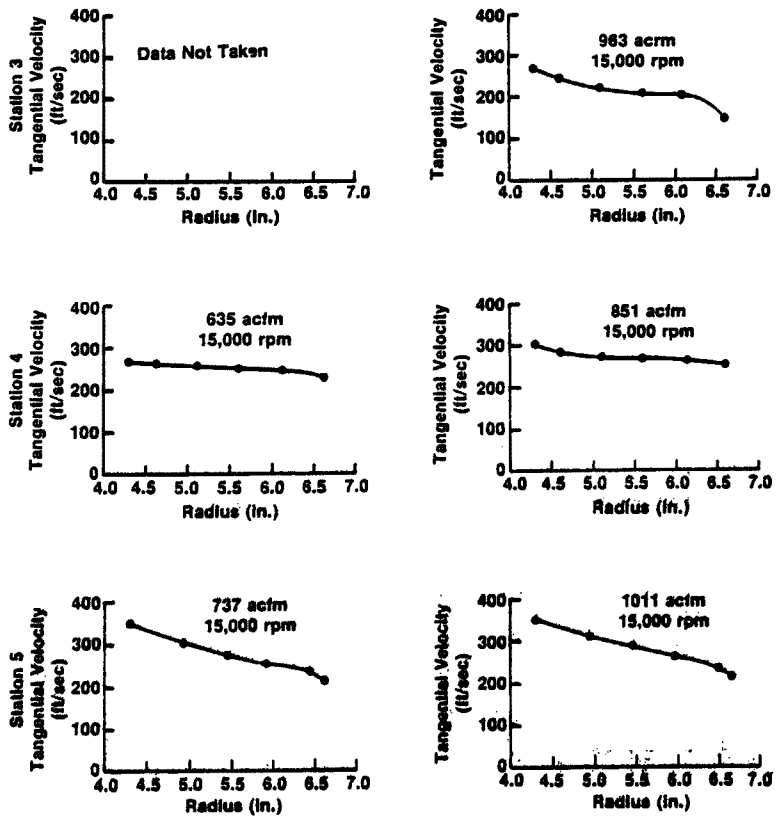


Fig. 5 Tangential Velocity Profiles Adjacent to the Swirl Augmentation Rotor for Various Flow Rates

Figure 5 shows the velocity profiles at the stations in the neighborhood of the swirl augmentation rotor for various flow rates. From this set of curves it can be seen that the tangential velocity increases as the flow passes axially through the centrifuge blades, and that a flow turndown ratio of 0.25 does not cause a substantial reduction in the maximum velocity at the end of the rotor.

A velocity map (Figure 6) taken near design point condition shows that the maximum tangential velocity of 350 ft/sec at Station 5, which is near the last blade row of the swirl rotor, is exceeded at Station 7 in the cone, and is almost equalled at the bottom of the cone at Station 9. Thus, the high centrifugal force that was generated by the swirl augmentation rotor acts to produce and maintain particle separation throughout the length of the Cyclocentrifuge. The plots on Figure 6 showing axial velocity indicate the boundary of the rising core of cleaned gas. At Station 7, the radius of the core is 3 in., which is equal to the radius of the hollow rotor that acts as the exit pipe. During the aerodynamic tests, the boundary of the core was studied and found to be a stable surface at design conditions. At Stations 7 and 9, the points of maximum tangential velocity, which correspond to the maximum separation force are inside the rising clean gas core. Considering the particle residence time, the magnitude of the force field, and the stability of the flow, a high percentage of particles ranging downward to a diameter of approximately 0.5 micron should reach, and be held in, the cyclone boundary layer.

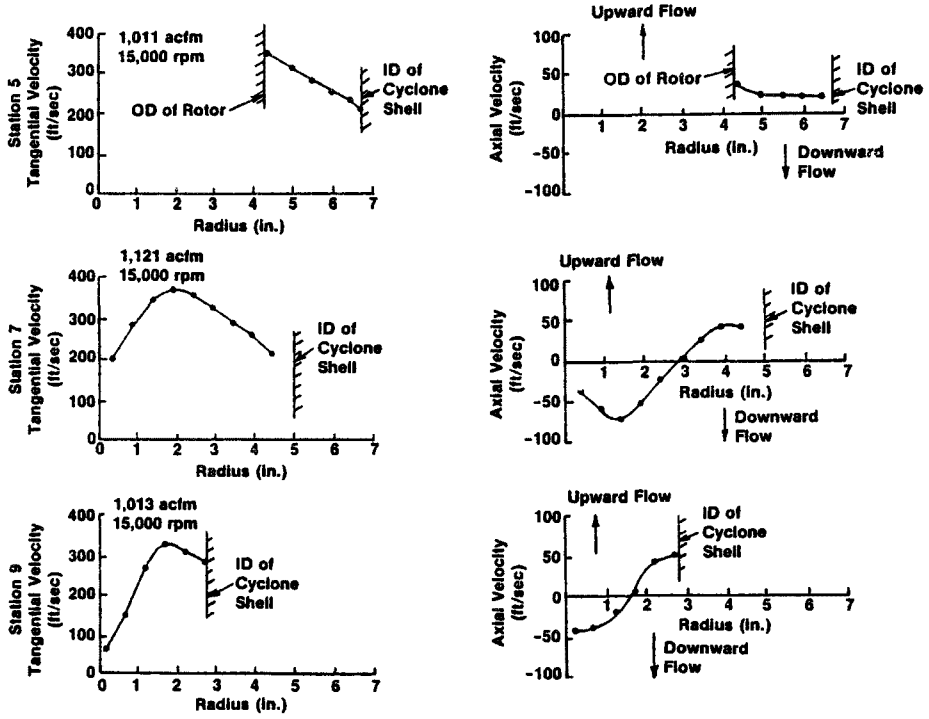


Fig. 6 Gas Tangential and Axial Velocity Profiles at Design Flow

The pressure drop through the Cyclocentrifuge is shown in Figure 7 as a function of rotor speed for different flow rates. The dashed lines in Figure 7 indicate the calculated pressure drop using the method described in Reference 1, with measured variables and an empirical correction factor for the

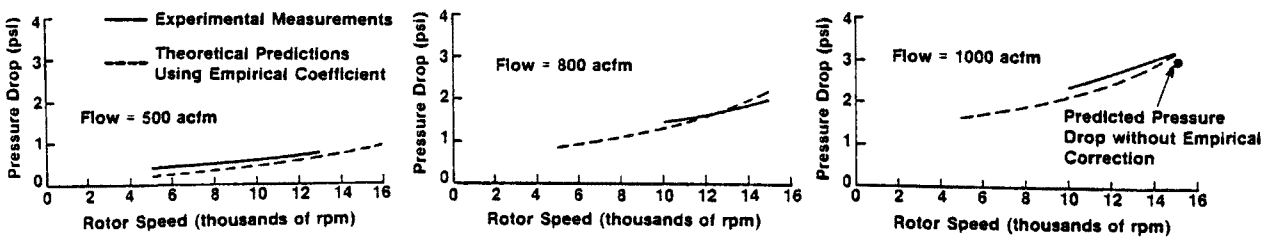


Fig. 7 Pressure Drop Versus Speed

Cyclocentrifuge. The point shown in the bottom curve of this figure is the calculated design point value for pressure drop without empirical correction. Note that about half the pressure drop would occur in a conventional cyclone operating at the same flow conditions. The other half of the pressure drop is taken across the rotor drive turbine.

## Dust Tests

### Methylene Blue Method

The dust tests were divided into two sections. The particulate generation and measurement methodology for the first section were selected on the basis of: (1) ease of generating a controlled monodispersed particle size distribution, and (2) rapid, accurate data reduction.

Several well-established techniques exist which will produce an aerosol of repeatable size distribution and predictable concentration. The Collison nubulizer/methylene blue dye aerosol generation system is one of the best established of these techniques and years of experience with this system have been used to formulate British Standard BS-2577 for its use [2]. A detailed description of the design of a Collison nebulizer is given by May [3].

The Collison nebulizer is an atomizer which is used to generate relatively uniform water droplets from a reservoir which contains dissolved methylene blue dye. The droplets from the nebulizer are mixed with a stream of moisture-free nitrogen gas in a drying column where the water is evaporated, leaving a methylene blue dust suspended in the gas. This dye is then injected into the test loop, and isokinetically fed impactors are inserted upstream and downstream of the Cyclocentrifuge to sample the aerosol. The collected particles are then washed from the various stages of the impactor with a small quantity of water, and the strength of the blue dye solution measured photometrically. A concentration of one part dye in $10^7$ parts water will produce sufficient coloration to be detected, allowing efficiencies to be determined by comparing the upstream and downstream mass of dye from equivalent-size isolation stages of the collector.

The total amount of aerosol injected during this section was 6.6 mg/hr. Preliminary tests with a cascade impactor indicated that well over 3/4 of the mass was in the aerodynamic size range below 3 microns in diameter, and no particles larger than 6 microns in diameter were detected. Similar results have been obtained during subsequent test runs. In general, 90% of the injected dye is within ± 0.5 micron of a prescribed value that depends primarily on the percent concentration of methylene blue in the water solution.

The filter holders, or May cascade impactor, are mounted at the exit of the ball valve, and a fraction of the inlet flow is sampled during each test to determine either the mass concentration when the filter is used or the size distribution of dye particles when the impactor is used. During preliminary testing, inlet flow was sampled for periods of 3, 6, 12, 24, 12, 6 and 3 minutes to determine the stability of the system. These tests indicate that 6 minutes of sampling is sufficient to accurately determine the rate of injected dye.

At the completion of the intial test sequence, a 0.4-micron-pore filter was substituted for the usual paper filter at stage five of the impactor. The Collisons were operated at their normal injection rate, and a two-minute exposure of the impactor stage was completed at design flow. The cascade impactor stages were then removed and, rather than washed for color analysis, they were examined microscopically using a Leitz Ultra Pak with total magnification of 800X. Transmitted light, with slight crossed polars in conjuntion with supplementary incident light, showed the methylene blue particles as easily identified, slightly flattened, shiny spheres. A Porton eyepiece was used to determine the equivalent diameter of particles larger than 0.4 micron in diameter by traditional counting techniques. The optical procedure was used to verify the calibration of the more rapidly executed photometric analysis.

A similar cascade impactor sampling system is located in the cylindrical duct downstream of the centrifuge. A three-probe integrated sampling system is used to verify the absence of stratification or other similar phenomena. Because of the low particle loading downstream of the Cyclocentrifuge, a minimum of 30 minutes of sampling time is required to obtain a measurable concentration of dye. The mass of dye measured on each stage of the impactor at inlet and discharge is compared, and the efficiency of the Cyclocentrifuge is then determined for each size class.

### Methylene Blue Test Results

The dust tests were conducted at the design point flow while varying the rotor speeds and blowdown flow. The rotor speeds at which tests were conducted were 10,000, 12,500, and 15,000 rpm. The blowdown flows were approximately 2 and 3% of the main stream flow.

The tests at each combination of parameters were repeated ten times, and the average of the ten runs was used as the datum point for each combination. The results of the individual tests were generally found to be repeatable within 10% of average.

Figure 8 shows the measured grade-efficiency curve for the Cyclocentrifuge operating at design poin conditions with a 3% blowdown flow, and using methylene blue dust suspended in air. The vertical line of the curve represent the standard distribution of the ten test runs. The dashed line shown on thi curve is the theoretical grade efficiency for this dust calculated by the method described in Referenc 1.

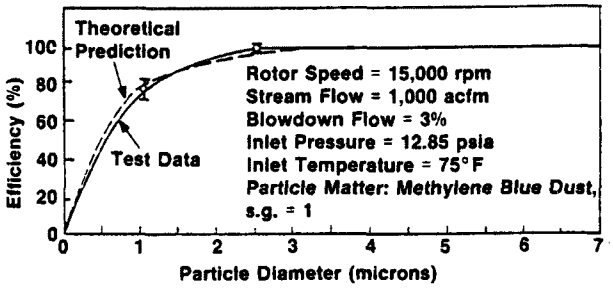


Fig. 8 Grade-Efficiency Curve for Design Point Conditions

SUMMARY OF SEPARATION EFFICIENCY FOR PARTICLES 1/2, 1, AND 2 MICRONS IN DIAMETER

| Rotor Speed | 2% Blowdown Flow Separation Efficiency (Percent) | | | 3% Blowdown Flow Separation Efficiency (Percent) | | |
|---|---|---|---|---|---|---|
| rpm | 1/2 micron | 1 micron | 2 micron | 1/2 micron | 1 micron | 2 micron |
| 10,000 | 22 | 44 | 80 | 32 | 55 | 82 |
| 12,500 | 25 | 47 | 80 | 38 | 60 | 85 |
| 15,000 | 25 | 47 | 80 | 54 | 73 | 92 |

Microscopic examination of the impactor plates revealed that some of the larger particles (>4 microns) tended to bounce through the impactor and get trapped in the final filter. Attempts to correct this situation by coating the collection plates of the impactor led to erroneous readings on the photometer. The microscopic analysis of the collection plates indicated that some of the particles that should have been intercepted by the 0.5-micron plate had passed through to the final filter. Thus, the photometric analysis of this plate indicated a higher separation efficiency than actually existed. These points are shown on the 0.5-micron line of the separation efficiency curves given on Figure 9. However, the plotted curves statistically correct this situation using the microscopic data. The data given on these curves generally show an increase in particle separation efficiency as the rotor speed and blowdown flow increase. The above table shows this trend clearly.

The effect of rotor speed and blowdown flow on the overall efficiency, and on the efficiency for all particles less than 1.4 microns, is shown in Figure 10. The upper curve shows a general increase in overall efficiency with increasing rotor speed and blowdown flow. The lower curve, however, shows a different trend. In this curve, when 3% of the process gas flow is used for continuous blowdown, the

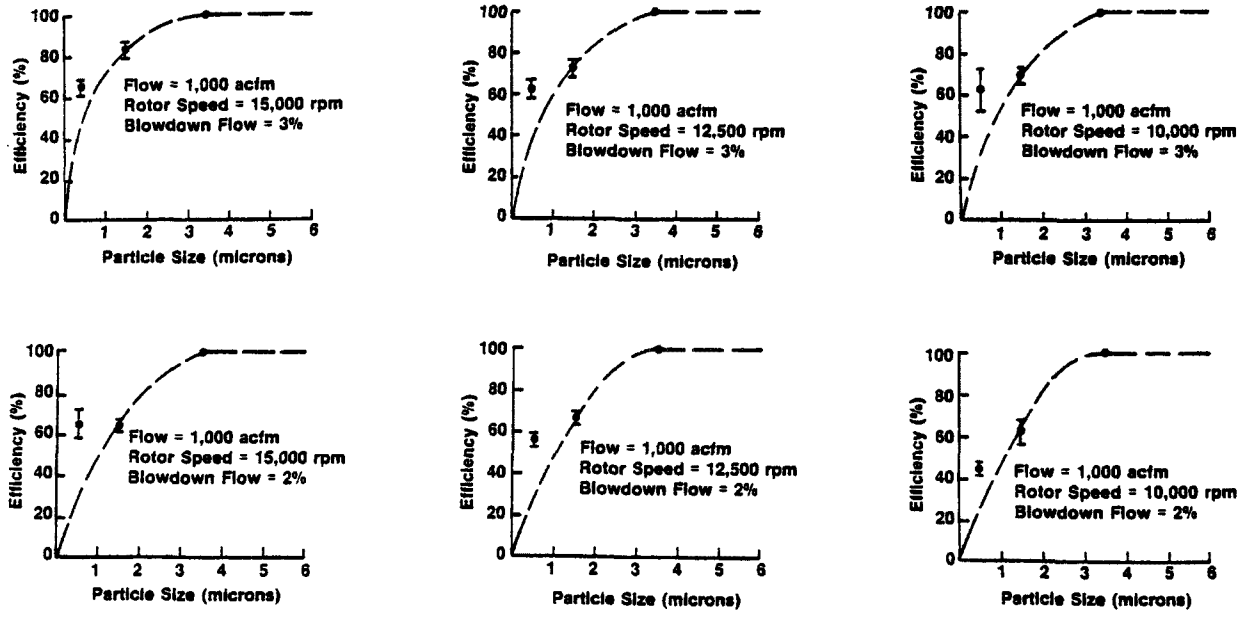


Fig. 9 The Effects of Rotor Speed and Blowdown Flow Rate on Grade Efficiency

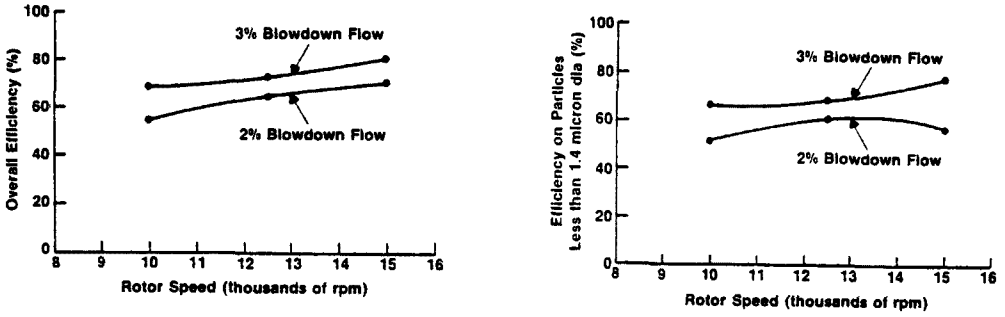


Fig. 10 Rotor Speed Versus Efficiency for 2% and 3% Blowdown

efficiency increases the rotor speed up to the speed test limit. But when the blowdown flow is decreased to 2%, the efficiency shows a maximum value at about 13,500 rpm. The decrease in efficiency after 13,500 rpm can probably be attributed to increased particle reentrainment in the blowdown hopper with increased vortex strength.

Figure 11 shows the calculated grade-efficiency curves for high-pressure, high-temperature gasification conditions based on extrapolating the cold-flow test results. The theoretical performance curves for the Cyclocentrifuge and a high-efficiency cyclone are the curves published in the Phase I Final Report [1]. The curve labeled "Based on Cyclocentrifuge Cold-Flow Test Results" is the solid line curve from Figure 8 corrected for the conditions listed. The theoretical curve and the performance curve based on the cold-flow test results are in close agreement, and are substantially better than a theoretical high-efficiency cyclone, based on Reference 4.

Fly Ash Tests

The second set of dust tests used fly ash recovered from an electrostatic precipator used by Rochester Gas and Electric on one of their coal-fired boilers. The fly ash was injected into the loop from a fluidized bed at a rate of about 1.5 grains per actual cubic foot (3.5 grams/$m^3$) or about 3500 ppm. The inlet and discharge were sampled isokinetically and the sample was collected on filters for subsequent analysis. The samples were weighed for total mass, and centrifugal sedimentation techniques were used for size analysis.

Fly Ash Test Results

Testing with fly ash is still in progress and grade efficiency data is still subject to some refinements. However, Figure 12 shows average grade efficiency for several test runs at 13,000 rpm rotor speed (approximately 85% design speed). Also shown on this figure is the methylene blue results for similar conditions. Further testing at design speed is in progress.

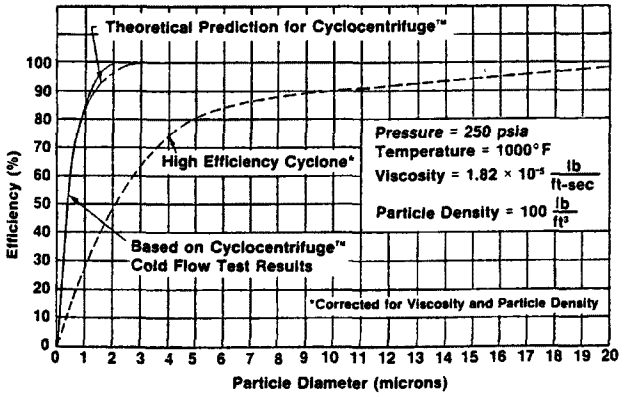


Fig. 11 Grade Efficiency Curves for Gasification Conditions

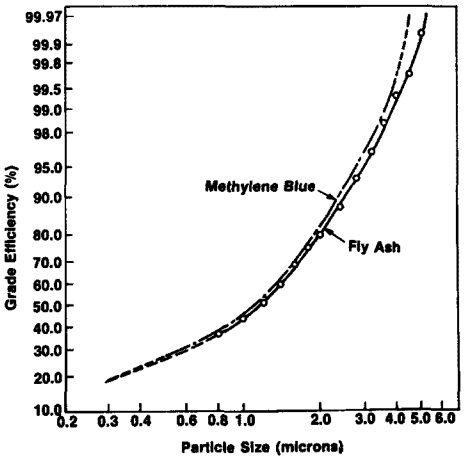


Fig. 12 Grade Efficiency for Fly Ash and Methylene Blue Tests at 13,000 rpm

## SUMMARY

Laboratory tests were made that show the vortex flow in a conventional cyclone can be accelerated by an aerodynamically designed rotor to a stable tangential velocity that is three to five times greater than a high through-put conventional cyclone. The tests also showed the separation efficiency was increased to the level that would be expected from the increased centrifugal force and that the penalty for this efficiency increase was increased pressure drop. Design analysis completed to date indicates a durable mechanical design for the planned 1000°F tests is feasible.

## ENDNOTES

1. McCabe, J.T. Centrifuges for Coal Conversion and Related Processes. Phase I, Feasibility Study. Mechanical Technology Incorporated, DOE Report FE-2428-10, Contract No EF 76-C-01-2428.

2. British Standard For Methylene Blue Tests For Respirator Canisters. British Standards Institution, B52577; 1955.

3. May K.R. The Collision Nebulizer: Description, Performance and Application. Aerosol Science, Vol. 4, 1973.

4. Kotch, H., and Licht W. New Design Approach Boosts Cyclone Efficiency. Chemical Engineering, Nov 7, 1977.

# DEMONSTRATION OF THE USE OF CHARGED FOG IN CONTROLLING FUGITIVE DUST FROM LARGE-SCALE INDUSTRIAL SOURCES

By: Edward T. Brookman
Project Engineer
TRC - Environmental Consultants, Inc.
Wethersfield, CT 06109

R.C. McCrillis, D.C. Drehmel
Industrial Environmental Research Laboratory
U.S. Environmental Protection Agency
Research Triangle Park, NC 27711

## ABSTRACT

A unique device for the control of particulate emissions works on the principle that most industrial pollutants acquire an electrostatic charge as they are dispersed into the air. If this charged airborne material is exposed to an oppositely charged water fog, the charges act to enhance the contact between the particulates and the fog droplets, resulting in rapid agglomeration and particle fallout. A device that generates charged fog has now been substantially developed and is being offered commercially by The Ritten Corporation.*

TRC-Environmental Consultants, Inc. has been contracted by EPA/IERL-RTP to test The Ritten Corporation's Fogger IV on several large-scale fugitive dust sources. This paper discusses the initial test at a sand and gravel operation and then describes current and future test sites. Preliminary test results are presented in terms of percent reduction in total suspended particulates (TSP). Changes in fogger effectiveness due to variations in operational parameters are discussed. Initial tests indicate overall fogger efficiencies of approximately 70 percent.

## INTRODUCTION

A spray of fine water droplets is a well-known means of airborne dust removal. Unfortunately, water sprays are not very efficient in removing dust from ambient air. One means of improving the efficiency of water sprays is by applying a charge to the spray that is opposite in polarity to that of the dust to be suppressed. Most industrial pollutants and naturally occurring fugitive dusts acquire an electrostatic charge as they are dispersed into the air. Exposing this charged airborne material to an oppositely charged water spray enhances contact between the particulates and the water droplets. After contact is made, the wetted particulates agglomerate rapidly and fall out of the atmosphere.

---

* The Ritten Corporation, 40 Rittenhouse Place, Ardmore, PA 19003

Charged sprays can be improved further by atomizing the water droplets to produce a fog. The fineness of the particles enhances their charge carrying capabilities in the spray. Furthermore, Hoenig (1) has demonstrated that the greatest effectiveness is obtained when the size of the water droplets is similar to that of the dust particles to be controlled. Lastly, less water is required when fog is used, thus reducing operating costs.

A device capable of producing this fine spray and applying a charge to it is known as a charged fogger. The charged fogger is intended primarily for fugitive dust sources that cannot reasonably be controlled using conventional means such as hooding. Such sources include materials handling operations (transfer points and conveyors), truck and railroad car loading and unloading, front end loaders, ship loading, grain silos, and mining operations. The charged fog concept has been applied to operations as small as a hand grinder and as large as a quarry.

Although the charged fog concept has been widely applied to industrial souces of fugitive dust, little data is available on fogger control efficiency. To obtain such data, the Industrial Environmental Research Laboratory of the Environmental Protection Agency at Research Triangle Park, North Carolina EPA/IERL-RTP contracted TRC-Environmental Consultants, Inc. to conduct a full scale demonstration of a charged fogger on several industrial fugitive emission sources. In particular, EPA/IERL-RTP was interested in testing the largest fogger, "Fogger IV," manufactured by the Ritten Corporation, on several sources in the iron and steel and sand and gravel industries.

Sources considered for testing included materials transfer, conveying, grinding, crushing, and truck and railroad car loading and unloading. Requirements for a test site included isolability from other dust sources, availability of necessary utilities, relative difficulty of control by other methods, representativeness to the general industry, relatively continuous operation, and fairly heavy dust production to facilitate sampling.

Following numerous visits to iron and steel and sand and gravel sites, several suitable sources were selected for field testing the charged fogger. The source chosen for the first test was the primary rock crusher operation at a sand and gravel site in Connecticut.

## DESCRIPTIONS OF SITE AND TEST EQUIPMENT

Figure 1 is a plot plan of the primary crusher operation showing the locations and dimensions of the various structures. The site and test equipment are described in the following subsections.

### Test Site

The inital fogger test site was a primary rock crusher. Approximately 100 dump trucks per day, each carrying loads of approximately 45 Mg (50 tons) of quarry rock (basically basalt) mixed with dirt, back up to the crushing pit to unload. Unloading times vary from 30 to 60 seconds,

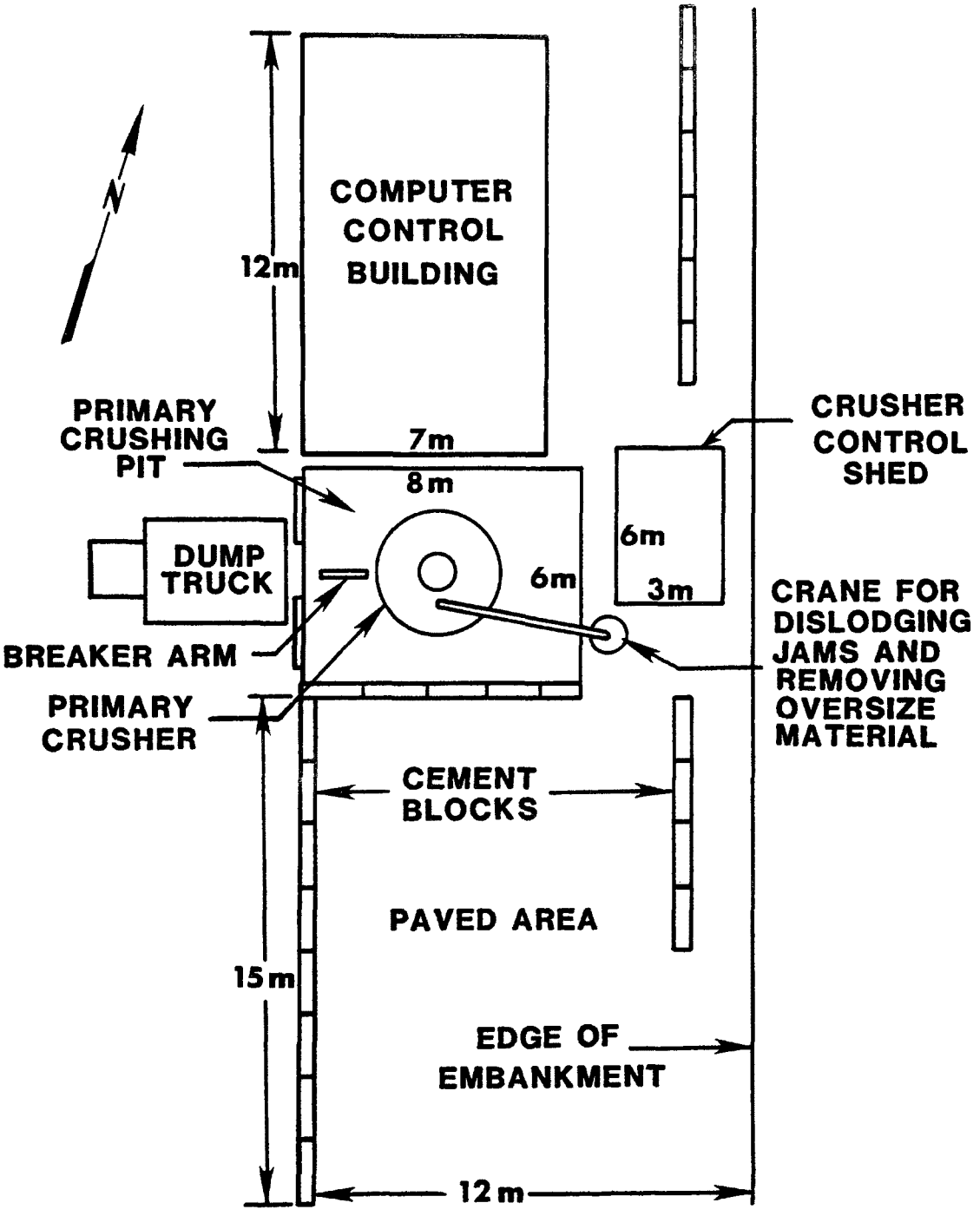


Figure 1. Primary crusher plot plan

depending on conditions in the pit. The pit itself is roughly 8 meters long and 6 meters wide. The crushing is done by a Superior 4265 gyrotory rock crusher. There is a two story computer control building north of the crushing pit, a control shed to the east, and a large paved area to the south. All approach roads and areas around the buildings and pit are paved and kept reasonably clean through frequent sweepings and waterings.

Fugitive dust emissions result from the dumping and crushing operations. The truck unloading is the primary source of dust with the major portion coming from dust boil-up at the rear of the pit. There is also dust at the rear of the truck during the dump. The crushing procedure itself also produces dust, but to a much lesser degree than the unloading process.

Charged Foggers

Two identical foggers were designed especially for TRC and EPA by the Ritten Corporation. Ritten's standard Fogger III was modified and upgraded to allow for variations of parameters. The final configuration, "Fogger IV," is shown schematically in Figure 2.

In the generation of the charged fog by the Fogger IV, water is atomized by compressed air and ejected from a nozzle. As the fog leaves the nozzle, it passes through an induction ring where either a positive or negative charge, depending on the nature of the dust, is applied to the spray. A flow of air around the nozzle, provided by a centaxial fan, projects the fog toward the dust source. A control panel, on the back of the fogger, allows for fogger operation and parameter variability.

The requirements for and capabilities of the operational parameters are:

- Air supply to nozzle - A compressed air supply of 5.6-8.8 $kg/cm^2$ (80-125 psi) is required. For the tests the air was supplied by a 2 hp compressor. The air flow through the nozzle is variable from 0 to 11.3 $m^3/hr$ (0 to 400 scfh).

- Water flow - The water supply to the fogger should be around 3.5 $kg/cm^2$ (50 psi) which is typical "shop" water pressure. The water flow through the nozzle is variable from 0 to 151 l/hr (0 to 40 gph).

- Power - The foggers require a power supply of 230 volts, single phase, 60 Hz. Current requirements do not exceed 35 amps.

- Centaxial fan - The fan, driven by a 5 hp explosion-proof motor, operates at a maximum of 79 $m^3/min$ (2800 scfm). The maximum output air velocity is approximately 3048 m/min (10,000 fpm). The fan flow rate is variable from 0 to 100 percent of capacity.

- Charge per droplet - Assuming an average droplet size of approximately 60 μm, the average number of elementary charges per droplet was calculated to be approximately $8 \times 10^4$ for 75 l/hr (20 gph) water flow. This can also be expressed as a charge/mass ratio of 0.11 μC/g.

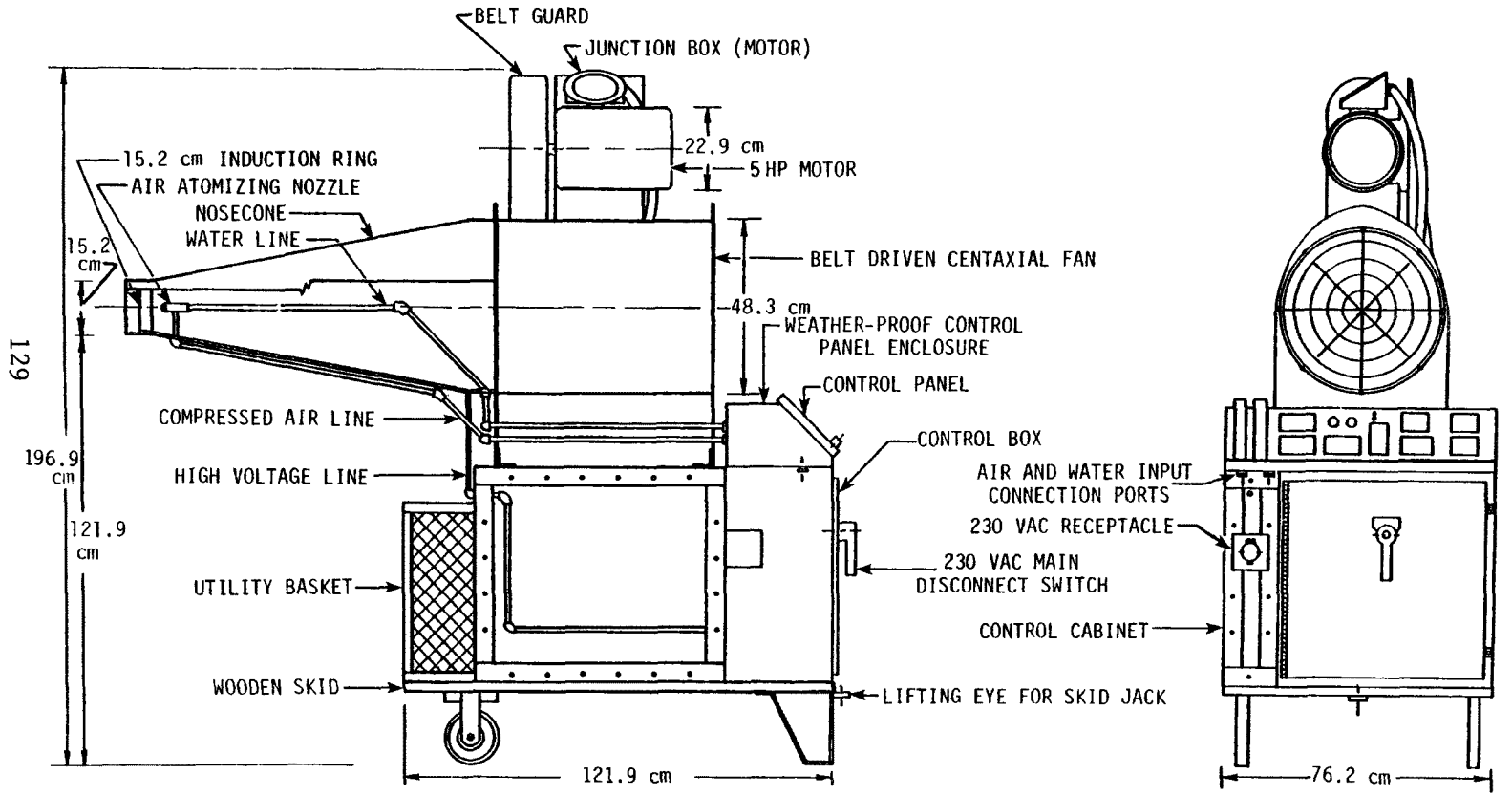


Figure 2. Schematic of The Ritten Corporation's Fogger IV.

- Flow spectra - Two different flow nozzles were used for the tests, both manufactured by Delavan.* One nozzle produced a conical spray of droplets estimated to be in the 50-70 μm size range; the other had a heavier flow capacity and produced a conical spray of droplets estimated to be in the 60-80 μm size range. A third nozzle, which produces a flat spray, was not available for the tests, but may be used later.

The two foggers were tested at various locations around the pit to determine the arrangement for optimum dust control. Placement was also dependent on wind direction. The most effective positions seemed to be at the rear corners of the pit with one fogger aimed at the dust boil-up and the other, at the rear of the truck.

Sampling Equipment

The equipment used for particulate measurements included seven high-volume samplers (hi-vols) and a wind recording system. The hi-vols were manufactured by Misco Scientific** and had automatic flow control, enabling the mass flow rate to be held constant regardless of filter loading, atmospheric conditions, and line voltage changes. Two of the hi-vols were fitted with Andersen Model 7000 Size Selective Inlets (SSIs) which are designed to remove all particulates larger than 15 μm from the sampled air before filtering the remaining particulates onto a standard hi-vol filter. Two other hi-vols were fitted with Sierra Instruments Series 230 four-stage cascade impactors (CIs). By using the SSIs and CIs, the charged fogger efficiency could be examined for various particle size ranges.

The wind velocity and direction measurements were recorded using a Climatronics Mark III wind system. Wind speed is measured with a three-cup anemometer coupled to a light chopper. The chopper output is converted to DC voltage and recorded on a chart. The wind direction is measured by a wind vane coupled to a precision low-torque potentiometer. The wiper voltage of the potentiometer is recorded on another chart.

The hi-vols were at various locations and in various combinations around the pit, depending on wind direction. The locations were selected to provide variation in downwind distance.

## TEST PROGRAM AND PROCEDURE

The test program consisted of 32 runs during 6 days of testing. Tests were run with no charge, with fog only, with uncharged fog, with positive fog, and with negative fog. Water flow, air flow, and fan speed were only varied slightly since conditions at the crusher prevented extensive parameter variations. Water was provided by a tank with a small pump which limited nozzle flow to approximately 80 l/hr. Fan speed was reduced to 80 percent of capacity to help reduce excessive dust reentrainment in the pit.

* Delavan Mfg. Co., 811 4th St., West Des Moines, IA 50265
** Misco Scientific, 1825 Eastshore Highway, Berkeley, CA 94710

The sampling procedure was essentially the same for each test. Upon arrival at the test site, the wind recording system was set up and the wind direction determined. The hi-vols were then positioned in a sampling array downwind of the crushing pit. The foggers were positioned to control the dust cloud while not spraying directly into the samplers. Once the equipment was positioned, the pre-weighed hi-vols were placed in the samplers. The samplers were turned on simultaneously just prior to the first truck dump of a predetermined sequence of trucks (typically eight trucks provided sufficient material for sampling purposes). For the runs with the foggers in operation, the foggers were also turned on at this time and adjusted to the predetermined fogger operational parameter conditions. After the last truck of the sequence had dumped into the pit and crushing was completed, the samplers and foggers were all stopped and the filters removed. At the end of the day, all of the filters were returned to TRC's chemistry laboratory where they were subsequently desiccated and weighed.

## PRELIMINARY RESULTS AND DISCUSSION

The majority of the test runs at the primary crusher, numbers 7-31, were completed before the final filter weights were available from the chemistry laboratory. Examination of the data revealed several important factors. In almost all cases, the TSP levels, as measured by the various samplers, showed increases above the uncontrolled levels when uncharged fog was applied to the crushing operation. Although this result was unexpected, further analysis revealed the problem: the fans in the foggers which create the airflow that projects the fog toward the dust source are so powerful that they were actually creating an artificial wind effect. The uncontrolled dust plume was subject only to the ambient wind; whereas, the controlled plume was being "directed" radically by the fogger air jets. This discovery produced the need for a final series of tests wherein the uncontrolled baseline TSP levels were recorded with the fans on with no water added.

Another concern that developed was with the intermittent nature of the truck dumps. In some cases, eight trucks would unload within 20 minutes; at other times it would take 30 or 40 minutes. The data was therefore reduced on a per-truck basis since the unloading and crushing times, the times when the vast majority of the dust is produced, were essentially the same for all dumps. The data were also adjusted slightly to account for deviations of the actual sampler flow rates from the design flow of 1.1 $m^3$/min (40 cfm).

While the data from runs 7-31 did not reveal information regarding overall fogger efficiency, they did provide insight into the increase in efficiency due to charging the fog. This efficiency could be further examined with regards to particle size, distance from the pit, and charge polarity. Not all of the runs produced usable data: the fog impinged on the samplers during some tests.

The data from runs 32-39 were used to determine fogger efficiency with respect to uncharged fog. The spacing of the samplers also allowed for the examination of efficiency versus distance from the pit. This information was then combined with the data from runs 7-31 to calculate overall fogger efficiency.

Attempts were made to obtain information on visibility improvement using EPA Method 9 (visual determination of opacity). It was found that the opacity of the fog was similar to that of the uncontrolled dust plume so that no real visibility improvement was noted.

Figure 3 presents the preliminary test results from the initial charged fogger tests at the primary crusher site. The left side of the figure shows the percent reduction in TSP levels when an uncharged water fog was used to control the fugitive dust. The right side of the figure shows the additional percent reduction in TSP levels when a charge was applied to the fog. The data from this figure reveal several important results, as discussed in the following subsections.

Uncharged Fog Efficiency

Based on the limited amount of data for fan-only versus uncharged fog, it appears that a water spray alone is approximately 30-40 percent efficient in reducing fugitive dust levels from the primary crusher. It also appears that this efficiency is independent of particle size and distance from the pit.

Efficiency Increase Due to Charging of Fog

Applying a charge to the water spray reduced the fugitive dust levels 40-70 percent over those recorded using uncharged fog. There appears to be a trend of increasing reduction with increasing distance from the pit. This apparent phenomenon is not explainable at this time, but it may have something to do with agglomeration and particle fallout. This possible distance factor will be examined further in future tests.

Figure 3 also shows that TSP reduction due to charging is essentially the same regardless of the polarity of the charge applied to the spray. This indicates that the dust cloud contains a mixture of particles, some negative and some positive. This is consistent with the findings of other researchers, namely Hoenig (1) and Kunkel (2).

TSP reduction appears to be the same for the respirable size range ($\leq$ 15 μm), as measured with the hi-vols with size selective inlets, as for the size range sampled with the standard hi-vol ($\leq$ 30 μm). It was hoped that using cascade impactors would provide additional information on efficiency versus particle size, but the results proved unusable. Almost all of the material collected by the hi-vols fitted with the impactors was collected on the back-up filter, indicating severe particle bounce between the impactor stages. Perhaps tests at sources with finer dust will yield more useful information.

Overall Fogger Efficiency

By combining the results presented in Figure 3, it is possible to calculate an overall collection efficiency for the charged foggers. Based on the preliminary data, the use of charged fog can reduce the fugitive dust levels

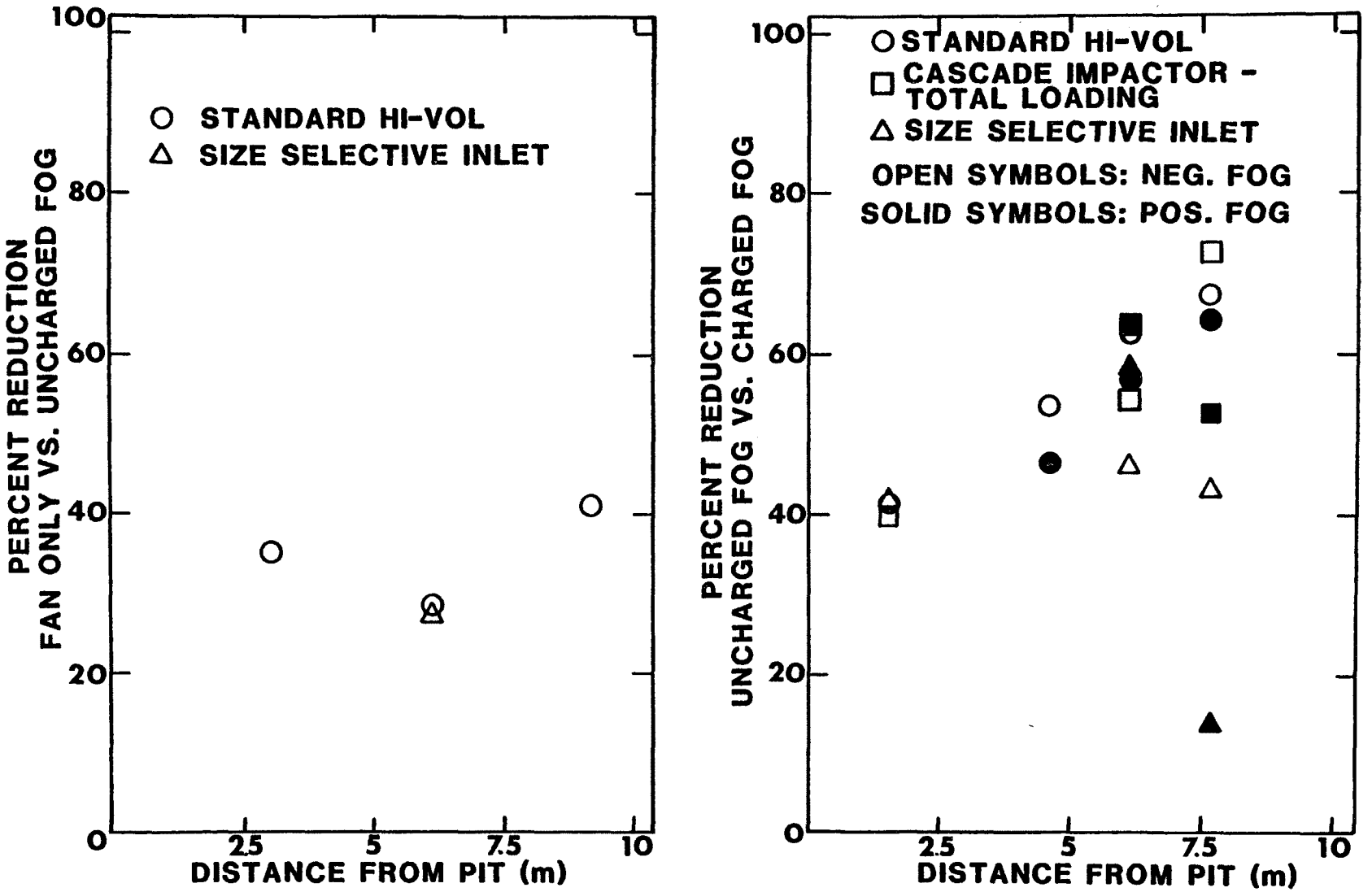


Figure 3. Percent reduction in TSP levels due to fogging of primary crusher.

that result from the primary rock crushing operation approximately 65-75 percent. It is felt that this reduction could be even greater through the use of additional foggers, wind baffles to reduce turbulence, and increased water flow.

## FUTURE WORK

The foggers are currently being tested on two different sources in U.S. Steel plants near Pittsburgh, Pennsylvania. One source is a sinter plant pug mill which mixes water with baghouse dust for dust suppression before recycling the material back through the plant. Even with water addition, there is a significant amount of fugitive dust around the source. The second source is the hot fume that results in a cast house from the filling of a ladle car with molten iron from a cast. Following the tests at U.S. Steel, a coke screening operation at Stelco in Hamilton, Ontario, will be tested. At this site, coke is transferred onto a shaker screen where it is sorted by size. The shaking results in copious amounts of dust.

The steel company tests mentioned above will most likely be completed by this summer. Following completion of all field tests, a final report will be prepared for the EPA presenting the results.

## ENDNOTES

1. Hoenig, S.A. Use of Electrostatically Charged Fog for Control of Fugitive Dust Emissions. The University of Arizona, Tucson, AZ. EPA-600/7-77-131 (NTIS PB 276-645). November 1977.

2. Kunkel, W.B. The Static Electrification of Dust Particles on Dispersion into a Cloud. Journal of Applied Physics. Volume 21. August 1950. pp. 820-832.

# THE CONTROL OF FUGITIVE EMISSIONS USING WINDSCREENS

By: David Carnes
Project Scientist
TRC - Environmental Consultants, Inc.
Wethersfield, CT 06109

Dennis C. Drehmel
Industrial Environmental Research Laboratory
U.S. Environmental Protection Agency
Research Triangle Park, NC 27711

## ABSTRACT

TRC-Environmental Consultants, Inc., was contracted by EPA/IERL-RTP to perform a project that would provide information on the velocity distributions downwind of windscreens. This was accomplished via field testing of several windscreen sections erected on smooth terrain. This paper presents the results of these tests as well as a discussion of windscreen theory in general. A theoretical case study of the potential reduction of emissions from a coal storage pile using a windscreen as a control measure is also presented. The results of this case study indicate 80 percent fugitive emission reduction.

## INTRODUCTION

Despite extensive controls on traditional point sources, the National Ambient Air Quality Standard (NAAQS) for total suspended particulate (TSP) is still being exceeded in many areas of the country. Among the reasons for these excessive TSP levels is the fugitive dust that is generated from non-traditional sources such as unpaved parking lots, construction sites, exposed plant areas, and storage piles. To reduce the impact of these sources on ambient air quality, EPA/IERL-RTP has undertaken a program of area source control technology research and development. One of the control methods under investigation is a windscreen.

Wind-generated fugitive dust is the result of wind pressure against surface particles overcoming the force of gravity on the particles and the force of adhesion between the particles. For each size and type of dust particle, there is some "threshold" velocity below which no wind erosion will occur. Windscreens or wind barriers function as do other surface barriers in providing wind erosion control; i.e., they take up or deflect a sufficient amount of the wind force to lower the wind velocities to leeward below the threshold required for initiation of soil movement.

## THEORY

A windscreen exerts a drag force on the incident wind field, causing a net loss of momentum and a sheltering effect in the lee of the screen.

Airflow characteristics within the sheltered area vary with:

1. windscreen height and width;

2. windscreen permeability;

3. size of the elements or openings in the windscreen;

4. terrain roughness; and

5. turbulence intensity in the incident wind field and in the airflow downwind of the screen.

The design and siting of a wind fence for a specific application should reflect the optimum combination of the above. Typical field data presented by Raine and Stevenson (1) indicate that an effective windscreen should give a mean velocity reduction of 50 percent up to 10 fence heights downstream and a maximum reduction of 70 to 80 percent 1 to 5 fence heights downstream (measurements taken at 0.5 fence heights above ground).

Windscreen Height and Width

The downwind extent of sheltering is typically reported in terms of the number of equivalent fence heights. Figure 1 depicts isotachs for a 4.9 meter high windscreen (50 percent porosity) that is 122 meters long. The data was collected by Radkey and MacCready (2) for an incident wind of 17 m/sec. Using this case as an example, wind velocity is reduced by 50 percent or greater for a distance of 55 meters downwind. Doubling the height of the fence will double the distance downwind for the 50 percent isotach.

The fence width determines the lateral extent of the sheltered area. The downwind isotachs are essentially parallel to the windscreen, with the exception of edge effects which reduce the effectiveness of the windscreen locally. Edge effects consist of displacement of the adjacent flow and the development of turbulent eddies.

Windscreen Permeability

Air that passes through the windscreen elements is referred to as "bleed flow." Air that is displaced upward and passes over the fence is referred to as "displacement flow." As the permeability of a windscreen is reduced, the "bleed flow" through the windscreen decreases and the drag force increases. Also, there is a greater upward deflection of the incident wind. As the permeability approaches zero, a region of large-scale separated flow in the lee of the windscreen develops, turbulence in the separation zone intensifies, and stagnation occurs downstream in the "bleed flow." The lower the permeability of the wind break, the closer behind it lies the stagnation point. The mean flow pattern in the vicinity of the stagnation point is poorly defined. With a solid fence, there is a well-defined recirculating eddy in the separation zone. A less permeable windscreen may cause a greater reduction in mean wind speed; however, the

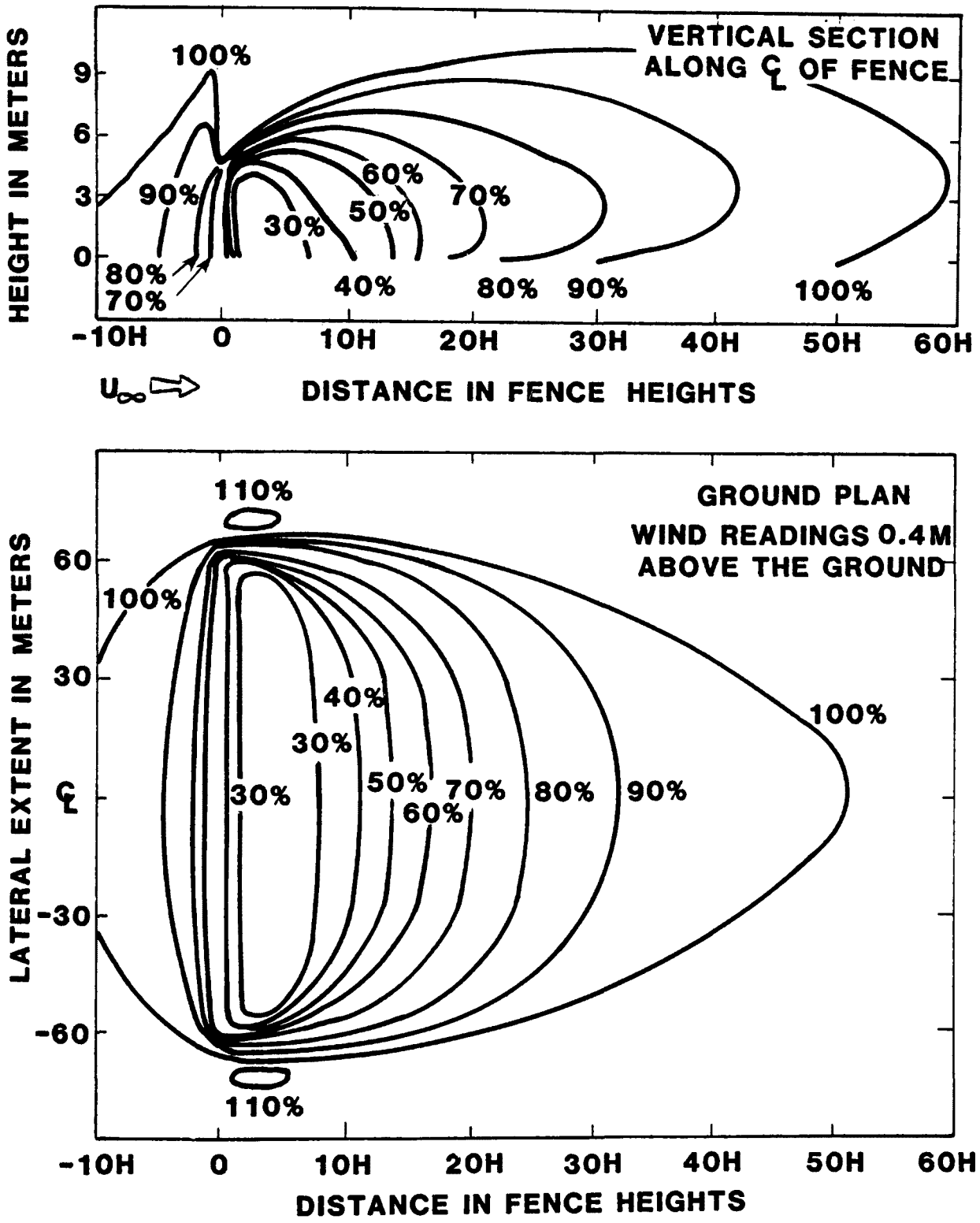


**NOTE: VELOCITIES ARE % OF UPSTREAM VELOCITY AT THE SAME HEIGHT**

Figure 1. Wind velocity pattern above a mown field during a 17 m/sec wind blowing at right angles to a 4.9 m high wood fence 122 m long of 50% porosity.

greater turbulence in its wake may make it less effective for overall wind protection than a more permeable one.

With a more permeable fence and consequently higher "bleed flow" velocity, there is less shear in the flow at the fence top and thus weaker streamwise momentum transfer from the "displacement flow" back into the sheltered region. As a result, there is less reduction in mean wind speed and lower turbulence intensity in the near wake, but a slower recovery to the upstream condition in the far wake. Above a geometric permeability of 35 to 50 percent, a zone of stagnated flow and large scale eddying is no longer evident in the leeward flow.

Size of the Elements in the Windscreen

The high shear initiated at the fence top is the dominent source of turbulent velocity fluctuations in the leeward flow, even with the most permeable fence. However, the size of the elements in the windscreen significantly affects the turbulent structure in the "bleed flow." For a windscreen of a given geometric permeability, the turbulence intensity and scale at a given location downstream increases with the size of the elements in the barrier; i.e., with the coarseness of the permeability.

Terrain Roughness

The smoother the terrain on which a windscreen of given height and permeability is erected, the greater will be the reduction in mean velocity in the leeward flow. It has been found that with increasing upstream terrain roughness and more turbulent approach flow, the smaller is the zone of reduced wind velocity downstream of the wind break. Also, experimental data from field and wind tunnel tests show that drag increases with an increase in the fence height to the effective terrain roughness ratio.

Turbulence Intensity of the Incident Wind Field

In fully aerodynamically rough, neutrally stable flow, windscreen leeward flow patterns should be independent of approach flow velocity. However, decreasing the turbulence intensity in the approach flow increases the zone of reduced velocity downwind of the screen.

Turbulence Intensity Downwind of a Windscreen

At any downstream point the root mean square velocity fluctuation, u', varies much less with windscreen permeability than does mean velocity, U. This indicates that higher values of u'/U behind denser fences are due more to a large reduction in U than to higher u' levels. Therefore, regions of high turbulent intensity tend to be regions of low mean velocity. Also, the high shear initiated at the fence top is the dominent source of turbulent velocity fluctuations, even with the most permeable fence. For a given approach flow, u'/U tends to be slightly higher with less permeable fences, apparently due to stronger shear in the flow at the fence top.

## TESTING PROGRAM

TRC completed tests on two commercially available polyester windscreens provided by Julius Koch, USA, Inc.* The windscreens had permeabilities of 65 percent and 50 percent, respectively. Testing was completed at the state airport in Quonset, Rhode Island. The windscreens were erected on a flat open field which was located adjacent to Narragansett Bay. Each fence was 1.8 meters high, with the 65 percent permeable fence 55 meters wide, and the 50 percent permeable fence, 59 meters wide.

The objective of the field testing was to document the effectiveness of a commercially available windscreen. Measurements were also made of wind acceleration on the slope of a hill located on the Quonset airport grounds. Measurements were made using either Teledyne or Climatronics wind anemometers and wind direction sensors. Data were recorded on Soltec strip chart recorders.

### Windscreen Results

Results for the 65 percent permeable windscreen are presented in Figures 2 and 3. For an average incident wind ($U_O$) of 3.0 m/sec, the observed wind velocity reduction was 70 percent in the adjacent area downwind of the windscreen. A reduction of 40 percent was observed as much as 14 fence heights (H) downwind. A second test was completed for an average incident wind of 5.2 m/sec. The observed reduction in wind speed adjacent to the windscreen was only 40 percent. For an elevation of 1/2H, the downwind distance experiencing a 40 percent reduction extends to approximately 6H for $U_O$ = 3.0 m/sec, and 20H for $U_O$ = 5.2 m/sec. With increasing incident wind speed, the area experiencing a 40 percent reduction is reduced significantly. The decrease in fence efficiency is attributed to an increase in the turbulence intensity within the incident wind field. Fluctuations of the instantaneous velocity in the incident flow field was 25 percent greater for the $U_O$ = 5.2 m/sec case.

For $U_O$ = 3.0 m/sec, the data collected at 0.5H, 1H, and 2H downwind shows that there is a loss of momentum in the "bleed flow" and development of a zone of stagnation. However, the few data points collected for the $U_O$ = 5.2 m/sec case exhibit no apparent zone of stagnation. The increased mixing behind the windscreen and possibly the very coarse nature of the elements in the windscreen contribute to the elimination of the area of stagnation.

Data for the 50 percent permeable fence (Figure 4) were collected for an incident wind of 4.2 m/sec. The downwind area adjacent to the windscreen shows a reduction in wind velocity of 60 percent, which is comparable to the efficiency of the 65 percent permeable fence for an incident wind of 3.0 m/sec. However, there is no apparent zone of stagnation separating the "bleed flow" from the "displacement flow." Also, recovery of the incident flow strength downwind occurred relatively fast.

---

* Julius Koch, USA, Inc., 387 Church Street, New Bedford, MA 02741

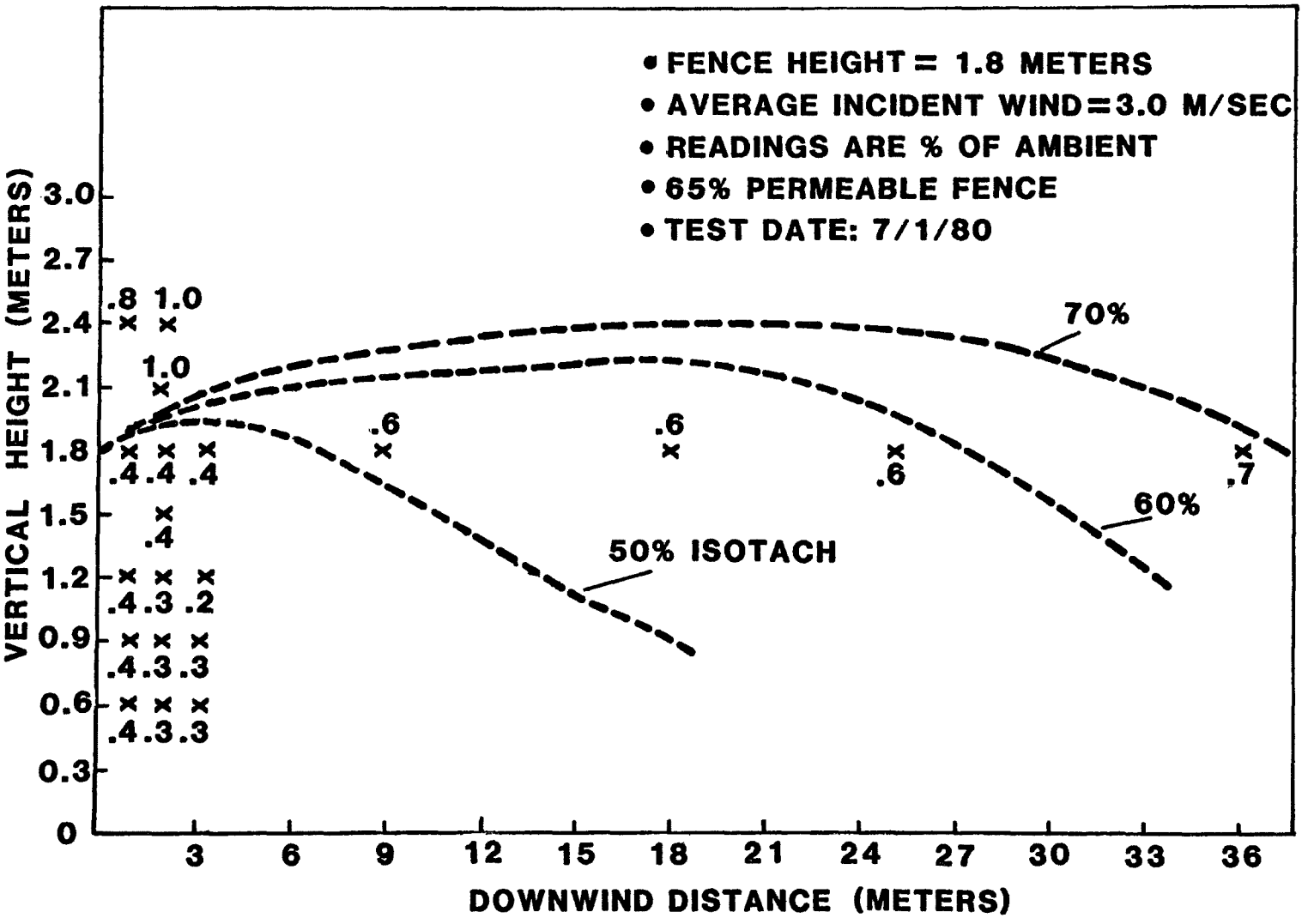


Figure 2. Measured velocity reductions due to a 65% permeable windscreen with an average incident wind speed of 3.0 m/sec.

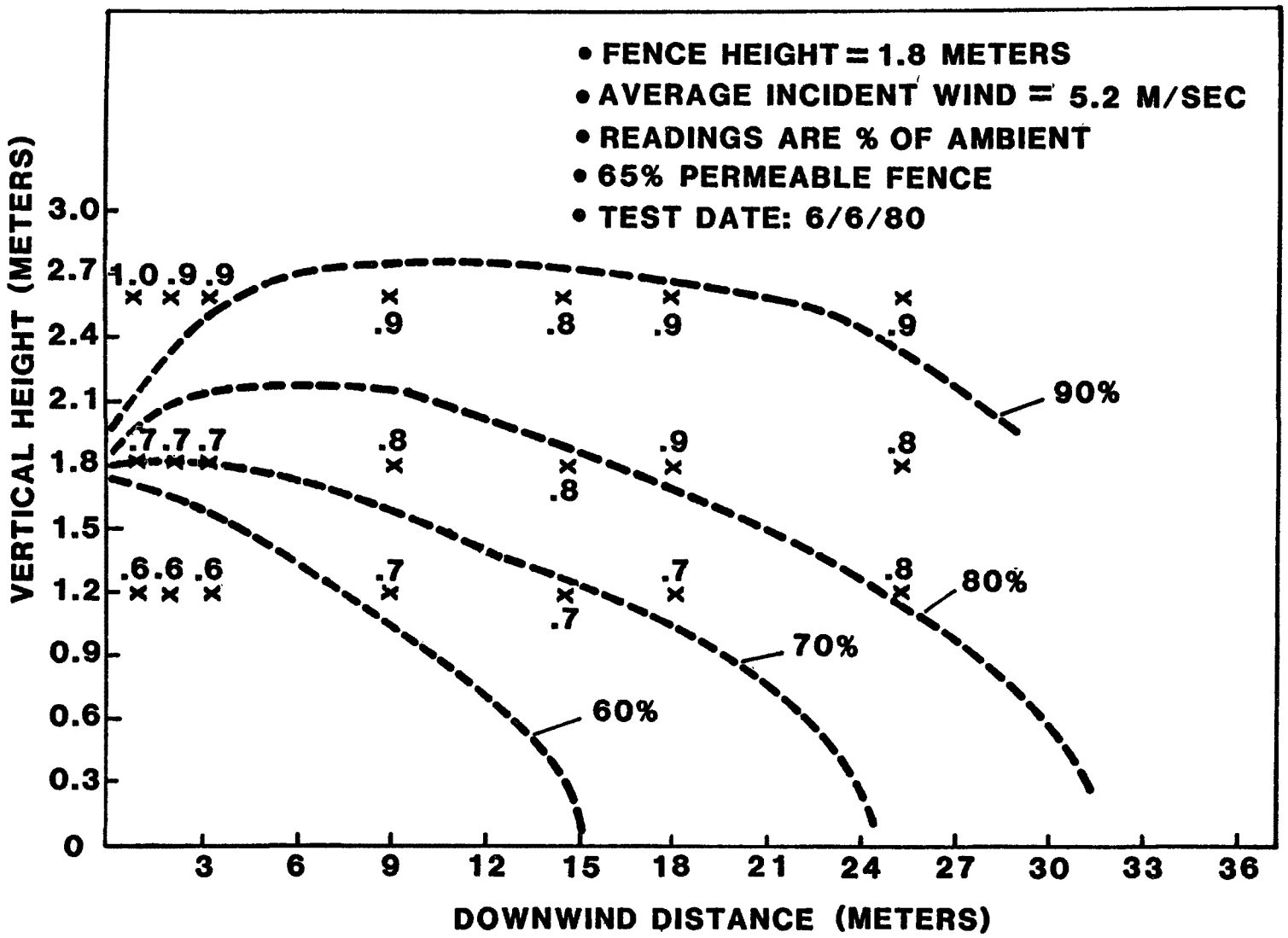


Figure 3. Measured velocity reductions due to a 65% permeable windscreen with an average incident wind speed of 5.2 m/sec.

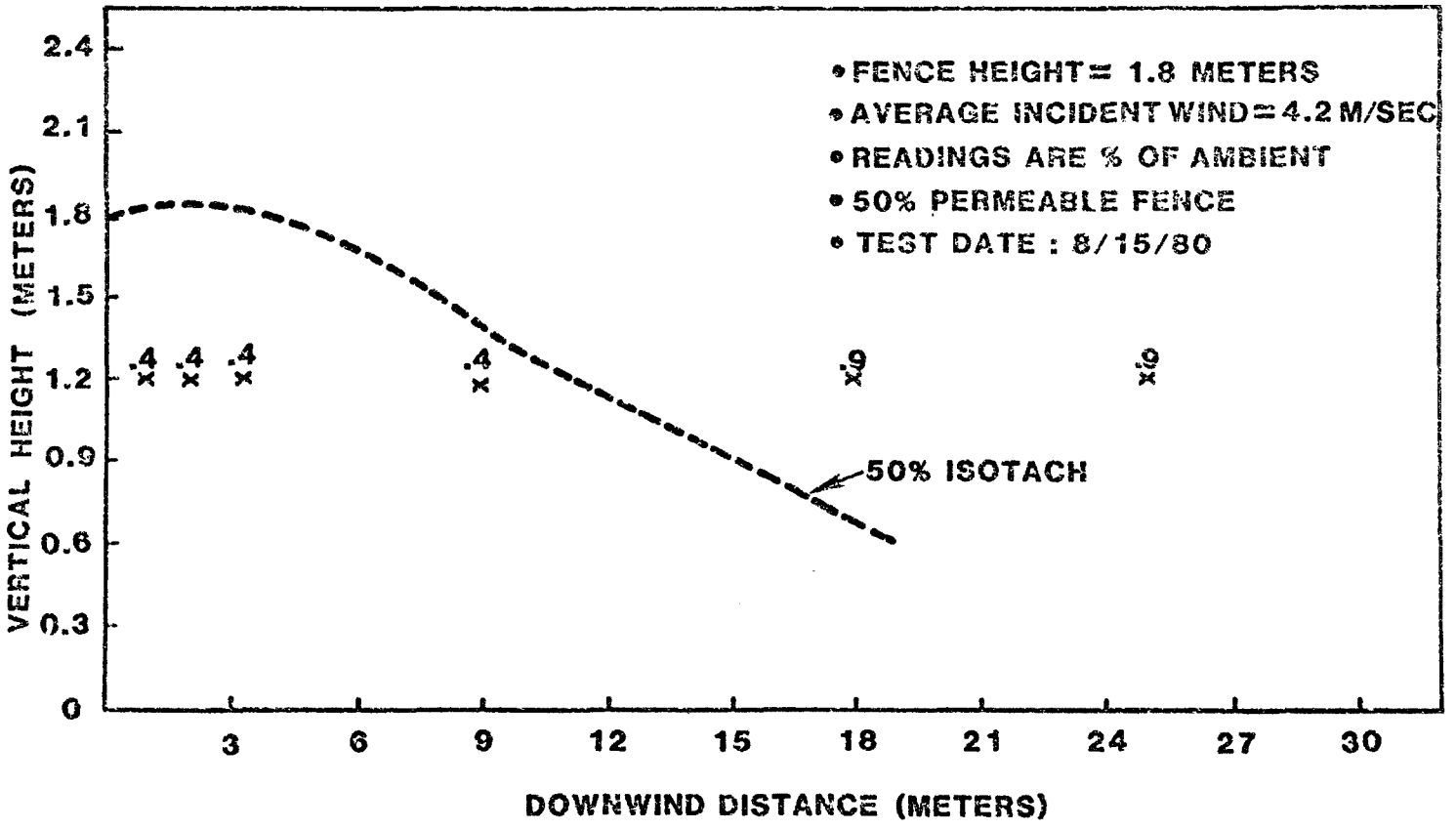


Figure 4. Measured velocity reductions due to a 50% permeable windscreen with an average incident wind speed of 4.2 m/sec.

The test results suggest that, in practical application, fence efficiency in the region where "displacement flow" predominates is less than predicted. The lower efficiencies observed are attributed to the higher turbulence intensity observed for higher incident wind velocities and shearing at the fence top. Both of these effects extend the penetration of the turbulent eddies into the sheltered zone which, in turn, transfers momentum and increases mixing.

## APPLICATION OF WINDSCREEN - CASE STUDY

The effectiveness of a windscreen to control fugitive emissions from a coal storage pile was appraised using the equations developed by Blackwood and Wachter (3). Solutions were obtained for a 54,000 metric ton coal pile with an 8 meter high windscreen. The surface area of the coal pile was determined from the following relation:

$$S = T_c/P_bH$$

For this equation, S is the surface area of the pile; $T_c$ the weight of the coal stored; $P_b$ the bulk density (800 $kg/m^3$); and H the pile height (7.6 m). For the study case, S equals 8900 $m^2$.

The incident wind velocity distribution under consideration is presented in Table 1. Average velocities were multiplied by a factor of 1.5 to account for wind acceleration along the upwind slope of the pile. The particulate emission rate was estimated from the following equation:

$$Q = \frac{336\ u^3\ P_b^2\ S^{0.345}}{(P-E)^2}$$

For this equation, Q is the entrainment/emission rate; u is the wind speed; and (P-E) is the precipitation-evaporation index.

The total estimated emissions from the coal pile using no control measures were 26.3 metric tons. The total estimated emissions using the 8 meter high windscreen were only 5.4 metric tons. Using the windscreen offers the potential of reducing fugitive emissions by 80 percent.

TABLE 1. VELOCITY DISTRIBUTION FOR THE COAL STORAGE PILE

| Velocity Interval (m/sec) | Average Velocity (m/sec) | Percent Time of Occurrence | Average Velocity x 1.5* (m/sec) |
|---|---|---|---|
| 0 - 2.2 | 1.3 | 19 | 2.2 |
| 2.2 - 4.5 | 3.6 | 38 | 5.4 |
| 4.5 - 6.7 | 5.8 | 19 | 8.9 |
| 6.7 - 8.9 | 8.0 | 10 | 12.1 |
| 8.9 - 13.4 | 11.2 | 10 | 17.0 |
| >13.4 | 15.6 | 4 | 23.7 |

* Multiplier of 1.5 applied to account for wind acceleration along the upwind slope of the storage pile.

## ENDNOTES


1. Raine, J.K. and D.C. Stevenson. Wind Protection by Model Fences in a Simulated Atmospheric Boundary Layer. Journal of Industrial Aerodynamics Vol. 2, 1977, pp. 159-180.

2. Radkey, R.L. and P.B. MacCready. A Study of the Use of Porous Wind Fences to Reduce Particulate Emissions at a Coal-Fired Generating Station. Prepared by Aerovironment, Inc. February 1979.

3. Blackwood, T.R., and R. A. Wachter. Source Assessment: Coal Storage Piles. EPA-600/2-78-004k (NTIS PB 284 297). May 1978.

# THE INFLUENCE OF AGGREGATE PILE SHAPE AND ORIENTATION ON PARTICULATE FUGITIVE EMISSIONS

By: Dennis Martin
Principal Engineer
TRC - Environmental Consultants, Inc.
Wethersfield, CT 06109

## ABSTRACT

While it has long been recognized that pile shape and orientation have some influence on the amount of particulate matter emitted, quantitative data have been lacking. This is due primarily to the inherent difficulties of any field program which would attempt to establish such a relationship. To correct this lack, studies were conducted in a wind tunnel to determine quantitatively how pile shape influences emissions. It was found that the slope of the pile played an important part with respect to the acceleration of the wind up the front of the pile. Also, it was shown that emissions from the top of the pile were dependent upon the orientation of the pile with respect to the wind. The implications of this study are that significant reductions in fugitive emissions from a pile can be accomplished simply by changing its shape slightly and reorienting it with respect to the wind. Estimates of the potential reduction are given.

Also, it is shown that use of water sprays, chemical stabilizers, and wind screens can be made more cost effective by selectively applying them to the high emission areas of the piles.

## INTRODUCTION

The fugitive particulate emissions from active and inactive storage piles can be a significant portion of the total emissions from a facility such as a coal port, power plant, steel mill, or coal mine. As with most other fugitive emission sources, however, past efforts to precisely quantify them with respect to those parameters which affect their rate of emission have met with little success. It has been only recently that factors such as silt and moisture content have been taken into account in predictive equations. However, large inconsistencies are still evident in the work done by the various researchers.

As part of a research project for the Particulate Technology Branch of EPA's Industrial Environmental Research Laboratory at Research Triangle Park, North Carolina, TRC - Environmental Consultants, Inc. (TRC) investigated several control strategies applicable to various fugitive areas

sources. It was during this work that the aforementioned inconsistencies were noted. Special interest was taken in the wide variation with which researchers related air velocity to emissions. Since it had been previously observed that pile contour and alignment probably had some impact upon the magnitude of the emissions, it was decided that a more detailed study of this effect was now in order.

A better understanding of how fugitive emissions are generated is now necessary since the quantification of fugitive sources is part of many prevention of significant deterioration applications and offset type situations. With various factors available in the literature for any given operation, the potential for unnecessary confrontation exists between EPA or state enforcement officials and industry representatives. It is not unusual for a situation to occur where enforcement will choose an emission factor available for an operation that is two orders of magnitude higher than that picked by industry. Through a better understanding of how emissions are generated, more accurate factors can be obtained through a planned testing program and such conflicts can be avoided in the future.

## EMISSION FACTORS FOR STORAGE

Table 1 lists some of the more frequently referenced emission factors for wind erosion from aggregate storage piles. Two of the factors do not include wind speed directly in the equation. Another factor relates emissions to the cube of the velocity while the final one does not include a velocity term at all. Investigations performed in wind tunnels and in the field have related particulate fugitive emissions from piles to the air speed raised to the 2.1, 2.7, 3, and 9.0 powers (Reference 4).

The above variations indicate that those factors which influence the emissions from piles are complex in nature and in interaction and are probably not accurately characterized by the parameters used in the equations. Partially, this is due to the use of surrogates acting in place of what might be the preferred factor. For example, it is obvious that high surface moisture content of dust would act in a number of ways to inhibit emissions. The surface moisture content of a material varies with its physical properties and those meteorological conditions such as rainfall, temperature, and incident radiation levels particular to a given area. Rather than measure the surface moisture contents of the dust during testing programs and relating the result to emissions, however, Thornthwaite's precipitation-evaporation index is commonly used, as can be seen in Table 1. While there are good and compelling reasons to use this index, it must be realized that its use could impart considerable inaccuracy to the resulting factor. A second reason for such variations is that the velocity was measured in different locations around the pile and at different heights during the different programs. This, of course, could lead to a scatter in the results. A third reason for variation in emission factors is that the sampling is usually performed by the upwind-downwind technique. Due to the inherent imprecision of this method, short-term testing programs could result in factors which are only appropriate to the sites tested being developed.

TABLE 1. WIND EROSION EQUATIONS

| Factor | Parameter Definition | Reference | Comments |
|---|---|---|---|
| $E = \frac{0.11}{\left(\frac{PE}{100}\right)^2}$ | E = emission factor, lb/ton placed in storage<br>PE = Thornthwaite's index | 1 | Test performed at sand and gravel plants. Upwind-downwind test method used. |
| $E = 0.05 \left(\frac{s}{1.5}\right)\left(\frac{d}{235}\right)\left(\frac{f}{15}\right)\left(\frac{D}{90}\right)$ | E = emission factor, lb/ton put through storage<br>s = silt content, %<br>d = No. of dry days per year<br>f = % of time wind speed exceeds 12 mph at 1 foot above ground<br>D = duration of storage, days | 2 | Does not include emissions caused by pile maintenance and traffic. Iron pellet and coal piles were sampled. |
| $E = \frac{6.16 \times 10^6 \left(\frac{e}{50}\right)\left(\frac{s}{15}\right)\left(\frac{f}{25}\right)}{\left(\frac{PE}{50}\right)^2}$ | E = emissions of suspended particulate, lb/acre/year<br>e = soil erodibility<br>s = silt content, %<br>f = % of time wind speed exceeds 12 mph at 1 foot above ground<br>PE = Thornthwaite's index | 3 | Portable wind tunnel used to modify original soil loss equation |
| $Q = \frac{336 \left(u\right)^3 \left(\rho_b\right)^2 \left(S\right)^{0.345}}{\left(PE\right)^2}$ | Q = emissions, mg/sec<br>u = wind speed, m/sec<br>$\rho_b$ = bulk density, g/cm$^3$<br>S = surface area, m$^2$<br>PE = Thornthwaite's index | 4 | Limited testing performed at a coal pile |

Having reviewed the available emission factors along with experimentally derived relationships between emissions and velocity, it remains unclear exactly what role wind velocity plays in the particulate emissions from storage piles.

## PARTICLE TRANSPORT

To properly understand why pile shape and orientation could have an effect upon emissions caused by wind erosion from storage piles, it is first necessary to understand those forces which act upon the particles causing them to become airborne. Basically, there are four forces which act upon a particle immersed in a moving fluid. The first force is caused by the impact of the fluid upon the particle and is called the impact pressure or form drag for a particle lying on the ground. The second force acts as a negative pressure on the leeward side of the particle and is termed the viscosity pressure. This pressure varies with the velocity of the fluid as well as its density and its coefficient of viscosity. This pressure is also termed the skin friction drag. Together, these two forces are the total drag exerted on the particle and are symbolized by the term $F_c$ in Figure 1. The third force acting upon the particle is the lift force ($L_c$) caused by the Bernoulli effect which states that whenever the fluid velocity is increased, as at the top of a particle, the pressure transverse to the direction of the fluid motion is reduced. Since the air speed increases travelling over the top of the particle, the decrease in pressure at the top of the particle causes a lifting force. This force acts through the center of gravity as is shown in Figure 1. The final force acting on the particle is that of gravity.

To get the particle airborne, particle movement must first be initiated. From Figure 1, the threshold drag acting on a particle would be:

$$F_c = (0.52\ g\ D^3\rho' - L_c) \tan \phi \qquad (1)$$

where:

$F_c$ = threshold drag
$g$ = acceleration due to gravity
$D$ = particle diameter
$\rho'$ = immersed density of the particle
$L_c$ = lift force
$\phi$ = angle of repose of the particle with respect to the average drag level of the fluid

It has been experimentally determined that $L_c = 0.75\ F_c$ for any size of spherical particle. Also, since the drag and lift forces per unit of horizontal area acting on the topmost particle are larger than drag and lift for the entire bed, the equation is modified to include a factor n which expresses this ratio. Another factor, T, is introduced to express the ratio of maximum to mean lift and drag on the particle. This factor is important since it has been observed that the longitudinal turbulence intensity is about 33 percent near the bed. If a normal distribution is assumed for velocity fluctuations, then instantaneous velocities would be twice the mean while instantaneous drag values would be four times the mean (Reference 6).

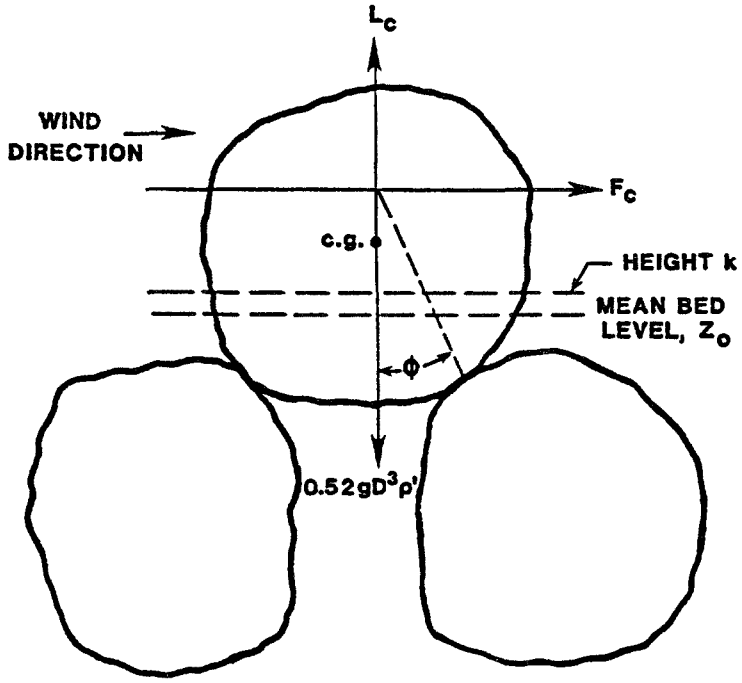


Figure 1. Forces of lift, drag and gravity acting on a soil grain in a windstream at the threshold of movement of the grain.(Ref. 5)

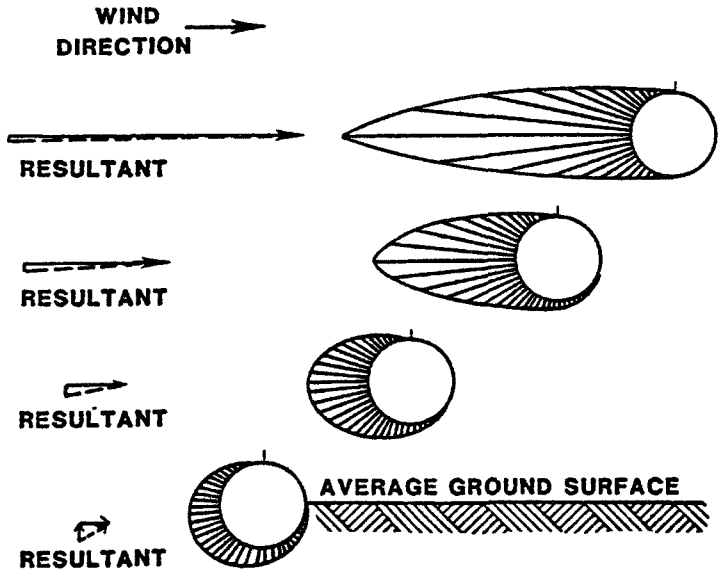


Figure 2. Pattern of approximate pressure differences. (Ref. 5)

Combining all of these factors and dividing by the area of the particle ($0.7854D^2$) gives:

$$\tau_c = \frac{0.66\ g\ D\ \rho'\ n\ \tan\phi}{(1 + 0.75\ \tan\phi)\ T} \qquad (2)$$

where $\tau_c$ is the mean threshold drag per unit horizontal area of the whole bed of material. Since the wind induced surface shear stress is:

$$\tau = \rho\ U_*^2 \qquad (3)$$

where:

$\rho$ = density of air

$U_*$ = friction velocity

$$= \frac{U}{2.5\ \ln\ (z/z_o)}$$

$U$ = mean wind velocity at height $z$

$z_o$ = height where $U = 0$

it can be seen therefore that the force necessary to initiate particle movement is directly related to the air velocity squared.

Having initiated movement, the forces acting on the particle change as the particle moves upwards. The drag force increases with height as does the velocity while the lift force due to the Bernoulli effect decreases rapidly. This is shown in Figure 2. It is expected that at sites such as a coal pile thermal drafts would help to raise the particles still higher into the air.

In summary, therefore, a relationship between the square of the velocity and emissions is indicated by theory.

## RESULTS OF STUDIES

Since it has been shown that the air velocity is the primary force governing individual particle transport, the question remains why such a relationship is not more evident in the available emission factors. Seeking to show that pile shape and orientation have an effect upon the local velocity field around a storage pile, two studies were undertaken. The first study was performed in a wind tunnel and its purpose was to determine if the velocity at the top of a model storage pile was affected by the angle of the slope leading to it. A second part of this study was to determine if emissions from the model varied according to its orientation. The wind tunnel and measurement methods used were described previously (Reference 7).

The second study was a field program performed to measure the wind flow over a hill. The purpose of this study was to determine if the velocity increases noted in the wind tunnel study would also be observed.

Wind Tunnel Study

Figure 3 shows the results of the effect of the slope of the leading edge upon the air velocity at the top of the storage pile. In the ratio $V_p/V_o$, $V_o$ is the velocity taken at the same height as the top of the pile but 6 inches in front of it. Little or no change in the value of $V_p/V_o$ with increasing wind speed was noted for very shallow (10°) or steep (90°) leading edge slopes, but marked increases were observed for the intermediate (30°, 45°, and 60°) slopes.

To determine the effect of pile orientation upon emissions, 50g of coal dust were sprinkled on the top of the model at each orientation, and the tunnel free stream velocity was set to 20 mph. Although various sizes of coal dust were used, all of the results were within about 20 percent. When the pile was placed length-wise in the tunnel, emissions averaged 0.008 $g/ft^3$. When placed width-wise, the emissions were about 0.02 $g/ft^3$. It was obvious from observation that the leading edge of the pile was where most of the erosion took place. By placing the pile width-wise in the air stream, the area of the high erosion zone more than doubled.

Wind Flow Over a Hill

The incident wind speed ($V_1$) was monitored approximately 15m to one side of the hill, at an elevation of 1m. For various locations on the hill, wind velocity measurements ($V_2$) were also obtained at 1m above the surface (Figure 4). The data recorded at each monitoring location are presented in Table 2. In addition, average $V_2/V_1$ ratios are noted in Figure 4.

As the incident wind approached the hill, $V_2/V_1$ was observed to decrease at the foot of the hill. On the upwind slope of the hill, $V_2/V_1$ values increased, with a maximum of 1.6 recorded at the hill crest. $V_2/V_1$ values then decreased to the lee of the hill crest.

TABLE 2. MEASURED WIND ACCELERATION ALONG THE SLOPE OF A HILL

| Location, X, M from Crest | Incident Wind Speed ($V_1$) | Measured Wind Speed ($V_2$) | $V_2/V_1$ | Average $V_2/V_1$ |
|---|---|---|---|---|
| 4.90 | 8.1 | 6.6 | 0.8 | 0.8 |
| 3.25 | 6.5 | 6.9 | 1.1 | |
| 3.25 | 7.0 | 6.5 | 0.9 | 1.1 |
| 3.25 | 6.2 | 7.8 | 1.2 | |
| 1.38 | 6.5 | 8.5 | 1.3 | 1.3 |
| 0 | 7.0 | 9.6 | 1.4 | |
| 0 | 8.1 | 11.6 | 1.4 | |
| 0 | 6.2 | 10.4 | 1.7 | 1.6 |
| 0 | 5.5 | 8.6 | 1.6 | |
| 0 | 6.7 | 11.6 | 1.7 | |
| -1.71 | 5.5 | 8.1 | 1.5 | 1.5 |
| -3.20 | 6.7 | 8.7 | 1.3 | 1.3 |

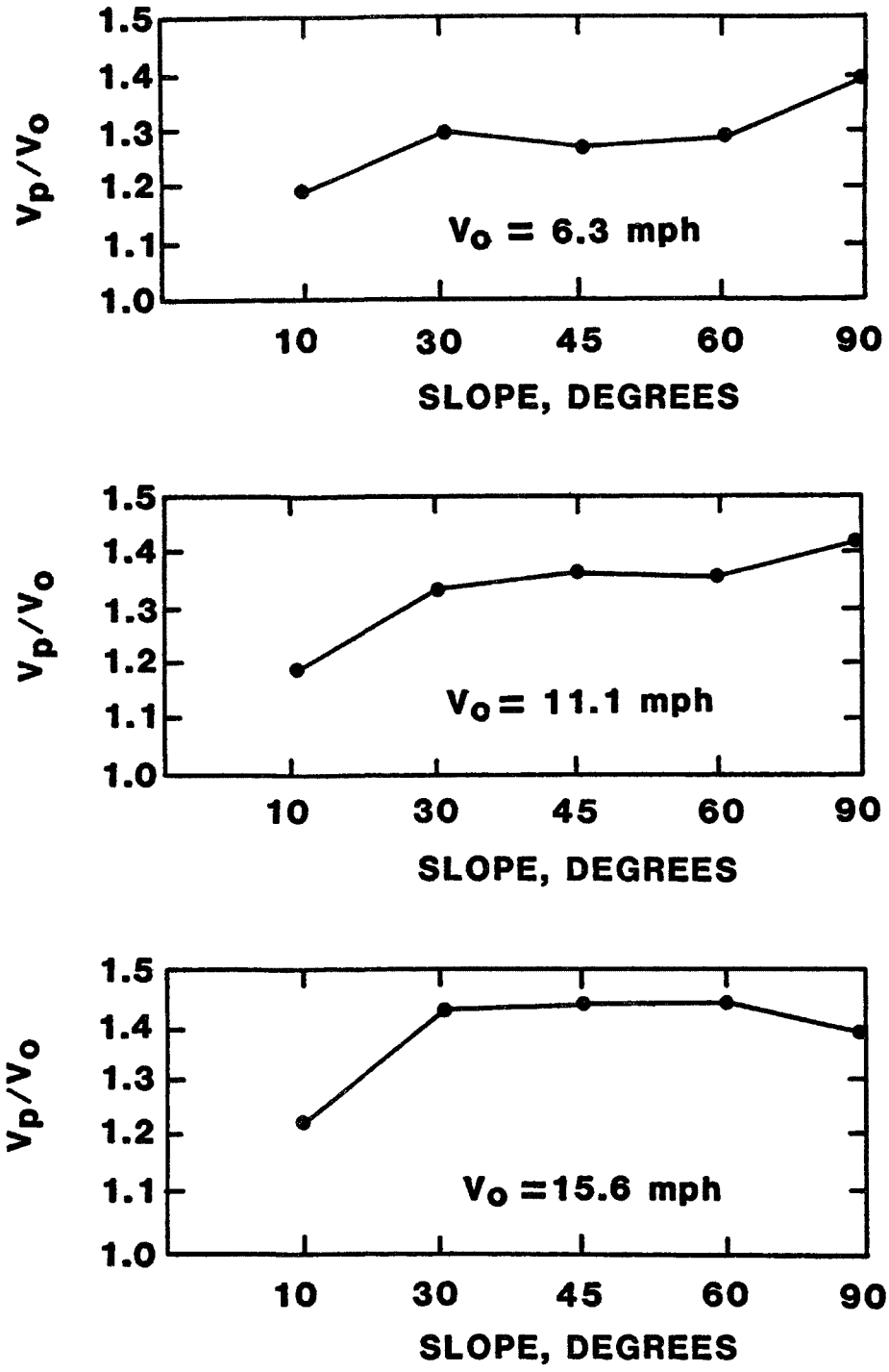


Figure 3. Relationship between velocity at top of pile (Vp) divided by upstream velocity at same height (Vo) vs. angle of slope of leading edge.

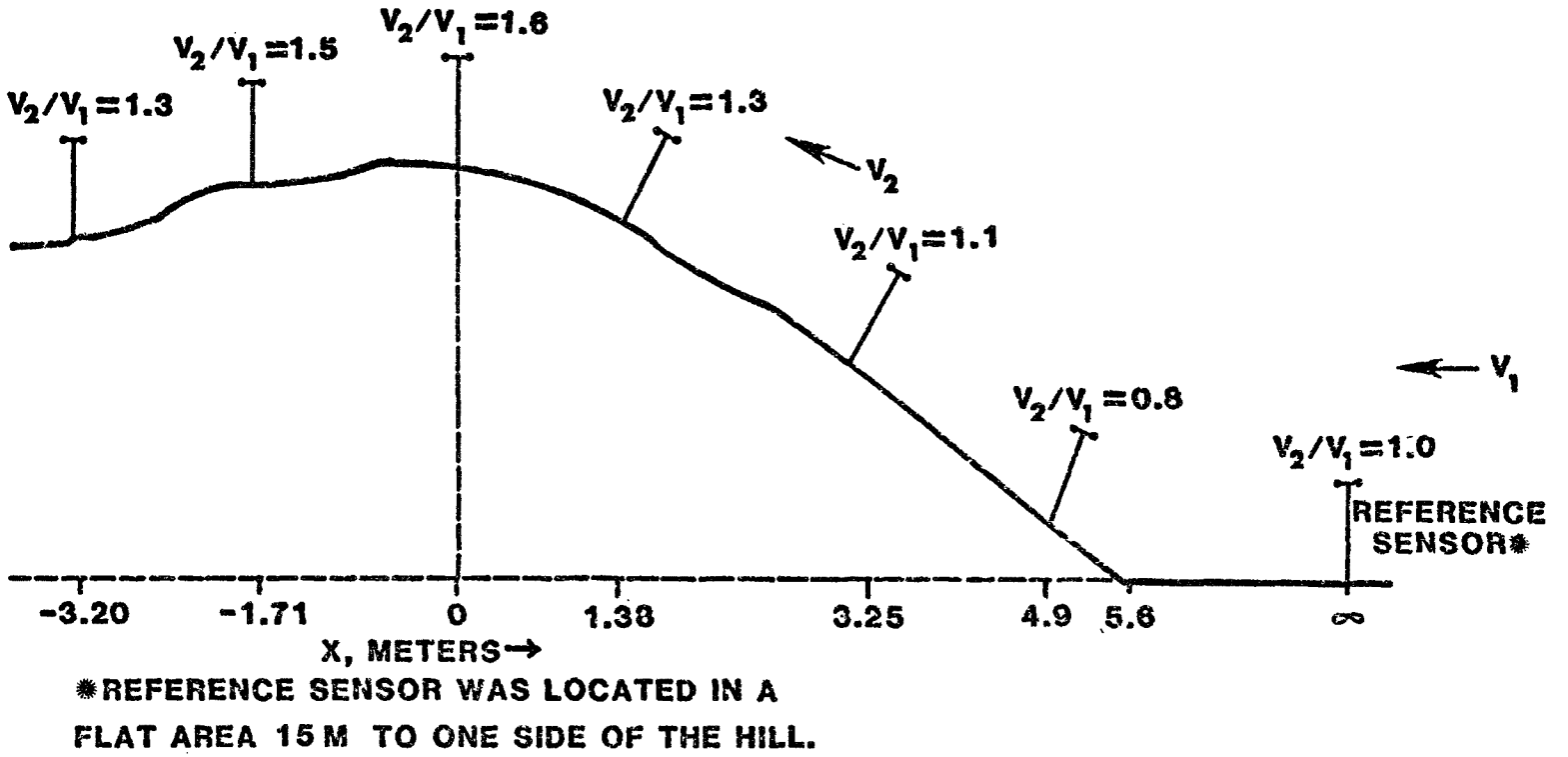


Figure 4. Location of sensors for monitoring wind velocities over a hill.

## CONCLUSIONS

From theoretical consideration it was shown that the square of the velocity is related to the initiation of particle movement and subsequent transport. From the results of our study it was shown that the orientation of the pile could affect the emissions by as much as a factor of 2.5. Also, it was observed that the air will accelerate up the sides of these piles making velocities at the top 20 to 50 percent higher than anticipated. These results could explain why emission factors developed from field studies do not correlate well with $V^2$ since this relationship is masked by the effects of pile shape and orientation. A further result of this study is the possibility that the existing emission factors could be modified to account for the orientation effect. If it is assumed that the field studies which developed the data for these factors were performed with the samplers placed parallel to the length of the pile then the factors represent a maximum emission rate potential. If the prevailing wind direction is perpendicular to the length of the pile then the emission factor should be able to be reduced by about 60 percent.

Control techniques applicable to storage piles can be better applied if the effect of shape and orientation are taken into account. Windscreens placed on top of the pile would control the acceleration effect and reduce or eliminate the zone of high erosion. Watering or chemical stabilization should be concentrated on the edge of the pile most affected by the wind. The slope of the pile in the prevailing wind direction should be limited to less than $10^{o}$.

## REFERENCES


1. U.S. Environmental Protection Agency. Compilation of Air Pollutant Emission Factors. Third Edition. AP-42 (NTIS PB 275525). August 1977.

2. Cowherd, C., Bohn, R., and T. Cuscino. Iron and Steel Plant Open Source Fugitive Emission Evaluation. Midwest Research Institute. EPA-600/2-79-103 (NTIS PB 299385). May 1979.

3. Cowherd, C., Cuscino, T., and D. Gillette. Development of Emission Factors for Wind Erosion of Aggregate Storage Piles. APCA Paper No. 79-11.1 Presented at the 72nd Annual Meeting of the Air Pollution Control Association. June 1979.

4. Blackwood, T.R. and R.A. Wachter. Source Assessment: Coal Storage Piles. Monsanto Research Corporation. EPA-600/2-78-004k May 1978.

5. Chepil, W.S. and N. P. Woodruff. The Physics of Wind Erosion and Its Control. Advances in Agronomy, Vol. 15, pp 211-302. 1963.

6. Lyles, L. and R. K. Kraus. Threshold Velocities and Initial Particle Motion as Influenced by Air Turbulence. Transactions of the ASAE, Vol. 14, pp 563-566. 1971.

7. Martin, D. and D. Drehmel. Control Methods for Fugitive Area Sources. In: Proceedings, Fourth Symposium on Fugitive Emissions: Measurement and Control, New Orleans, LA, May 1980. TRC - Environmental Consultants, Inc. EPA 600/9-80-041. pp 402-415, December 1980.

# SPRAY CHARGING AND TRAPPING SCRUBBER FOR FUGITIVE PARTICLE EMISSION CONTROL

By: Shui-Chow Yung and Seymour Calvert
Air Pollution Technology, Inc.
4901 Morena Blvd., Suite 402
San Diego, CA 92117

Dennis C. Drehmel
Particulate Technology Branch
Industrial Environmental Research Laboratory
U.S. Environmental Protection Agency
Research Triangle Park, NC 27711

## ABSTRACT

The control of fugitive process emissions (FPE) with Spray Charging and Trapping (SCAT) scrubber was evaluated both theoretically and experimentally. The SCAT uses air curtain and/or jets to contain, convey, and divert the FPE into a charged spray scrubber.

Experiments were performed on an 8000 cfm bench-scale spray scrubber to verify the theory and feasibility of collecting fugitive particles with charged water spray. The effects of charge levels on drops and particles, nozzle type, drop size, gas velocity, and liquid/gas ratio on collection efficiency were determined experimentally. The results of the experiments and the comparison between theory and data are presented.

An air curtain was developed for conveying the FPE to the spray scrubber, deflecting the crosswind, and containing hot buoyant plume. The design and air flow field for the air curtain are presented.

NOTE: Published in the Journal of the Air Pollution Control Association, 30:1208-11, November 1980.

# IMPROVED STREET SWEEPER FOR CONTROLLING URBAN INHALABLE PARTICULATE MATTER

By: S. Calvert, H. Brattin, S. Bhutra, R. Parker
Air Pollution Technology, Inc.
4901 Morena Blvd., Suite 402
San Diego, CA 92117

D. Drehmel
Particulate Technology Branch
Industrial Environmental Research Laboratory
U. S. Environmental Protection Agency
Research Triangle Park, NC 27711

## ABSTRACT

Dust emissions from paved roads are a major source of urban inhalable particulate matter. A.P.T. is conducting an experimental program to develop design modifications which can be used to improve the ability of municipal street sweepers to remove inhalable dust particles from the street.

A commercial regenerative air sweeper has been purchased and modified. Major modifications include a charged spray scrubber for fine particle collection and a gutter broom hood to help contain redispersed dust particles. Design information and preliminary test data are presented.

## INTRODUCTION

Dust emissions from paved roads are a major source of urban air pollution. Draftz (1978) estimated that 40 to 70% of the total suspended particulate matter in many urban areas comes from dust particles redispersed by road traffic. Pitt (1978) estimated that city streets can contribute from 5 to 50 $\mu g/m^3$ of particulate matter to the urban air.

The existing types of street sweepers include broom, vacuum, regenerative vacuum, and water flushing sweepers. These generally have low-to-moderate efficiency for removing inhalable particulate matter (IPM) from streets and test data scatter widely. Buchwald and Schrag (1967) sampled the air inside the driver's cab and determined that there is a serious exposure to respirable dust. Closing the windows and the use of a cyclone separator for dust collection had small effect on respirable dust concentration in the cab. It is clear that urban street dirt can cause air pollution, water pollution from rain water runoff, and an occupational hazard for the sweeper operator.

When evaluated with regard to IPM removal, each of the conventional types of sweepers has a significant deficiency, as indicated below.

| Type of Sweeper | Deficiency |
|---|---|
| Broom | Disperses IPM while sweeping. |
| Vacuum | Either emits IPM or must clean a large volume of vent air. Gutter broom disperses IPM into air. |
| Regenerative vacuum | Disperses IPM while sweeping. |
| Water flush | Moves IPM to gutter and causes water pollution. |

## OBJECTIVE

Under E.P.A. contract, A.P.T. has conducted a research and development program with the primary objective of developing practical means for improving the efficiency of a suitable street sweeper for the removal of IPM from urban streets.

A.P.T. evaluated the problem and proposed to develop a street sweeper which would use a regenerative air flow system, gutter broom hooding, and a low-volume scrubber on a vent air stream. The use of a vent air stream would permit a positive inward flow of air from the sweeping area into the sweeper body rather than allowing this dusty air to be dispersed. The applicability of the SCAT (Spray Charging and Trapping) system was to be investigated.

The SCAT system uses combinations of air curtaining, hooding, and spray scrubbing (with or without electrostatic augmentation) to capture and retain particles for subsequent disposal. Specific circumstances dictate the SCAT features which are used in each case.

Additional objectives of the program were to:

1. Build a modified street sweeper and demonstrate its capabilities for urban street sweeping.

2. Develop and use methods for evaluating sweeping efficiency.

## APPROACH

The general approach of the program was consistent with the premise that a suitable scrubber could be designed if one knew what air flow rate and particle collection capability were required. In other words, much more was known about scrubber design than about street sweeping in terms of IPM

control parameters. Consequently, the main effort was placed on determining:

1. Background information on street sweeping.

2. The street sweeper best suited for study.

3. A tentative set of design criteria to use for designing the experimental street sweeper, including:

   a. Air flow rates required to control dust emissions.
   b. The total air flow rate which has to be scrubbed.
   c. Particle size distribution and particle concentration in the uncontrolled effluent air.
   d. Utilities limitations.

4. Design concepts for the modifications needed for IPM control.

5. An experimental procedure for determining the efficiency of removing IPM from urban streets.

A limited effort was expended on charged spray scrubbing and scrubber design. Some experimental work was done to confirm earlier experiments and to evaluate concepts for atomizers and drop chargers which could produce smaller charged drops than used in previous work. The further development of a mathematical model for particle collection by charged spray also received some effort.

## RESULTS

A literature search and interviews of qualified persons were conducted to determine:

1. The nature of dirt on paved streets, including information on the sources of particulate matter, the methods of deposition, and various methods of removal.

2. The prevalent types of street sweepers available, their cost, and the potential for improving them.

3. Methods for sampling and analysis of the IPM on the street and in the air.

There is abundant literature on street dirt and its contribution to air and water pollution. There is, however, very little on the subject of street sweeper efficiency as a function of dust particle size. Brookman and Martin (1979) present an extensive literature review and recommendations for research areas. Some of the works which provide useful quantitative information are those of Axetell and Zell (1977), Cowherd et al. (1977), Draftz (1978), Pitt (1978), Sartor and Boyd (1972), and Sehmel (1973).

At the time the research began, broom sweepers were the type most commonly used. However, the trend appeared to be toward the use of regenerative vacuum sweepers, so this was the type selected for our use.

Street sweeping effectiveness has been determined in several ways, such as:

1. Ambient air was sampled upwind and downwind from the street to determine the contribution of dust from the Street (e.g., Cowherd et al., 1977, and Pitt, 1978).

2. Street dirt loading was measured by vacuum-cleaned sample areas before and after sweeping (e.g., Cowherd et al., 1977).

3. Street dirt loading was measured by a combination of sweeping and water-flushing sample areas before and after street sweeping (e.g., Sartor and Boyd, 1972).

## Preliminary Design Criteria

Observation of street sweeper operation clearly showed that gutter brooms (GB) and leakage from the "pickup hood" were the major sources of IPM emissions from the regenerative vacuum sweeper (RVS). In order to design the vent air scrubber and the GB hoods, the required air flow rate was estimated from industrial ventilation practice to be about 28 to 56 $m^3$/min (1 to 2 x $10^6$ $ft^3$/min) vented through the scrubber.

The sweeper has a blower which the manufacturer rated at 280 to 340 $m^3$/min (10 to 12 x $10^6$ $ft^3$/min). Our tests showed that it can move about 50% of the rated capacity. This proved to be adequate for venting about 30 $m^3$/min while providing effective dust pickup in the hoods.

The SCAT scrubber uses preformed spray drops to collect the fine particles, and an entrainment separator to collect the drops and large partiles. The particles may be charged in an ionizing section before reaching the spray section, and the spray may be charged with induction electrodes near the nozzle water outlet.

The scrubber needs about 0.9 $\ell/m^3$ (3 gal. water/1,000 $ft^3$ air handled). For convenience, this translates to a 0.76 $m^3$ (200 gal.) capacity to allow once-through operation, and a reasonable time between refills. An existing 0.12 $m^3$ (30 gal.) tank plus an additional 0.64 $m^3$ (170 gal.) auxiliary will provide the required water. The scrubber comes equipped with a water pump which can provide 0.9 $\ell$/min (3 gpm) at 3,450 kPa (500 psi). For the first experimental sweeper, it was assumed that the existing water pump would suffice and that once-through water use would be acceptable.

## Experimental Apparatus

The basic sweeper was analyzed for air flow and dirt conveyance. Extra ducting was needed to transport the dirt from the RVS recirculating airflow system to the scrubber. Hoods were designed to contain the dust generated by the gutter brooms, and ducting was designed to carry this dirt to an appropriate place in the hopper.

It was necessary to develop a hood arrangement that allowed normal broom operation and also reduced fugitive broom emissions to an acceptable level. An abbreviated hood was designed that allowed brushing on the curb side. This hood operates with a high velocity suction airflow similar to a vacuum cleaner, and also uses the interaction of the rotating broom and street dirt to capture dust. The captured dust is conveyed to the main hopper with piping and flexible hose. A damper valve in the pipe section controls the airflow from the hood to the hopper.

Several street dust samples were taken from the plumes dispersed by broom and vacuum type sweepers. The representative particle size distribution had a geometric mean diameter, $d_{pg}$, of 4 μmA and geometric standard deviation, $\sigma_g$, of 2. Experiments on charged spray scrubbing were conducted to verify and extend the results of previous studies.

Predictions of scrubbing efficiency based on the preliminary information on street dust size indicated that a minimum of 90% efficiency could be obtained within the constraints of the available power, space, and water.

The scrubber and accessories were designed conservatively so that enough space was allowed for additional airflow. Other main elements, such as the entrainment separator, were also designed so that their capacity could be increased if the need arose.

The sampling system provides for the measurement of airflow from the gutter brooms to the scrubber inlet. Particle size and concentration were measured with cascade impactors. Sample ports were provided for the scrubber inlet and outlet at locations at least 8 duct diameters from upstream transitions or bends. Sample trains of the type used for EPS Method 5 were used. Scrubber and GB airflow rates were measured with Venturi meters and were controlled by dampers.

The positive displacement water pump was calibrated in terms of auxiliary engine speed. Additional utilities (such as the electrical power supplies for sampling pumps and scrubber charging, water tank and transfer pump, sampling personnel station, and platform for sampling trains) were placed on a trailer pulled by the street sweeper.

## Street Dust Sampling

Initial full scale operation of the sweeper and auxiliary equipment in San Diego was used to observe the modified components in use, and to provide more data on the nature of street dirt. Later, as the apparatus was refined, additional samples were gathered on other streets, and eventually more were

gathered in heavy industrial areas in Los Angeles.

Twelve sampling runs were made, and results are summarized in Table 1. As can be seen, the concentration and particle size distribution vary greatly from location to location. Sampling results agree with visual observations in that dirtier streets resulted in higher particle concentrations and larger particles.

The data in Figure 1 show the effect of vent rate on mass concentration at the scrubber inlet. These data were taken from the same street site; only the vent rate varied. Run 18/7 had a higher vent rate and a higher mass concentration than Run 18/11.

Street samples collected so far indicate a difference in characteristic size dirt when neighborhoods are considered. The major distinction noticed between neighborhoods is the amount of traffic; street dirt is reduced in size by continuous traffic.

## Vent Air Rate

During the initial sampling runs it was noted that "puffs" of dust escaped from the main pickup hood, suspended dust was continuously generated by the G.B.'s, and the G.B. water sprays were ineffective for reducing fugitive emissions. When the pickup head travels on uneven street surfaces, dust puffs emerge from the pickup head.

These dust puffs are eliminated by opening the vent valve. This decreases the pressure on the discharge side of the blower and increases the suction in the hopper. As a result, the average pressure in the pickup head is reduced and air flows into the hood through any openings between the rubber seals and the pavement.

To minimize the scrubber size and water consumption, the air flow to be vented through the scrubber should be kept at a minimum. However, the air flow should not be so low that dust puffs occur around the gutter broom and the pickup head.

The minimum air flow needed to be vented through the scrubber to prevent the occurrence of dust puffs was determined when the gutter broom hoods were turned either ON or OFF. When ON, the air flow in each hood was maintained at 0.17 $m^3/s$ (350 acfm), which was the minimum required flow for satisfactory hood operation.

It was found that the minimum air flow to be vented through the scrubber to prevent dust puffs with the gutter broom hoods OFF was about 0.33 $m^3/s$ (700 acfm), and about 0.38 $m^3/s$ (800 acfm) with the gutter brooms ON.

## Efficiency Measurement Method

To determine the sweeping efficiency of the sweeper, a method is needed which measures the amount of dust that can be dispersed into the ambient air

by the mechanisms actually occurring on streets. The mechanisms of street dust removal are (Brookman and Martin, 1979):

1. Reentrainment (by air currents around moving vehicles).
2. Wind erosion (similar to 1, but due to natural air currents).
3. Displacement (similar to 1, re-deposition near street).
4. Rainfall runoff.
5. Street cleaning.

The first three mechanisms result in airborne dispersal of street dirt so the sampling method should measure the amount of IPM which can be dispersed by these.

Preliminary experiments were performed to measure street dust density with a brush-type vacuum cleaner, as performed by Dahir and Meyer (1974). The dust on the street was first loosened with a brush, and then taken up and filtered by the vacuum cleaner. The dust density (mass/unit street area) was determined from filter weight gain.

This method was found to have several deficiencies. The vacuum cleaner can remove dust which is deposited deeply in cracks and is not normally reentrained. Further, the amount of dust vacuumed increases with each pass of the vacuum nozzle; therefore, there is no logical end point for sampling.

Consequently, the above method was abandoned and a new method developed. The new method is a vacuum cleaner and a modified pickup nozzle. The pickup nozzle is shown in Figure 2. The nozzle is shaped to create a uniform 97 km/hr air flow field at the street surface. The dust dislodged by the airflow is sucked into the vacuum and filtered by the vacuum bag. This method should simulate the dust reentrainment mechanisms.

A detailed definition of reentrainment would require a complex model of airflow around an automobile. Assuming that the maximum air velocity caused by the passage of an automobile will not exceed its velocity, and that 97 km/hr (70 mph) is a reasonable maximum automobile velocity, the resultant maximum reentrainment velocity would be 97 km/hr.

Wind speeds are generally much less than 97 km/hr (27 m/s), so this velocity is conservatively high to represent the influence of wind erosion.

The displacement mechanism is essentially similar to that for reentrainment, and due to the same vehicular motion. The definition differs in that the particles stay in suspension only long enough to reach the area immediately adjacent to the street. An air velocity of 97 km/hr would adequately represent this vehicle-induced mechanism.

Efficiency Data

The jet nozzle street dust sampling method was used; representative results are shown in Figure 3, a plot of street dust density before and after sweeping. Street dust is concentrated in the gutter area. The street sweeper sweeping efficiency can be calculated from the results presented in

Figure 3. The sweeping efficiency ranges from 75% to 97% for measurements to date.

## CONCLUSIONS

Results to date show that the application of SCAT to the control of fugitive road dust emissions is feasible. The regenerative vacuum sweeper (RVS) is ideally suited to the SCAT technique, as it allows a discharge stream of air to be cleaned and recycled into the atmosphere. This feature reduces the size and power requirements necessary for control of fugitive emissions of IPM.

Gutter broom dust emissions can be substantially improved with an advanced, interactive gutter broom hood. Since most of the dirt is in the gutter, this improvement is very significant. Additional power requirements for the SCAT system are minimal. Existing standard equipment pumps, blowers, and auxiliary power are sufficient to do the job.

## END NOTES


1. Axetell, D., and T. Zell. "Control of Reentrained Dust from Paved Streets". U. S. Environmental Protection Agency, Washington, DC, NTIS. PB 280325, July 1977.

2. Brookman, E. T., and D. K. Martin. "Assessment of Methods for Control of Fugitive Emissions from Paved Roads". EPA-600/7-79-239 (NTIS PB80-139330), November 1979.

3. Buchwald, H., and K. R. Schrag. "Dust Exposure in Mechanical Street Sweepers". J. of A.I.H.I., 28, pp. 485-487, 1967.

4. Cowherd, C., et al. "Quantification of Dust Entrainment from Paved Roadways". U. S. Environmental Protection Agency, Washington, DC, EPA-450/3-77-027, NTIS PB 272613, July 1977.

5. Dahir, S. H. and W. E. Meyer. "Bituminous Pavement Polishing". The Pennsylvania State University, University Park, PA. November 1974.

6. Draftz, R. "The Impact of Fugitive Dust Emissions on TSP Concentrations in Urban Areas". In Third Symposium on Fugitive Emissions: Measurement and Control, U. S. Environmental Protection Agency, Research Triangle Park, NC. EPA-600/7-79-182 (NTIS PB 80-130891), August 1979.

7. Pitt, R. "Demonstration of Non-Point Pollution Abatement Through Improved Street Cleaning Practices". Prepared for the City of San Jose, Public Works Department, San Jose, CA. August 1978.

8. Sartor, J. D. and G. B. Boyd. "Water Pollution Aspects of Street Surface Contaminants". U. S. Environmental Protection Agency, Washington, DC. EPA-R2-72-081, November 1972.

9. Sehmel, G. A. "Particle Resuspension from an Asphalt Road". Atmospheric Environment, pp. 291-309, March 1973.

TABLE 1. SUMMARY OF SAMPLING RESULTS FROM LOS ANGELES AREA

| Industry | Traffic Conditions | Scrubber Flow Rate acfm | Total Mass Concentration mg/DNm$^3$ | Mass Median Diameter µmA | Geometric Standard Deviation $\sigma_g$ | Street Loading |
|---|---|---|---|---|---|---|
| Refinery | Medium-heavy | 710 | 3,190 | 10.0 | 4.5 | Heavy |
| Bridge | Very heavy | 710 | 770 | 5.2 | 3.5 | Heavy |
| Steel plant | Light-medium | 1,130 | 3,503 | 26.0 | 15.3 | Heavy |
| Refinery | Heavy | 1,130 | 684 | 65.0 | 8.1 | Medium |
| Coke plant | Heavy | 1,130 | 132 | 42.0 | 7.1 | Light-medium |
| Coke plant | Heavy | 1,130 | 193 | 100.0 | 8.7 | Light-medium |
| Steel plant | Light-medium | 710 | 386 | 7.7 | 7.0 | Heavy |
| Steel plant | Medium | 710 | 265 | 17.5 | 4.9 | Medium |
| Steel plant | Medium-heavy | 710 | 362 | 13.1 | 5.0 | Medium |
| Warehouse and steel plant | Medium | 710 | 134 | 15.4 | 4.3 | Medium |
| Grain mill | Heavy | 1,130 | 556 | 170.0 | 9.4 | Medium heavy |
| Warehouse | Medium | 1,130 | 2,186 | 47.0 | 5.4 | Heavy |

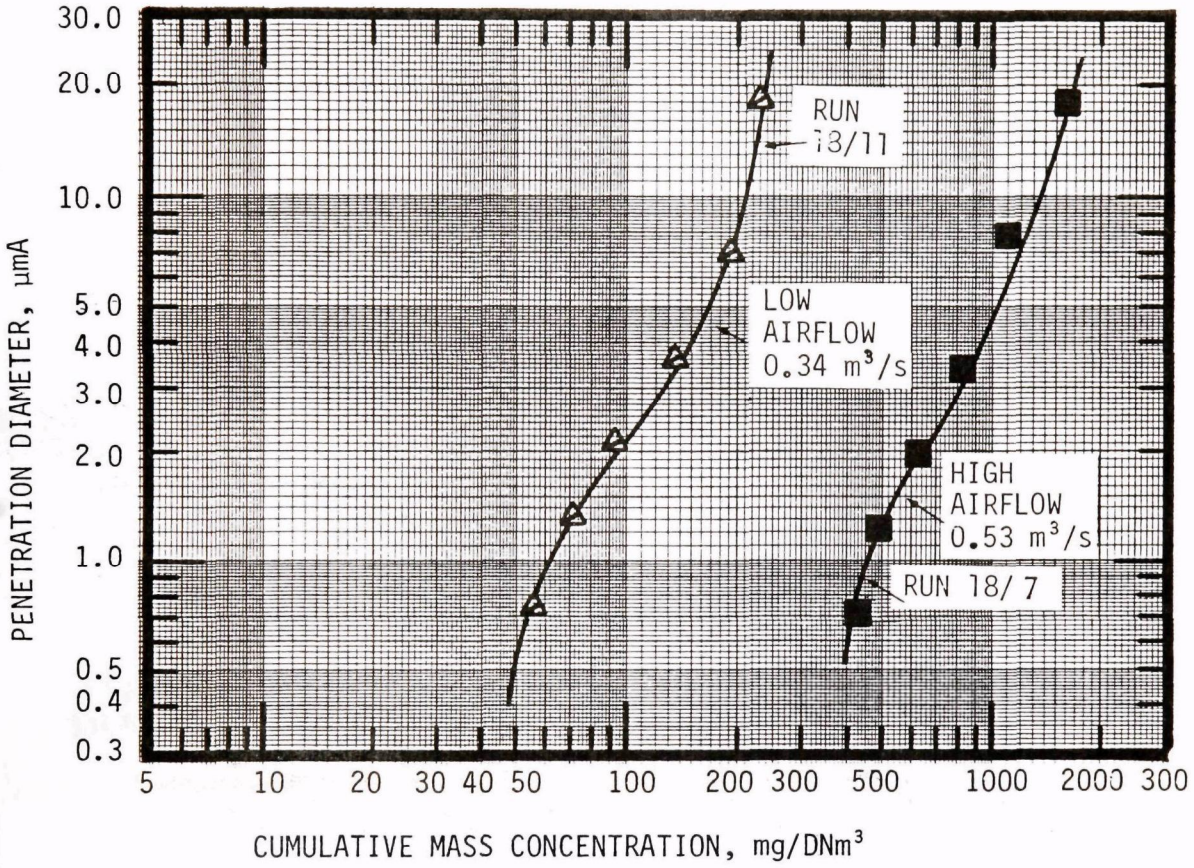


Figure 1. Effect of vent air flow on scrubber inlet dust concentration.

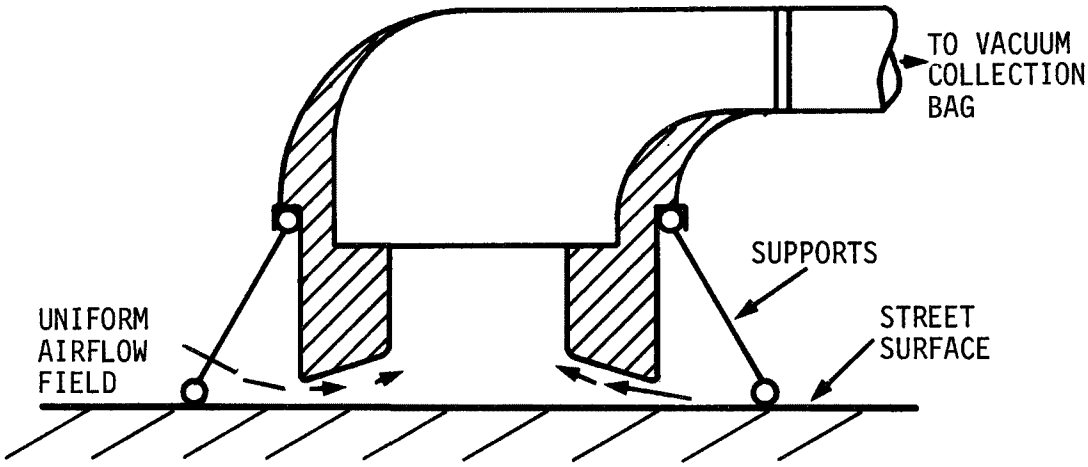


Figure 2. Uniform airflow vacuum nozzle.

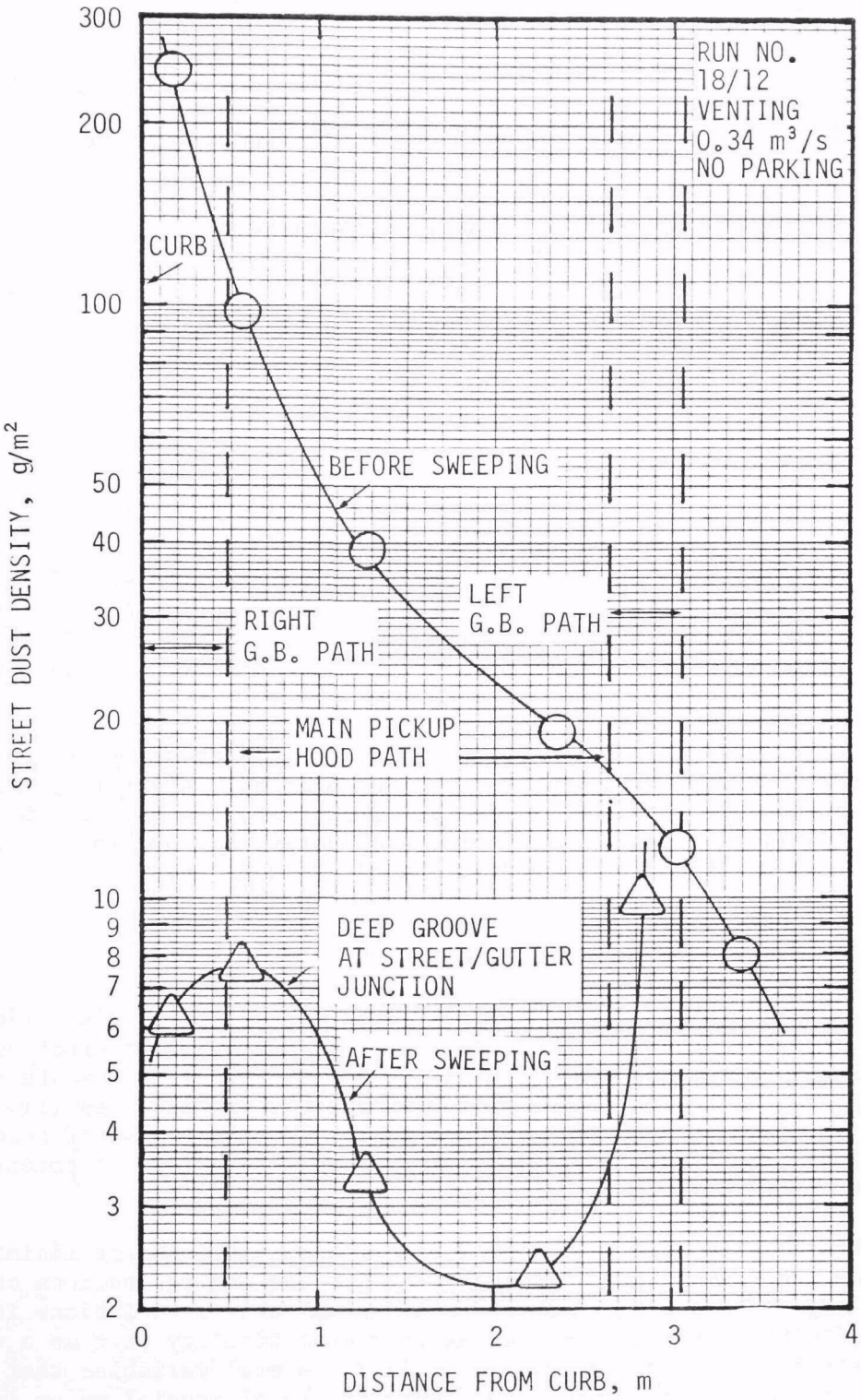


Figure 3. Street dust distribution before and after sweeping.

# A WIND TUNNEL FOR DUST ENTRAINMENT STUDIES

By: A.S. Viner, M.B. Ranade
Research Triangle Institute
P.O. Box 12194
Research Triangle Park, North Carolina 27709

E.J. Shaughnessy
Department of Mechanical Engineering
Duke University
Durham, North Carolina 27706

D.C. Drehmel, B.E. Daniels
Industrial Environmental Research Laboratory
U.S. Environmental Protection Agency
Research Triangle Park, North Carolina 27711

## ABSTRACT

A wind tunnel facility has been fabricated at the Industrial Environmental Research Laboratory (IERL) of the Environmental Protection Agency (EPA) at Research Triangle Park, NC, to assess potential emissions from different dust types and source configurations, and to evaluate control techniques to reduce emissions.

The aerodynamics of the wind tunnel is designed to study the effects of velocity profiles and turbulence on dust entrainment. A sampling protocol was developed to measure emission rates from several model sources. The aerodynamics of the wind tunnel, experimental procedures, and prelimianry experimental data on dust entrainment are described in this paper.

## INTRODUCTION

Dust entrainment from open sources first gained major scientific attention when wind erosion caused the dust bowls of the 1930's in the Great Plains of North America. Entrained dust from soils, storage piles, and waste sites has been recognized as a significant source of ambient particulates (1). Control of these fugitive dust emissions is desirable to prevent loss of resources (such as coal from storage piles) and to prevent the spread of potentially toxic dusts from waste dumps.

The EPA is responsible for developing control options for minimizing the impact from these emissions. Evaluations of these control options on a field scale are expensive and the measurements are subject to variations in atmospheric conditions. A reduced-scale experimental facility such as a wind tunnel is desirable to allow controlled study of several variables that influence erosion in the open atmosphere. This approach is of special value in screening control options.

A wind-tunnel facility was considered to be ideal for such investigations. Gillette (2) described a wind tunnel used to study threshold velocities for erosion. His tunnel was a portable, open-floored unit in which soil formed the floor. Soo, Perez, and Rezakhany (3) also used a wind tunnel to study the use of wind barriers for reducing entrainment from coal-dust piles.

## Description of the Wind Tunnel

Review of past work on particle entrainment by wind indicated that the dust entrainment test facility should be characterized by a long, square test section and should offer maximum access and visibility throughout its length. The flow near the floor over the dust sample should have a thick, turbulent boundary layer with a logarithmic velocity profile to simulate the form of the atmospheric boundary layer.

Options for design were somewhat limited because the test section would be a modification to the existing aerodymanic test facility which could be best described as an environmentally controlled, closed-loop wind tunnel. Because of the size of the fan already in place, the maximum available airflow was 680 $m^3$/min. With a fixed flowrate, a trade-off had to be made between the tunnel cross-sectional area and the wind velocity. A large cross-section was desirable because it would eliminate the boundary-layer effects of the side walls and ceiling. However, a conflicting concern was that a sufficient velocity be available to entrain, say, coal dust with an entrainment-reducing coating applied.

Based on these requirements, a new test section with a 60 cm x 60 cm cross-section was designed and constructed. This cross-sectional area allows a maximum velocity of 30 m/sec and is of sufficient size to minimize ceiling and wall effects. The whole assembly, shown in Figure 1, is a bolt-on replacement for the original wind-tunnel test section. The structure is 9.8 m long and is constructed of aluminum, plexiglass, and plywood. The primary elements are aluminum channels and angle beams which ensure straightness and rigidity. The walls of the wind tunnel are virtually all plexiglass for maximum visibility. The plexiglass sheets are mounted on aluminum frames to form swinging doors which provide access to all points in the test section. Each door is 1.2 m long and there are eight doors to a side. The plexiglass ceiling is suspended from cross supports so that the height can be adjusted by adjusting the ceiling height at different points down the length of the tunnel. A larger floor-to-ceiling height may be provided at the tunnel exit than at the tunnel inlet. This divergence permits a uniform static pressure while slightly decreasing the velocity. Keeping the static pressure slightly below atmospheric eliminates sealing difficulties and ensures that dust entrained in the gas stream stays in the tunnel.

Several ways of generating a thick, turbulent boundary layer near the floor were considered. In short wind tunnels, complex vortex generators are required to get the necessary boundary layer. In this tunnel, however, the length was sufficient to develop the logarithmic profile using roughness elements. Two different types of roughness elements were tried; the first were lengths of 2.5 cm aluminum angle and the second were 1.25 cm, quarter-round wooden strips. The roughness elements were attached to the floor and placed

across the width of the tunnel. The first element was placed at the inlet, the second one 30 cm downstream, and so on until the last one located 4.6 m downstream of the inlet. The dust sample tray is 45 cm downstream of the last roughness element.

Velocity profiles were measured with a pitot tube and a hot-film anemometer to verify the aerodynamic design. The velocities were measured vertically from the floor, just upstream of the test section along the vertical centerline. The profile of mean velocities as measured at different nominal velocities is shown in Figure 2. The indicated flow settings correspond to the nominal flow speed in ft/sec. The nearly 30 cm thick boundary layer resulting from the 2.5 cm roughness elements is evident. Although not shown in these measurements, the ceiling boundary layer is less than 5 cm thick. Hot-film anemometer studies indicate that the flow is laminar between 30 and 55 cm from the floor. Horizontal velocity profiles, the profiles between the walls and parallel to the floor, are shown in Figure 3. The mean velocity is uniform to within 5 percent over the central 45 cm of the tunnel, and virtually constant over the central 30 cm.

The atmospheric boundary layer has a velocity profile which can be represented by:

$$U = \frac{U^*}{k} \ln (Y/Y_o) \qquad (1)$$

where $U$ is the velocity at height $Y$,

$U^*$ is the friction velocity,

$k$ is Von Karman's constant ($k=0.4$), and

$Y_o$ is the roughness length.

The vertical profiles as measured with a hot-film anemometer were compared to Equation 1. Figure 4 shows the vertical velocity profile resulting from 2.5 cm roughness elements at a nominal velocity of 23 m/sec. Figure 5 shows similar data for the 1.27 cm elements. A best-fit line through the data points indicates that $U^* = 3.5$ m/sec and $Y_o = 1.7$ cm for the 2.5 cm elements. For the 1.27 cm elements, $U^* = 1.5$ m/sec and $Y_o = 0.33$ cm. From the definition of friction velocity ($U^* = \sqrt{\tau_o/\delta}$), the shear stress can be calculated for known $U^*$ and $\delta$. The 2.5 cm surface roughening elements produce a shear stress of 14.4 N/m$^2$ and the 1.27 cm elements produce a value of 2.7 N/m$^2$. These values are typical of values encountered in the atmosphere.

The turbulence intensity was measured as a function of height from the floor. The results of these measurements are shown in Figure 6. The turbulence is greatest near the floor and rapidly drops to zero at the centerline of the tunnel.

## Experimental Setup and Procedure

A test procedure was developed to measure dust emissions and evaluate control options. The advantage of reduced-scale tests is that they offer the ability to determine the sensitivity of dust entrainment to individual para-

meters. The disadvantage of reduced-scale tests is that the relationship between data from wind-tunnel tests and data from actual performance tests in the open atmosphere is uncertain at best.

The most important parameter with regard to particle entrainment is the shear stress at the surface of the dust sample. As noted above, the shear stress at the surface is related to the shape of the velocity profile. Therefore, a change in the shape of the velocity profile would result in a change of the shear stress. For example, when wind flows over a pile, eddies introduced in the flow affect the shear stress. The inclusion of secondary flows would complicate the comparison of results from tests on different control options.

A dust tray was designed which could be inlaid in the floor of the test section as seen in Figure 7. When the tray is filled, the top surface of the dust is flush with the floor of the tunnel and the velocity profile is not appreciably altered. The tray has an area of 900 $cm^2$ and is 2.5 cm deep. It is equally spaced between the walls of the tunnel and 46 cm downstream of the last surface roughening element. At this location, the tray is not affected by the wall or ceiling boundary layers. The tray can be lifted out of the tunnel either to be filled with dust or to be weighed on a triple beam balance.

To measure the emissions from the dust sample, two sets of sample ports were drilled. There are two ports in each set, one in the floor and one in the wall of the tunnel. The first set of ports is located 2.44 m downstream of the dust tray and the second set is located 4.88 m downstream of the tray. A probe connected to either a Climet optical particle counter or a filter may be inserted into a port to determine the particle size distribution or mass. A similar set of ports located 15 cm upstream of the sample tray is used to measure the velocity profile.

Each test of entrainment involved filling the sample tray with dust and smoothing the surface. Then the tray was placed in the tunnel and exposed to a known velocity profile. Three methods to measure the rate of dust emission from the sample were investigated. For Methods 1 and 2, a probe was inserted in one of the ports located downstream of the tray. In Method 1, the probe was used to collect mass samples. In Method 2, the probe was used to collect samples for size-distribution analysis with an optical particle counter. A large number of particles were blown off very soon after the beginning of the test; after this initial phase, hardly any dust was entrained. These emission-measurement methods are sensitive to the transient structure of the sample surface; consequently, the results obtained with these methods were virtually impossible to reproduce. Method 3 was much more direct. By measuring the pre-test and post-test weights of the sample tray, it was possible to calculate the amount of mass entrained per unit area per unit time averaged over the duration of the test. A drawback of pre-test and post-test weighings is the requirement that the dust tray be removed from the tunnel for each data point to be obtained. Consequently there is the possibility of errors due to handling.

## Preliminary Results

Preliminary results on dust entrainment which were obtained using this facility are shown in Figure 8. A variety of dust types and sizes were used for these verification studies including flyash, flyash mixed with glass beads, and coal dust. The threshold velocities shown in Figure 8 compare well with the results of Gillette (2) who reported threshold friction velocities on the order of 50 cm/sec for grains with 1 mm diameter. The most important feature to note in Figure 8 is the higher velocities, and consequently higher shear stresses, required to entrain the smaller particles. These results agree with the observations of Chepil and Woodruff (4) who note, "Loose particles smaller than 0.01 mm (10 μm), if not mixed with coarser particles and if placed in a bed that is thoroughly smoothed, are not moved even by an exceedingly strong wind."

To entrain a small particle, the inertial and adhesive forces acting on it must be overcome by the shear stress of the wind. The shear stress in the laminar sub-layer which is present at the surface is considerably less than the shear stress in the turbulent layer surface. For this reason, a particle which is too small to protrude above the laminar layer is less likely to be entrained than a larger particle.

## Summary

In summary, we were able to design and construct a wind-tunnel section for modification of the EPA aerodynamic test facility. The design offers access to all points of the tunnel and visibility throughout its full length. The tunnel is long enough for surface roughening elements to generate turbulent boundary layers with a wide range of friction velocities.

Preliminary tests indicate that dust emissions can be measured in the tunnel and the shear stresses generated are sufficient to cause entrainment of particles of various sizes. Detailed tests of the effectiveness of emission control options are being studied.

## References


1. Cuscino, T.A., C. Cowherd, and R. Bohn. Fugitive Emission Control of Open Dust Sources. In: Proceedings: Symposium on Iron and Steel Pollution Abatement Technology for 1980, EPA-600/9-81-017, pp.71-84, March 1981.

2. Gillette, D. Tests with a Portable Wind Tunnel for Determining Wind Erosion Threshold Velocities. Atmos. Env. V. 12, pp.2309-2313, 1978.

3. Soo, S.L., J.C. Perez, and S. Rezakhany. Wind Velocity Distribution Over Storage Piles and Use of Barriers. In: Proceedings: Symposium on Iron and Steel Pollution Abatement Technology for 1980, EPA-600/9-81-017, pp.85-106, March 1981.

4. Chepil, W.S. and N.P. Woodruff. The Physics of Wind Erosion and its Control. Advances in Agronomy, V. 115, pp.211-302, 1963.

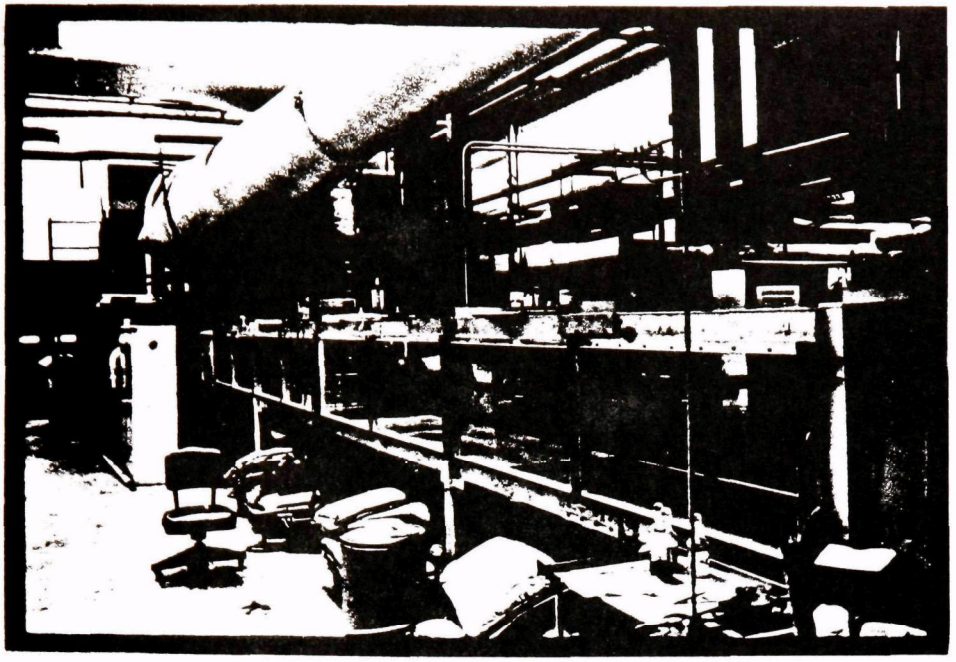

Figure 1a. The wind tunnel.

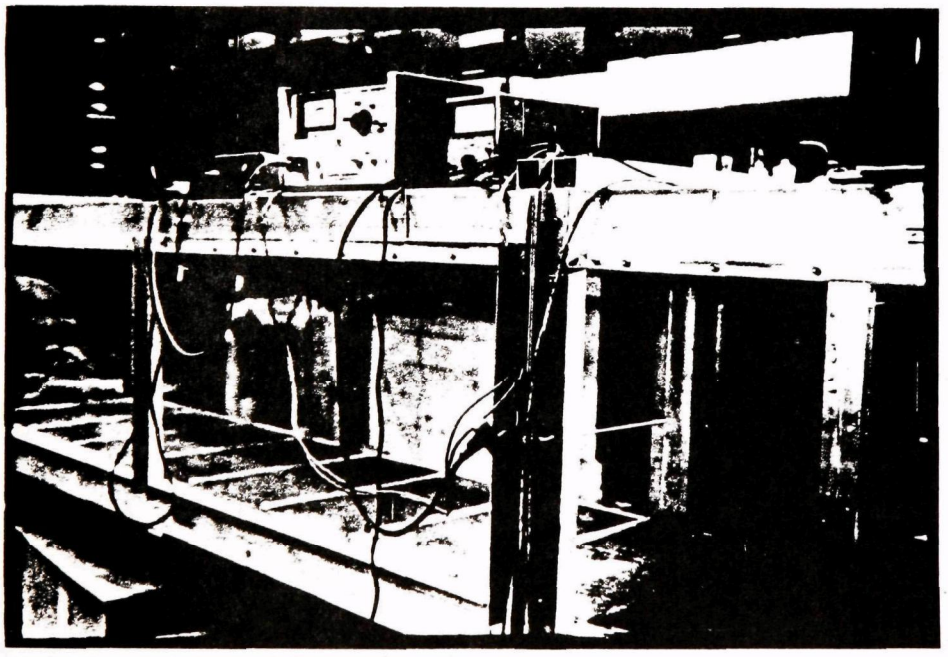

Figure 1b. Profile forming roughness elements.

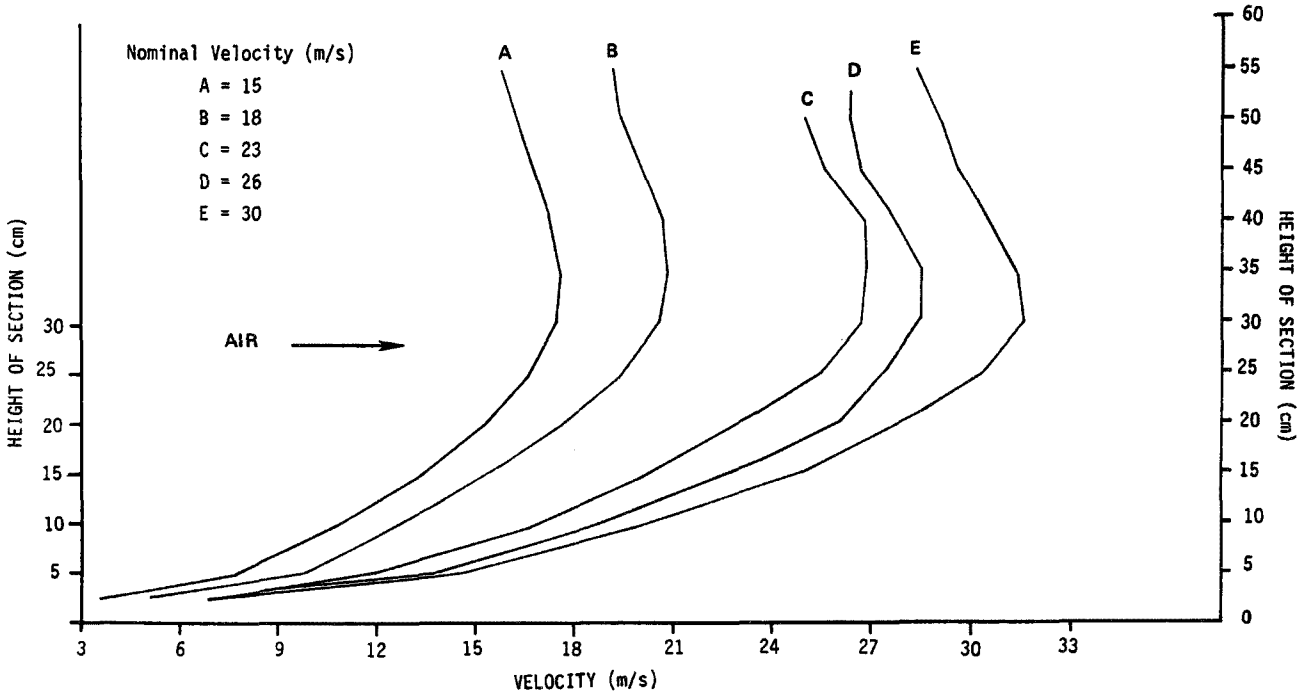


Figure 2. Vertical mean velocity profile at tunnel centerline.

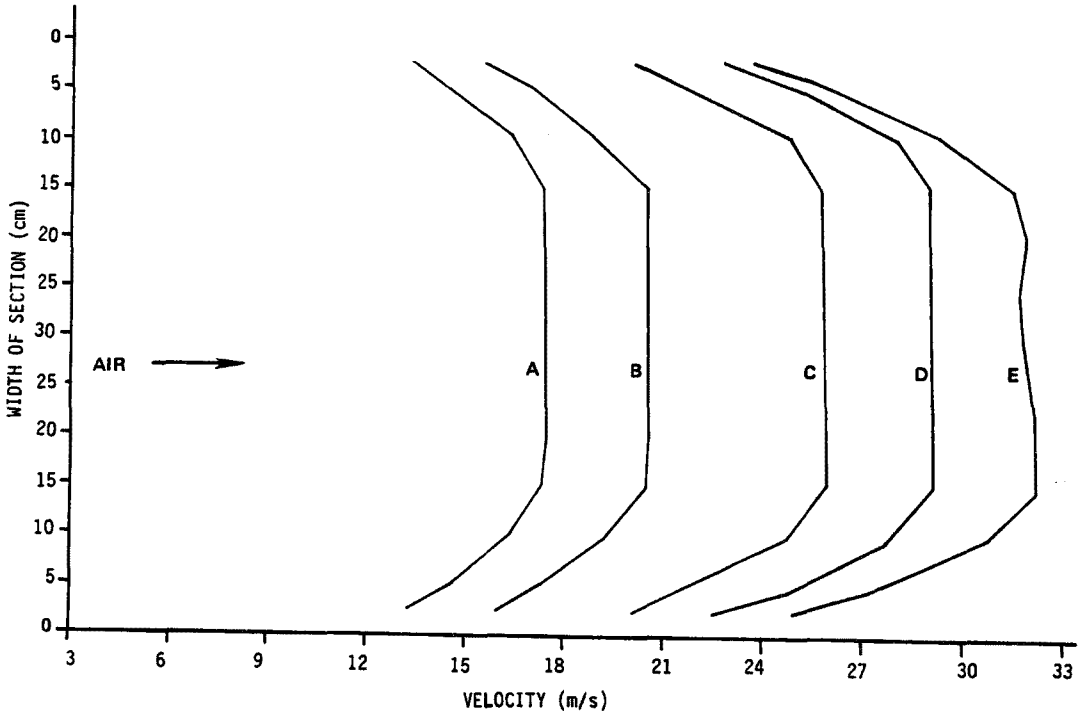


Figure 3. Horizontal mean velocity profile at tunnel centerline.

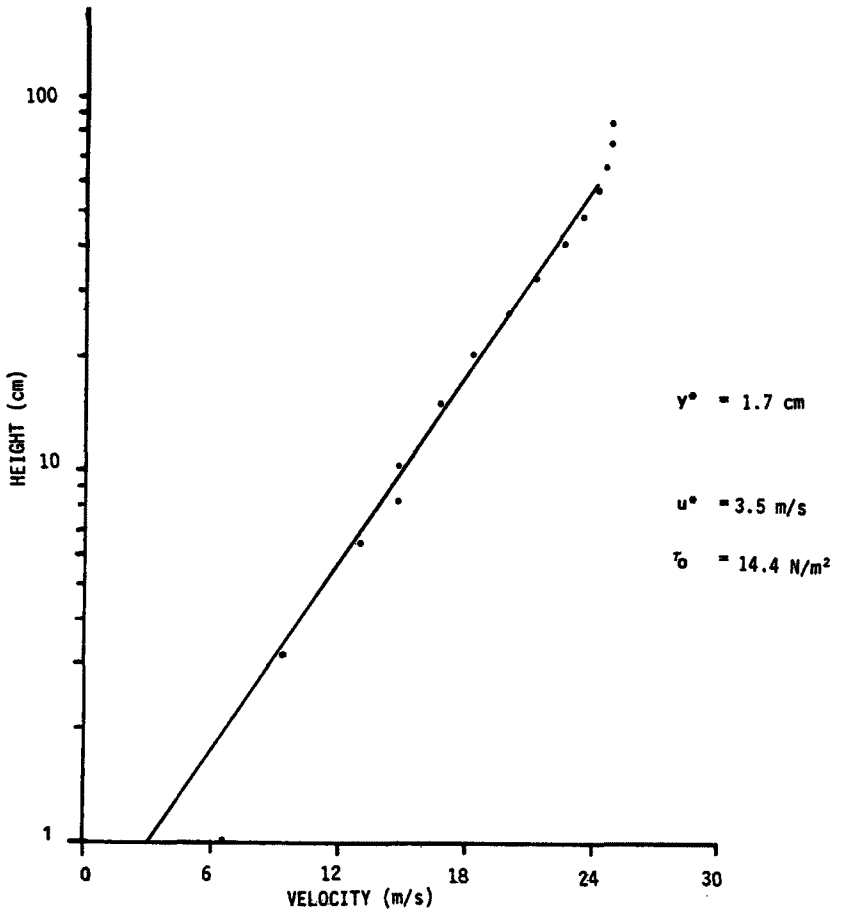


Figure 4. Boundary layer profile at 23 m/s, 2.5 cm roughness elements.

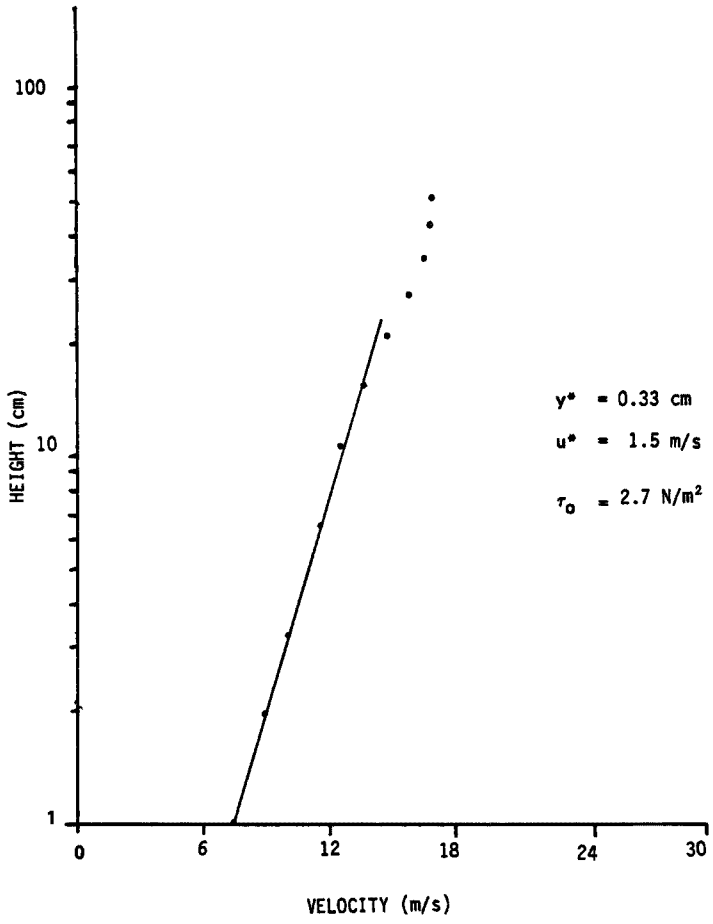


Figure 5. Boundary layer profile at 12 m/s, 1.27 cm roughness elements.

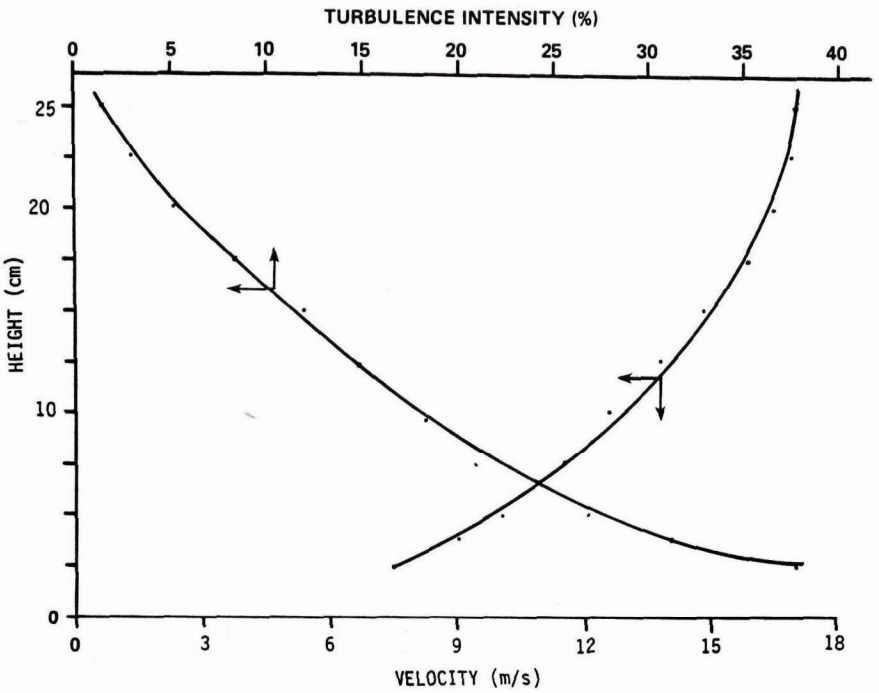


Figure 6. Boundary layer profile at 18 m/s, 1.27 cm roughness elements.

Figure 7. Dust tray in the wind tunnel.

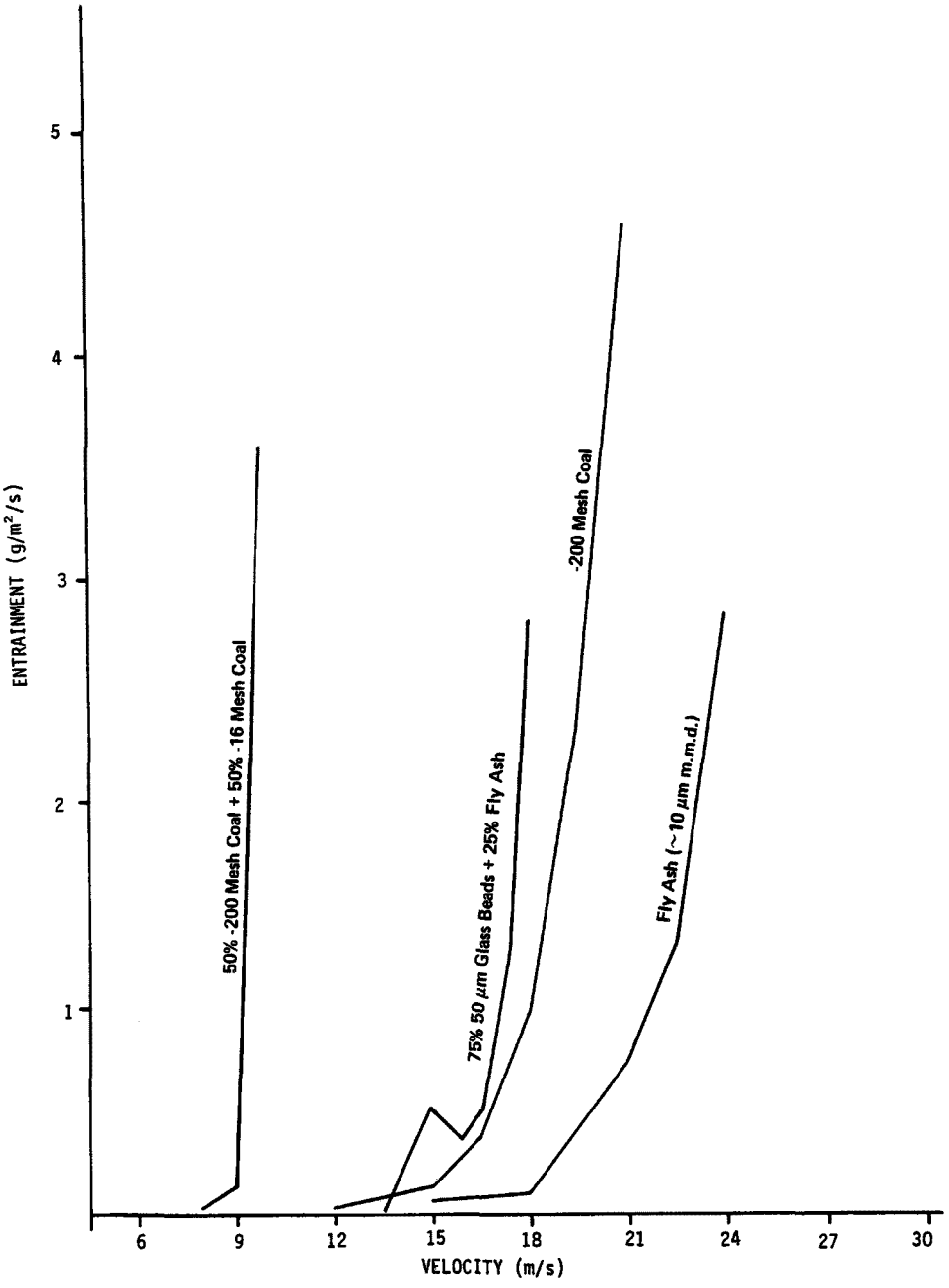


Figure 8. Preliminary results of entrainment tests.

# TECHNIQUES AND EQUIPMENT FOR MEASURING INHALABLE PARTICULATE FUGITIVE EMISSIONS

By: Henry J. Kolnsberg
TRC - Environmental Consultants, Inc.
Wethersfield, CT 06109

## ABSTRACT

The United States Environmental Protection Agency has initiated an extensive program to measure inhalable particulate matter (IP) emissions from a large number of industrial sources to obtain data for the development of IP emission factors. About half of the effort has been reserved for fugitive emissions measurements at a variety of industrial sites.

To respond to the special demands of sampling in the limited IP size range, the recognized sampling methods have been modified or restricted and a number of specialized sampling devices have been developed. It is expected that the modified sampling methods and special devices will provide the bases for future standard sampling procedures once an IP standard has been adopted.

This paper describes the sampling techniques and modifications being employed in the program. The IP sampling devices are also described, along with the results achieved in their initial applications.

## INTRODUCTION

One result of the Environmental Protection Agency's current review of the criteria and standards for the regulation of particulate matter emissions is a proposed revision of the existing standard for total suspended particulate matter (TSP). The proposed revision will either replace the TSP standard with one based on the fraction of particulate matter in the inhalable size range (currently defined as 15 micrometers and smaller in aerodynamic diameter) or modify the TSP standard to include inhalable particulate matter (IP) limitations for specific areas or sources.

To obtain background data for the proposed IP standard, the Agency has initiated a program to measure IP emissions from sources in a variety of industries, prioritized in consideration of their estimated impact. The measurements will be used to update emission factors for industrial processes and operations as published in EPA's Compilation of Air Pollutant Emission Factors, commonly referred to by its report number, AP-42. The measurement program, which is divided about equally between point and fugitive sources, will include simultaneous determinations of TSP and IP from each

source; and will thus provide bases for comparison and guidance in the proposed revision of the standard.

The measurement of the fugitive IP emissions presents some rather unique problems. Point source IP emissions can, in most instances, be quantified quite readily using the standard techniques and equipment currently employed for point source TSP - or relatively simple modifications of such techniques and equipment. There are no such "standard" measurement methods for fugitive emissions, however, and most of the equipment employed in the recognized techniques is designed for sampling TSP. The starting point for the fugitive IP measurement portion of the program then had to be the definition and specification of the techniques and equipment to be employed. This paper summarizes the measurement techniques and sampling equipment for IP fugitive emissions currently being used in the program and described in an as yet unpublished draft version sampling protocol prepared by TRC - Environmental Consultants, Inc. as the initial phase of the program effort.

## MEASUREMENT TECHNIQUES

There are four basic measurement techniques for airborne fugitive emissions generally recognized by the air pollution community as capable of providing acceptable data. Each is used to determine the generation rate of emissions from a source as the product of a measured concentration and the volume flow rate of the air carrying the emissions past the measurement location. While most of the measurements made until very recently have been designed to quantify emission rates of TSP, the four basic techniques may be employed for IP measurements with only minor modifications to program designs and sampling procedures and the utilization of some specifically designed size-selective sampling equipment.

The most accurate fugitive emissions measurements can usually be made at the source before the emissions begin to diffuse into the atmosphere. The quasi-stack sampling technique provides a means for the capture of the emissions in a small volume of transport air and for the control of the emissions flow from the source to the sampling location. The next most accurate measurements can be obtained after the emissions have diffused into a larger, enclosed volume of air, such as that inside a plant structure. The roof monitor sampling technique is used in such instances. The least accurate measurements are those made after the emissions have diffused extensively into the ambient air at significant distances from the source, where the upwind downwind sampling technique may be employed. The fourth technique, exposure profiling, is a specialized form of downwind sampling restricted to a specific category of sources. Its accuracy is comparable to roof monitor sampling.

The IP sampling program prioritizes the application of the techniques in their order of accuracy--quasi-stack, roof monitor and upwind/downwind sampling. Exposure profiling receives higher priority for applicable sources than upwind/downwind sampling.

The basic techniques their applicabilities and limitations, and the modifications or special sampling equipment required for IP measurements are

described in the following subsections. Descriptions of the IP sampling equipment are provided under Sampling Equipment, below.

Quasi-Stack Sampling

In this technique the fugitive emissions are captured at their source in a temporarily installed hood or enclosure and transported by the capturing air to an exhaust duct or stack of regular cross-sectional area. The emissions are measured in this ductwork using standard stack sampling procedures such as EPA Method 5.

The precision and accuracy limits of the quasi-stack method are the best of the noted sampling techniques and are also the best defined. The accuracy of the quasi-stack method is only slightly less than that of a normal stack test in that fewer points are usually sampled and that a constant bias may be introduced by a failure to capture all of the emissions from the source being tested. Care in the design of the capturing system can reduce the latter error to a negligible amount. A tolerance in the isokinetic sampling range of $\pm$20 percent, rather than the $\pm$10 percent allowed in stack sampling, is usually permitted.

Quasi-stack sampling is necessarily limited to sources that can be isolated from other sources and effectively enclosed or hooded to capture their emissions. Careful consideration must be made in the design of the enclosure or hood to ensure total capture of the emissions and to provide a volume of emission-transporting air sufficient to carry the emissions intact to the sampling equipment. The hooded enclosure design should not interfere with normal plant operations, and the capturing air flow across the process should not be so large as to alter the nature of the process or affect the amount or character of the emissions.

No major modifications to the quasi stack sampling method procedures are required for IP measurement. A small, dual- cyclone probe to provide for particle size fractionation has been designed for use with the EPA Method 5 or 17 trains for in-stack sampling. The probe is ideally suited for IP quasi-stack sampling and is described under Sampling Equipment, below. Standard cascade impactors may be used with the addition of a cyclone to provide the 15 micrometer cut.

Roof Monitor Sampling

This method is used to measure the emissions generated by sources located within a building or similar structure as they are transmitted into the atmosphere through a roof monitor or other opening. The total emission rate for all sources within the structure is determined as the product of the emissions concentration measured in the air at the opening and the air flow rate through the opening. Most roof monitor sampling programs require the collection of samples and the measurement of air velocities simultaneously at a number of points in the plane of the opening to ensure that representative average values of concentration and flow rate are obtained.

Roof monitor sampling is most effectively employed for larger sources located within structures with only a few openings. It requires sampling and measurement devices capable of making accurate determinations of relatively small masses of emissions and very low air velocities. It may be utilized for the characterization of specific sources within an enclosure if operating schedules include or permit the arrangement of emissions generation by only that specific source.

The accuracy and precision of this technique vary with characteristics of the sources and are definable only in general terms for each source tested. In general, the roof monitor method is not as accurate as the quasi-stack method since a significant portion of the emissions may escape through other openings before reaching the measurement point and since a much higher degree of dilution with transport air occurs before measurement.

No procedural modifications to the roof monitor method are required for IP measurements. The method is probably more effective for particles in the smaller IP size range since a smaller proportion of such particles will be lost to fallout resulting from relatively low entrainment velocities and large vertical transport distances inherent in roof monitor arrangements. Size-selective devices, such as a horizontal elutriator to reject particles larger than 15 micrometers and cascade impactors to provide size-fractionated samples, are employed with high volume (hi-vol) filter samplers to obtain concentration measurements. Transport air velocities for calculating volume flow rates are determined by traversing anemometers across the monitor opening.

Upwind/Downwind Sampling

This method is utilized in the measurement of emissions after they have entered the ambient atmosphere from open or area sources, or from enclosed sources not amenable to quasi stack or roof monitor sampling. The emission rate for such sources is determined by measuring the concentration of the emissions in the ambient air downwind of the source, subtracting the portion of the concentration attributable to other sources and that measured as background upwind of the source, and using the thus-determined concentration in proven diffusion equations or mathematical models to back-calculate the source's rate of emission. Measurements of other contributing parameters, such as wind speed and direction during the emission sampling, location of samplers relative to the source, and atmospheric and topographic conditions, are also required.

The upwind/downwind method is the least accurate of the methods described, since only a very small portion of the emissions are captured for measurement after an extreme degree of dilution in the transporting ambient air. Careful sampling system design is required to approach the accuracy of the equations or models used in calculating the emission rate.

Upwind/downwind sampling is probably the most universally applicable of the fugitive emissions measurement techniques, since it is not usually limited by source location or geometry.

Procedure modifications required for IP sampling are limited to allowances for longer sample collection periods to permit the collection of sufficient particulate material mass for analysis, required by the rejection of particles larger than 15 micrometers. Longer sampling period requirements can sometimes be relieved by locating samplers closer to the emissions source where the concentration is higher. A size-selective inlet for standard hi-vol samplers has been developed and is already commercially available. It is described under Sampling Equipment, below. More detailed particle size data may be obtained by adding a cascade impactor.

Wind speed and direction measurements are made throughout the sampling period using standard meteorological devices with recorders.

Exposure Profiling

The exposure profiling technique is employed in the sampling of line or moving point sources and relatively small virtual point or area sources where the samplers can be located in the ambient atmosphere within a few meters downwind.

Samples are taken at a number of points within the emission plume at near-isokinetic sampling velocities, selected to approximate the measured local mean wind speed. The plume boundaries are determined by spatial extrapolation of the measured exposures and the source strength is determined by integration of the measured exposures over the cross-sectional area of the plume.

The exposure profiling method is not as accurate as the quasi stack method since only portions of the total emissions and transport air are sampled or measured. Its use of near-isokinetic sampling and provisions for correcting to isokinetic conditions in the exposure calculations tend to minimize errors, making the method about as accurate as the roof monitor method.

IP exposure profiling requires only that the larger particles be rejected from the sample while maintaining the near-isokineticity of the sampling. This is readily accomplished by the use of either a horizontal elutriator or a cascade impactor in the inlet to a hi-vol type sampler. Sampling velocities are matched to transporting air velocities by an inlet nozzle of suitable dimensions with the constant-flow rate samplers.

## SAMPLING EQUIPMENT

The modifications to adapt the basic fugitive emissions measurement techniques for IP measurements all involve the addition of size-selective devices for the rejection of most of the particulate matter larger than 15 micrometers from the samples before they are collected for gravimetric analysis. Each of the devices makes some provision for the determination of the mass of large particles included in the IP catch, usually as a function of the mass of larger particles collected by the device. The devices include the dual cyclone train for quasi-stack measurement; a horizontal elutriator for roof monitor and exposure profiling measurements; and a size selective

inlet for hi-vol samplers for upwind-downwind measurements. Each of these devices has been developed specifically for the IP measurement program and is being used by the program's contractors. Possible modifications to eliminate excess particle bounce and carry-over in existing cascade impactors designed to be used with hi-vol samplers are being investigated by the Process Measurements Branch of EPA's Industrial Environmental Research Laboratory at Research Triangle Park, North Carolina.

Each of the devices is described in some detail in the following subsections, along with some of the procedural or operational techniques involved in its application to IP measurements.

## Dual Cyclone Train

The dual cyclone train was designed and fabricated by the Southern Research Institute (SoRI) of Birmingham, Alabama, as their IP Cyclone Sampler specifically for the IP measurement program. It consists of two cyclones and a backup filter arranged in series, and can be connected directly to an EPA Method 15 or Method 17 sampling train. The initial cyclone has a $D_{50}$ of 15 micrometers at the design flow rate of 23 liters (0.8 $ft^3$) per minute at 150°C (300°F). The second cyclone has a $D_{50}$ of 2.5 micrometers. The backup filter may be either a 2.5 inch disc or a Method 17 thimble type.

In operation, the selection of one of a set of 11 inlet nozzles of different diameters permits sampling at near-isokinetic conditions over a wide range of gas velocities at the design flow rate. The initial cyclone separates the portion of particles larger than 15 micrometers from the sample and passes the IP fraction. The second cyclone then separates the fraction between 15 and 2.5 micrometers and passes the fine fraction to the filter. The overall diameter of the IP Cyclone Sampler with any of the inlet nozzles is just under 6 inches so that two 6-inch diameter sampling ports are required for the recommended four-sampling-point array for round or rectangular ducts.

## Horizontal Elutriator

A horizontal elutriator consists of a stack of horizontal plates, spaced so that each pair of plates forms a settling chamber. As particles are transmitted through the chambers at a velocity determined by their carrier-gas volumetric flow rate, the larger particles are deposited on the chamber bottom as the result of gravitational acceleration, while smaller particles are carried through. The elutriator designed by SoRI for the IP program has a collection efficiency of 50% for 15 micrometer particles when used as a directional inlet for a standard 8 x 10 hi-vol sampler operating at 40 CFM (1.13 $m^3$/min). The elutriator, since it is a passive device, requires no special calibration but must be kept level during sampling to ensure proper operation. A modified design has been developed that will provide 15 micrometer particle separation at 20 or 40 CFM sampling rates and allow the use of impaction type samplers in series with the elutriator and hi-vol sampler.

## Size-Selective Inlet

Designed for non-directional sampling applications as a precollector of 15 micrometer particles with a standard hi-vol sampler, the size-selective inlet (SSI) is commercially available from at least two manufacturers. The SSI draws its sample through a circumferential inlet slot that eliminates almost all wind speed and direction effects, and transmits it through a buffer chamber into an impaction chamber where all particles larger than 15 micrometers are collected. Smaller particles are transmitted through the impactor chamber's vertical vent tubes to the hi-vol filter for collection. The SSI thus provides a measure of the IP concentration as a single mass/sampled-air-volume ratio in the same manner as hi-vol sampling for TSP.

## Cascade Impactors

At least two manufacturers currently market multi-stage impaction devices for use with standard hi-vol samplers. Theoretically capable of separating the particulate matter into as many as six different size ranges within the IP category, most of the impactors have been found to provide cut points different from their design or calibrated values due to excessive bouncing of larger particles and the resultant carry-over to subsequent stages. Experiments by the EPA and manufacturers have indicated that the bounce problem can be largely eliminated by operating at reduced sampling rates, but this also results in a shift in the SSI cut point to greater than 15 micrometers. The Process Measurements Branch of EPA's Industrial Environmental Research Laboratory at Research Triangle Park is currently conducting tests to evaluate impactors modified to eliminate the bounce problem while operating at the standard hi-vol sampling rate of 40 CFM (1.13 $m^3$/min.). Such modified impactors will provide particulate size distribution information in addition to the IP fraction concentration when used in conjunction with an SSI on a standard hi-vol sampler.

# APPLICATIONS AND RESULTS

To date, only the SSI's and cascade impactors designed for use with hi-vol filter sampler have been used in the sampling of fugitive emissions. Three SSI/impactor/hi-vol samplers were included in an array of 25 samplers used to determine the fugitive emissions generation rate of a large, active utility coal storage pile in a TRC project to evaluate the cost-effectiveness of the upwind/downwind technique. The combined samplers were installed at locations side-by-side with standard TSP hi-vols and operated simultaneously with them. The combined samplers were operated through five successful test runs at 20 CFM (0.57 $m^3$/min.) after a trial run at 40 CFM (1.13 $m^3$/min.) indicated so much bounce and carry-over that almost all of the sample was deposited on the final hi-vol filter.

Results of the five sampling runs are summarized in Table 1 as average values of the IP sampled at three distances downwind of the emissions source. The increasing percentages of particles in the smallest size range displayed as the distance from the source increases is indicative of effective operation of the combined samplers, reflecting the settling of larger particles in the diffusing cloud of emissions.

Current plans to increase the effort on the IP measurement program will provide additional applications data to either verify the effectiveness of the procedures and equipment designated in the IP sampling protocol or indicate changes to make them more effective.

TABLE 1. INHALABLE PARTICULATE MASS IN COAL PILE FUGITIVE EMISSIONS

| SAMPLER LOCATION Meters downwind of source | PERCENT IP SAMPLE IN SIZE RANGE 16 to 10.2μm | 10.2 to 4.2μm | 4.2 to 2.1μm | 2.1 to 1.3μm | 1.3-0μm |
|---|---|---|---|---|---|
| 210 | 25.4 | 22.0 | 6.4 | 6.5 | 39.6 |
| 470 | 15.1 | 18.8 | 3.6 | 6.4 | 56.0 |
| 600 | 17.6 | 21.2 | 1.2 | 2.5 | 57.4 |

# BALLOON SAMPLING TO CHARACTERIZE PARTICLE EMISSIONS FROM FUGITIVE SOURCES

by
James A. Armstrong
Denver Research Institute
University of Denver
Denver, Colorado 80208

and
Dennis C. Drehmel
U. S. Environmental Protection Agency
Industrial Environmental Research Laboratory
Research Triangle Park, North Carolina 27711

## ABSTRACT

A balloon sampling method being developed to characterize fugitive particle emissions from line, point, and area sources is presented. The method consists of using a series of tethered balloon sampling systems positioned at selected distances downwind from the source being sampled. Three lightweight wind directional samplers will be flown simultaneously at different heights by each balloon system with a fourth sampler located at ground level at each launch site. The samplers will utilize horizontal elutriation to obtain a 15 μm aerodynamic diameter particle cut and will be capable of sequential filtration to provide a second cut to separate the fine and coarse size fractions of the inhalable particles sampled. The multiple balloon sampling technique will be coupled with the exposure profiling method to determine improved source emission factors. In addition, the balloon network will be used to characterize the downwind transport of fugitive emissions.

## INTRODUCTION

It is now widely recognized that fugitive particle emissions contribute significantly to the measured levels of total suspended particulates (TSP) found in both urban and rural environments. These emissions are believed to be responsible for the failure of many areas to attain the national primary air quality standards for TSP. Major open sources of fugitive emissions include unpaved roads, paved roads, surface mines, storage piles, construction activities, agricultural tilling, wind erosion of harvested cropland, and forest and brush fires, including both wildfires and prescribed burns(1). Other sources include iron and steel foundries, smelters, and refineries(2,3,4).

Of the fugitive sources listed above, open sources (except forest and brush fires) emit particles primarily in a coarse size range of greater than approximately 2.5 μm in equivalent aerodynamic diameter. These particles, classified as mechanically generated, are believed to be the most significant sources of fugitive emissions contributing to measured ambient TSP levels. Fugitive particle emissions produced by combustion processes,

such as from forest and brush fires and from furnace operations at foundries and smelters, are typically in a fine particle size range less than 2.5 μm. The chemistry of the coarse versus fine particles also differs: coarse particles are usually more basic; and fine particles, more acidic(5).

The traditional method of monitoring airborne particles from fugitive sources has been to use ground-based high-volume (hi-vol) samplers. The samplers are usually at considerable distances both upwind and downwind from the source being sampled. Dispersion modeling is normally used to interpolate the source strength from the hi-vol data. Considerable error can be incurred when using this technique because of the often limited number and location of sampling sites and due to the current simplicity of the atmospheric dispersion models(6). Complications are further increased when the source is not well defined.

Samplers mounted on towers have been used successfully to characterize fugitive dust emissions from paved and unpaved roads employing an "exposure profiling" technique which is based on the isokinetic profiling concept used for conventional source testing(7). Particulate emissions are measured directly downwind of the source being sampled by placing a grid of samplers in the effective cross-section of the plume. Emission factors are subsequently determined by a mass-balance calculation. The exposure profiling technique eliminates the need to use dispersion models to estimate emission rates from fugitive sources. A two dimensional vertical array of samplers must be used when sampling a point or area source with this technique while line sources (e.g., haul roads) require a one dimensional vertical grid of samplers. Major limitations of the exposure profiling technique are the practical height of the sampling towers and their lack of mobility.

A tethered balloon sampling system has been developed which overcomes these limitations so that the exposure profiling technique can be extended to a larger number of fugitive sources. This sampling system basically consists of a tethered balloon, three wind vane samplers, and a ground-based sampler. The wind vane samplers attach to the balloon and its tetherline at different sampling heights. The balloon is positioned at selected distances downwind from a source being sampled. The ground-based sampler is located near the balloon launch site to monitor dust concentration at ground level. This sampling method has been successfully employed to investigate the vertical extent of fugitive dust emissions from various operations at a surface coal mine(8). A program has been started to extend this method by using a series of four balloon systems equipped with newly designed inhalable particulate (IP) samplers capable of sequential filtration. The multiple balloon sampling method will be coupled with the exposure profiling technique to determine improved emission factors from line, point, and area sources.

## SYSTEM DESIGN

The sampler design parameters are presented. This is followed by a detailed discussion of the IP wind vane samplers and the tethered balloon systems.

## Sampler Design Parameters

EPA is in the process of establishing a new ambient air quality size specific particulate standard(5). Particles classified as "inhalable" form the basis of the proposed standard. Inhalable particles are currently defined as those having an aerodynamic diameter of 15 μm or less. The 15 μm diameter constitutes a conservative upper limit for the size of inhaled particulate matter that can affect the human lower respiratory system. Consequently, the new wind vane particle samplers are being designed for 50% capture of 15 μm aerodynamic diameter particles by means of horizontal elutriation. Inhalable particles can further be subdivided into groups of coarse and fine fractions with a cut point of approximately 2.5 μm. The fine particles are primarily responsible for air quality visibility degradation and are primarily produced by combustion processes. The coarse-fraction inhalable particles are those between 2.5 and 15 μm and are normally classified as mechanically generated. Most wind generated dust, for example, would consist of coarse size particles. Depending on the type of source being sampled, it may sometimes be desirable to be able to separate inhalable particles into coarse and fine fractions. For example, fugitive particulate emissions from an iron foundry are expected to be a mix of fine and coarse particles. By being able to quantify the fractions in terms of amount and chemical composition, the actual emission sources should be able to be identified. When desired, the balloon samplers will employ sequential filtration to separate inhalable particles into coarse and fine fractions.

The samplers are also being designed such that their performance will be independent of wind speed and direction. Sampler weight will allow three units to be flown by each balloon. A fourth unit will be stationed at the winch site of each balloon system to monitor ground-level dust concentrations.

## IP Wind Vane Samplers

A schematic of the sampler type being developed for this program is shown in Figure 1. The vertical tube of the sampler attaches to the horizontal tube at a point where the wind vane balances the forward tube extension such that the extension is always horizontal. The tubes are fiberglass; the wind vane consists of aluminized Mylar sheets stretched over a wire loop. A particle sampling assembly, consisting of a fiberglass entrance cone, a horizontal metal tube elutriator, and a polystyrene cassette capable of holding one or two filters, attaches to the front end of the horizontal tube. The wind vane configuration ensures that the entrance cone always points into the wind during sampling. A housing containing a diaphragm pump, battery pack, and voltage regulator is attached to the lower end of the vertical tube. The weight of these components ensures that the sampler maintains the orientation shown in Figure 1. The pump voltage will be regulated so that a constant flow rate of 2 ℓ/min through the sampling assembly will be maintained. The pump can operate for ~10 hours before the lithium battery pack needs replacement. Nylon lines equipped with swivels and quick disconnect clamps will be used to attach the samplers to the balloons or tetherlines. A prototype IP wind vane sampler, weighing ~320 g, is nearing completion and will be laboratory

tested before mass production of additional units commences. The sections that follow discuss horizontal elutriation, sequential filtration, entrance cone considerations, and the planned laboratory evaluation of the IP wind vane sampler.

## Horizontal Elutriation

Several types of inertial mechanisms, such as centrifugal force and impaction, were considered for separating particles having aerodynamic diameters larger and smaller than 15 μm. Due to weight and pressure drop limitations of the pumps capable of being used for the IP wind vane samplers, however, it was decided to use horizontal tube elutriators.

The governing equation for predicting the collection efficiency of particles from a laminar airstream passing through a circular horizontal tube is (9):

$$\text{Eff.} = \frac{2}{\pi}[2\varepsilon\sqrt{1-\varepsilon^{2/3}} - \varepsilon^{1/3}\sqrt{1-\varepsilon^{2/3}} + \arcsin \varepsilon^{1/3}] \quad (1)$$

where $\varepsilon = (3V_s L/8a\bar{V})$, $V_s$ is the particle settling velocity, L is the tube length, a is the tube radius, and $\bar{V}$ is the average air velocity. The settling velocity of spherical particles in air is:

$$V_s = \frac{C g \rho d^2}{18\mu} \quad (2)$$

where C is the slip correction factor, g is the gravitational constant, ρ is the particle density, d is the particle diameter, and μ is the viscosity of air.

For a 15 μm diameter aerodynamic particle, $\rho = 1$ g/cm$^3$ and $C \simeq 1$. From Equation 2, $V_s = 0.67$ cm/s. Now by specifying the average air velocity through a tube of a given radius and by setting Eff. = 0.5, the tube length can be calculated using Equation 1. The horizontal elutriator for this program will consist of a matrix of 19 thin wall stainless steel tubes, each having a radius of 2.3 mm. The total flow rate through the elutriator will be 2 ℓ/min so that $\bar{V}$ through each tube will be 10.9 cm/s. From Equation 1, L = 3.5 cm.

Figure 2 shows the horizontal elutriator in detail. The 19 tubes will be housed in a thin wall aluminum tube having an outside diameter of 2.5 cm. Interstitial spaces between adjacent elutriator tubes will be filled with epoxy.

## Sequential Filtration

Sequential filtration for use by the balloon-borne particle samplers is based on the work of the Air Quality Group at the University of California, Davis(10). This group has developed a stacked filter unit in which particles are collected on two 47 mm filters mounted in a commercially available sequential filter holder. Nuclepore filters are employed where the first filter, having a pore size of 8.0 μm, is used to collect coarse particles and the second filter, having a pore size of 0.3 μm, is used to collect

fine particles. Nuclepore filters are excellent for this application since their low blank weight and low hygroscopicity facilitate gravimetric and elemental analyses. By controlling the face velocity of air passing through the filters, it is possible to obtain a good size cut between coarse and fine particles. For the 8.0 μm Nuclepore filter, a face velocity of 2.8 cm/s results in 50% capture efficiency for 3.1 μm aerodynamic diameter particles. If the face velocity is increased to 7 cm/s, the cut point shifts to 2.8 μm while a face velocity of 15 cm/s results in a cut point of 2.2 μm(11). A thin coating of Apiezon grease is used on the 8.0 μm filter to prevent particle bounce.

For this program, 25 mm diameter Nuclepore filters having the above pore sizes will be used. Sequential filter cassettes are commercially available for this filter size. (The filter cassette in Figure 2 shows only the base section of the stacked filter assembly. This configuration would be used when sequential filtration is not employed.) The actual filtration area of the filters is 2.4 $cm^2$ so for an air flow rate of 2 ℓ/min, the face velocity would be 14 cm/s resulting in a cut point of ~2.3 μm. The outer cassette cap will be epoxied to the back of the elutriator housing tube.

Entrance Cone Considerations

The diverging entrance cone of the particle sampling assembly will have a total included angle of 30° or less to ensure that separation from the walls will not occur as the air is decelerated prior to entering the elutriator. The cone will slip over the front of the elutriator housing tube as shown in Figure 2.

An error analysis, which considered the ratio of sampled particle concentration to true concentration, was conducted to determine the effects of anisokinetic sampling(12). The analysis showed that one cone having a set inlet diameter was insufficient for the anticipated range of wind speeds (2 to 10 m/s) which will be encountered during balloon sampling. In order to reduce the potential sampling error to less than 20% for 15 μm aerodynamic diameter particles, three interchangeable cones having different inlet diameters will be used. The decision of which cone to employ will be dictated by the average wind speed encountered at the start of a sampling period. Table 1 shows the calculated sampling error for three different cone inlets. Since the sampling error is proportional to the particle diameter squared, the error will be much less for particles <15 μm.

The samplers' wind vanes should keep the entrance cones aligned to ±10° of the wind direction. Since the maximum sampling error is equal to 1 minus the cosine of the angle, the maximum error for misalignment will be 1.5%(13).

Laboratory Evaluation of the IP Wind Vane Sampler

The particle collection performance of the prototype IP wind vane sampler will be evaluated in the laboratory prior to field use. A

closed-loop experimental electrostatic precipitator will be used as a wind tunnel for this evaluation. The test section, where the wind vane will be suspended, will be the precipitator collector section. The collector plates and corona wire frame assemblies will be removed from the precipitator prior to these tests. The length of the collector section is 2.1 m while its height and width are 1.5 and 1.8 m, respectively. Diffuser screens in the precipitator inlet cones ensure a uniform average airflow velocity of 1.5 m/s through the collector section. Fly ash, injected upstream of the precipitator, will be used for the sampler performance evaluation. The mass loading and particle size distribution of the suspended fly ash will be measured in the precipitator inlet and outlet sampling ports by means of a cascade impactor. Results will be used to determine the aspiration efficiency of the sampler, the effectiveness and accuracy of the horizontal elutriator, and the performance of the sequential filter assembly.

TABLE 1

CALCULATED SAMPLING ERRORS FOR THREE CONE INLETS

| Wind Speed (m/s) | Inlet Dia. (cm) | Stokes No. for d=15 μm | Velocity Ratio | Sampling Error (%) |
|---|---|---|---|---|
| 2 | 0.45 | 0.31 | 1.0 | 0 |
| 3 | 0.45 | 0.46 | 0.67 | -16 |
| 4 | 0.29 | 0.95 | 1.25 | +18 |
| 5 | 0.29 | 1.2 | 1.0 | 0 |
| 6 | 0.29 | 1.4 | 0.83 | -14 |
| 7 | 0.23 | 2.1 | 1.14 | +12 |
| 8 | 0.23 | 2.4 | 1.0 | 0 |
| 9 | 0.23 | 2.7 | 0.89 | -10 |
| 10 | 0.23 | 3.0 | 0.80 | -18 |

The sequential filter collection efficiency will be evaluated by weighing the dust catch of both the 8.0 and 0.3 μm Nuclepore filters by means of a Cahn electrobalance. Scanning electron microscopy will also be employed to evaluate the size cut performances of the elutriator and the 8.0 μm filter by determining the size distributions and concentrations of particles collected on each filter.

Tethered Balloon Systems

Blimp-shaped, red polyethylene balloons, inflated with 3.25 $m^3$ of helium, will be used to carry aloft the IP wind vane samplers. The balloons attach to portable winches by means of lightweight tetherlines having a breaking strength of 535 newtons. The winches, which weigh 27 kg, contain forward/reverse variable speed motors and rechargeable, sealed lead/acid battery packs.

This size balloon has a lifting capacity of 1.2 kg to altitudes of 800 to 1,000 m in winds of 6 to 8 m/s. Balloon flight performance is still

reasonable in winds of 10 to 12 m/s but the maximum altitude attainable is somewhat reduced. The balloons are designed to survive in winds up to 20 m/s. Four balloon systems are being developed for this program.

## FIELD PROGRAMS

A demonstration program, monitoring emissions from an unpaved road, will be conducted first in order to evaluate and establish sampling parameters and analysis techniques. This will be followed by a field program at a site where chemical surface treatments for unpaved roads are being evaluated. Later field programs will characterize fugitive emissions from point and area sources.

### Demonstration Program

An initial demonstration field program is planned to evaluate the balloon sampling method using dust emissions from an unpaved road. Since this is a line source, only a one dimensional analysis need be applied. The present site being considered for this demonstration is a lightly travelled unpaved county road located along the north perimeter of the DRI Cherry Creek Field Site (CCFS) in Englewood, Colorado. This well maintained gravel road runs in an east-west direction in an open area which is bordered to the north by a Colorado state recreation area. Winds are normally from either the north or the south so that downwind sampling sites would be either on DRI or State of Colorado property. Permission to conduct sampling tests on state property is currently being requested. The CCFS is located ~16 km southeast of the University of Denver. This location is ideal since inflated balloons can be stored indoors at the CCFS overnight or during inclement weather.

The objectives of the demonstration program are to evaluate the performance and reliability of the balloon systems during actual field operations, to determine appropriate sampling heights at selected downwind sampling distances, and to establish sampling times versus road traffic necessary to collect sufficient dust samples for the exposure profiling analysis.

Parameters controlling the emission levels from unpaved roads include: the silt and moisture contents of the surface road material, the average weight and number of wheels of vehicles passing over the road, the average vehicle speed, and the local wind speed(14). For this demonstration, as many of these parameters as possible will be held constant. The maximum speed limit for this road is 65 km/hr. During non-rush hour periods the average traffic on the road is ~2 to 4 automobiles or light duty trucks per hour. It is planned that during balloon sampling, a DRI truck will be continuously driven at 65 km/hr across a 200 m test section of this road (20 to 30 passes/hr). Dust emissions due to other vehicles should have a minor impact on the test results. Time lapse movies of the road test section will be taken to record all traffic during sampling.

All demonstration tests will be conducted under dry road conditions. At least 2 days of dry weather will precede any test. Samples of the road

surface material will be analyzed for silt content and type of soil. Field operations will be conducted over periods in which the wind is relatively steady and predominately from either the south or the north. A meteorological station will be located at the test site to record wind speed, direction, and temperature during all tests.

The sampling network for the demonstration is shown in Figure 3. Separation distances of 25 m between the road and first balloon and between the three balloons will be evaluated first, followed by other separation distances. Tests over a 2 to 3 week period will be conducted where the IP wind vane samplers will be operated both with single and sequential filters. Emphasis will be placed on determining appropriate sampling heights and times for selected "source to balloon" separation distances.

It is believed that three to four people will be required to operate the balloon systems. This demonstration will allow the field personnel requirements to be established.

All dust samples collected by the IP wind vane samplers during the demonstration tests will be analyzed gravimetrically. Background particulate matter collected by the upstream samplers will be subtracted from the downwind sampler catches. Scanning electron microscopy will be used to analyze selected samples from both single and sequential filters to determine particle size distributions and number concentrations. The mass emission rates of inhalable particles per unit length of the unpaved road will be calculated by the exposure profiling method for each of the downwind balloon systems. Comparisons of the calculated mass emission rates will be made between the three downwind balloon systems as well as with published results for unpaved roads.

Treated Unpaved Road Study

Following the demonstration program, balloon sampling will be employed to monitor fugitive emissions from an unpaved road which has a number of test sections treated with different chemical stabilizers. A long term sampling program has been started at the test road located at the Fort Carson Army installation, south of Colorado Springs, Colorado. An extensive ground-based network of hi-vol and dichotomous samplers is being used to monitor emissions from the road test sections. A direct comparison between the ground-based and balloon sampling results at this site will be possible.

Later Field Studies

The balloon sampling method will be used to monitor and characterize fugitive emissions from an open area source, such as a coal pile that is actively worked or a construction site, during the second program year. The area source will require two dimensional sampling and analysis. Efforts will be made to select a field test site which is isolated from other particle emission sources. The sampling network which will be employed for the field program is shown in Figure 4. This first test of an area source can again be considered a demonstration program in that considerable

effort will be made to define the two-dimensional envelope of the resultant particle plume for selected downwind locations and to establish appropriate sampling times for the collection of adequate particle mass loadings for gravimetric analysis. The total mass emission rate of inhalable particles from the area source will be calculated and compared to past investigations. Again, all sampling operations will be documented using time lapse photography.

Future field studies will be conducted to sample particle emissions from both paved and unpaved roads and both process and open sources. It is anticipated that fugitive particle emissions will be monitored and analyzed at sites such as copper and lead smelters, iron and steel foundries, and aluminum mills. The sequential filtration capability of the IP wind vane samplers will be extremely useful in identifying the fractions of coarse versus fine particles from such sites. This will aid in the identification of the specific sources of the emissions. All collected samples will be gravimetrically analyzed. In addition, selected filter samples from process sources could be analyzed by x-ray fluorescence to determine major, minor, and trace elements, and by scanning electron microscopy/energy dispersive x-ray spectrometry to determine particle size distributions, concentrations, and compositions. Transmission electron microscopy/selected area electron diffraction may also be employed to determine the species of individual particles.

Further studies at open pit mining sites are also envisioned as well as investigations at oil shale extraction and process operations, which are just now being developed.

## REFERENCES


1. Evans, J.S., D.W. Cooper, M. Quinn, and M. Schneider. Setting Priorities for the Control of Particulate Emissions from Open Sources. Symposium on the Transfer and Utilization of Particulate Control Technology, Vol. 4. EPA-600/7-79-044d (NTIS PB 295229), February 1979, pp. 85-103.

2. Scott, W.D., and C.E. Bates. Measurement of Iron Foundary Fugitive Emissions. Symposium on Fugitive Emissions: Measurement and Control. EPA-600/2-76-246 (NTIS PB 261955), September 1976, pp. 211-237.

3. Lindstrom, R.N., and S.E. Sundberg. Fugitive Particulate Emission Rate and Characterization for Electric Arc Steelmaking Furnaces. (Presented at the 72nd Annual Meeting of the Air Pollution Control Association, Cincinnati, Ohio. 79-39.3, 1979.)

4. Kalika, P.W., R.E. Kenson, and P.T. Bartlett. Development of Procedures for the Measurement of Fugitive Emissions. EPA-600/2-76-284 (NTIS PB 263992), December 1976.

5. Miller, F.J., D.E. Gardner, J.A. Graham, R.E. Lee, W.E. Williams, and J.E. Bachmann. Size Considerations for Establishing a Standard for Inhalable Particles. JAPCA 29:610-615, June 1979.

6. Zeller, K.F., D.G. Fox, and W.E. Marlatt. Estimating Dust Production from Surface Mining. Third Symposium on Fugitive Emissions: Measurement and Control. EPA-600/7-79-182 (NTIS PB 80-130891), August 1979, pp. 103-117.

7. Cowherd, C., C.M. Maxwell, and D.W. Nelson. Quantification of Dust Entrainment from Paved Roads. EPA-450/3-77-072 (NTIS PB 269944), July 1977.

8. Armstrong, J.A., P.A. Russell, and D.C. Drehmel. Particle Production from Surface Mining - Part 1: Vertical Measurements. Proceedings: Fourth Symposium on Fugitive Emissions: Measurement and Control. EPA-600/9-80-041 (NTIS PB 81-174393), December 1980, pp. 37-63.

9. Cushing, K.M. Development of Horizontal Elutriators for Sampling Inhalable Particulate Fugitive Emissions. Proceedings: Fourth Symposium on Fugitive Emissions: Measurement and Control. EPA-600/9-80-041 (NTIS PB 81-174393), December 1980, pp. 208-242.

10. Cahill, T.A., L.L. Ashbaugh, J.B. Barone, R.A. Eldred, P.J. Feeney, R.G. Flocchini, G. Goodart, D.J. Shadoan, and G.W. Wolfe. Analysis of Respirable Fractions in Atmospheric Particulates via Sequential Filtration. JAPCA 27:675-678, July 1977.

11. Barone, John B. Air Quality Group, Crocker Nuclear Laboratory, University of California, Davis, California. Personal communication, June 1980.

12. Belyaev, S.P., and L.M. Levin. Techniques for Collection of Representative Aerosol Samples. J. Aerosol Sci. 5:325-338, 1974.

13. Durham, M. Isokinetic Sampling of Aerosols from Tangential Flow Streams. Ph.D. Dissertation, University of Florida, Gainesville, Florida, 1978.

14. Cowherd, C. Jr., K. Axetell, Jr., C.M. Guenther, and G. Jutze. Development of Emission Factors for Fugitive Dust Sources. EPA-450/3-74-037, 1974.

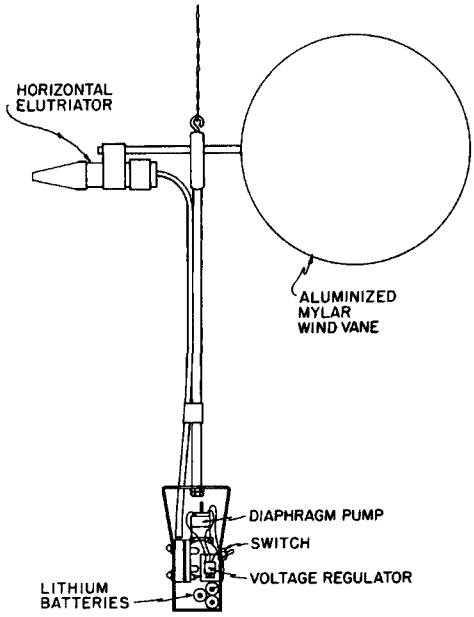


Figure 1. Schematic of the IP wind vane sampler.

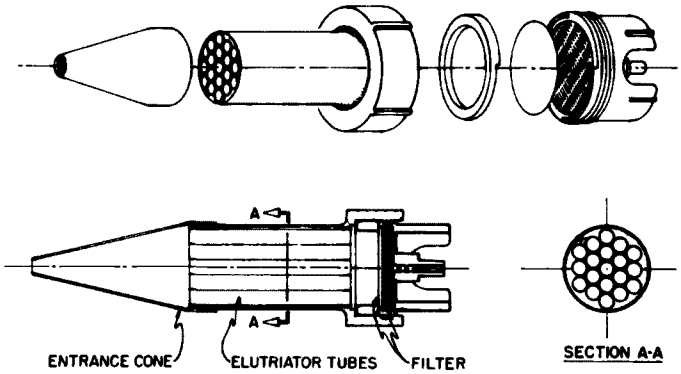


Figure 2. Isometric and sectional views of the particle sampling assembly.

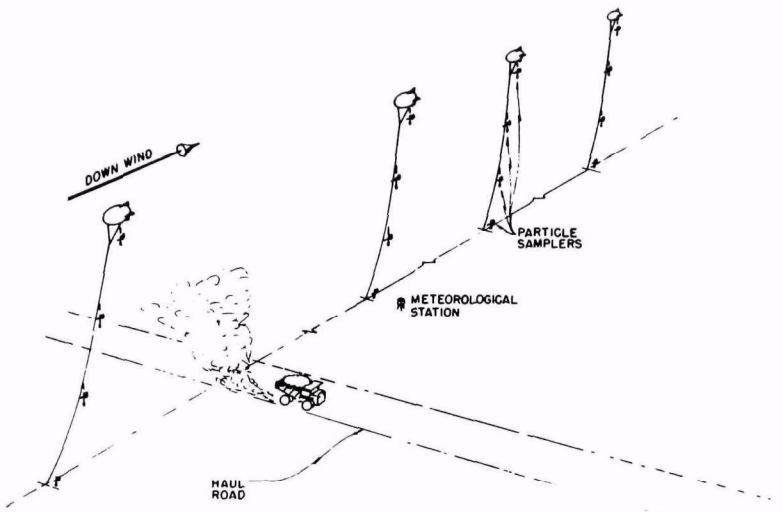


LAYOUT OF TETHERED BALLOON SAMPLING SYSTEM FOR PROFILING THE PLUME FROM A LINE SOURCE AND FOR DETERMINING THE DOWNWIND TRANSPORT OF PARTICLES

Figure 3.

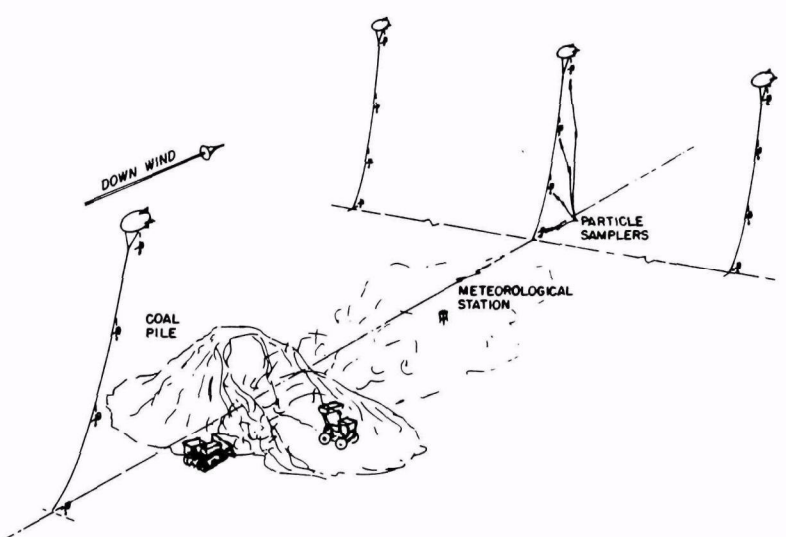


LAYOUT OF TETHERED BALLOON SAMPLING SYSTEM FOR PROFILING THE PLUME FROM AN AREA SOURCE.

Figure 4.

# AN ELECTROSTATICALLY CHARGED FOG GENERATOR FOR THE CONTROL OF INHALABLE PARTICLES

By:

C.V. Mathai
L.A. Rathbun

AeroVironment Inc.
145 Vista Avenue
Pasadena, California 91107

and

D.C. Drehmel

Industrial Environmental Research Laboratory
U.S. Environmental Protection Agency
Research Triangle Park, North Carolina 27711

## ABSTRACT

Devices using electrostatically charged water droplets for the control of inhalable particulate matter from fugitive emission sources have recently been introduced commercially (Foggers). This paper introduces a new spinning cup fog thrower (SCFT) which uses a different method for droplet charging and overcomes certain drawbacks of commercial Foggers.

The new SCFT is a modified Ray Oil Burner. Centrifugal forces and a high velocity air stream generate fine water droplets from water flowing into an atomizing cup. These droplets are charged by directly connecting a high voltage power supply to the inflowing water and electrically isolating the water until it becomes fog. The typical charge-to-mass ratio recorded is $1.2 \times 10^{-6}$ C/g, with a median mass diameter of 200 µm. The fog covers an area of approximately 20 sq. ft. and the water flow rate can be varied from 8 to 68 lph.

The SCFT, which requires less than 1 kW power, is being field-tested to evaluate its potential to control inhalable particles from certain fugitive emission sources where conventional methods of control cannot be applied effectively.

## INTRODUCTION

Although significant progress has been made in the past in controlling emissions from conventional industrial sources, air pollution regulatory agencies are becoming increasingly concerned with the non-attainment of ambient total suspended particulate matter standards, due mainly to fugitive emissions from various sources. In the past, fugitive emissions have been of concern only from a nuisance standpoint, increasing soiling potential and decreasing atmospheric visibility only in the immediate vicinity of the source. It has also been recognized that inhalable particles ($< 15\ \mu m$), fine particles ($< 2.5\ \mu m$) in particular, have a dominant role in causing hazards to human health (1) and degradation of visibility. The fine particles can remain in the atmosphere for extended periods and can be transported over long distances.

Indiscriminate spraying of large amounts of water has been the most common control method used in mines and other fugitive emission sources and it has been only marginally successful (2). In a mine atmosphere, 30-40% is the accepted value for the dust control efficiency of water sprays (3). However, even this method has problems with clogged water spray nozzles and the need for large quantities of water.

It has recently been shown that most industrial pollutants and naturally occurring fugitive dusts acquire electrostatic charges as they are dispersed into the air (4). Hoenig (4) has also shown that the charge on the particles of fugitive emission is usually negative. Therefore, if positively charged water droplets are sprayed on the dust to be suppressed, the particles which collide with the charged droplets will agglomerate rapidly and settle out of the atmosphere. The collection efficiency of water sprays can thus be improved significantly if well-charged water droplets (fog) of approximately 20 to 200 $\mu m$ diameter can be generated. Commercially available instruments to generate charged fog, called Foggers are manufactured by the Ritten Corporation, Ardmore, Pennsylvania. These Foggers use either a standard pressure-type or twin-fluid nozzle to atomize the water, thus necessitating a substantial supply of high pressure water or air for proper atomization. These types of nozzles have a tendency to clog if the water supply contains a high concentration of suspended solids (5).

Under EPA sponsorship, AeroVironment Inc., in consultation with S.A. Hoenig of the University of Arizona, developed an instrument called the spinning cup fog thrower (SCFT). This instrument was tested in a wind tunnel facility during 1979 and these test results were reported by Kinsey (5). Since then the SCFT has been completely redesigned and is now capable of generating well-charged water droplets which guarantees a greatly increased collection efficiency. This paper reports the details of this modified SCFT and the field-testing program currently under way.

## THEORETICAL BACKGROUND

A mathematical relationship describing the collection efficiency, E, of suspended particles by water droplets is given by (6, 7)

$$E = 1 - \exp\left[-\frac{3}{2} \cdot \frac{Q_l}{Q_g} \cdot \frac{L}{D} \cdot \eta\right]$$

where $Q_l$ is the volumetric water flow rate, $Q_g$ is the volumetric gas flow rate, L is the characteristic length for the total capture process, D is the mass mean droplet diameter, and $\eta$ is the single droplet collision efficiency.

The single droplet collision efficiency depends on the droplet diameter and its lifetime in the air. It is determined by several mechanisms of interaction between the droplet and the particles which collide with it. These mechanisms include direct interception, inertial impaction, Brownian diffusion, and electric, diffusiophoretic, and thermophoretic forces (8-11). The dominant mechanism for large particles ($>1\,\mu m$ radius) is impaction and interception and for small particles it is Brownian diffusion. To obtain best collection efficiency, the droplets must be small enough to provide both an adequate spray rate per volume of gas treated and sufficient contact time, yet large enough not to evaporate too quickly. The lifetime of a water droplet depends on the temperature and relative humidity of the medium into which it is introduced.

Single droplet collection efficiency (which is assumed to be equal to the collision efficiency) has been investigated by many (8-11). Figures 1A, B, and C show the collection efficiency plotted as a function of particle radius with droplet radius, relative humidity, and electric charge on the droplet as varying parameters, respectively (8). From Figure 1A, it may be noticed that the collection efficiency of larger particles is greater for larger droplets while the collection efficiency of smaller particles is greater for smaller droplets. The minimum in E occurs near a particle radius of $\sim 1\,\mu m$ (due to the ineffectiveness of different interaction mechanisms) and, for droplets less than $\sim 55\,\mu m$ radius, E becomes infinitely low giving rise to the so called "Greenfield gap." Figure 1B shows that the collection efficiency increases with decreasing relative humidity for smaller particles and E is independent of relative humidity for larger particles. Figure 1C, the most interesting one to us, shows that the introduction of electric charge on the aerosol particles and water droplets completely eliminates the minimum in E and substantially increases the collection efficiency depending on the amount of charge. Figure 2 shows a comparison of calculated and experimentally measured values of the single particle collection efficiency as a function of droplet radius for aerosol particles of $0.25\,\mu m$ at about 20% relative humidity and there is good agreement between them.

The collection efficiency over a continuous distribution of aerosol particle sizes by water droplets having a spectrum of radii may be quite different from that shown above for the case of a single droplet. Very little data are currently available from an operating system. Therefore, our field tests of the spinning cup fog thrower are even more significant.

## THE MODIFIED SPINNING CUP FOG THROWER

As mentioned earlier, Kinsey (5) presented the results of wind tunnel tests of an earlier version of the SCFT. The poor collection efficiency of that

instrument has been attributed to: (1) the induction ring method of charging the droplets gave a charge-to-mass ratio of only $1 \times 10^{-11}$ C/g; (2) non-uniformity of the charge on the droplets -- the outer edges of the spray pattern exhibited a slight negative charge whereas the droplets in the center of the pattern exhibited a positive charge; and (3) only a small fraction of the inflowing water was converted to droplets suitable for the capture and removal of dust while the large fraction ended up as large satellite drops which simply hit the tunnel walls. Because of these problems, we have developed a completely different instrument.

The new spinning cup fog thrower is a modified Ray Oil Burner (type AG) which consists of only one movable part, a hollow steel shaft upon which are mounted the atomizing cup, the fan, and the motor rotor. Figure 3 is a schematic representation of the new SCFT. The modifications to the oil burner include replacement of the fuel tube, air cone, and the spinning cup with non-conducting materials. The water inlet tube is attached to the spinning cup and its rear end is connected to the water supply using a rotating seal. We thus have a completely closed water system which is kept at a high potential of 15 kV by direct connection to the positive terminals of a d.c. high voltage supply (12).

Water from the water tube falls into the 3,600 rpm spinning cup whose inside is fabricated to a gradual smooth taper. Because of the centrifugal forces, the water becomes a thin film and moves forward into a high velocity air stream where it breaks up into fine droplets. These droplets are projected forward by the air stream from the fan and an air butterfly is used to set the airflow speed, thus controlling the spray pattern. Figures 4A and B show typical fog patterns obtained with the modified SCFT. The spray patterns cover approximately 20 sq. ft. and the water flow rate was about 8 lph when water was flowing under gravity alone. With the addition of an optional small pump we were able to increase the water input to 68 lph. The total power requirement of this instrument is less than 1 kW. The whole instrument is mounted on a portable platform for easy transport to a remote location. With the addition of a small generator, the SCFT can be operated where commercial electric power is not available.

The droplets were charged by directly connecting the positive terminal of a 15 kV d.c. power supply to the inflowing water. The charge-to-mass ratio was measured using a sample train designed at AeroVironment. This consisted of a stainless steel probe tip mounted on a glass midget impinger. The probe was connected to copper wool packing placed inside the midget impinger and also to an electrometer. The impinger was immersed in a grounded Dewar flask containing dry ice. A sample of droplets was isokinetically collected inside the impinger where the droplets transfer their charge to the copper wool. The current produced in the copper wool was measured with the electrometer and the mass of water collected inside the impinger was obtained gravimetrically. Then the charge-to-mass ratio was calculated. This procedure was repeated several times and the typical value obtained for a 200 µm droplet (see later) was $1.2 \times 10^{-6}$ C/g.

The size distribution of the water droplets was measured using a cloud optical array probe for droplets in the range of 30 to 300 μm (diameter) and a precipitation optical array probe for droplets in the range of 125 to 1,875 μm. These measurements gave a concentration median droplet diameter of 100 μm and a mass median droplet diameter of ~200 μm. These determinations were supplemented by microscope measurements of droplets collected on greased glass slides, with a correction factor of 1.26 applied to account for the change in shape of droplets on slides. This method gave a value of ~90 μm for concentration median droplet diameter.

To determine the particle control efficiency of the SCFT, a field test program has been designed. The field tests are currently under way. Fog from the SCFT will be applied to the sample volume and the SCFT's dust control efficiency will be determined under various experimental conditions. It will be tested with no fog, with uncharged fog, and with charged fog, for a total of 104 test scenarios as shown in Figure 5. The variable parameters for these scenarios are wind conditions, relative humidity, water flow rate into the SCFT, fog pattern, and nature and amount of charge on the droplets.

A sample train has been assembled to extract a representative sample isokinetically. This sample train consists of an elutriator to cut off particles over 15 μm and a five-stage cascade impactor. The samples collected on the filters will be analyzed gravimetrically to determine both the total mass concentration and particle size distribution for each test scenario. From these measurements, we can calculate the control efficiency of the SCFT under various experimental conditions.

## CONCLUSIONS

The new spinning cup fog thrower is a Ray Oil Burner modified to generate electrically charged water droplets for the control of inhalable particles. We were successful in developing a well charged fog which should ensure excellent particle control efficiency. The total power requirement of the SCFT is under 1 kW; therefore, with the addition of a small generator, it can be operated from a moving vehicle such as a road sweeper or a front-end loader.

This modified spinning cup fog thrower is being field tested to determine its particle control efficiency as a function of various field conditions and water and power requirements. These results will be analyzed to evaluate the effectiveness of the spinning cup fog thrower in controlling dust from certain types of sources where other conventional methods can not be applied effectively and economically.

## ACKNOWLEDGEMENTS

The authors are grateful to S.A. Hoenig, J.S. Kinsey, and C. Lyons for their contributions to the Fogger project at AeroVironment.

## REFERENCES


1. Cowherd, C. The Technical Basis for a Size-Specific Particulate Standard. J. of Air Poll. Cont. Assn. 30: 971, 1980.

2. Emmerling, J.E., and R.J. Seibel. Dust Suppression with Water Sprays During Continuous Coal Mining Operations. Bureau of Mines Report of Investigations, RI 8064, 1975.

3. Courtney, W.G., and L. Cheng. Control of Respirable Dust by Improved Water Sprays. Bureau of Mines Information Circular, IC 8753, 92, 1976.

4. Hoenig, S.A. Use of Electrostatically Charged Fog for Control of Fugitive Dust Emissions. University of Arizona. EPA-600/7-77-131, (NTIS PB 276645), November 1977.

5. Kinsey, J.S., C.E. Lyons, S.A. Hoenig, and D.C. Drehmel. A New Concept for the Control of Urban Inhalable Particulate by the Use of Electrostatically Charged Fog. In Proceedings: Fourth Symposium on Fugitive Emissions, Measurement and Control, New Orleans, La, May 1980 (OTRC -- Environmental Consultants, Inc., EPA-600/9-80-041, pp. 388-402, December 1980.

6. Calvert, S., J. Goldschmid, D. Leith, and D. Metha. Wet Scrubber System Study. Volume I, Scrubber Handbook EPA-R2-72-118a, (NTIS PB 213016), August 1972.

7. Cheng, L. Collection of Airborne Dust by Water Sprays. Ind. Eng. Chem. Process Develop. 12: 221, 1973.

8. Wang, P.K., S.N. Grover, and H.R. Pruppacher. On the Effect of Electric Charges on the Scavenging of Aerosol Particles by Clouds and Small Rain Drops. J. of Atmospheric Sciences. 35: 1735, 1978.

9. Young, S.C., S. Calvert, and D.C. Drehmel. Fugitive Dust Control Using Charged Water Spray. (Presented at the 72nd Annual Meeting of the Air Pollution Control Association, Cincinnati, Ohio, 1979.)

10. Wang, P.K., and H.R. Pruppacher. The Effect of an External Electric Field on the Scavenging of Aerosol Particles by Cloud Drops and Small Rain Drops. J. of Colloid and Int. Science. 75: 286, 1980.

11. Pilat, M.J. Collection of Aerosol Particles by Electrostatic Droplet Spray Scrubbers. J. of Air Poll. Cont. Assn. 25: 176, 1975.

12. Mathai, C.V., and L. Rathbun. New Concepts of Control Applied to Urban Inhalable Particulates. Phase I Preliminary Report Submitted to U.S. EPA Contract No. 68-02-3145 EPA, IERL-RTP, December 1980.

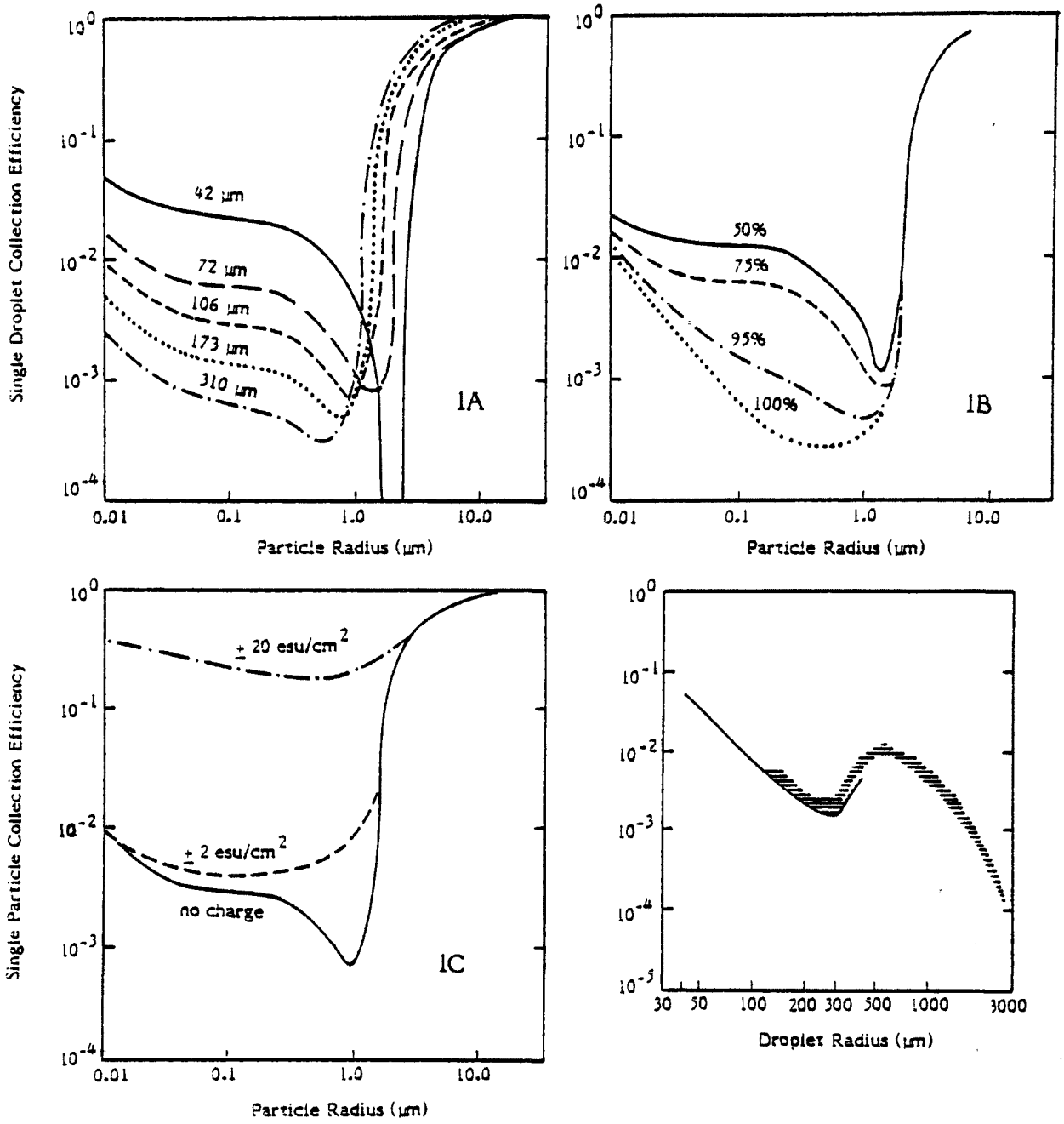


FIGURE 1. Calculated single droplet collection efficiency (8) in air at 10°C and 900 mb as a function of particle radius: A) for various droplet radii and at 75% R.H.; B) for a 72 µm droplet and various R.H.; C) for a 102 µm droplet with various charges and 75% R.H.

FIGURE 2. Comparison of calculated (smooth line) and measured (shaded) single droplet collection efficiency (8) as a function of droplet radius for uncharged aerosol particles of 0.25 µm radius in air (22°C, 1000 mb, and ~20% R.H.)

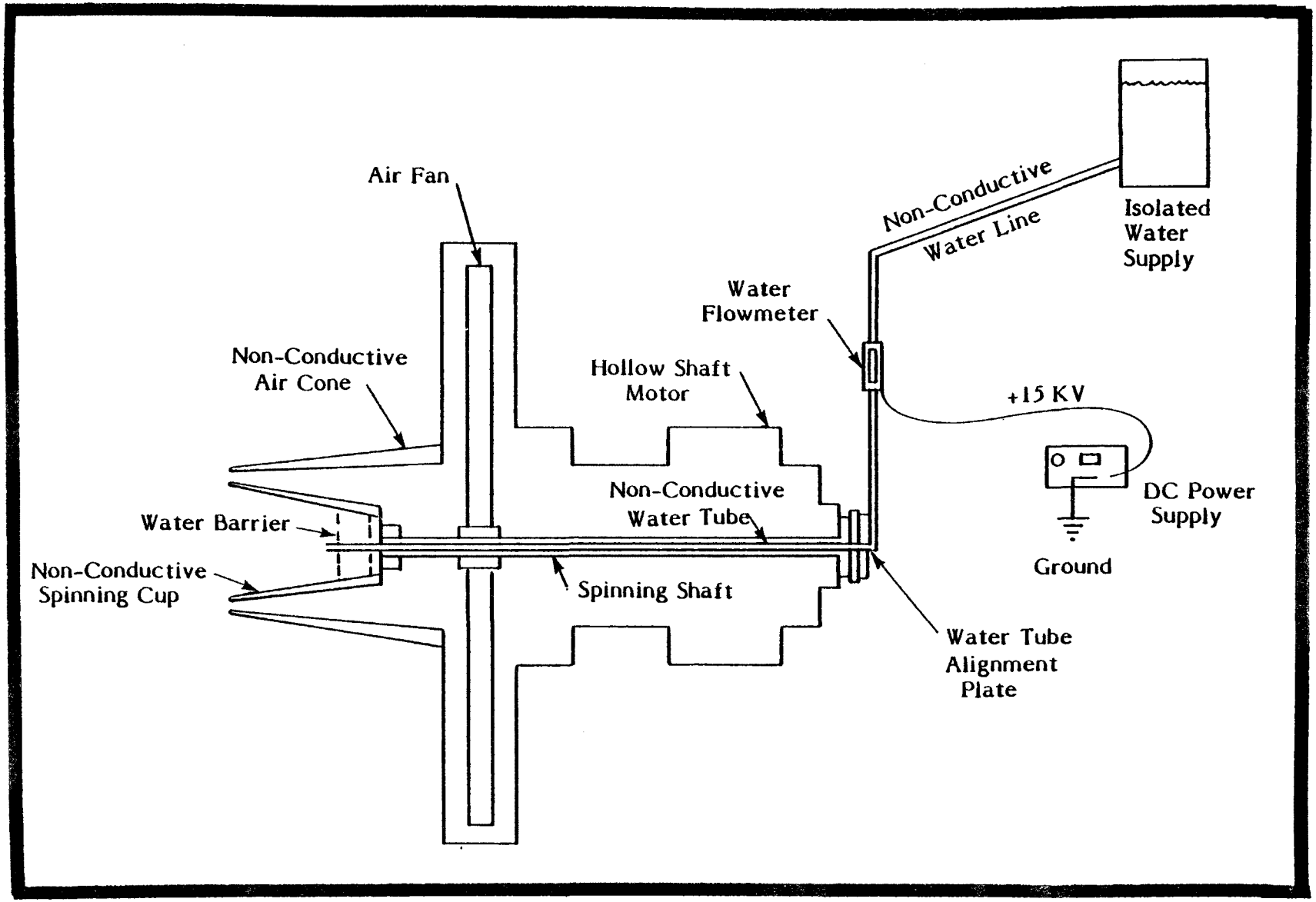


FIGURE 3. Schematic diagram of the SCFT.

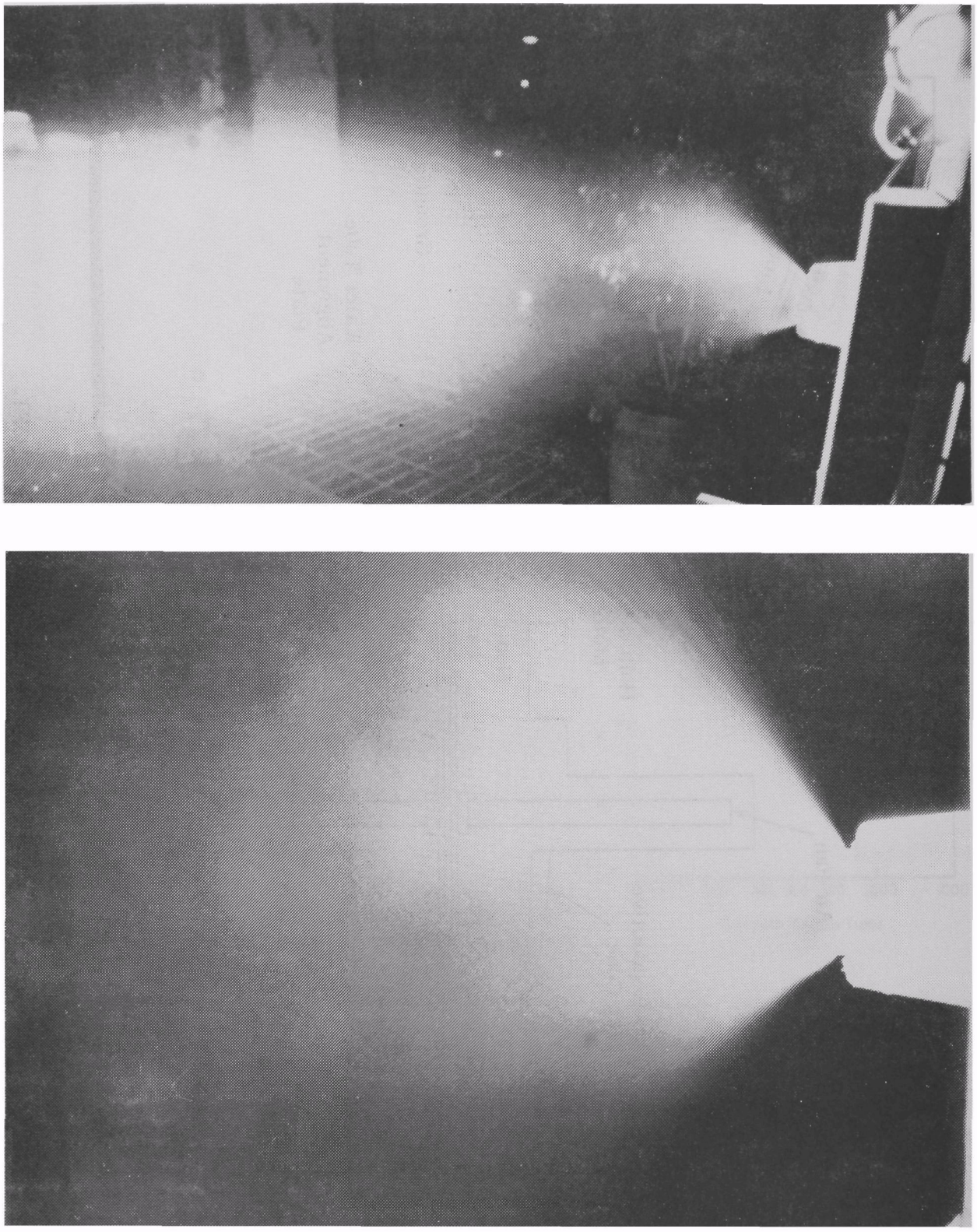

FIGURES 4A and B. Typical spray patterns of the SCFT.

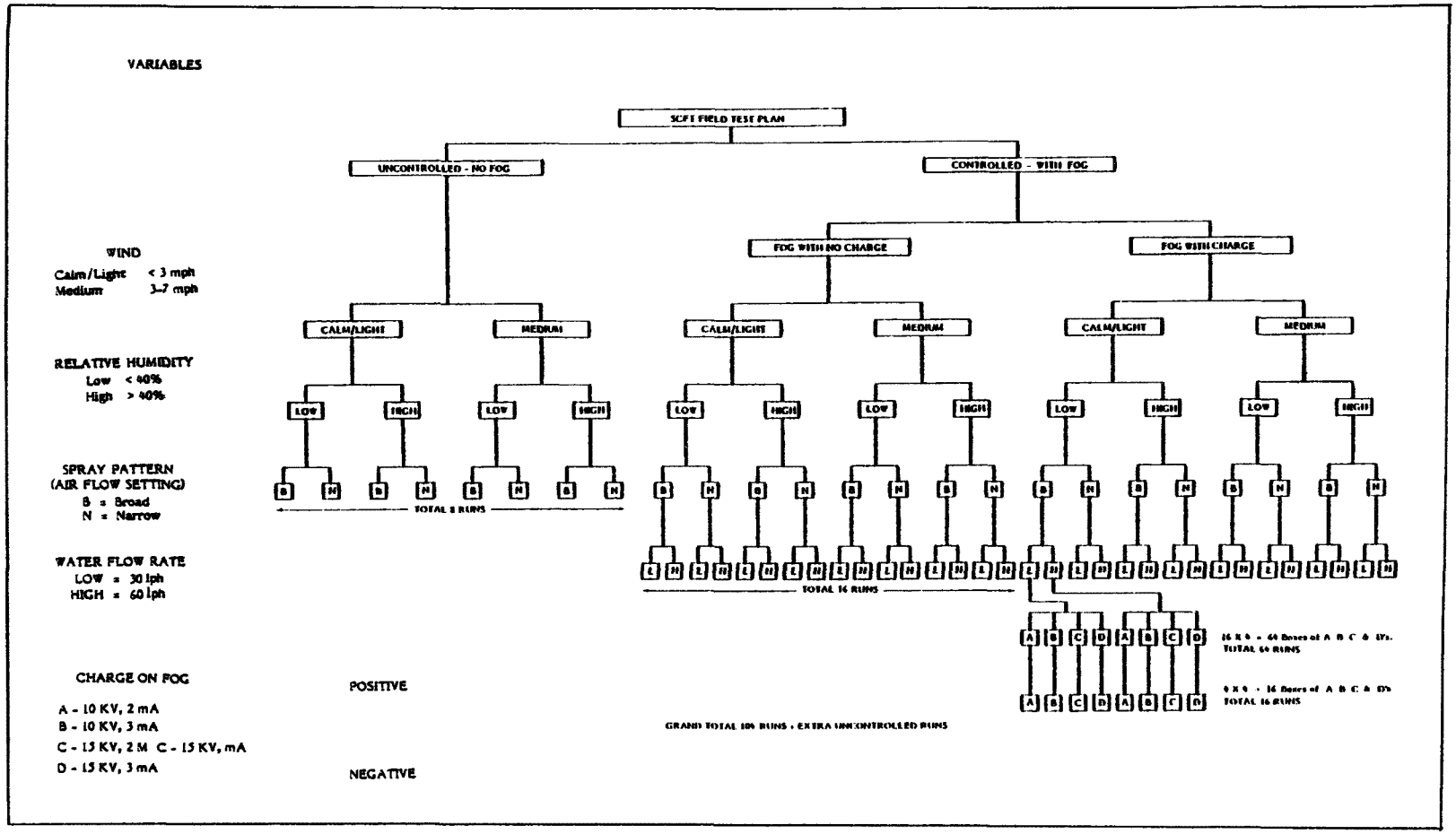


FIGURE 5. Field-test program of the SCFT.

# RELATIVE EFFECTIVENESS OF CHEMICAL ADDITIVES AND WIND SCREENS FOR FUGITIVE DUST CONTROL

By: Dennis C. Drehmel, Bobby E. Daniel
U.S. Environmental Protection Agency
Industrial Environmental Research Laboratory
Research Triangle Park, North Carolina

## Introduction

It has been estimated that in 1976 particulate emissions from open sources were 580 million tons[1] as compared to emissions from ducted sources of 15 million tons.[2] Even if most of the particulate emissions from open sources are large and will settle out quickly, it is evident that open sources will make a substantial impact on ambient air quality. Consequently, the Environmental Protection Agency is investigating control methods for open sources including road carpet for unpaved roads,[3] improved street sweeping for paved roads,[4] charged sprays for industrial fugitives,[5] and wind screens for storage piles.[6] In conjunction with those studies, the control of dust from unpaved roads and storage piles with water and chemical additives must be determined.

The purpose of this work is to evaluate the cost effectiveness of chemical additives and wind screens as opposed to other control methods. Before this can be accomplished, it is necessary to evaluate the wide range of additive properties and effects. The results reported in this paper are from wind tunnel experiments planned to determine the extent of diversity of chemical additives. Future work on the effects of aging and weathering on additives will be needed to allow comparisons between additives and wind screens for control of dust from storage piles. Comparisons for control of dust from unpaved roads will require tests of vehicular wear in addition to aging and weathering tests. Thus, the current study should be seen as beginning a series of studies to evaluate best practice for fugitive dust control.

## Experimental

All tests were conducted in a wind tunnel with a 2 ft square cross section. The active section of the tunnel was 32 ft long. The first 16 ft was used for establishing the desired velocity profile. Next was the 2 ft square dust holder with a 1 ft square recess below the level of the floor of the tunnel. Past the dust holder was a 14 ft long disengagement section. Besides the active section of the

tunnel is an air return loop. In the air return section is a baghouse to clean recycled air to the active section of the tunnel. Design of the active section was intended to produce a turbulent boundary layer similar to that found for wind passing over open ground or a storage pile. Details of this design are given by Shaughnessey et al.[7]

The dust holder located in the active section was a removable section of the tunnel floor. The dust holder was weighed, filled with coal dust, treated, reweighed, and mounted in the tunnel. The dust holder was always filled loosely with dust, even with the top, so that the top of the dust would be even with the floor of the tunnel. Excess dust was pushed horizontally and brushed off. The treated coal layer would dry overnight before testing. The wind tunnel would be operated at several velocities beginning at the lowest and advancing monotonically. After maintenance of a velocity for 3 min, the tunnel would be shut down to remove and reweigh the dust holder. With the dust holder put back, the next velocity was tested. The process was repeated until the maximum test velocity was reached or until the emission rate exceeded 200 gr/min. During some runs, isokinetic sampling after the disengagement section was compared to dust loss results.

For testing the effects of chemical additives, two types of coal dusts were used to determine the importance of dust particle size. The mass median diameters of these two coals were different by a factor of 3. For testing wind screens, the test dust was road silt with a mass median diameter of 148 μm. Ten types of chemical additives were tested as listed in Table 1. These additives were organic salts, oils, acrylics, synthetic polymers, or copolymers. While the recommended total application rates (water + additive) ranged from 0.016 to 8 gal./100 sq ft, the additive rate would vary more widely because of recommended dilution factors ranging from 1 (no dilution) to 6000. For these tests, the additives were diluted with water within the recommended range and applied with either a spray bottle or a spray gun. The application rate was within the recommended range and verified by the volume applied and the weight gain of the coal layer in the holder.

## Results

The emission rate from road dust is shown in Figure 1 for several cases using wind screens. With no wind screen, the loss of dust began at 24 ft/sec and accelerated with increasing velocity. With a 2 in. solid barrier in front of the road dust, incipient reentrainment was in front of the road dust, slightly delayed but the loss of dust accelerated faster than before so that the free stream case and the solid barrier case were very similar in reentrainment profiles. With 1 in. high and 2 in. high mesh wind screens of 50 percent porosity in front of the road dust, the threshold velocity for reentrainment was delayed and the reentrainment profiles were significantly different. A 2 in. high fence of 50 percent porosity was also tested; it gave similar results to the 2 in. high mesh screen. Examination of the velocity profiles before and after the 2 in.

Table 1. TYPES OF CHEMICAL ADDITIVES TESTED

| Additive | Chemical | Additive Supplier | Range of Cost $/gallon | Recommended Total Application Rate gallons/100 sq ft | Recommended Range of Dilution Factors |
|---|---|---|---|---|---|
| Arquad 2C-75 | dimethyldicocoamonium chloride | Armak | 1.66-2.16 | - - - | 30 |
| Coal Dyne | - - - | Aquadyne | 4.25-4.75 | 0.016 | 6000 |
| Coherex | petroleum resin in water | Witco | 1.60-2.55 | 0.4 - 8 | 4 - 5 |
| CPB-12 | acrylic latex | Wen Don | 3.50-4.75 | 0.7 - 4 | 10 - 20 |
| Gantrez An-119 | polymeric anhydride | G.A.F. | 4.41 | | |
| Lignosulfonate | liqnosulfonate | Wen Don | 2.00 | 0.7 - 6 | 1 - 4 |
| Oil & Water | mineral oil | Wen Don | 2.00 | 1.1 | 1 |
| SP-301 | synthetic polymer | Johnson & March | 2.8 - 3.0 | 1 | 1 |
| Pentron DC-3 | acrylic in water | Apollo | 4.00 | 0.4 - 3 | 4 - 10 |
| Polyco 2151 | synthetic copolymer | Borden | 2.95 | | |

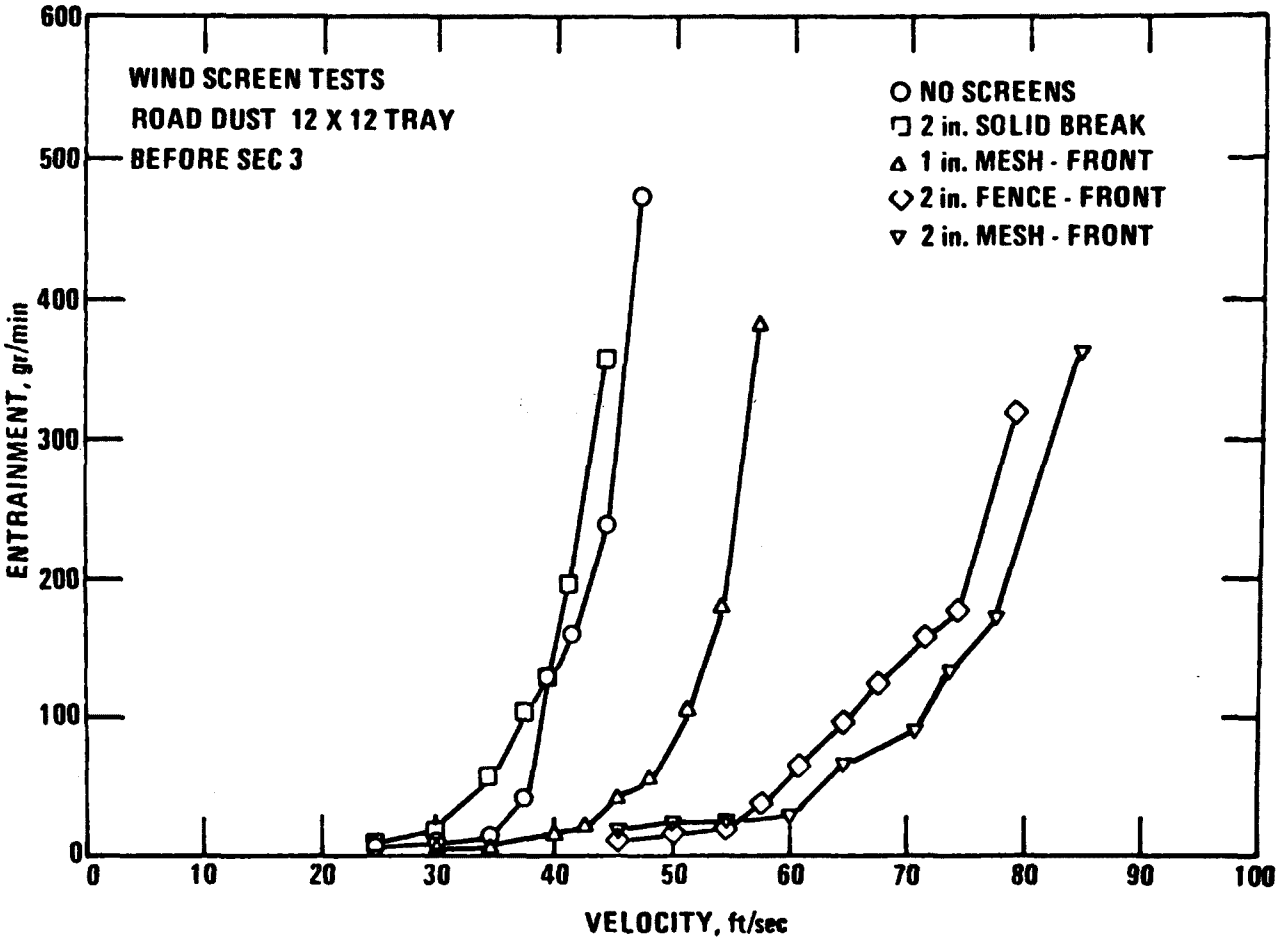


Figure 1. FUGITIVE DUST EMISSIONS (WIND SCREEN TESTS)

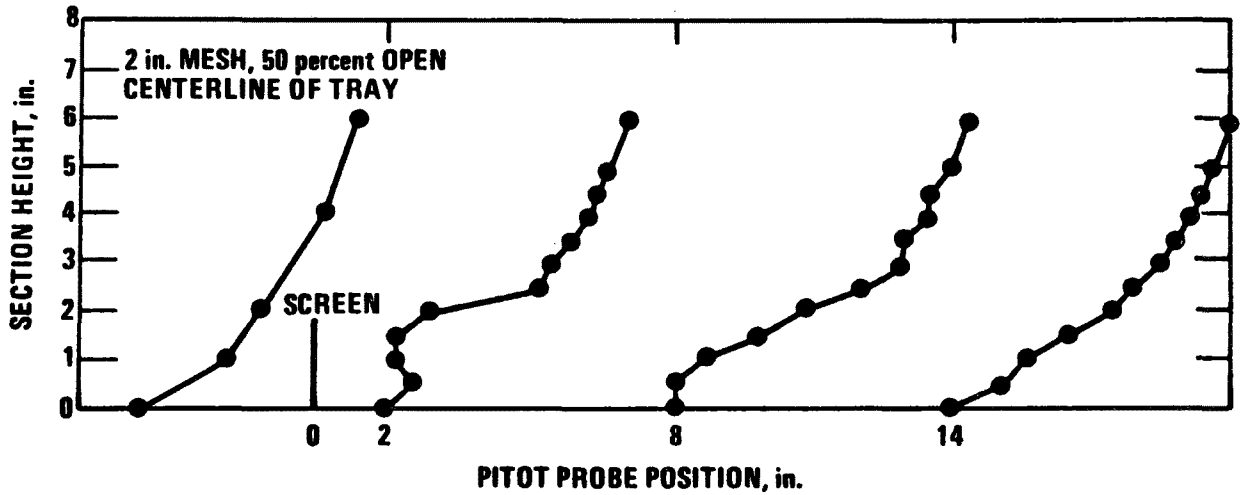


Figure 2. VELOCITY PROFILE AROUND A WIND SCREEN

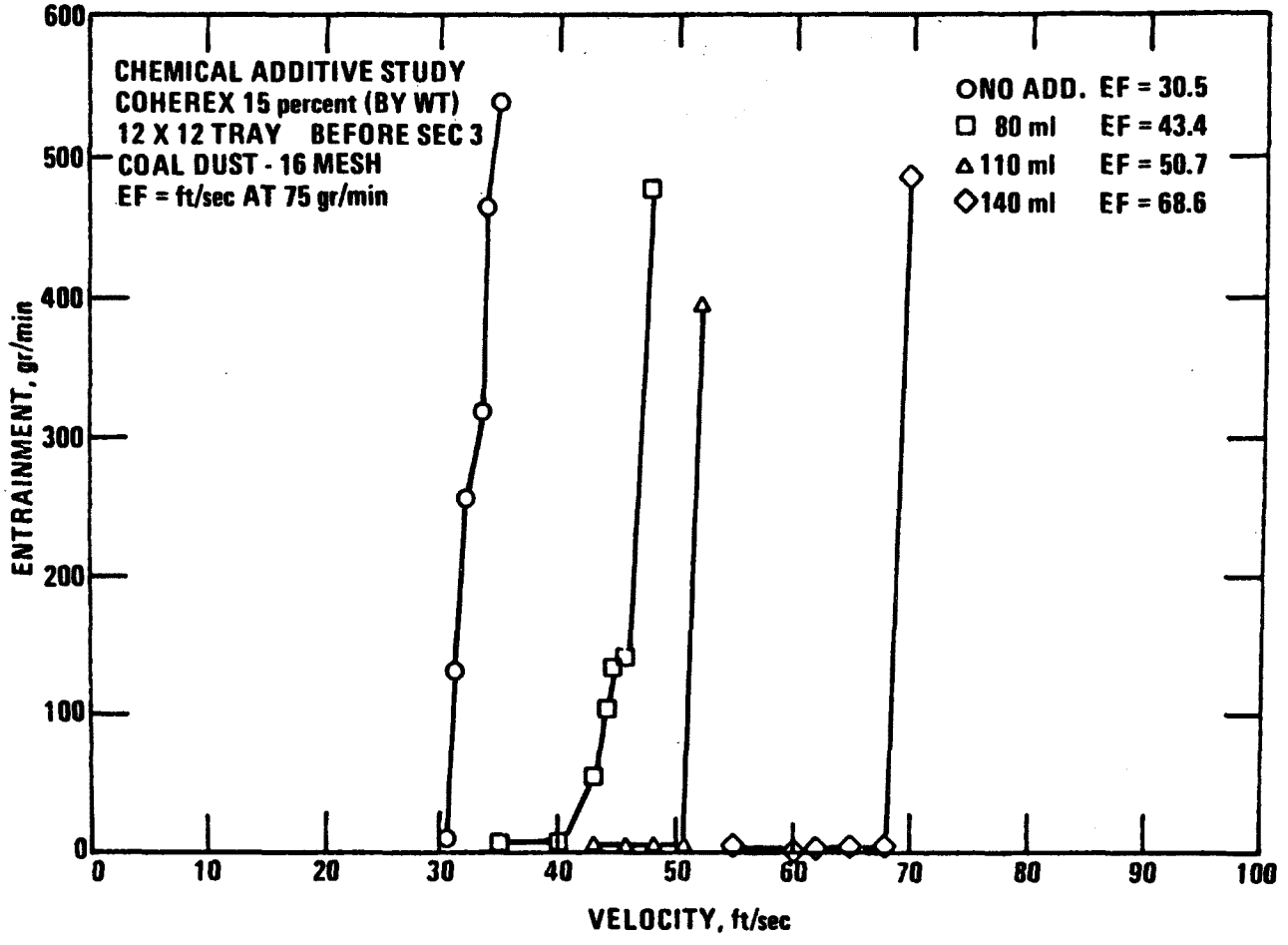


Figure 3. FUGITIVE DUST EMISSIONS (CHEMICAL ADDITIVE STUDY)

high mesh screen provides an explanation of these results. As shown in Figure 2, the upstream velocity profile and the profile at 14 in. down from the screen are almost the same. At 2 in. down from the screen, the air velocity is nearly zero up to a height of 1.5 in. At 8 in. down from the screen, the air velocity is still near zero for the first 0.5 in. above the test dust. Hence the 2 in. high screen is providing a wind shadow of 8 to 14 in. which should protect the 12 in. long section of test dust. If the 1 in. high screen provided a wind shadow at the same ratio, it would protect only the first half of the test dust section from reentrainment. Typical results of treatment with chemical additives are shown in Figure 3. With or without additive, the entrainment rate rises rapidly with wind velocity. Increasing the amount of additive increases the threshold velocity and the placement of the profile. For each combination of coal type, additive type, and application method, there is a set of curves as shown in Figure 3.

To reduce a set of curves, several measures of the velocity-entrainment profile were studied. First, the data was fit with either a second or third order polynomial and solved for the threshold velocity. Second, the lowest velocity causing 75 gr/min reentrainment was recorded. Third, the data was replotted on log-log paper to extrapolate back to the velocity giving 1 gr/min reentrainment. In general the curve fitting for threshold velocity and the back extrapolation on log-log paper gave nearly the same result: the lowest velocity at 75 gr/min was usually 50 percent higher. The last number, the lowest velocity causing 75 gr/min entrainment, was named the entrainment velocity (or EV) to distinguish it from the threshold velocity. As an example of the relationship between the entrainment velocity and the threshold velocity, the EV of the coarse coal dust was 28 ft/sec (19 mph) and the threshold velocity was 19 ft/sec (11.5 mph). Because the velocity-entrainment profiles often varied greatly in slope (for example, see Figure 1), it was felt that a measure of both the intercept and the rate of rise was needed to characterize performance. Hence, the entrainment velocity was used primarily for comparison. Note that entrainment rate varies inversely with entrainment velocity.

1) The addition of water without additive had little effect on entrainment velocity.
2) Compacting the coal with 5 lb/sq ft decreased the entrainment rate by a factor of 4.
3) The coarser coal dust had a 50 percent lower entrainment velocity.

The last result agrees with previous work. As noted by Chepil,[8] for sizes smaller than the most erodible (about 100 μm for soil), erodibility decreases with particle size.

Results for chemical treatment are shown in Table 2. Costs vary over four orders of magnitude with Coal Dyne (the cheapest by virtue of a high dilution factor) and SP-301 (the most expensive). All but Coal Dyne appear to be effective at the manufacturer's recommended rate. In comparing the entrainment factor at a standard cost of $300/acre, the most cost effective additives are Lignosulfonate, Oil and Water, Coal Dyne, and Polyco 2151. Of this group, Polyco 2151 is also effective at a lower cost of $68/acre.

## Discussion of Results

A large number of agents to prevent wind erosion and air pollution have been previously reported.[9,10,11] It is evident from these papers that the effectiveness of a chemical additive to water for fugitive dust control will vary dramatically according to the extent of dilution, application rate, and method of application. Moreover, the optimum conditions for one additive is often unlike that for another. The problem is that for each additive, changes in dilution, application rate, and method of application have different advantages and disadvantages. The greatest cost effectiveness for a given additive may only be determined after the effects of all parameters are understood. Consequently, results as shown in Table 2 must be taken only within the context of the parameters varied during this study.

Method of application was varied only by changing spray technique. The effects of multiple applications and multiple applications with mixing of the top layer were not tested. The two application techniques tested were application with a spray bottle and with a spray gun. One of the additives, Gantrez, could not be applied with a spray bottle. Water modified with this additive would not atomize with the spray bottle application. For some additives there was no apparent difference in the effectiveness using different sprays; these were CPB-12, Pentron, and Coal Dyne. For Coherex, the spray bottle application was more effective. For Arquad, Lignosulfonate, Oil and Water, and SP-301 the spray gun application was more effective.

The effect of dilution appeared to be discontinuous in relation to application rate. If the dilution was too low in combination with a low application rate, poor coverage would result. The poor coverage was evidenced by a non-uniform crust which would have crusted areas in patches, lumps, or "ropes." Between the crusted areas would be uncovered areas ranging from cracks to patches as large as a dime.

The effects of application rate on different additives can be categorized in three groups, depending on the general shape of the curve relating effectiveness to the rate. In all cases but SP-301, this curve is either linear or tending to level off. For SP-301 the curve rose sharply. The three groups are those in which:

Table 2. RESULTS OF CHEMICAL TREATMENT

| Chemical Additive** | Cost at Recommended Rate $/acre | Entrainment Velocity* At Manufacturer's Recommended Rate | Entrainment Velocity* At a Cost of $300/acre |
|---|---|---|---|
| Coal Dyne | 0.15 | 19 | 755 |
| Coherex | 470 | 55 | 44 |
| CPB-12 | 354 | 35 | 32 |
| Lignosulfonate | 460 | 61 | 61 |
| Oil & Water | 968 | 61 | 60 |
| Pentron DC3 | 667 | 44 | 30 |
| Polyco 2151 | 68 | 48 | 50 |
| SP-301 | 1223 | 55 | 21 |

*Lowest wind velocity in mph causing 75 gr/min reentrainment.

**Manufacturer's recommended rates not available for Arquad 2C-75 and Gantrez An-119.

a) Increased rate caused a proportionate rise in effectiveness: Lignosulfonate, Coherex, CPB-12, Polyco, Coal Dyne.

b) Increased rate caused little or no rise in effectiveness: Arquad, Pentron, Gantrez.

c) Increased rate caused a rapid rise in effectiveness: SP-301 only.

It was expected that effectiveness would be proportional to additive rate and this response was the most common. The response of Arquad, Pentron, and Gantrez was not expected. This tendency to produce less effect with more additive may also be viewed as producing more effect at lower application rates than expected. Either interpretation carries the warning that merely using more additive may not solve a problem and that the most cost effective additive rate may not be assumed but should be found by experiment. Lastly, the response of SP-301 may be understood in the content of its chemical nature. As a concentrated latex, SP-301 was observed to form a leathery layer on top of the coal. At increasing additive rates, this layer becomes more uniform with fewer imperfections to the point where the coal covered absolutely. Just before that point, the imperfections in the crust layer are important sites for disturbing the air flow and for weakening the strength of the crust. With a small increase in additive, these imperfections are eliminated with a concomitant dramatic improvement in the effectiveness of control.

## Conclusions

This study helped determine that:

1. Wind screens and fences are effective for prevention of reentrainment and hence for fugitive dust control.

2. A 50 percent porosity screen or fence will cast an effective wind shadow of 4 to 7 times its height.

3. A solid barrier provides no protection against fugitive dust reentrainment. A 50 percent porosity barrier provides protection in that the free stream wind velocity can be doubled before encountering emissions equivalent to those with no barrier.

4. All chemical additives studied significantly increased the threshold velocity and entrainment velocities and hence are effective for fugitive dust control.

5. All chemical additives except Coal-Dyne were effective at the recommended dilution and application rate. Coal Dyne could be made cost effective by lowering the dilution rate to a more typical value (from 6000:1 to 4:1).

6. The effectiveness of additives was strongly dependent on application rate, dilution ratio, and method of application.

7. Too high a dilution ratio may render the additive ineffective and be coupled with run-off problems; too low a dilution ratio may give poor coverage.

8. Increasing the total application rate does not affect the performance of all additives in the same way. Although a proportionate improvement is most common, some additives will not benefit from increasing application.

Table for Conversion to Metric Units

| To convert | to | multiply by |
|---|---|---|
| acfm | $am^3/hr$ | 1.70 |
| in. | cm | 2.54 |
| gal. | liter | 3.79 |
| mile | km | 1.61 |
| mph | km/hr | 1.61 |
| gr | g | 0.065 |
| acre | hectares | 0.405 |
| ft | m | 0.305 |
| sq ft | sq m | 0.093 |

References

1. Evans, J. S. and Cooper, D. W., An Inventory of Particulate Emissions from Open Sources, JAPCA, 30 (12) December 1980.

2. Monitoring and Data Analysis Division, U.S. EPA, National Air Quality and Emissions Trends Report, 1976, EPA-450/1-77-002, December 1977.

3. Levene, B. and Drehmel, D. C., Civil Engineering Fabrics Applied to Fugitive Dust Control Problems. In Proceedings: Fourth Symposium on Fugitive Emissions, Measurement and Control, New Orleans, LA, May 1980, EPA-600/9-80-041 (NTIS No. PB 81-174393), August 1980.

4. Calvert, S. et al., Improved Street Sweepers for Controlling Urban Inhalable Particulate Matter. Presented at Third Symposium on the Transfer and Utilization of Particulate Control Technology, March 9-12, 1981, Orlando, Florida

5. Yung, S., Calvert, S., and Drehmel, D. C., Spray Charging and Trapping Scrubber for Fugitive Particle Emission Control, JAPCA, 30 (11), November 1980.

6. Carnes, D. H. and Drehmel, D. C., The Control of Fugitive Emissions Using Wind Screens. Presented at Third Symposium on the Transfer and Utilization of Particulate Control Technology, March 9-12, 1981, Orlando, Florida.

7. Shaughnessey, E. J. et al., A Wind Tunnel for Dust Entrainment Studies. Presented at Third Symposium on the Transfer and Utilization of Particulate Control Technology, March 9-12, 1981, Orlando, Florida.

8. Chepil, W. S. and Woodruff, N. P., Journal of Advances in Agronomy, Vol. 15, pp 211-302, 1963.

9. Ambrust, D. V. and Dickerson, J. D., Temporary Wind Erosion Control, Journal of Soil and Water Conservation, July-August 1971, pp 154-7.

10. Canessa, W., Chemical Retardants Control Fugitive Dust Problems, Pollution Engineering, 9 (7) pp 24-26, July 1977.

11. Cross, F. L., Control of Fugitive Dust from Bulk Loading Facilities, Pollution Engineering, 12 (3) pp 52-53, March 1980.

# PARTICULATE IMPACT COMPARISON BETWEEN CONTROLLED STACK EMISSIONS FOR A 2000 MW ELECTRICAL GENERATING STATION

By
Dr. Howard E. Hesketh, P.E.
College of Engineering
Southern Illinois University
Carbondale, Illinois 62901

Frank L. Cross, P.E.
Cross/Tessitore and Associates, P.A.
1611 E. Hillcrest St.
Orlando, Florida 32803

## ABSTRACT

The impact on air quality is evaluated in regard to the National Ambient Air Quality Standards (NAAQS) and PSD increments for a coal burning 2000 mw electrical generating station. The hypothetical western station discussed is in mountainous terrain, with elevation of up to 1800 m (6000 ft.) within 35 km (20 miles). The comparison is based on the use of NSPS control for the boilers and BACT control for the fugitive emissions. The "valley" model is used for the impact evaluation.

Combustion emissions are estimated using two different stack heights. The flue gas emission control system consists of cold side electrostatic precipatators followed by limestone flue gas scrubbers. Fugitive emissions include estimates of controlled emissions from the coal and limestone piles, conveyors, stackers, cooling towers, dumpers, and waste ponds plus vehicular traffic in the various work areas. The importance of fugitive emission control relative to stack emissions in meeting PSD and air quality requirements is shown.

## INTRODUCTION

It is difficult to comprehend the magnitude and significance of particulate emissions from large emission sources. In order to compare the effects of elevated controlled stack emissions and low level controlled fugitive emissions this study assumes a hypothetical 2000 mw coal fired utility located in mountainous western terrain.

Both the National Ambient Air Quality Standards (NAAQS) and the new Prevention of Significant Deterioration (PSD) regulations are applicable to utilities and mean that many millions of dollars in control system costs must be expended. In addition, the costs will differ by millions of dollars dependent upon the actual impacts and the specific alternate control technologies deemed necessary to meet these needs. The effects are reflected in all of capital, operating and energy costs.

The PSD particulate increment restrictions which exist for Class I, II, and II areas respectively in $\mu g/m^3$ are 5, 19, and 37, for geometric annual mean and 10, 37, and 75 for the 24 hr maximum.(1)

## Stack Emissions and Height

NSPS dictate that the allowable particulate emissions should not exceed (0.03 lb/$10^6$ btu).(2) At full load this is equivalent to approximately 1.93 x $10^{10}$ btu/hr heat input or 73.4g/sec (582 lb/hr) of particulate emissions. This requires a control efficiency of about 99.6% which can be obtained by ESPs, scrubbers or fabric filters. Filters would be most efficient, however they do not remove the required $SO_2$ without incorporation of alkali spray dry facilities which are currently in a demonstration phase of development. ESPs can achieve this level of particulate control but a large SCA is required and ESPs do not remove $SO_2$ (spray dry systems can use ESPs for the solids removal, but this technology has not been accepted). The new type FGD scrubbing systems, which incorporate gas conditioning, have been shown to achieve 99.6% particulate removal with simultaneous $SO_2$ control when operated with good mist elimination.(3) For emission comparisons, this study assumes that ESPs are used in parallel with limestone FGD wet scrubbers and that the scrubbers have good mist eliminators. No plume reheat is assumed.

Stack emission plume height is dependent upon stack height, stack diameter, type of control system used, exit vel. and temp., and meteorological conditions. This is to say that wet scrubbing emissions would be at adiabatic saturation temperatures of about 328°K (130°F) unless plume reheat is used. For purposes of the comparisons presented in this paper, it is assumed that the plumes are unheated and to evaluate the results of reheat, two stack heights are used. These heights are 114.4m (350 ft.) and 152.5m (500 ft.).

For this facility, four separate stacks are assumed, one for each boiler, each having an exit velocity of 25.2 m/s (82.6 ft/sec) at full load. These data are summarized in Table I for each of the four stacks.

TABLE 1. EMISSION INVENTORY AND STACK DATA FOR FOUR STACKS

| | Comparison | |
|---|---|---|
| Parameter | A | B |
| Stack Height, m | 114.4 | 152.5 |
| Stack Diameter, m | 5.2 | 5.2 |
| Exit Velocity, m/sec | 25.2 | 25.2 |
| Exit Temperature, °K | 328 | 328 |
| Particulate Emissions, g/s | 73.4 | 73.4 |

## Fugitive Emissions

Because of the theoretical nature of this report, certain assumptions on the general arrangement of the power station and the types of equipment for coal handling had to be assumed. Figure 1 is a sketch of the general arrangement of the plant indicating the size and location of coal piles,

conveyors, cooling towers, and train unloading facilities. Table II includes a list of the control systems considered for the fugitive sources of emissions, and the estimated emission from these sources. A 90 day coal and chemical storage pile quantity is assumed. A 1.1 limestone supplied to $SO_2$ removed stoichiometry is assumed.

It is assumed that two 100 car unit trains could be dumped each day at full load operation of the utility. This would amount to a transfer of 20,000 tons coal per day. Actual transfer would occur over a 6 to 8 hr period of time. The values shown in the table are shown as if unloading were continuous so values are lower than actual during unloading periods.

## Dispersion Modeling

### Models and Wind Data

Mountainous terrain is assumed for the location of the power station, and therefore the EPA Valley Model is used to estimate downwind ground level concentrations (GLC). The meteorological data used in the Valley Model calculations for the 3 hr winds is presented as a frequency distribution in Table III. These data are restrictive, but are reported in the mountainous regions of the western United States. EPA "default" data are used for the 24 hr meteorology. A 10 meter plume height is used in these calculations for all ground level emissions sources that are actually less than 10 m high. The fugitive emission sources were considered to originate at 4 locations throughout the area as shown in Figure 1, and appropriate coordinates for these are used as inputs to the Valley Model.

All models are subject to certain imperfections and deficiencies. Yet certain models do consider factors that at least attempt to correct for conditions not considered in other models. It is recognized that Williams and others are in the process of developing high terrain models which may be more accurate, yet at this time the EPA accepts the Valley Model as being most applicable to mountainous terrain modeling. Data basis are being obtained for attempted validation of the EPA Valley and CRSTER (for conventional terrain) models and for other comparable models such as the "Texas" and "Small Hill" models. It is not the intent of this paper to attempt to validate the Valley Model nor is it desired to extend the dispersion predictions to the 1 $\mu g/m^3$ level over hundreds of miles as has been done by others. The Valley Model is used here as it is the only high terrain model accepted by the EPA without validation[7].

### Terrain

A schematic of the downwind terrain showing relative distances and elevations is given in Figure 2. This figure is not to scale and shows only the specific locations corresponding to the wind directions used in Table III. Obviously, other wind directions and terrain conditions could be used.

FIGURE 1

POSSIBLE PLANT ARRANGEMENT
(Simplified Flow Diagram)

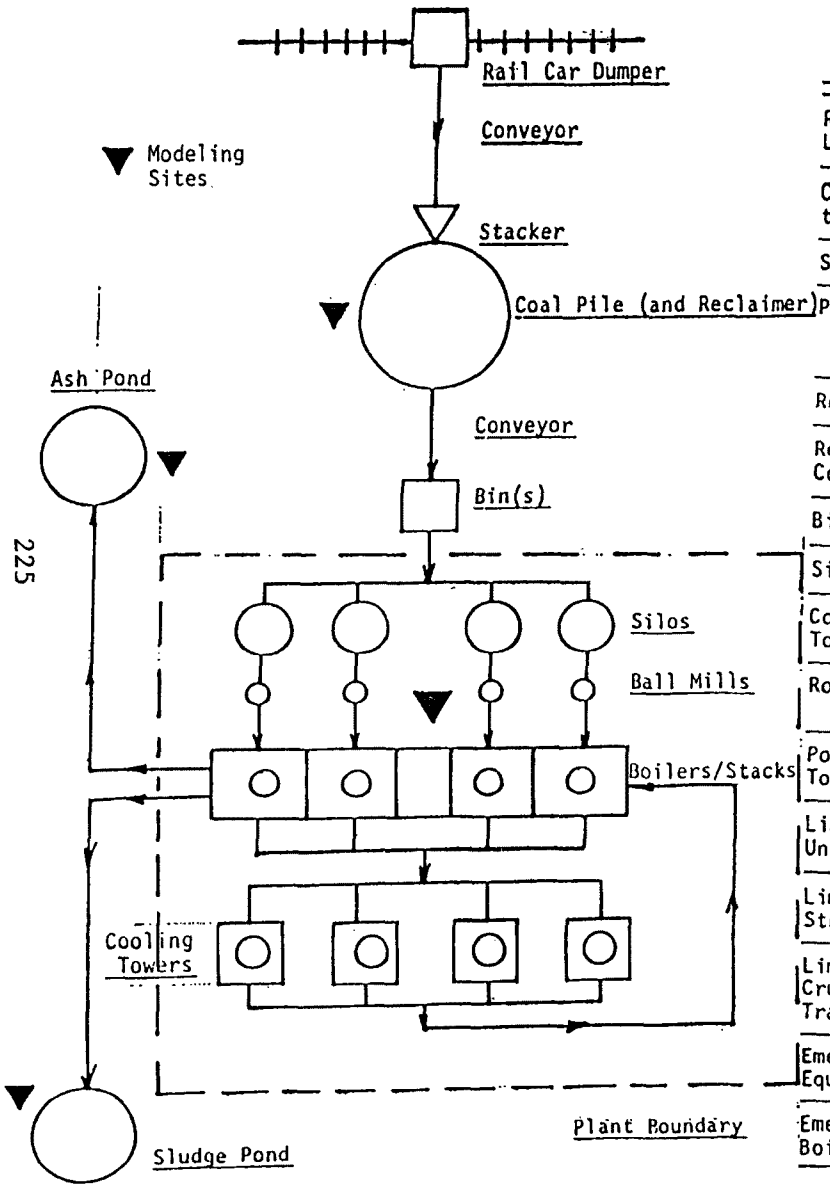


TABLE II — INVENTORY OF FUGITIVE EMISSIONS

| EMISSION SOURCE | BASIS OF EMISSION CALCULATION | EMISSION FACTOR (lbs/ton) Uncontrolled | BACT (%) | EMISSION RATE (lbs/hour) |
|---|---|---|---|---|
| Rail Car Unloading | 200 car dumps/day | 0.007 | zero | 6 |
| Conveyors to Pile | 0.5 miles | 0.2[4] | 90[4] | 17 |
| Stacker | 20,000 TPD | 0.037 | zero | 30 |
| Pile | 40' high, 30.6 acres (90 day supply) | 6.4 lb/acre hr[6] | 90 (enclosed) | 20 |
| Reclaimer | 20,000 TPD | 0.2[4] | 90[4] | 17 |
| Reclaimer Conveyor | 0.5 miles | 0.2[4] | 90[4] | 17 |
| Bins | Single | 0.0002[4] | 95[4] | --- |
| Silos | Four (4) Units | 0.0002[4] | 95[4] | -- |
| Cooling Towers | Four (4) Units | 5.5 lbs/hr per tower[3] | -- | 22 |
| Roads | Estimation 300 Miles Per Day | 2.4 lb/Veh. miles | Yes | 29 |
| Ponds, Total | 100 Acre (Dry) | 1.2 lb/Acre hour[6] | 90 (enclosed) | 12 |
| Limestone Unloading | 1.6 lb/100 lb coal | 0.007 | zero | 0.1 |
| Limestone Storage | 90 day supply | 6.4 lb/hr[6] | 90 | 0.4 |
| Limestone Crushing & Transfer | 0.5 miles & crushing | 0.2[4] | 90[4] | 0.3 |
| Emergency Equipment | 50 hr/yr | 0.2 | zero | 0.2 |
| Emergency Boiler | oil fired/40 days | 1 | zero | 1 |

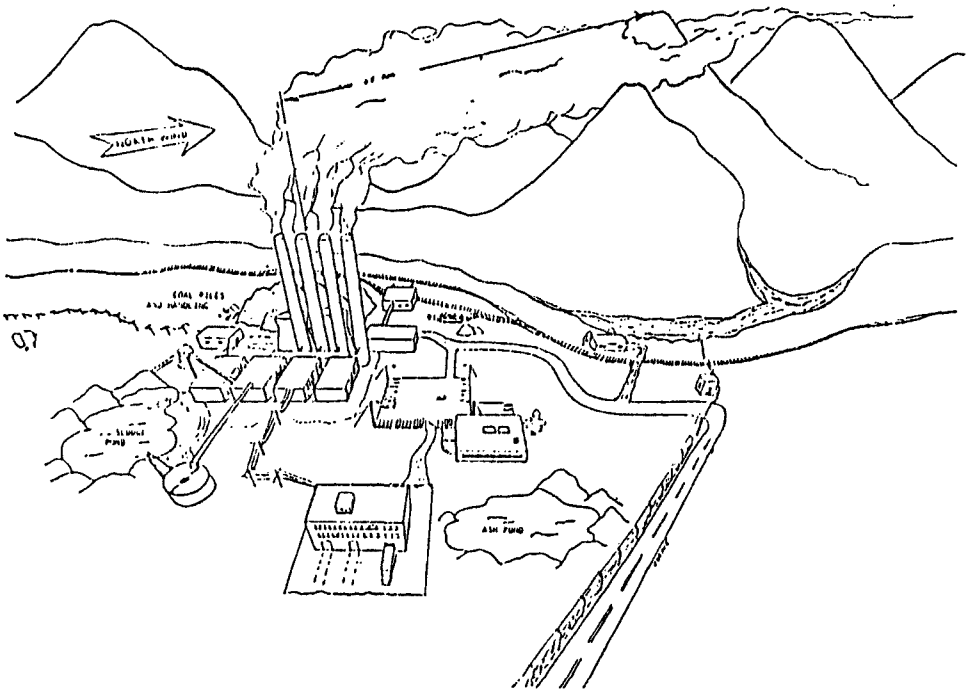

Figure 2. Panoramic Sketch of Generating Station and Local Topography

TABLE III

METEOROLOGY 3 HOUR WIND MATRIX *

| CASE NO. | DESCRIPTION | WIND SPEED | WIND DIRECTION | STABILITY CLASS |
|---|---|---|---|---|
| | | m/sec | | |
| 1 | Low wind speed Unstable | 1.0 | 206 | 1 |
| | | 2.0 | 192 | 1 |
| | | 2.2 | 203 | 1 |
| 2 | High wind speed Unstable | 8.9 | 185 | 4 |
| | | 8.4 | 179 | 4 |
| | | 10.1 | 183 | 4 |
| 3 | Low wind speed Stable | 0.7 | 181 | 6 |
| | | 1.8 | 179 | 6 |
| | | 1.8 | 187 | 6 |
| 4 | Medium wind spd Stable | 2.6 | 189 | ** 6 |
| | | 2.5 | 186 | 6 |
| | | 2.8 | 182 | 6 |

* Personal files

** Case 4 is most restrictive; these data are average for this case and are used for their GLC effects study

Figure 3A - North Receptors

24 Hour Downwind Particulate GLC's Due to North Wind and EPA Star Meteorological Data for Receptor Locations as noted from 2000 MW Utility

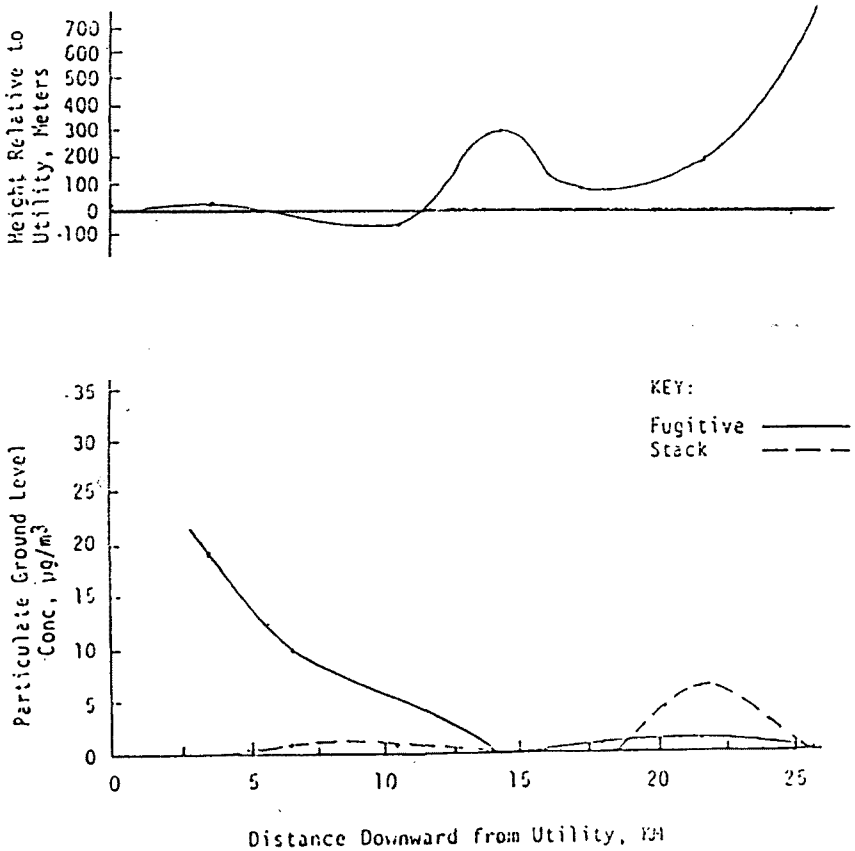


Figure 3B - NNE Receptors

24 Hour Downwind Particulate GLC's Due to North Wind and EPA Star Meteorological Data for Receptor Locations as noted from 2000 MW Utility

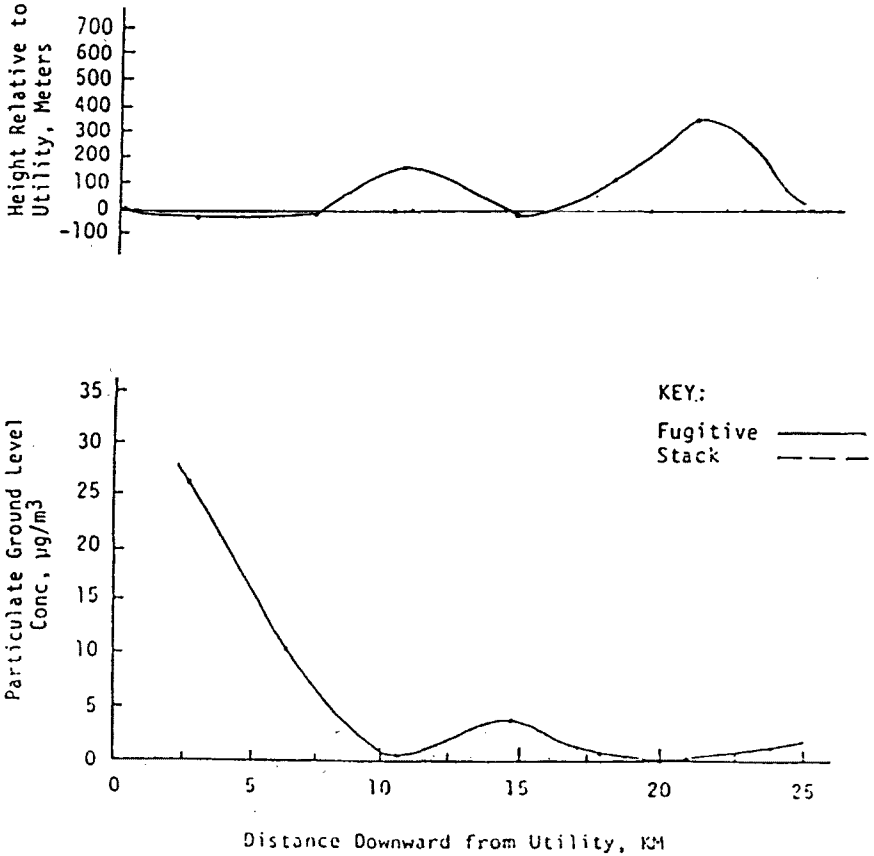

Figure 3C - NE Receptors

24 Hour Downwind Particulate GLC's Due to North Wind and EPA Star Meteorological Data for Receptor Locations as noted from 2000 MW Utility

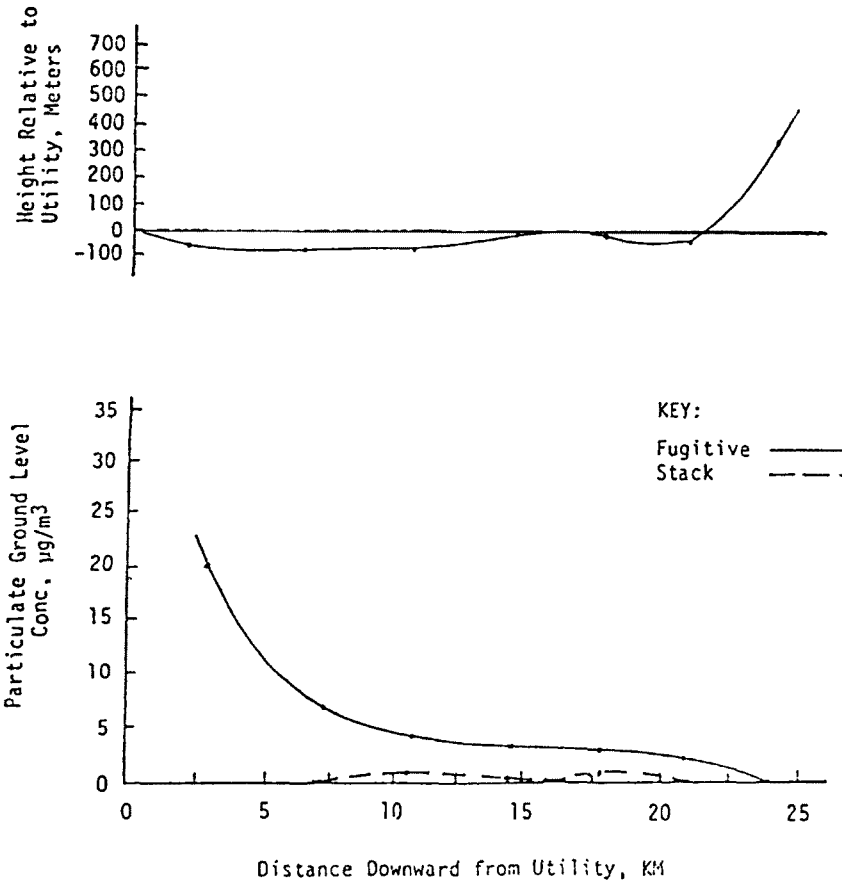


Figure 3D - NNW Receptors

24 Hour Downwind Particulate GLC's Due to North Wind and EPA Star Meteorological Data for Receptor Locations as noted from 2000 MW Utility

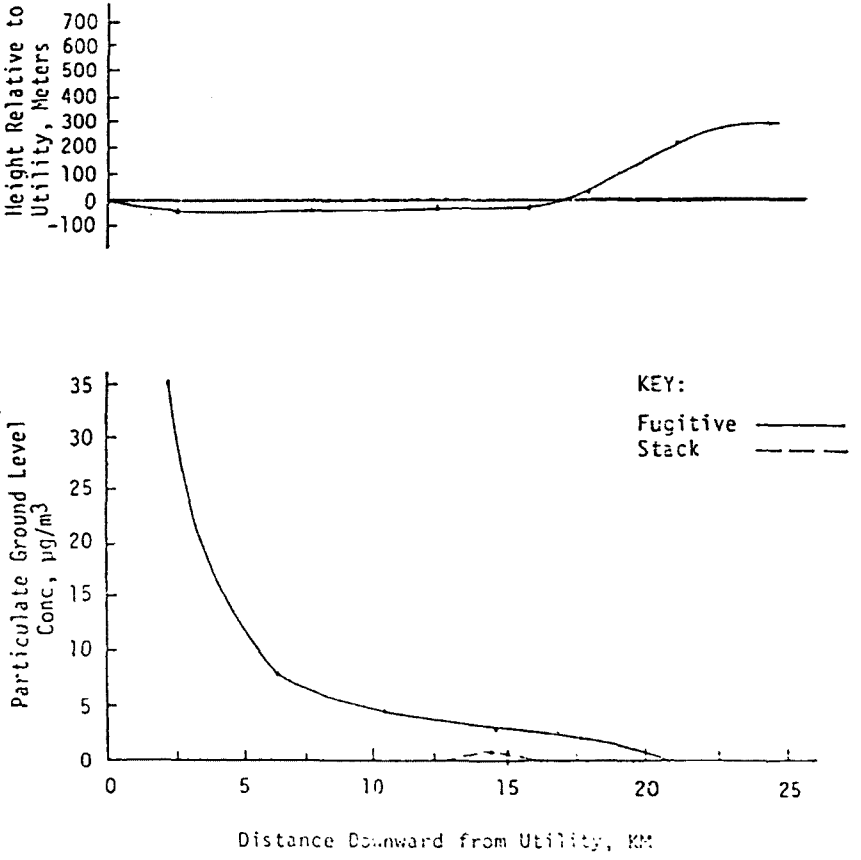

Figure 3E - NW Receptors

24 Hour Downwind Particulate GLC's Due to North Wind and EPA Star Meteorological Data for Receptor Locations as noted from 2000 MW Utility

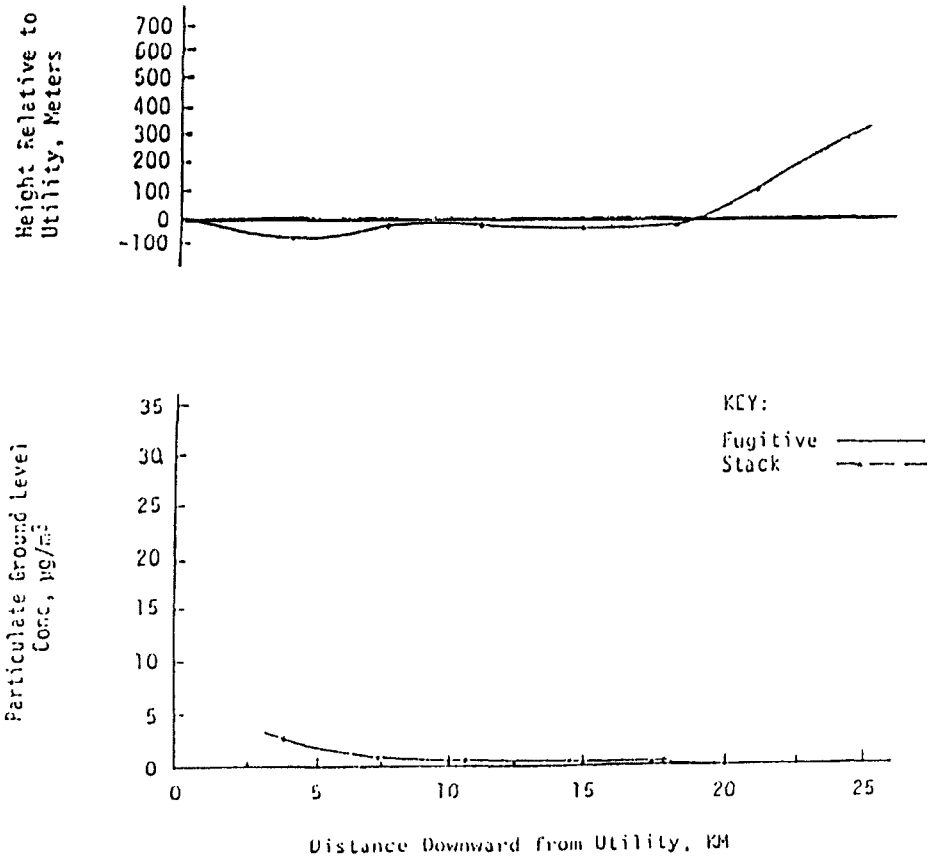


## Impact Analysis Results

Most data show only GLC's for stack emissions. These data show GLC's for the fugitive and the elevated stack emissions. The complete data are given in the figures for all receptors for 24 hour wind persistance averaging times for the most restrictive meteorological conditions. A screening series of model runs were made to establish the most restrictive meteorological data-which turned out to be Case No. 4 as shown in Table III for the particular wind directions and terrain chosen for this study. An actual wind speed of 2.6 m/s and stability Class 6 are used.

Figure 3 shows these data for GLC's due to ground level and elevated emissions. The total emission increases at the specific ground receptors would be the sum of the two individual effects noted in Figure 3. A profile of receptor heights is superimposed on each part of Figure 3. Note that only the 114.4 m elevated source height impact is shown as the impact from the 152.5 m stack are very similar.

Figure 3C shows that for relatively smooth terrain the downwind GLC's of fugitive dust decrease exponentially with distance as would be expected. This figure further shows that effects of controlled elevated emissions are much less than the effects of the fugitive emissions for all distances shown (up to 25km). A comparison of Figures 3A-E show all GLC's decrease with deviation from source wind direction. Figure 3A indicates that a large elevation receptor would block further significant transport of fugitive emissions whereas Figure 3B suggests that a lesser receptor elevation could result in higher fugitive downwind GLC's at greater distances.

GLC's from elevated emissions are more significant at remote receptors. Figure 3A shows the effects of both distance and plume height. This figure shows source emissions could be more significant than fugitive emissions, under these circumstances, only when high elevations exist downwind.

It is apparent from this type of comparisons that coal burning facilities must not overlook fugitive emissions when considering their air impact analyses.

Summary

Comparisons of downwind particulate GLC's from a hypothetical 2000 mw coal burning utility show that "controlled" fugitive emissions can have a much greater impact on air quality than controlled elevated stack particulate emissions. The data from this study are summarized in Figures 3A-E, and show that Class I PSD increments would be exceeded because of fugitive emissions and depending upon the terrain, distance, and meteorological conditions, Class II increments may also be exceeded.

In addition, the following comparisons are shown relative to controlled fugitive dust and controlled stack particulate emissions from a large coal fired utility on downwind particulate GLC air quality:

- fugitive dust can be much more significant
- fugitive dust GLC decreases with downwind distance for relatively smooth terrain
- fugitive dust GLC decreases as source wind direction deviates from source-receptor direction
- a large elevation receptor (>200 m above source) may prevent further downwind transport of fugitive dust
- substantial downwind elevations of <200 m may result in higher fugitive GLC's at greater distances
- GLC's from elevated emission become more significant at remote receptors
- GLC's from elevated emissions may dominate when downwind receptor elevations are "very" high.

## Bibliography


(1) Prevention of Significant Deterioration, Clean Air Ammendments of 1977, PL-95-95.

(2) U.S. Federal New Source Performance Standards, Subpart Da, for New Electric Utility Steam Generating Units started after Sept. 18, 1978, promulgated 6/11/79, CFR 44 FR 33580.

(3) Grimm, C., et al, "The Colestrip Flue Gas Cleaning System", CEP, Vol. 85, No. 5, pp. 51-57, Feb., 1978.

(4) Evaluation of Fugitive Dust Emission from Mining, IERL, EPA, Contract 68-02-1321, April, 1976.

(5) Potential Site Study for a 1500MW Coal Fired Generating Station near Creston, Washington. Prepared for the Energy Facility Site Evaluation Council, Olympia, Washington, prepared by URS Company, (1979).

(6) Currier, E.L., and Neal, B.D., "Fugitive Emissions from Coal Fired Power Plants", paper NO. 79-11.4, proceedings 72nd Annual APCA meeting, Cincinnati, Ohio, June 24-29, 1979.

(7) "Winds of Change Reshape Air Pollution Modeling", Chemical Engineering, Vol. 87, No. 24, pp. 35-37, December 1, 1980.

# OPERATING EXPERIENCE AND THE TECHNIQUES IN THE CONTROL OF COAL DUST EMISSIONS FROM LARGE STORAGE PILE AT NANTICOKE TGS

By: N. Krishnamurthy
Ontario Hydro Corporation
700 University Avenue
Toronto, Ontario
Canada, M5G 1X6

W. Whitman
Nanticoke Thermal Generating Station
Nanticoke, Ontario
Canada

Y.V. Nguyen
Ontario Hydro Research Division
800 Kipling Avenue
Toronto, Ontario
Canada, M8Z 5S4

## ABSTRACT

The large coal storage and handling operation at Nanticoke Thermal Generating Station has caused significant coal dust control problems. Investigations were made to identify the principal sources of airborne coal dust. The dust emission rates and particle size distribution from different sources were measured and dispersion calculated. An estimate of the impact of these emissions on the area surrounding the station were made. Physical model studies were carried out in an open channel water flume to determine the optimum shape of the coal pile and derive optimum techniques in operation. Several coal dust control agents to reduce the dusty character of the coal were tested and evaluated. The application of these results to the Nanticoke TGS coal pile management and experience are discussed.

## INTRODUCTION

Nanticoke TGS is a 4 000 MW coal-fired generating station located on the north shore of Lake Erie. Although this station has not operated at its full capacity to date, ultimately it will receive a total of over 7 000 000 Mg of eastern US and western Canadian coals per year and store 4 500 000 Mg on the stockpiles for the winter peak period when the lake is closed to shipping. During the shipping season, on average, a 30 000 Mg shipload is received each day. Material handling of this coal is accomplished with conveyers, 2 stacker-reclaimers, 1 radial stacker, 10 tractor-scrapers, and other mobile equipment.

Since 1976, Ontario Hydro has received a number of complaints from the cottagers in the northeast of the plant that coal dust is being blown from the plant coal piles onto their properties. The dustfall rate in the cottage area was in the range of 2.5 Mg/($km^2$.mo) to 5.9 Mg/($km^2$.mo)/1/ which is below the Ontario ambient air quality criterion of 7 Mg/($km^2$.mo)/2/ but coal dust is a nuisance problem and the Ontario Environmental Protection Act prohibits adding any contaminent to the environment which can cause impairment to the quality of the natural environment. The Ontario Ministry of the Environment expressed concern about this problem to Ontario Hydro and accordingly Ontario Hydro formed a task force to study the problem and recommend solutions. This paper outlines the findings on the sources and control of coal dust emissions. The control technology is not complex, but for such a large materials handling operation, an organized, integrated approach was required. The approach taken was to identify the principal sources of coal dust emissions, estimate the impact of emissions on the surrounding environment, and then modify the coal handling operation to minimize the dust generation.

## COAL HANDLING OPERATION AND SOURCES OF COAL DUST

### Coal Handling Operation

Figure 1 shows schematically the coal handling operations at Nanticoke in 1977. Coal was unloaded at the dock hopper from a self-unloading ship at a maximum rate of 5500 Mg/h. This operation was dusty under high wind conditions.

From the dock hopper coal was conveyed to the transfer house in two covered conveyors and then either to the plant or to two stacker-reclaimers for stockpiling. Each stacker-reclaimer is rail-mounted and forms two long and narrow temporary surge piles, one on each side of the rail track. This stockpiling operation generated dust especially under high wind conditions. From the surge piles, coal was moved to the main storage pile by tractor-scrapers to provide the winter coal requirement for the plant. The tractor-scrapers weigh 100 Mg when loaded and pulverize the coal on the haul roads to a fine dust which can be picked up in the wake of moving vehicles. Haul roads were identified as sources of airborne dust. After the coal was unloaded from the tractor-scrapers onto the main coal pile, the coal surface was smoothed out and compacted by a rubber-tired bulldozer and sprayed with water using a water wagon. This reduced the amount of airborne dust but under high wind conditions and with dry coal, dust emissions could still be seen from the top surface of the coal pile as well as from the sides and at the leading edges. In the winter, when the lake is closed to shipping, coal was reclaimed from the main storage pile by the tractor-scrapers running down the slope of the pile. This operation generated significant amounts of dust due to the wind turbulence at the reclaiming area.

Figure 2 shows a recent modification to the coal pile handling operation to accommodate western Canadian coal. This coal contains a much larger proportion of fine particles than the eastern US coal and worse problems were anticipated with this coal. This coal is received at a separate dock and transferred to a temporary surge pile created by a radial stacker. This

stacker is equipped with a water spray system which forms a curtain around the falling coal. The dock hopper is fitted with a dust hood and rubber curtains at the opening. These facilities control and contain dust effectively.

Airborne Dust and Impact of Emissions

Airborne dust sampling was carried out at the locations identified above viz stacker and reclaimer, haul roads, and on top surface and sides of the piles. The results of the dust concentrations at these locations are shown in Table 1. The geometric mass mean diameters of the samples collected were:

(a) Stacker-reclaimers surge piles - 18 μm-26 μm

(b) Haul roads with vehicle travelling - 12 μm-30 μm

(c) Top and sides of coal pile due to turbulent wind conditions - 12 μm-35 μm

These particles were small enough to be dispersed to the cottage area and thus had to be controlled.

The impact of these dust emissions on the area surrounding the station was assessed using a downwash dispersion model/2/. The maximum coal dust deposition rate is a function of wind speed and distance downwind from the coal pile, and it was estimated that the maximum deposition at the nearest cottage was between 3.8 Mg/($km^2$.mo) and 5.2 Mg/($km^2$.mo) which is similar to the monthly dustfall measurements made by Ontario Ministry of the Environment, 2.5 Mg/($km^2$.mo) to 5.6 Mg/($km^2$.mo)/1/. This agreement was probably fortuitous but it did indicate that dust from the coal pile could be a nuisance problem for the cottage area and furthermore, the dispersion model showed that dust can be dispersed to as far as 3 km downwind from the plant. This indicated strongly that there was a need to control coal dust from the Nanticoke coal pile operation.

## PHYSICAL MODELLING STUDY

As one step in the control program, Ontario Hydro hired a consultant to examine the effect of wind turbulence on the coal pile by constructing a physical model, 720 times reduction of the coal pile and placing it in an open channel water flume to simulate the effect of wind turbulence on the coal pile.

This modelling study allowed local wind flows to be visualized and permitted modifications to be introduced without difficulty into the coal pile model to reduce the wind blowing coal dust. The transport of coal particles was simulated by the introduction of silica sand into the model area. Areas of scouring or quiescence could be easily identified visually and problem areas could be examined by the introduction of a coloured dye at the problem spot.

The above study made the following recommendations for reducing the wind blown dust around the coal pile.

(a) The coal pile surface should be smooth and erosion should be controlled.

(b) The coal pile should have gentle slopes, as low as 1:7 or should be treated with a dust suppressant.

(c) Semi-permeable fences with 50 percent open area should be installed on and around the coal pile to reduce the wind velocity and turbulence.

(d) Operation of equipment which creates dust should be restricted to wind protected areas.

Practical applications of these recommendations were considered when modifying the coal pile operation. The pile building techniques were changed to allow compaction of the coal on the sides and sealing the surface with waste oil to give a smooth surface and prevent wind and water erosion.

Due to space limitations, the gentle sloping coal pile with a gradient of 1:7 was not possible.

The semi-permeable fences with 50 percent open area, would need to be at least 4 m high and portable. The fence would be too costly to construct to withstand the expected wind load and not practical for regular operation. Thus, the use of these fences has been postponed pending further studies of other coal dust control techniques.

The major application to the coal pile of the results of the modelling study was a complete revision of the coal reclaiming technique so that the operation of equipment that creates dust can be restricted to wind protected areas. In previous years, coal was reclaimed from a bowl surrounding the reclaim hopper by driving the tractor-scrapers down the slope. Modelling studies showed that there was considerable turbulence in the bowl and that dust generated by the scraper movement would not settle out. In 1977/1978, the coal pile was redesigned so that the pile itself acted as a protective berm allowing drifting coal to settle.

## COAL DUST SUPPRESSANT EVALUATION

A wide range of coal dust suppressant agents were studied in both the Research Division laboratory and on experimental coal piles at Nanticoke. Weight loss data and the capability of the suppressant agent to retain its dust binding properties for longer periods were used as performance indicators.

A bitumastic emulsion, and waste oil were selected for trials on the Nanticoke coal pile. The bitumastic emulsion was used to seal the sides of the coal pile and the initial characteristics of the treated surface were most satisfactory. But after about two months, weathering began to deteriorate the quality of the surface crust and large sheets of the treated surface were slipping down the pile sides exposing an unsealed surface. Waste oil was used to seal the haul roads on the coal pile, at an application rate of approximately 1 $L/m^2$. The resulting coal surface had no crust, but the small coal particles were well retained on the coal surface. The effectiveness of the oil depended on how soon the tractor-scrapers were allowed to travel on

these haul roads after they were oiled, and the extent of coal spillage from tractor-scrapers. At Nanticoke the haul roads need to be oiled every two weeks to maintain their dust-free character.

## COAL DUST CONTROL PROGRAM AT NANTICOKE

Following the identification of the sources of airborne coal dust at the coal pile, a coal dust control program was implemented which took into account the results of the modelling and coal dust suppressant studies as far as practically possible. This program involves modifications to the coal handling operation at the dock hoppers, stacker-reclaimers, and at the main coal pile areas.

At the dock hopper for receiving the eastern US coals, the distance that coal falls through the air has been minimized by lowering the height of the ship boom as the ship unloads. The ships have installed sprays, hoods, and side screens around the end of the boom. At the dock hopper for receiving the western Canadian coal, the hopper is equipped with two rotating sector screened hoods to provide a totally protected environment when unloading coals from the ship boom. Any airborne dust particles in the hood can be collected by a baghouse filter.

At the stacker-reclaimer surge piles, dust generation has been reduced by lowering the free fall distance of the coal. A water spraying to agglomerate any remaining dust from this falling coal is under consideration. Water spraying has also been applied to the radial stacker for the western Canadian coal and is found to be effective for dust control.

On the main eastern US and western Canadian coal piles, the wind turbulence along the pile sides has been reduced by a revised method of compacting coal and using waste oil to retain dust on the surface. The dust from the haul roads on the coal piles is being controlled by using waste oil and the dust from the top surface of the pile is being controlled by using two water wagons. The water wagons are used whenever there is any coal movement on the coal pile in the summer as well as in the winter.

The coal reclaiming technique from the main coal piles has been completely revised, as mentioned earlier, to permit the coal to be reclaimed from the lee side (Figure 2) of the pile so that the pile itself acts as a protective berm for any airborne coal dust to settle out.

The effectiveness of this control program has been monitored by a particulate monitoring network which has been in operation since 1977.

## COAL DUST MONITORING NETWORK

The monitoring network includes nine monitoring sites located between 0.2 km and 4.2 km from the coal pile. All sites monitor dustfall, the one site about 1 km to the northeast of the coal pile, has additional monitoring equipment consisting of a standard hi-vol, an isokinetic hi-vol sampler and wind velocity and direction instrumentation/4/.

The dustfall data show no significant change following implementation of the coal dust control program but the coal fraction (by volume) in dust has decreased since 1978. The total carbon fraction are in the range of 10 percent to 30 percent of the total dustfall sample.

The hi-vol data between July 1977 and April 1979 show four exceedances of the 24 h Ontario air quality criterion of 120 $\mu g/m^3$; however, in only one case was the free carbon content of the dust sample high (40 percent); the other three samples contained less than 10 percent free carbon. The hi-vol sampling data were of limited value in characterizing the impact of coal pile operations in the cottage area because the sampler has a low collection efficiency at high wind speeds. Only at consistently low wind speed (< 10 km/h) is a representative sample of airborne particulate likely to be collected and these are not the conditions likely to result in significant fugitive emissions from the coal pile.

The isokinetic hi-vol sampling data are the only data considered to be of value in characterizing the impact of coal pile operations in the cottage area. This sampler, developed by Ontario Hydro, Research Division, consists of a cyclone collector ahead of the standard hi-vol sampler/5/. This sampler collects dust samples isokinetically over a wind speed range of 15 km/h to 45 km/h whenever wind is from the direction of the coal pile. The sampler was in operation after the implementation of the coal dust control program and therefore, the sampling data cannot be used to assess the effectiveness of the control program. However, the data point out that high dust concentrations (> 150 $\mu g/m^3$) occurred infrequently, were of short duration (< 10 hours) and the highest frequency of occurrences was in the winter months. Even during these high dust episodes our very limited data show that the free carbon contents of the dust were about 12 percent.

Since the implementation of the coal dust control program, the number of complaints of coal dust in the cottage area to the northeast of the coal pile have reduced. Ontario Hydro is continuing to operate this monitoring network to examine the effect of significantly greater usage of the fine western Canadian coals on particulate levels in the cottage area and the monitoring data obtained to date will provide a basis for comparison of the relative dust levels.

## CONCLUSIONS

1. The main sources of airborne coal dust are the operation of the tractor-scrapers on the haul roads and the wind blown dust from the top surface and sides of the coal piles.

2. Dispersion model studies indicate that if coal dust emissions are not controlled, dust can be dispersed as far as 3 km downwind from the coal piles.

3. The windblown dust from the sides of the coal pile has been reduced by a revised method of compacting coal and covering it with waste oil. The dust from the top surface of the pile has been controlled by spraying water from two water wagons and the dust from the haul roads controlled by spraying waste oil on the roads.

4. The coal reclaiming operation has been completely redesigned and coal is now being reclaimed from the leeward side of the pile so that the coal pile itself acts as a protective berm to allow any airborne coal dust to settle out.

5. The particulate monitoring network is a valuable tool to assist in designing coal dust control strategy, but conventional dust sampling equipment such as hi-vol and COH tape samplers are of very limited value.

## ACKNOWLEDGEMENTS

The authors acknowledge the contributions of the members of the task force on coal dust control, including Messrs. G.R. Taber, D.W. Hotchkiss, T.B. Walls, M.J. Northfield, J.R. Ryan, M.R. Booth, R.W. Glass, and others. Modelling studies were performed by Morrison, Hershfield, Theakston, and Rowan Limited.

Permission for publication of this paper has been given by Ontario Hydro. The opinions stated are those of the authors and do not necessarily reflect official Ontario Hydro policy.

## REFERENCES

1. Nguyen, Y.V. Airborne Coal Dust at Nanticoke GS. In: Summer Operating Conditions. Ontario Hydro Research Division Report, 77-467-K, 1977.

2. The Environmental Protection Act, Ontario Regulation 872/74, 1971.

3. Nguyen, Y.V. Evaluation of Coal Dust Control Agents. Ontario Hydro Research Division Report, 78-70-K, 1978.

4. Glass, R.W. Nanticoke TGS Coal Dust Monitoring. Ontario Hydro Research Division Report, 79-556-K, 1979.

5. Glass, R.W. An Isokinetic Hi-Vol Air Sampler. Ontario Hydro Research Division Report, 78-79-K, 1978.

6. Booth, M.R. Report of Task Force on Coal Dust Control. Thermal Generation Division Report, NA59-07112.

7. Booth, M.R., Whitman, W.N., and Krishnamurthy, N. Coal Dust Management at Nanticoke TGS. Report TG-07112. This paper was presented at the Canadian Electrical Association, Thermal and Nuclear Power Section Meeting, in Calgary, October 15-17, 1979.

TABLE 1. SUMMARY OF COAL DUST CONCENTRATIONS AT VARIOUS SAMPLING LOCATIONS DURING HANDLING OF US AND WC COAL

| Date | Location | Type of Coal | Dust Concentration $mg/m^3$ | Comment on Location |
|---|---|---|---|---|
| Aug 3,77 | 1 | US | 1.2 | Near the stacker pile, |
| 12,77 | 2 | WC | 7.3 | during stacking. |
| Aug 4,77 | 3 | US | 1.3 | Near the north stacker |
| 12,77 | 4 | WC | 18.9 | coal pile in a breeze. |
| Aug 4,77 | 7 | US | 75.3 | In the wake of a van |
| 4,77 | 8 | US | 97.2 | travelling on the haul |
| 12,77 | 9 | US | 146.7 | roads and ramps. |
| 12,77 | 10 | US | 171.4 | |
| 12,77 | 11 | US | 194.4 | |
| 12,77 | 12 | US | 185.8 | |
| Aug 3,77 | 14 | US | 7.7 | On the side of the main |
| 3,77 | 15 | US | 0.9 | coal pile in a breeze. |
| Aug 2,77 | 5 | US | 0.9 | On top of the main coal |
| 3,77 | 6 | US | 0.3 | pile. |

Note:

Airborne dust samples were collected 1.5 m above the ground level near the sources identified above by drawing air through a 0.8 cm diameter nozzle onto a millipore filter paper, 0.45 μm pore size. Isokinetic samples were obtained by measuring the wind speed at about 15 cm above the sampling nozzle with a portable anemometer and the sampling rate adjusted to match the wind speed.

Legend

mo - Month
// - Reference Number

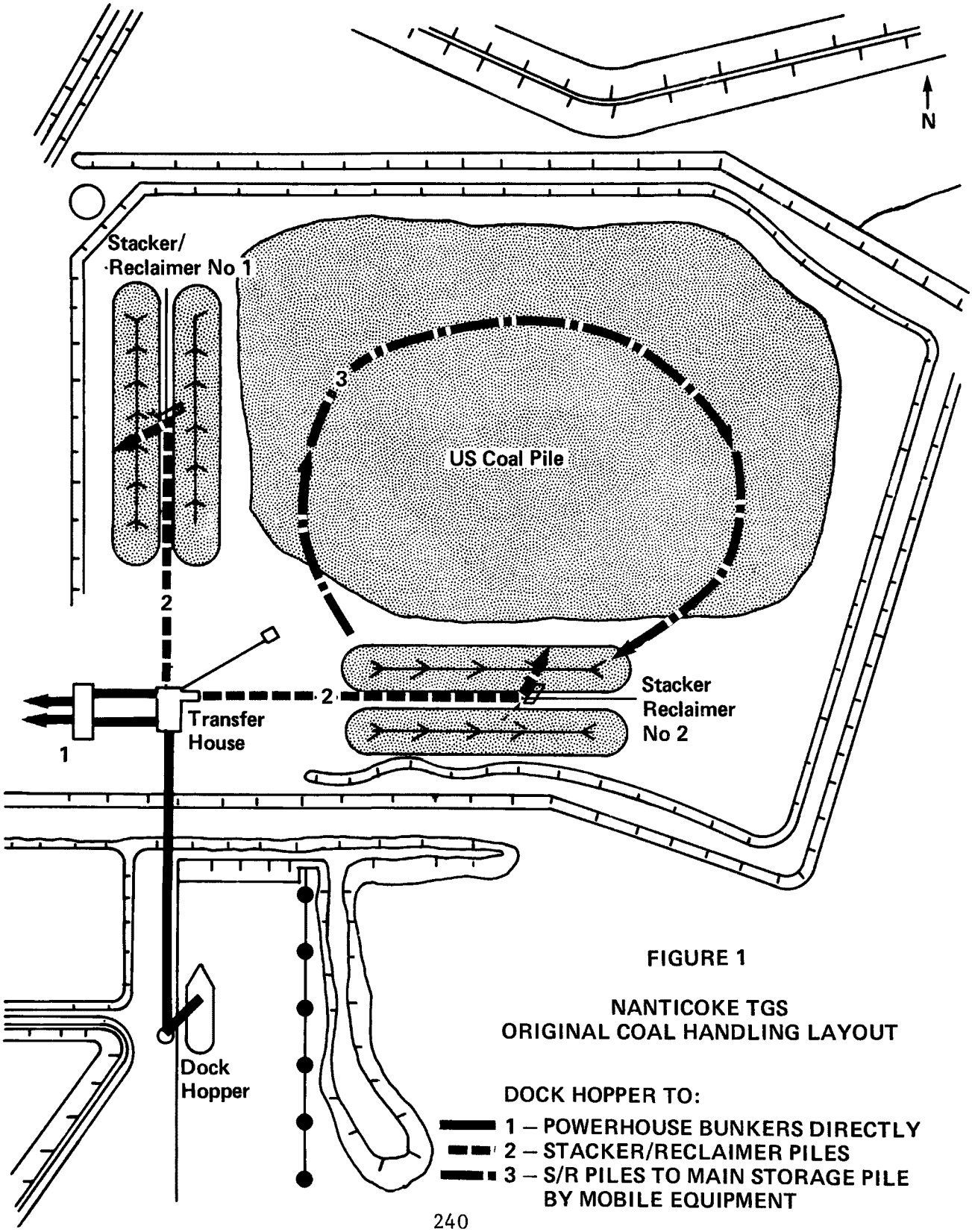


FIGURE 1

NANTICOKE TGS
ORIGINAL COAL HANDLING LAYOUT

DOCK HOPPER TO:

1 – POWERHOUSE BUNKERS DIRECTLY
2 – STACKER/RECLAIMER PILES
3 – S/R PILES TO MAIN STORAGE PILE BY MOBILE EQUIPMENT

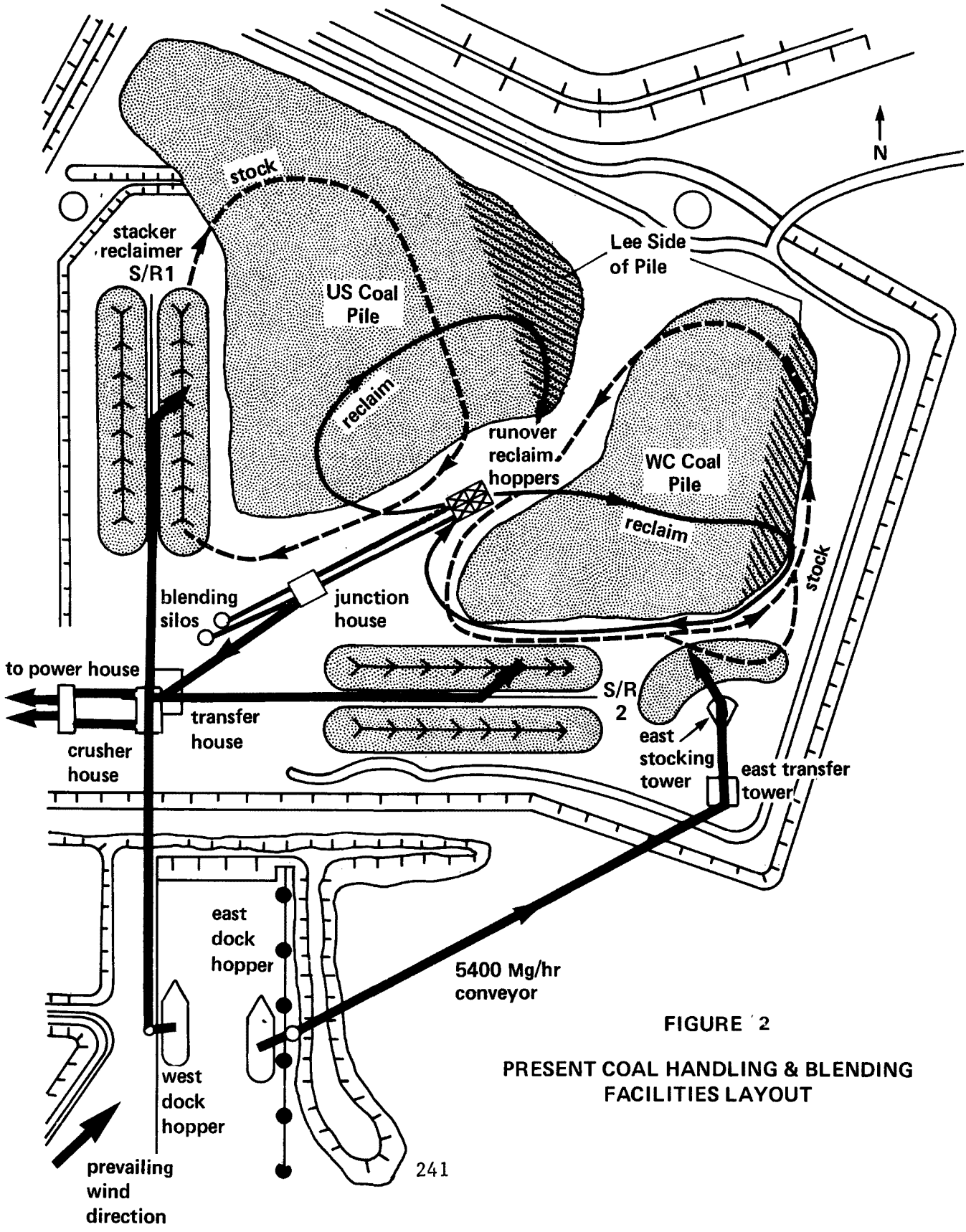


FIGURE 2

PRESENT COAL HANDLING & BLENDING FACILITIES LAYOUT

# MODELING SMOKE PLUME OPACITY FROM PARTICULATE CONTROL EQUIPMENT

By: David S. Ensor and Phil A. Lawless
Research Triangle Institute
P. O. Box 12194
Research Triangle Park, North Carolina 27709

Stanton J. Cowen
Atmospheric Research Group
464 West Woodbury Road
Altadena, California 91001

## ABSTRACT

The ability to predict plume opacity from control equipment is important in meeting air pollution regulations. This paper describes the applications of a model to electrostatic precipitators and the implications to the mass/opacity relationship for variation in inlet size distribution.

## INTRODUCTION

### Objective

The objective of this research was to develop convenient and accurate methods to permit the design of control devices to meet opacity limitations. Included are methods implemented on computation equipment such as programmable calculators, personal interactive microcomputers, and large computers.

### Background

The opacity determined by observation of the smoke plumes emitted from stationary sources has long been used as a means of regulation in the United States. The Clean Air Act currently specifies that, if a source meets the mass emission standards, a special regulation can be developed for that stack. Thus, an understanding of the significant causes of opaque plumes is important for the application of the regulation. Also, it has been observed that identically designed plants may yield plumes with differing opacities. A systematic investigation of the causes of excessive opacity requires the development of scientific tools. The current research traces its history to the work of Ensor.(1) Ensor assumed that the particle size distributions were lognormal and the particles were spherical. Results of extensive computer calculations were reported in graphs to allow an estimation of opacity.

A different approach was adopted by Cowen et al.(2) They wrote general opacity prediction programs for programmable calculators, which allowed computations without the restriction of a lognormal particle size distribution.

Work is in progress to apply these programs to microcomputers.(3)

## COMPUTATION OF OPACITY

The present discussion is limited to in-stack opacity as measured by a transmissometer. Even with this restriction, the light scattering equations that form the basis of opacity are complex and require modern computational equipment.

### Light Scattering

Opacity is defined by the light transmitted through the smoke by:

$$O_p = (1 - I/I_o)\ 100 \qquad (1)$$

where $O_p$ is percent opacity, $I_o$ is incident light intensity, and I is transmitted light intensity.

The light transmittance is related to the aerosol or particulate concentration by:

$$I/I_o = \exp\ (-\ b_{ext}\ L) \qquad (2)$$

where $b_{ext}$ is the extinction coefficient ($m^2/m^3$) and L is the light pathlength, the stack diameter in this case.

For computational work and data analysis, it is useful to express the extinction coefficient in terms of mass concentration as:

$$b_{ext} = \frac{S_v}{\rho} W \qquad (3)$$

where $S_v$ is specific volume extinction coefficient, $m^2/cm^3$; W is mass concentration, $g/m^3$; and $\rho$ is particle specific gravity, $g/cm^3$. The $S_v$ is the reciprocal of the "K" used previously by Ensor.(1) The $S_v$ is a function of only the particle size distribution and refractive index. The $S_v$ is computed by:

$$S_v = \frac{3\int D^2\ Q(D,\lambda,m)\ N(D)\ dD}{2\int D^3\ N(D)\ dD} \qquad (4)$$

where D is particle diameter, μm; N(D) is particle size distribution by number; Q is light scattering efficiency, the effective light scattering area divided by the projected particle area; λ is the wavelength of light, usually 0.55 μm for visible light; and m is the particle refractive index (a complex number), the real part of which is the ratio of the speed of light in media divided into the speed in vacuum and the imaginary part of which describes the absorption or conversion of light to heat. The Q is computed by applying

the Mie equations; the solution involves a series of spherical Bessel's functions. The details of the computation are described by Ensor(1) and Cowen et al.(2) and will not be covered here.

The magnitude of the specific extinction coefficient is a measure of opacity expected per unit particle volume. The relative nature of the parameter is very useful in analysis of opacity problems. The extinction coefficient is a function of concentration as well as size distribution and refractive index. Thus, the extinction coefficient is not as useful as the specific extinction coefficient for opacity prediction.

### Control Device Models

Each type of air pollution control equipment acts on the inlet aerosol in its own way. The reader is referred to Mosley et al.(4) and Lawless et al.(5) for detailed descriptions of the electrostatic precipitator models.

## ELECTROSTATIC PRECIPITATOR/OPACITY MODELING

### Combustion Aerosol

The aerosol from the combustion of coal is composed of two distinct populations of particles: The fly ash mode in the 5 to 50 μm particle diameter range, formed from the gaseous phase and composed of fused ash; and the accumulation mode in the 0.08 to 0.2 μm diameter range, composed largely of condensed materials. Typically, the accumulation mode contains less than 2 percent of the total mass. The physical basis of aerosol formation from coal combustion has been extensively reviewed by Flagen and Friedlander.(6) Experimental results from field measurements of the aerosol size distribution were reported by Markowski et al.(7)

Ensor(8) reported a relationship between the geometric mean diameter of the fly ash mode of the distribution and the ash content of the coal. The distribution appears to be a stronger function of the ash concentration than was predicted by the Flagen-Friedlander theory.

### Size Distribution Case Studies

The model fly ash distributions were compiled from the literature relying heavily on Gooch and Marchant(9), and Ensor et al.(10,11) These size distributions are idealized but are a good representation of expected size distribution for coals of low, medium, and high ash content. The model fly ash size distributions used in this study are summarized in Table 1.

### Computational Results

The electrostatic precipitator conditions are summarized in Table 2. The precipitator parameters were constant for computation of all three particle size distribution cases.

## Specific Extinction Coefficient Distributions

The behavior of the specific extinction coefficient as a function of particle diameter provides insight into how an electrostatic precipitator affects the opacity-to-mass concentration relationship. The convention first used by Ensor et al.(12) for atmospheric aerosol is a plot of the $\Delta b_{ext}/\Delta \ln D$ as a function of diameter on semilogarithmic paper. If $\Delta S_V$ is plotted, the area under the curve is a portrayal of the total specific extinction coefficient. In Figure 1 the incremental curves are presented for the medium ash coal model size distribution. The specific extinction distribution is shown for the inlet and the outlet conditions. For each model aerosol, the extinction distributions have the same behavior. As the aerosol passes through the precipitator, the relative importance of the submicron particles becomes less for opacity, while the $\simeq$ 6-μm particles dominate opacity. This observation is contrary to the popular conception that submicron particles determine the opacity and large particles determine the mass concentration. The explanation is the dominance of the rapping re-entrainment for both mass concentration and opacity. The precipitator is effectively acting as a source of aerosol in the $\simeq$ 6-μm particle diameter region.

## Specific Extinction Coefficient as a Function of Specific Collection Area

In Figure 2 the specific extinction coefficient is shown for the inlet and after each section as a function of cumulative specific collection area (plate area/gas volume flow rate). The aerosol distribution is transformed to approximately the same shape in each case. The emissions gradually assume the properties of a rapping puff as the primary aerosol is removed.

The significance of the rapping puff in determining the outlet opacity characteristics requires an examination of rapping. Extensive data on the rapping size distribution were reported by Gooch and Marchant(9) for six sites and by Ensor et al. (10,11) for rapping distribution at single sites. The striking conclusion is that the rapping puffs have quite similar size distributions for a wide range of equipment designs and test sites. The range of the rapping puff distributions and corresponding specific extinction coefficients are shown in Table 3.

The expected specific extinction coefficient (and extremes) computed from the rapping distribution is $0.85 \pm 0.3$ $cm^2/m^3$ and this variation can explain much of the reported variability of opacity-to-mass correlations.

The in-stack opacity as a function of outlet mass concentration is shown in Figure 3. Two features of the curves are apparent: the test cases produce similar opacity-to-mass curves, a consequence of the similar outlet $S_V$ values; and the curves, although computed with much different inlet conditions, are consistent with the federal regulations.

The present analysis indicates that, for high efficiency electrostatic precipitators, the outlet optical properties will generally be dominated by the properties of the rapping puff. There are three reasons why this would not occur: 1) with low efficiency precipitators, the properties of the inlet distribution dominate the outlet; 2) precipitation problems occur such as back

corona, excessive sneakage, and sparking; and 3) the second mode of the size distribution makes an optically significant contribution to the emissions. The effects of low efficiency precipitators on mass-to-opacity relationships generally have not been considered in studies such as those reported by Brennan et al.(13) In fact, one popular way of varying opacity and concentrations to develop correlations is to shut off sections of the precipitator.

This could be an explanation of why correlations for an individual stack may be excellent, but correlations of one stack to another may be poor.

The second consideration of pathological precipitator operation is less likely on high efficiency installations. However, one interesting well-documented case was reported by Ensor et al. (11) for a large cold-side precipitator operating in extreme back corona. The submicron particles were collected with abnormally low efficiency in the precipitator. The specific extinction coefficient was about twice as large as calculated for a rapping puff. (The rapping puff data are consistent with those measured at other installations.)

The importance of the accumulation mode (0.1 μm) on in-stack opacity is worthy of discussion. The fly ash cases were computed without consideration of the accumulation mode. The specific extinction coefficients for the condensed metal oxides and soot are shown in Table 4 with estimates of the contribution to the emission. Soot is very effective in screening light as indicated by the magnitude of the specific extinction coefficient. For this reason, the optical properties of soot and amorphous carbon are an active topic of research.(14)

For widely separated distributions as reported here, the total specific extinction coefficient is a sum of the mass fraction times the specific extinction coefficient for each component. As shown in Table 5, the contribution of the case of the accumulation mode is small and much less than 15 percent for the soot case.

## CONCLUSION

The in-stack opacity/mass concentration relationships have been explored for electrostatic precipitators. The opacity for high efficiency precipitators will be determined by the rapping puffs. The relationship of opacity-to-mass concentration for these precipitators may be quite similar because rapping puffs have similar particle size distributions. Low efficiency precipitators will retain the specific extinction coefficients of the inlet ash. Nonideal conditions such as back corona may alter the specific extinction coefficient by reducing the efficiency of submicron particles.

The combustion aerosol accumulation mode is believed to have an insignificant effect on opacity from high efficiency electrostatic precipitators unless soot is present.

ACKNOWLEDGEMENTS

This research was supported by U. S. Environmental Protection Agency Grant No. R-806718010 to the Atmospheric Research Group, U. S. Environmental Protection Agency Cooperative Agreement No. R-805897-03 with the Research Triangle Institute, and Research Triangle Institute program development funds.

ENDNOTES

1. Ensor, D. S. Smoke Plume Opacity Related to the Properties of Air Pollutant Aerosols. Ph.D. Dissertation, University of Washington, 1972.

2. Cowen, S. J., D. S. Ensor, and L. E. Sparks. TI-59 Programmable Calculator Programs for In-Stack Opacity, Venturi Scrubbers, and Electrostatic Precipitators. U. S. Environmental Protection Agency. EPA-600/8-80-024 (NTIS PB80-193147), May 1980.

3. Cowen, S. J., D. S. Ensor, and L. E. Sparks. In-Stack Opacity Computer Programs. Report in preparation under U. S. Environmental Protection Agency Cooperative Agreement No. R-806718010.

4. Mosley, R. B., M. H. Anderson, and J. R. McDonald. A Mathematical Model of Electrostatic Precipitation (Revision 2). U. S. Environmental Protection Agency. EPA-600/7-80-034 (NTIS PB80-190994), February 1980.

5. Lawless, P. A., J. W. Dunn, and L. E. Sparks. A Computer Model for ESP Performance. (Presented at the EPA Third Symposium on the Transfer and Utilization of Particulate Control Technology, Orlando, Florida, March 9-12, 1981.)

6. Flagan, R. C. and S. K. Friedlander. Particle Formation in Pulverized Coal Combustion--A Review. In: Recent Developments in Aerosol Science, Shaw, D. T. (ed.). New York, John Wiley, 1978.

7. Markowski, G. R., D. S. Ensor, R. G. Hooper, and R. C. Carr. A Submicron Aerosol Mode in Flue Gas from a Pulverized Coal Utility Boiler. EST. 14:1400-1402, 1980.

8. Ensor, D. S. Aerosol Emissions Due to the Combustion of Coal. (Presented at the Symposium on Plumes and Visibility: Measurements and Model Components, Grand Canyon, Arizona, November 10-14, 1980.) Submitted to Atmospheric Environment.

9. Gooch, J. P. and G. H. Marchant. Electrostatic Precipitator Rapping Re-Entrainment and Computer Model Studies. Electric Power Research Institute Report No. EPRI FP-792, 1978.

10. Ensor, D. S., P. A. Lawless, and L. E. Sparks. Evaluation of the United McGill Electrostatic Precipitator. (Presented at the EPA Third Symposium on the Transfer and Utilization of Particulate Control Technology, Orlando, Florida, March 9-12, 1981.)

11. Ensor, D. S., S. J. Cowen, R. G. Hooper, G. R. Markowski, R. Scheck, J. D. Farrell, and J. Burnham. Evaluation of the George Neal No. 3 Electrostatic Precipitator. Electric Power Research Institute Report No. EPRI FP-1145, August 1979.

12. Ensor, D. S., R. J. Charlson, N. C. Ahlquist, K. T. Whitby, R. B. Husar, and B. Y. H. Liu. Multiwavelength Nephelometer Measurements in Los Angeles Smog Aerosol: I. Comparison of Calculated and Measured Light Scattering. In: Aerosols and Atmospheric Chemistry, Hidy, G. M. (ed.). New York, Academic Press, 1972.

13. Brennan, R. J., R. Dennis, and D. R. Roeck. Review of Concurrent Mass Emission and Opacity Measurements for Coal-Burning Utility and Industrial Boilers. U. S. Environmental Protection Agency. EPA-600/7-80-062 (NTIS PB80-187420), March 1980.

14. Cowen, S. J., D. S. Ensor, and L. E. Sparks. The Relationship of Fly Ash Absorption to Smoke Plume Opacity. (Presented at the EPA Third Symposium on the Transfer and Utilization of Particulate Control Technology, Orlando, Florida, March 9-12, 1981.)

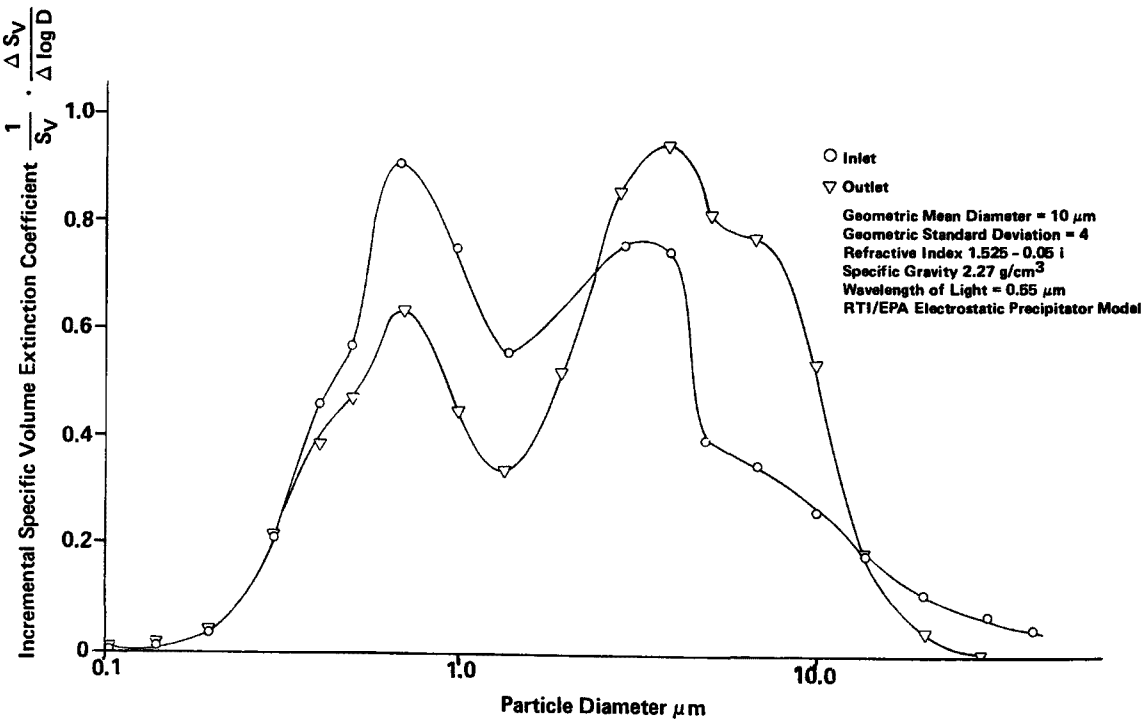


Figure 1. Incremental specific extinction coefficient as a function of particle diameter at the inlet and outlet of an electrostatic precipitator.

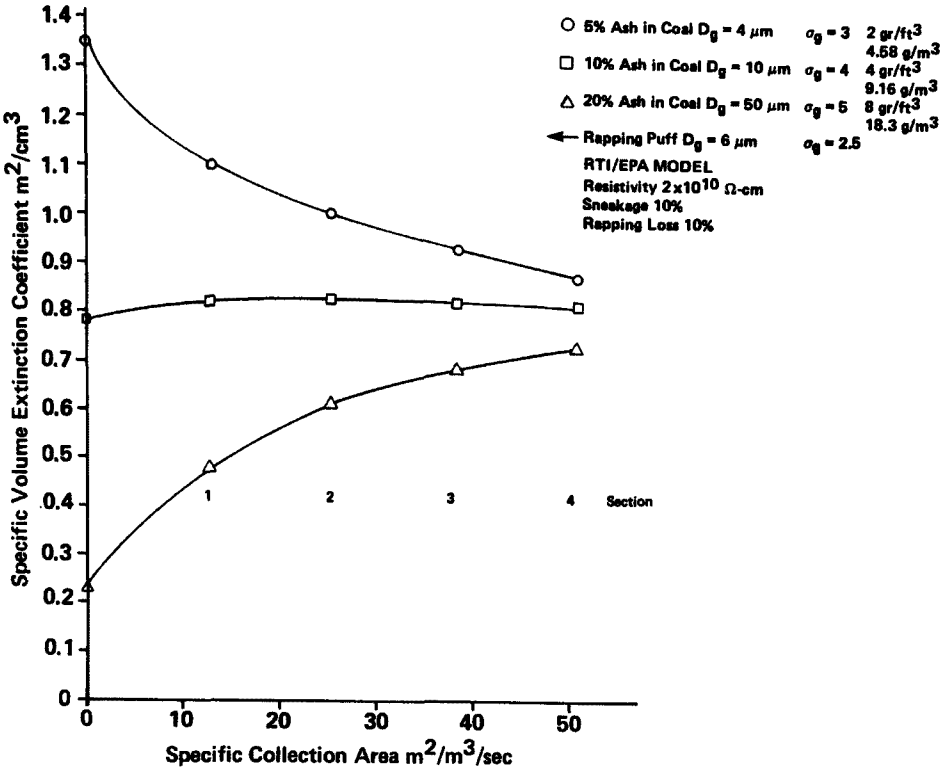


Figure 2. Change in specific volume extinction coefficient as a function of precipitator collection area.

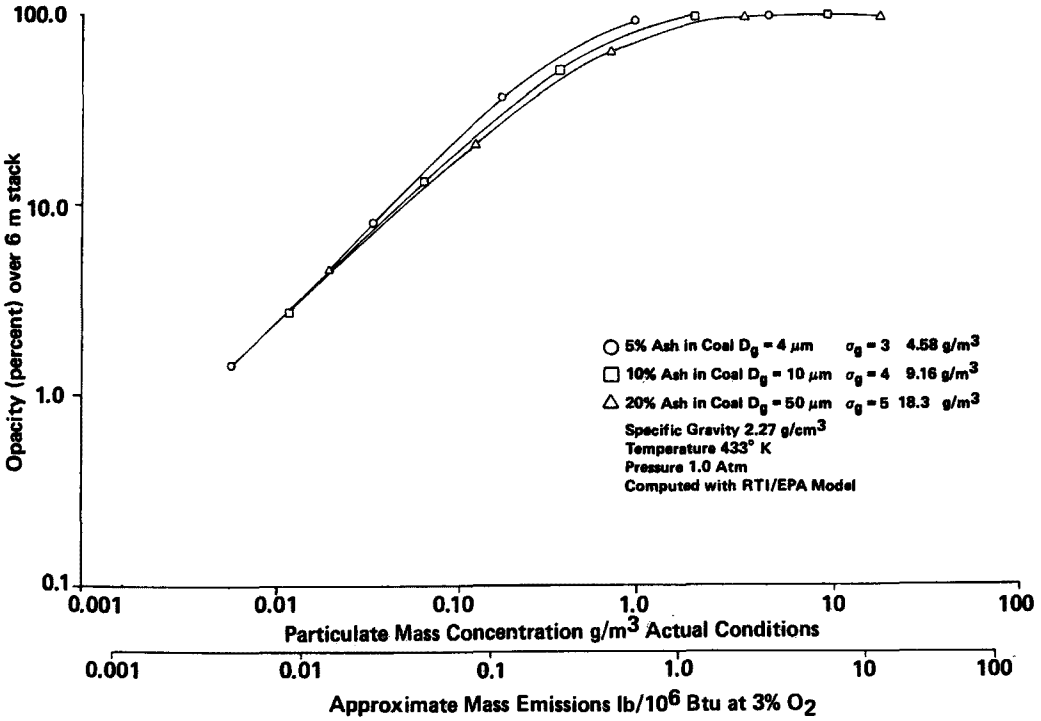


Figure 3. In-stack opacity as a function of outlet mass concentration for the example size distribution.

TABLE 1. MODEL AEROSOL SIZE DISTRIBUTIONS FOR THE FLY ASH MODE*

| Case | Concentration | $D_g$ (μm) | $\sigma_g$ | $S_v$ ($cm^2/m^2$) |
|---|---|---|---|---|
| Very low ash coal, 5% | 4.6 $g/m^3$ (2 $gr/ft^3$) | 4 | 3 | 1.447 |
| Average ash content coal, 10% | 9.2 $g/m^3$ (4 $gr/ft^3$) | 10 | 4 | 0.784 |
| High ash content coal, 20% | 18.3 $g/m^3$ (8 $gr/ft^3$) | 50 | 5 | 0.231 |

* Particle specific gravity = 2.27 $g/cm^3$; refractive index = 1.525-0.05 i; wavelength of light = 0.55 μm.

TABLE 2. SUMMARY OF ESP PARAMETERS

| | |
|---|---|
| Wire-to-plate spacing | 0.127 m |
| Wire radius | $2.54 \times 10^{-10}$ m |
| Area per section | 1477 $m^2$ |
| Sections | 4 |
| Gas flow rate | 117 $m^3/sec$ |
| Temperature | 433° K |
| Pressure | 1.0 atm |
| Length of section | 9.76 m |
| Resistivity | $2 \times 10^{10}$ Ω-cm |
| Applied voltage (depending on section and operating conditions) | up to 55 kV |
| Current density (depending on section and operating conditions) | up to $4 \times 10^{-4}$ $A/m^2$ |
| Sneakage/section | 10% |
| Rapping re-entrainment/section [An average cold-side puff size distribution from Gooch and Marchant(9) was used.] | 10% |
| Sigma (standard deviation of gas velocity) | 0.34 |

TABLE 3. RANGE OF SPECIFIC VOLUMETRIC EXTINCTION COEFFICIENTS EXPECTED FOR RAPPING PUFFS

| Diameter (μm) | $\sigma_g$ | Specific volumetric extinction coefficient |
|---|---|---|
| 5.0 | 1.5 | 0.784 |
| | 2.5 | 1.17 |
| * 6.0 | 1.5 | 0.637 |
| | 2.5 | 0.896 |
| 7.0 | 1.5 | 0.534 |
| | 2.5 | 0.761 |

* Generally believed to be the most representative.

TABLE 4. PROPERTIES OF ACCUMULATION MODE*

| | Condensed material | Soot |
|---|---|---|
| Maximum contribution by mass (%) | 2.0 | 10 |
| Geometric mean diameter (μm) | 0.1 | 0.08 |
| Geometric standard deviation | 1.2 | 2.0 |
| Specific gravity ($g/cm^3$) | 2.6 | 2.0 |
| Refractive index | 1.50 | 1.96-0.66 i |
| Specific volume extinction coefficient ($cm^2/m^3$) | 2.86 | 11.15 |

* Wavelength of light is 0.55 μm.

TABLE 5. CONTRIBUTION OF THE ACCUMULATION MODE TO SPECIFIC VOLUME EXTINCTION COEFFICIENT

| Case | $S_V$ ($cm^2/m^3$) | Percent increase |
|---|---|---|
| Low ash-soot | 0.961 | 9.9 |
| Medium ash-soot | 0.894 | 9.8 |
| High ash-soot | 0.833 | 15.5 |
| Low ash-condensed mode | 0.884 | 1.4 |
| Medium ash-condensed mode | 0.899 | 0.5 |
| High ash-condensed mode | 0.748 | 3.8 |

# TETHERED BALLOON PLUME SAMPLING OF A PORTLAND CEMENT PLANT

By
James A. Armstrong
Philip A. Russell
Myron N. Plooster
Denver Research Institute
University of Denver
Denver, Colorado 80208

## ABSTRACT

A remote-controlled tethered balloon sampling system was used to collect aerosols from a Portland cement plant which was experiencing a persistent plume opacity problem. The persistent plume was always associated with the prior formation of a water condensate plume which at times would be detached from the stacks of the plant's electrostatic precipitator. When the ambient air temperature was high enough that the water condensate plume did not form, the plume was clear.

Aerosol samples were collected from both persistent and clear plumes. The plume sampling was conducted concurrently with in-stack gas sampling. The plume samples were analyzed by scanning and transmission electron microscopy to determine the concentration and composition of the collected aerosols. The field program is discussed as well as analytical results and a proposed hypothesis of the persistent plume formation.

## INTRODUCTION

The existence of a high-opacity persistent plume from a Portland cement kiln located in Glens Falls, New York, is dependent upon whether or not a water condensate plume is first formed when exhaust gases exit the plant's electrostatic precipitator. When the ambient air temperature is sufficiently cold, quenching of the stack gases leads to the formation of a water condensate plume. This plume prevails for a few tens of meters until it evaporates due to mixing with drier ambient air. From this point on, a very dense, bluish-white plume persists for kilometers downwind of the plant. Depending upon the ambient air temperature, the water condensate plume often is detached from the precipitator stacks. The persistent plume opacity is observed to decrease when this occurs. When the ambient temperature is warm enough that the water condensate plume does not form at all, a clear plume from the precipitator stacks results.

The water condensate plume and the persistent plume occur consistently during cold winter periods but are not observed during the summer. In the spring and fall, when the morning ambient air temperature is sufficiently cold, the plume formations occur until the air temperature rises above an appropriate level.

An electrostatic precipitator is used to control particulate emissions from the exhaust gases of the cement kiln. The kiln is fired using No. 6 fuel oil. The plant utilizes the "dry" process in which crushed raw materials are fed into the kiln in their dry state. The precipitator, however, was designed for controlling emissions from a "wet" process kiln in which crushed raw materials are mixed with water and fed in a slurry to the kiln. The plant utilized the wet process when the precipitator was first installed, but soon after changed over to the dry process. In lieu of replacing the precipitator, a water injection system was installed downstream of the kiln and upstream of the precipitator to condition and cool the exhaust gases to the precipitator.

Each of the two stacks of the precipitator is equipped with a transmissiometer to continuously monitor in-stack opacity levels. Under normal plant operations these levels are less than 10%. The production of the persistent plume with an opacity often as high as 85% occurs outside of the stacks, however, which indicates that additional control strategies are in order to eliminate the problem. Before such strategies can be instituted, however, definitive knowledge concerning the formation process and composition of the persistent plume need to be established. A number of past in-stack sampling programs had been conducted at this plant to obtain this knowledge but the results were inconclusive(1,2).

During April 1979, the Denver Research Institute (DRI) conducted a field study using a tethered balloon sampling system to collect particles directly from both persistent and clear plumes of this plant, in order to determine the nature of particles causing the visibility problem. The DRI field study was sponsored by the Particulate Technology Branch of the Industrial Environmental Research Laboratory, U.S. Environmental Protection Agency, Research Triangle Park, North Carolina. The plume sampling was conducted concurrently with in-stack gas sampling by a Northrop Services field team sponsored by the Gaseous Emissions Research Section of the Environmental Sciences Research Laboratory, U.S. Environmental Protection Agency, Research Triangle Park, North Carolina. In-stack measurements of $H_2SO_4$, $SO_2$, sulfur salt ions, $NH_3$, and HCl were made by the EPA/ESRL sponsored team(3).

## TETHERED BALLOON SAMPLING SYSTEM

A detailed description of the tethered balloon sampling system used during the investigation is presented elsewhere(4). The system basically consists of a remote controlled particle sampler which is carried aloft by a balloon tethered to a portable winch. The sampler, which weighs 950 g, contains eight 37 mm diameter filters in cassette holders which are connected through a motor-driven rotary valve to a piston-type suction pump. The filter being sampled and the sampling time are controlled via a ground-based

transmitter and an airborne receiver/servo system. An airborne verification transmitter and ground-based receiver monitor the sampler for correct operation. Collection substrates for this program included 0.4 μm Nuclepore filters and prefired glass fiber filters. The sampling flow rates were 3.9 ℓ/min and 4.1 ℓ/min for the Nuclepore and glass fiber filters, respectively. This sampler also contains a heated-surface semiconductor gas detector, the output of which is coupled to the verification transmitter, so that continuous relative information of the sampler position in a plume envelope is provided to the ground-based receiver.

A blimp-shaped, red polyethylene balloon, which is inflated with 3.25 $m^3$ of helium, is used as the airborne platform for the particle sampler. The balloon is attached to a battery-powered winch by means of a lightweight tetherline having a breaking strength of 535 newtons.

## FIELD OPERATIONS

The sampling operations took place on April 24 and 25, 1979. Weak surface radiation inversions occurred in the early morning hours of both days, during which time light winds of 0.5 to 1.5 m/sec were from the north. The topography of the area where the cement plant is situated slopes down to the Hudson River, which is located a few kilometers south of the plant. As the ambient air temperature increased from ~8°C to ~13°C on both days, the wind remained light but shifted to a southerly direction. This occurred by 0800 hours EST on April 24 and by 0900 hours on April 25. The persistent plume existed and was sampled during the time that the winds were from the north.

The plant electrostatic precipitator is oriented in a north-south direction with the two stacks on the west side of the unit. The stacks are 1.83 m in diameter and are separated by approximately 8.7 m. The north stack was sampled by the EPA/ESRL sponsored field team. With the winds from the north, the individual plumes of the two stacks merged soon after the exhaust gases exited the stacks.

Limited plume sampling was accomplished on April 24. The sampling operations were started at 0607 hours from the open field to the south of the precipitator. The visible persistent plume was sampled at a location just downwind of the zone where the condensed water plume evaporated. The plant was experiencing operational problems, and by 0628 hours shut down due to a blockage in the cement kiln. The plant was out of service until 0300 hours on April 25. The samples collected on April 24 were not analyzed.

Sampling of the persistent plume at a location just downwind of the condensate plume was started at 0516 hours on April 25. The cement plant operated continuously during the entire plume sampling period which ended at 1015 hours. During this time, the kiln feed rate varied between 1,630 and 1,660 kg/min, the fuel feed rate varied between 85.9 and 87.1 ℓ/min, and the opacity of the north and south precipitator stacks varied between 8 and 9% and 3 and 4%, respectively. The kiln exhaust gas temperature to the spray tower was 288°C and the precipitator inlet temperature was 111°C during the sampling period.

Balloon sampling operations were documented by photographic slides and time-lapse movies. A 16 mm movie camera, equipped with a zoom lens and an intervalometer, was positioned at a site ~100 m west of the precipitator. The movies proved to be invaluable in verifying the vertical position of the balloon in the persistent plume; in determining the residence time of a parcel of gas passing through the condensate zone; in clearly showing the phenomenon of the condensate plume becoming more detached from the stacks and the persistent plume becoming less intense or opaque as a function of time as the ambient air temperature increased; in determining the horizontal and vertical sampling distances from the precipitator stacks; and, finally, in confirming that the balloon was indeed in the clear plume during the later morning sampling operations. This was evidenced by observing the flight behavior of the balloon in the clear but turbulent plume.

The ambient air temperature was 5°C at the start of plume sampling operations on April 25. At this time the water condensate plume formed within the first 3 m and evaporated at ~45 m downwind (south) of the stacks. From 0516 to 0651 hours, four samples of the persistent plume aerosols were collected by the balloon system with sampling times ranging between 5 and 20 minutes. The estimated average horizontal and vertical sampling distances from the top of the precipitator stacks were 55 and 35 m, respectively, for these samples. By 0700 hours, the ambient air temperature had increased to 8°C, causing the condensate plume to form and evaporate at estimated downwind distances from the stacks of 10 and 25 m, respectively. At this time the wind was beginning to shift to the northeast. Between 0756 and 0823 hours, one 20 minute and one 5 minute sample of the less intense persistent plume were collected. For these samples the balloon was located at average horizontal and vertical distances from the stacks of 30 and 35 m, respectively. By 0900 hours the ambient temperature was 13°C, the wind had shifted to the south, and clear plume conditions existed. Two 30 minute samples of the clear plume aerosols were taken between 0903 and 1015 hours. The estimated average horizontal and vertical sampling distances from the stacks were 25 and 50 m, respectively.

## LABORATORY ANALYSIS

Examination of materials collected on the Nuclepore and glass fiber substrates was first made using a scanning electron microscope (SEM) equipped with an energy dispersive X-ray spectrometer (EDXS) capable of detecting elements with the atomic number of sodium or greater. All substrates were precoated with approximately 20 nm of carbon by vacuum evaporation prior to SEM examination. Particle size parameters, concentration, morphology, and elemental composition were estimated using the information provided by this examination. The discussion that follows concerns the selected Nuclepore substrates containing aerosols collected in the persistent plume over a 20 minute period starting at 0523 hours on April 25 (Sample 25-2) and in the completely clear plume over a 30 minute sampling period starting at 0903 hours on the same date (Sample 25-9).

These selected samples were further examined using a transmission electron microscope (TEM). Selected area electron diffraction (SAED) patterns

were obtained from crystalline materials. Substrates to be examined by TEM were coated with a thin layer (∿ 10 nm) of carbon by vacuum evaporation, transferred to a TEM grid, wicked with chloroform to dissolve the Nuclepore polycarbonate filter, and covered with another thin layer of carbon by vacuum evaporation. Particles collected on Samples 25-2 and 25-9 were also subjected to treatment with $NH_3$ vapor and heat (100°C for 30 minutes and 150°C for 42 hours) with subsequent TEM-SAED examination.

SEM-EDXS Results

In Sample 25-2 the dominant particles by number had submicrometer diameters and were observed to be of a liquid nature. SEM micrographs of this sample are presented in Figures 1 and 2. Figure 1 shows these particles when examined by SEM at a low tilt angle to the normal electron beam axis; Figure 2 illustrates the droplet or liquid morphological characteristics of these particles when examined at a high tilt angle.

An examination of the individual liquid particles by EDXS showed that they were rich in sulfur. These particles were observed to be stable in all but the most intense SEM beam, where some decomposition was observed. The liquid morphology of these sulfur-rich particles strongly suggested that $H_2SO_4$ was the dominant component. $H_2SO_4$ possesses an extremely low vapor pressure and will exist as a liquid in the vacuum necessary for SEM analysis(5,6).

Mineral particles, with diameters ranging from 0.2 to 15 μm, were observed in Sample 25-2 but at concentrations much lower than the liquid particles. The composition of the mineral particles, which were sometimes alone but usually in agglomerates, included quartz, clays, feldspars, and calcites.

The characteristic morphology of the most numerous particles on Sample 25-9 is illustrated in Figures 3 and 4. These particles were again submicrometer in size. They, however, were roughly spherical and did not "wet" or spread on the collection media surface. Figure 3 is a low tilt angle view of these particles while Figure 4 is taken at a higher tilt angle. The round submicrometer particles were rich in sulfur and were stable in an intense electron beam. As in Sample 25-2, mineral particles in a size range of 0.2 to 15 μm in diameter were observed at concentrations much lower than the sulfur-rich particles.

It was assumed that the liquid particles of Sample 25-2 existed as spheres in the persistent plume. In order to determine the equivalent spherical diameters of the liquid particles on the Nuclepore substrate, the volumes of these droplets as observed on high tilt SEM micrographs were estimated assuming they had the shape of spherical segments. The diameters of spheres having equal volumes to the spherical segments were then calculated. The equivalent spherical diameters of a significant number of liquid droplets were used to plot a cumulative number distribution on a log-probability graph. The resulting geometric median diameter by count, $d_{gc}$, for the liquid particles of Sample 25-2 was 0.32 μm with a geometric standard

Figure 1. SEM micrograph, Sample 25-2 at ~25° tilt angle to normal beam axis.

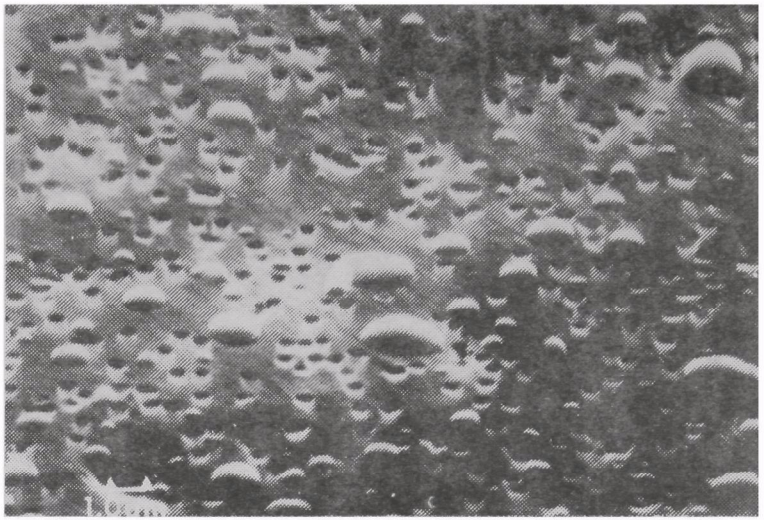

Figure 2. SEM micrograph, Sample 25-2 at ~60° tilt angle to normal beam axis.

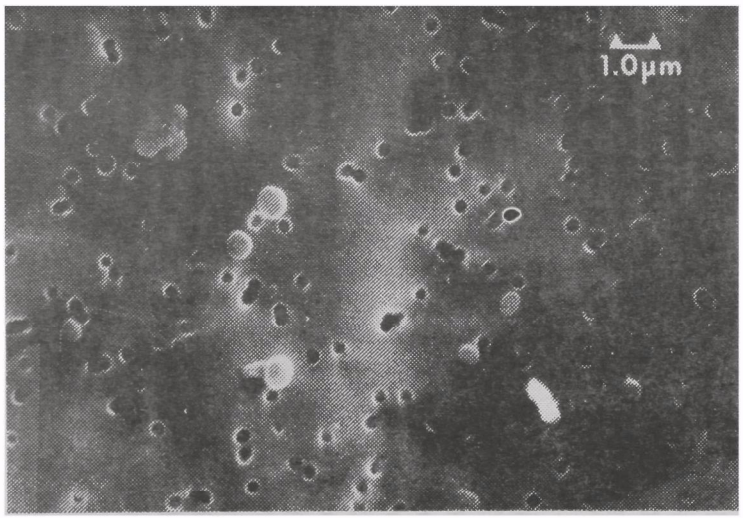


Figure 3. SEM micrograph, Sample 25-9 at ~20° tilt angle to normal beam axis.

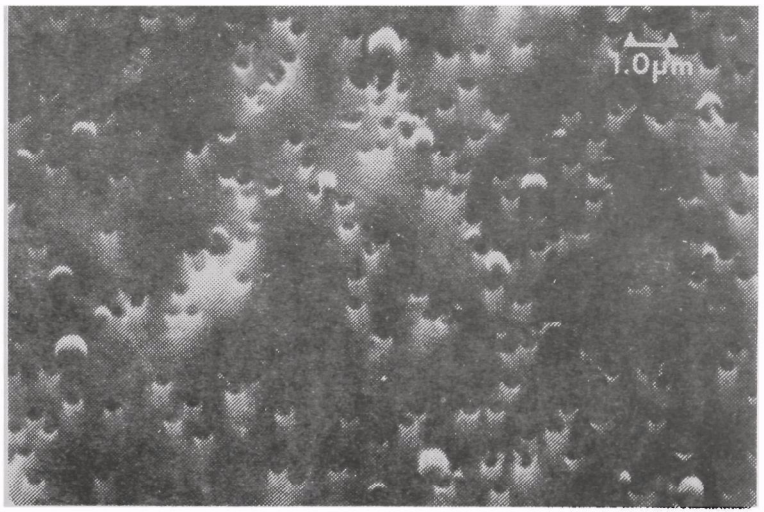


Figure 4. SEM micrograph, Sample 25-9 at ~55° tilt angle to normal beam axis.

deviation, $\sigma_g$, of 1.69. The number concentration of these particles was calculated to be $1.46 \times 10^6$ particles/ℓ of sampled air.

The cumulative number distribution of the sulfur-rich particles from Sample 25-9 was also plotted on a log-probability graph. For this sample, $d_{gc} = 0.35$ μm and $\sigma_g = 1.4$. The particle number concentration was calculated to be $1.18 \times 10^5$ particles/ℓ.

The size distributions of the two samples were unexpectedly similar and the persistent plume sulfur-rich particle concentration was only one order of magnitude larger than that of the clear plume. Based upon these facts, the difference in opacity between these plumes would not be expected. A possible explanation for the high opacity of the persistent plume is discussed later.

TEM-SAED Results

TEM-SAED examination of Sample 25-2 particles indicated that many of the original particles on the Nuclepore substrates became connected during the transfer process to TEM grids to form "bridges" of material. Some particles were relatively unchanged and were observed to still be oblate when examined at high tilt angles. While particle morphology was altered by the chloroform dissolution of the polycarbonate substrate and the addition of the second carbon coating, the composition appeared unchanged. The material in the particles was heat labile in a more intense electron beam. No residues were left after the material evaporated and no SAED patterns were observed. This is shown in Figures 5 and 6.

No major changes were observed for Sample 25-9 particles in comparing SEM and TEM micrographs. These particles under TEM examination appeared to have thick shells surrounding less electron-dense matrices. They were not heat labile. The particles were also not crystalline since they produced no SAED patterns. Electron density appeared homogeneous; i.e., there were no obvious inclusions of different material. A TEM micrograph of one of these particles is shown in Figure 7.

After discovering the liquid nature of the sulfur-rich persistent plume particles, portions of both the persistent and clear plume samples were exposed to ammonia gas in order to determine if the particles would transform into crystals. If the particles contained $H_2SO_4$, it would be expected that exposure to $NH_3$ would cause ammonium salts of sulfur oxides to form. TEM grid-mounted samples were either exposed to vapors from $NH_4OH$ in a petri dish or had a gentle jet of $NH_3$ gas directed onto their surfaces. Both aerosol samples reacted with $NH_3$ to form stable crystals. Depending if the particle samples were precoated with carbon or not and/or if the samples had been subjected to a heat treatment before being exposed to $NH_3$, the resulting crystals possessed different structural characteristics (microcrystalline structure, often showing preferred orientation, versus thin rod-like crystals) and produced different SAED patterns. Rigorous crystal indexing was not conducted on the crystalline particles generated by $NH_3$ exposure but it was established that similar diffraction patterns could have been produced by crystals of ammonium sulfate $[(NH_4)_2SO_4]$, ammonium hydrogen

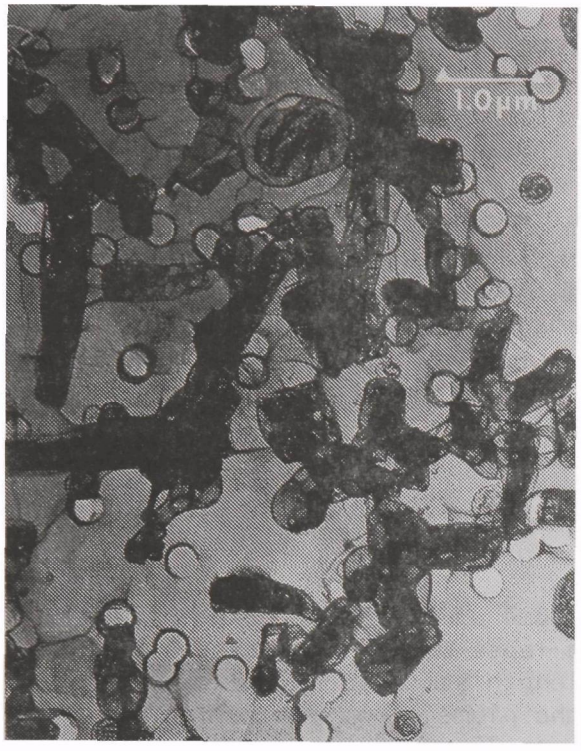


Figure 5. TEM micrograph, Sample 25-2, chloroform filter dissolution only, low electron beam current.

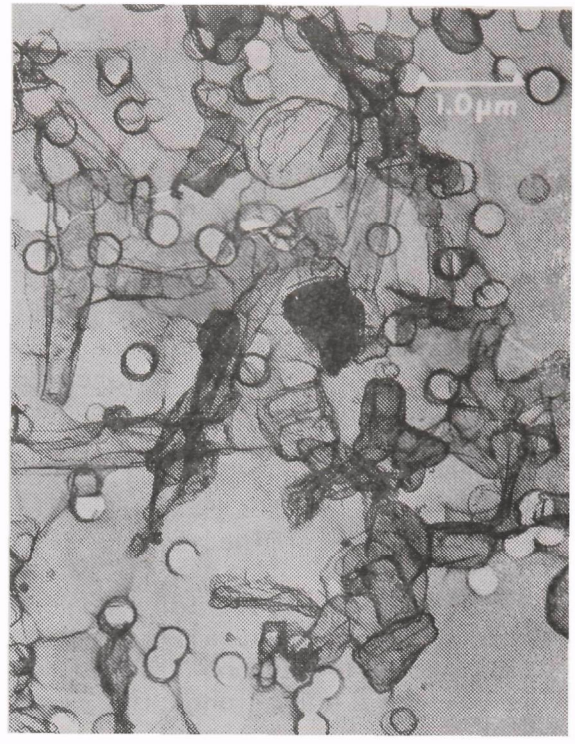


Figure 6. TEM micrograph, Sample 25-2, after exposure to higher beam current.

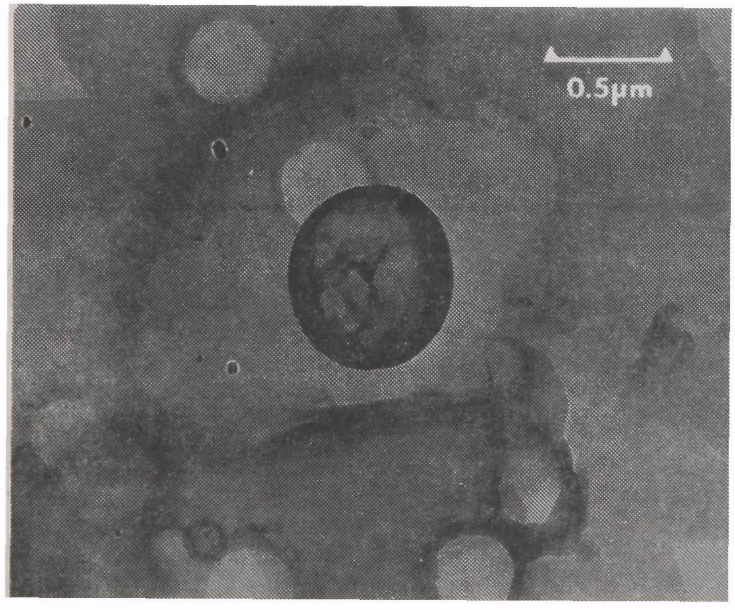


Figure 7. TEM micrograph, Sample 25-9.

sulfate [$NH_4HSO_4$], ammonium sulfamate [$NH_4SO_3NH_2$], ammonium dithionate [$(NH_4)_2S_2O_6$], sulfamic acid [$NH_3SO_3$], and ammonium hydrogen sulfate sulfamate [$(NH_4)_2SO_4 \cdot HSO_3NH_2$]. A more detailed discussion concerning the generation of the stable crystals from the persistent and clear plume aerosol samples is presented elsewhere(7).

## SULFUR MASS BALANCE

To make any estimate of the mechanism of formation of the particles in the persistent plume it was necessary to compare the quantity of matter in the particles with the quantity of the "raw material" in the stack gases. Since sulfur was the main identifiable element in the particles sampled from the persistent plume, and the $SO_2$ concentration in the stack gases was measured, a sulfur mass balance computation was carried out.

The effluent from the electrostatic precipitator was released into the atmosphere through two 1.83 m diameter stacks. The total stack cross-sectional area was thus 5.25 $m^2$. The $SO_2$ concentration in the stack gas was ~200 ppm as determined by the EPA/ESRL sponsored in-stack measurements(3).

The mean diameter of the persistent plume at the sampling point was determined from several frames of the time lapse movie taken at the time of sampling. The balloon itself provided a length scale for plume measurements. The balloon is 4 m long; the diameter of the plume, from the movie, was about 7.5 times the length of the balloon, or 30 m. Assuming that the plume was cylindrical, its cross-sectional area was then ~700 $m^2$. The dilution ratio (plume area/stack area) was thus 700/5.25 = 133. The average concentration of $SO_2$ at the sampling point was then 200 ppm/133 = 1.5 ppm.

The filter sampler was in the persistent plume for 20 minutes. Since the sampling rate was 3.9 ℓ/min, the total volume of air processed for this filter sample was 78 ℓ.

To make an estimate of the mass of the particulate matter collected on the filter sample, it was necessary to make some assumptions as to its chemical composition and density. For the purposes of this calculation, it was assumed that the particles were pure $H_2SO_4$ (molecular weight 98, density 1.834 g/$cm^3$). (This means that this calculation probably gave an upper limit for the quantity of sulfur present in the particles in the plume.) Integration of the particle size distribution gave a total mass of $2.67 \times 10^{-11}$ g. This particle size distribution was obtained by counting and sizing the particles on a filter area of $1.1 \times 10^{-5}$ $cm^2$. The total filter area was 8.55 $cm^2$. The mass loading of particles per unit volume of air was thus:

$$\frac{2.67 \times 10^{-11}\ g}{1.1 \times 10^{-5}\ cm^2} \times \frac{8.55\ cm^2}{78\ \ell} = 2.65 \times 10^{-7}\ \frac{g}{\ell}$$

The volume of $SO_2$ gas needed to generate this mass loading was easily found using the ideal gas law; the result was $6.4 \times 10^{-8}$ ℓ $SO_2$/ℓ air, or a volume concentration of 0.064 ppm. This was about 4% of the quantity of $SO_2$ estimated to be present in the plume, a relatively small fraction.

A similar calculation was carried out for the particles observed on Sample 25-9, taken in the clear plume later in the day. The mass loading of particulate matter on this filter sample was smaller by almost exactly a factor of 10. However, it is not possible to conclude from this that the relative ratio of sulfur in the particles to sulfur available in gaseous form was also smaller by a factor of 10, for two reasons: 1) the physical characteristics of the particles in Sample 25-9 were different in the electron microscope studies, suggesting a somewhat different chemical composition (i.e., less like $H_2SO_4$); and 2) because the plume was invisible, it was not possible to estimate the plume size from the photographic records, so that the dilution ratio at the sampling point is not known.

## POSSIBLE MECHANISMS OF AEROSOL FORMATION

The combined results of the in-stack and plume sampling investigations have generated nearly as many questions as answers. Nevertheless, a plausible case can be made for the hypothesis that the particles in the persistent plume were sulfuric acid most likely containing some dissolved ammonium sulfate and/or ammonium hydrogen sulfate, created by the aqueous oxidation of $SO_2$ in the presence of ammonia. In addition to an average $SO_2$ concentration of 200 ppm, the stack gases contained about 20% water vapor and 170 ppm of $NH_3$ (3). They also were known to contain a low concentration of mineral particles from the cement-making process, and very probably also contain trace quantities of heavy metals from the fuel oil. $NH_3$ is known to catalyze the aqueous oxidation of $SO_2$ to $H_2SO_4$; more precisely, it acts as a buffer in the solution to limit the hydrogen ion concentration and thus keep the concentration of sulfite ions (reportedly the most readily oxidizable species) high(8). Some heavy metal ions (Mn, V, etc.) which are commonly found in fuel oils, are also known to catalyze the sulfite-to-sulfite oxidation reaction(9).

The laboratory investigation of the persistent plume particles by electron microscopy also was consistent with the above hypothesis, although not conclusive. Morphologically, the particles appeared to be droplets; they behaved in the electron beam in much the same way as $H_2SO_4$; and they reacted with $NH_3$ vapor to give a crystalline deposit whose behavior in the electron beam was similar to that of ammonium sulfate. (Incidentally, if this hypothesis is even only partially correct, the particle size distribution in the plume could be quite different from the "size" distribution" on the filters. At the relative humidities present in the plume, $H_2SO_4$ droplets could contain a considerable quantity of water, which would evaporate when the particles were placed in a vacuum environment for electron microscopy. The persistent plume itself was bluish-white in color, which is consistent with scattering from a median particle size about twice that estimated from the SEM micrographs; humidification of an $H_2SO_4$ aerosol distribution reported above could easily enlarge the median particle size to this extent.)

The time-lapse movies suggest a residence time of 20 to 30 seconds for gases and particles in the condensate plume, which seems very short. On the other hand, the high concentrations of both $SO_2$ and, especially $NH_3$, plus the almost certain presence of heavy metal ions from the fuel oil, and the fact that the above mass balance calculation showed that only a very few percent

of the available $SO_2$ needed to react to produce the particles observed, make the situation at least plausible. This is also supported by calculations made by the EPA/ESRL sponsored research team who performed the in-stack gas measurements at the time of the plume sampling. The calculations indicated that, in the presence of an aqueous environment containing the measured level of $NH_3$, all of the $SO_2$ present in the stack gases could have been oxidized to sulfate in ~15 seconds(3).

The particles in the clear plume are at present somewhat of an enigma. They were high in sulfur, appeared to be solid, and were much more stable to high temperatures and electron bombardment than the persistent plume aerosol. Yet they too reacted with $NH_3$ to give crystals similar to those formed from the persistent plume aerosol. Moreover, particles with these properties were not found in the persistent plume aerosol, which suggests that they did not survive the water condensation/evaporation cycle which gave rise to the persistent plume. A more detailed study of these "strange" particles could possibly shed some light on the overall chemistry of the plume from this cement plant.

## CONCLUSIONS

Tethered balloon sampling of the persistent plume from the Glens Falls Portland cement plant revealed the plume to be dominated by submicrometer, sulfur-rich liquid particles. These particles reacted with $NH_3$ gas to form stable crystals which were similar to $(NH_4)_2SO_4$, $NH_4HSO_4$, and other ammonium salts of sulfur oxide. It is proposed that these liquid particles consisted of $H_2SO_4$ most likely containing some dissolved $(NH_4)_2SO_4$ and/or $NH_4HSO_4$, created by the aqueous oxidation of $SO_2$ in the presence of $NH_3$.

Sampling of the clear plume from this plant revealed the presence of submicrometer, sulfur-rich spherical particles which were more stable to electron bombardment than the persistent plume particles. The clear plume particles also reacted with $NH_3$ to form stable crystals which were similar to ammonium salts of sulfur oxide.

More refined collection and analysis procedures based upon the findings of this investigation should lead to a more complete definition of the nature and formation processes of the persistent and clear plume particles from this Portland cement plant.

## REFERENCES

1. Kawahata, M.. Study on Rotary Kiln Exhaust Gas Emissions in Relation to Blue Haze Formation. Environment/One Corp. Report to Glens Falls Portland Cement Company, November 1974.

2. Aggarwal, V., B. Pine, D. Daoust, H. Potter, B. Gould, and T. Clark. New York State Stack Test Report, Glens Falls Cement Company, Glens Falls, N.Y. New York State Department of Environmental Conservation Report, September 1975.

3. Dellinger, B., G. Grotecloss, C.R. Fortune, J. L. Cheney, and J. B. Homolya. Sulfur Dioxide Oxidation and Plume Formation at Cement Kilns. Environ. Sci. Technol. 14: 1244-1249, October 1980.

4. Armstrong, J.A., P.A. Russell, L.E. Sparks, and D.C. Drehmel. Tethered Balloon Sampling Systems for Monitoring Air Pollution. Submitted to JAPCA for publication, August 1980.

5. Lodge, J.P. Jr. Identification of Aerosols. In: Advance in Geophysics, Vol. IX, Landsberg, H.E. and J. Van Migham (eds.). New York, Academic Press, 1962. p. 97-139.

6. Gras, J.L. and G.P. Ayers. On Sizing Impacted Sulfuric Acid Aerosol Particles. J. Appl. Meteor. 18: 634-638, May 1979.

7. Armstrong, J.A., P.A. Russell, M.N. Plooster, and L.E. Sparks. Balloon Borne Particulate Sampling of a Portland Cement Plant Plume. In preparation.

8. Hegg, D.A.. Atmospheric Sciences Department, University of Washington, Seattle, Washington. Personal communication, June 1980.

9. Hegg, D.A. and P.V. Hobbs. Oxidation of $SO_2$ in Aqueous Systems with Particular Reference to the Atmosphere. Atmos. Environ. 12: 241-253, February 1978.

# THE RELATIONSHIP OF FLY ASH LIGHT ABSORPTION TO SMOKE PLUME OPACITY

By: Stanton J. Cowen
Atmospheric Research Group
Altadena, California 91001

David S. Ensor
Research Triangle Institute
Research Triangle Park, North Carolina 27709

## ABSTRACT

Measuring the fly ash light absorption for coal-fired boilers with the Integrating Plate Method (IPM) is discussed. Measurement of the optical properties of fly ash may be useful for stack opacity modelling and identifying the relative contribution of particle light absorption to downwind visibility impairment. The IPM technique is defined as comparing the light absorption through a clean filter to one with a single layer of aerosol by integrating the scattered light so only absorption is measured. Since the light absorption is a strong function of particle size, careful sizing is required for accurate measurement. Preliminary calibration and fly ash data are reported.

## INTRODUCTION AND SCOPE

Smoke stack opacity regulations have become an important regulatory issue, and compliance can be difficult for stationary sources. The ability to predict opacity depends on the quality of particle size and refractive index data of the emission aerosol. A careful examination of the complex index of refraction is necessary to improve the accuracy of opacity prediction.

This paper discusses a preliminary measurement of the optical properties of fly ash from pulverized-coal-fired boilers as part of work to determine the relative importance of light absorption compared to light scattering. Such work is needed, since the optical absorption of fly ash has been measured by Volz (1973) and Nolan (1977) under very limited conditions. The large variability in the composition of fly ash, especially carbon content, prompted further investigation of optical properties of this aerosol.

This paper is, an initial, not comprehensive, examination of light absorption by fly ash from different types of coals and combustion conditions. This information will help opacity modelers to more accurately predict stack opacity.

## EXPERIMENTAL PROCEDURE

This study includes the experimental measurement of fly ash absorption and the theoretical modeling of smoke plume opacity. The experimental technique is an application of the Integrating Plate Method (IPM), as developed by Lin et al. (1973), to fly ash. Preliminary measurements were undertaken to determine the importance of fly ash light absorption. Absorption measurements and analysis of the carbon content of the ash (assumed to be "graphitic") were performed to determine the correlation between absorption and carbon content. This "graphitic" assumption is valid, because little "organic" carbon is thought to be present in the fly ash. The measurement strategy has two assumptions regarding the nature of fly ash and its optical properties:

First, samples were collected from electrostatic precipitator hoppers downstream of a coal-fired boiler and stored in hard plastic containers for future analyses. It is assumed that this sample is representative of the ash emitted from the stack and that storage of the sample does not change its optical properties.

Second, the absorption technique was used to examine submicron fly ash deposited on a filter. The assumptions are that the submicron ash has optical characteristics similar to other size particles and that fly ash light absorption on a filter can be related to its behavior while suspended in a gaseous medium. Work is needed to assess the size dependency of carbon in fly ash to certify that absorption properties of submicron ash are representative for opacity calculations.

Lin et al. (1973) developed the Integrating Plate Method to measure the absorption coefficient of ambient aerosol. Weis et al. (1978) further tested and calibrated this technique with monodisperse aerosols of methylene blue. A main goal of this study is to examine the application of the IPM procedure to source aerosols such as fly ash.

IPM is a simple direct measurement of aerosol light absorption based on comparing the transparency of a clean nuclepore filter with one containing a thin layer of particles. A Hitachi Model 60 double-beam spectrophotometer with a specially designed filter holder was used for the comparison. Opal glass behind each filter integrates the transmitted light as a function of angle so that only absorption is recorded. Back scattering probably can be neglected, because the reflectivity of the filter is unchanged by the fly ash particle; i.e., the real refractive indices of particles and filters are similar. The double-beam automatically gives the ratio of the aerosol absorption to the blank filter. The optical arrangement for the beam measuring the sample is shown in Figure 1.

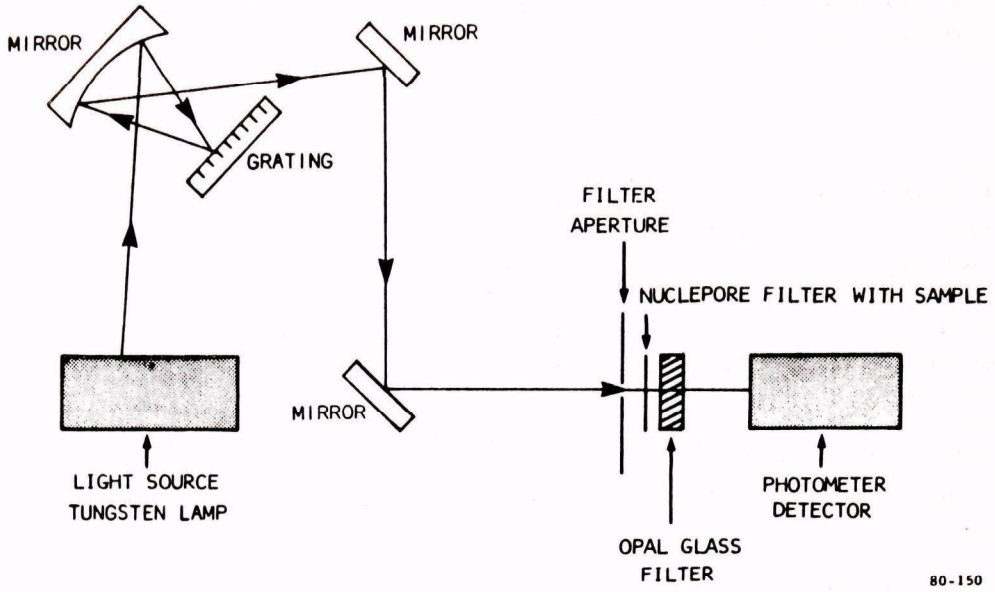


Figure 1. Schematic diagram of the optical system incorporating the integrating plate method.

The real part of the index of refraction is measured with oil immersion techniques. The ash sample is spread over a microscope slide so that individual particles can be identified. The particle is then immersed in an oil of known refractive index. The Becke line test shows the particle index of refraction to be lower or higher than the immersion oil.

Converting the specific absorption coefficient to an imaginary refractive index with an aerosol of spherical ammonium sulfate particles containing methylene blue dye is discussed at the end of Section 3, Data Analysis.

Bulk ash samples obtained from electrostatic precipitation required resuspending before measurement. A common sandblast gun was used as a simple technique for deagglomerating fly ash by producing a high pressure aerosol stream.

A single layer of submicron aerosol is required to easily evaluate the light absorption effects. The absorption for submicron aerosol is simply proportional to the product of the imaginary refractive index and volume of particles as described by Weis et al. (1978). The resuspended fly ash was first drawn through an impactor to remove large particles and then through a Model 3071 Thermo System Incorporated Electrostatic Classifier to obtain a near monodisperse aerosol with a particle diameter of approximately 0.8 $\mu$m. Transmission Electron Microscope photographs (Figure 2) show the coagulation of very small ash speres (particle diameter $\sim$ 0.07 $\mu$m) on the surface of larger 0.8 m particles. The quantity of material collected on each filter was approximately 50 to 100 micrograms as measured by Cahn 25 balance. A dry gas meter downstream of the filter measured gas volume passing through the

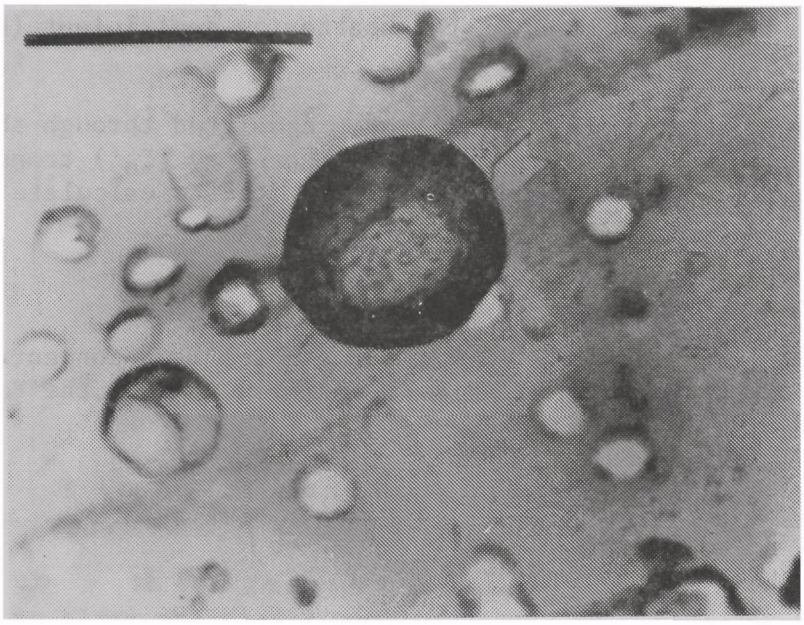

Figure 2. Transmission electron microscopy photograph of submicron fly ash particle at a magnification of 44,350X. The length of the line is approximately 1 micron.

filter. The gas volume was used with the filter area to compute an effective optical path length, which was used to calculate the absorption coefficient.

West Paine Laboratories performed a carbon analysis of the ash samples by standard methods. Approximately 1.0 gram was accurately weighed and placed in a tube furnace. The furnace was heated to 800°C until the samples were completely ashed. The carbon dioxide given off was trapped in a $CO_2$ free NaOH solution. The carbon dioxide was then measured by a Beckman Total Organic carbon analyzer.

## DATA ANALYSIS

Data reduction for the Integrating Plate Method uses Mie theory to determine absorption effects. It is assumed that the filter does not interfere with the light absorption of the particles. Nuclepore membrane filters were used, because the particles are on the surface of the filter and not embedded as they would be in a fiberglass filter.

The transmission of light through a volume containing an aerosol is described by the Beer-Lambert Law:

$$\text{Light transmittance} = I/I_o = \exp(-b_{ext}L)$$

where I is the transmitted light, $I_o$ is the incident light, $b_{ext}$ is the light extinction coefficient, and L is the illumination path length. The light extinction coefficient is the sum of the scattering coefficient ($b_{scat}$) and the absorption coefficient ($b_{abs}$).

The ratio of intensity (I') of light transmitted through the opal glass and a filter deposited with aerosol to the intensity ($I_o'$) transmitted through an opal glass and blank filter can be used to calculate the absorption coefficient:

$$I'/I_o' = \exp(-b_{abs}L)$$

Ensor and Pilat (1971) have shown that the aerosol mass concentration is related to optical transmittance through a modified form of the Beer-Lambert Law:

$$\frac{I}{I_o} = \exp\left(-\frac{M\ L\ S_{ve}}{\rho}\right)$$

where M is the particle mass concentration, $S_{ve}$ is the ratio of the light extinction coefficient to the specific particulate volume ($m^2/cm^3$), (reciprocal of "K" in the original paper), is the average particle specific gravity, and L is the optical path length. Optical absorption can similarly be formulated by

$$\frac{I'}{I_o'} = \exp\left(-\frac{M\ L\ S_{va}}{\rho}\right)$$

where $S_{va}$ is the ratio of the light absorption coefficient to the specific particulate volume. The optical path length is determined by the length of the volume of sampled air of cross-sectional area equal to the filter.

The specific absorption coefficient ($S_{va}$) is converted to an imaginary refractive index (n") by calibrating the instrument with a laboratory aerosol of similar particle shape and size as fly ash with known absorption characteristics. This was accomplished with an aerosol of spherical ammonium sulfate particles containing various amounts of methylene blue dye to obtain various degrees of light absorption. The calibration $S_{va}$ is then proportional to the product of imaginary refractive index (n") of methylene blue and its weight percent in the ammonium sulfate aerosol, a nonabsorbing material. The imaginary refractive index of the ash sample is calculated in the following manner: The specific absorption coefficient ($S_{va}$) of the ash sample is plotted on the methylene blue ammonium sulfate calibration curve (Figure 3). The fraction of methylene blue corresponding to this plotted point multiplied

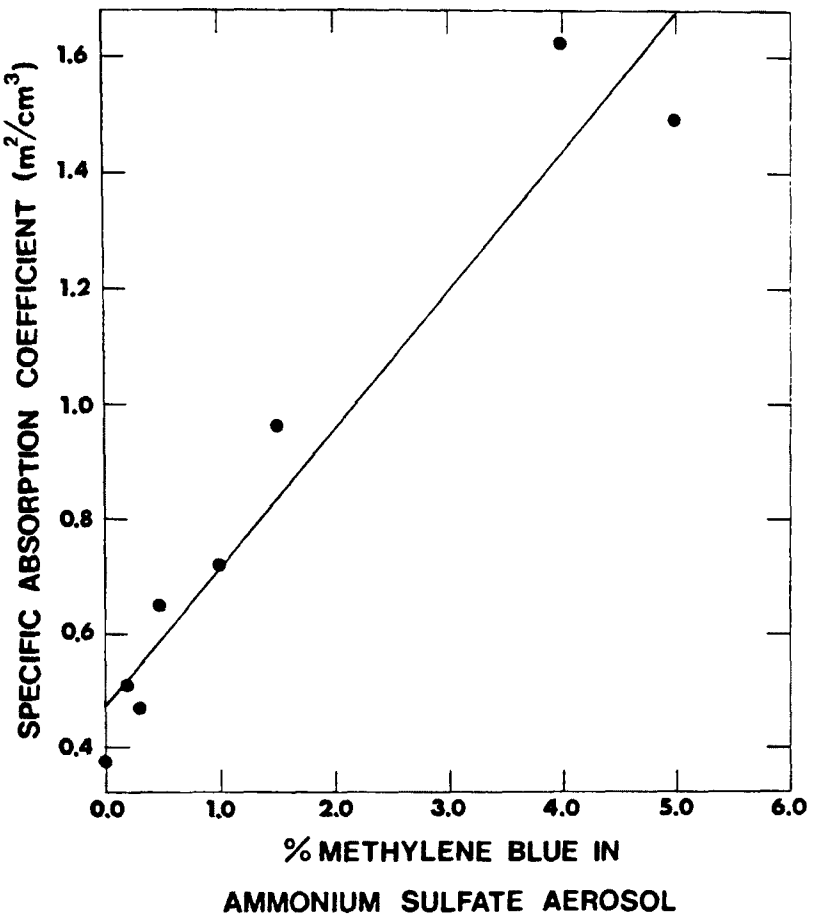


Figure 3. The absorption per unit volume ($S_{va}$) as a function of methylene blue content.

by the imaginary refractive index of methylene blue (in this case, 0.1) equals the imaginary refractive index of the ash sample. There is very little dependence on the real part of the refractive index because the Integrating Plate Method diminishes scattering effects by comparing a blank filter to one with a layer of aerosol where the real refractive indices of aerosol and filter are similar. The computed imaginary refractive index may then be used to calculate its effect on stack opacity with the opacity model described earlier.

## RESULTS

The absorption measurement of the calibration methylene blue/ammonium sulfate aerosol are presented in Figure 3. Samples weighing from 100 to 500 micrograms were generated at the 1st International Workshop on Light Absorption by Aerosols at Colorado State University Cloud Simulation and Aerosol Laboratory. The correlation coefficient of the line with the least squares fit to the absorption data is 0.96. (One is a perfect correlation.) The linear relationship is predicted by Mie theory for this submicron absorption

aerosol. The particle size was determined by scanning electron microscopy and an Electrical Aerosol Size Analyzer.

This experimental technique has been calibrated with monodisperse pure methylene blue 0.8 to 2 $\mu$m particles with absolute error of ten percent as reported by Weis et al. (1978). Our experiments with pure methylene blue particles with a mass mean diameter of 1.5 $\mu$m and 200 microgram filter loadings produced absorption readings approximately twenty-five percent higher than predicted by Mie theory. The high absorption readings may indicate interference from multiple scattering effects for high mass loadings (greater than 100 micrograms on a 47 mm filter). The difficulty of separating scattering from absorption effects, especially for low absorption aerosols, precludes a simple determination of fly ash absorption.

The interference effects are indicated in Figure 3 by the apparent absorption for the nonabsorbing pure ammonium sulfate samples. The high correlation for the absorbing aerosols indicates a systematic offset related to light scattering of the particles on the filter.

The coal, combustion conditions, and refractive indices for the fly ash samples are listed in Table 1. These characteristics are probably not as important in determining light absorption as the quantity of soot emissions. These carbonaceous emissions are more important for determining fly ash absorption than the mineral content of the ash.

Results of five fly ash samples analyzed for absorption and carbon content are shown in Figure 4. The absorption measurements were performed on submicron ash sample with a mass mean diameter of approximately 0.8 $\mu$m as indicated by Transmission Electron Microscopy. Although the trend indicates increasing absorption with increasing carbon (graphitic) content, as expected, the limited number of samples precludes statistical analysis. The scatter may be the result of small differences in the particle size distributions and the nonuniform distribution of carbon in the submicron ash compared to the hopper ash.

The absorption measurements of the ash samples produce results similar to the absorption calibration measurements of methylene blue ammonium sulfate aerosol. The similarity in particle size and the similar low absorption of these aerosols may explain their similar behavior. Again interference effects like those in the calibration curve are noted by the back extrapolation of the curve in Figure 4 to 0 percent carbon. Also the linear results are present in both calibration and fly ash curves as predicted by Mie theory.

The effect of imaginary refractive index on opacity was estimated by computing the ratio of opacity from pure soot to the opacity from transparent material (Table 2). The calculated ratio of the specific aerosol volume to the extinction coefficient reported by Pilat and Ensor (1971) was used to compute the effect of light absorbing material on opacity less than 20 percent. The opacity equation can be approximated for opacity less than 20 percent by taking Taylor's expansion of an exponential as follows:

Table 1

DESCRIPTION OF COAL AND COMBUSTION CONDITIONS FOR FLY ASH SAMPLES

| Power Plant | COAL PROPERTIES | | | COMBUSTION CONDITIONS | | Refractive Index* |
|---|---|---|---|---|---|---|
| | Heating Type | Heating Valve (BTU/lb) | Ash Content (%) | Boiler Type | Unit Rating (MW) | |
| Power Plant A | Sub-bituminous, pulverized, western | 10,000 to 11,000 | 3 to 7 | Front-fired | 40 | 1.565 - 0.0055i |
| Power Plant B | Sub-bituminous, pulverized, western | 10,500 | 19 | Reheat, natural-circulation steam generator | 314 | 1.57 - 0.0012i to 0.0025i |
| Power Plant C | Bituminous, pulverized, eastern | 12,000 | 20 | Controlled circulation steam generator | 540 | 1.5 - 0.0043i |
| Power Plant D | Bituminous, pulverized, western | 12,000 | 10 | | 320 | 1.61 - 0.0004i |

*Real part of the refractive index determined by oil immersion techniques. Imaginary part of the refractive index determined by Integrating Plate Method. Methylene blue has an imaginary refractive index equal to 0.1 at 0.56 $\mu$m wavelength reported by J. Gillespie (1980).

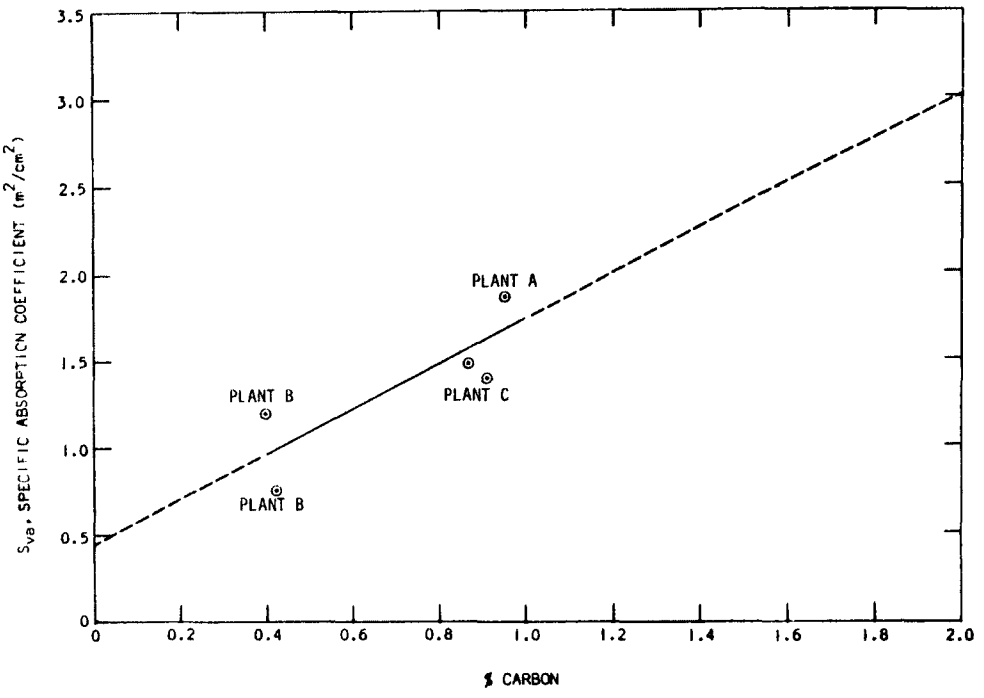


Figure 4. Absorption per unit volume ($S_{va}$) as a function of carbon content.

$$\text{Opacity} = \left[1 - \exp\left(-\frac{S_{ve}\ M\ L}{\rho}\right)\right] \times 100$$

$$\text{Opacity} = \left[1 - \left(1 - \frac{S_{ve}\ M\ L}{\rho}\right)\right] \times 100 \text{ for opacity } <20\%$$

$$\text{Opacity} \approx \frac{S_{ve}\ M\ L}{\rho} \times 100$$

$$\frac{\text{Opacity (soot)}}{\text{Opacity (transparent)}} \approx \frac{S_{ve}\ \text{(soot)}}{S_{ve}\ \text{(transparent)}}$$

Table 2. THE EFFECT OF ABSORBING MATERIAL ON OPACITY AS A FUNCTION OF PARTICLE SIZE

| g \ $\bar{r}_{gw}$ | 0.1 | 0.5 | 1.0 | 5 | 10 |
|---|---|---|---|---|---|
| 1 | 6.5 | 1.08 | 0.895 | 0.977 | 1.0 |
| 2 | 3.38 | 0.95 | 0.929 | 0.996 | 1.0 |
| 3 | 3.09 | 1.29 | 1.0 | 0.974 | 0.985 |
| 4 | 3.11 | 1.56 | 1.32 | 1.02 | 0.99 |
| 5 | 3.33 | 1.75 | 1.47 | 1.12 | 1.0 |

If aerosols are compared with similar particle mass concentration (M), path length (L), and particle specific gravity ($\rho$), the ratio of their opacities is then simply the ratio of their specific extinction coefficients ($S_{ve}$). Table 2 is a calculation ratio of $S_{ve}$ for transparent aerosol with refractive index equal to 1.5. These results show the absorbing refractive index is most significant for the monodisperse aerosol with a mass mean radius equal to 0.1.

## SUMMARY AND CONCLUSIONS

Applying the Integrating Plate Method to a source aerosol such as fly ash requires careful treatment, especially in the area of particle sizing. Scanning or transmission electron microscopy may be required for certain measurement of the actual deposited particle size. Coagulation, especially for larger particle mass concentrations, can change the effective particle size on the filter. The application of this experimental technique to low absorbers can create problems with filter interferences and scattering differences between the filter substrate and the particulates. The measured absorption may be an overestimation of actual absorption because of these interference problems. More work is required to quantify these interference effects and to develop a sound theoretical basis for this quantification. Fortunately, these interferences seem to be consistent for a given particle size and absorptive range, thus allowing an empirical correction.

The usefulness of this technique for fly ash absorption requires that the optical properties of submicron ash represent the bulk sample emitted from the stack, especially for modeling purposes. Additional research is required to compare the carbon content and other absorbing species of the bulk ash to the submicron ash concentrations. Careful work may require direct source sampling rather than resuspension of bulk samples.

This preliminary work indicates that imaginary refractive index is related to carbon content in a manner similar to that reported for atmospheric aerosol by Weis et al. (1978) and Salder (1979). However, the number of samples needs to be expanded to include the range of carbon content expected in fly ash (up to 20 percent or more). Also in cases of good combustion with low carbon carryover from the boiler, matrix elements such as calcium, titanium, and iron are believed to affect imaginary refractive index.

## ACKNOWLEDGMENTS

We wish to thank G. Woffinden, G. Markowski and E. Hindman for technical advice. This research was supported by the Environmental Protection Agency under grant number R806718010 under the direction of L. E. Sparks.

## ENDNOTES

Berstrom, R. W. (1972): Predictions of the spectral absorption and extinction coefficients of an urban air pollution aerosol model. Atmos. Environ., 6, 247-258.

Lin, C., M. Baker and R. J. Charlson (1973): Absorption Coefficient of atmospheric aerosol: A method for measurement. Appl. Optics, 12, 1356-1363.

Ensor, D. S., and M. J. Pilat (1971): Calculation of smoke plume opacity from particulate air pollutant properties. J. Air Poll. Contr. Assn., 21, 496.

Gillespie, J., Personal Communication (1980).

Nolan, J. L. (1977): Measurement of light absorbing aerosols from combustion sources. M. S. Thesis, University of Washington.

Pilat, M. J., and D. S. Ensor (1971): Comparison between the light extinction aerosol mass concentration relationship of atmospheric and air pollutant emission aerosols. Atmos. Environ., 5, 209-215.

Sadler, M. S. (1979): A comparative study of light attenuation, filter media, and total carbon content. M. S. Thesis, University of Washington.

Twitty, J. T., and J. A. Weinmen (1971): Radiative properties of carbonaceous aerosols. J. Appl. Meteor., 10, 725-731.

Volz, F. E. (1973): Infrared optical constants of ammonium sulfate, Sahara dust, volcanic pumice, and fly ash. Appl. Optics, 12, 564-568.

Weis, R. E., A. P. Waggoner, R. J. Charlson, D. L. Thorsell, J. S. Hall and L. A. Riley (1978): Studies of the optical, physical, and chemical properties of light absorbing aerosols. Presented at Conference on Carbonaceous Particles in the Atmosphere, Berkley, CA, 20-22 March.

# A SPECIFIC METHOD FOR THE ANALYSIS OF SULFURIC ACID MISTS

By: P. Urone, R.B. Mitchell, J.E. Rusnak, R.A. Lucas, J.F. Griffiths
Environmental Engineering Sciences Department
University of Florida, Gainesville, FL 32611

## ABSTRACT

A number of organic dye precursors were investigated for their use as specific reagents for the detection and measurement of sulfuric acid mists in air. The underlying principle of the method was to have the sulfuric acid react with the precursor to form a sulfonated product with a specific color that could not be caused by other acids or pollutants in air. At least five organic dyes were found to react with sulfuric acid to form a uniquely colored sulfonation product. In all cases, reversal of the reaction was a serious problem. It was found that heating of the filter holder while sampling with a precursor coated glass fiber filter fixed the sulfonated product. Fifty μg $H_2SO_4$ aerosol are readily observed by a color change on the filter. Basic theory, methodology, sensitivity, and reproducibility are discussed.

## INTRODUCTION

The sampling and analysis of sulfur trioxide and sulfuric acid in emission sources continues to be a source of difficulty. At present a number of methods are used to determine sulfuric acid mist in either emission sources or ambient air. These methods can generally be divided into two basic operations: 1) the sampling or collection of the aerosol; and 2) the analysis or measurement of the collected aerosol (1).

The major methods of collection of sulfuric acid aerosols are: absorption into isopropyl alcohol or alkaline solutions, controlled and uncontrolled condensation, impaction, and filtration.

The major methods of measurement and their chemical basis for the analysis of $H_2SO_4$ at present are:

sodium hydroxide titration (1); barium ion titration (2); chloranilate (1); turbidimetric (1); flame photoluminescent detector (1,5); ammonium vanadate (3); bromphenol blue (4); coulometry (5) and conductimetry (1,7).

The major difficulties encountered by the presently available methods are due generally to the sampling methods with their inherent interferences from copollutants and sampling efficiency. Recently Jaworowski and Mack evaluated the performance of EPA's Method 8, the controlled Condensation Method, and the Dew Point Measurement Method (7).

## SULFONATION

A specific analytical technique for the analysis of sulfuric acid is possible due to the sulfonating ability of sulfuric acid with aromatic and heterocyclic compounds. Sulfonation by definition is the process of replacement of a hydrogen atom in an organic compound with the sulfonic group ($SO_3H^+$). The replaced hydrogen atom and the hydroxyl ion ($OH^-$) from sulfuric acid form a water molecule (8, Fig. 1).

There is no clear cut guideline to follow when considering reaction temperatures, concentrations, percent product recovery and reaction rates when the sulfonation of species not generally dealt with in industrial applications are studied. However, sulfonation of rings which are substituted with electron withdrawing groups ($-Cl^-$, $-Br^-$, $-SO_3H$, $-CO_2H$, $-NO_2$) proceeds with difficulty since the ring is already electron poor. Electron donating groups ($-NH_2$, $-OH$, $-OR$, $-O^-$) attached to the ring aid sulfonation and are ortho and para directing.

Kinetic and mechanistic studies of the sulfonation of aromatic compounds have led to the conclusion that it is an $S_E2$ reaction with monomeric $SO_3$ as the effective reacting species, not only with $SO_3$ itself, but also when sulfuric acid or oleum are used. It has been proposed that in sulfuric acid an acid solvate of $SO_3$ is the active species. This is considered possible, but less likely than free $SO_3$ (8).

Aromatic compounds can be sulfonated with concentrated $H_2SO_4$, but as the concentration of the water increases during reaction, the rate of sulfonation steadily decreases, the reaction rate being inversely proportional to the square of the water concentration. The reaction ceases when the acid concentration reaches a level characteristic of each compound. Sulfonation differs from most other types of electrophillic substitution in that the process is readily reversible under mild conditions (9). Desulfonation of some aromatic compounds proceeds rapidly and in good yield by simple dilution in aqueous medium. Therefore, to carry sulfonation reaction to completion, the removal of water formed from the reaction is essential. However, the hydrolysis of sulfonated aromatics will not occur if the acid strength is kept high.

## EXPERIMENTAL

Five indicator dye precursors were studied because their reactions with sulfuric acid produced a sulfonated product having a distinctive and intense color. The compounds were: acid orange A, phenolphthalein, thymolphthalein, methylene blue, and o-cresolphthalein. The reactions of all gave satisfactory color changes with intensities useful for both source and ambient air concentrations. Problems with reversibility of the sulfonated products were encountered in all cases making it desirable to develop a technique for preventing the reversal of the reaction.

O-cresolphthalein was selected as one of the more promising of the precursors. It was easily available in relatively pure form as a dry slightly yellow powder. It reacted with sulfuric acid to give an intense red-orange color. It did not react with concentrated solutions of hydrochloric or phosphoric acids. Tests were designed: 1) to study the optimal method for dissolving and coating the o-cresolphthalein on a glass fiber filter; 2) to use the coated filter to sample a highly dilute sulfuric acid aerosol under conditions that would promote and fix the reaction of the sulfuric acid aerosol particles with the o-cresolphthalein; and 3) to selectively extract the sulfonated product from the filter for spectrophotometric study.

Materials and Apparatus

The acids used were HCl, $HNO_3$, $H_2SO_4$, and $H_3PO_4$. They were all concentrated and laboratory grade, or better. A 0.045 M $H_2SO_4$ solution was used in generating the acid aerosol to be sampled.

The solvents used were acetonitrile, dimethyl sulfoxide, and methanol. They were selected from solubility tests with ortho-cresolphthalein powder. They were all laboratory grade, or better.

The standard solution for the calibration curve was prepared by mixing 0.03531 gm. of ortho-cresolphthalein powder with 5 ml. of 18 M $H_2SO_4$ in a 100 ml volumetric flask. It was gently heated until all the OCP had gone into the solution. The flask was immersed in an ice water bath and 95 ml. of 12 M HCl was added, at first drop by drop until the violent reactions ceased. Then the dilution proceeded normally.

The aerosol generating and sampling train system is shown in Figure 2. The Dwyer type rotameters and the critical orifice, Type # 22-F, were calibrated using a precision wet test meter. The aerosol was generated by a DeVilbis nebulizer Model 40. The manufacturer has rated the aerosols generated to have a mean diameter of 4.5 microns with a geometric standard deviation of 1.8 at 5 psi. Aerosol flowrates and concentrations were measured using distilled water and various molarities of $H_2SO_4$. Heat checks were made before and after each run.

Purified compressed air was used for aerosol generation and a Thomas vacuum pump, Model/Serial #907CA18-2, for sampling. The filter holder was an in-line stainless steel Gelman Type 303. The plastic inlet and outlet nipples were replaced with metal nipples to withstand temperatures not to exceed 110°C. The inlet dispersing screen was removed to avoid any loss of aerosol.

The type of filter used to collect the sulfuric acid aerosol was the Gelman Type A/E glass fiber filter. These filters are devoid of any organic binders and have a minimum retention efficiency of 99.7% for 0.3 μm particles as measured by the dioctyl phthalate penetration test. Barton and McAdie developed a method of treatment of the glass fiber filters by soaking in 20% sulfuric acid followed by gentle boiling for

10 minutes, rinsing with distilled water, 80% isopropanol, and finally acetone (10-13). The filters are then dried for 15 minutes at 105°C and stored in a desiccator (14). This method of filter treatment was used in this study.

The heating unit was made from a copper pipe coupler covered with alternate layers of asbestos and nichrome wire. The voltage to the heater was controlled by a Powerstat. Two wooden caps were cut to fit the inlet and outlet ends and to hold a thermometer. A four-liter Pyrex bottle was used to receive and mix the aerosol. All excess gases were exhausted to a laboratory fume hood.

Each filter was weighed and placed for approximately 2 minutes in various solutions of ortho-cresolphtalein powder (OCP) in acetonitrile (OCP-A), dimethyl-sulfoxide (OCP-D) or methanol (OCP-M). They were drained of any excess solution by touching the edge of the beaker, placed on Petri dishes or watch glasses, and allowed to air dry. Then the filters were either placed directly in a desiccator or after oven drying at 105°C for approximately 15 minutes.

Sulfuric Acid Aerosol Sampling

A pre-weighed and coated filter was placed in the filter holder, the filter holder encased in the heater unit, and the Powerstat switched on and set to a predetermined positon that would yield the desired sampling temperature of 105°C.

Approximately 5 ml. of 0.045 M $H_2SO_4$ was placed in the nebulizer. Just before achieving the desired sampling temperature the aerosol generating system was turned on with the compressed air valve. The desired flowrate of 2.89 lpm, used in all of the experiments, was regulated with the calibrated rotameter. This compressed air flowrate produced an average sulfuric acid aerosol flowrate of 0.178 ml/min., giving a concentration of 0.272 mg $H_2SO_4$ per liter of undiluted aerosol. Dilution of the aerosol with one cubic foot air per minute produced a concentration of 26.0 µg $H_2SO_4$/l air. The aerosol was sprayed into the mixing chamber, diluted when desired, and vented to the hood. When assured that the sulfuric acid aerosol was evenly and well dispersed, the sampling pump was turned on. The sample flowrate was controlled by the critical orifice at 1.913 lpm. Sampling periods were timed such that 48-520 µg of sulfuric acid was collected on the sampling surface. Immediately following the sampling run, room air was pulled through the filter for 1 minute. Then the filter was kept in the heater unit for an additional 10 minutes at 105°C.

The filters showed a light to a strong red-orange color of o-cresolsulfonphthalein, tests were performed on them. The tests were for (1) color stability by exposing a filter to either room air, oven drying at 105°C, dessication, or combinations of each; (2) solvent extraction by various organic and inorganic solvents, and (3) spectrophotometry of the solutions.

The same sampling procedure was used with a 12 M HCl solution with no dilution air added. One-minute samples were taken at temperatures in the filter holder of 50°C and 100°C. The 50°C samples showed some coloration but the 100°C samples showed none. Solutions of OCP in concentrated HCl and $H_3PO_4$ gave no color. Concentrated nitric acid gave a yellow color.

## RESULTS

It was found that the prescribed method gave a stable and very sensitive red-orange color of o-cresolsulfonphthalein on the filter. The color was specific for sulfuric acid, and was easily discernable in the range of 50 to 500 micrograms of sulfuric acid. This would cover the range of one to 10 parts per million for a 10 liter (5 minute) stack sample. Higher or lower concentrations can be measured with shorter or longer sampling times. Field tests could be quickly and easily conducted by comparison of the color obtained with those on a series of standards.

The color is not, at present, easily separated from the filter and the organic precursor. Extraction of the filters with concentrated hydrochloric acid can give semi-quantitative results when the extracted color is compared to that of a blank run. Extraction with water causes reversal, but titration of the ensuing sulfate is easily possible. Recent work shows that phosphoric acid dissolves the o-cresolphthalein without dissolving the sulfonated product. Such a separation would be most useful for exact laboratory measurements.

The method has not as yet been field tested or tested for the possible interference of volatile bisulfate salts. The latter should easily be removed at higher temperatures by filtration if their interference is significant.

## ACKNOWLEDGMENTS

This work was supported by grants from the Environmental Protection Agency and the Smelter Environmental Research Association.

## REFERENCES


1. Urone, P., "Source and Ambient Air Analysis of $SO_3$ and $H_2SO_4$: State of the Art Report," Health Lab. Sci., 11;246 (July 1974).

2. Barton, S.C., and McAdie, H.G., "An Automated Instrument for the Specific Determination of Ambient $H_2SO_4$ Aerosol," Presented before the Divison of Water, Air and Waste Chemsitry, ACS, New York (1972).

3. Baviha, C.J., and Shinkararenka, L.S., "Determination of Sulfuric Acid in Air by a Vanadate Method," Neftepererab Neftehhim, 9;40-41, (1971).

4. Barrett, W.J., Miller, H.C., Smith, J.E., and Guin, C.H., "Development of a Portable Device to Collect Sulfuric Acid Aerosol," Interim Report from EPA (February 1977).

5. Scaringelli, F.P., and Rehme, K.A., "Determination of Atmospheric Concentrations of Sulfuric Acid Aerosol by Spectrophotometry, Coulometry and Flame Photometry," Anal. Chem., 41:707-713 (June 1969).

6. Thomas, R.L., Dharmarajan, V., Lundquist, G.L., and West, P.W., "Measurement of Sulfuric Acid Aerosol, Sulfur Trioxide, and Total Sulfate Content of Ambient Air," Anal. Chem., 48:639-642 (April 1976).

7. Jaworowski, R.J., Mack, S.S., "Evaluation of Methods of Measurement of $SO_3/H_2SO_4$ in Flue Gas," J. Air Pollu. Control Assoc., 29:43-46 (Jan. 1979).

8. Gilbert, E.E., Sulfonation and Related Reactions, Interscience Publishers, New York (1965).

9. Butler, G.B., and Berlin, K.D., Fundamentals of Organic Chemistry Theory and Application, Ronald Press Company, New York (1972).

10. Gelman Instrument Company Catalog (1975).

11. Scaringelli, F.P., and Rehme, K.A., Anal. Chem., 41:707 (June 1969).

12. Byers, R.L., and Davis, J.W., "Sulfur Dioxide Adsorption and Desorption on Various Filter Media," Air Poll. Control Assoc., 20:236 (April 1970).

13. Pate, J.B., Ammons, B.E., Swanson, G.A., and Lodge, J.P., Jr., "Nitrite Interference in Spectrophotometric Determination of Atmospheric Sulfur Dioxide," Anal. Chem., 37:942 (1965).

14. Barton, S.C., and McAdie, H.G., "Preparation of Glass Fiber Filters for Sulfuric Acid Aerosol Collection," Env. Sci. Tech., 4:769-770 (September 1970).

## SULFONATION REACTION

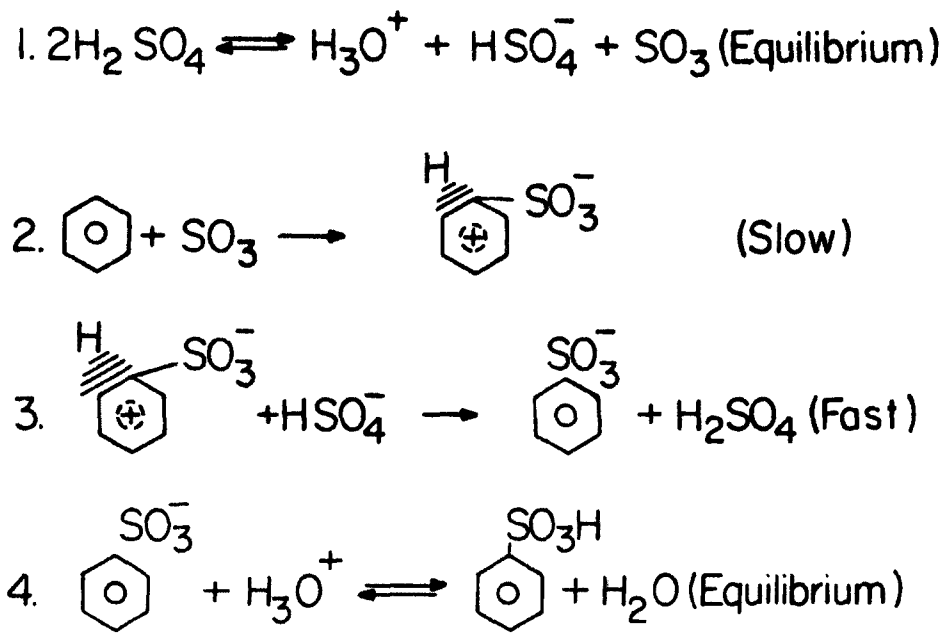


## DESULFONATION REACTION

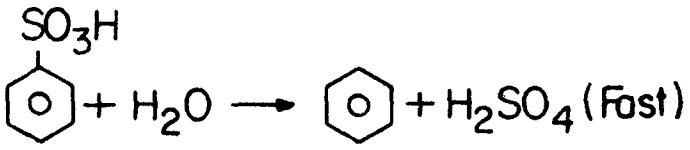


Figure 1. The Sulfonation Reaction

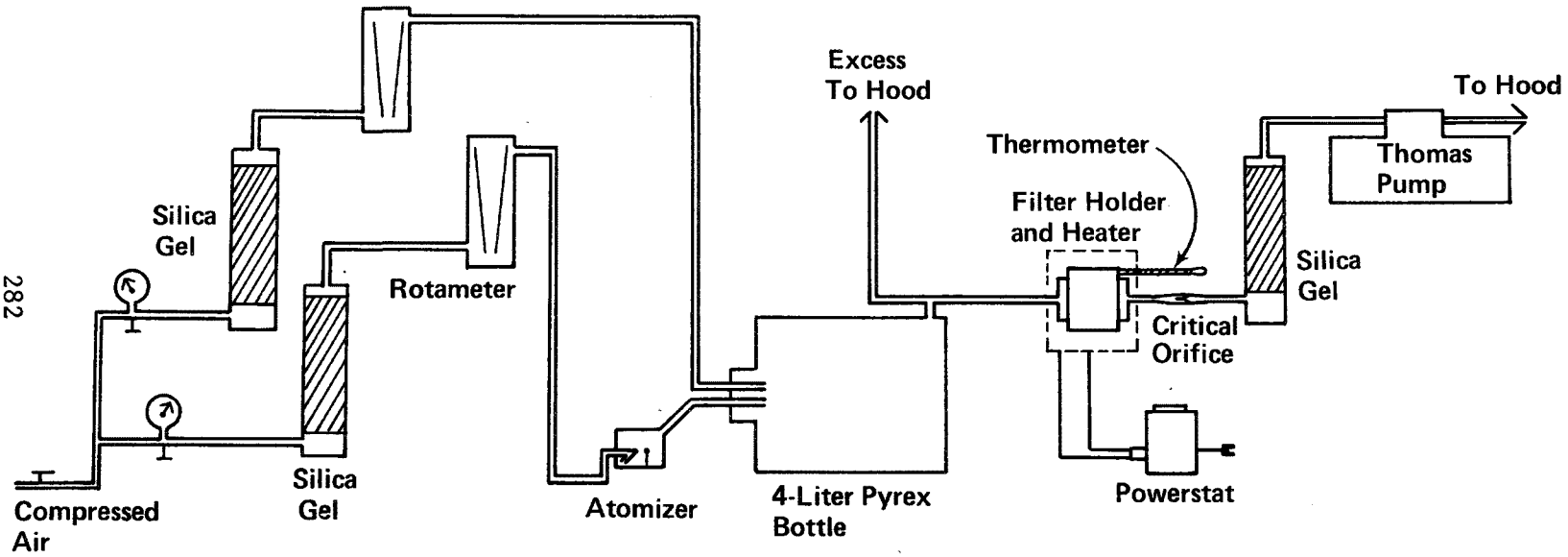


Figure 2. Experimental Apparatus

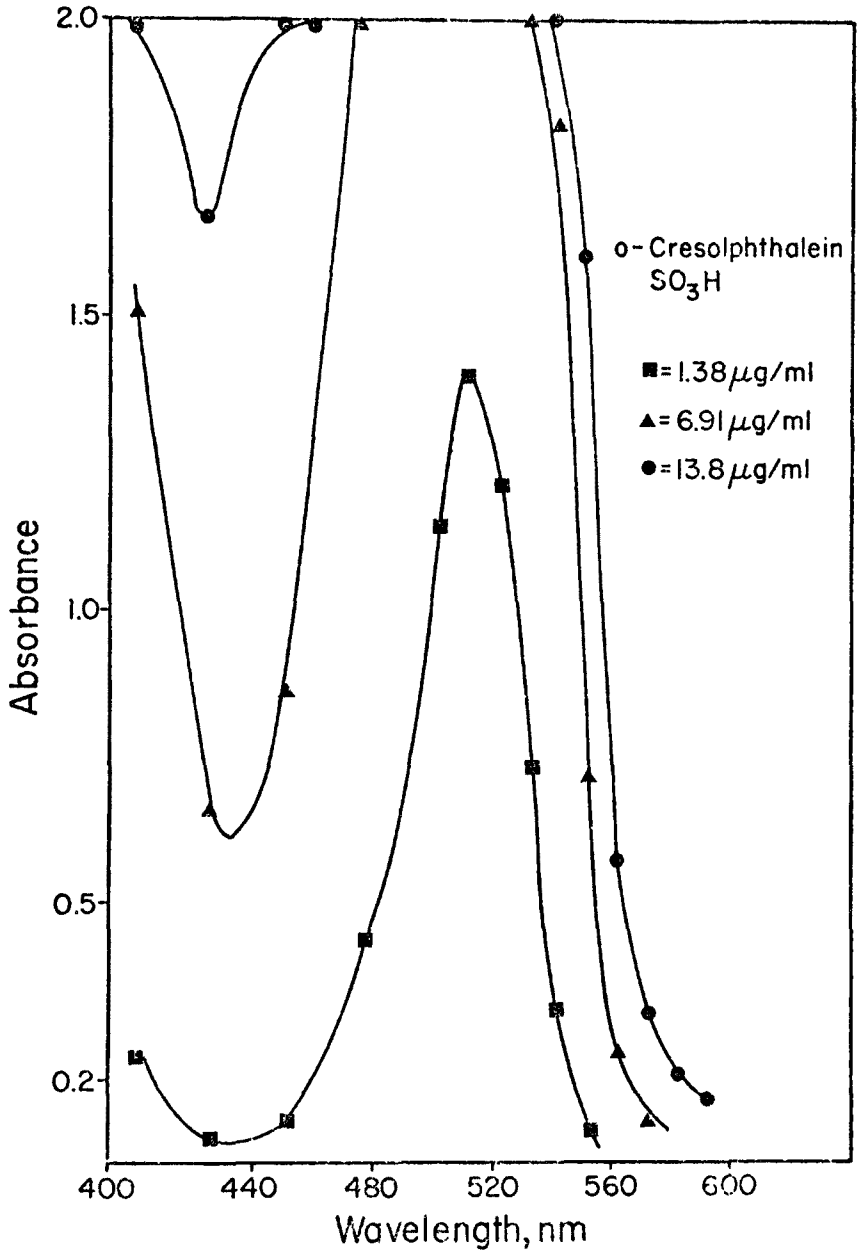


Figure 3. o-Cresolsulfonphtalein Adsorption Curves

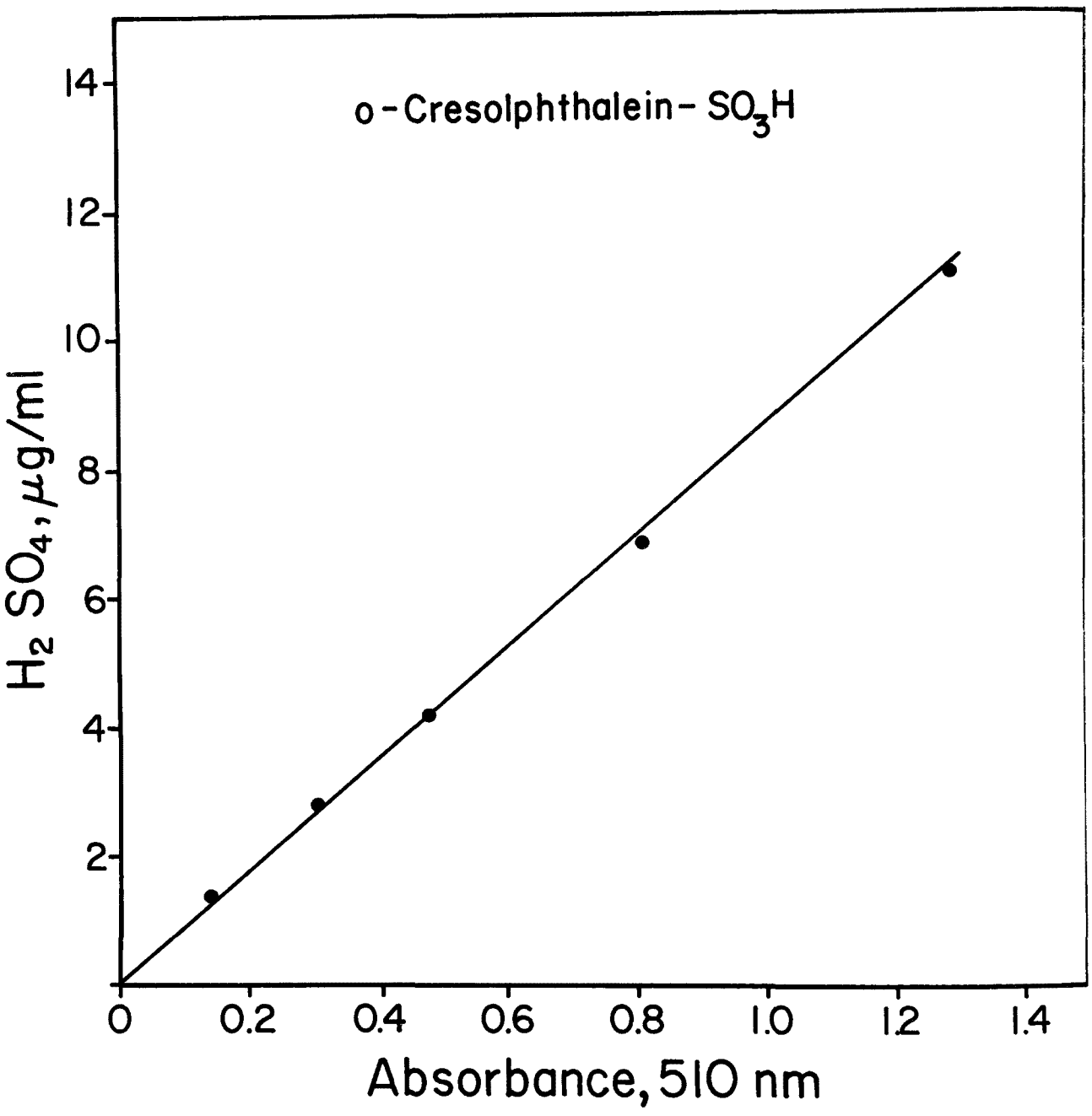


Figure 4.
Standard Curve for the $H_2SO_4$ - o-Cresolphthalein Reaction Product

# A MICROCOMPUTER-BASED CASCADE-IMPACTOR DATA-REDUCTION SYSTEM

By: Michael Durham
Scott Tegtmeyer
Ken Wasmundt

Denver Research Institute
University of Denver
P.O. Box 10127
Denver, Colorado 80210

Leslie E. Sparks
Industrial Environmental Research Laboratory
U.S. Environmental Protection Agency
Research Triangle Park, N.C. 27711

## ABSTRACT

This paper describes a cascade-impactor data-reduction system incorporating the Radio Shack TRS-80* computer. The system provides the computational facilities required to reduce raw impactor data to a particle size distribution. The program first calculates the 50% cut-points for each stage and then determines the cumulative mass distribution. A linear regression analysis is then applied to this distribution in log-normal space to determine the log-normal distribution parameters. A spline-fit routine is used to mathematically describe the cumulative distribution and to generate the differential distribution. A mathematical function is used to extrapolate the data to the maximum particle diameter in order to determine the amount of mass below the Inhalable Particulate Matter (IP) 15 μm cut. Additional programs provide the capability to statistically combine similar runs and to calculate the efficiency of a control device as a function of particle size by comparing impactor runs from the inlet and outlet. The system provides hard copy of input and results in a combination of tables, line printer graphics, and/or plotter graphics.

## INTRODUCTION

Cascade impactors have become the standard instrument for measuring size distributions of particulate matter entrained in gas streams. However, since impactors measure the aerodynamic characteristics rather than particle size, elaborate data reduction procedures are required to obtain particle size data from an impactor run. This is due to the fact that the aerodynamic characteristics of particles are dependent upon interactive functions of such variables as: particle size and density; gas composition, density, viscosity, temperature, pressure, and mean free path; and impactor flow rate, number and diameter of jets, and stage-calibration constant. Even using the simplest data-reduction procedures, these variables must be taken into account.

---

*TRS-80 is a trademark of Tandy Inc.

Another problem that exists is that, since the cut points on each stage are a function of sampling conditions, even if the same impactor is used, it is unlikely that the cut-diameters will be the same for two runs. This means that, in order to statistically combine similar runs or to compare data from different conditions, it is necessary to interpolate between data points.

Because of the extensive nature of the data reduction required for cascade-impactor runs, a computer-based system was developed not only to reduce the time required in making these tedious calculations, but also to provide a measure of data-quality assurance. The system was designed for a microcomputer to eliminate the necessity of a full-sized computer. Besides a savings in cost, the microcomputer is physically small and portable and thus can be transported to the source of the data and provide quick feedback to the field-test program.

## TRS-80 CASCADE-IMPACTOR DATA-REDUCTION SYSTEM

The TRS-80 cascade-impactor data-reduction system is designed to function on a Tandy Model I TRS-80 microcomputer system equipped with 48k bytes of central memory (RAM), two or more diskette drives, and a line printer. In addition, some of the programs have options for plotting data on either a Houston Instruments DP-1 plotter or an HP 7225A plotter using the TRS-80 serial interface.

The system is intended to provide the computational facilities required to reduce raw cascade-impactor data (stage weight gains, etc.) to a particle size distribution at a consistent set of particle sizes, and then to combine multiple impactor runs and compare the results of the inlet and outlet samples to calculate the collection efficiency of an air-pollution control device as a function of particle size. The system allows the user to select whether the data are reduced according to physical diameter, classical aerodynamic diameter, or impaction aerodynamic diameter depending on how the data are to be used. Each program, as appropriate for the data forms, provides hard copy in a combination of tables, line printer graphics, and/or plotter graphics.

The programs use a "menu" format for data entry in which the operator is presented with a list of variables and their values. The user may review and change any parameter up until the time that he initiates the calculations. Figure 1 is a flow chart depicting the general organization of the system showing the interactions between the programs (boxes) and the files produced by the programs (circles).

### GO

The "GO" program provides a central directory for the other programs in the system. It provides a list of the other programs, and can be used to give a brief description of each, or to initiate the execution of the other programs. All of the other programs automatically return to this program unless the return is disabled by the system manager.

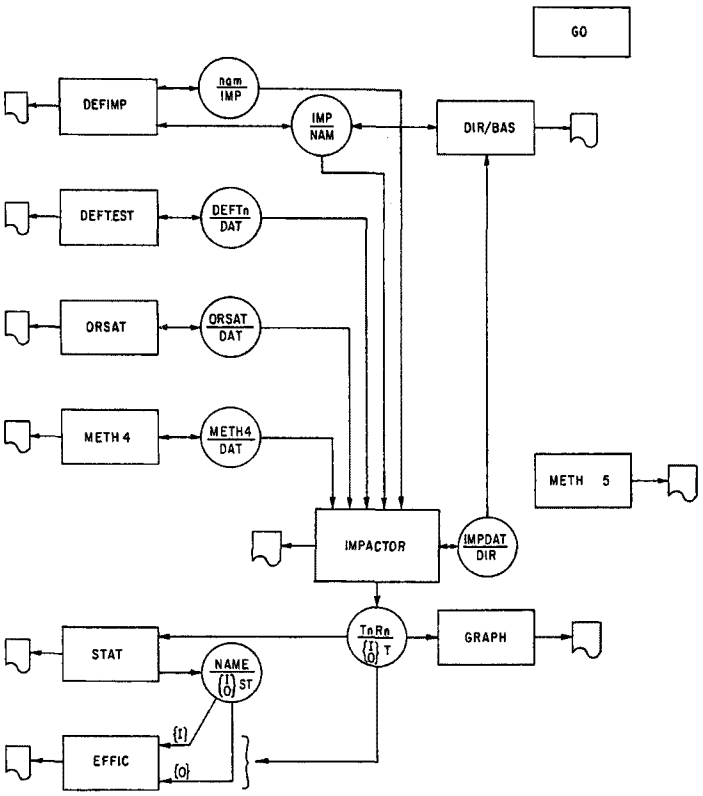


Figure 1. Impactor Data-Reduction System Flow Chart

DEFIMP

In order to make the system versatile enough to handle any type of impactor, the "DEFIMP" or "Define Impactor" program was written. This program creates a permanent file for an impactor which includes all the information that will be required to reduce data from the particular impactor. Table I shows the type of data required for each impactor. The operator first provides a name for the impactor which will be used in the IMPACTOR program to identify the correct impactor file. A brief description of the impactor is also included to help the operator distinguish between similar impactors. The shape of the jets (circular or rectangular) and the number of stages are defined by the operator. Then for each stage the number of jets, a calibration constant (square root of PSI), and the jet diameter for circular jets or the slot length and width for rectangular jets are input. The calibration constant, PSI, is defined as:

$$PSI = D_p^2 \frac{C\rho_p V}{18\mu D_j} \qquad (1)$$

where

$D_p$ = Particle diameter (cm),

$C$ = Cunningham slip factor,

$\rho_p$ = Particle density ($g/cm^3$),

$V$ = Jet velocity (cm/sec),

$\mu$ = Gas viscosity (poise), and

$D_j$ = Jet diameter (cm).

PSI is a dimensionless value and can be obtained empirically (Harris, 1977) or theoretically (Marple, 1970; Ranz and Wong, 1958). Empirical values for several of the commercial impactors are presented in Cushing et al., (1976).

A pressure drop calibration constant (K) is input from the equation:

$$DP = K\ P\ Q^2 \qquad (2)$$

where DP = Impactor pressure drop (in. Hg),

P = Density of the gas stream ($g/cm^3$), and

Q = Actual flow rate ($ft^3/min$).

If the value for K in not known, zero is entered, and the measured value is then input after each test.

After all the data are input, the operator initiates the calculation of stage constants. The stage constants are purely a function of the geometry, and for given sampling conditions will be proportional to the cut diameter of the stage. The stage constants are compared in order to determine if there will be any overlapping of stage cut-points. When this occurs the masses of the overlapping stages will be combined and assigned the smaller of the two cut-points. Information concerning stage overlapping as well as geometric and calibration data are then stored in a file for later retrieval by the IMPACTOR program. The data are also output on the line printer in the form of Table I. DEFIMP can be run for as many impactors as desired. Since it has been found that the stage calibration constants (PSI) vary for different collection substrates (Balfour, 1977) by changing the name, the same impactor can be defined for different substrates.

DEFTEST

This program is used to provide the specification for each test performed by the data-collection facility. A "test" is a series of impactor runs made on a single source while that source is operating with a fixed nominal set of operating parameters (e.g., flow rate, boiler condition). For each test DEFTEST creates a file of documentation of the source, control device, and test conditions. This eliminates the necessity to repeat the test documentation for each impactor run. Table II is an example of the output of this file. Besides the documentation, the operator also selects which diameter definition will be used in the calculations for this particular test. The particle density is also input but is only used in the calculations if the physical, or Stokes, diameter is used.

TABLE I. OUTPUT OF DEFIMP PROGRAM

| | |
|---|---|
| YES | HARD COPY |
| YES | DISK UPDATE: FILENAME MRI165/IMP |
| MRI165 | IMPACTOR NAME |
| DESCRIPTION: | DRI IMPACTOR CALIBRATION |
| CIRCLE | SHAPE OF JETS (CIRCLE/RECTANGLE) |
| 7 | NUMBER OF STAGES |
| 8860.000 | K IN 'DP=K*P*Q*Q' (0 IF UNKNOWN) |

| STAGE # | # OF JETS | SQR ROOT (PSI) | JET DIAMETER | STAGE CONSTANT |
|---|---|---|---|---|
| 1 | 8 | 0.1100 | 0.8700 | 0.2325 |
| 2 | 12 | 0.2700 | 0.4770 | 0.2838 |
| 3 | 24 | 0.3400 | 0.1980 | 0.1352 |
| 4 | 24 | 0.3200 | 0.1190 | 0.0593 |
| 5 | 24 | 0.3200 | 0.0838 | 0.0350 |
| 6 | 24 | 0.3400 | 0.0539 | 0.0192 |
| 7 | 12 | 0.3600 | 0.0542 | 0.0145 |

MASS ON STAGES 1 AND 2 WILL BE ASSIGNED THE CUTPOINT OF STAGE 1

TABLE II. DEFTEST OUTPUT

| | |
|---|---|
| ***** | DEFTEST VER-3.0 ***** |
| YES | HARD COPY |
| YES | DISK UPDATE OF FILENAME: DEFT30/DAT |
| 29 | TEST NUMBER |
| 2.430 | PARTICLE DENSITY (G/M[3) |
| SOURCE DESC.: | 230 MW COAL FIRED BOILER |
| LOCATION: | ASPEN COLORADO |
| CONTROL DEV.: | APC ELECTROFORCE ESP 375 SCA |
| TEST PURPOSE: | DETERMINE FRACT. EFFICIENCY DURING S03 CONDIT. |
| REMARKS: | IMPACTOR PROGRAM DEMONSTRATION |
| PHYSICAL | PARTICLE DIAMETER TYPE (I, C, P) |

## ORSAT, METH4, AND METH5

ORSAT, METH4, and METH5 are programs to calculate the results of tests for molecular weight, moisture content, and mass concentration using EPA Reference Methods 3, 4 and 5 (Federal Register 1971 and 1977), respectively. The values of the molecular weight and moisture content are stored in files and used by the IMPACTOR program. The METH5 data are not required by any other programs, and so the program creates no files but outputs results to the line printer.

## IMPACTOR

This is the main program in the system. It is used to perform all of the calculations required to reduce the data from an impactor run to the particle distribution at a specified set of diameters. The program uses the contents of files created in the DEFTEST, DEFIMP, METH4, and ORSAT programs along with the operator input, and produces optional disk files, CRT graphics, and listings.

The input menu for this program is on three pages. The first page contains descriptive data, which are also used to gather data from the test-desciptor file (after the test number is specified), and from the impactor descriptor file (after the impactor name is given). The run number is used to form the output file name and therefore must be unique for each run in a test series. The second page of the input is used to describe the sampling conditions. The third page is used to enter the mass gain for each stage and the final filter of the impactor. The number of stages is derived from the impactor description file.

After reviewing and correcting any incorrect data, the operator initiates the calculations. The FLOW subroutine calculates the actual flow rate through the impactor, the flow rate corrected to standard conditions, and the percent isokinetic sampling rate. The JET subroutine then calculates the jet velocity and pressure drop for each stage of the impactor. The pressure drop for each stage is equal to the sum of the pressure drops across all stages preceding and including the stage being considered. Since only the total drop across the entire impactor is known (measured or calculated), it is necessary to estimate the fraction of the pressure drop occuring at each stage. Because the gas flow through the impactor is accelerated and decelerated at each stage, it is reasonable to assume that the pressure drop is due to a loss of velocity pressure, and therefore the pressure drop at each stage is proportioned according to the square of the jet velocity.

The VISCOSITY subroutine calculates the viscosity of the gas stream as a function of the temperature and gas constitution. The viscosities of each component of the gas stream are first calculated as a function of temperature and then are combined into the viscosity of the total gas stream.

The CUT subroutine then calculates the 50% cut-point for each stage (based on the selected diameter definition) and the cumulative frequency of particles collected up to each stage. An iterative loop is used to determine

the Cunningham correction factor. During the CUT routine, the stage number is displayed to keep the operator confident that the program's progress is satisfactory. Finally, the cumulative mass frequencies are computed for each stage, and the results are displayed for the operator to confirm. The data are then ready for the spline fit of the data.

Spline-Fit Subroutine

The Spline-Fit subroutine is used to extrapolate between the data points to determine values of the distribution at a given set of diameters. The program uses a spline routine described by Lawless (1978) which first transforms the data to log-normal space and then fits the data with a natural cubic spline curve. This is different from the routine used by Johnson et al. (1978) in which a series of parabolas was used to fit the data in log-log space.

In this program the impactor data are first transformed to log-normal space; that is, the logarithm of the cut-point diameters is used and the normal transform of the cumulative probabilities is used. In other words a curve is fit to the data as plotted on log-probability paper. In this manner, the spline will fit a true log-normal distribution exactly, and the inherent errors in fitting near-log-normal distributions are substantially reduced. Fitting the curve in log-normal space in no way forces the conditions of log-normality on the data.

The natural cubic-spline-curve-fitting method is used to fit the transformed data. The properties of such splines are well defined mathematically; these splines are the smoothest curves that can be passed through all the data points, and they are capable of fitting non-log-normal distributions with small error.

The third-order natural spline that is used in the program consists of a series of cubic polynomials, joined at the data points with continuous first and second derivatives and with the second derivatives at the first and last data points equal to zero. Outside the data range, the cubic polynomial is reduced to a linear polynomial, so that the natural spline has some utility in situations calling for extrapolation. Another interesting characteristic of this spline is its insensitivity to variations at a single point. Changes at a single point in the value of the function being fitted change the value of the spline function only at that point and only affect the first and second derivatives of its nearest neighbors. Thus, an error in the original data does not propagate throughout the entire fitted region, as can happen with the interpolating polynomial.

Once the cumulative distribution is fit and values are determined for the specific diameters, the differential distribution (deltaM/delta(logD)) is determined by calculating the values of the first derivative at the same diameters. The data are then transformed back to linear space.

In addition to the spline fit, a linear-regression analysis is performed on the data in log-normal space. This is done to obtain values of mass-median diameter and geometric-standard deviation. These log-normal characteristics are calculated so that the data can be used in the computer models

for control devices. The correlation coefficient is also calculated to give an estimate of how close the data fit a log-normal distribution.

Extrapolation of Data for Inhalable Particulate Information

Since the largest cut-point diameter of most commercial impactors is on the order of 10 μm aerodynamic diameter, it is necessary to extrapolate beyond the last data point in order to provide useful data for the inhalable-particulate program (i.e., cumulative mass less than 15 μm aerodynamic diameter). To provide a degree of control on the extrapolation, the inhalable-particulate program committee decided that the mathematical routine should be based on the following steps:

1. Obtain an estimate of the maximum particle diameter, $d_{max}$.
2. Set the cumulative mass fraction less than $d_{max}$ equal to 1.
3. Set the slope of the cumulative-size distribution curve at $d_{max}$ equal to zero.
4. Draw a smooth curve between $d_{max}$ and the last impactor data point.
5. Match the slope of the extrapolated curve with the slope of the spline-fit curve at the last impactor data point.

To meet these criteria, the extrapolation was given the general form of a hyperbola plus a quadratic. In log-normal space the cumulative distribution approaches 1 at infinity. Therefore, steps 2 and 3 required that the curve approach infinity at $d_{max}$ and bend over at infinity so that the slope was zero. The hyperbola was incorporated to satisfy these requirements. To provide a smooth transition from the hyperbola to the last data point the quadratic was added. With the combined spline and extrapolated curve, it is then possible to calculate the amount of mass less than 15, 10, 5, and 2.5 μm.

Presentation of Data from the IMPACTOR Program.

Following the calculations, the results of the spline fit are displayed on the screen. The operator can select to store the data on diskette for later use in the GRAPH, STAT, and EFFIC programs. The program then displays a graph of the cumulative distribution on the CRT. The display consists of the points calculated by the spline fit routine, plus the actual points calculated at the stage cut-points which blink on the screen. The differential distribution is then displayed showing the points calculated in the spline-fit routine. Finally the operation is given an option of line-printer output of the results. Table III shows an example of output from the IMPACTOR program which consists of three pages of data. The first page is documentation and input data. The second page is calculated results including sampling rate, percent isokinetic, cut-points, and spline fit results. The third page gives the results of the extrapolation for inhalable-particulate matter and the results of the linear regression to determine the log-normal-size distribution parameters.

# TABLE III. LINE PRINTER OUTPUT OF THE RESULTS FROM THE IMPACTOR PROGRAM.

IMPACTOR VER-3.0

INPUT DATA

| | |
|---|---|
| DATE OF TEST | 1/6/81 |
| TIME OF TEST | 13:30 |
| LOCATION OF TEST | PORT 3A |
| TEST NUMBER | 29 |
| SOURCE DESCRIPTION: | 230 MW COAL FIRED BOILER |
| SOURCE LOCATION: | ASPEN, COLORADO |
| CONTROL DEVICE: | APC ELECTROFORCE ESP 375 SCA |
| TEST PURPOSE: | DETERMINE FRACT. EFFICIENCY DURING SO3 CONDIT. |
| TEST REMARKS: | IMPACTOR PROGRAM DEMONSTRATION |
| PART. DIAM. IS | CLASS. AERO. |
| TEST TYPE | OUTLET |
| RUN NUMBER | 1 - FILE NAME: T29R1/OT |
| RUN REMARKS: | GREASED SUBSTRATES |
| IMPACTOR TYPE | MRI165 |
| | DRI IMPACTOR CALIBRATION |
| WATER VAPOR | 8.88% (FROM 'METH4') |
| CARBON DIOXIDE | 4.00% CARBON MONOXIDE 2.00% |
| OXYGEN | 20.00% NITROGEN 73.00% |
| PARTICLE DENSITY | 1.00 GRAMS/CM |
| GAS METER VOLUME | 10.200 CUBIC FEET |
| IMPACTOR DELTA P | 1.70 INCHES HG (CALCULATED) |
| ORIFICE DELTA P | 3.60 INCHES H20 |
| STACK PRESS. (BELOW ATMOS.) | 14.00 INCHES H20 |
| BAROMETRIC PRESS. | 24.75 INCHES HG |
| STACK TEMPERATURE | 302 DEGREES F |
| METER TEMPERATURE | 78 DEGREES F |
| IMPACTOR TEMPERATURE | 260 DEGREES F |
| SAMPLE TIME | 30.00 MINUTES |
| AVERAGE VELOCITY OF GAS | 240.00 FEET/MINUTE |
| GAS METER PRESSURE | 2.85 INCHES HG |
| NOZZLE DIAMETER | 0.60 INCHES |
| MAXIMUM AERODYN. DIAMETER | 60.00 MICRONS |
| MASS GAIN OF STAGE 1 | 12.20 MG |
| MASS GAIN ON STAGE 2 | 13.80 MG |
| MASS GAIN OF STAGE 3 | 14.46 MG |
| MASS GAIN ON STAGE 4 | 13.13 MG |
| MASS GAIN OF STAGE 5 | 6.23 MG |
| MASS GAIN ON STAGE 6 | 1.81 MG |
| MASS GAIN OF STAGE 7 | 0.72 MG |
| MASS GAIN ON FINAL FILTER | 0.43 MG |

RESULTS

| | |
|---|---|
| DATE OF TEST | 1/6/81 |
| TIME OF TEST | 13:30 |
| LOCATION OF TEST | PORT 3A |
| TEST NUMBER | 29 - IMPACTOR PROGRAM DEMONSTRATION |
| RUN NUMBER | 1 |
| ACTUAL FLOW RATE (STACK CONDITIONS) | 0.461 CFM |
| FLOW RATE (STANDARD CONDITIONS) | 0.244 CFM |
| PERCENT ISOKINETIC SAMPLING | 103.57% |

VISCOSITY OF GAS STREAM 0.0002171 GRAMS/CM-SEC

| STAGE | CCF | DP(CLASS. AERO) | DP(IMP. AERO) | CUM FRACTION |
|---|---|---|---|---|
| 1 | 1.029 | 9.344 | 9.480 | 0.8057 |
| 2 | 1.024 | 11.433 | 11.569 | 0.5859 |
| 3 | 1.051 | 5.378 | 5.513 | 0.3555 |
| 4 | 1.120 | 2.283 | 2.416 | 0.1464 |
| 5 | 1.212 | 1.296 | 1.427 | 0.0471 |
| 6 | 1.442 | 0.646 | 0.776 | 0.0183 |
| 7 | 1.725 | 0.434 | 0.570 | 0.0068 |

NOTE: THE MASS ON STAGES 1 AND 2 WILL BE COMBINED AND ASSIGNED TO THE OUTPUT ON STAGE 1, FOR SPLINE FITTING ANALYSIS.

TOTAL MASS PER DRY NORMAL CUBIC METER 332.1070 MG/CUBIC METER

| CLASS. AERO. PARTICLE SIZE (MICRONS) | CUMFR (STD. DEV.) | CUMFR (PER CENT) | CUM. MASS MG/DRY N. CU. METER) | DM/DLOGD |
|---|---|---|---|---|
| 0.20 | -3.3870 | 0.0 | 0.1180 | 1.2862 |
| 0.25 | -3.1214 | 0.1 | 0.3002 | 3.0528 |
| 0.40 | -2.5620 | 0.5 | 1.7313 | 14.9665 |
| 0.50 | -2.3191 | 1.0 | 3.3895 | 22.8497 |
| 0.75 | -1.9951 | 2.3 | 7.6472 | 25.5045 |
| 1.00 | -1.8472 | 3.2 | 10.7483 | 32.5045 |
| 1.50 | -1.5301 | 6.3 | 20.9196 | 112.0330 |
| 2.00 | -1.1978 | 11.5 | 38.3563 | 188.5060 |
| 2.50 | -0.9636 | 16.8 | 55.6704 | 194.3580 |
| 4.00 | -0.6012 | 27.4 | 90.9565 | 200.0610 |
| 5.00 | -0.4321 | 33.3 | 110.5450 | 250.5770 |
| 7.50 | -0.0332 | 48.7 | 161.6490 | 370.7900 |
| 10.00 | 0.3247 | 62.7 | 208.3240 | 506.7230 |
| 15.00 | 0.9977 | 84.1 | 279.2380 | 363.4890 |
| 20.00 | 1.5722 | 94.2 | 312.8610 | 222.7530 |
| 25.00 | 2.1738 | 98.5 | 327.1680 | 101.7230 |
| 40.00 | 5.2478 | 100.0 | 332.1070 | 0.0049 |
| 50.00 | 12.1548 | 100.0 | 332.1070 | 0.0000 |

RESULTS (CONTIUNED)

| | |
|---|---|
| TIME OF TEST | 13:30 |
| LOCATION OF TEST | PORT 3A |
| TEST NUMBER | 29 |
| RUN NUMBER | 1 |

INHALABLE PARTICULATE MATTER

CUM. MASS LESS THAN 2.5 MICRON: 55.67 MG/DRY NORMAL CU. METER (16.8%)
CUM. MASS LESS THAN 5.0 MICRON: 110.55 MG/DRY NORMAL CU. METER (33.3%)
CUM. MASS LESS THAN 10.0 MICRON: 208.32 MG/DRY NORMAL CU. METER (62.7%)
CUM. MASS LESS THAN 15.0 MICRON: 279.24 MG/DRY NORMAL CU. METER (84.1%)

NOTE: DIAMETERS FOR INHALABLE PARTICULATE ARE CLASSICAL AERODYNAMIC DIAMETERS.

LOG-NORMAL SIZE DISTRIBUTION PARAMETERS

LEAST SQUARES LINE: Y=1.77-1.98X

| | |
|---|---|
| MASS GEOMETRIC MEAN DIAMETER | 7.846 |
| GEOMETRIC STANDARD DEVIATION | 3.192 |
| CORRELATION COEFFICIENT | 0.995 |

GRAPH

This program is used to graph the output of the IMPACTOR program using either the Radio Shack line printer, a Houston Instruments DP-1 plotter, or a Hewlett Packard 7225A plotter. The program first plots the cumulative distribution in log-normal space for diameters from 0.3 to 30 μm. The differential distribution is then plotted in log-normal space from 0.3 to 30 μm. Figures 2 and 3 are examples of plots from the HP plotter.

STAT

This program is used to combine several impactor runs into a single file for later processing by the EFFIC program. This program first checks to see if the data being combined were calculated based on the identical diameter definition. The program then proceeds to calculate the mean and the confidence intervals for each of the diameters in the impactor file. The statistical calculations are performed twice, with points which are widely separated from the data ("outliers") eliminated from the second set calculations. The standard deviation is then converted to a confidence interval range using an abbreviated table of the t-test for significance at the 90% level. Von Lehmden and Nelson (1976) describes the criteria for outliers.

EFFIC

This program is used to compute the particulate collection efficiency of particulate control equipment by comparison of simultaneous tests at the inlet and outlet of the control device. The calculation can be done for single impactor runs or multiple runs combined by the STAT program as long as all data are based upon the same diameter definition. Calculations are made for both total particulate mass and as a function of particle size, and the results are expressed both in terms of fractional penetration and percent efficiency. The results are displayed on the screen of the TRS-80, and are optionally available as line-printer listings, line-printer plots, and/or plots from one of the plotters. Figure 4 shows an example of the plot produced by the HP plotter.

DIR/BAS

This program is used to examine and modify the directories IMP/NAM and IMPDATA/DIR. The first of these is a list of the file names and descriptions of the impactors in the system, and the second is a list of the files produced by the IMPACTOR program. One file is produced by IMPACTOR each time it is run. The program can be used to provide a detailed listing of the names and remarks for the files in the IMPDATA/DIR file, or it can be used to delete file names and the associated files from either of these files.

## CONCLUSIONS

The TRS-80 cascade-impactor data-reduction system provides an inexpensive computerized system to reduce raw cascade-impactor data to size

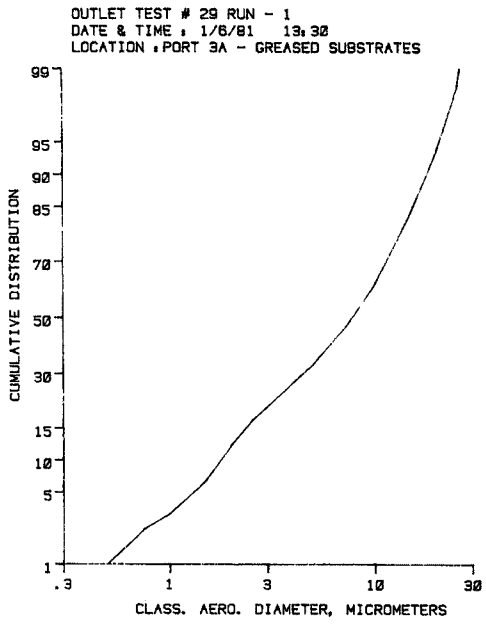


Figure 2. Cumulative Distribution*

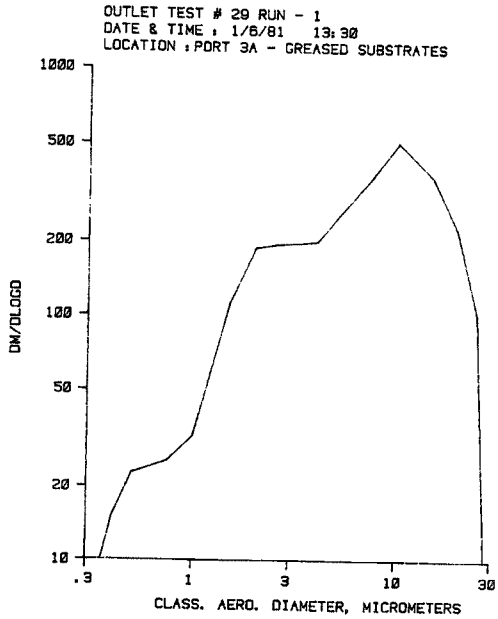


Figure 3. Differential Distribution*

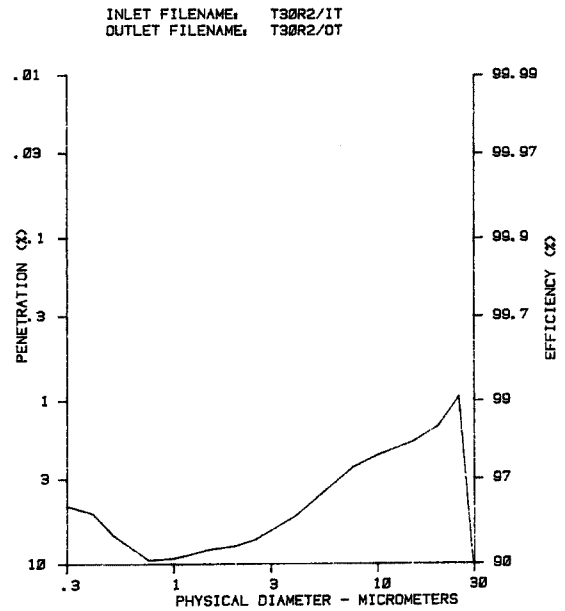


Figure 4. Fractional Efficiency Plot*

* Actual plots on 8-1/2 by 11 inch paper.

distributions, reducing the time required for the necessary calculations and providing a measure of quality control for the data processing. Besides standardizing the listing of input data and results, the system provides report quality plots of the results. The hardware for the system is available through Radio Shack and the software is currently available through the Denver Research Institute and will soon to be available through NTIS.

## REFERENCES


Balfour, W.D., (1977): "Use and Limitations of In-Stack Impactors," Masters Thesis, University of Florida, Gainesville, Florida.

Cushing, K.M., G.E. Lacey, J.D. McCain, and W.B. Smith, (1976): Particulate Sizing Techniques For Control Device Evaluation: Cascade Impactor Calibrations. EPA-600/2-76-280 (NTIS PB 262849), October.

Federal Register, (1971): "Standards of Performance for New Stationary Sources," Vol. 36, No. 247, December 23.

Federal Register, (1977): "Standards of Performance for New Stationary Sources: Revision to Reference Methods 1-8," Vol. 42, No. 160, August 18.

Harris, D.B., (1977): "Procedures for Cascade Impactor Calibration and Operation in Process Streams," EPA-600/2-77-004 (NTIS PB 263623), January.

Johnson, J.W., G.I. Clinard, L.G. Felix, and J.D. McCain, (1978): A Computer-Based Cascade Impactor Data Reduction System. EPA-600/7-78-042 (NTIS PB 285433), March.

Lawless, P.A., (1978): "Analysis of Cascade Impactor Data for Calculating Particle Penetration," EPA-600/7-78-189 (NTIS PB 288649), September.

Marple, V.A., (1970): A Fundamental Study of Inertial Impactors. Ph.D Thesis, Mechanical Engineering Department, University of Minnesota, Minneapolis, Minnesota 55455.

Ranz, W.D., and J.B. Wong, (1958): Impaction of Dust and Smoke Particles, Ind. and Eng. Chem., 50, No. 4, April.

Von Lehmden, D.J., and C. Nelson, (1976): "Quality Assurance Handbook for Air Pollution Measurement Systems," EPA-600/9-76-005 (NTIS PB 254658), March.

# DEVELOPMENT OF A SAMPLING TRAIN FOR STACK MEASUREMENT OF INHALABLE PARTICULATE

By: A.D. Williamson and W.B. Smith
Southern Research Institute
2000 Ninth Avenue South
Birmingham, AL 35255

## ABSTRACT

A new system, consisting of two cyclones operated in situ followed by a diluter operated outside the process stream, has been developed to measure the emission of inhalable particles from stationary pollution sources. Collection efficiency of 50% for 15 μm particles was achieved in the initial cyclone at flow rates of 11, 20, and 23 ℓ/min, respectively, at temperatures of 23°C, 93°C, and 150°C. At each condition the collection efficiency of the second cyclone was found to be 50% for particles of 2.5 ± 0.6 μm diameter. From the second cyclone the fine particles pass through a heated probe into the dilution device. The temperature and relative humidity of the dilution air are adjustable, and dilution ratios from 10:1 to 40:1 are possible, with standard operation at a dilution of 25:1. Provision is made to sample the resulting "plume" in the diluter with absolute filters, cascade impactors, electrical aerosol analyzers, optical particle counters, or diffusion batteries.

## INTRODUCTION

In reassessing the ambient air standards for suspended particulate, health effects professionals have suggested that particles having aerodynamic diameters of 15 μm or less are most likely to be deposited in the human respiratory system.[1] These particles, called inhalable particulate (IP), are considered to represent the primary health hazard for airborne pollution.

In order to estimate the impact of sources of IP upon the environment, the U.S. Environmental Protection Agency is sponsoring a large sampling program to measure emission factors of IP from source categories of significant interest. The objectives of this program include measurement of total mass smaller than 15 μm, the condensable fraction of total emissions, mass in discrete size fractions within the IP range, and continuous size distribution up to 15 μm or up to 80 μm. Lower priority goals include chemical and biological characterization of the sized particulate. As part of the program to measure emission factors, standardized methods are being developed to sample stack, ambient, and fugitive aerosols. The methods that are currently considered to be appropriate for stack sampling include cyclones, impactors with appropriate precollectors, and dilution for recovery of condensables.

The minimum requirements of the instack sampler are that the IP be separated into two fractions: one fraction with aerodynamic diameters lying between 2.5 and 15 μm, and the other, fine-particle, fraction with diameters smaller than 2.5 μm. The condensable fraction of the aerosol is included with the fine particles. The aerosol fractions larger and smaller than 15 μm must be separated using an inertial device having an efficiency (Eff. vs. dia.) curve bounded by two cumulative log-normal curves with geometric standard deviations, $\sigma_g$, of 1.0 and 1.7 and median diameters ($D_{50}$) of 13 and 17 μm aerodynamic. It has been shown that the measured IP concentration, for a wide range of typical aerosols, is rather sensitive to the value of the median diameter but much less sensitive to the $\sigma_g$ of the sampler's collection efficiency curve.[2,3]

This paper contains a brief description of the systems that have been developed for sampling in process streams (instack).. The systems consist of two cyclones, or a cyclone and impactor in series, followed by a dilution device.

## TECHNICAL DISCUSSION

Three cyclones were developed for use in the IP sampling program: two for use in a dual series-cyclone sampler, and the other for use as an IP precutter with cascade impactors. Their dimensions are given in Figure 1.

Each of the cyclones was calibrated at three temperatures using monodisperse dye particles generated with a vibrating-orifice aerosol generator. The aerosol was passed through a heated tube into the test cyclone and a filter which were inside an oven. For the larger cyclones, particles of 15 μm diameter were generated and sampled over a range of flowrates until the flowrate for 50% efficiency was found at each temperature. Tests were also made with the cyclone axes in different orientations to determine if particle settling was important. The data from these experiments are summarized in Figures 2 and 3. After the proper flowrates were determined for the IP cyclone, the small cyclone ($D_{50} \approx 2.5$ μm) was calibrated at the same flowrates and temperatures to quantify its performance. Data from these tests are shown in Figure 4.

The data from calibration tests of the IP cyclone and the IP precutter cyclone are shown plotted as flowrate (for $D_{50}$ = 15 μm) vs. gas viscosity in Figure 5. The curves fitted to the data will allow the operators to interpolate between the calibration points in choosing the flowrate corresponding to a $D_{50}$ of 15 μm at different temperatures.

In order to meet the IP program goal of obtaining measurements of condensable matter, a dilution system has been designed and prototypes tested under laboratory and field conditions. The design objective of this Stack Dilution Sampling System is to simulate the plume/ambient mixing process as closely as possible within the size constraints of a field sampling train. The dilution system is illustrated schematically in Figure 6 and its specifications are summarized in Table 1. The principal component of the diluter is a cylinder in which flue gas is mixed with filtered air and the resulting

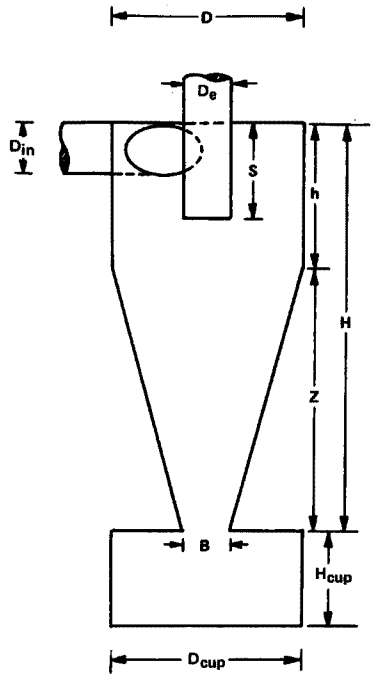


DIMENSIONS (CENTIMETERS)

| CYCLONE | D | $D_{in}$ | $D_e$ | B | H | h | Z | S | $H_{cup}$ | $D_{cup}$ |
|---|---|---|---|---|---|---|---|---|---|---|
| SRI-X | 6.14 | 1.83 | 2.17 | 2.92 | 8.47 | 2.82 | 5.65 | 2.40 | 2.635 | 6.14 |
| SRI-III | 3.11 | 0.75 | 0.83 | 0.76 | 4.91 | 1.40 | 3.51 | 1.08 | 2.22 | 3.10 |
| SRI-IX | 5.12 | 1.53 | 1.81 | 2.43 | 7.06 | 2.35 | 4.71 | 2.00 | 2.26 | 5.12 |

4181-22

Figure 1. Dimensions of cyclones used in sampling for inhalable particles.

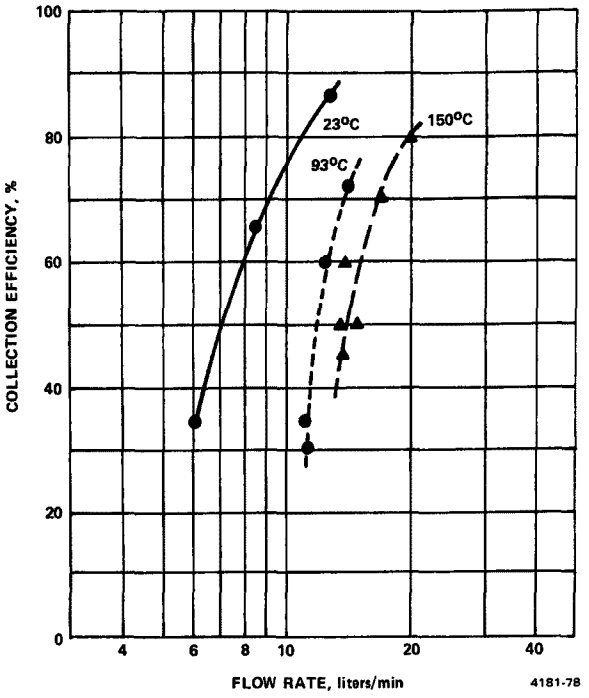


Figure 2. Determination of flow rate at three temperatures for $D_{50}$ = 15 μm in Cyclone IX.

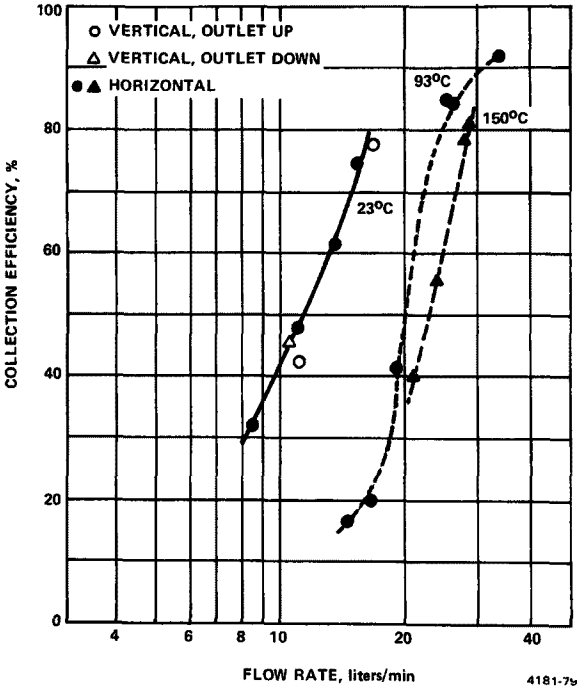


Figure 3. Determination of flow rate at three temperatures for $D_{50}$ = 15 μm in Cyclone X.

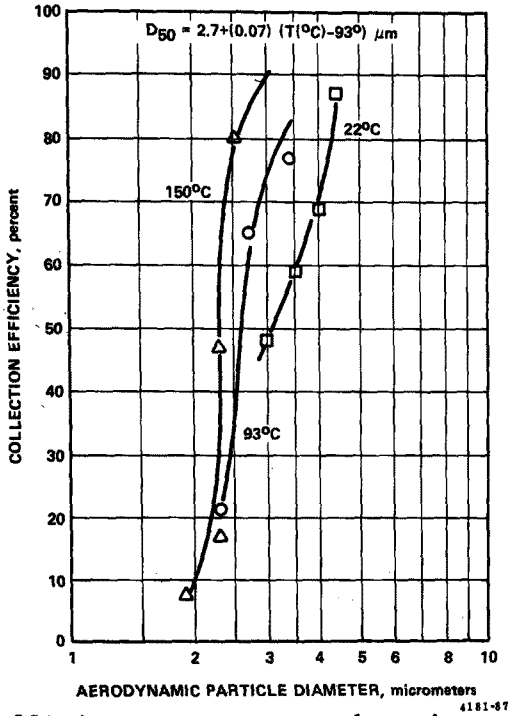


Figure 4. Collection efficiency versus aerodynamic particle diameter for smaller IP cyclone at 22°C and 11.3 ℓ/min (□), 93°C and 19.8 ℓ/min (○), and 150°C and 22.7 ℓ/min (△).

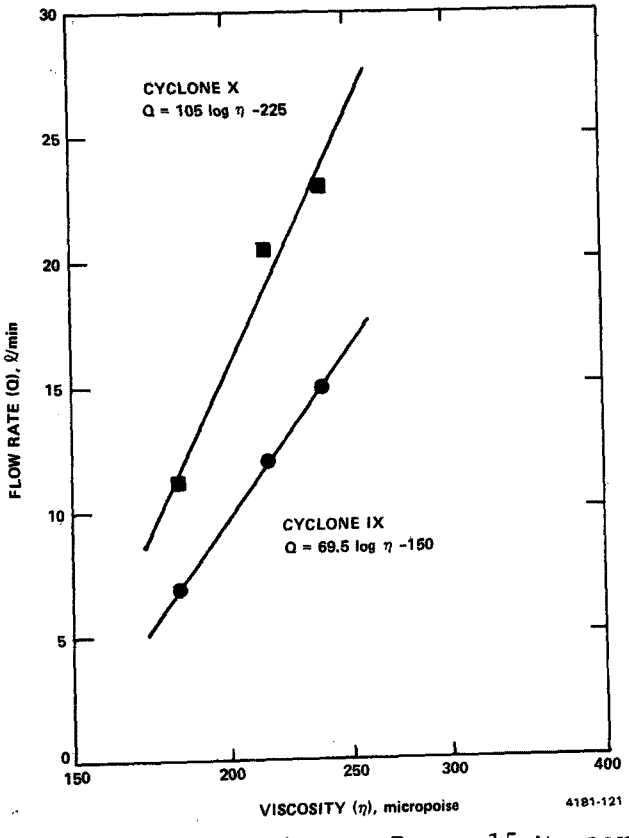


Figure 5. Gas flow rate versus viscosity at $D_{50}$ = 15 μm aerodynamic for IP cyclones IX and X.

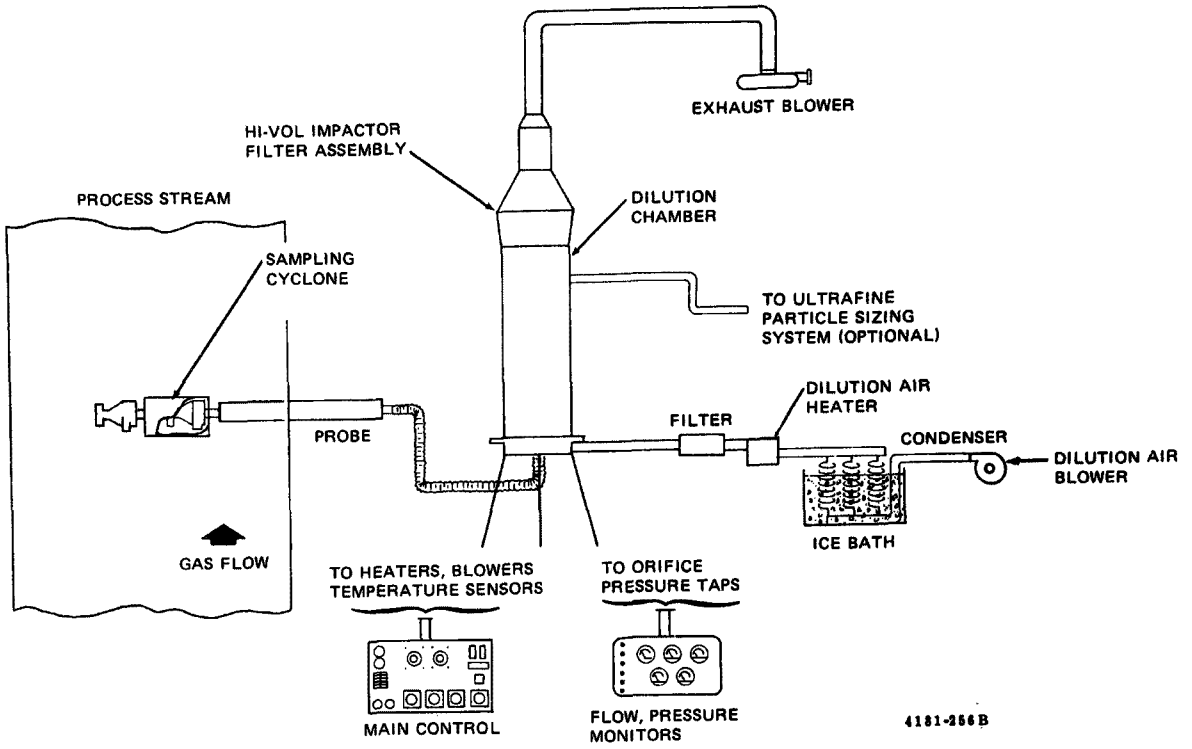


Figure 6. Diagram of Stack Dilution Sampling System.

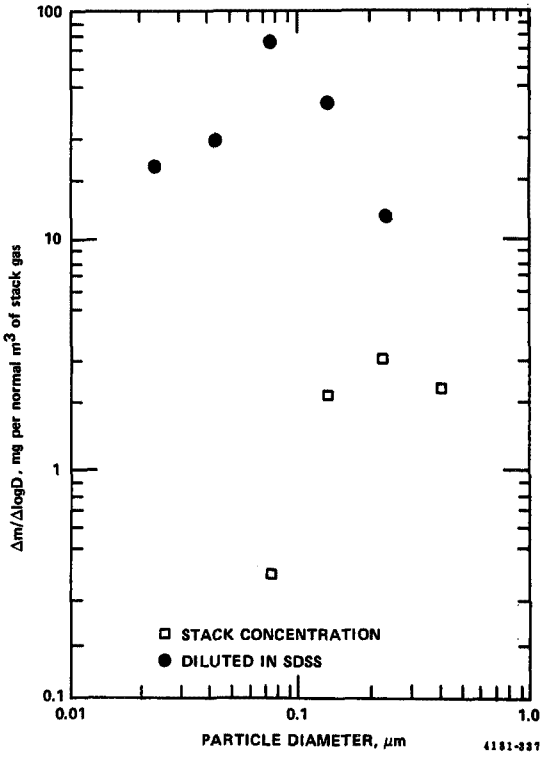


Figure 7. Submicron size distribution in stack gas from a coal-fired boiler before and after dilution in Stack Dilution Sampling System. Note evidence of sulfuric acid condensation mode.

TABLE 1. SPECIFICATIONS FOR DILUTION SAMPLING SYSTEM

| | |
|---|---|
| **GEOMETRIC** | |
| • Active length of dilution chamber: | 122 cm |
| • Diameter of dilution chamber: | 21.3 cm |
| • Diameter of sample inlet tube: | 4.27 cm |
| • Active dilution volume: | 43600 $cm^3$ |
| **FLOW** | |
| • Sample flow (determined by IP cyclone train): | ∿17 ℓ/min |
| • Sample velocity: | ∿27 cm/sec at 150°C |
| • Dilution air flow: | 425 ℓ/min |
| • Dilution air velocity: | 20 cm/sec |
| • Dilution ratio: | ∿25:1 (up to 40:1 possible) |
| • Residence time: | 6.2 sec |
| **GAS CONDITIONS** | |
| • Sample gas: T <250°C; particles >2.5 μm removed by cyclones | |
| • Dilution air: T = 21.1°C; relative humidity 24%; filtered ambient air | |
| **SAMPLE COLLECTION** | |
| • Particulate collected on glass fiber filter | |
| • Optional impactor gives cuts at 0.5, 1.0, 2.0, 4.0 μm | |
| • Optional extraction of diluted stream for sizing by optical counter, electrical mobility analyzer, CN counter, etc. | |

aerosol-laden mixture analyzed. The sample gas is introduced through a tube oriented along the axis of the cylinder and the dilution air is introduced as an annular sheath around the sample. As the sample is cooled by dilution, condensable vapors form particles under conditions close to those which occur in actual plumes. The system is designed for a "standard" dilution air at 21°C, 24% relative humidity, mixing time of 6.2 seconds, and a dilution ratio of 25:1. All of these parameters can be adjusted to some extent. The diluter can be adapted to a variety of sampling devices to measure the condensed and diluted aerosol. The total flow can be directed into a cascade impactor or filter, or portions of the diluted stream can be extracted, further diluted if necessary, and sampled using electrical aerosol analyzers, optical particle counters, or diffusion batteries with condensation nuclei counters.

The Stack Dilution Sampling System has been subjected to a variety of laboratory and field tests. Using a transparent prototype, the formation and mixing of a condensation plume were studied. For sample gas at typical stack temperatures, thorough mixing was found to occur before the diluted stream reached the top of the dilution chamber.

After laboratory characterization, the Stack Dilution Sampling System was tested at the EPA facilities in Research Triangle Park, North Carolina. The SDSS was one of a battery of devices used to sample the effluent of a domestic oil-fired heater. Other sampling devices included SASS trains, gas analyzers, and an automotive dilution tunnel. Analysis of extracts from the

SASS solvent module demonstrated that the majority of the emissions were light (TCO fraction) organic compounds, whose vapor pressure was too high to be captured in any of the particulate sampling devices including the dilution systems. However, both the SDSS and the automotive dilution tunnel captured about 25% more mass than the SASS trains, indicating that condensation did significantly increase the particulate loading under the conditions similar to those at the flue exit.

A more dramatic confirmation of the operating behavior of the system was obtained in a test at a power plant fueled by high-sulfur coal. The dilution sampling system was used to sample the emissions of a 50 MW boiler downstream of the electrostatic precipitator. Since independent measurements recorded $SO_3$ levels of 7 to 8 ppm in the same duct during the sampling periods, it was anticipated that a measurable amount of sulfuric acid would be detected in the SDSS. Since the duct did not have the 6 in. (15 cm) ports required for the IP dual cyclone train, only the smaller cyclone was used on the probe of the dilution sampling system. In addition, a Teflon membrane hi-vol filter was used in order to ensure low sulfate background and minimize artifact sulfuric acid formation due to the high concentrations of $SO_2$ in the stack gas. Aside from these changes the dilution sampler was operated in a standard manner. All data from this field test have not been analyzed at this time; however, preliminary results are summarized in Table 2. The mass train and impactor measurements are consistent with a stack particulate loading of 36 $mg/m^3$ actual gas volume during the approximate time period of the SDSS test, with approximately 2 $mg/m^3$ in the fine fraction as defined by the cut of stage 4 of the U.W. Mark V impactors used. In contrast, the fine particulate plus condensable mass as measured by the SDSS was about 26 $mg/m^3$. Although some differences are to be expected due to the fact that the impactors and mass trains were run at different times in different positions in the duct, the order of magnitude increase in mass is clearly beyond experimental uncertainty. To obtain further evidence that sulfuric acid condensation was occurring in the SDSS, a portion of the diluted stream was extracted into the Southern Research Institute Ultrafine Particle Sizing System for size analysis of the particulate matter smaller than 1.0 μm. As shown in Figure 7, the size distribution of particulate after dilution was dominated by a mode centered at about 0.08 μm. In contrast, the size distribution in the stack peaks at larger diameters with an integrated mass roughly 5% that observed in the diluted sample. The data in Figure 7 indicate that a sulfuric acid mist is formed by condensation in the Stack Dilution Sampling System and, presumably, in the plume of the power plant under test.

The Stack Dilution Sampling System will be tested at a variety of stationary emission sources in the course of the IP emission factor measurements program. We anticipate that this program will provide extensive field validation of all the devices described in this paper. In addition, independent laboratory and field characterization of each device is continuing.

TABLE 2. COMPARATIVE MASS LOADINGS (IN MG/ACM) IN TEST OF UTILITY BOILER BURNING HIGH SULFUR COAL - PRELIMINARY DATA

| Sample | | Fine (<2 μm) | Coarse (>2 μm) | Total |
|---|---|---|---|---|
| Method 17 | (2/4/81) | | | 35.7 |
| Impactor | (2/3/81) | 2.0 | 21 | 23 |
| Impactor | (2/4/81) | 2.2 | 25 | 27 |
| SDSS | (2/3/81) | 25 | | |
| SDSS | (2/4/81) | 27 | | |

ENDNOTES


1. Miller, F.J., D.E. Gardner, J.A. Graham, and R.E. Lee, Jr. Size Considerations for Establishing a Standard for Inhalable Particles. J. Air Pollut. Contr. Assoc., 29(6): 610 (1979).

2. Kapadia, A., D.Y.H. Pui, and K.T. Whitby. Modeling of Impactor Data and Calculation of IP Concentration. Final report on subcontract to Southern Research Institute, EPA Contract No. 68-02-3118, November 1979.

3. Johnson, J.W., B.E. Pyle, and W.B. Smith. Extending Precision in a Computer-Based Cascade Impactor Data Reduction System. (Presented at the Second Advances in Particle Sampling and Measurement Symposium, Daytona Beach, Florida, October 1979, EPA-600/9-80-004, January 1980).

# INHALABLE PARTICULATE MATTER SAMPLING PROGRAM FOR IRON AND STEEL AN OVERVIEW PROGRESS REPORT

By: R.C. McCrillis
Metallurgical Processes Branch
Industrial Environmental Research Laboratory
U.S. Environmental Protection Agency
Research Triangle Park
North Carolina 27711

## ABSTRACT

EPA's Office of Research and Development has entered into a major program to develop inhalable particulate matter (IP) emission factors, where IP is defined as airborne particles of <15 μm aerodynamic equivalent diameter. The Metallurgical Processes Branch of EPA's IERL-RTP is responsible for the iron and steel industry segment of this program. This paper presents a summary of efforts to date. Every effort is being made to mesh the IP requirements with those of other EPA sampling programs, thus reducing overall cost to EPA and minimizing inconvenience to the host plants.

A preliminary literature review indicated the existence of particle size data for several of the major iron and steel sources. However, none of these data were obtained using current measurement technology: most of it does not cover the full IP size range and, in many cases, there is insufficient documentation to determine test procedures followed and to adequately define the process operation during the tests. A thorough compilation and review of existing data, currently underway, will be completed in June 1981. This will augment the current field test program which is directed toward those sources with the combination of high priority and low existing data quality. To date, processes tested are basic oxygen furnace (BOF) charging and tapping, hot metal desulfurization, blast furnace cast house (building evacuation approach), and BOF main stack (limited combustion system after scrubber). Open sources tested are paved and unpaved roads and coal storage pile wind erosion and maintenance, all both with and without controls, and an uncontrolled open area. Discussions are now underway with several plants to test other high priority sources. If funds allow, duplicate tests will be undertaken at another plant of at least the highest priority sources.

## INTRODUCTION

The U.S. Environmental Protection Agency is required, under the amended Clean Air Act of 1977, to review the scientific basis for the total suspended particulate ambient air quality standard. Major consideration is being given to a size-specific particulate standard focusing on inhalable particulate (IP) matter, defined as airborne particles of $\leq 15$ μm aerodynamic equivalent diameter.[1] EPA has initiated an extensive program to compile and review existing data and, where necessary, conduct field sampling programs from which reliable emission factors for IP can then be determined.

EPA's Office of Research and Development is responsible for developing these IP emission factors. A major part of this effort is directed toward the steel industry. This paper discusses briefly the review of existing iron and steel source particle size data and the field sampling program being undertaken. The rationale and approach being followed to select test sites are discussed and results obtained to date are summarized. Conceptual plans for the remainder of the program are presented.

## DISCUSSION

### Source Selection

At the outset of the iron and steel sampling program, the decision was made to proceed with field test site selection voluntarily, rather than through the application of Clean Air Act, Art. 114. Industry contact was initiated through the American Iron and Steel Institute (AISI) who established an ad hoc coordinating committee. Meetings with this committee were held to present an overview of the whole program and, following resolution of outstanding issues, to review sources selected for testing.

The EPA/AISI cooperative effort has thus far resulted in the mounting of an extensive field sampling program at Armco, Inc.'s Middletown Works. Discussions will soon be initiated with several other companies; several field test programs should be getting underway soon. The source selection priority list, shown in Table 1, was developed based on estimated controlled particulate emissions from each source on a nationwide basis. This prioritization represents an average of emission factors developed under separate efforts: one represented factors from specific short term emission tests [2]; the other, presented values which might be termed typical for long term operation [3]. It is only fair to say that, at best, this procedure is only qualitative, but does nevertheless provide a rational approach to source selection.

### Review of Existing Data

The source selection priority list is based on total particulate data due to the paucity of particle size data. Only six data sets are currently contained in EPA's Fine Particle Emissions Information System (FPEIS)[4]. These data sets, consisting of three open hearth furnace stack tests, two electric arc furnace tests, and coke oven pushing shed tests, are summarized in Figures 1-3, respectively. These data are judged to be good, although

consideration must be given to when they were obtained (1974-77) and the advancements made in particle size sampling technology since then. These three sources should be tested again but not before other equally high priority sources with no existing data are tested.

A thorough review of both published and unpublished literature is currently underway in a concerted effort to ferret out all existing particle size data. A first cut at the review has produced 30 unpublished test reports containing particle size data. It is felt that there may be a significant amount of additional data still to be located. It is apparent that some of these data are of sufficient quality to warrant delaying new tests until other sources with little or no data are tested. None of these old data were obtained using the current measurement technology embodying a straight nozzle into a 15 μm cyclone precutter. Thus, if funding permits, all significant sources will be tested under this program.

In addition to the selection procedure coordinated with AISI, every effort has been made to combine measurement of IP with other EPA sampling programs. Not only does this serve to reduce EPA expenditures, it also reduces inconvenience to the host companies. During the initial stages of the program these "piggy back" projects constituted the greatest area of activity due primarily to the fact that initial groundwork had already been laid by the Agency, making it possible to mount the field effort relatively quickly.

## Results To Date

### Kaiser Steel Corporation

The first two sources tested under the iron and steel IP program were the hot metal desulfurization (HMDS) and BOF charging and tapping emission control systems recently installed at Kaiser Steel Corporation's Fontana, CA, plant. These tests, performed in coordination with EPA's Office of Enforcement through the Region V office, consisted of total particulate by EPA Method 5 and particle size before and after the control device which was, in both cases, a baghouse. EPA's contractor was Acurex Corporation.

Particle size before control was measured with the EPA two-cyclone IP train developed for EPA by Southern Research Institute. Due to the low particulate concentration, baghouse outlet particle size in both cases was measured with an Andersen Mark III impactor fitted with the 15 μm cut point cyclone precutter.

Results of the HMDS tests were reported in detail at an earlier EPA-sponsored symposium[7]. In summary, the data showed an average uncontrolled total particulate emission factor of 1.01 kg/Mg of hot metal desulfurized (range: 0.23 to 1.82 kg/Mg) with an average IP fraction of 25 percent. Nonsimultaneous measurements of the baghouse discharge showed an average controlled total particulate emission factor of 0.0045 kg/Mg of hot metal desulfurized (range: 0.0025 to 0.0055 kg/Mg) with an average IP fraction of 62 percent. Thus the baghouse collection efficiency averaged 99.6 percent for total particulate and 98.9 percent for the IP fraction.

BOF fugitive emissions from hot metal charging and tapping of finished steel were measured separately. Charging measurements did not include the addition of scrap. Results of the tests will be reported later in this session[8].

Armco, Inc., Middletown

The extensive testing program undertaken for EPA by Midwest Research Institute at Armco, Inc.'s Middletown Plant encompassed both open dust sources and ducted process sources; emphasis was on the former. Specifically, emissions from paved and unpaved roads were measured before and after the initiation of emission reduction procedures. For paved roads, the emission reduction consisted of flushing with water and/or sweeping -- vacuuming at regular intervals. Berms of paved roads were treated with Coherex®. The unpaved roads were treated either with Coherex® or water to suppress emissions. Tests of the Coherex® treated road were conducted on the second and third days after application of the suppressant. Additional tests would be required to determine the long term control efficiency decay. Preliminary results of the paved and unpaved road tests are currently under review; final results should be available in May.

In addition to the road tests, measurements were made of windblown emissions from the coal pile and emissions arising as a result of coal pile maintenance activities. These data, still being analyzed, should also be available in May.

All of these open source measurements were made using the MRI source exposure profile technique. Road surface silt and moisture content were sampled to allow correlation with the measured emission rates. Numerous samples were taken from other inplant roads to develop an idea of the representativeness of the sampled road segments and also to allow a more realistic extrapolation of the test data to the whole plant.

Ducted process emissions measured at Middletown were from the BOF main stack[9]. Although the IP protocol calls for measurements before and after the control device, the nature of the limited combustion BOF operation at Middletown precluded measurements before the scrubber. Measurements after the scrubber included total particulate and particle size as per the protocol. Results are shown in Table 2. The results are presented for two production rates, normal and intermediate. The ratios of IP to total particulate are 69 percent and 57 percent, respectively, for the controlled emission.

Dominion Foundries and Steel Company (DOFASCO)

DOFASCO first installed cast house emissions controls several years ago. Their No. 1 blast furnace cast house control system, installed in 1975, was tested by EPA[10] in 1976. This system employs the total building evacuation concept. Although particle size measurement of uncontrolled emissions was attempted, the data were not reliable due to particle bounce (no precutter was used). Using present techniques, which employ the 15 μm cyclone precutter ahead of the cascade impactor, has solved this problem for

the ongoing IP program. The combined control system for cast houses No. 2 and 3 was started up in November 1978. These cast houses are evacuated by a common fan and baghouse sized to control emissions in either one by isolation valves. Cast house No. 4 is currently being used to evaluate concepts for local emission control.

The IP emission tests were run during the week of November 10, 1980, on the combined control system serving cast houses No. 2 and 3; however, measurements were made only when furnace No. 3 was casting. Emission tests followed the protocol for ducted sources. Measurements were made for EPA by GCA/Technology Division in the duct upstream of the baghouse; the open monitor discharge on the baghouse was not tested due to the perceived difficulty in obtaining meaningful results. A detailed discussion of the results is the subject of the next paper[11].

Bethlehem Steel Corporation, Sparrows Point

GCA/Technology Division is planning to conduct emission tests for EPA at the new "L" furnace cast house at Sparrows Point this month. This is a large modern furnace employing close-fitting hoods and covers over the trough, iron runners, and spouts, a practice pioneered in Japan. Emissions are ducted to a large baghouse. Emissions, following the ducted source protocol, will be measured in the duct upstream of the baghouse. Since this baghouse also controls emissions from numerous other fugitive sources, no attempt will be made to sample the open monitor discharge. Installation of scaffolding and ports was completed in February, several months later than planned, causing the delay in testing from the original November date. Results will be available in draft form within 3 months following completion of field tests.

Future Tests

EPA is continually reviewing the overall status of the field testing program in light of the source priority list and tests already completed or firmly planned[12]. Future tests will continue to address the highest priority sources first. Testing of high priority sources suspected of containing a significant fraction of condensible emissions (e.g., sinter plant windboxes, electric arc furnaces, and coke ovens) will be initiated in a few months when the condensible emission sampling equipment becomes available. In the meantime, noncondensible sources (e.g., Q/BOP and full combustion BOF main stack, material stock piles, and coke pushing) will continue to be tested as rapidly as possible.

Once the field tests are completed, all data, new and old, will be pulled together in one source category document giving emission factors versus particle size for all major sources in the iron and steel industry. In additon to the source test data, emission factors will be summarized in formats appropriate for AP-42[13]. The current schedule calls for testing to be completed in September 1981 and the source category report published in January 1982.

TABLE 1. IRON AND STEEL SOURCE PRIORITY RANKING FOR IP STUDY, CONTROLLED EMISSIONS

| Rank | Process | Industry total particulate emissions, Mg/yr |
|---|---|---|
| 1 | Coke quenching | 34,500 |
| 2 | Blast furnace cast house | 22,700 |
| 3 | BOF stack | 20,000 |
| 4 | Material stockpiles | 16,300 |
| 5 | Roadway travel | 16,300 |
| 6 | Coke combustion stack | 16,300 |
| 7 | BOF charge and tap | 14,500 |
| 8 | Coke pushing | 8,900 |
| 9 | Sinter, misc. fugitives | 8,700 |
| 10 | Sinter windbox | 8,200 |
| 11 | EAF charge, tap, slag | 7,600 |
| 12 | Coal preparation | 7,400 |
| 13 | OH stack | 7,300 |
| 14 | Coke door leaks | 7,100 |
| 15 | EAF stack | 6,600 |
| 16 | Sinter discharge end | 5,700 |
| 17 | Blast furnace top | 3,700 |
| 18 | Teeming | 3,700 |
| 19 | Ore Screening | 3,300 |
| 20 | BOF misc. fugitives | 2,200 |
| 21 | Coke topside leaks | 2,100 |

(Continued)

TABLE 1. IRON AND STEEL SOURCE PRIORITY RANKING FOR IP STUDY, CONTROLLED EMISSIONS (Continued)

| Rank | Process | Industry total particulate emissions, Mg/yr |
|---|---|---|
| 22 | Reheat furnaces | 2,000 |
| 23 | Blast furnace combustion | 2,000 |
| 24 | OH roof monitor | 2,000 |
| 25 | Coal charging | 1,800 |
| 26 | Open area | 1,100 |
| 27 | Machine scarfing | 670 |
| 28 | BOF HMT | 650 |
| 29 | OH misc. fugitives | 640 |
| 30 | Soaking pits | 570 |
| 31 | EAF misc. fugitives | 540 |
| 32 | OH - HMT | 190 |

TABLE 2. SUMMARY OF LIMITED COMBUSTION BOF MAIN STACK PARTICULATE EMISSION FACTORS[9]

| Date | Run Nos. | Cumulative emission factor, kg/Mg (lb/ton) steel[a] | | | | Low carbon steel produced, Mg (tons) |
|---|---|---|---|---|---|---|
| | | <2.5 μm | <10 μm | <15 μm | Total | |
| 7/11/80 through 7/14/80 | PSD-1[b] - PSD-6 | 0.010 (0.020) | 0.010 (0.021) | 0.011 (0.022) | 0.016 (0.031) | 196 (216) |
| 7/14/80 | PSD-7[c] and PSD-8 | 0.007 (0.013) | 0.007 (0.014) | 0.008 (0.015) | 0.014 (0.027) | 152 (168) |

[a] Steel produced.

[b] Results are the average of the first three heats and are considered to represent emissions during normal production rates.

[c] Results are for the last heat tested and represent emissions for intermediate production rates.

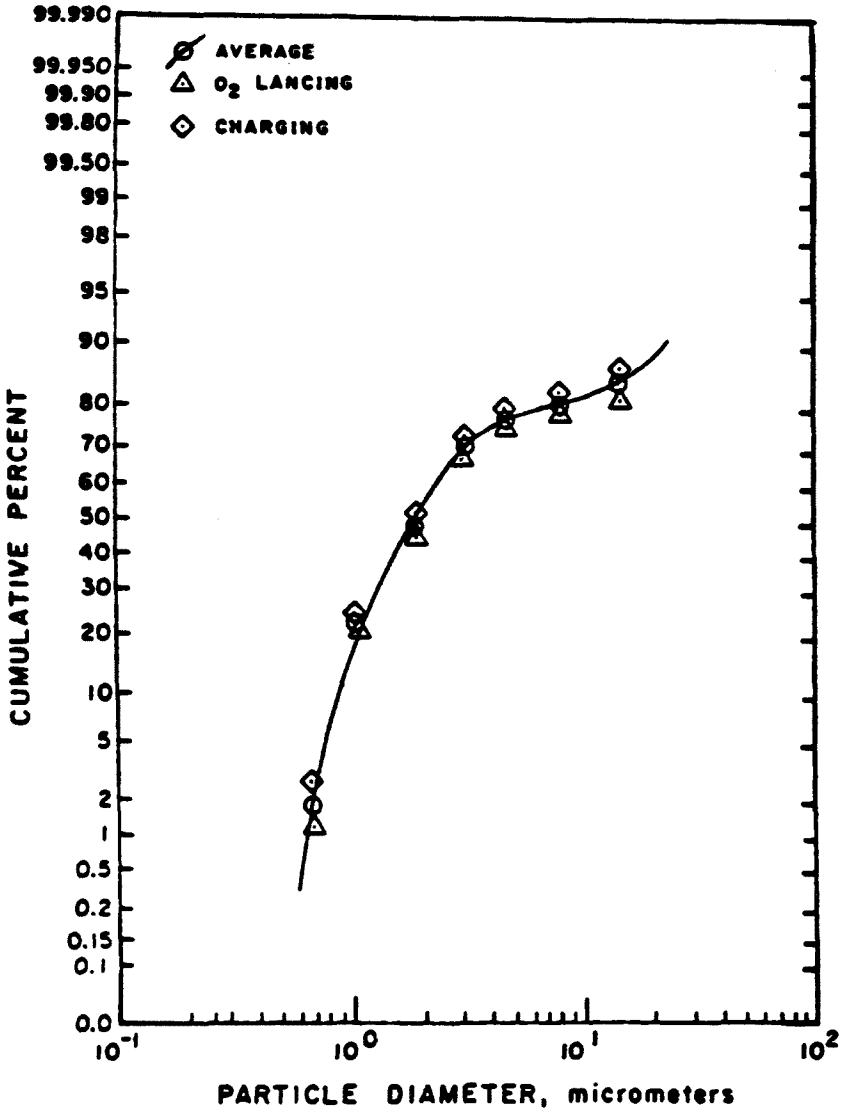


Figure 1.[5] Average size distribution - open hearth furnace emissions, uncontrolled.

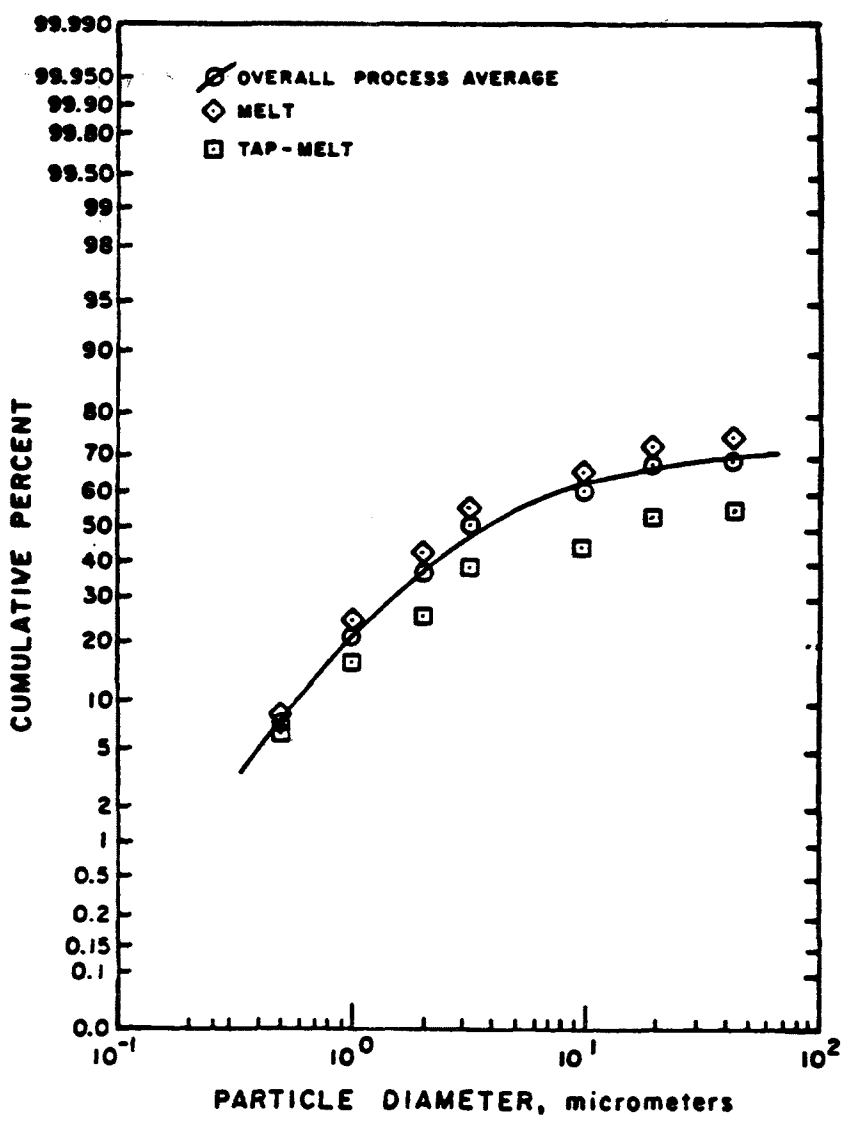


Figure 2.[5] Average size distribution - Marathon LeTourneau Electric arc facility.

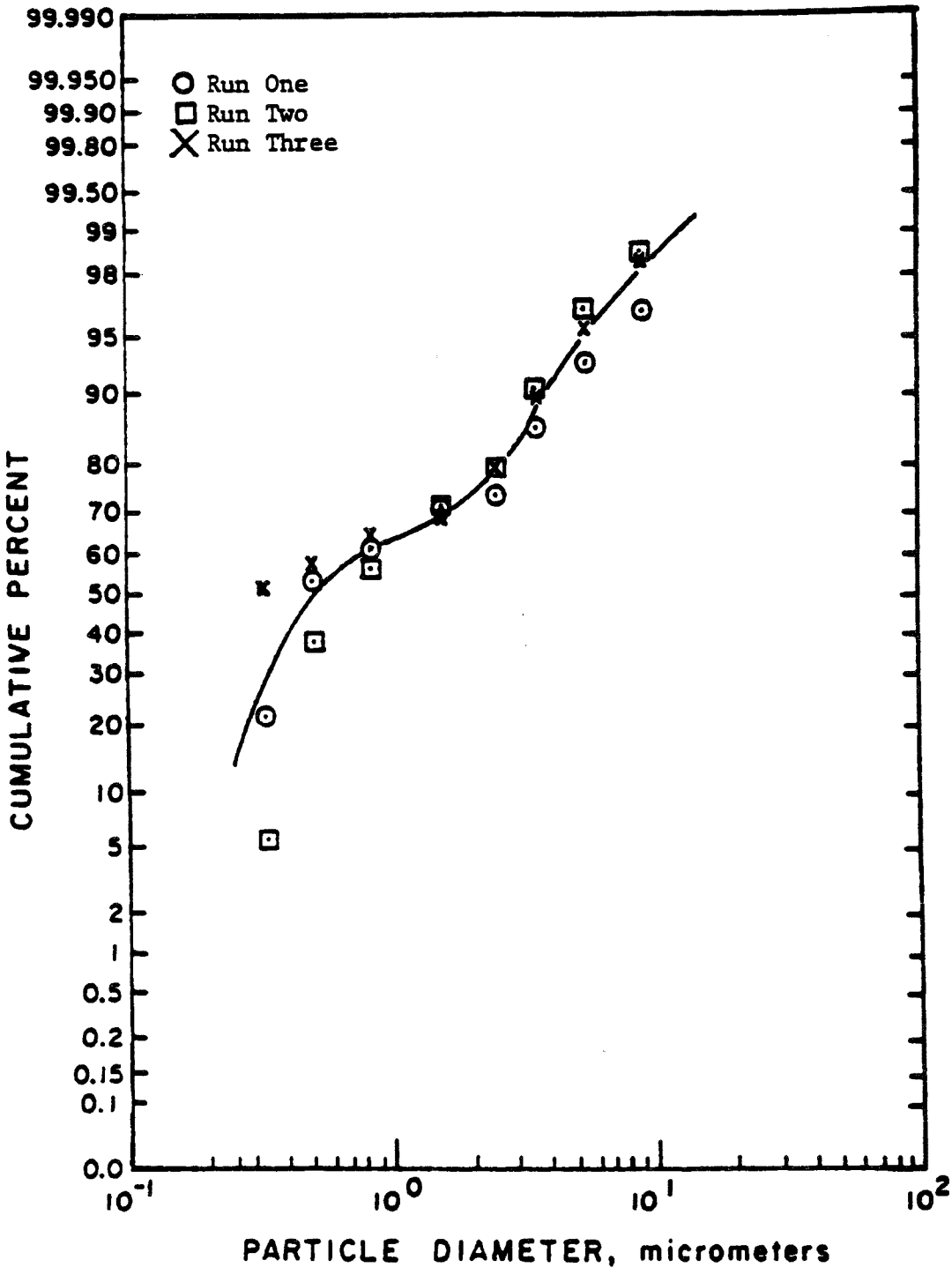


Figure 3.[6] Average particle size distribution--coke oven pushing.

ENDNOTES

References


1. Miller, F.J. et al. "Size Consideration for Establishing a Standard for Inhalable Particles," J. Air Pollu. Contr. Assoc., 29(6): 610 (1979).

2. Cuscino, T. A., Particulate Emission Factors Applicable to the Iron and Steel Industry, EPA-450/4-79-028, Midwest Research Institute, August 1979.

3. Barber, W.C., Particulate Emissions from Iron and Steel Mills, EPA/OAQPS Internal Memorandum, dated November 6, 1978.

4. Reider, J. P., and R. F. Hegarty, Fine Particle Emissions Information System: Annual Report (1979), EPA-600/7-80-092 (NTIS PB 80-195753), Midwest Research Institute, May 1980.

5. Fitzgerald, J., D. Montanaro, and E. Reicker, Development of Size-Specific Emission Factor (Draft), EPA Contract 68-02-3157 TD 3, GCA/-Technology Division, October 1980.

6. Gronberg, S., Test Program Summary for Characterization of Inhalable Particulate Matter Emissions (Draft), EPA Contract 68-02-3157 TD 5, GCA/Technology Division, September 1980.

7. Steiner, J., and D. Bodnaruk, "Particulate and $SO_2$ Emission Factors for Hot Metal Desulfurization," Symposium on Iron and Steel Pollution Abatement Technology for 1980 (November 1980, Philadelpia, PA).

8. Steiner, J., "Inhalable Particulate Emission Factors for BOF Furnaces in the Iron and Steel Industry," Third Symposium on the Transfer and Utilization of Particulate Control Technology (March 1981, Orlando, FL).

9. Inhalable Particulate Emission Characterization Report: Armco Steel's No. 16 Basic Oxygen Furnace, Middletown, OH (Draft), Prepared by PEDCo Environmental, Inc. under subcontract, EPA contract 68-02-3158 TD 6, Midwest Research Institute.

10. May, W. P., Blast Furnace Cast House Emission Control Technology Assessment, EPA-600/2-77-231 (NTIS PB 276999), Betz Environmental Engineers, November 1977.

11. "Inhalable Particulate Emission Factors for Blast Furnace Casthouses in the Iron and Steel Industry," Third Symposium on the Transfer and Utilization of Particulate Control Technology (March 1981, Orlando, FL).

12. Preparation of Overall Iron and Steel Industry Inhalable Particulate Test Plan (Draft), EPA Contract 68-02-2687 TD 13, GCA/Technology Division, December 1980.

13. Compilation of Air Pollutant Emissions Factors: Third Edition, No. AP-42 (NTIS PB 275525), US Environmental Protection Agency, August 1977.

## ACKNOWLEDGEMENTS

The three sampling contractors for EPA's IP program are GCA/Technology Division, Midwest Research Institute, and Acurex Corporation. The AISI and its member companies (in particular Armco, Inc., Bethlehem Steel Corporation, Dominion Foundries and Steel, Ltd., and Kaiser Steel Corporation) have been most helpful.

# DEVELOPMENT OF IP EMISSION FACTORS

BY: D. L. Harmon
Industrial Environmental Research Laboratory
U. S. Environmental Protection Agency
Research Triangle Park, N. C. 27711

## ABSTRACT

In response to the Clean Air Act Amendments of 1977, EPA is considering an inhalable particulate (IP) ambient air standard. It will be necessary to have emission factors for IPs to provide for implementation of the standard. Steps have been taken to develop IP sampling techniques, extrapolate existing data on particulate characteristics to the IP size range, and select sampling strategies for major sources based on national and regional impacts within budgetary constraints. Three year contracts were awarded to three contractors in September 1979 to conduct plant surveys and characterize sources for IPs. A priority list of major sources has been developed and testing is underway to provide data for IP emission factors for the priority sources.

## INTRODUCTION

EPA is considering an inhalable particulate (IP) ambient air standard. Particulate emission factors, as compiled in AP-42 (1) ("Compilation of Air Pollutant Emission Factors"), estimate the emission of total suspended particulates from uncontrolled sources. It will be necessary to have similar emission factors for IP to provide for implementation of an IP standard. Early in 1978, a task force on Particulate Emission Characterization was formed to develop a program for determining emission factors based on cut-off size for IPs from both controlled and uncontrolled sources.

In September 1978, a draft plan (2) was completed by EPA's Office of Research and Development (ORD) for a program to obtain the IP data as specified by a priority listing developed by EPA's Office of Air Quality Planning and Standards (OAQPS). Since the amount of money required for this program was obviously not available, both ORD and OAQPS decided that a second draft was needed which would present potential strategies for partial characterization of the priority list based on the amount of resources available. The second draft (3) was produced and is the basis for the ongoing IP emission factor development program.

During the time the IP emission factor program was being developed, it became apparent that the measurements problem for obtaining IP source data was much more difficult than originally believed. It was determined that a sizeable effort would have to be devoted to this area before any field measurements were actually undertaken. To this end a meeting was sponsored by EPA's Industrial Environmental Research Laboratory and Environmental Sciences Research Laboratory, both of Research Triangle

Park (IERL-RTP and ESRL), bringing together many of the nation's measurements experts to develop a program to provide the necessary measurement and sampling techniques and expertise.

Three steps were deemed necessary to achieve the objectives of the program proposed to develop IP emission factors:

1. Develop sampling techniques to allow assessment of the particulate characteristics based on the inhalable potential.

2. Extrapolate existing data on particulate characteristics to the inhalable size range where possible.

3. Select sampling strategies for major sources based on national and regional impacts within budgetary constraints.

## DISCUSSION

The IP Emissions Factor Task Force Executive Committee has been meeting about once a month since February 1979 to direct the work for development of IP emission factors. The committee has members from the following EPA organizations:

Office of Air Quality Planning and Standards (OAQPS)
Industrial Environmental Research Laboratory-RTP (IERL-RTP)
Industrial Environmental Research Laboratory-Cincinnati (IERL-Cin)
Environmental Sciences Research Laboratory (ESRL)
Division of Stationary Source Enforcement (DSSE)

An early task for the committee was to establish a list of priority sources to be tested for IP emissions. Since the range of sources emitting IP emissions was large and the time and resources available were limited, it was necessary to make use of existing data to the maximum extent practical and test those sources which would provide the highest practical level of return. The priority sources identified early in the program are listed in Table I. The only change made in the priority list since it was developed has been to add Iron Foundries as a source to be tested. Also, a recommendation to remove primary non-ferrous zinc smelters from the priority list is being considered. At the time the original priority list was developed and funding levels were established, funds were included for lower priority sources to be added when identified. Delays in testing and increased testing costs have eliminated any testing beyond that now planned unless additional funds are made available for this program.

At the beginning of the IP emission factor program, IP's were defined as those having aerodynamic diameters less than 15 $\mu$m. In addition to the IP size cut it was also desired to collect data for a

possible future secondary fine particulate standard. Fine particles were defined tentatively as less than 2.5 μm in diameter.

A large data bank of particle size data on various industrial sources is in existence. The most useful data was taken with impactors which have an upper stage cut-off of 10 μm or less. For this data to be used to develop IP emission factors it was necessary to extrapolate from existing data to 15 μm. An extrapolation procedure has been developed and data from the Fine Particle Emissions Information System (FPEIS), a data bank developed for EPA containing much of the existing particle size data, is now being extrapolated to 15 μm. This data should be adequate to provide IP emission factors for some industrial sources without additional testing.

The measurement experts assembled to recommend IP test methods decided that a 2-stage cyclone set would be the best device to use for point source sampling. Such a system was developed for EPA by Southern Research Institute to provide 15 μm and 2.5 μm size cuts. Before fabrication of these cyclone sets was complete, however, questions began to arise as to selection of a 15 μm upper limit for IPs. In the spring of 1980 it was determined that the definition of IP might be revised to some cut point less than 15 μm so that the cyclones could no longer be used. At this time, the approved point source sampling method became an impactor with a 15 μm cyclone precutter. Data is reported as a continuous plot of emission factor vs particle size from 15 μm down. When the IP cut point is finalized the appropriate emission factor can be read from the graph. An example curve is shown in Figure 1.

It is necessary to obtain IP fugitive emission data on industrial sources as well as point source data. Four test methods have been approved for sampling IP fugitive emissions depending on the characteristics of the site to be sampled:

Quasi-Stack Sampling
Roof Monitor Sampling
Upwind/Downwind Sampling
Exposure Profiling

Where cooling and dilution of ducted gas streams result in the formation of condensed particles, it is necessary to measure these condensibles. One of the early tasks in the IP program was to develop a condensibles sampler. A prototype device has been designed, fabricated, and laboratory tested by Southern Research Institute for EPA. This device is currently being field tested and should be available for testing by early spring.

Draft copies of protocols for these test methods have been developed for those doing the IP testing. (4)(5)(6)(7)

In the spring of 1979 a competitive procurement was issued for three IP characterization contractors to conduct plant surveys and source assessments for IPs and to support OAQPS in the development and implementation of an IP standard. The continental U.S. was divided into three separate geographical areas for contract award purposes:

| Area A | Area B | Area C |
|---|---|---|
| EPA Regions 1, 2, 3, and 4 | EPA Regions 5, 6, and 7 | EPA Regions 8, 9, and 10 |

Separate proposals were required for each area an offeror wished to be considered for. The level of effort for each area was estimated to be 43,500 direct technical labor hours with a period of performance of 36 months.

Contracts were awarded in September 1979 to three contractors, each with a major subcontractor:

| | Area A | Area B | Area C |
|---|---|---|---|
| Contractor | GCA Corp. | Midwest Res. Inst. | Acurex Corp. |
| Subcontractor | TRC Env., Inc. | PEDCo Env., Inc. | TRC Env., Inc. |

The scope of work for these contracts required the contractor to conduct on-site plant inspections or surveys for the purpose of defining and evaluating the particulate pollution problems and for determination of the fugitive sources. After approval of a test plan the contractor was to make all necessary studies as directed. Testing would vary from site to site but could include:

(1) Ducted Particulate Matter - When required, grainloading measurements by mass and particle size and particulate samples for chemical analysis would be obtained with the approved sampling train. Whenever particulate control equipment was present, measurements would usually be taken simultaneously up- and downstream of the control device. Generally, four independent measurements at each sampling location would be required for particle size measurements.

(2) Fugitive Emissions - Particulate emissions from both fugitive process sources and fugitive dust sources would be determined using the measurement methods approved by EPA. In the case of fugitive emissions, sampling would include a full cycle of the process during representative operation. In the case of fugitive dust emission, measurements would be made under varying wind, moisture, and/or traffic conditions.

(3) Condensible Particulate Matter - Where cooling and dilution of ducted gas streams resulted in formation of condensed particles, mass measurements of such material may be required in addition to conventional mass and particle size measurements of primary particulate.

(4) Hazardous Particulate Matter - Where significant emissions of hazardous materials were part of the IP, it may be required to include determination of the composition of the particles. This determination would be for inorganic materials such as lead, arsenic, beryllium, and mercury.

When the IP characterization contracts were initiated, it was planned to use EPA personnel from IERL-RTP and IERL-Cin who were familiar with the industries to be tested to make test site selections. This did not work out in most cases because many of the EPA personnel did not have adequate time to devote to test site selection. It was necessary to direct the IP characterization contractors to develop priority lists of various industries and recommend specific sites for testing. Early in the program, it was decided to try to work on a cooperative basis with industrial organizations to gain access to test sites rather than use Clean Air Act Section 114 letters to gain access. Most of the industrial organizations contacted have been willing to work on this project on a cooperative basis but working out such agreements has been time consuming.

It was originally planned that much of the testing would be done early in the contract period but this has not been possible. In addition to the delays in test site selection and gaining access to test sites, significant delays have resulted from the need to develop IP sampling equipment including a condensibles sampler and size selective inlets and elutriators for use in the fugitive measurements program.

Table II shows the current target dates for completing the high priority source tests and the source category reports giving IP emission factors. This testing is scheduled to be completed in 1981. If additional funds are made available in FY-82 then testing will be extended to include other sources.

As each source test is completed an individual test report is written. When all testing is completed for a given source category, such as Iron and Steel, then one of the three IP characterization contractors will be given the task of preparing a final report providing emission factors for that source category. This contractor will combine test results from all contractors, extrapolate valid pre-existing data, develop source category IP emission factors, and prepare a report which will be used for AP-42 input.

Budgetary constraints limit the number of source categories and number of sources within a category to be tested. Where possible, tests for IP emissions are combined with other EPA field tests to stretch the limited funds. Table III lists the IP tests which have been completed to date. Table IV lists the tests which are in process or scheduled. Several of these tests were "piggybacked" onto other EPA sponsored tests.

Most of the Paved Road tests for IP emissions have been completed. Testing on unpaved roads will begin this spring. Midwest Research Institute has developed predictive emission factor equations for traffic-entrained dust from paved and unpaved roads based on field tests of a variety of uncontrolled roads. Sufficient data will be collected from a small number of field tests of industrial paved and unpaved roads to verify or revise the emission factor equations. During most field tests samples of silt from road surfaces will be taken and other data will be collected so the emission factor equations can be used to develop industrial road emission factors for various industries.

Tests at three different steel mills have been completed on different sources and tests at a fourth plant are scheduled. An overall test plan for the remainder of the Iron and Steel Industry tests has been submitted to EPA by one of the characterization contractors. Tests at a lime plant with one kiln controlled by a fabric filter and one kiln controlled by an ESP have been completed. Tests at a wet cement plant are scheduled. One secondary lead plant has been tested and site surveys to select remaining secondary lead plants for testing are scheduled. One primary copper plant has been tested and site surveys are scheduled to select sites for other primary nonferrous smelter tests. Tests of two ferroalloy plants are scheduled. Test sites for the Pulp and Paper testing have been selected and testing will start as soon as the condensibles sampling system is ready.

The categories not included in Tables III and IV which list completed or scheduled tests are Iron Foundries, Asphaltic Concrete, Combustion, and Incineration. Technical Directives have been issued to IP characterization contractors to prepare overall test plans for Iron Foundries and Asphaltic Concrete. A report giving IP emission factors for combustion sources based on existing data extrapolated to 15 μm is due in March. Any field tests required to fill gaps in the existing data base for combustion sources will be scheduled after this report is received. A Technical Directive will be issued to one of the IP contractors in March to prepare an overall test plan for Incineration. With this directive, work will be initiated for all sources included on the priority list.

## REFERENCES


1. Compilation of Air Pollutant Emission Factors, Third Edition and Supplements, AP-42, U. S. Environmental Protection Agency, Research Triangle Park, N. C. August 1977.

2. Kashdan, E., Emission Factors for Inhalable Particulate Matter: Draft Proposal Plan, U. S. Environmental Protection Agency, Research Triangle Park, N. C., 1978.

3. Abbott, J. H., D. C. Drehmel, E. Kashdan, and M. D. Ranade Emission Factors for Inhalable Particulate Matter: Draft Proposal Plan, U. S. Environmental Protection Agency, Research Triangle Park, N. C., 1979.

4. Harris, D. B., Procedures for Cascade Impactor Calibration and Operation in Process Streams-Revised 1979, 2nd Draft, U.S. Environmental Protection Agency, Research Triangle Park, N. C., 1979.

5. Protocol for the Measurement of Inhalable Particulate Fugitive Emissions from Stationary Industrial Sources, Draft, U. S. Environmental Protection Agency, Research Triangle Park, N. C., March 1980.

6. Wilson, R. R., W. B. Smith, Procedures Manual for Inhalable Particulate Sampler Operation, Draft, U. S. Environmental Protection Agency, Research Triangle Park, N. C., November 1979.

7. Williamson, A. D., Procedures Manual for Operation of the Dilution Stack Sampling System, Draft, U. S. Environmental Protection Agency, Research Triangle Park, N. C. October 1980.

TABLE I. IP EMISSION FACTOR PRIORITY SOURCES

1. Paved and Unpaved Roads
2. Iron and Steel
3. Secondary Lead Smelters
4. Portland Cement
5. Lime Manufacture
6. Asphaltic Concrete
7. Ferroalloy
8. Primary Nonferrous
   a. Copper
   b. Lead
   c. Zinc
   d. Aluminum
9. Kraft Pulp Mills
10. Combustion (Coal/Oil)
    a. Utility
    b. Industrial
    c. Commercial/Residential
11. Incineration

TABLE II. IP EMISSION FACTOR PROGRAM TESTING SCHEDULE

| | Industry | Complete Testing | Complete Source Category Report |
|---|---|---|---|
| 1. | Paved and Unpaved Roads | 8/81 | 9/81 |
| 2. | Industrial Roads | 5/81 | 7/81 |
| 3. | Iron and Steel | 9/81 | 1/82 |
| 4. | Iron Foundries | 11/81 | 3/82 |
| 5. | Secondary Lead Smelters | 9/81 | 12/81 |
| 6. | Portland Cement | 5/81 | 7/81 |
| 7. | Lime Manufacture | 5/81 | 7/81 |
| 8. | Asphaltic Concrete | 8/81 | 12/81 |
| 9. | Ferroalloy | 6/81 | 10/81 |
| 10. | Primary Nonferrous | 9/81 | 12/81 |
| | a. Copper | | |
| | b. Lead | | |
| | c. Aluminum | | |
| 11. | Kraft Pulp Mills | 8/81 | 12/81 |
| 12. | Combustion (Coal/Oil) | 12/81 | 4/82 |
| | a. Utility | | |
| | b. Industrial | | |
| | c. Commercial/Residential | | |
| 13. | Incineration | 12/81 | 4/82 |

TABLE III. COMPLETED IP EMISSION TESTS

| Source Category | Sources Tested |
|---|---|
| Paved and Unpaved Roads | Paved Roads |
| Iron and Steel | BOF<br>Hot Metal Desulfurization<br>Paved Roads<br>Coal Storage Pile<br>Cast House |
| Cement and Lime | Lime Plant<br>Kiln-ESP<br>Kiln-Fabric Filter<br>Material Transfer<br>Product Loading |
| Primary and Secondary Nonferrous | Secondary Lead-various ducted and fugitive sources<br>Primary Copper-matte tap, slag tap, and idle ladle |

TABLE IV. IP EMISSION TESTS IN PROCESS OR SCHEDULED

| Source Category | Sources Being Tested |
|---|---|
| Cement and Lime | Wet Cement Plant<br>Kiln-ESP<br>Product Grinder<br>Raw Material Transfer<br>Clinker Transfer<br>Product Loading<br>Mill Building |
| Ferroalloy | Silicon Metal Furnace<br>FeMn Furnace |
| Iron and Steel | Cast House |
| Pulp and Paper | DCE Furnace<br>Non-DCE Furnace<br>Smelt Dissolve<br>Lime Kiln |

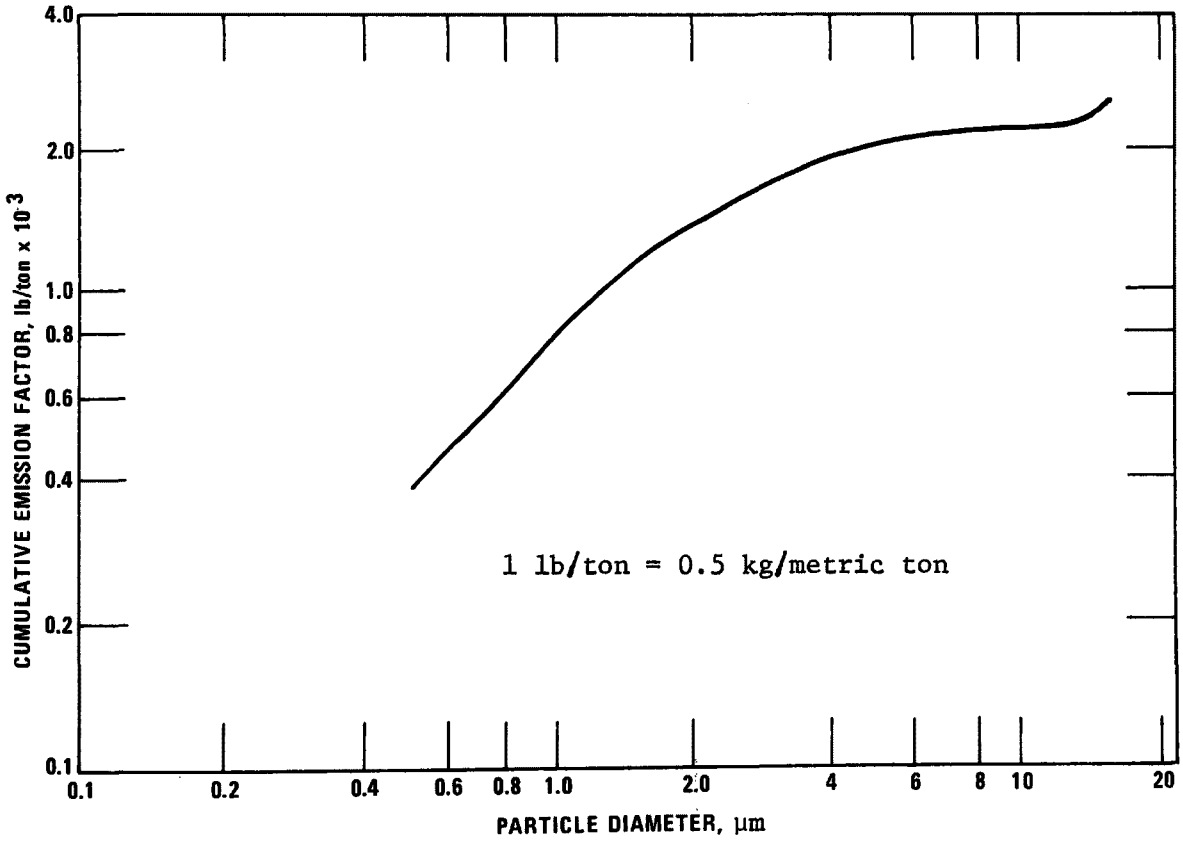


Figure 1. Emission factor for controlled emissions from hot metal desulfurization plant based on one test.

# INHALABLE PARTICULATE EMISSION FACTOR PROGRAM PURPOSE AND DEVELOPMENT

By: Frank M. Noonan and James H. Southerland
U.S. Environmental Protection Agency
Office of Air Quality Planning and Standards
Monitoring and Data Analysis Division
Air Management Technology Branch (MD-14)
Research Triangle Park, NC 27711

## ABSTRACT

The Environmental Protection Agency is in the process of reviewing the technical criteria and data bases to determine whether the establishment of a particle size based National Ambient Air Quality Standard (NAAQS) for particulate matter is warranted. Upon adoption of such a size specific particulate standard, the Clean Air Act requires the States to develop and submit revisions to their State Implementation Plans to define how they will carry out a program to attain and maintain such a standard. Such revisions would necessitate the collection and use of information related to size selective particulate emissions from existing and future sources. Thus a need exists to initiate development of an emission factor data base to allow meeting such objectives.

A review of the basis and objectives of EPA's Inhalable Particulate (IP) program currently underway to obtain emission factors is presented. Due to the limitations of resources and the large number of sources to be characterized, a prioritization of source categories had to be developed for the emissions testing program. The criteria for selection of and prioritization of source categories for particle size characterization are presented.

## INTRODUCTION

The basis of the IP emission factor program is to provide data to support and meet the legal requirements of the Clean Air Act as amended in 1977.[1] The 1977 Amendments require the Administrator to complete reviews of all existing National Ambient Air Quality Standards (NAAQS) and the air quality criteria upon which they are based before the end of 1980 and at five year intervals thereafter, and to revise NAAQS as appropriate. The air quality criteria documents contain the latest scientific knowledge useful in indicating the kind and extent of all identifiable effects on public health or welfare. The law provides that the primary NAAQS must be based on health effects criteria and provide a reasonable margin of safety to ensure protection of the public health. Secondary NAAQS define levels of air quality which the Administrator judges necessary to protect the public welfare from any known or anticipated adverse effects of a pollutant.

In late 1977, EPA's Office of Research and Development (ORD) initiated review of the existing criteria documents. To date, ozone, carbon monoxide, hydrocarbons, lead, and nitrogen oxides have been completed, and sulfur oxides, particulate matter draft documents are in the process of review.

The major concern regarding the current particulate standard is with the human health effects associated with size specific particulate exposure. In addition to total suspended particulates the agency is examining the effects of several size fractions including IP matter, $\leq$ 15 micrometer (μm) aerodynamic equivalent diameter and fine particulate $\leq$ 2.5 μm aerodynamic equivalent diameter and fractions between these size cut points.[2] The IP fraction is based on particulate matter which can deposit in the conducting airways and gas exchange areas of the human respiratory system during mouth breathing. A fine fraction $\leq$ 2.5 μm is based upon chemical composition and the bimodal size distribution of airborne particles and the predominant penetration of particles $\leq$ 2.5 μm into the gas exchange region of the respiratory tract.[3]

Program Development

In order to provide for attainment of these standards, States are charged with the responsibility of developing and implementing emission control programs for individual sources through the mechanism of State Implementation Plans (SIP) which are subject to EPA approval. A stepwise development of the SIP process is briefly presented in Figure 1. The legal time requirement for the States to submit a plan to attain and maintain a NAAQS after promulgation by the agency is nine months. Upon receipt of the SIP, the EPA has four months to approve or reject the plan.

Should a size specific particulate standard be established, it will be necessary for States to develop and submit revisions to their SIP to demonstrate attainment and maintenance of the standard. These revisions will entail the development and utilization of emission inventories, air quality simulation models, and air quality baseline data for purposes of control strategy development. Emission inventories of the stationary source IP fraction of emissions will be needed for controlled as well as uncontrolled sources, similar to those presently inventoried for the existing particulate standard. Emission limitations and control measures must be adopted by the States to ensure attainment and maintenance of air quality standards through rules and regulations legally enforceable by the State agency. Additionally, the SIP revisions must set forth legally enforceable procedures for review of new sources and modification of existing sources based upon control requirements anticipated necessary to meet the NAAQS.

Therefore, formulation of a size specific particulate control strategy if needed begins with development of a baseline emission inventory of existing particulate emission sources (including both ducted and nonducted fugitive emissions) within a study area. Projected size specific emission inventories will also be required for five year forecast periods, taking into account source growth, more stringent controls, etc. The baseline inventory would be input information to appropriate air quality simulation models or

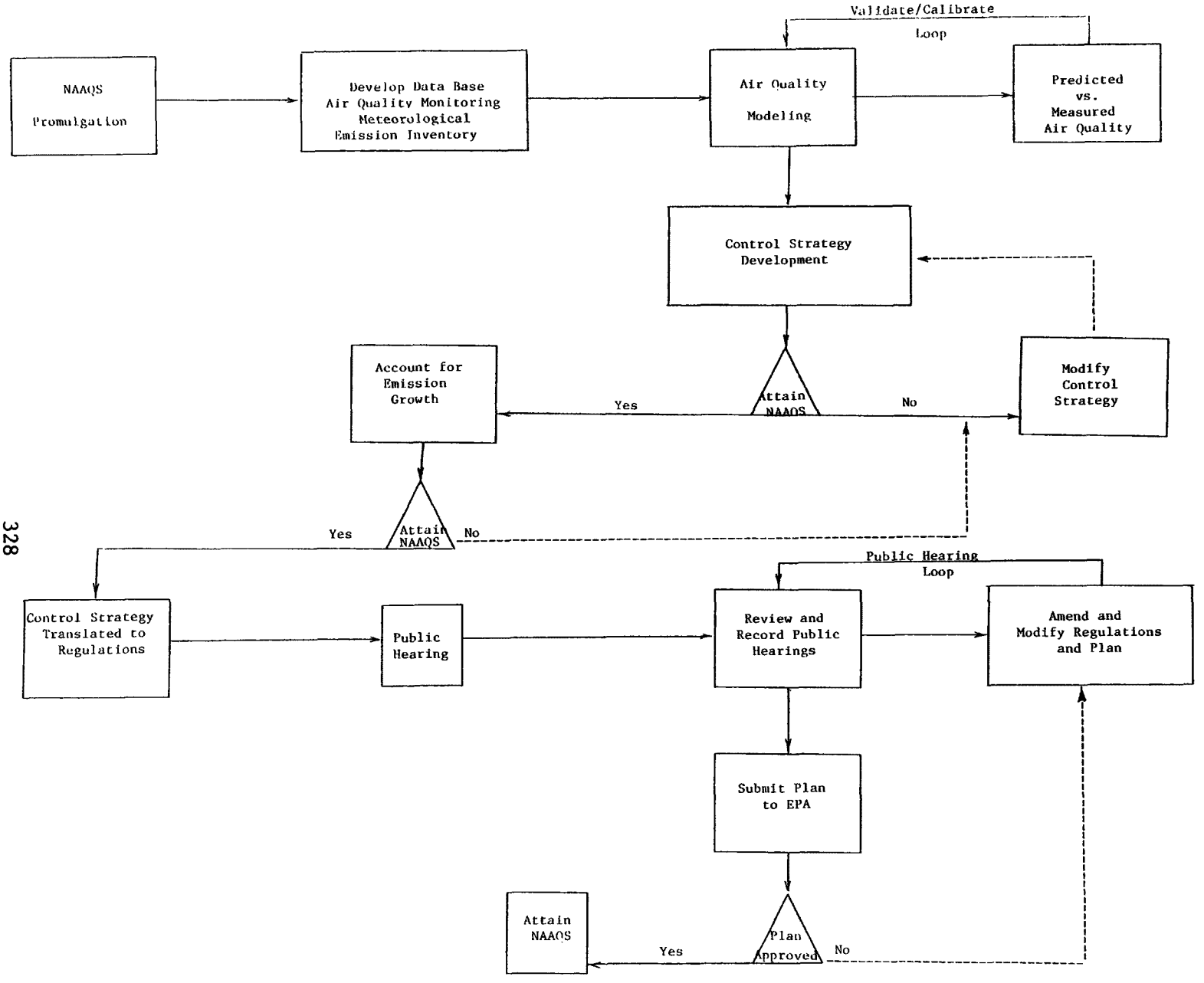


Figure 1. STATE IMPLEMENTATION PLAN DEVELOPMENT PROCESS

techniques which would be calibrated against observed ambient size specific particle concentrations. The calibrated models would then be used in conjunction with baseline air quality data and projected emissions from the sources to determine the source specific (or source category) emission reductions needed to attain and maintain the particulate standard.

It is too costly for States to conduct exhaustive source by source monitoring to determine size specific particulate emission rates. Thus emission or estimation factors to be utilized in estimating these emissions are required. EPA has historically provided a compendium of emission factors that can be used to estimate source emissions; AP-42,[4] "Compilation of Air Pollutant Emission Factors." This document provides emission data for typical, uncontrolled, existing sources. Data are presented for most major source categories, and are listed for each significant process within the source category. Individual source category sections of AP-42 are periodically updated as new information become available. The IP testing program underway is directed toward producing size specific emission factors for many major particulate source categories, which will be published in AP-42, or in a similar format for use by the States in development of SIP revisions. Resource constraints prevent this program from addressing all possible source categories at the present time. Therefore, some data gaps will remain.

Early in the IP program, a search for reliable particulate mass fraction data for uncontrolled and controlled process emissions was conducted. Computerized data bases that contain mass emission data and particle size distribution data such as the Source Test Data System (SOTDAT), Regional Air Pollution Study (RAPS), and the Fine Particle Emission Information System (FPEIS) were searched. Also, support document or New Source Performance Standards, other published data, such as Handbook of Emissions, Effluents, and Control Practices for Stationary Particulate Pollution Sources,[5] and other related EPA documents were reviewed for applicable particle size source related data. Particle size distribution data found in the existing data bases were considerable for some source categories, (e.g., coal fired power plants and some metallurgical foundries) but rather limited to non-existant for many expected significant emission sources. Some of the existing data bases were incomplete or not useful because the limited data for sources of interest lacked detailed information pertaining to sampling characteristics, particle sizes tested and reported (data was typically confined to the 0.2 to 2.0 μm range), and source operating conditions. Much of the data provided only particle size emissions information after controls. The available particle size data was generally confined to ducted sources, and obtained mostly by cascade impactors designed for particle size classifications, well below the tentative 15 μm value for IP. Data on process fugitive emissions, and on open dust sources were sparse. Moreover, little data exists regarding condensible particulate which may be a major contribution to ambient fine particulate ($\leq$ 2.5μm) levels.

Due to the lack of sufficient technical data to develop IP emission factors, Office of Air Quality Planning and Standards (OAQPS) requested ORD's Industrial and Environmental Research Laboratory (IERL) to support development of a program which would meet these objectives. A list of

industrial source categories was compiled, which OAQPS viewed as potentially significant source categories based on the following criteria:

- °Source particulate emissions characteristically found by existing measurements or judgements were estimated to have substantial portions less than 15 μm.
- °Source particulate emissions in the National Emission Data Systems (NEDS) were reported to have high mass emissions with implied national and regional impact.
- °Sources where particle size data and characterization is virtually nonexistant.
- °Fugitive emissions from processes are usually associated with the source category.
- °Source categories where condensible emissions, were expected and thus no appropriate data base, could be anticipated, (e.g., metal fume, sulfate, etc.)

Efforts were also made to identify and separate sources which characteristically produce particulate emissions totally greater than 15 μm or totally less than 15 μm since currently available emission factors compiled in AP-42 would potentially be sufficient in such cases, assuming final selection of a 15 μm upper limit.

The priority list of source categories recommended to IERL for inclusion in the test program included Iron and Steel, Primary and Secondary Nonferrous Smelters, and selected sources such as cement manufacturing, mineral (ore) extraction and beneficiation, etc. The list did not recommend early sampling of combustion sources because it was believed that available particle size data might be sufficient for development of an IP emission factor should sound data extrapolation methods become available. Also it was believed that combustion sources are largely being addressed by existing control programs. Further, a time delay before testing could be initiated was anticipated due to the necessity for development of a suitable condensible particulate test measurement method and development of methods to obtain a 15 μm upper limit, since available particle sizing techniques were not then applicable above about 10 μm.

During the program development, the question of balancing program resources and anticipated source emission characterization testing requirements was considered. A first estimate of costs to perform the work necessary for developing IP emission factors for the complete initial priority list of sources submitted by OAQPS was in excess of resources available to ORD or OAQPS for this purpose. Additionally, time considerations for development of IP emission testing equipment and methods along with strategies for sampling listed source categories led to revisions in the priority list. OAQPS and IERL jointly reviewed the budget constraints and selected a final priority list of source categories, presented in Table 1, which were expected to have the greatest impact on the SIP process. This priority list was developed with the expectation that, from time to time, revision of source

priorities would be made as the IP testing program progresses and data become available from various source assessment projects.

The IP emission factor priority list emphasizes fugitive emissions (process and dust) since the quantity and size distribution of these emissions are uncertain and are expected to be a significant factor in the implementation of IP standards. For some sources, total particulate "mass" emission data are available but particle size data are not. Efforts on these sources would routinely be expected to require particle size characterization only. This is not an ideal situation, but is generally conceded to be a reasonable approach. Thus, further cost adjustments had to be made. When the final plan was being firmed up, it was decided that emission factors would be developed not only for the 15 μm cut point but also for 2.5 μm as this information would be needed should a "fine" particulate standard be developed in the future and size distribution data between 2.5 and 15 μm be required. Provision for collection and storage of particulate samples for future chemical analyses and characterization was made. There was also a consensus on the desirability to conduct a number of separate emission tests rather than conducting single tests because multiple data points would provide more confidence in the emission factors. This is especially true since emission rates can vary by a factor of 2-3 among similar sources within the same source category.

TABLE 1. PRIORITY LIST OF SOURCE CATEGORIES[a]

| |
|---|
| Paved and Unpaved Roads |
| Iron and Steel |
| Portland Cement |
| Lime Plants |
| Asphaltic Concrete |
| Ferroalloy |
| Secondary Nonferrous Lead |
| Primary Nonferrous |
| Copper |
| Lead |
| Zinc |
| Aluminium |
| Kraft Pulp Mills |
| Combustion (Coal-Oil) |
| Utility |
| Industrial |
| Commercial and Residential |
| Incineration |
| Lower Priority Sources |

[a]Priority list not in absolute order of data needs or source category's potential impact.

To ensure that the testing phase would yield desired objectives, requirements for plant surveys and source characterization reports to IERL project officers would be made available prior to testing so that the relationship of the plant to "typical" existing plants could be assessed. Plant survey reports and preliminary assessments include process descriptions, production and operating data, current operating practices, emission estimates, number and kinds of fugitive sources and plant representativeness of the industry. Source category reports include review of available emission data published in literature, EPA data files (e.g., FPEIS, NEDS, etc.), and AP-42 emission factors.

Source characterization requires using sampling protocols developed by EPA for both ducted and fugitive emissions. Where control equipment is present, IP measurements shall be taken simultaneously up stream and downstream so that uncontrolled and controlled emission factors are developed. All pertinent process equipment operating parameters required to support the emission factor development are required as part of the test report. Generally, four independent measurements at each sampling location are required. In the case of fugitive process emissions, the sampling must include a full cycle of the process during representative operation, with process equipment parameters recorded. Fugitive dust emission measurements shall be made under varying wind, moisture, and other (e.g., traffic) characterizations as appropriate.

Program Progress

From mid 1978 to date, implementation of the IP program has gone forward at the direction of the IP Emission Factor Task Force Executive Committee, which is composed of members of Office of Air Quality Planning and Standards, Industrial Environmental Research Laboratory, Environmental Sciences Research Laboratory, and Division of Stationary Source Enforcement. The purpose of this committee has been to direct the overall program, keep its members informed of how the program is proceeding and, to decide on issues related to the IP program such as source testing schedules and review of lists of tasks necessary to finalize IP emission factors. Several major steps have been successfully realized since the beginning of the program. EPA and many of the nation's particulate measurement experts have developed necessary sampling techniques for measurement of IP particulate matter. During the intervening time, formulation of particle size extrapolation techniques, which can be applied to existing data bases such as the FPEIS to estimate IP emissions have been developed. Measurement protocols for sampling IP have become available and are presently in use in source characterization tests today.

Performance of the IP testing program as specified in the established protocols will result in reports and will be summarized in a format that presents the emission factors over the entire particulate size distribution ranges up to 15 μm for each measured process in the source category. The necessity for developing the emission factors over the entire range is due to the possibility that some cut points other than 15 μm (or 2.5 μm) may be

adopted as IP standards. The final step will be the compilation and publication of IP emission factors for each source category in a format that will be appropriate to supplement AP-42 along with a background documentation for the emission factors. Table 2, lists major elements of the IP emission factor program development.

TABLE 2. INHALABLE PARTICULATE EMISSION FACTOR PROGRAM DEVELOPMENT

- ° Priority List of Source Categories
- ° Development of IP Measurement Equipment and Sampling Protocols
- ° Source Site Selection and Evaluation Reports
- ° Specific Plant Survey with Recommended Plans
- ° Testing Program Implemented
- ° Data Analysis and Development of IP Emission Factors for Processes Tested
- ° Emission Factors for Source Category Compiled and Formated for AP-42
- ° IP Emission Factor Guidance for SIP Preparation When Standard Is Promulgated

This paper has focused on the requirements and development of the IP emission factor program, and provides a brief rationale for prioritization of resources available for this characterization effort. The ultimate purpose of the IP emission factor program is to provide assistance to the States who will need guidance in the preparation of their emission inventories and SIPs, should a size specific National Ambient Air Quality Standard be adopted by the agency. As a result of this program the Agency will provide States guidance information through size specific emission factors for a wide range (though not exhaustive) of source categories that may be impacted by a size specific particulate matter standard.

References

1. The Clean Air Act as amended August 1977 (42 U.S.C. 7414).

2. Staff Paper Outline for Particulate Matter, Office of Air Quality Planning and Standards, U.S. Environmental Protection Agency, Research Triangle Park, NC, July 31, 1980.

3. F. J. Miller, et al., "Size Considerations for Establishing a Standard for Inhalable Particles", Journal of the Air Pollution Control Association, 29(6): 610-615, 1979.

4. Compilation of Air Pollutant Emission Factors, Third Edition and Supplements, AP-42, U.S. Environmental Protection Agency, Research Triangle Park, NC, August 1977.

5. A. E. Vandergrift, et al., Handbooks of Emissions, Effluents and Control Practices for Stationary Particulate Pollution Sources, National Air Pollution Control Administration, U. S. Department of Health, Education and Welfare, Cincinnati, OH, November 1970.

# INHALABLE PARTICULATE EMISSION FACTORS FOR BLAST FURNACE CASTHOUSES IN THE IRON AND STEEL INDUSTRY

Peter D. Spawn

Stephen Gronberg

Stephen Piper

GCA/Technology Division
213 Burlington Road
Bedford, MA 01730

## ABSTRACT

Total mass emissions and the inhalable particulate fraction were measured in the baghouse inlet ductwork at the No. 3 blast furnace casthouse emission control device at DOFASCO in Hamilton, Ontario. The tests were sponsored by EPA's Industrial Environmental Research Laboratory as part of the inhalable particulate (IP) measurement program. The uncontrolled mass emission rate, measured in the inlet ductwork, averaged 0.39 lb particulate per ton of hot metal cast for four Method 5 test runs. Results of 12 Andersen impactor runs, conducted concurrently with the mass tests, found 0.24 lb/ton of inhalable particulate (less than 15 μm aerodynamic diameter). These measurements did not include drilling and plugging emissions. Less than 100 percent capture of the total uncontrolled emissions by the control system was noted. Some casting emissions escaped capture and were not measured in ductwork.

## BACKGROUND

Under the Clean Air Act Amendments of 1977, the U.S. EPA is required to review the scientific basis for the total suspended particulate ambient air quality standard. A size-specific ambient standard based on inhalable particulate matter (IPM), defined as airborne particles ≤ 15μm aerodynamic equivalent diameter, is being considered.

EPA's Office of Research and Development (ORD) is responsible for developing IPM emission factors for possible use by states in revising State Implementation Plans if an ambient standard based on particle size is promulgated. A major portion of ORD's IPM program is directed towards establishing size-specific emission factors for major iron and steel making processes.

Based on a survey of best available emission factors, the blast furnace casting operation is considered the second largest particulate emission source in the integrated iron and steel industry, generating about 22,000 metric tons of total particulate per year, industry wide. Casting emissions are not controlled at most U.S. blast furnaces, and are discharged to the atmosphere through open roof monitors. Consequently, accurate measurement of total mass emissions and particle size distributions has historically been unfeasible or

quite difficult.

The first casthouse control system on a basic iron-producing furnace in North America entered service at Dominion Foundries and Steel, Ltd. (DOFASCO) in Hamilton, Ontario 1975. A blast furnace that produced ferromanganese, operated by Bethlehem Steel, was fitted with controls in the early 1970s; the furnace was retired later in the decade.

By the Fall of 1980, three new and seven retrofit casthouse emission control systems had been installed in North America, and a number of prototype systems were under evaluation by steel companies and EPA. By 1981, the industry had made committments to install controls on an additional 58 furnaces in the U.S.

As casthouse control technology began to develop in North America, it became possible to accurately measure emission rates in the control device ductwork. When the inhalable particulate program was initiated in 1979, DOFASCO operated the only continuous-service control systems in North America, and was a logical choice for measuring uncontrolled mass and inhalable particulate emissions.

## PLANT DESCRIPTION

### Process Description

DOFASCO operates four blast furnaces at the Hamilton, Ontario plant to supply molten (pig) iron to the two BOF steelmaking shops. A typical blast furnace and casthouse is shown in Figure 1. The furnace is continuously charged at the top with iron ore pellets, coke, and limestone. Preheated blast air blown through the furnace supports combustion of the coke, and smelting of iron from the ore. Molten iron accumulates in the hearth (furnace bottom). After several hours, a taphole in the furnace base is drilled open, molten iron flows from the furnace through refractory-lined runners in the casthouse floor, and into waiting railcars.

The No. 3 furnace is rated at 2150 tons of hot metal per day. It has a working volume of 32,346 $ft^3$ and a hearth diameter of 22 feet, 3 inches. Entering service in 1956, its most recent reline at the time of testing was in 1972. Furnace charge composition, operating parameters and hot metal chemistry data are summarized later in this paper.

### Casthouse and Emission Control Description

Figure 2 shows the runner layout at the No. 3 casthouse. Casting emissions result from the hot metal flow through the brick-lined runners and the interface of the hot metal with the ambient air inside the casthouse. Emissions consist of micron-sized particles of iron oxide and graphitic carbon. If not captured, casting emissions discharge to the atmosphere through open roof monitors.

Casting emissions at the No. 3 blast furnace are controlled by a total casthouse evacuation system which entered service in November 1978. A down-

stream fan supplies an exhaust flowrate of about 480,000 acfm to a roof-level intake plenum, withdrawing casting fumes into a 10 ft. duct leading to the baghouse. Efforts were made to seal potential leakage paths that would allow casting emissions to bypass the intake plenum. The total enclosed casthouse volume is 365,000 $ft^2$, and the 480,000 acfm exhaust rate measured in these tests provides 1.3 casthouse air changes per minute.

The baghouse serving No. 3 furnace also controls No. 2 furnace. Dampers in the ductwork are activated so only one casthouse is controlled at any one time. The tests were conducted when No. 3 was controlled, and no exhaust was supplied to No. 2 furnace.

The baghouse is a positive pressure unit, with an air-to-cloth ratio of 3.3:1 (at 400,000 acfm). The 1,360 polyester bags measure 11-3/4 inches in diameter and 30 feet, 7 inches in length. The exhaust fan is designed for 400,000 acfm at a static pressure of 16 in. W.G. using a 2,500 hp, 900 rpm direct drive motor. When not casting, the fan idles with dampers 90 percent closed.

Shortly after these tests, the No. 3 blast furnace was taken out of service for a reline. DOFASCO was planning to convert the total evacuation system to a local hood system. The No. 2 casthouse, which shares the baghouse with the No. 3 furnace, was also being converted to local hoods. Since local hoods require less exhaust flowrate ($\sim$200,000 acfm), the existing 400,000 acfm baghouse will be able to control both furnaces simultaneously.

## SAMPLING EQUIPMENT

### Total Particulate Sampling

EPA Methods 1 through 5 were used to measure total mass emissions. RAC Stacksampler$^{TM}$ sampling trains were used in conformance with EPA Method 5 specifications. Each train consisted of a stainless steel, heat-traced probe with a stainless steel button hook nozzle, thermocouple, pitot tubes, and a Method 3 sampling probe attached as per EPA Method 5. Following the probe was a glass fiber filter/cyclone bypass assembly installed in the hot box. A Reeves Angel type 900AF 4-inch diameter filter was used in a filter compartment maintained at 248$^{o}$F $\pm$ 24$^{o}$F. The gas sample exits the hot box into impingers where condensible materials are removed. The first, third, and fourth impingers were modified Greenburg-Smith designs; the second was a standard Greenburg-Smith. The first two impingers each contained 200 ml of distilled deionized water, the third was empty, and the fourth contained silica gel. Following the impingers, the sample gas flow rate and volume were measured at the control box containing the pump, a calibrated orifice, and dry gas meter.

An integrated multipoint gas sample was collected in a tedlar bas as part of each Method 5 test run and analyzed with an Orsat analyzer. The samples were obtained and analyzed in accordance with EPA Method 3 - Gas Analysis for Carbon Dioxide, Oxygen, Excess Air, and Dry Molecular Weight.

Particle Size Distribution: Andersen Impactors

Particle size in the 0.8 to 15 micron range was determined using Andersen Mark III cascade impactors equipped with a 15 micron cyclone inlet (precutter), or button-hook nozzle. This in-stack fractionating sampler provides eight size range measurements, and a cutpoint of greater than 15 microns. The substrates and backup filters were Reeve Angel type 934AH glass fiber filters, and were preconditioned for sulfate adsorption.

SAMPLING PROCEDURES

The test site was located in the horizontal inlet ductwork leading to the baghouse, 11 diameters downstream and 2.6 diameters upstream of any flow disturbance. The horizontal duct was traversed from ports located on the side and the bottom. A bottom port was used instead of a top port; top port sampling was impossible due to interference with an ore yard crane. A preliminary velocity traverse determined the following:

- Absence of cyclonic flow conditions
- Average flow and temperature points for particle size measurements
- Proper sized nozzles needed to perform isokinetic sampling

Four mass tests were performed, each requiring two casts per run. Concurrent with the mass tests, a total of 12 Andersen runs were conducted, each requiring about 15 minutes sample time to obtain a minimum of 50 mg sample, per impactor. Leak checks were performed before and after each sampling run, and after changing or disconnecting any train component.

The signal to begin sampling was provided by radio communication from the process engineer stationed inside the casthouse. The inside observer carefully documented the origin and magnitude of all emissions generated within the casthouse. An outside observer recorded the opacity of emissions that escaped capture and were emitted to the atmosphere.

TEST RESULTS

Mass and Visible Emissions Data

Mass emissions data for the four Method 5 test runs are summarized in Table 1. Each test run sampled two casts, excluding the initial drilling and final plugging operations. The average uncontrolled mass emission rate for the four test runs during eight casts was 118 lb/hr, or 0.39 lb/ton of hot metal cast.

Table 2 elaborates on the mass sampling data, showing the gas volume sampled, particulate mass actually collected, and grain loading in the inlet ductwork. The back-half analyses were low, ranging from 0.4 to 4.6 lb/hr.

The Method 9 opacity observations indicated that less than 100 percent capture was achieved by the TE system. The average opacity of emissions escaping the No. 3 casthouse during these tests was about eight percent (Method 9)

Although it is not possible to quantitatively determine system capture efficiency, the GCA engineers on-site felt that the uncontrolled emission measurements may be 5 to 15 percent lower than the total emission.

DOFASCO has conducted long-term weight measurements of the baghouse hopper catch and converted these data to emission factors. Unlike the GCA emission factors reported herein, the baghouse catch data includes captured drilling and plugging emissions, but excludes the small amount of baghouse emissions. Review of the baghouse catch data, and comparison with the GCA Method 5 tests of only four casts suggests that the Method 5 tests represent individual casts and may not be representative of long-term average casthouse emissions at DOFASCO.

Particle Size Distribution Results

Figure 3 shows the average particle size distribution for 12 Andersen impactor runs conducted during 8 casts. Aerodynamic diameter is shown on the horizontal axis, and the cumulative percentages are shown on the left. The right-hand scale shows the uncontrolled emission factor for each particle cut size.

Visual inspection of the Andersen substrates showed that particles less than about 2 μm were red in color, typical of iron oxide fume. Particles greater than about 2 μm were black, probably graphitic carbon.

Table 3 provides a numerical summary of the particle size data. Inhalable particulate, less than 15 μm aerodynamic diameter, averaged 62 percent of the total mass emissions.

Process Parameters During Testing

To facilitate comparison of the DOFASCO tests to other furnaces Table 4 shows the average of furnace process data during testing. Table 5 summarizes hot metal characteristics. The sulfur content during these tests was approximately 2-3 times greater than normally encountered in domestic furnaces since DOFASCO uses external desulfurization for sulfur control.

Casthouse emissions tend to increase as hot metal sulfur content increases However, the sulfur levels during the DOFASCO tests varied over a narrow range, and no conclusions could be drawn regarding the influence of sulfur on measured emission rates. Assessment of other process parameters relative to the emissions data found no statistically significant relationships. This may be due, in part, to the limited amount of test data, i.e., only four mass emission test runs.

CONCLUDING COMMENTS

The following comments summarize the results of the DOFASCO No. 3 casthouse tests for uncontrolled emission rates.

- Total mass emissions averaged 0.39 lb/ton of hot metal, excluding drilling, plugging, and clean-up operations.

- Inhalable particulate fraction, i.e., < 15μm, averaged 0.24 lb/ton, or 62 percent of the total mass emission.
- Capture efficiency varied somewhat between casts, and overall, somewhat less than 100 percent capture was generally achieved. This tended to bias the emission rates reported herein slightly low.
- The data showed no discernable impact of hot metal temperature sulfur, or other process parameters on mass emissions or particle size distributions.

The Final Report to EPA contains additional information describing this program.

ACKNOWLEDGEMENT

This study was partially funded by the U.S. EPA under IERL's inhalable particulate program (Contract No. 68-02-2687, Technical Directive No. 011 and Contract No. 68-02-3157, Technical Directive No. 002), with Mr. Robert C. McCrillis of IERL serving as Task Manager. EPA's Division of Stationary Source Enforcement provided some of the funding under EPA Contract No. 68-01-4143, Technical Service Area 1, Task No. 96C with Mr. Thomas J. Maslany serving as Task Manager. Mr. Richard Craig, also of EPA, served as Task Coordinator.

A high level of cooperation was received from DOFASCO during the field tests, and planning efforts, especially from Al Kruzins, Murray Greenfield and Warren Rombough. The contents of this paper do not necessarily reflect the views or policies of the U.S. EPA, nor does mention of trade names, commercial products, or organizations imply endorsement by the U.S. Government.

TABLE 1. MASS EMISSION DATA-FRONT-HALF

| TEST NUMBER | TONS IRON CAST | TOTAL MASS EMISSIONS | |
|---|---|---|---|
| | | LB/HR | LB/TON OF IRON |
| 1 | 500 | 86 | 0.27 |
| 2 | 488 | 108 | 0.39 |
| 3 | 496 | 134 | 0.46 |
| 4 | 458 | 131 | 0.45 |
| Average | 485 | 118 | 0.39 |

TABLE 2. TOTAL MASS PARTICULATE TEST DATA-FRONT-HALF

| TEST NUMBER | GAS VOLUME SAMPLED (dscf) | TOTAL PART. COLLECTED (mg) | PART. CONC. (gr/dscf) | PART. EMISSION RATE, (lb/hr) |
|---|---|---|---|---|
| 1 | 106 | 144 | 0.021 | 86 |
| 2 | 114 | 202 | 0.027 | 108 |
| 3 | 118 | 249 | 0.032 | 134 |
| 4 | 102 | 227 | 0.034 | 131 |

NOTE: BACK-HALF CATCH RANGED FROM 0.4 - 4.6 LB/HR FOR FOUR TESTS

TABLE 3. COMPARISON OF TOTAL MASS AND IP (<15 μm) FRACTIONS

| TEST NUMBER | IP MASS EMISSIONS, LB/TON IRON | TOTAL MASS EMISSIONS, LB/TON IRON | % IP IN TOTAL MASS EMISSION |
|---|---|---|---|
| 1 | 0.14 | 0.27 | 51 |
| 2 | 0.29 | 0.39 | 74 |
| 3 | 0.28 | 0.46 | 61 |
| 4 | 0.30 | 0.45 | 65 |
| AVERAGE | 0.24 | 0.39 | 62 |

TABLE 4. FURNACE OPERATION DURING FOUR TEST DAYS

| | |
|---|---|
| COKE RATE, LB/NTHM | 961 |
| OIL RATE, LB/NTHM | 149 |
| CARBON, LB/NTHM | 1014 |
| FLUX, LB/NTHM | 282 |
| BLAST TEMP., $^{o}$F | 1457 |
| TOP TEMP., $^{o}$F | 423 |
| BLAST PRESSURE, PSI | 24.0 |
| TOP PRESSURE, PSI | 5.1 |
| $O_2$ IN BLAST, % | 21.9 |
| AVERAGE WIND, CFM | 89,500 |

TABLE 5. HOT METAL CHEMISTRY DURING FOUR TEST DAYS

| RUN NUMBER | TONS CAST | RUNNER TEMP. $^{o}$F | S %† | Si % | Mn % |
|---|---|---|---|---|---|
| 1 | 500 | 2725 | .095 | 0.75 | 0.85 |
| 2 | 488 | 2735 | .090 | 0.69 | 0.79 |
| 3 | 496 | 2710 | .113 | 0.53 | 0.77 |
| 4 | 458 | 2720 | .089 | 0.55 | 0.85 |
| AVERAGE | 485 | 2720 | .097 | 0.63 | 0.82 |

†Percent by weight.

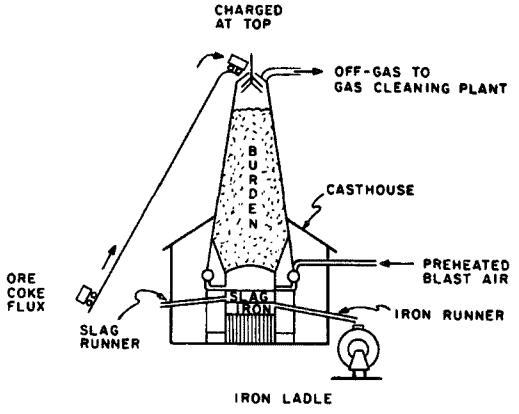


Figure 1. Typical blast furnace plant layout (side-view).

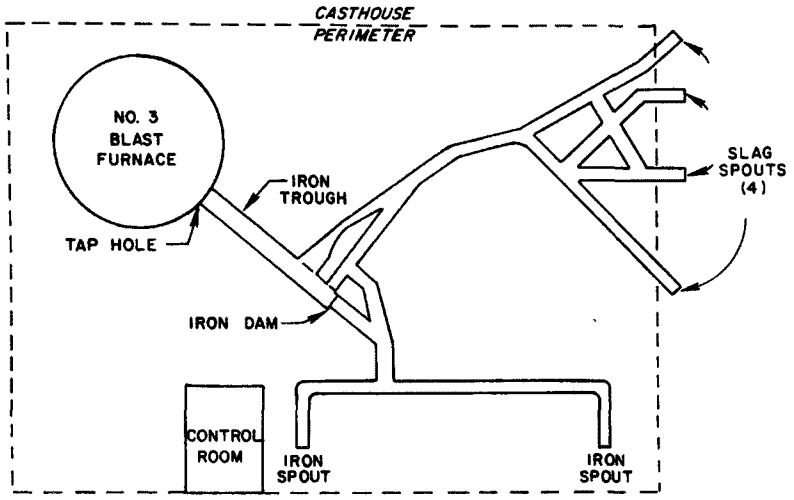


Figure 2. Runner Layout, No. 3 Casthouse.

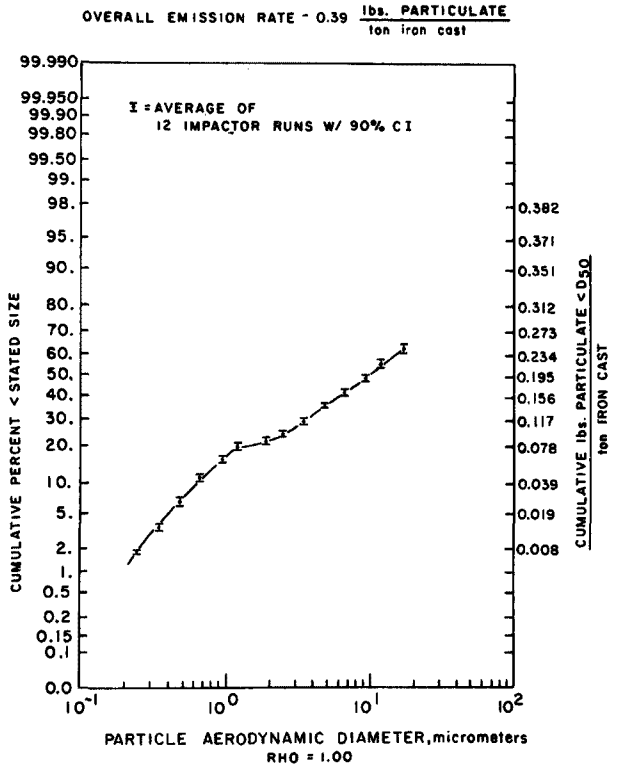


Figure 3. Average size distribution of casting fumes at DOFASCO No. 3 Blast Furnace Casthouse, Hamilton, Ontario.

# INHALABLE PARTICULATE EMISSIONS FROM VEHICLES TRAVELING ON PAVED ROADS

By: Russel Bohn
Midwest Research Institute
425 Volker Boulevard
Kansas City, Missouri 64110

## ABSTRACT

This paper presents the results of a field sampling program designed to test the quantity of dust emissions from vehicles traveling on paved urban roadways. The sampling protocol used in this program focused on the exposure profiling technique. Emission factors were determined for inhalable particulate, i.e., particles less than 15 micrometers in aerodynamic diameter. Testing was performed in the winter and spring seasons of the year in Kansas City and St. Louis, Missouri, respectively.

Samples of the dust found on the road surfaces were collected to determine total loading and silt content. The relationship of measured emission factors to road surface silt loadings and vehicle characteristics was investigated.

## INTRODUCTION

Traffic entrained particulate from vehicles traveling on paved roadways has been identified as a major cause of nonattainment of air quality standards for total suspended particulates (TSP) in urban areas. Therefore, the quantification of this source is necessary to the development of effective strategies for the attainment and maintenance of the TSP standards, as well as for the potential standard for inhalable particulate, i.e., particles less than 15 micrometers in aerodynamic diameter.

The following paper summarizes the methods used to quantify and characterize the nature of the traffic entrained dust emissions. Preliminary results are presented showing the variability in the measured emission factors and road surface dust loadings.

## METHODS

### Sampling Sites

Roadway sites which were selected for this study were located in TSP nonattainment areas in the Kansas City and St. Louis metropolitan areas. In Kansas City, three general site locations were chosen. They were

7th Street and Osage, an industrial park area; Volker Boulevard and Rockhill Road, an urban arterial; and 4th Street in Tonganoxie, Kansas, a small rural town. These roadways were sampled in February and March of 1980.

In St. Louis, four general site locations were chosen. Interstate 44, a high speed expressway; Kingshighway at Penrose Park, an urban arterial; 24th and Madison, a commercial arterial; and Benton Road, an urban arterial. The last two sites were in Granite City, Illinois. These roadways were sampled in May of 1980.

Emissions Sampling Equipment

The Exposure Profiling Technique was used as the protocol for the source sampling. Previous roadway sampling using this technique and an explanation of the sampling methods are reported elsewhere (1,2,3). Downwind of the roadway, in addition to the vertically distributed exposure profiling samplers, size selective inlets (SSIs) for the high volume air sampler were located at two heights in the dust plume. These SSIs were fitted with slotted high volume cascade impactors to measure particle size distribution. The substrates of these impactors were greased to mitigate particle bounce.

Upwind of the roadway, the SSIs were placed at two heights to determine vertical profile IP concentrations. In addition to the previously mentioned sampling equipment, one standard high volume air sampler and one dichotomous sampler were placed upwind and downwind of the roadway. These instruments were used to measure TSP and elemental concentrations, respectively. Figure 1 presents the general sampling equipment deployment for the roadway testing.

Road Surface Dust Sampling Equipment

Samples of the dust found on the road surface were collected by using a portable hand-held vacuum cleaner. A typical length of 5 feet was sampled for every roadway travel lane. All travel lanes of the roadway were sampled in the vicinity of the air sampling equipment. An exception was the high speed expressway travel lanes in St. Louis. Due to safety constraints, only one travel lane could be hand vacuumed during the study.

The collected total road particulate was weighed and then sieved to determine physical particle size and silt content. Samples of the silt were further analyzed for elemental composition.

## RESULTS AND DISCUSSION

### Particulate Emissions

Inhalable particulate emission factors for the 19 roadway tests are presented in Table 1. The emission factor units are pounds of particulate per vehicle mile traveled. The information is tentative and subject to change before the final report for this study is submitted to U.S. EPA in the spring of 1981.

Concerning the ratio of IP to TSP particulate concentrations, the average ratio of downwind IP/TSP was 0.47 with a standard deviation of 0.13. The upwind IP/TSP particulate concentration ratio was 0.57 with a standard deviation of 0.15. The above values are reported for a 2-meter sampling height. The data indicates that background TSP contains a higher fraction of IP than the TSP found 5 to 10 meters from the roadway edge.

### Street Loadings

For each of the 19 source tests, a sample of the road surface dust in the immediate area of the sampling site was collected. The sample consisted of a representative strip across all the travel lanes. The total particulate sample was subsequently sieved to determine silt content. Table 2 presents the 19 total surface loadings, silt contents, and silt loadings. The loading values are based on mass of material per area.

### Vehicle Characteristics

Throughout the source testing, the amount and type of vehicular traffic was monitored. Vehicle counts by type (cars, light trucks, and heavy trucks) were tabulated. Vehicle speed was monitored with a radar gun. Vehicle weights were estimated by vehicle type. Table 3 presents the monitored vehicle characteristics for the 19 tests.

### Emission Factors and Adjustment Parameters

A previously developed predictive emission factor equation for paved roads was developed which accounted for the major adjustment parameters which control the extent of vehicular entrained TSP emissions. Figure 2 presents the equation (3). An objective of this study is to develop an equation of a similar form for inhalable particulate. Multiple regression analysis will be used to establish the dependence of the emission factors with the source adjustment parameters of road surface silt loading and the vehicle characteristics of speed and weight. The equation will be developed in a predictive form, i.e., by quantifying the values of the adjustment

parameters for a road segment, a source specific emission factor can be estimated to aid emission inventory development.

## SUMMARY

In this study, inhalable particulate emission factors were determined for traffic entrained paved roadway emissions. A total of 19 source tests were performed in the Kansas City and St. Louis metropolitan areas using the Exposure Profiling Sampling Protocol. In addition to the collected airborne particulate, samples of the dust loading on the paved road surface were collected and characterized. Measured inhalable particulate emission factors varied from 0.00026 lb/VMT for an expressway to 0.036 lb/VMT for an uncurbed road adjacent to an unpaved parking area in a small rural town. Measured silt loadings found on the paved roads ranged from 0.022 g/sq m for the expressway to 2.6 g/sq m for the road in the rural town. Typical average emission factors and silt loadings for an urban arterial would be summarized as 0.0042 lb/VMT and 0.47 g/sq m, respectively.

## ACKNOWLEDGMENT

This work was supported by the U.S. Environmental Protection Agency's Industrial Environmental Research Laboratory under EPA Contract No. 68-02-2814, Work Assignment No. 32. Dr. Dennis C. Drehmel, Particulate Technology Branch, was the requester of this work.

## ENDNOTES

1. Cowherd, C., Jr., C. M. Maxwell, and D. W. Nelson. Quantification of Dust Entrainment from Paved Roadways. EPA-450/3-77-027. U.S. Environmental Protection Agency. July 1977.

2. Bohn, R., T. Cuscino, and C. Cowherd. Fugitive Emissions from Integrated Iron and Steel Plants. EPA-600-2-78-050. U.S. Environmental Protection Agency. March 1978.

3. Cowherd, C., Jr., R. Bohn, and T. Cuscino. Iron and Steel Plant Open Source Fugitive Emission Evaluation. EPA-600/2-79-103. U.S. Environmental Protection Agency. May 1979.

TABLE 1. INHALABLE PARTICULATE EMISSION FACTORS

| Test No. | Location | IP Emission Factor (lb/VMT) |
|---|---|---|
| Kansas City | | |
| M-1 | 7th St. | 0.013 |
| M-2 | 7th St. | 0.0036 |
| M-3 | 7th St. | 0.0072 |
| M-4 | Volker Blvd. | 0.00070 |
| M-5 | Volker Blvd. | 0.0020 |
| M-6 | Rockhill Rd. | 0.0037 |
| M-7 | Volker Blvd. | 0.011 |
| M-8 | Tonganoxie, Ks. | 0.036 |
| M-9 | 7th St. | 0.0078 |
| St. Louis | | |
| M-10 | I-44 | 0.00073 |
| M-11 | I-44 | 0.00080 |
| M-12 | I-44 | 0.00026 |
| M-13 | Kingshighway | 0.0011 |
| M-14 | Kingshighway | 0.0017 |
| M-15 | Kingshighway | 0.0037 |
| M-16 | I-44 | 0.00066 |
| M-17 | 24th St.-Granite City | 0.00080 |
| M-18 | 24th St.-Granite City | 0.0016 |
| M-19 | Benton Rd.-Granite City | 0.0010 |

TABLE 2. PAVED ROAD SURFACE DUST LOADINGS

| Test No. | Total Surface Loading (g/sq m) | Silt Content (%) | Silt Loading (g/sq m) |
|---|---|---|---|
| M-1 | 4.3 | 10.7 | 0.46 |
| M-2 | 4.2 | 6.2 | 0.26 |
| M-3 | 4.2 | 3.5 | 0.15 |
| M-4 | 4.9 | 18.8 | 0.43 |
| M-5 | 4.7 | 21.4 | 1.0 |
| M-6 | 3.3 | 21.7 | 0.72 |
| M-7 | 2.7 | 22.7 | 0.61 |
| M-8 | 17.6 | 14.5 | 2.6 |
| M-9 | 2.5 | 12.2 | 0.31 |
| M-10 | 0.047 | 46.0 | 0.022 |
| M-11 | 0.047 | 46.0 | 0.022 |
| M-12 | 0.047 | 46.0 | 0.022 |
| M-13 | 0.77 | 13.7 | 0.11 |
| M-14 | 0.58 | 8.1 | 0.047 |
| M-15 | 0.58 | 8.1 | 0.047 |
| M-16 | 0.047 | 46.0 | 0.022 |
| M-17 | 13.9 | 5.7 | 0.79 |
| M-18 | 10.1 | 7.1 | 0.72 |
| M-19 | 10.5 | 8.6 | 0.90 |

TABLE 3. VEHICLE CHARACTERISTICS

| Test No. | Number of Vehicle Passes | | | Speed (mph) | Weight (tons) |
|---|---|---|---|---|---|
| | Cars | Light Trucks | Heavy Trucks | | |
| M-1 | 2,100 | 330 | 320 | 30 | 5.6 |
| M-2 | 1,800 | 120 | 120 | 30 | 3.8 |
| M-3 | 1,900 | 120 | 200 | 30 | 4.5 |
| M-4 | 2,800 | 50 | 0 | 35 | 2.1 |
| M-5 | 2,400 | 60 | 0 | 35 | 2.2 |
| M-6 | 3,800 | 40 | 0 | 30 | 2.1 |
| M-7 | 3,100 | 50 | 20 | 35 | 2.3 |
| M-8 | 1,500 | 30 | 0 | 20 | 2.2 |
| M-9 | 2,100 | 230 | 150 | 30 | 4.1 |
| M-10 | 10,050 | 450 | 1,090 | 55 | 4.5 |
| M-11 | 9,280 | 470 | 1,160 | 55 | 4.8 |
| M-12 | 17,400 | 1,200 | 1,140 | 55 | 3.8 |
| M-13 | 5,000 | 40 | 150 | 35 | 2.7 |
| M-14 | 3,800 | 30 | 110 | 35 | 2.7 |
| M-15 | 3,900 | 30 | 110 | 35 | 2.7 |
| M-16 | 13,200 | 1,010 | 1,220 | 55 | 4.3 |
| M-17 | 3,390 | 0 | 0 | 30 | 2.0 |
| M-18 | 3,670 | 0 | 0 | 30 | 2.0 |
| M-19 | 5,500 | 300 | 0 | 30 | 2.4 |

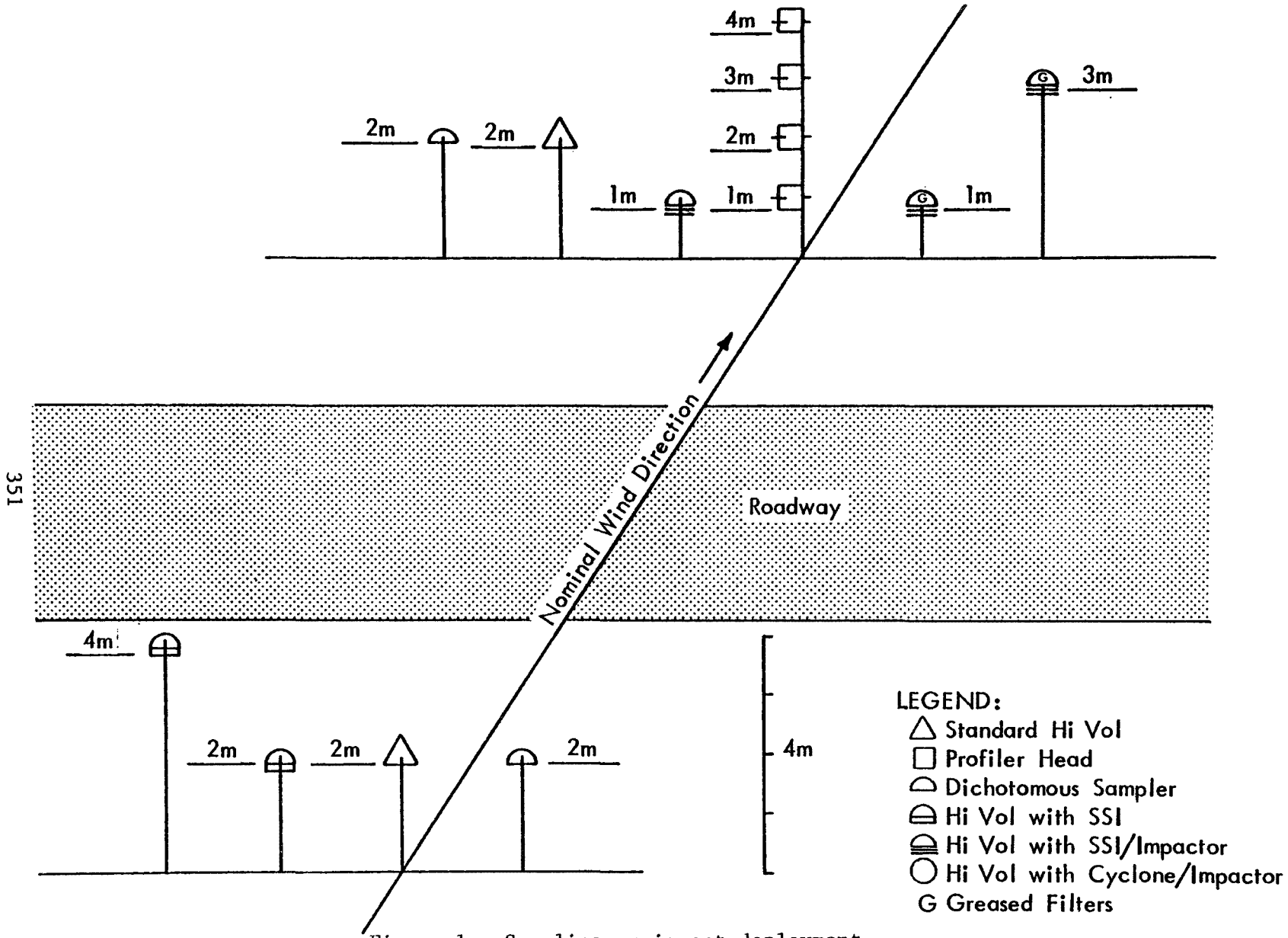


Figure 1. Sampling equipment deployment.

OPEN DUST SOURCE: Vehicular Traffic on Paved Roads
QA RATING: B for Normal Urban Traffic
C for Industrial Plant Traffic

$$EF = 0.026\, I \left(\frac{4}{n}\right)\left(\frac{s}{10}\right)\left(\frac{L}{280}\right)\left(\frac{W}{2.7}\right)^{0.7} \text{ kg/veh-km}$$

$$EF = 0.090\, I \left(\frac{4}{n}\right)\left(\frac{s}{10}\right)\left(\frac{L}{1000}\right)\left(\frac{W}{3}\right)^{0.7} \text{ lb/veh-mi}$$

Determined by profiling of emissions from traffic (mostly light-duty) on arterial roadways with values for s and L assumed.

Assumed by analogy to experimentally determined factor for unpaved roads.

Determined by profiling of emissions from industrial plant traffic yielding higher than predicted emissions, presumably due to resuspension of dust from vehicle underbodies and from unpaved road shoulders.

Determined by profiling of emissions from light-duty vehicles on roadway which was artificially loaded with known quantities of gravel fines and pulverized topsoil.

| | metric | non-metric |
|---|---|---|
| EF = suspended particulate emissions | kg/veh-km | lb/veh-mi |
| I = industrial road augmentation factor (see text) | - | - |
| n = number of traffic lanes | - | - |
| s = silt content of road surface material | % | % |
| L = surface dust loading on traveled portion of road | kg/km | lb/mi |
| W = average vehicle weight | tonnes | tons |

Figure 2. Predictive TSP emission factor equation for vehicular traffic on paved roads.

# QUALITY ASSURANCE FOR PARTICLE-SIZING MEASUREMENTS

By: C. E. Tatsch
Systems and Measurements Division
Research Triangle Institute
Research Triangle Park, NC 27709

## ABSTRACT

Quality assurance for particle-sizing measurements comprises three components: planning, implementation, and appraisal. The first two components relate to activities designed to ensure that data generated will satisfy project requirements. The latter component concerns assessment and documentation of the data quality. Suitable resources for routine field calibration of entire particle-sizing systems are not readily available. Only certain subsystem parameters, such as flow rates, may be checked in the hostile environments generally associated with such tests. Thoughtful execution of a well-designed test plan is thus crucial to the production of data of the required quality.

Several constraints are important in the design of a test plan that will ensure the collection of high quality data. Qualified personnel must be available who are experienced with equipment-specific details, aware of anticipated process fluctuations, and capable of evaluating the consequences of changing the test plan to accommodate unforeseen circumstances. The capabilities of available equipment (including adequate spare parts, tools, etc.) together with the characteristics of the field facility must also be considered. Support of a comprehensive, consistent data quality program must include consideration of additional factors such as the necessity for laboratory aerosol calibration and adequate resources for assembly, operation, and disassembly of the particle-sizing measurements system(s). There must be the capability for timely (preliminary) data reduction in order to provide the necessary feedback for execution of an adaptable test plan.

Appraisal of data quality consists of qualitative and quantitative checks on operations that are critical to measurement data quality. Qualitative checks include reviewing the adequacy of, and adherence to, written operating procedures, consistent with the particular project data requirements and site. Quantitative checks may include checks of various subsystem components, such as flow rate, nozzle quality, weighing checks, and collocated measurements. At present, emphasis must be on the comparability of test data, but there is increasing potential for improved precision and accuracy of particle-sizing data.

## INTRODUCTION

Particle-sizing measurements of all types are fundamentally scientific observations, whether they are made in the laboratory or in the field. They have an initially well-defined end use, such as characterization of the performance of a scrubber or validation of a model of a precipitator. But in research programs the goal frequently shifts before the end of the proj-

ect, testing conditions are not what was desired, and the data are used by someone with quite different motives than were expected. Data analysis may occur long after data collection, and many things which were obvious earlier in the project are forgotten. Discrepancies become more obvious as data are available for extensive review and analysis, which is increasingly prevalent in our data-base-oriented society. Unless we are willing to accept the validity of nonrepeatable data, a conscious effort must be made to ensure and document the quality of data, whether in the laboratory or in the field.

Adding weight to this is EPA's recent commitment to a mandatory Agency-wide Quality Assurance program. Following issuance of memos from the Agency Administrator in May and June 1979 requiring QA for "...all environmentally-related measurements which are funded by EPA or which generate data mandated by EPA," the Quality Assurance Management Staff (QAMS) was created in the Office of Research and Development. The QA program being developed by QAMS is motivated by EPA's need to have data of documented, adequate quality. The program is being applied from "the top down" through QA programs for Laboratories and Regional Offices to the project level. QA requirements for contracts were developed late last year and will be part of all new EPA contracts involving environmentally related measurements. QAMS is establishing consistent, specific QA guidelines for routine measurements. Although particle-sizing measurements do not fall into the routine category, evaluation for QA aspects of particle-sizing measurement is closely related to the basic scientific issues of planning for, and documenting, project data quality.

The five basic data quality criteria being scrutinized by QAMS are shown in Figure 1. Accuracy and precision are defined in familiar terms. Completeness, although frequently applied to automated monitoring networks, also applies to manual methods.

Two key concepts in the Quality Assurance program are Quality Control and Quality Assurance. Quality control activities are those quality-related activities conducted internally by the testing organization. Quality assurance activities are those quality-related activities conducted externally by the testing organization. Many of the quality-related activities are similar. The distinguishing feature is the organization responsible: personnel of the testing organization may perform quality control functions, but it requires personnel from an outside organization to perform quality assurance functions. Because of this objectivity, the QA program is a tool by which management may ensure and assess the quality of the measurement data.

Management commitment to data quality assurance must be demonstrated to all personnel of the organization to ensure the success of the program. Responsibility must be delegated for checking on data quality, but <u>all</u> personnel, beginning with management, must realize and accept their personal responsibility for producing high quality data.

Figure 2 depicts QC and QA activities at various stages in the life of a project. The project team is responsible for all test preparation and execution. The project QC personnel frequently evaluate all aspects of the

project. QA personnel normally interact infrequently with both the project team and the project QC personnel, with followups only if data quality problems are discovered.

The goal of the project QA program is to ensure and assess that project data are of adequate quality. If the majority of the QA effort is aimed at ensuring project data quality, the job of assessing and documenting it will be a straightforward and inexpensive one. For this reason, a proper, cost-effective QA program is integral to a well-designed measurement program and provides a tool for ensuring and evaluating project data quality before and during data production activities, as well as at the end of the project.

## PLANNING

Figure 3 outlines the problems faced in designing any measurement program: the real focus is not on the sample collection or analysis, but on the data analysis, which is the result of these activities. Obtaining useful data as a final result is the motivation for the measurement effort; if any of the links between the "real world" and the data interpretation fail, the entire effort may be wasted. The principle of continual, logical cross-checking and critiquing of the entire data collection effort should be applied--not just by project management, but by each team member, at each phase of a project.

The data quality question central to the entire sample collection and analysis effort is how accurately the accepted data reflect the real world. Conscious consideration of this criterion throughout the project will enhance development and implementation of an acceptable quality assurance program.

Figure 4 is an outline of quality control planning applicable to field tests. The level of acceptable data quality will affect the planning of many operations and can be helpful in avoiding later misunderstandings with the customer. Therefore, it should be established very early in the life of a project. Tested procedures for routinely performed operations should be available and should be followed by the test crew.

There are three major, and obvious, considerations of any sampling and analysis effort, regardless of the particle-sizing method being used. Despite the fact that they are obvious, we have encountered so many omissions of them in our audits that it seems worthwhile to review them here. It is useful to recall that all measurement programs suffer from the 'weak-link' phenomenon: omission of certain key considerations can easily invalidate excellent efforts in every other area of a project.

The measurement system component, which is the limiting factor in the quality of data that can be obtained, is the team personnel. The best test conditions and the best and most elaborate equipment cannot substitute for personnel who are trained, experienced, and motivated to obtain high quality data. Often there are too few of these people available, and the test crew is made up of inexperienced, although well-intentioned, individuals. This would be fine if no problems occurred during the test; but problems are the

rule, rather than the exception. Training and experience are traditionally considered to be key personnel qualifications. However, it has been demonstrated repeatedly that workers also must be motivated to high quality work.

The equipment available to the test crew must be known to produce as high a quality of data as possible. In some disciplines there are Standard Reference Materials available that can be used to verify a total sampling-measurement system. However, only selected component checks can be made for particle-sizing equipment. That is all the more reason to check and document the performance of every possible component of the measurement system. Laboratory calibration of instrumentation before and after field use is highly desirable and should be omitted only if cost is clearly prohibitive. Careful documentation of calibration procedures and comparison of trends may be useful. For example, if the calibration constant for an orifice suddenly changes by 20 percent, there may be corrosion problems. Similarly, a sudden shift in the calibration constant of a dry gas meter may indicate internal problems. This information can then be used to develop a rational maintenance program. Anticipating and preventing equipment failure improves the completeness of the data, which is an aspect of the quality assurance program being evaluated by QAMS.

The third important general aspect of a QA program for particle-sizing is timely and valid data reduction. The reduced data and inferences made from them are the "product" received and used by your customer. As the sophistication of your data processing increases, so does the potential for undetected errors. It is especially important to remember that no computer program can ever be proven correct; it only takes one counterexample to demonstrate a weakness. One of the most effective means of validating a program is to have a variety of users with a variety of data use a program. Also, it is now feasible to compute quite respectable results in the field. This may be done using one of the first-generation hand-held computers, a desktop microcomputer, or a portable terminal and telephone link to the home laboratory computer. In any case, provision should be made for physically and mathematically appropriate data reduction in as short a time as possible for the final report. Only in this way can a test crew make informed decisions during the progress of a test. Since the purpose of the intermediate calculations is different from the final calculations, their content and format need to be tailored to this purpose. For example, in the operation of a dilution system for conditioning stack gas, a program for calculating dilution flow, given the various orifice constants and pressure drops in a multiple dilution system, would be helpful. The program could be designed to allow changing (and entering) only the new flow value, with all the previous data retained in continuous memory. The dilution rate results would be available within seconds, thus allowing a trained operator to fine-tune his adjustments in a knowledgeable manner.

Other common sense aspects of a measurement program, which may actually be considered as part of the QA program, include allowing adequate time for test crew planning, travel, setup, shakedown, operation, and critiquing of test results as they are recorded. Provision for adequate utilities and workspace (which are part of good operating practice) is also part of the

data quality program. Considering the many possible sources of error, it is a good investment of time to map out and document a flow chart of activities, including reasonable alternatives, as part of the test plan. Suitable forms for data collection should be included. Although development of these forms and flow charts is time-consuming, they serve as good tools for reviewing operations and pinpointing potential data quality problems. They also provide materials for organizing subsequent tests at a fraction of the effort yet with no relaxation of the quality planning. This approach to methodical data collection will require some adjustment for you and your crew members. At first, there may be a tendency not to complete data forms "until later"--which seemingly never arrives. Perhaps this early development stage of the QA program is the best time to demonstrate your commitment to the QA management system by reviewing and critiquing some of the incoming worksheets. This is also a good time to include each of the crew members in the quality planning. Especially as new systems and forms are developed, implementation of feedback concerning the ease of use, items to be added or deleted, and format changes will clearly demonstrate that management is committed to making the new system work. The people who use these tools generally have useful suggestions for their improvement that may improve your data quality.

Figure 5 shows an example of an impactor test plan that includes quality assurance considerations. This is essentially a one-sheet directory that serves as a pointer to related test information. It covers not only the aspects of data quality that factor into calculations, but the additional operating aspects of a test that impinge on data quality and that are easy to overlook. This sheet points to additional test-related documentation that may be useful in substantiating the test. For example, recordkeeping may be adequate with one notebook per test crew member; at least the hazards of recording data on available scraps of paper can be avoided. The matter of reweighing frequency can be evaluated and provided for before the test. Transportation of the substrates, both from the preweighing to the impactor assembly and from impactor disassembly to the postweighing area, can be evaluated and a decision made on whether to do the weighings onsite or at the home laboratory.

Because each of these decisions involves different resource requirements, preliminary cost-benefit types of information should be used; for example, if substrates are to be weighed at the home laboratory, a set of preweighed loaded substrates should be transported to the test site and reweighed upon their return to determine typical effects of transport on the substrate weights. The effects observed must then be compared with the desired data quality before a decision can be made to exclude a portable balance from the test equipment. Similarly, provision for near real-time data processing should be evaluated. This provides the only secure means of evaluating the progress of a test in the field. A distinct time lag occurs after an impactor run until the substrates with samples can be conditioned and reweighed; however, provision should be made for data analysis very shortly following the postweighing. This may be performed using hand-held calculators, desktop computers, or large mainframe computers, and one of several available programs. However, if this is done, the program should be

verified to give the correct results with a minimum of user effort. The latter criterion will be well received by the users and is an important factor in ensuring the quality of the results--the fewer user inputs to a valid program, the fewer chances there are for mistakes.

One approach to data analysis that we have been developing with the Fine Particle Emissions Information System is to have all data reduction performed on EPA's computer at Research Triangle Park, with all data entry in response to a prompt from the computer. This permits the software program to be well-documented and provides users with comparable and accurately reduced data. It is available in a uniform manner to the person doing the preweighings, to the test crew who have recorded the impactor run parameters, and to the person doing the postrun weighing. Various validation checks can be built in to assist in evaluating the quality of the raw data. It is also designed to permit significant changes and extensions as better algorithms are developed for processing fine particle data. The output is designed to provide useful summary information to the test crew during a test, as well as report-ready raw and reduced data on completion of the test. And all data are entered only once and retained by the system for subsequent use, which should enhance the quality of the calculated results.

## IMPLEMENTATION

Following the extensive planning activities that have been outlined, it is important that the plans actually be carried out. Insofar as these are developed and agreed on by management, the test leader, and test crew, much of the implementation effort of quality assurance will be simplified. These plans, implemented by those qualified, motivated crew members, who are cross-checking and supporting each other in collecting good data and responding to changing test conditions, will reliably lead to high quality data. The only other activity which is needed to complete the QA program is project appraisal.

## APPRAISAL

Appraisal of the project for its quality aspects is the final part of the QA effort. Appraisal can be performed by project personnel--and then it is discussed as part of the project quality control. If it is performed by personnel who are not organizationally involved in the project, it is known as a quality assurance activity, and will most likely be requested by your project officer as part of the routine Agency-wide QA program. The types of activities will remain similar, and so I will briefly outline the approach you may take to quality control, or internal QA, appraisals.

Appraisal activity necessarily requires a degree of objectivity on the part of the person assigned to this job. On a large project, it may require the full-time effort of a crew member. On smaller ones, explicit assignment of data quality responsibilities to one person is sufficient. In any case, the purpose of this assignment is to have clear delegation of responsibility for quality control and adequate time for review and assessment of project data quality without conflict from other commitments. The basic tool to be used is project documentation and its comparison with actual practice, assuming, of course, that there has been adequate documentation.

Review of completed data forms, observation of the performance of specific tests, comparison of instrument readings against available standards, and other checks that may be developed are all part of the reasonable routine for an internal (or external) auditor. Especially as your quality system is being established, the auditor can provide useful information on the fine-tuning of the system to your own data quality needs. As the internal audit program is implemented and documented, the credibility of the data that you generate will be enhanced.

## SUMMARY

In summary, aspects of Quality Assurance that can be applied to specific programs, and that are consistent with EPA's Agency-wide Quality Assurance program as applied to particle-sizing measurements, have been described. In particular, use of feedback mechanisms for collecting, processing and evaluating data were mentioned as an effective tool by which qualified, motivated personnel can evaluate and improve data quality.

| | |
|---|---|
| Accuracy: | The degree of agreement of a measurement (X) with an accepted reference or true value (T) usually expressed as the difference (X−T). |
| Precision: | A measure of mutual agreement among individual measurements of the same property, usually under prescribed similar conditions. |
| Representativeness: | A numerical statement of how well a sample or group of samples or the data derived therefrom represent the actual parameter variations at the sampling point, and how well that sampling point represents the actual parameter variations under study. |
| Completeness: | The amount of valid data obtained from a measurement system compared to the amount that was expected to be obtained under correct normal conditions. |
| Comparability: | The measure of how well data may be compared within a study and with data from other studies. |

**Figure 1. Basic quality criteria.**

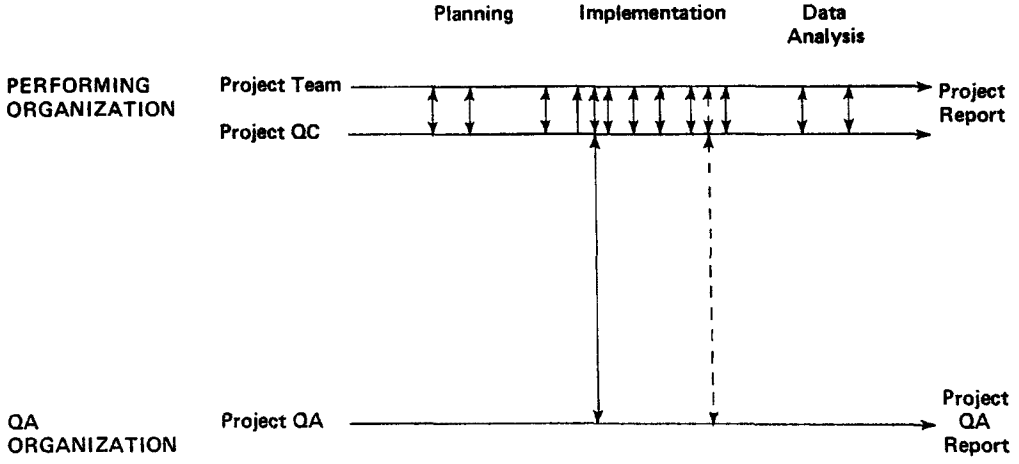


**Figure 2. Relationships of project QA and QC.**

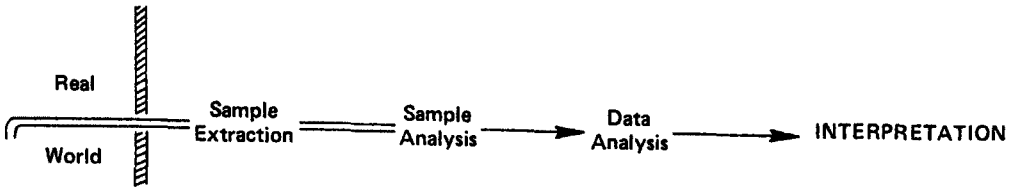


The purpose of SAMPLE extraction and analysis is to obtain DATA for analysis.

**Figure 3. Summary of sample/data flow.**

## QUALITY CONTROL

- Specify data quality required
- Establish and evaluate adequacy of procedures
- Make sure procedures are followed
- Employ trained and motivated personnel
- Ensure that equipment and supplies are adequate, calibrated and properly maintained
- Perform independent check of experiment
- Use controls and blanks
- Provide for field data reduction
- Initiate corrective action based on field data reduction
- Establish chain of custody of data and samples

**Figure 4. Outline of field test Quality Control planning.**

GENERAL

- Procedures available to test crew
- Data forms—velocity traverse, gas composition, impactor operation
- Provision for range-finding runs
- Recordkeeping

CALIBRATION

- Impactor
- Dry gas meter and orifice
- Pitot tube
- Analytical balance

WEIGHING (pre/post)

- Filter conditioning
- Transport provisions
- Comparison of samples with blanks and substrates
- Reweighing checks
- Stage loadings appropriate?

ASSEMBLY

- Leak check (train assembled) Nozzle/flow rate selection
- Impactor at desired temperature

OPERATION

- Constant flow rate
- Blank—appropriate timing, location (using filtered stack gas, etc.)
- Isokinetic operation
- Orientation: absolute and with respect to flow

DISASSEMBLY

- Filter handling/storage
- Transport to weighing?
- Probe/impactor brushdown
- Check for re-entrainment

DATA ANALYSIS

- Model matches sampling train
- Minimize user effort
- Real-time capability/use

**Figure 5. Outline of cascade impactor test plan.**

# PARTICULATE EMISSIONS CHARACTERIZATION FOR OIL-FIRED BOILERS

By: Dominick Mormile
Consolidated Edison Company of NY Inc.
4 Irving Place
New York, NY 10003

Stuart Hersh and Bruce F. Piper

KVB Incorporated - A Research-Cottrell Company
175 Clearbrook Road
Elmsford, NY 10523

Michael McElroy
Electric Power Research Institute
3412 Hillview Avenue
Palo Alto, CA 94303

## ABSTRACT

The size distribution and composition of particulate matter emissions from three oil-fired boilers, representative of utility usage, were determined for nominal operation under full-load operating conditions. The selected boilers were a 360 MW tangentially fired boiler, a 346 MW face-fired boiler and a 150,000 lb/hr steam flow steam sendout boiler. In addition, assessments of the variability of these particulate characteristics with changes in excess air level and atomization quality were obtained as an indication of the fluctuations which could be anticipated as a result of operating practices. Sizing characteristics were established with a low pressure, cascade impactor system (University of Washington), an electric aerosol analyzer (which classifies size according to electric mobility) and electron microscopy techniques with automatic counting. Particle composition analyses utilized atomic absorption on bulk samples and electron dispersive X-ray (EDX), Auger Microprobe and electron spectroscopy (ESCA) on individual particles.

## INTRODUCTION

Despite the move towards increased coal utilization by the utility industry, many regions of the country rely on existing oil-fired power plants as their principal energy source and are likely to continue to do so for many years. Historically, oil-fired plants have been viewed as clean sources of energy compared to conventional coal-fired plants. However, oil-fired plants may represent an increasingly significant source of utility particulate matter emissions as advanced high efficiency particulate controls for coal-fired units continue to be developed and enter into service. Furthermore, since oil-fired units are situated predominately in metropolitan areas with large populations, the potential impact of particulate matter emissions from these sources is of special concern.

In this context, a detailed understanding of the physical and chemical characteristics of particulate matter emissions from oil-fired boilers is important for a number of reasons. First, there is growing concern about the

particle size dependent nature of possible health effects from particulate matter emissions as evidenced by regulatory interest in fine "inhalable" particulates in the respirable size range (<10 micrometer diameter). Secondly, to formulate emission control strategies, the size distribution of particulate matter is of critical importance due to the size dependent collection performance of various control options. Third, from the standpoint of reducing plume opacity and visibility, the size and composition of particulate matter emissions play a key role due to the highly size dependent nature of particle light scattering and plume formation mechanisms. Detailed particulate matter emission data from oil-fired boilers, similar to the data developed for coal, are virtually nonexistent and has resulted in a major gap in the utility's emission data base.

## Purpose and Scope

The objective of this project was to quantify the size and chemical composition of particulate matter emissions from representative oil-fired utility boilers. Specifically, the size distribution and composition of emissions from three boilers operated by the Consolidated Edison Company of New York were measured for normal (baseline) operation under full load conditions. In addition, measurements were performed under conditions of low furnace excess air and deteriorated fuel atomization to provide an indication of fluctuations in particulate matter which could be anticipated as a result of daily boiler operating practices. Polycyclic organic material (POM), $SO_3$, CO and NO emissions were also measured to provide a more complete characterization of the boiler emissions.

This project was jointly funded by the Consolidated Edison Company and EPRI. The test program was conducted by personnel of the East Coast Division of KVB Inc. This is the first phase of a continuing research effort at Consolidated Edison to characterize particulate emissions. Future phases will consist of obtaining effects of fuel additives, off nominal operation such as low NOx and ultimately to correlate particulate characteristics and other flue gas properties with stack opacity.

## Program Description

### Test Boilers

The three test boilers, a 360 MW tangentially fired unit (Ravenswood 10), a 345 MW face-fired unit (Arthur Kill 20) and a 150,000 lb/hr steam sendout package boiler (East River 114) were selected because of the distinct differences in their combustion designs. The objective of this selection was to determine if major differences in the particulate size characteristics could be attributed to specific boiler types. The excess air and atomization quality tests were conducted only on the tangentially fired unit. All the boilers were equipped with steam atomized oil burners.

The fuel burned in all of the boilers tested was a low sulfur (maximum 0.3 percent) relatively light No. 6 oil currently used throughout the Consolidated Edison sytem. While different fuels might be expected to influence the overall level of particulate emission and composition, the particu-

late size characteristics presented in this report may be generic to conventional oil-fired utility systems due to the suspected commonality of the particle formation mechanisms involved.

### Measurement Methods

Three complementary measurement techniques were used to measure particulate matter size distributions: 1) in-situ low pressure cascade impactor (particle segregation via inertial separation), 2) electric aerosol analyzer (based on charged particle mobility in an electric field) and 3) electron microscopy with automated particle sizing utilizing samples collected with a miniature electrostatic precipitator. For the latter two approaches, a prototype dilution-probe sampling system, specifically designed by KVB, was used. Total mass loading was measured using EPA method 5. Particulate matter chemical composition was determined for bulk samples and individual particles by X-ray analysis, scanning Auger mircoprobe (with argon ion milling) and electron spectroscopy (ESCA).

### Field Test Procedure

At each boiler test condition a minimum of two replicate samples were obtained with each of the particulate measurement techniques to demonstrate repeatability. The actual test procedure consisted of two phases. The first phase verified the desired boiler operating condition through inspection of the burner front and flue gas measurements of $O_2$, CO and NO. The second phase consisted of performing the various particulate measurements as the boiler conditions were held constant.

Baseline operating conditions at the three boilers were generally repeatable from day to day as evidenced by the consistency of the emission results. However, the reduced excess air and deteriorated fuel atomization test conditions were not as repeatable due to the unavoidably subjective nature of specifying these conditions. The reduced excess air tests were conducted as close as practical to the boiler smoke threshold. The poor atomization condition was established by decreasing the atomizing steam supply pressure to the burners and adversely adjusting the fuel oil temperature, thereby producing large oil droplets.

## Results and Discussion

### Influence of Boiler Operating Variables

Typical particulate mass size distributions at Ravenswood Unit 10 under baseline, low excess air and poor fuel atomization conditions are compared in Figure 1-1. The data are presented in a so-called "differential" plot where the differential emission rate is plotted versus the log of the particle diameter. For purposes of interpretation this format can be viewed as an emission rate histogram where the area under the curve is equal to the total emission rate in units of $lb/10^6$ Btu.

A striking feature of the data is the concentration of fine, submicron size mass emissions in a narrow "peak" at approximately 0.2 micrometer dia-

meter. For baseline conditions, virtually all the particulate emissions are generated in this size range. This baseline distribution is in great contrast with coal fired boilers where the mass mean particle diameter typically ranges between 10 and 20 micrometers. It is also important to note that the submicron peak is at a size region which can contribute significantly to plume opacity due to the light scattering characteristics of these particle sizes.

A typical photomicrograph of baseline particulate matter in Figure 1-2 shows spherical shaped particles with a relative size uniformity consistent with the size distribution results. Chemical analysis indicates mostly sulfate compounds with smaller quantities of carbon and oil ash mineral constituents.

Poor Fuel Atomization: Deteriorated fuel atomization resulted in the generation of a substantial mass of large particulates (greater than 10 micrometer diameter) as indicated in Figure 1-1. The fine submicron distribution and composition was essentially unaltered compared to baseline. Significantly, no changes in stack opacity were noted despite an up to a 10-fold increase in total particulate emissions. Photomicrographs of the large particles as typified by Figure 1-3 indicate irregularly shaped, porous particles with sponge-like appearance. Surface analysis of individual large particles indicated mostly carbon, but with an abundance of sulfur and oxygen (sulfate) and lesser quantities of trace elements. However, particle depth analysis illustrated in Figure 1-4 revealed that the dominant portion of the sulfate was contained in a surface layer while the bulk of the particles consisted mainly of carbon.

These results indicate that reducing the fuel atomization quality produces large particulates which appear to be derived from the carbonization of large fuel droplets which neither completely vaporize nor burn out in the furance. Thus, the presence of large porous carbonaceous particulates in the emissions from an oil-fired boiler may indicate the existence of an atomization deficiency or mismatch between the furnace burnout characteristics and the type of atomizer used. Measurements of the type made in this study might be utilized as a diagnostic procedure in situations where excessive particulate emissions are encountered.

Reduced Excess Air: Referring again to Figure 1-1, the low excess air test conditions produced a particle size distribution very similar to baseline, but the generation of a small quantity of large particles was apparent. Chemical analysis showed a measurable increase in carbon compared to baseline measurements. Nevertheless, it appears that the particulate matter is fundamentally similar in size to that produced under baseline conditions and that carbon soot generated during low excess air operations does not necessarily produce larger size particles. This conclusion may not be applicable to extreme low excess air conditions (smoking) where large carbonaceous particles might be expected. Unlike poor fuel atomization, increases in-stack opacity were noted during reduced excess air conditions.

Summary: A summary of the overall particulate matter emission rates and composition for the three Ravenswood Unit 10 test conditions is shown in

Figure 1-5. Compared to baseline, increased carbon accounts for the slight increase in emissions under low excess air conditions. Higher emission rates with poor fuel atomization result from increases in both carbon and sulfate. It is speculated that the large surface area associated with the atomization-derived carbonaceus particles provide sites for deposition of additional sulfate compounds.

Comparison of Boiler Designs

The particulate emissions size distribution for the three test boilers under full load baseline operation are shown in Figure 1-6. These results indicate that both the face-fired and steam sendout boilers exhibit a bimodal distribution with a large size particle peak similar, but lesser in magnitude, to that obtained from the tangentially fired boiler under reduced atomization quality conditions. Photomicrographs of the large particles from both the face-fired and steam sendout boilers show a sponge-like appearance typical of the atomization derived particulates from the tangentially fired unit. Chemical composition of these particulates were also similar to those of the reduced atomization tests. Thus, both of these units appear to have deficient atomization and/or furnace design characteristics less conducive to carbon burnout. For the steam sendout unit this conclusion is further reinforced by visual flame observations which indicate the presence of numerous large burning droplets throughout the furnace.

The baseline particulate mass emission rates and composition for three boilers are summarized in Figure 1-7. Compared to federal New Source Performance Standards of 0.03 $lb/10^6$ Btu, the emission rates are generally low, reflecting the low ash, low sulfur properties of the fuel. The differences among the three units can be attributed mainly to differences in particulate carbon content. Reduction in carbon emissions from the face-fired and steam sendout boilers is presently being pursued.

Polycyclic Organic Matter

POM emissions were measured at Ravenswood Unit 10 during the three previously discussed test conditions: baseline, low excess air and poor atomization. Although POM analyses must be interpreted with caution due to sampling and analytical uncertainties, emission rates were small, varying from .0000013 to .0000131b/$10^6$ Btu. No definitive correlation with boiler operating condition was established. Up to 15 individual POM species were detected.

## CONCLUSIONS

Based on the results of this program, the particulate matter emissions from oil-fired boilers (at least firing fuels similar to those tested) can be expected to exhibit 1) relatively narrow submicron size distributions with a mass mean diameter in the 0.1 to 1.0 micrometer range and 2) a potential for the addition of a large particle distribution, depending upon fuel atomization quality and boiler design characteristics which affect particle burnout. The large particles generated as a result of these latter affects have a distinctly different structure and composition than the submicron

size particulates. The large particles are porous, roughly spherical and are composed principally of carbon with a surface layer of sulfates. This is in contrast to the submicron particles which appear to be generally spherical solids of sulfate, carbon and trace amounts of fuel metals.

These test results also indicate the value of using particulate matter size distribution measurements as a diagnostic indicator of potentially resolvable emissions problems. However, substantial work remains to be performed to further differentiate between operational and design generated emissions, to quantify fuel and additive influences and to integrate particulate, flue gas and ambient properties into an opacity model.

FIGURE 1-1 PARTICLE SIZE MASS DISTRIBUTIONS
Ravenswood Unit 10 - Comparing Baseline, Low Excess Air and Deteriorated Fuel Atomization Quality

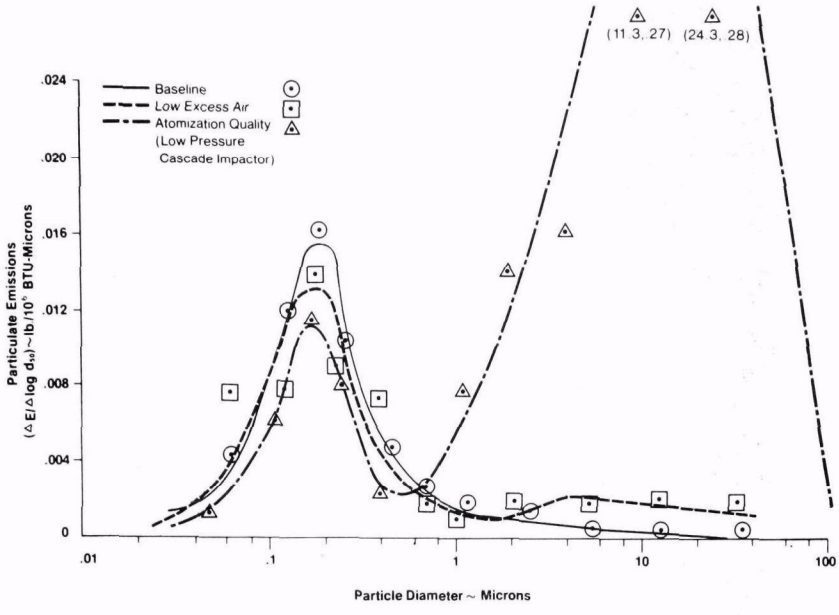


FIGURE 1-2 TYPICAL SEM PHOTOMICROGRAPH
Of Baseline Particulate Matter Illustrating Relatively Uniform Submicron Size Particles
(Ravenswood Unit 10)

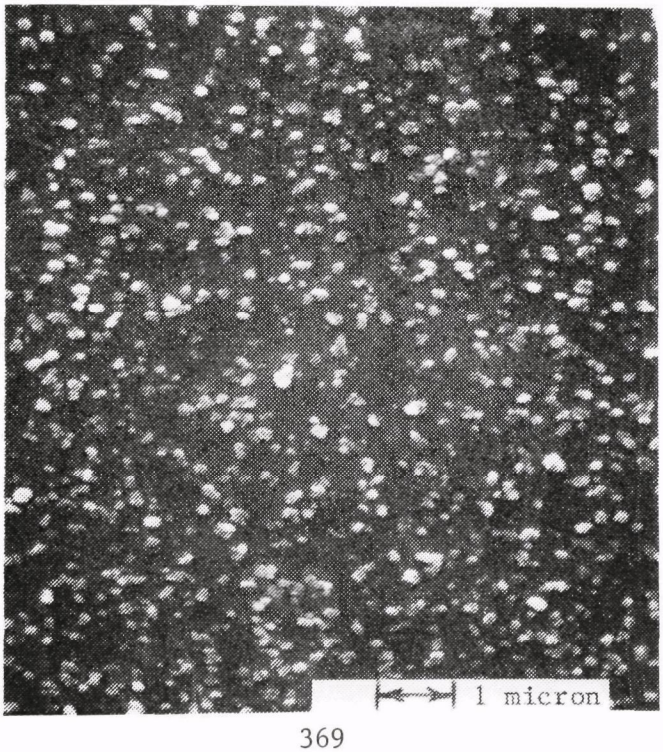

FIGURE 1-3

TYPICAL SEM PHOTOMICROGRAPH
Of Large Carbonaceous Particles Resulting From
Poor Fuel Atomization
(Ravenswood Unit 10)

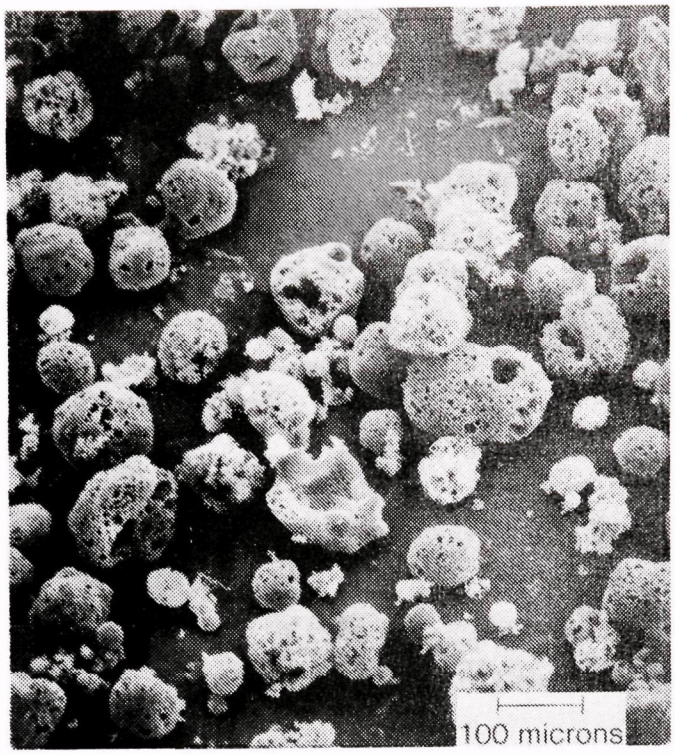


FIGURE 1-4

CHEMICAL DEPTH ANALYSIS
Of Large Atomization Derived Particle

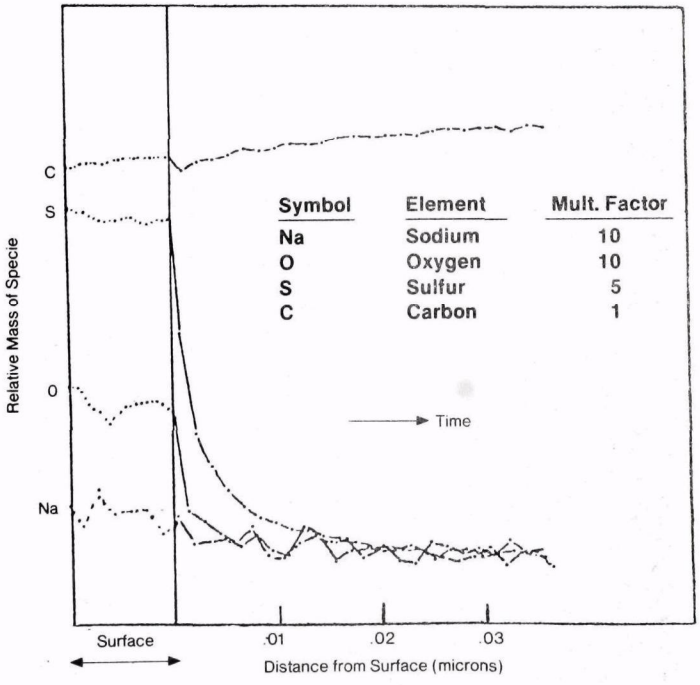

FIGURE 1-5 COMPARISON OF PARTICULATE MATTER
Emission Levels and Composition Under Baseline,
Low Excess Air And Deteriorated Fuel Atomization Conditions
(Ravenswood Unit 10)

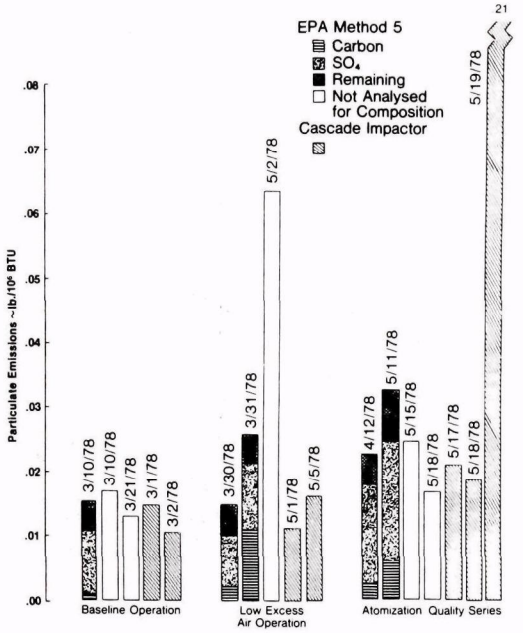


FIGURE 1-6 COMPARISON OF PARTICULATE SIZE DISTRIBUTION
Normal Baseline Operation For Three Oil Fired Utility Boilers

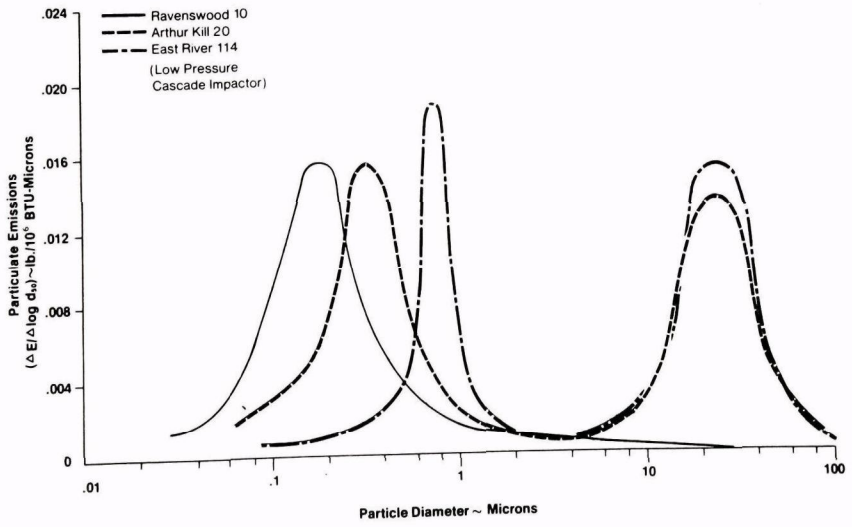

FIGURE 1-7 COMPARISON OF BASELINE PARTICULATE MATTER
Emission Levels and Composition
For Three Oil-Fired Boilers

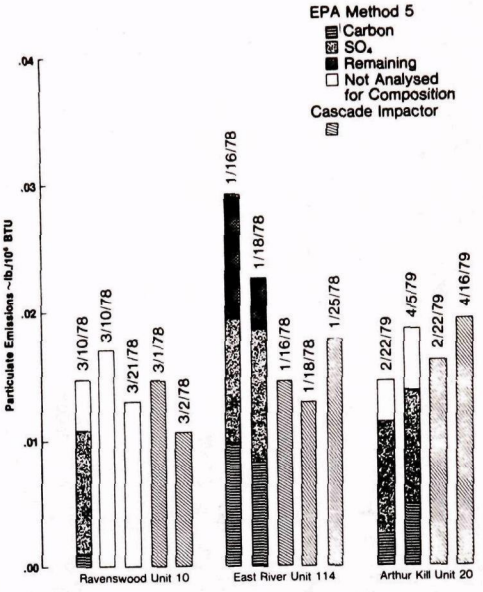

# A CONTINUOUS REAL-TIME PARTICULATE MASS MONITOR FOR STACK EMISSION APPLICATIONS*†

By: James C. F. Wang
Combustion Research Division
Sandia National Laboratories, Livermore, CA

Harvey Patashnick and Georg Rupprecht
Rupprecht and Patashnick Company
Englewood, CO

## ABSTRACT

The mass loading and size distribution of particulate emissions from industrial stacks are critical parameters which the EPA uses for air pollution monitoring and control. Commercially available instruments for detection of particulates are either optical types, which do not measure particle mass directly, or sampling types which do not provide real-time measurements. Last year we demonstrated the feasibility of using the tapered-element oscillating microbalance (TEOM) for real-time particle mass measurements at room temperatures. Currently, we are developing a new TEOM for high temperature applications (up to 300 C). Other features of this new real-time mass monitor include periodic backflush for long-duration continuous operations and an interface to a multi-staged cyclone-train for real-time aerodynamic particle size distribution measurements. Fractional particulate mass loadings, at 50% cut size of 1, 3 and 10 μm, are obtained using the modified cyclones in the Source Assessment Sampling System (SASS). Test data on the performance of this new TEOM/cyclone system are reported.

## INTRODUCTION

The mass loading and size distribution of particulate emissions from industrial stacks are the critical parameters which the EPA uses for air pollution monitoring and control. Presently, commercial particle detectors are either optical devices which do not measure particle mass directly, or physical sampling devices which do not provide real-time measurements. Furthermore, the accuracy of these measurements suffers from many inherent shortcomings in the instruments when they are adapted from the laboratory bench to an industrial stack. For example, the optical properties of the particulate matter are required for optical techniques, but in a stack exhaust, these properties are generally not known a priori and many also

*Presented at the Third Symposium on the Transfer and Utilization of Particulate Control Technology, Orlando, Florida, March 9-12, 1981.
†This work supported by the Department of Energy, the Office of Fossil Energy.

change in time. Maintaining a clean window for optical access is also a very difficult task.

Physical sampling techniques, on the other hand, involve sample withdrawal by a probe, with consequent dilution or cooling of the sample, or both. Also, the particle size in the sample may change because of agglomeration and condensation of gaseous species during dilution or cooling. Furthermore, the particle analysis is usually performed off-line and may be biased or dubious because of difficulties associated with redispersion of the particles in the analyzer.

Recently, at Sandia National Laboratories we have demonstrated the feasibility of using the tapered-element oscillating microbalance (TEOM) for real-time particle mass measurements at room temperature.(1) This mass monitor measures the actual weight of the particles collected from a sampled gas stream in real time. Thus, measurement biases of the type encountered in conventional physical sampling techniques are minimized.

To further improve the measurement accuracy of the physical sampling technique, we are developing a new TEOM for high-temperature applications (up to 300°C) in which the sampled gas can be kept at the stack gas temperatures during measurements. Furthermore, the new TEOM is designed to be interfaced to a multistaged cyclone train (one TEOM per cyclone) for real-time aerodynamic particle size fraction measurements. This new TEOM/cyclone system has been designed, laboratory tests on various components have been conducted, and preliminary results on these tests are reported in this paper.

## NEW TEOM/CYCLONE SYSTEM

The new TEOM detector operates on the same principle as that of the room temperature device reported previously.(1) Figure 1 shows the schematic of the TEOM detector. Briefly, the tapered fiber element is clamped rigidly at the wide end with high-temperature cement. A dust collection cup is mounted rigidly on top of the narrow end of the tapered element, which is set in oscillation between a set of electrically charged plates. The oscillation of the fiber element is monitored by an LED and a photo-transistor at 90° to the direction of the oscillation. Because of the temperatures encountered, the LED and photo-transistor are placed in a box outside the detector assembly. Two high-temperature optical fibers are used to transmit the LED signal and to carry the oscillation signal to the photo-transistor, respectively. The oscillation signal from the photo-transistor is then amplified and fed to the conductive surface of the TEOM fiber. This feedback arrangement maintains the fiber oscillation, whose natural frequency will change in relation to the mass deposited on the dust collection cup. The sensitivity and frequency can be chosen at will by proper dimensioning of the oscillating tapered element.

Three cyclones used to aerodynamically separate particles in the sampled stream were originally part of a Source Assessment Sampling System from Acurex Corp. They are modified here to interface with TEOM detectors for real-time particle fraction measurements. The 50 percent cut sizes of these cyclones at room temperature and atmospheric pressure are 1, 3, and 10 μm . With modifications to accommodate the TEOM detectors and changes in operating

conditions, the 50 percent cut sizes and collection efficiency curves of these cyclones are expected to change.(2) A calibration test for the cyclones with modifications for high-temperature and high-pressure conditions is planned.

Figure 2 shows the interface between the 3 μm cyclone and the TEOM detector. A funnel is placed under the dust outlet of the cyclone to guide the dust onto the dust collection cup. Our flow visualization tests indicate that a gap of less than 6 mm between the bottom of the funnel and the cup is desirable to ensure complete dust collection on the cup. A high-speed air jet is designed to blow the dust out through the side holes periodically to clean the TEOM detector. Currently, we are testing this concept for self-cleaning operation and have not finalized the design yet.

Figure 3 shows the schematic of the total assembly of the TEOM/cyclone system. An oven housing the cyclone train and TEOM detectors is capable of keeping the internal temperature at levels up to 230C. A secondary sampling line in the exhaust of the third cyclone is designed to be connected to a fourth TEOM detector, which will be operated with a positive suction filter attached to the tapered element to measure particles less than 1 μm. However, this secondary sampling line is currently not implemented.

Because the cyclone cut size depends on the sampling velocity, in our preliminary tests we decided to sample the gas at a fixed flow rate for consistent particle size-fraction measurements. This introduces a nonisokinetic sampling error which must be accounted for in the data interpretation.

## PRELIMINARY TEST RESULTS

In laboratory tests of the TEOM/cyclone system, conducted on the atmospheric combustor exhaust simulator (ACES) (3) at Sandia, fly ash from the Exxon pressurized Fluidized Bed was injected into the ACES by a cyclone-type fluidized bed dust feeder. The weight loss of the dust feeder was measured in real time by an electronic scale and was related directly to the dust loading in the sampled stream. The rate of dust injection was controlled by the fluidizing air velocity in the dust feeder and could be changed within a few seconds. With this feeder assembly, the dust loading density in the test section of the ACES can be varied between 0 and 15 $g/m^3$. The fly ash used was classified at a mean diameter of 5 μm and a standard deviation of 1.5 μm.

An original SASS train sampling system from the Acurex Corporation was used, including sampling probe, cyclones, and oven. Only the 3 μm cyclone was modified to have a TEOM detector coupled at its dust outlet. Regular dust collectors were used for the 10 and 1 μm cyclones. The sampling flow was established with a vacuum pump and measured with a mass flow meter. Because of the size distribution of the fly ash, most of the particles were collected by the 3 μm cyclone. The accumulated weight of the dust collected at the 3 μm cyclone was measured in real time by the TEOM detector and compared with the weight loss of the dust feeder.

The sampling system was tested in three temperatures, 20, 130 and 190 C. During each test, the dust feeding rate was changed to test the time response of the TEOM detector. At the end of each test, the dust collection cup of the

TEOM detector was removed and weighed to compare the total dust weight with that from the TEOM frequency shift measurement. Close agreement of the total dust weight with that measured by the TEOM detector was obtained in every test; the discrepancy between the two was always less than 2 percent. However, the calibration factor which converts the frequency shift measured by the TEOM detector to the dust weight must be obtained in the actual measurement environment to achieve this accuracy.

Figure 4 shows typical real-time measurements of the dust collected at the 3 μm cyclone compared with the weight loss of the dust feeder at room temperature. At the end of the test, the total weight loss from the feeder and the total weight gain from the dust collected on the TEOM were compared, and the ratio of these two final weights yielded a constant factor used to scale both measurements for comparison throughout each test. It is noteworthy that this scale factor changes for tests performed at different conditions and/or arrangements. Moreover, this scale factor, SF, is proportional to (1) the ratio of the total flow rate, $Q_T$, in the test section and the sampling flow rate, $Q_S$, and (2) wall losses of sampled particles in the sampling probe and cyclones, $W_L$.

$$SF = \frac{Q_T}{Q_S}\left(1 + \frac{W_L}{W_C}\right) \qquad (1)$$

where $W_C$ = weight gain on the TEOM dust collection cup. If one has fixed total and sampling flow rates, the scale factor provides a direct measurement of wall losses of the sampling system.

Figure 4 shows close agreement between the dust collected at the TEOM and the weight loss in the dust feeder as a function of time. The same slope changes were obtained from the TEOM output at the instant the dust feed rate changed. Similar results were obtained at 130 and 190 C, as shown in Figures 5 and 6, respectively. The closeness of the agreement shown in these figures indicates that the TEOM/cyclone arrangement works properly and is capable of providing real-time particle size fraction measurements at conditions which simulate power plant exhaust stack environments.

Because only one scale factor was used in each test, the results shown in Figures 4 through 6 indicate that the ratio of dust collected on the TEOM cup to the wall loss of particles in the sampling probe and cyclones is constant throughout each test. If particles come off from walls of the sampling probe and cyclones during operation, the TEOM detector should pick up these particles and the weight gain should deviate from the weight loss curve of the dust feeder. Similarly, if the particle wall loss is not related by a constant factor to the particles collected, the TEOM output will not closely follow the weight loss curve of the feeder. However, there may be an incubation time required for the particle deposition on the wall to reach a saturation or equilibrium state. We did not test the TEOM/cyclone system long enough to observe these conditions.

Figure 7 shows the effect of temperature on particle wall loss, which is calculated from Eq. (1) based on the measured flow rates, $Q_T$ and $Q_S$, and the TEOM weight gain, $W_C$. In the present sampling system, it is evident that the

particle wall loss is reduced as the temperature of the sampled gas is increased. This result can be attributed to the fact that the fly ash used becomes less sticky at higher temperatures. It is also an important reason to insist that stack sampling be performed at the characteristic temperature of the stack gas for minimizing measurement errors.

## CONCLUSIONS

The new TEOM detector has been demonstrated to measure particle mass in real time at stack gas temperatures (up to 200 C). The combination TEOM and cyclone also provides aerodynamic particle size-fraction measurements. The importance of sampling at stack gas temperatures and in real time has also been clearly shown. A complete real-time TEOM/cyclone particle size-fraction monitor is being assembled and is scheduled to be tested in the near future.

## ACKNOWLEDGEMENTS

The authors wish to thank E. Porter for his help in performing the experiments and M. A. Libkind for many helpful discussions. This work is sponsored by the Office of Fossil Energy, U.S. Department of Energy, and is a part of the Sandia National Laboratories Diagnostics Assessment for Advanced Power Systems Program.

## ENDNOTES

1. Wang, J.C.F., H. Patashnick, and G. Rupprecht, "A New Real-Time Isokinetic Dust Mass Monitoring System," APCA Journal, Vol. 30, No. 9, September 1980, pp 1018-1021.

2. Parker, P., R. Jain, S. Calvert, D. Drehmel, and A. Abbott, "Particle Collection in Cyclones at High Temperature and Pressure," submitted to Environmental Science and Technology, October 15, 1980.

3. Wang, J.C.F., "Combustor Exhaust Simulation Facilities," Sandia Combustion Research Program Annual Report 1979, UC-96, Sandia National Laboratories, Livermore, CA, pp 15-16.

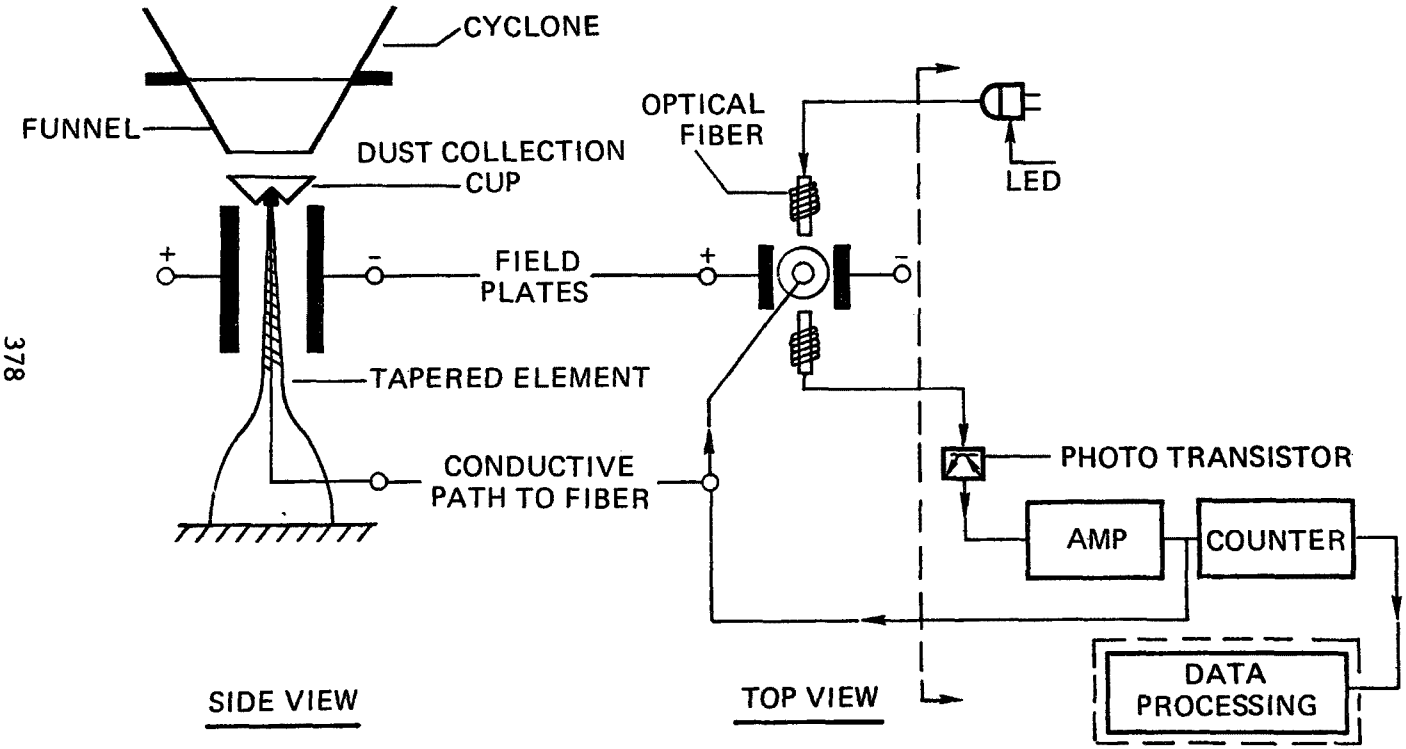


Figure 1. Schematic of the High Temperature TEOM Detector

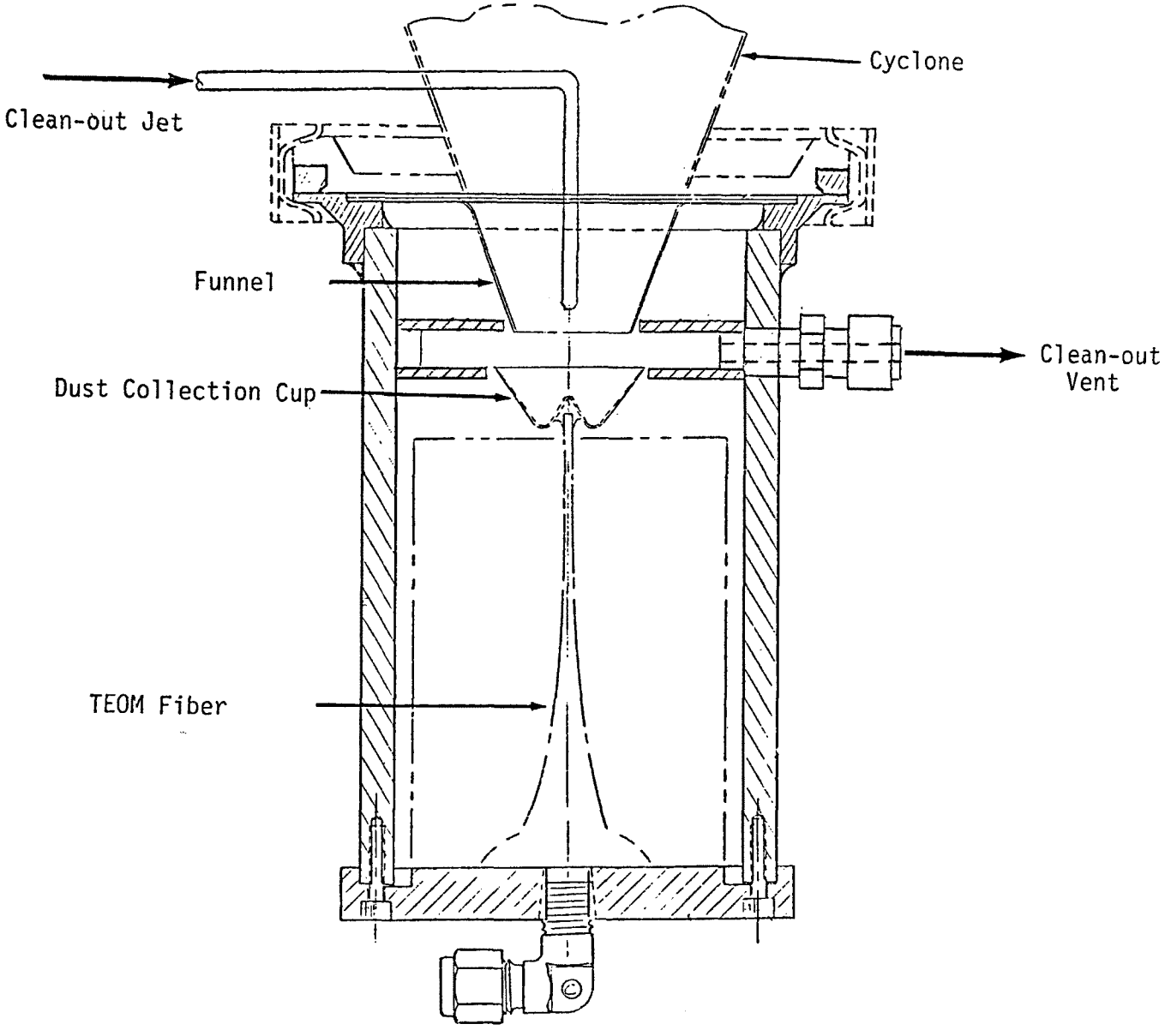


Figure 2. Schematic of the Interface Between Cyclone and TEOM

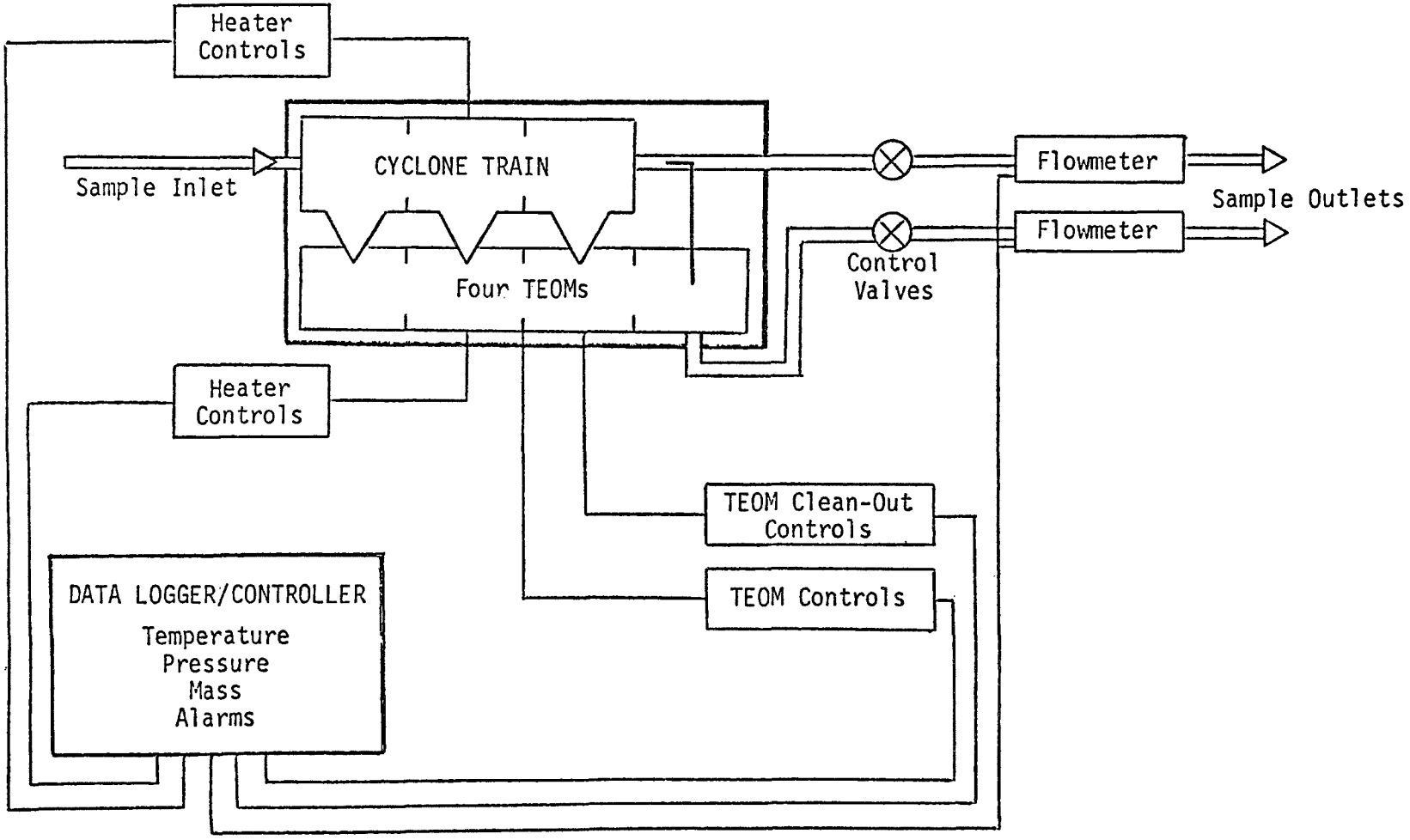


Figure 3. Schematic of the Real-Time Particle Mass Monitor

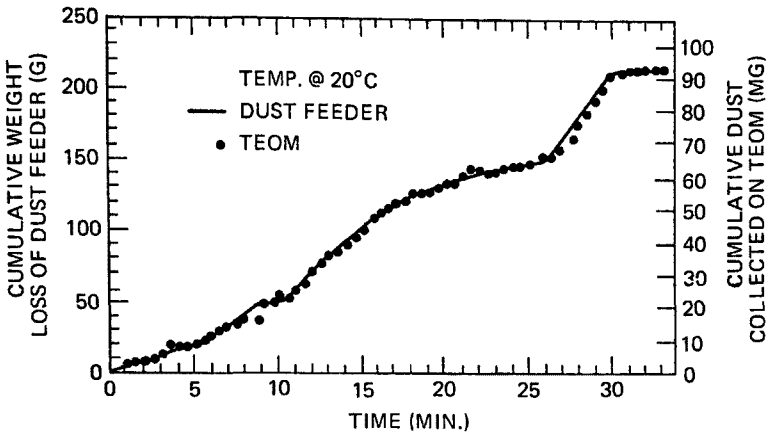


Figure 4. Real-Time Test Results of the TEOM/Cyclone System at 20°C

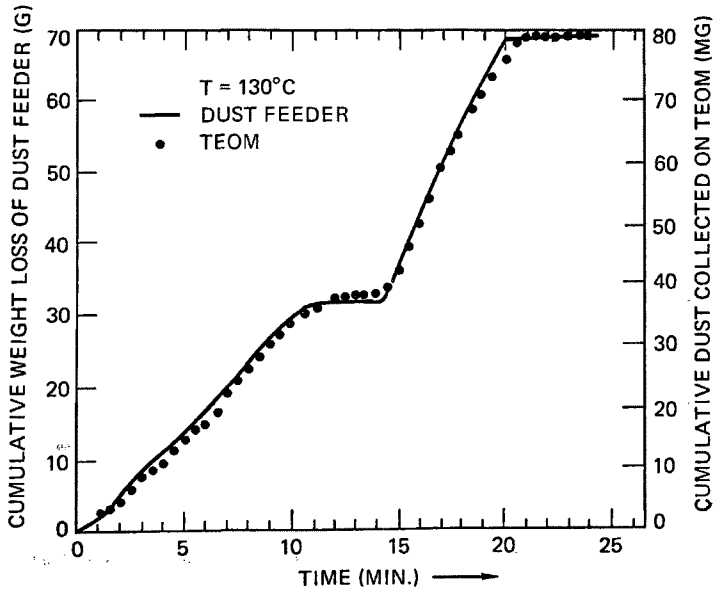


Figure 5. Real-Time Test Results of the TEOM/Cyclone System at 130°C

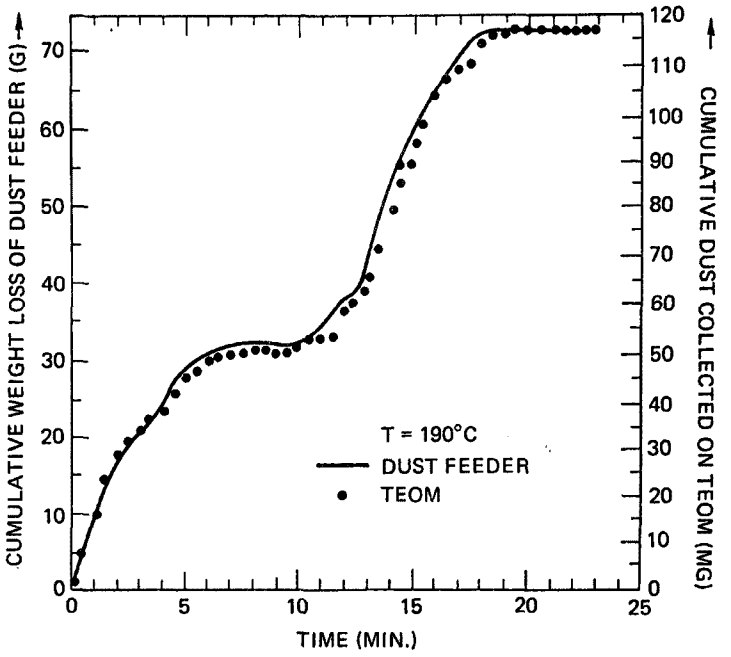


Figure 6. Real-Time Test Results of the TEOM/Cyclone System at 190°C

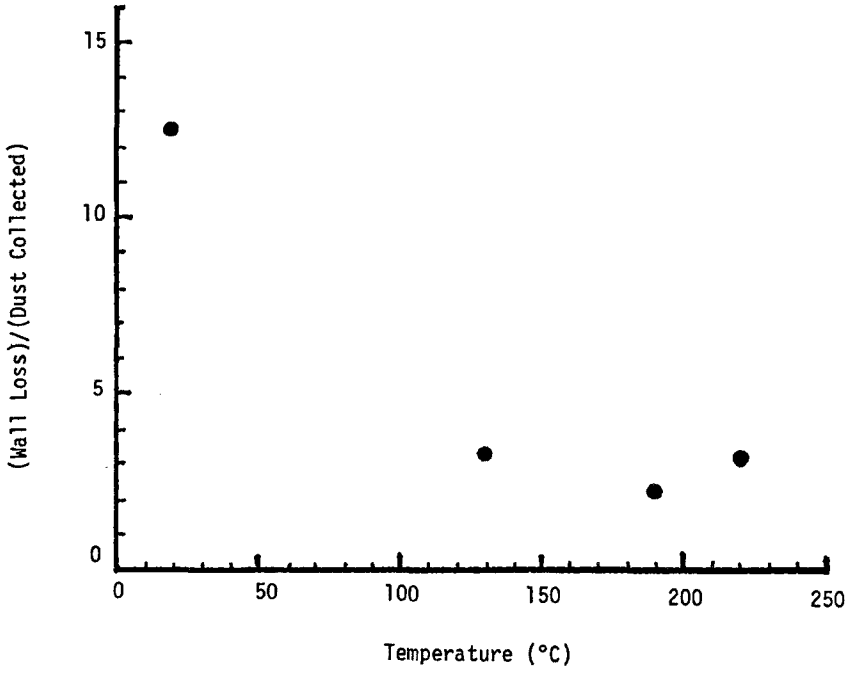


Figure 7. Effect of Sampling Temperature on Particle Wall Loss

# STUDIES OF PARTICULATE REMOVAL FROM DIESEL EXHAUSTS WITH ELECTROSTATIC AND ELECTROSTATICALLY-AUGMENTED TECHNIQUES

By: James L. DuBard, M. Greg Faulkner, Jack R. McDonald
Southern Research Institute
2000 Ninth Avenue, South
Birmingham, Alabama 35255

Dennis C. Drehmel, James H. Abbott
Industrial Environmental Research Laboratory
U.S. Environmental Protection Agency
Research Triangle Park, N.C. 27711

## ABSTRACT

Laboratory experiments on a 5.7 liter GM diesel truck have established the concept of removing particulate emissions from diesel exhaust by a combination of agglomeration and trapping devices. A two-stage electrostatic precipitator (ESP) is used to agglomerate the primary particulate matter, resulting in an order-of-magnitude increase in mass median diameter. The agglomerated particulate is characterized. Aerosol sampling data are presented for the variation in particle size distribution and the efficiency of trapping the agglomerated particulate in cyclones, fiber filters, and a granular bed filter. Overall mass removal efficiencies greater than 80% have been achieved with an ESP/granular bed filter system for a duty distance greater than 800 km (500 miles) at a constant highway speed of 88 km/hr (55 mph). Methods of cleaning the devices and removing collected particulate are discussed.

## INTRODUCTION

This paper will discuss the application of electrostatic gas cleaning technology to the aftertreatment of vehicular diesel exhaust. Electrostatic precipitation has the possible advantage of high-efficiency collection of submicron diesel particulate matter with low engine backpressure and the expenditure of low electrical power. On the other hand, the low resistivity of the diesel particulate matter leads to the possible difficulties of surface current leakage through sooty deposits on insulators and poor particle adhesion to the collection plates. Electrostatic gas cleaning devices were tested on the exhaust from a 5.7 liter GM diesel pickup truck mounted on a chassis dynamometer.

## ELECTROSTATIC PRECIPITATOR

An electrostatic precipitator (ESP) was developed and tested at Southern Research Institute in Birmingham, Alabama(1). The ESP is a cylindrical, two-stage device designed to obtain maximum collecting plate area in a small volume (Figure 1). It is designed to be periodically wet-flushed in a vertical orientation. The internal diameter (ID) of the cylinder is 20 cm (8 in.). A volume gas flow of 6.2 $m^3$/min (220 ACFM) at 88 km/hr (55 mph)

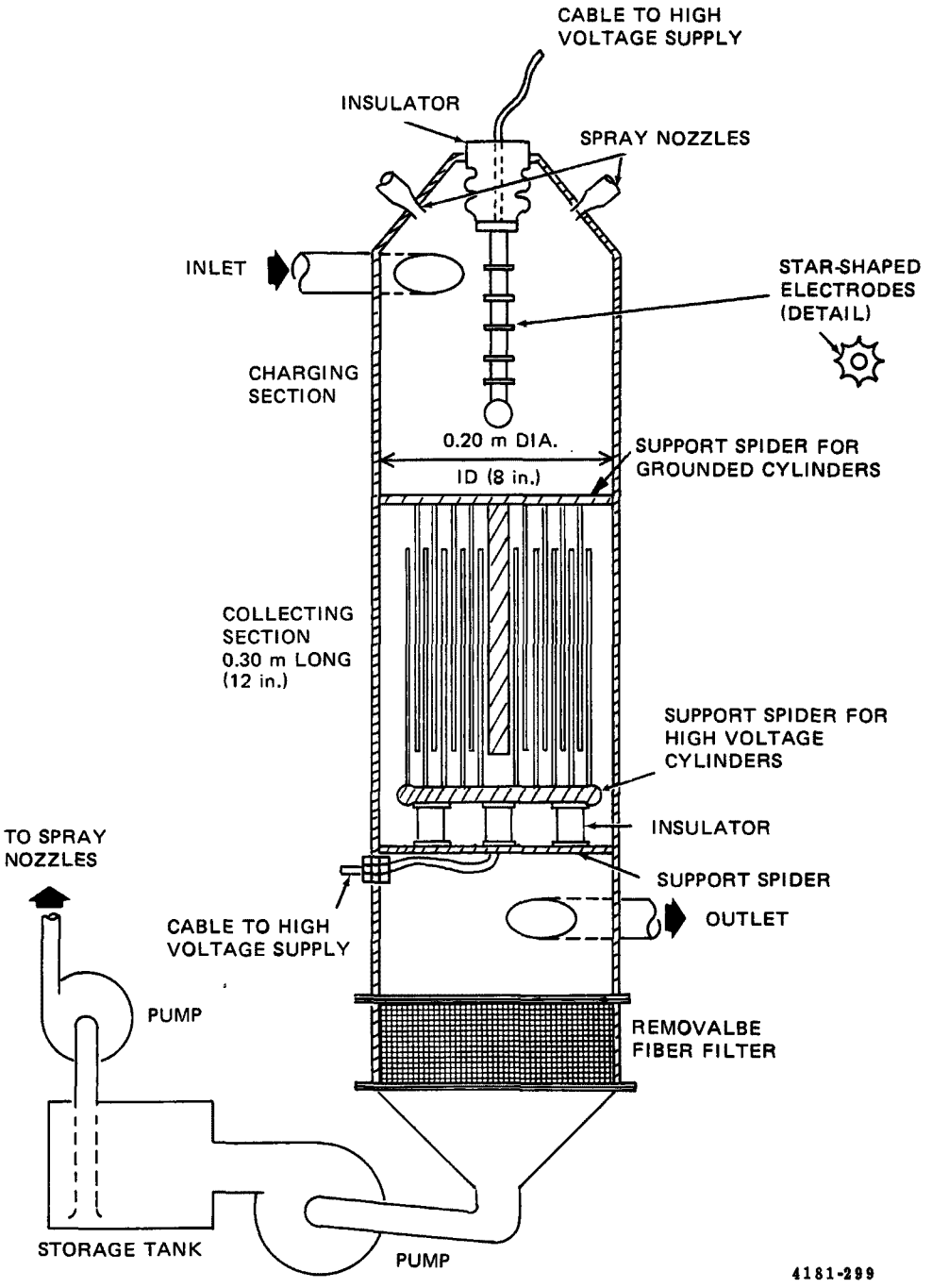


*Figure 1. Schematic diagram of the electrostatic precipitator.*

gives an average linear gas flow down through the ESP of 3.2 m/sec. For the charging section, five star-shaped corona electrodes are mounted on a vertical high-voltage rod chosen for mechanical strength. The corona electrodes are typically operated at 40 kV (negative) and about 250 μA. The product of negative ion density and gas treatment time in the corona section is

$$N_0 t \simeq 0.6 \times 10^{13} \text{ sec/m}^3,$$

at an electric field of approximately $4 \times 10^5$ volt/m. The electric field for particle charging could be increased with the use of improved high voltage insulation.

The collector section is a set of concentric cylinders (overlapping length 28 cm), alternately grounded and biased negative. The total collecting area is 1.18 $m^2$ (12.7 $ft^2$). For a volume flow of 6.2 $m^3$/min (220 ACFM), the specific collection area is about 11.3 $m^2/(m^3/sec)$ (58 $ft^2$/1000 ACFM). The collector cylinders have a nominal spacing of 0.6 cm. After wet-flushing loose particulate, the cylinders will hold about 6 kV without arcing. In order to increase the collecting electric field, the voltage is increased typically to 15 kV, with steady arcing carrying about 1.5 mA. Then the collecting electric field is about $24 \times 10^5$ volt/m.

Early tests of the ESP produced little permanent collection of diesel particulate. Preliminary mass train sampling (non-isokinetic) indicated an overall mass removal efficiency in the neighborhood of 30 to 40%. Later measurements (with cascade impactors and a backup filter) of the mass removal efficiency of the ESP gave values of about 26%. While the ESP achieved only low collection of diesel soot, there was on the other hand a substantial agglomeration of the particles. Electrical aerosol size analyzer data showed roughly 50 to 70% removal of particles of aerodynamic diameter on the order of 0.1 μm. This phenomenon was easily confirmed by visual observation of some macroscopic agglomerates. Microscopic examination of particles at the ESP outlet showed a preponderance of very loose and fluffy agglomerates on the order of 25 μm in actual size. Settling velocity experiments with large agglomerates indicated that the aerodynamic diameter was roughly 1/10 the physical particle diameter. This was consistent with later cascade impactor measurements of the mass median diameter (mmd) at the ESP outlet. Subsequent testing of the ESP was designed to emphasize its role as an agglomerator, with the ESP followed by some other device for trapping the agglomerated diesel soot.

The electrical resistivity of the diesel soot is of concern in regard to surface conduction through sooty deposits on insulating standoffs in the ESP. The resistivity of a bulk sample of diesel soot collected at the ESP outlet was measured in moist air using an ASME PTC-28 test cell. The soot was compacted as little as possible. With temperature and moisture content comparable to those of the diesel exhaust gas, the resistivity of the fluffy agglomerated soot measured about $10^7$ ohm-cm.

Several common cleaning fluids were bench-tested for effectiveness in cleaning the ESP. The fluids were tested both on bulk samples of diesel soot and on soot layers impacted on metal parts. Perchloroethylene, a common dry

cleaning fluid, was chosen for cleaning the ESP because it is effective, nonflammable, and of relatively high boiling point and low toxicity.

The ESP was occasionally flushed after the device had cooled down overnight. About 1 gallon (4 liters) of perchloroethylene was pumped directly from a supply container through four spray nozzles in the top of the ESP. The dirty fluid flowed directly from an outlet in the bottom of the ESP into a take-up container. Teflon insulators were thoroughly cleaned, but there always remained a thin film of soot on metal surfaces which could not be removed by any cleaning fluid (without rubbing).

One problem in the aftertreatment of diesel exhaust is the collection and handling of the large volume of low bulk density soot (roughly 120 $kg/m^3$). An advantage of wet flushing with perchloroethylene is that the collected soot is left in a highly compacted state when the dirty cleaning fluid is evaporated (to be followed by condensation in a closed system). The measured bulk density of dry residue from the wet-flushing procedure was 1300 $kg/m^3$.

## ESP/CYCLONE

Three series of tests were conducted on three different ESP/cyclone combinations, with the diesel truck running at 88 km/hr (55 mph). First, a Fisher-Klosterman XQ-4 industrial cyclone was connected in the exhaust line after the ESP. The cyclone was calibrated by the manufacturer under ambient conditions to have a $D_{50}$ cutpoint of 2.0 μm for a volume gas flow of 5 $m^3$/min (180 ACFM). By Lapple's law, the $D_{50}$ cutpoint extrapolates to 1.6 μm under actual operating conditions (175°C, 2.5 x $10^{-5}$ Pa•sec, 6.2 $m^3$/min, 36.5 m/sec). Performance of the ESP/cyclone combination was tested by extracting samples of the exhaust gas through cascade impactors. Three test stations were used to accumulate data simultaneously at the outlets of the diesel truck, the ESP, and the cyclone. Average results of several tests are shown in Figure 2.

The agglomeration of carbon soot by the ESP is demonstrated in Figure 2 in that the aerodynamic mmd at the ESP outlet is increased by roughly one order of magnitude to about 2.5 μm. (On the basis of electrical aerosol size analyzer data combined with cascade impactor data, the mmd of the primary diesel particulate is known to be approximately 0.3 μm.(1)) The total mass loading of the impactor stages plus backup filter was 37.0 mg/scm at the truck outlet and 27.2 mg/scm at the ESP outlet. The ESP alone achieved about 26% mass removal efficiency.

Figure 2 shows that about 56% of the diesel particulate at the ESP outlet had an aerodynamic diameter greater than the extrapolated $D_{50}$ cutpoint of the cyclone. However, the total mass loading at the cyclone outlet was 34.7 mg/scm, 28% greater than at the ESP outlet. There was evidently substantial hydrocarbon condensation in the gas stream passing through the cyclone. Figure 2 shows also that the mmd of the diesel particulate was greatly reduced (to about 0.9 μm) in passing through the cyclone. This was not due to collection of large particles in the cyclone because only a very small amount of diesel soot was retained in the cyclone catchpot. The decrease in mmd could have resulted both from hydrocarbon condensation and from

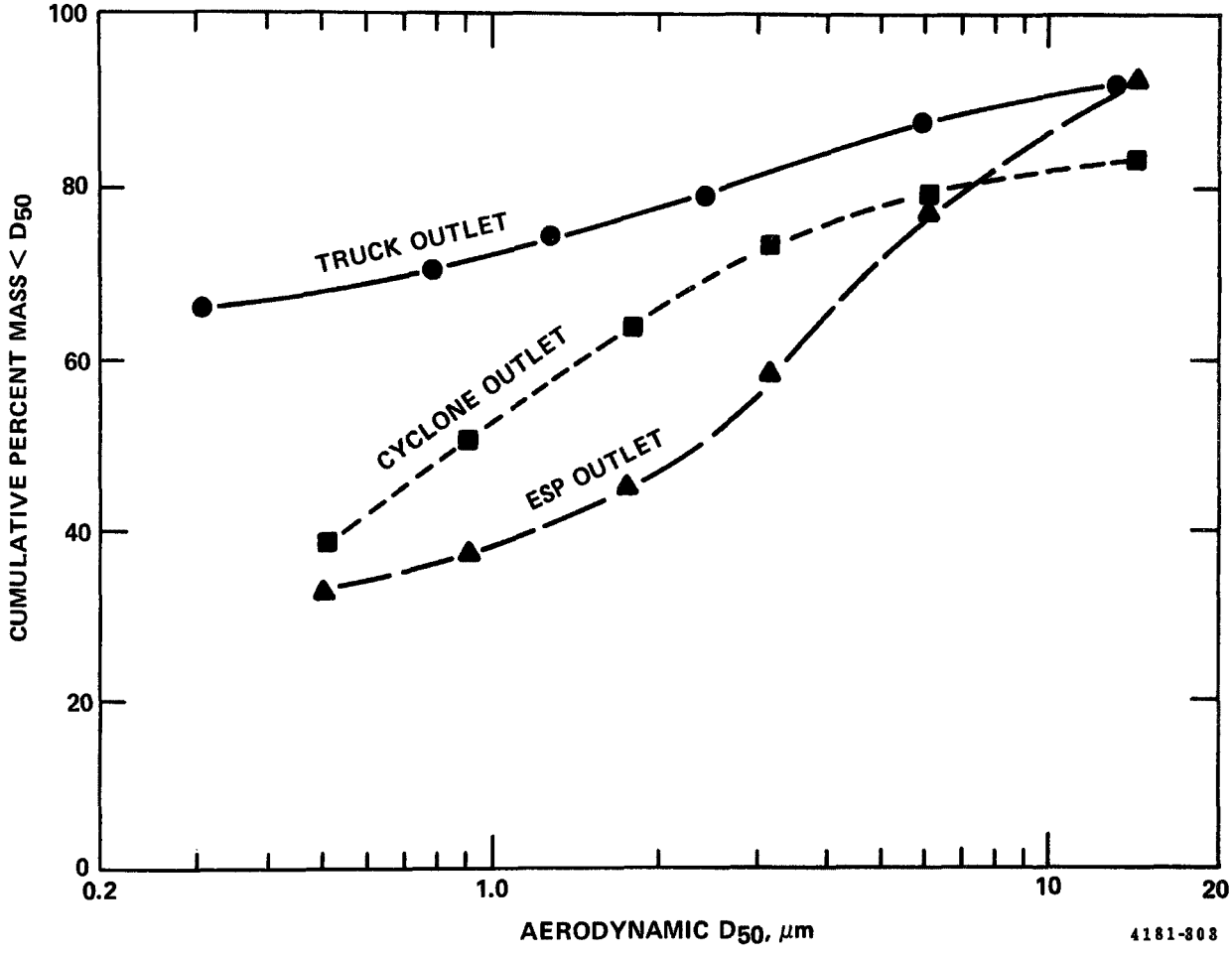


*Figure 2. Impactor testing of ESP/cyclone combination cumulative percent mass of aerodynamic diameter less than the $D_{50}$ cutpoint.*

breakup of the fluffy, agglomerated soot particles in the vortex of the cyclone, in reentrainment from the cyclone catchpot, or in the impactor jets.

The concept of an ESP/cyclone combination was tested further with a small five-stage cyclone system designed and calibrated for in situ stack sampling. In this case, a gas sample at the ESP outlet was extracted through the five-stage cyclone at 170°C and 0.03 $m^3$/min (1 ACFM). The corresponding calibrated $D_{50}$ cutpoints are 8.3, 3.9, and 2.5 μm for the first three cyclones, and an estimated 1.1 and 0.5 μm for the last two cyclones. A total of 136 mg of diesel particulate was collected in the cyclones (57%) and on the backup filter (43%). The measured mass distribution is displayed in Table 1. The five-stage cyclone data are compared with the cascade

TABLE 1. CUMULATIVE PERCENT MASS > $D_{50}$ OF DIESEL SOOT AGGLOMERATED BY THE ESP

| | 8.3 μm | 3.9 μm | 2.5 μm | 1.1 μm | 0.5 μm |
|---|---|---|---|---|---|
| Cascade Impactors (From Figure 2) | 17% | 35% | 49% | 61% | 67% |
| Five-Stage Cyclone | 24% | 35% | 44% | 50% | 57% |

impactor data, where the cumulative percent mass of aerodynamic diameter greater than the $D_{50}$ cutpoint is extracted from the ESP OUTLET curve of Figure 2. The five-stage sampling cyclone collects roughly the expected amount of agglomerated diesel particulate.

Finally, tests were conducted on various combinations of sampling cyclones, with diesel exhaust gas samples (at the ESP outlet) pulled through the cyclones at much higher flow rates than that for which they were designed. The concept under investigation was that if such a cyclone could collect agglomerated diesel particulate efficiently at a flow rate of .55 to .85 $m^3$/min (20 to 30 ACFM), then the total exhaust gas flow out of an ESP agglomerator could be passed through a parallel array of perhaps 10 such cyclones.

The tests were conducted with the diesel truck running at 88 km/hr (55 mph) and cyclone sampling gas temperatures approximately 170°C (340°F). The cyclone combinations were tested at flow rates of .55 and .80 $m^3$/min (20 and 28 ACFM). Particulate masses collected in the cyclone catchpot and in a backup filter were measured. The three cyclones used were designated 9, 3, and 4, with specifications as follows:

Cyclone 9 - Large IP (inhalable particulate) Cyclone
$D_{50}$ = 15 μm at .015 $m^3$/min, 22°C

Cyclone 3 - Small IP Cyclone (mounted inside Cyclone 9)
$D_{50}$ = 2.5 μm at .015 $m^3$/min, 22°C

Cyclone 4 - Cyclone 4 of the Five-Stage Sampling Cyclone
$D_{50}$ = 0.6 μm at .03 $m^3$/min, 22°C
$D_{50}$ ≃ 1.1 μm at .03 $m^3$/min, 170°C

Results of testing the cyclones at high flow rates are given in Table 2. These tests indicate that an ESP agglomerator followed by cyclonic trapping

TABLE 2. SUMMARY OF TESTING SMALL CYCLONES AT HIGH GAS FLOW RATES

| Cyclone | Flow Rate $m^3$/min | Pressure Drop kPa (in. $H_2O$) | Mass in Catchpot % |
|---|---|---|---|
| 9 | 0.55 | 1 (4) | 23 |
| 9 and 3 | 0.55 | 56 (14) | 52 |
| 9 and 3 | 0.80 | 96 (24) | 52 |
| 4 | 0.80 | 96 (24) | 37 |

of agglomerated particulate is a viable concept for aftertreatment of diesel exhaust. The mass removal efficiency of such a device is at least 50%. The mass removal efficiency can be improved by extensive engineering and testing to match the cyclone performance to the characteristics of the agglomerated diesel particulate. Methods for disposal of the trapped diesel particulate require further investigation. An ESP will require cleaning sooner or later, by wet flushing or air jet scouring. Soot collected in the cyclone catchpot will have to be removed and compacted. During the tests of the ESP in combination with other devices, it was necessary to clean the collector cylinders by wet flushing with perchloroethylene after 16 to 20 hours of operation with the diesel truck running at 88 km/hr.

## ESP/GRAVEL BED FILTER

The gravel bed filter, previously tested on primary diesel exhaust(2), was connected in the exhaust line after the ESP to test the concept of using a granular filter to trap diesel particulate that had been agglomerated in the ESP. Three series of tests were conducted with different configurations of the gravel bed and at different diesel truck speeds.

The ESP/gravel bed filter was tested first at a diesel truck speed of 88 km/hr (55 mph). The gravel bed consisted of a 10 cm depth of 2 mm steel

shot supported on a screen in a drum of diameter 45 cm (18 in.). Cascade impactor data for the ESP/gravel bed combination are shown in Figure 3. The combination was tested with and without stirring of the surface of the gravel with a rake to break up the cake of carbon soot that forms on the surface. Stirring resulted in a large puff of collected carbon soot passing through the exhaust line. The curve labeled WITH STIRRING represents average data for runs which included one stir in the middle of each 30 minute data collection run. The curve labeled WITHOUT STIRRING represents average data for runs taken over 3 days, with the gravel bed stirred once each day before the beginning of testing. This daily stirring typically reduced the engine backpressure from a maximum value of 17 kPa (68 in. $H_2O$) to about 12 kPa (48 in. $H_2O$). The mass removal efficiency did not vary measurably with the change in engine backpressure.

TABLE 3. TOTAL MASS LOADINGS MEASURED FOR THE ESP/GRAVEL BED COMBINATION

| Sampling Point | Total Mass Loading mg/scm |
|---|---|
| Truck Outlet | 37.7 |
| ESP Outlet | 27.7 |
| Gravel Bed Outlet | |
| with stirring | 20.7 |
| without stirring | 5.4 |

The total mass loading of the impactor stages plus backup filter is summarized in Table 3. The ESP alone achieved about 26% mass removal efficiency, as in previous cascade impactor testing of the ESP/cyclone combination. The overall mass removal efficiency, without stirring the gravel bed, was 86%. The data in Figure 3 show that the mmd of the agglomerated diesel soot (about 3.5 μm) greatly decreases when the gas stream passes through the gravel bed. This is the result of larger particulate being trapped in the gravel bed.

Figure 4 shows electrical aerosol size analyzer data for the ESP/gravel bed combination, with the diesel truck running at 88 km/hr. These data show the effect of the treatment devices on the very fine particulate matter that is predominant in the primary diesel exhaust. In the aerodynamic size range around 0.1 μm, the ESP alone achieved 60 to 70% removal of particulate mass. The addition of the gravel bed resulted in only a small improvement in mass removal in this small size range. The main function of the gravel bed is to trap the particulate mass which has been shifted to a larger size range by the ESP.

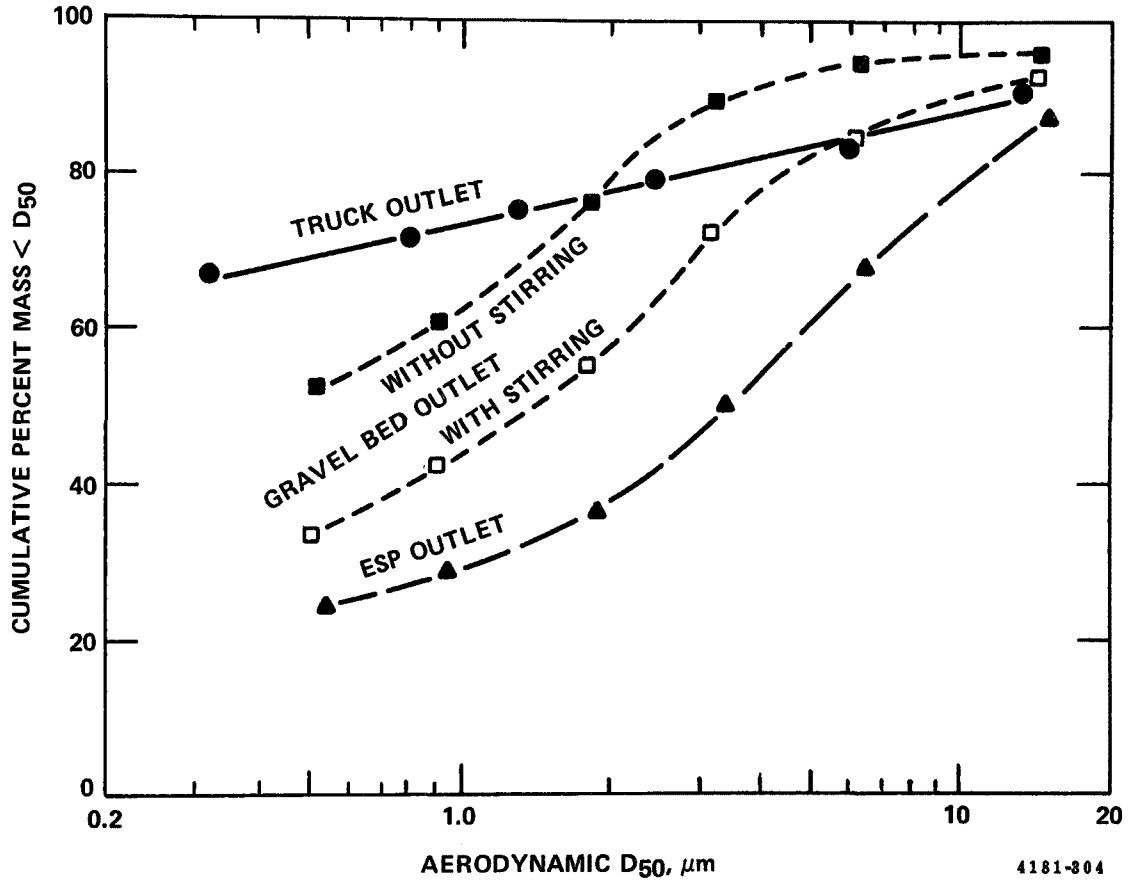


*Figure 3. Impactor testing of ESP/gravel bed combination cumulative percent mass of aerodynamic diameter less than the $D_{50}$ cutpoint.*

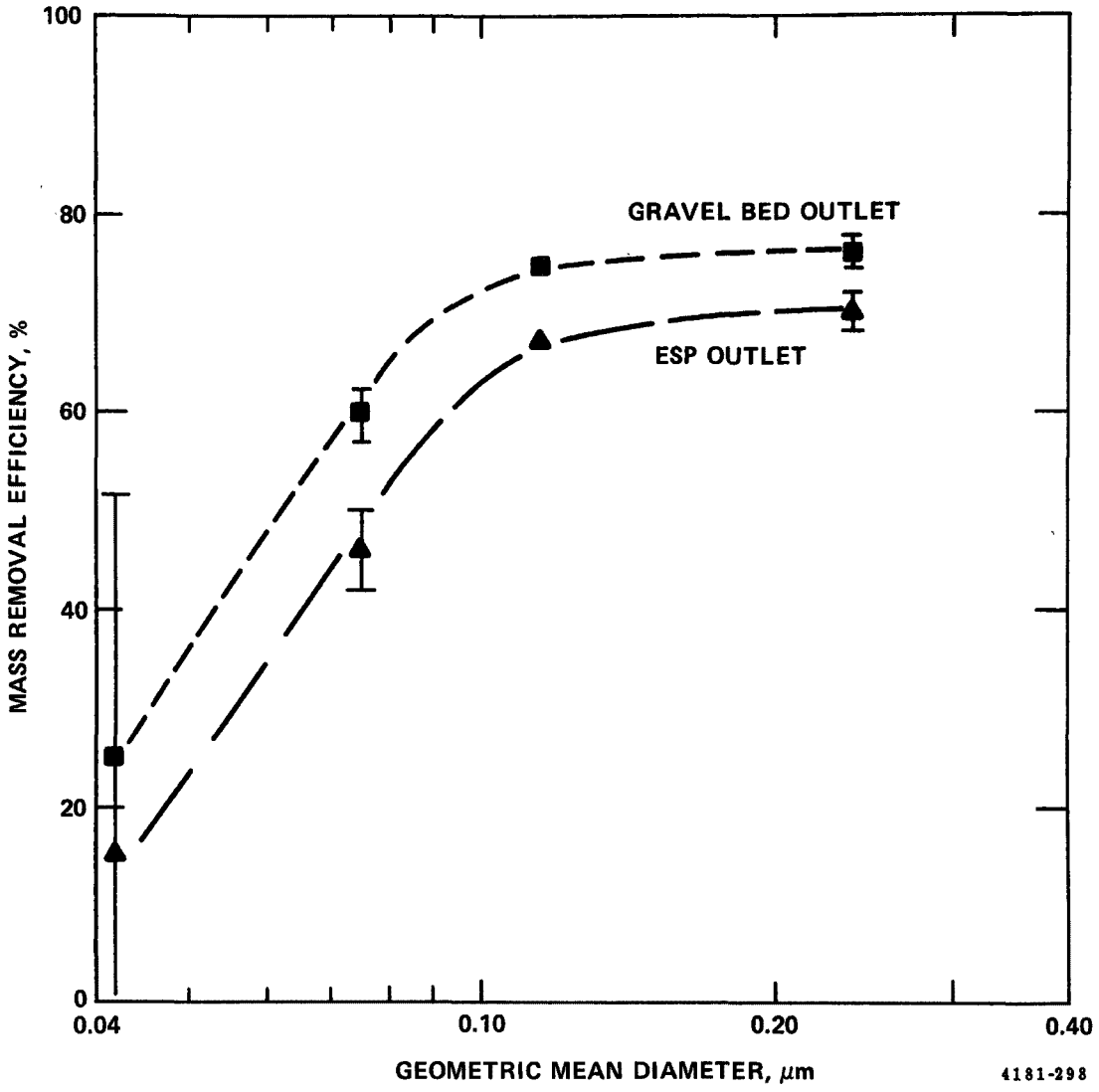


*Figure 4. Mass removal efficiency in small size ranges of diesel particulate.*

Secondly, the ESP/gravel bed combination was tested (without stirring) with the diesel truck running at 24 km/hr (15 mph). These tests were intended to simulate lower speeds and smaller displacement engines. The engine backpressure remained steady at about 2.5 kPa (10 in. $H_2O$). With the decrease in truck speed, the exhaust gas volume flow decreased from approximately 6.2 $m^3$/min (220 ACFM) to 2.2 $m^3$/min (80 ACFM) at 95°C (205°F). The particulate loading at the diesel truck outlet did not remain constant, but increased by roughly 75% to about 65 mg/scm. At the same time, the ESP/gravel bed combination collected more particulate mass per unit volume of gas flow at the lower gas flow. The overall mass removal efficiency was 83%, about the same as at 88 km/hr.

Finally, because the ESP/gravel bed combination had demonstrated high-efficiency cleaning of diesel exhaust gas for a practical operating time, the gravel bed was reduced to a more practical size. A gravel bed diameter of 20 cm was chosen, to correspond to the ID of the ESP and to achieve a reduction in filter area by a factor of 5. The diesel truck was operated at 88 km/hr. The mass removal efficiency was tested by mass train sampling at the diesel truck outlet and at the gravel bed outlet. Test results for gravel beds of depth 5 cm and 10 cm are summarized in Table 4.

TABLE 4. MASS REMOVAL EFFICIENCY OF THE ESP IN COMBINATION WITH AN 8-INCH DIAMETER GRAVEL BED FILTER

| Gravel Bed Depth cm | Engine Backpressure kPa (in. $H_2O$) | Outlet Mass Loading Truck mg/scm | Gravel Bed mg/scm | Efficiency % |
|---|---|---|---|---|
| 5 | 10 (40) rising to 15 (60) in 3 hours | 34.9 | 15.3 | 56 |
| 10 | 12 (48) rising to 16 (64) in 3 hours | 37.9 | 11.6 | 69 |

These tests indicate that a compact gravel bed filter can be contained within the housing of the ESP, directly below the collecting cylinders, and can achieve mass removal efficiency of 70%, or better, at acceptable levels of engine backpressure. The gravel bed filter can be cleaned simultaneously with the ESP by wet flushing with perchloroethylene. The mass removal efficiency of the ESP/gravel bed combination is largely independent of the running speed of the diesel truck. The higher mass loadings at lower exhaust gas flow rates are compensated by collection of greater particulate mass per unit volume gas flow by both the ESP and the granular filter. However, lower exhaust gas flow rates reduce the scouring of the insulating standoffs in the ESP and lead to more frequent cleaning periods.

## ESP/FIBER FILTER

Two types of ESP/fiber filter combinations were tested. First, the deep bed filter, previously tested on primary diesel exhaust(2), was loaded with fiberglass batts and connected in the exhaust line after the ESP. Then, the concept of agglomerating and trapping diesel particulate in a single compact device, with a removable cartridge filter, was tested with an electrified filter(1). This two-stage device was designed to transform high axial gas flow past a disk electrode in the corona charging section into a much lower radial gas flow in the collector section. The inner and outer sections of the collector assembly were loaded with various types of fiberglass filter media. The device had both electrical and mechanical forces acting to collect diesel soot.

The performance of these devices exhibited the behavior typical of all fiber filters tested: high mass removal efficiency (60 to 70%) but a lifetime of at most a few hours due to rising engine backpressure. The electrified filter experienced also deterioration of electrification because of diesel soot buildup in the electrified fiberglass filter. Two general conclusions derive from a variety of laboratory tests involving the aftertreatment of diesel exhaust with fiber filters: (1) high collection efficiencies and short operating periods will result from a dense cake of carbon soot forming on the surface of the filter material and causing a rapidly increasing pressure drop; and (2) exhaust gas leakage around the edges of the filter material, resulting from high pressure drop, will be a problem in the utilization of any replaceable cartridge filter.

## CONCLUSION

Conventional electrostatic precipitation is effective in the agglomeration of diesel particulate matter. An ESP can be used with either cyclones or a granular filter to obtain mass removal efficiency in the range of 50 to 85% at moderate engine backpressure and for a practical operating time between maintenance periods. Such a combination device can be made sufficiently compact to be used on stationary diesel engines or on large, heavy-duty diesel vehicles engaged in fleet operation where periodic maintenance can be performed at a central garage.

## ENDNOTES

1. M. G. Faulkner, E. B. Dismukes, J. R. McDonald, D. H. Pontius, and A. H. Dean, "Assessment of Diesel Particulate Control: Filters, Scrubbers, and Precipitators," EPA-600/7-79-232a (NTIS No. PB80-128655), U.S. EPA, IERL, Research Triangle Park, North Carolina, October 1979.

2. M. G. Faulkner, J. L. DuBard, J. R. McDonald, D. C. Drehmel, and J. H. Abbott, "Studies of Particulate Removal from Diesel Exhausts with Mechanical Techniques," at Third Symposium on the Transfer and Utilization of Particulate Control Technology, Orlando, Florida, 1981.

# STUDIES OF PARTICULATE REMOVAL FROM DIESEL EXHAUSTS WITH MECHANICAL TECHNIQUES

By: M. Greg Faulkner, James L. DuBard, Jack R. McDonald
Southern Research Institute
2000 Ninth Avenue, South
Birmingham, Alabama 35255

Dennis C. Drehmel, James H. Abbott
Industrial Environmental Research Laboratory
U.S. Environmental Protection Agency
Research Triangle Park, N.C. 27711

## ABSTRACT

A series of tests are discussed which were designed to characterize the collection of particulate emissions from diesel exhaust by several different mechanical methods. The source of particulate emissions is a 5.7 liter GM diesel truck mounted on a chassis dynamometer. The control devices which are discussed include fiber filters, gravel bed filters, and trap/cyclones. The overall mass collection efficiencies, fractional mass collection efficiencies, and operating characteristics of these devices were determined by measurements of inlet and outlet total mass loadings and particle size distributions.

A device containing a fiber filter was investigated with three different filter materials: long fiber glass wool, batts derived from fiberglass insulation, and stainless steel fiber mats. Collection efficiencies as high as 90% were achieved, coupled with a quick pressure rise culminating in gas sneakage. A device containing a gravel bed of 45.7 cm diameter and 10.2 cm depth was investigated with 2 mm steel shot. Efficiencies ranged from 45 to 70% and increased with increasing system backpressure.

## INTRODUCTION

The superiority in fuel economy of the diesel engine compared to a gasoline engine of the same displacement has created a widespread market for diesel powered light duty vehicles due to the increasing cost of fuel. In addition, automobile manufacturers view the diesel engine as a possible solution to the Federal Government's regulation requiring that the average fuel mileage for each auto manufacturer be at least 11.6 km/l. (27.5 mi/gal.) by the year 1985. Unfortunately, one characteristic of the diesel engine is a high level of combustion by-products, the most obvious of which is particulate matter*.

The particulate effluent of the diesel engine consists largely of agglomerates of very small particles of carbon which have condensed hydrocarbons adsorbed onto them. The mass median diameter (mmd) of the particles

*EPA has defined particulate matter as everything collected on a filter at 52°C (125°F) after dilution with ambient air in a dilution tunnel.

ranges from 0.3 to 0.5 μm, with about 70% occurring at diameters less than 1.0 μm(1). The small size of the particulate places it in a range where the collection efficiency of both filtration and electrostatic devices is reduced. The problem of particle collection is magnified by the large quantities of particulate produced, amounts ranging from 0.14 g/km for the Volkswagon Rabbit to 0.53 g/km for the General Motors 5.7 liter engine(2). The ultimate goal for particulate emissions set by EPA is 0.125 g/km(2), which would require that 76% of the particulate matter from the GM 5.7 liter engine be removed from the exhaust stream. Over a 8000 km (5000 mi.) service interval, this would amount to about 3.2 kg of particles. Using 120 $kg/m^3$ for the value of the bulk density of this collected material(1), this corresponds to about 27 liters (7 gal.).

Southern Research Institute (SoRI) has been studying non-regenerative aftertreatment devices. These devices include both devices which have been specifically developed for light duty vehicles and stationary-source devices which have been adapted to vehicular sources. The devices which were tested as part of this study can be classified as either electrostatic or purely mechanical in nature. The mechanical devices include a deep bed filter(3) which can accommodate up to a 15 cm depth of fibrous filter material, a granular bed filter, and a barrier filter. Also in this catagory are condensation traps developed by Eikosha Co. (Japanese Aut-Ainers)(3) which depend on gas stream cooling to condense particles on a relatively coarse wire mesh. Data on the mechanical devices are presented following a brief description of the test layout and particle sampling techniques used. Data on the electrostatic devices are presented elsewhere(4).

## TEST CONDITIONS

The diesel exhaust used in the control device tests was furnished by GM 5.7 liter diesel engines. At the SoRI facility in Birmingham, Alabama, a 1979 Chevrolet diesel pickup truck mounted on a chassis dynamometer provided the exhaust. For tests performed at the Department of Transportation (DOT), Transportation Systems Center, Cambridge, Massachusetts, an engine mounted in one of the engine dynamometer test cells was used.

The majority of the tests were run with the truck operating at a steady road speed of 88 km/hr (55 mph) in order to provide a high load for the control device. At DOT the engine was operated at 1700 rpm to achieve this same condition. This provided a gas flow rate of about 7.6 actual $m^3/min$ (270 acfm). For lower speed runs, the truck was operated at 24 (15) or 32 km/hr (20 mph). These speeds corresponded to flow rates of 2.4 and 3.2 $m^3/min$, respectively. The other engine speed used at DOT was 900 rpm corresponding to 48 km/hr (30 mph). Total mass and particle size distribution were measured before and after each control device to characterize the particle collection of the control device. The total mass loading information was obtained by using Gelman 47 mm stainless steel filter holders with glass fiber filters.

The particle size distribution data were obtained using modified University of Washington Mark V cascade impactors having seven stages with stainless steel inserts coated with Apiezon H grease to prevent particle

bounce. These instruments were used to obtain particle size distributions on a mass basis over the size range from about 0.2 to 4 μm. The impactors were either mounted in ovens close-coupled to the exhaust pipe or were wrapped in heating jackets which allowed them to be operated at the same temperature as the exhaust gas.

In addition to the cascade impactors, a Thermo Systems Model 3030 Electrical Aerosol Size Analyzer (EASA) was used to determine concentrations and electrical mobility derived size distributions of particles in the 0.01 to 0.3 μm size range. A Climet Model 208 optical particle counter was used to monitor concentrations in the fine particle size range. The SoRI SEDS III sample extraction, conditioning, and dilution system was used as an interface between these instruments and the exhaust stream. The system removes condensable vapors from the sample gas at elevated temperatures followed by controlled dilution to particle concentrations within the operating ranges of the measurement instruments. The optical data were not used for detailed sizing information but provided quick indications of efficiency in several size bands.

## DEEP BED FILTER

The first device to be fabricated and tested was the deep bed filter shown schematically in Figure 1. The dimensions of this device are based on a theoretical study which predicts 82% collection of diesel particulate when used with a 10 cm thick fiber mat of 10 μm fiber diameter and a porosity of 0.99(3). This device has a very large face area due to the downward gas flow. This geometry results in a greatly reduced flow velocity through the filter mat which enhances particle capture by the filter fibers and reduces reentrainment. In addition, should the filter be subject to blinding, the large face area should increase the lifetime of the device. The geometry would also be convenient for use with interchangeable filter elements.

The filter box was fabricated at Southern Research Institute for use in a joint testing program with the Automotive Research Laboratory of the DOT Transportation Systems Center in Cambridge, Massachusetts. A special stainless steel fiber mat was ordered from Bekaert Steel Wire Corp. in Belgium. However, when it became apparent that this material would not arrive in time for the first DOT test, screening tests were conducted at SoRI to determine substitute materials. Fiberglass batts derived from roll insulation and long fiber spun glass (angel hair) both demonstrated efficiencies in the 80-90% range and were used in the DOT test. The fiberglass batts had a fiber diameter of about 15 μm and, for the sample tested, a porosity on the order of 0.99. However, since the material was very compressible, the porosity was highly variable. The angel hair had a 20 μm fiber diameter and an undefinable porosity since it came compressed in 0.45 kg (1 lb) bags and could easily be pulled apart with the fingers.

The tests were run at engine speeds equivalent to 48 and 88 km/hr (30 and 55 mph). The pressure drop across the control device was monitored and the testing was discontinued if the pressure became too high or rose quickly and then leveled out or dropped, an indication that the gas was finding an alternate path through or around the filter material.

Initially, the deep bed filter demonstrated about 90% collection efficiency at 88 km/hr and 95% efficiency at 48 km/hr using 15 cm of fiberglass batts for the filter material. These values were degraded, however, as the pressure drop across the filter rose and gas sneakage was induced. On-site equipment modifications reduced the amount of sneakage present but were incapable of completely eliminating it. Figure 2 shows the pressure drop across the filter for one of the tests. In this example the pressure curve starts low, begins to rise quickly as the cake builds up, and then starts to level off. This pressure behavior proved to be typical for every run in the test series. Examination of the filter material showed some discoloration in the layers of fiberglass which implies that the particles were sifting through the mat. The front surface was very black and showed signs of building a cake of particulate. The edges, however, were also very black, which implies the presence of gas sneakage, an effect that would explain the leveling out of the pressure curve of Figure 2. Collection efficiencies measured after the pressure drop curve had leveled off were quite low. Figure 3 shows the collection efficiencies calculated from data taken early and late in the same test shown in Figure 2. The overall efficiency for the early data is 89%. The data taken late in the test, after the backpressure had leveled off, showed a 6% efficiency.

The behavior of the spun glass in the deep bed filter was very similar to that of the fiberglass batts. Initial efficiencies using about 15 cm of the material were in the 80-90% range for the 88 km/hr equivalent engine speed. This material appeared to be less susceptible to sneakage than the fiberglass batts. This is probably due to the less rigid form of the spun glass which should allow the material to flow to fit the container. Two runs were made with this material. In the first test, the pressure curve started to break over, an indication of the onset of sneakage. In the second run with spun glass, no break in pressure rise was evident. This run was terminated due to high backpressure (23 kPa or 92 in. $H_2O$). The efficiencies were essentially the same for both runs as the measurements were made before the onset of sneakage in the first run.

The second test with DOT was held in May 1980. During this test, the deep bed filter was run using the stainless steel fiber mat which had been ordered from Belgium for the November 1979 test. This material was composed of 12 μm stainless steel fibers which were spun into a 0.64 cm (0.25 in.) thick mat which was then sintered on both sides to give it some rigidity. The calculation called for a 10 cm thick bed but only 2.5 cm (four layers) were used in these tests. The first test was run at 88 km/hr equivalent speed with an upward gas flow to determine if the soot could be dislodged from the face of the filter mat by rapping the filter box. However, the test was cut short when the backpressure rose from 0.9 to 1.4 kPa (3.6 to 5.6 in. $H_2O$) in 25 minutes and then leveled out for the duration of the 1 hour test. After the test, the filter box was opened and the filter material was examined. There was obvious soot trails on the sides of the fiber bed indicating severe sneakage. There was no evidence of soot between the layers. The soot cake on the first surface of the fiber mat was very dense and tenacious. It could not be shaken off of the surface. Attempts to remove the cake by using a backflow of compressed air were only slightly successful but the compressed air permanently compressed the filter material.

Successful cake removal could only be achieved by scraping the face of the filter. The cake appeared denser here than it did with the fiberglass batts used in the November test but this is probably due to the smooth surface of the stainless steel. A retest of this device using a downward gas flow resulted in mechanical failure: pressure on the filter collapsed the support screen in the filter box.

## GRAVEL BED FILTER

The next device examined was a gravel bed filter. It was anticipated that the gravel bed would agglomerate the particulate matter so that it could be collected in a large particle separator such as a cyclone. A gravel bed offers the advantages of limited dust capacity (which should promote fast filling and subsequent reentrainment) and rugged filter material (which will allow stirring or other agitation of the filter bed to break up clogging and induce loss of collected particles). The device was constructed from a removable lid type 114 liter (30 gal.) drum having a 45 cm (18 in.) inside diameter. A platform covered with a steel screen supported the bed, which consisted of industrial grade steel shot. An exhaust pipe was welded to the side of the barrel near the bottom and another was welded to the lid. A stirring device consisting of a rake whose teeth extended 3 to 4 cm into the shot bed was added later in the test.

Initial tests were conducted with an upward gas flow to allow observation of the bed while the truck was running. The initial collection efficiency using 5 cm of 2 mm shot measured 22%. After 6 hours of operation, the backpressure dropped and localized boiling of the shot was observed. The efficiency was then 5%.

At this point the system was replumbed to a down draft. The bed was changed to 10 cm of 2 mm shot and was covered by a screen. The results of this test are shown in Figure 4. After 6 hours of operation, the unit was opened and inspected. Some rearrangement of the shot had occurred due to the direct blast from the inlet air. Consequently the screen was removed, the shot bed was smoothed out, and the screen was recut and replaced. It was observed at this point that, although the particulate had dispersed itself through the shot bed fairly evenly, it was also piling up on the top surface. This surface deposit was easily broken up when the bed was smoothed out and releveled. This mild stirring of the shot caused the break in the $\Delta P$ curve shown in Figure 4. However, the pressure quickly resumed its upward trend and reached 27 kPa (108 in. $H_2O$) after 10 hours of operation. Inspection again showed a thick surface layer of particulate. The collection efficiency measured at the end of the test was 72%.

At this point the system was modified to remove the screen on top of the bed, install a baffle so the gas stream would not dig holes, and install a rake so the top 3 cm of the shot could be stirred to break up the top layer. By stirring at 1 hour intervals, the pressure drop could be constrained to the 10-12 kPa (40-50 in. $H_2O$) range with efficiencies of about 40%. The emissions increased briefly each time the bed was stirred. Although the ratio of large to small particles increased considerably during

the stirring puff, no appreciable agglomeration effects were observed during the non-stirring portion of the operation cycle. Therefore the gravel bed filter must be considered a particle collector rather than an agglomerator.

## AUT-AINER

The Aut-Ainer, made by Eikosha Co. in Japan, is being developed specifically as a diesel exhaust control device. Figure 5 is a conceptual sketch of an Aut-Ainer with three bands of stainless steel mesh for soot collection. This mesh is a coarsely woven belt of 0.2 x 0.4 mm flat wire which has been rolled around the central tube and sandwiched between perforated plates. The device depends on cooling condensation for collection of particulate. The cooling is supplied by the central tube which acts as a ram air tube. Heat transfer is augmented by several perforated plates located across the gas flow and connected to the cooling tube. The exhaust gas flow is expected to tear agglomerates off of the wire mesh and swirl them through the cyclone to a catch bag on the side of the device, resulting in an effectively self-cleaning device. The only maintenance required would be periodic changing of the soot collection bag.

Three models of Aut-Ainer were tested. The first was the one shown in Figure 5. The first two bands of steel mesh are 5 cm thick and the third is 2.5 cm thick. The mixing of the cooling air with the exhaust at the end of the Aut-Ainer initially caused some concern as the effects on the condensable hydrocarbons in the exhaust stream were unknown. This difficulty was overcome by extending the cooling air tube down the center of the sampling port tube so that undiluted exhaust could be sampled. After this section, a baffle was placed in the exhaust pipe to promote mixing and another sampling tube was placed downstream to allow sampling of the diluted exhaust. The amount of dilution present was determined by examining the concentrations of CO, $CO_2$, and $NO_x$ present before and after dilution and deriving a correction factor based on the assumption that the quantities of these gasses were invariant.

The first Aut-Ainer was examined during the May, 1980, DOT test. According to the manufacturer, who was at DOT for the first week of testing, the Aut-Ainer requires about 12 hours of running-in time to obtain maximum efficiency. After 20 hours of running at 1700 rpm (88 km/hr equivalent), an efficiency of 12% was obtained for this speed. The manufacturer also pointed out that the device was designed for an engine in the 2-3 liter displacement range rather than the 5.7 liter GM engine being used. By scaling speeds and displacements, 48 km/hr (900 rpm) on the 5.7 liter engine can be considered the equivalent of the desired test speed of 88 km/hr for a 3 liter engine. Therefore a test was run at 900 rpm which yielded an efficiency of 32%. The efficiencies quoted are overall figures derived from filter and impactor data. Figure 6 shows size dependent efficiencies for both engine speeds. Ultrafine data indicate that the device was condensing but not collecting large quantities of small particles.

The second Aut-Ainer tested was designed after the DOT test by K. Aoi of Eikosha Co., who believed that a larger design would be more suitable

for an engine of 5.7 liter displacement. This device is essentially the same as the one shown in Figure 5 except that the three sections of mesh are 18 cm long for a total of 54 cm and that there is a bleed-off pipe connected to the back of the cyclone. The outlet used a double pipe which carried the cooling air past the sampling ports before allowing mixing. At the suggestion of Aoi the catch bags were enclosed so that the exhaust through the bags could be examined. The flow rates at the inlet and regular outlet were close to 7.6 actual $m^3$/min (270 acfm). The flow through the bags barely registered on the water manometer used with the pitot tube. Based on an estimated 0.13 cm (0.05 in.) deflection, a flow rate of 0.9 actual $m^3$/min (31 acfm) was obtained. This is only 14% of the total flow.

The large capacity Aut-Ainer was tested at SoRI using the conditions for which it was designed, i.e., a 5.7 liter vehicle operating at 88 km/hr. Filter data taken at the regular gas outlet indicated that the device was collecting 35% of the particulate after 40 hours of operation. EASA data taken at this point showed a negative efficiency for particles of less than 0.7 μm diameter, which suggests that this device, like its smaller counterpart, was condensing vapors to form small particles.

The filter samples taken from the exhaust through the catch bags were pale yellow. This implies that only negligible quantities of soot passed these bags which would indicate a high efficiency if opacity measurements were made. However, these filters showed a larger weight gain than the very black filters taken from the regular exhaust. The collection efficiency through the bags measured 22% with negative efficiency again occurring for the small particles. The temperature of the gas at this point was 84°C (184°F) compared to 132°C (271°F) at the regular outlet and 174°C (345°F) at the inlet. Since the temperature was less than 100°C, the filters were desiccated for several days and reweighed. The changes in weight were within the error of the weighing procedure which suggested that the weight gain was due to condensed hydrocarbons. Gas chromatography data taken from the residue collected on the filters support this by showing a distinct shift toward lighter, lower condensation temperature organic compounds in the sample taken from the catch bag exhaust filter compared to a sample taken from the regular outlet filter.

A different Aut-Ainer designed by S. Masuda was also tested. This device has no air pipe but is designed to maximize its surface area for cooling purposes. The device is 5 cm thick by 40 cm wide and contains three 27 cm long sections of the same steel mesh. There is no cyclone in this device and therefore any agglomerates which are reentrained should be discharged through the exhaust outlet. According to Masuda, the device was built for a 1 liter engine having a maximum gas flow rate of 3.5 $m^3$/min. Consequently, the truck was run at 32 km/hr which gave a gas flow of about 3.2 $m^3$/min.

After 20 hours of operation the efficiency was 36% with a backpressure of less than 3 kPa. EASA data indicate that the device is not agglomerating at all but is producing a condensation fog of very small particles.

## BARRIER FILTER

The barrier filter tested was a ceramic monolith made by Corning. The device was run at an engine speed equivalent to 48 km/hr (30 mph) and showed efficiencies of 92% using impactors and 97% using the electrical aerosol analyzer. However, its lifetime is very limited due to the rapidly rising pressure drop which reached 35 kPa (140 in. $H_2O$) in 7 hours.

## CONCLUSION

The use of a fine fiber filter to capture diesel soot does not appear to be practical due to the tendency toward formation of a cake on the face of the filter. This cake of particles reduces gas flow through the filter which results in an increase in the pressure drop across the device. The pressure continues to increase until either it impedes the operation of the engine or a lower pressure route around the filter mat is established. Once a route for gas sneakage is established, the collection efficiency of the device drops sharply.

The three Aut-Ainers tested were unable to achieve acceptable collection efficiency levels. In addition, there was no evidence that these devices were agglomerating particulate. Instead, they produced a fog of small particles as hydrocarbon vapors present in the diesel exhaust were condensed in the control device.

The granular bed filter is a concept which may prove applicable to the diesel exhaust problem. Although the collection efficiency was not as high as that of a fiber filter, the gravel bed has the important advantage of being cleanable, whether by mechanical or chemical means. The ceramic filter demonstrated a high collection efficiency but has a limited lifetime. This device is undergoing development by EPA at Ann Arbor, Michigan, and by several automobile manufacturers to extend its usable lifetime by regeneration.

## ENDNOTES


1. McCain, J. D., and M. G. Faulkner. Assessment of Diesel Particulate Control: Particle Size Measurements. EPA-600/7-79-232c (NTIS PB80-224256), U.S. Environmental Protection Agency, IERL, Research Triangle Park, North Carolina, December 1979.

2. Federal Register, 44 (33) February 1, 1979.

3. Faulkner, M. G., E. B. Dismukes, J. R. McDonald, D. H. Pontius, and A. H. Dean. Assessment of Diesel Particulate Control: Filters, Scrubbers, and Precipitators. EPA-600/7-79-232a (NTIS PB80-128655), U.S. Environmental Protection Agency, IERL, Research Triangle Park, North Carolina, October 1979.

4. DuBard, J. L., M. G. Faulkner, J. R. McDonald, D. C. Drehmel, and J. H. Abbott. Studies of Particulate Removal from Diesel Exhausts with Electrostatic and Electrostatically-Augmented Techniques, at the Third Symposium on the Transfer and Utilization of Particulate Control Technology, Orlando, Florida, 1981.

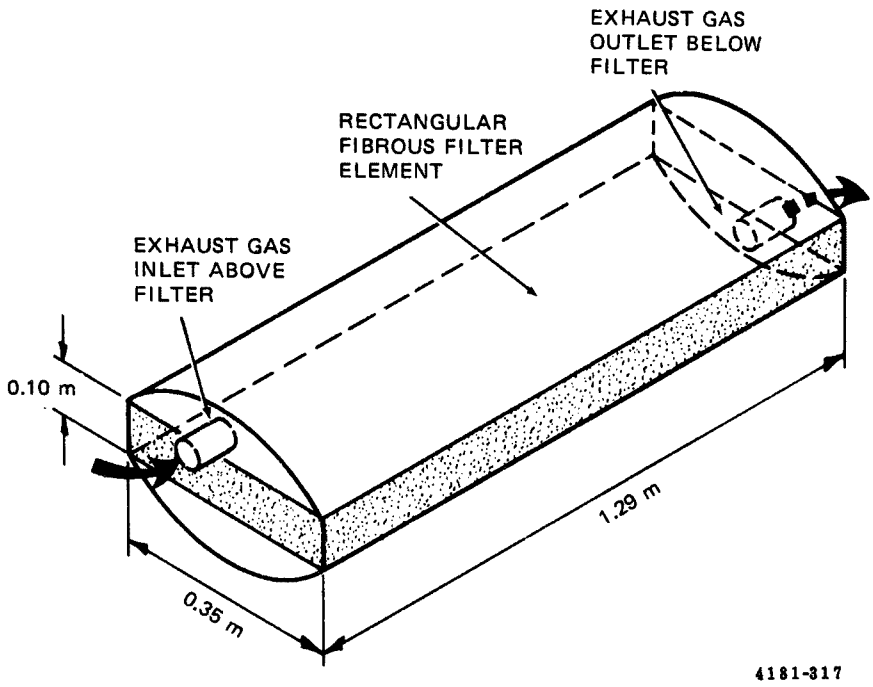


*Figure 1. Deep bed filter.*

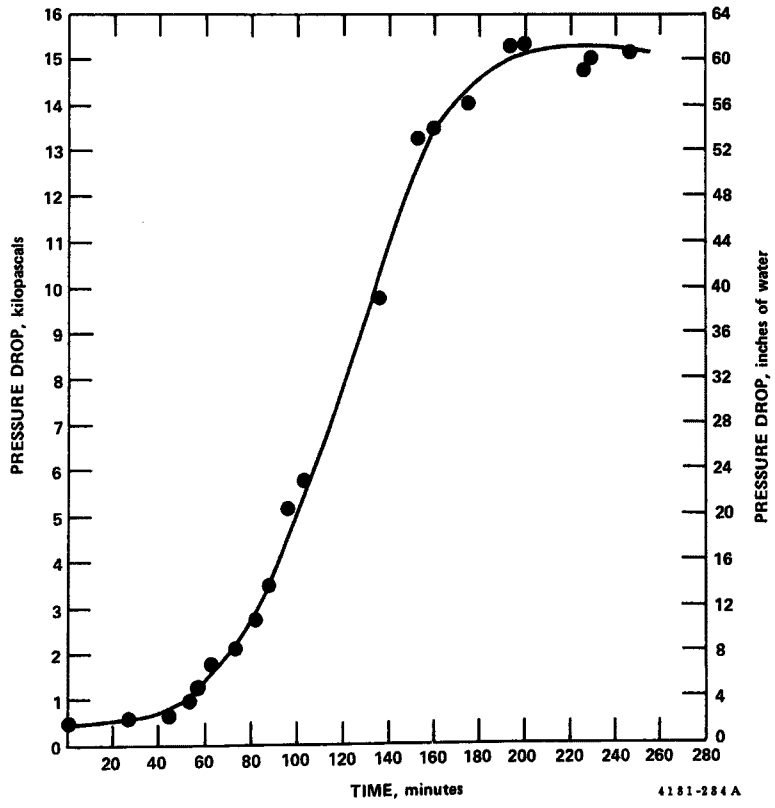


*Figure 2. Pressure drop across fiberglass batt.*

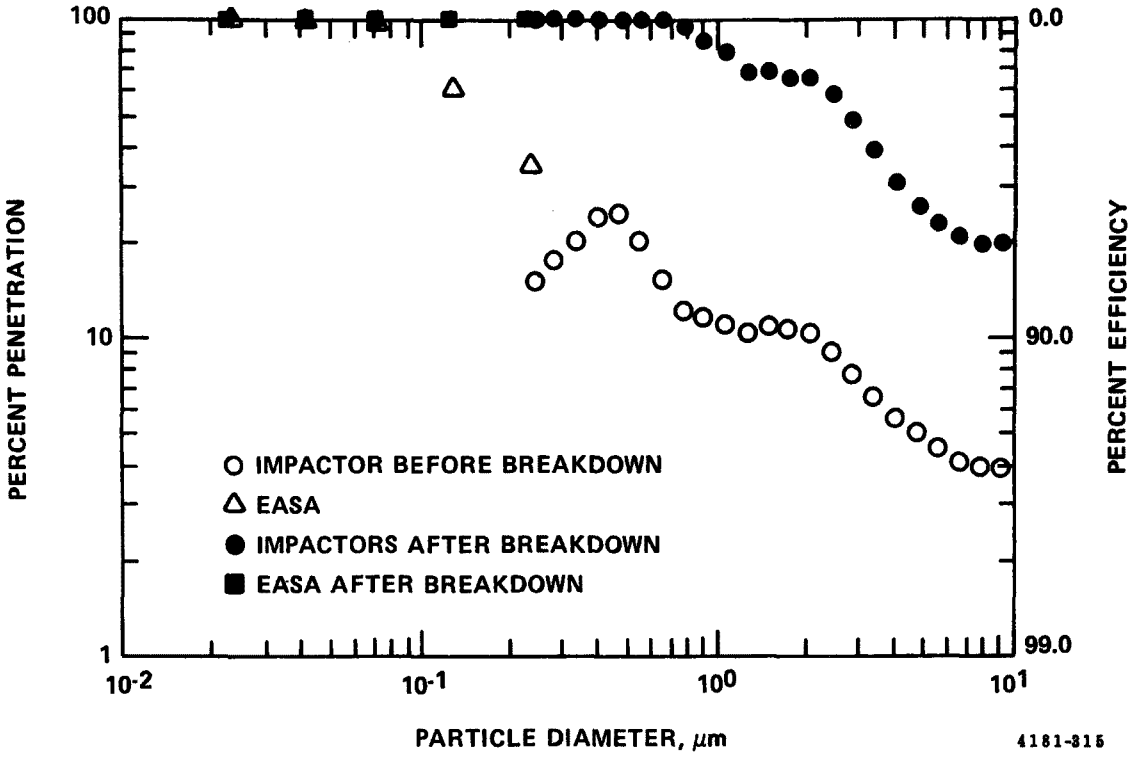


*Figure 3. Efficiencies before and after onset of sneakage for deep bed filter using fiberglass batts.*

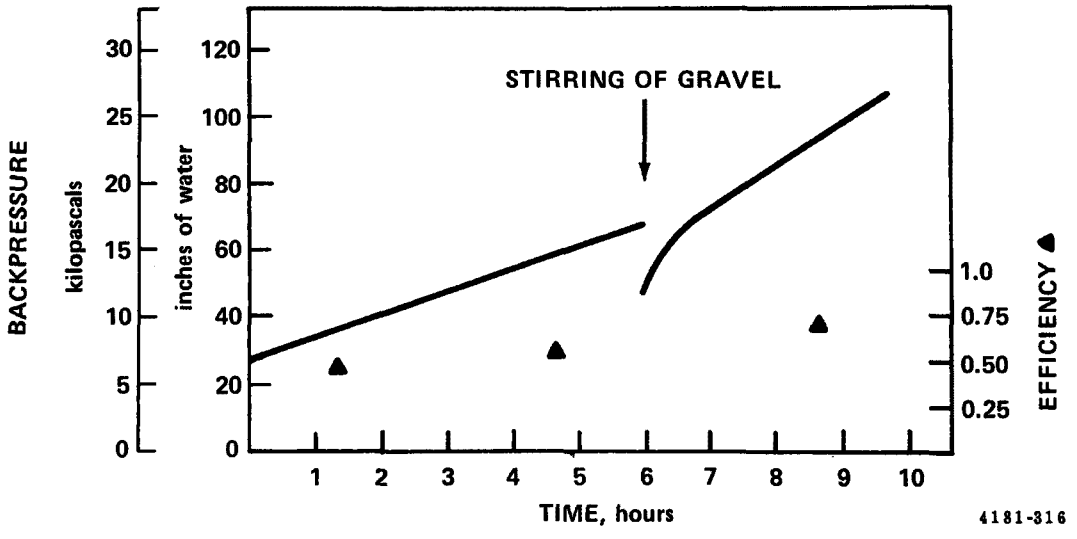


*Figure 4. Gravel bed filter efficiency and backpressure.*

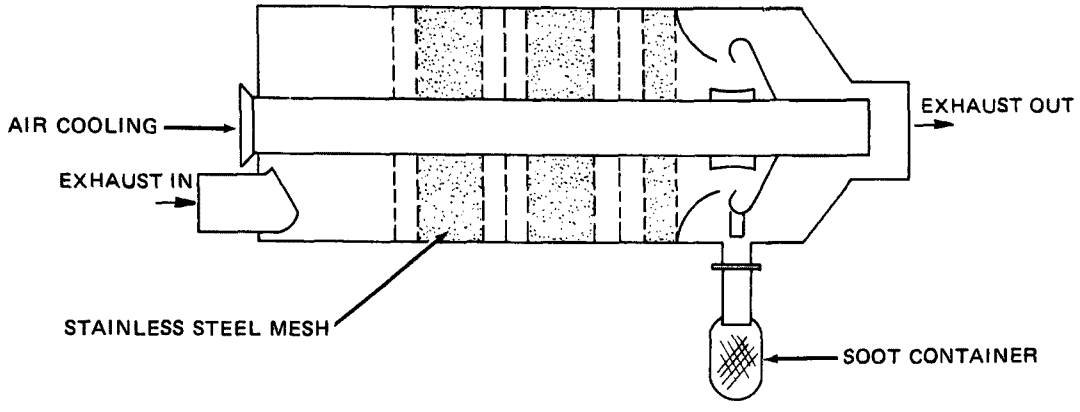


*Figure 5. Aut-Ainer.* 4181-297A

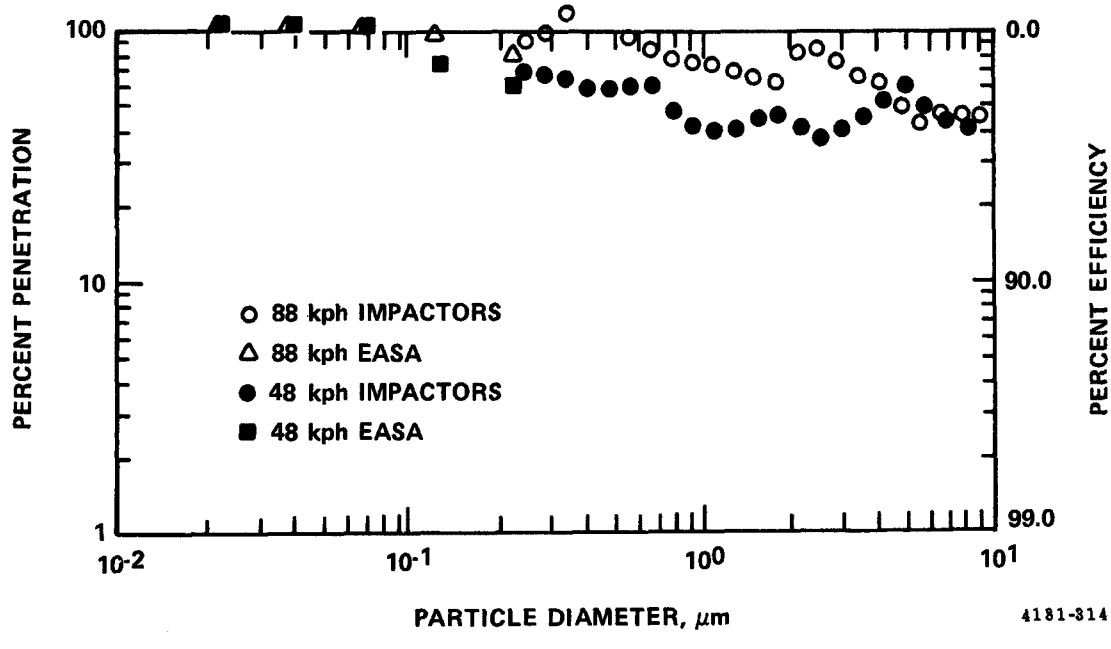


*Figure 6. Aut-Ainer efficiency for 88 and 48 km/hr speeds.*

# UPDATE ON STATUS OF CONNECTICUT'S CONTROL PROGRAM FOR TRANSPORTATION-RELATED PARTICULATE EMISSIONS

By: H. Ledger Chamberlain
Environmental Programs Department
Northeast Utilities
Berlin, CT

John H. Gastler
Bureau of Planning and Research
Connecticut Department of Transportation
Wethersfield, CT

## ABSTRACT

Connecticut's State Implementation Plan (SIP) indicated transportation related sources contribute more than half of total suspended particulate (TSP) emissions.

Our earlier paper, presented at the 1979 Symposium, discussed implications of this finding and identified additional efforts needed in two areas: measures to reduce and control emissions; and programs to better define and document the transportation sector's contribution to TSP emissions.

Control programs include both exhaust controls for exhaust emissions and fugitive controls for reentrained particulate material.

The success and cost of these controls are of interest both as means of achieving air quality standards and as a potential source of reductions for "offset" and "banking" programs. Potential interaction of mobile and stationary source controls exists.

Connecticut's unique program is presented. The results of extensive testing to further define transportation-related TSP emissions in Waterbury, Connecticut are summarized and preliminary conclusions regarding control strategies are discussed.

## TEXT

At the last symposium we presented a paper [1] which briefly described the TSP situation in Connecticut and then concentrated on the role which transportation played in bringing about that situation. In it we detailed the NAAQS compliance status of the state, the mode and extent of the transportation contribution to ambient TSP levels, and measures being taken to ameliorate the situation. Also presented were reservations about the technical analyses upon which the official description of the situation was based. This present paper updates progress which has been made and indicates areas where additional effort is required.

On the basis of readings from the statewide HiVOL monitoring network operated by the Connecticut Department of Environmental Protection, the city of Waterbury has been designated as noncompliance for the primary TSP

standard. A secondary standard noncompliance designation has been applied to the entire state. (2) Despite this, tremendous progress has been made in the past decade. The number of violations of the primary twenty-four hour standard has decreased from twenty-one in 1971 to one in 1979. During the same time period the number of secondary violations has decreased from thirty-four to seven. The severity of the violations has decreased as well. This improvement has been due in large part to a vigorous program of stationary source control.

The goals of Connecticut's particulate control program may be defined as: 1) achieving the primary standard in Waterbury; 2) achieving the secondary standard statewide; and 3) development of an accommodative SIP strategy. An accommodative SIP is one which will decrease pollutant levels so that they are demonstrably below the standards, thus leaving a margin to accommodate new growth.

The entire Connecticut portion of the New Haven-Hartford-Springfield interstate Air Quality Control Region was originally given a primary noncompliance designation, based on monitoring at the Waterbury permanent monitoring site. Subsequent examination of TSP levels at other sites in the region indicated that the primary nonattainment designation should be limited to the city of Waterbury. (2) The Waterbury monitoring site is strongly oriented to transportation sources, being located within an interchange of Interstate Route 84, immediately south of the highway mainline. The Connecticut Route 8 expressway is a short distance to the west of the site. The Waterbury Central Business District (CBD) lies to the north of the site and I-84.

The results of a number of analyses indicate that the high TSP levels encountered at the Waterbury site are the result of a one time situation. The apparent cause was a large construction project, consisting of widening and realigning I-84 immediately east of the monitoring site. This project involved a massive rock "cut and borrow" operation which began in November, 1976. Total completion of the project is scheduled for 1981. Although all legal controls and numerous special measures were employed there is tremendous potential for fugitive emissions from such operations as blasting, loading, on-site rock crushing, storing, unloading, and placement of material In many instances the material must be handled many times. The following table shows quantities of material removed (in thousand cubic yards) from the 1.2 mile project for each year of its duration. For reference, the

TABLE 1. MATERIAL QUANTITIES REMOVED FROM I-84 REALIGNMENT PROJECT

| Year | Earth (1000CY) | Rock (1000CY) | Total (1000CY) | Total Peak Mo. (1000CY) | Interchange Site [TSP]24 | Interchange Site [TSP]A | Typical Site [TSP]24 | Typical Site [TSP]A |
|---|---|---|---|---|---|---|---|---|
| 1975 | 0 | 0 | 0 | 0 | 180 | 84.7 | 173 | 65.5 |
| 1976 | 111 | 56 | 167 | 83(Dec) | 256 | 86.5 | 135 | 60.1 |
| 1977 | 312 | 406 | 718 | 80(May) | 255 | 81.3 | 147 | 70.0 |
| 1978 | 167 | 261 | 428 | 68(July) | 249 | 80.0 | 237 | 62.3 |
| 1979 | 186 | 31 | 217 | 62(Oct) | 174 | 69.6 | 147 | 49.8 |
| 1980 | 4 | 6 | 10 | 6(Jan) | | | | |

annual geometric mean and second high twenty-four hour TSP concentrations (in micrograms per cubic meter) from the Waterbury interchange site and a more typical Waterbury site are included.

A separate, but complementary, study was conducted by CONNDOT in an attempt to quantify particulate emissions from various construction activities. A HiVOL sampler was placed approximately twenty-five feet from the operations being monitored. Typical TSP concentrations are included in the following table.[3]

TABLE 2. TSP CONCENTRATIONS IN VICINITY OF SELECTED CONSTRUCTION OPERATIONS

| Operation | [TSP] ($ug/m^3$) |
|---|---|
| Rock Crushing/Trucking | 1000 |
| Paving | 150 - 200 |
| Hauling (Dry) | 500 |
| Hauling (Damp) | 70 |

While the precise contribution of the I-84 project to ambient TSP levels cannot be determined, the information presented above shows that a very large source of particulates existed in Waterbury for more than four years. Traffic was maintained on I-84 and most local streets throughout the construction period. Thus a mechanism was provided for reentrainment and transport of particulate matter throughout the area, as was reflected in TSP concentrations at the interchange monitoring site.

For a short time in 1979 the DEP operated a network of TSP monitoring sites encompassing the entire Waterbury area. Results of the monitoring indicate that the extremely high TSP levels measured at the interchange site are not representative of the city as a whole. We believe that the site's proximity to I-84 (it is a Zone A site), to the realignment project, and to the Waterbury CBD, resulted in the monitoring of a non-typical TSP episode With termination of construction activity the cause of the episode will have been eliminated. Reclassification of the city as primary attainment should then be possible, based on three consecutive years of monitored data.

Demonstration of secondary standard compliance and, thereafter, an accommodative growth margin will require reduction of monitored TSP concentrations at other sites more typical of the character of Connecticut than Waterbury. However, there are two possible sources of error to be encountered in determining the state's actual and equitable control requirements. They are passive sampling error and macroscale atmospheric transport.

Passive sampling error is the result of sampling methodology. As is standard practice, DEP operates its HiVOL samplers every sixth day, with the monitors being tended only once during each sampling cycle. In some critical areas samplers are operated every third day. During the inactive portion of the sampling cycle particles may collect on the filters, introducing a positive bias to the readings. This is known as passive sampling and the error introduced can be significant. Studies by DEP have shown that it can exceed twenty percent and is largely dependent on TSP concentration. Recent work by Sweitzer indicated average passive loading of 102 tests at two rural

Illinois sites as 16.3% and 17.2%. (4)

The DEP has begun using HiVOL samplers equipped with devices which cover the filter during passive periods. Data from these samplers show a decrease in TSP levels. The exact magnitude cannot be determined because of normal year-to-year variation and the lack of colocated monitors using a normal operating schedule. However, DEP has estimated a correction factor of 13%(2)

The implications of correcting for or eliminating passive sampling error are obvious. Application of DEP's correction relationship to Connecticut's monitor readings eliminates several of the secondary standard violations and reduces the primary violation to a secondary violation.

Efforts to account for macroscale atmospheric transport have thus far been minimal, having been almost exclusively devoted to oxidants and acidic precipitation precursors. These efforts must be expanded to include particulate transport. This is an especially critical issue for Connecticut because of its proximity to the New York City metropolitan area. Computer modeling and monitored data both provide evidence that a significant portion of the particulates in Connecticut were transported from the New York area.

The magnitude of the transport phenomenon is surely debatable, but its implications are obvious. Connecticut must implement controls which must be more severe than otherwise and must compensate for emissions over which it has no control. This imposes a competitive economic disadvantage on Connecticut's industries and businesses. These disadvantages would be compounded by a cut-off of federal funds should the NAAQS not be attained.

Consideration of passive sampling and transport will reduce the magnitude of our task. However, considerable disagreement remains concerning the portion of Connecticut's particulate emissions attributable to transportation and what measures should be undertaken to control them.

According to the emissions inventory prepared by DEP for the 1979 SIP revisions transportation sources were responsible for fifty-three percent of Connecticut's particulate emissions in 1976.(2) Assumed emission factors were used to calculate the emissions from transportation sources, i.e., motor vehicles. These emission factors consist of three components:

- exhaust or tailpipe emissions;
- tire wear; and
- reentrained road dust.

Tailpipe emissions consist of combustion products, primarily carbon particles and large aggregates of heavy hydrocarbon molecules. Lead-containing particles are emitted by vehicles burning leaded gasoline. Tire wear emissions are produced by friction between tires and the roadway surface. They consist of particles of rubber and other tire constituents. Reentrained road dust consists of particulate matter which is forced into suspension by vehicle-induced turbulence and natural air currents. The particles may be of any origin.

The emission factors used in inventory calculations are contained in the following table.

TABLE 3. VEHICULAR TSP EMISSION FACTORS

| Year | Tailpipe (gm/mile) | Tire Wear (gm/mile) | Reentrainment (gm/mile) | Total (gm/mile) |
|---|---|---|---|---|
| 1976 | 0.37 | 0.20 | 0.68 | 1.25 |
| 1982 | 0.25 | 0.20 | 0.68 | 1.13 |
| 1987 | 0.21 | 0.20 | 0.68 | 1.09 |

Vehicular emission factors are most commonly expressed as mass emitted per unit of distance traveled, usually grams per mile. The decrease in the tailpipe emission factor over time is due primarily to the phase-out of leaded gasoline.

We continue to have serious reservations concerning both the form and magnitude of these emission factors. All of the emission components are constant, rather than varying with the major factors which influence them. Our previous paper discussed these influencing variables and reviewed programs needed to better define vehicular emissions and measures to control them.

Much is already known about the age and type mix and the distribution of significant operating parameters of the vehicle population in Connecticut. This information is used to calculate emissions of other pollutants. What is not known is the effect that all of these variables have on the three TSP emission components. In most cases direct or inverse proportionality may be deduced, but the magnitude of the effects is unknown. Controlled testing and monitoring of all three emission components is necessary in order to establish emission factors upon which to base control strategies.

However, this is not enough. A significant portion of the emitted particulate mass consists of particles large enough to settle out of suspension rapidly, and thus cannot contribute to ambient TSP concentrations. Typical particle size/density distributions must therefore be developed in order to account for particle settling.

A reentrainment emission factor of 5.15 gm/mile has been recommended by EPA. To its credit, the DEP correctly assumed that it is too large if particle settling were not to be taken into account. It was assumed that a portion of the emissions was suspendable and the remainder was not. The suspendable emission factor of 0.61 gm/mile was developed using a simplified half-life analysis. The error inherent in this approach is that particle size is a continuum, not divisible into two portions at a discrete separation point.

Much study is required to determine typical particle size/density distributions which will complement the emission factors for each component, particularly reentrainment. From this information a model can be developed which will account for dispersion as well as particle settling.

Shortly after our previous paper was presented, both the Federal Highway Administration (FHWA) and the EPA indicated that they were planning to conduct programs aimed at better defining particulate emissions from transportation sources. Connecticut opted to await the results of these efforts rather than undertake the considerable expense of conducting duplicate studies. Unfortunately, both federal agencies cut back or eliminated these programs due to budget restrictions, leaving much to be accomplished.

In our previous paper we outlined several projects being conducted or proposed in the Waterbury area in an attempt to gain a better understanding of the area's TSP situation. Two of these are worth noting.

ConnDOT is participating in an interagency demonstration program examining the relationships between air quality and economic development. Agencies on the state, regional, and local level are taking part. An interesting concept being investigated is the use of transportation-related pollutants, particularly TSP, as offsets and/or banking credits for use by stationary sources. An example is a business gaining a TSP offset by implementing TSP-reducing transportation, such as vanpools, for its work force. A further example is implementation of less polluting transportation measures by a political body, thereby establishing "banked" emission rights which could be used to entice industry to locate or expand within the area. Such concepts may well be of interest in shaping the efforts of both stationary and transportation sources to achieve a common goal.

The other project is a monitoring study conducted by DEP at the interchange monitoring site in Waterbury. Daily TSP concentrations were measured for a period of several months, together with corresponding meteorological parameters and traffic counts on three streets in the vicinity of the monitor. Some data has been obtained from this study, but little analysis has been conducted as yet. However, preliminary investigation indicates that there is a positive proportionality between traffic volume and TSP concentration. The correlation however appears to be extremely weak. We hope that more detailed analyses of these data will provide some insight into the influence of vehicular traffic on TSP concentrations.

Connecticut's future programs for control of transportation-related particulate emissions will be influenced by several perspectives which have changed since our last paper was presented. We believe that monitoring results, when completely reviewed, will show that Connecticut is in compliance with the primary TSP standard statewide. However, attainment of the secondary standard must be achieved as expeditiously as possible. A comprehensive program for achieving the secondary standard will be formulated for the 1982 SIP revisions. Control efforts required of Connecticut will be less severe, as accounting for passive sampling error and interstate transport becomes more widespread.

As discussed earlier, the results of several studies indicate that Connecticut's primary nonattainment area (Waterbury) was the result of close proximity of a large one-time construction project to a sensitive monitoring site. Areas where monitored data indicate secondary standard violations will be carefully analysed to determine sources of ambient particulates and

appropriate control measures. Again, an accommodative SIP is a state goal.

The efforts needed to define vehicular emission factors for particulates have been discussed. Our decision-makers can only interpret the decision that previously scheduled federal programs were expendable as an indication that our earlier concerns were an over-reaction. We have already urged that one of the two federal agencies involved reconsider their cancelled programs because the scope of the problem is not limited to Connecticut. The task is also too complex and expensive for a single state to address adequately. We reiterate our plea that programs to quantify vehicular emissions be reinstated with the same priority as originally intended.

Efforts will be devoted to developing methodologies for analysing TSP in EIS preparation and in the state's Indirect Source Permit program. Here again, results from federal programs will be sought because more compelling problems will preempt available resources.

Attention will be given to various scenarios which are at present unpredictable. Many may force us to completely re-evaluate our present course. One such scenario is the adoption of new TSP standards for respirable particulates. Another could be an extensive amendment of the Clean Air Act by this session of Congress.

Finally, several trends have recently been taking shape which cause us concern. Significant increases in the use of coal and wood for home heating may increase TSP levels throughout the state. This could require compensating reductions in emissions from the transportation sector. The increased ambient TSP levels would also result in additional particulates settling onto roadways and being reentrained, thus compounding the problem.

Concern for fuel conservation has prompted a significant increase in the use of Diesel passenger vehicles. General Motors is projecting that twenty percent of its 1985 automobile sales will have Diesel engines. The particulate emissions from these vehicles are many times those of conventional vehicles. This trend is likely to have an adverse effect on progress toward attainment of Connecticut's particulate air quality goals.

References

1. Gastler, J.H., and Chamberlain, H.L., Status of Connecticut's Control Program for Transportation-Related Particulates, Second Symposium on the Transfer and Utilization of Particulate Control Technology, EPA-600/9-80-039D, September, 1980.
2. Connecticut Department of Environmental Protection, State Implementation Plan for Air Quality, June 22, 1979.
3. Connecticut Department of Transportation, A Study to Determine Particulate Concentrations From a Portland Cement Concrete Pavement Recycling Program, August, 1980.
4. Sweitzer, T.A., Characterization of Passively Loaded Particles on HiVOL Samples, JAPCA, 30: 1324-1325, December, 1980.

# AUTHOR INDEX


| AUTHOR NAME | PAGE |
|---|---|
| Albrecht, P.R. | IV-116 |
| Anderson, M.H. | II-334 |
| Arce-Medina, E. | II-76 |
| Ariman, T. | III-290 |
| Armstrong, J.A. | IV-188, IV-252 |
| Bakke, E. | I-236 |
| Balfour, W.D. | III-119 |
| Bamberger, J.A. | III-398 |
| Bergmann, L. | I-323 |
| Berlant, M.J. | II-218 |
| Bernstein, S. | II-405 |
| Beutner, H.P. | III-71, III-228 |
| Bickelhaupt, R.E. | I-165 |
| Boericke, R.R. | III-353 |
| Bohn, R. | IV-344 |
| Borenstein, M. | III-90 |
| Brookman, E.T. | IV-125 |
| Bump, R.L. | II-425 |
| Bush, P.V. | I-157 |
| Calvert, S. | III-1, III-10, IV-156 |
| Carnes, D. | IV-135 |
| Carr, R.C. | I-118 |
| Chamberlain, H.L. | IV-406 |

AUTHOR INDEX (cont.)


| AUTHOR NAME | PAGE |
|---|---|
| Chambers, R. | I-45 |
| Chiang, T. | III-250, III-261 |
| Chou, K.H. | IV-73 |
| Cowen, S.J. | IV-264 |
| Crippen, L.K. | I-148 |
| Crowson, F. | III-438 |
| Crynack, R.R. | II-242 |
| Czuchra, P.A. | IV-55 |
| Dalmon, J. | II-390 |
| Demski, R.J. | I-341 |
| Dennis, R. | I-1, III-140 |
| Dietz, P.W. | III-449, III-459 |
| Donovan, R.P. | I-11 |
| Drehmel, D.C. | III-341, IV-210 |
| DuBard, J.L. | IV-383 |
| Durham, M. | II-54, IV-285 |
| Ensor, D.S. | I-176, IV-242 |
| Eskinazi, D. | III-238 |
| Faulkner, M.G. | II-199, IV-395 |
| Feldman, P.L. | IV-3 |
| Ferrigan III, J.J. | I-197 |
| Finney, W.C. | II-358 |
| Fjeld, R.A. | II-179 |
| Fortune, O.F. | I-82 |

AUTHOR INDEX (cont.)


| AUTHOR NAME | PAGE |
|---|---|
| Frazier, W.F. | III-171 |
| Gardner, R.P. | III-128 |
| Gaunt, R.H. | I-216 |
| Gehri, D.C. | I-333 |
| Gentry, J.W. | III-406 |
| Giles, W.B. | III-468 |
| Hardison, L.C. | III-33 |
| Harmon, D.L. | IV-317 |
| Hawks, R.L. | III-221 |
| Helfritch, D. | I-75 |
| Henry, F. | III-301 |
| Henry, R.F. | IV-63 |
| Hesketh, H.E. | IV-222 |
| Hoenig, S.A. | III-382 |
| Hovis, L.S. | I-23 |
| Hyde, R.C. | I-129 |
| Iionya, K. | III-181, III-321 |
| Jaworowski, R.J. | I-185 |
| Jensen, R.M. | I-138 |
| Joergensen, H.J. | II-370 |
| Johnson, C.A. | I-352 |
| Kalinowski, T.W. | III-311 |
| Kanaoka, C. | III-280 |
| Kirstein, B.E. | III-373 |

AUTHOR INDEX (cont.)


| AUTHOR NAME | PAGE |
|---|---|
| Kolnsberg, H.J. | IV-179 |
| Krishnamurthy, N. | IV-232 |
| Ladd, K. | I-55, I-65 |
| Lagarias, J.S. | I-272 |
| Landham, Jr., E.C. | I-237 |
| Langan, W.T. | III-211 |
| Lawless, P.A. | II-25, II-35, II-44 |
| Leith, D. | III-270 |
| Leonard, G.L. | II-120 |
| Maartmann, S. | II-130 |
| Mahoney, D.F. | I-206 |
| Mappes, T.E. | III-150 |
| Martin, D. | IV-145 |
| Masuda, S. | II-189, II-380 |
| Mathai, C.V. | IV-200 |
| Mazumder, M.K. | II-160, II-169 |
| McCrillis, R.C. | IV-306 |
| McElroy, M.W. | I-94 |
| McLean, K.J. | I-265, II-304 |
| Menegozzi, L. | II-404 |
| Menoher, C. | III-111 |
| Mitchner, M. | II-97 |
| Moore, W.E. | IV-105 |
| Mormile, D. | IV-363 |

AUTHOR INDEX (cont.)


| AUTHOR NAME | PAGE |
|---|---|
| Moslehi, G.B. | II-109 |
| Mosley, R.B. | II-1, II-13 |
| Musgrove, J.G. | III-193, III-201 |
| Noonan, F.M. | IV-326 |
| Oglesby, H.S. | III-80 |
| Ostop, R.L. | I-107 |
| Parker, R. | III-51, IV-2 |
| Parquet, D. | III-363 |
| Parsons, Jr., E.L. | I-303 |
| Patton, J.D. | III-160 |
| Pearson, G.L. | I-120 |
| Pedersen, G.C. | III-60 |
| Petersen, H.H. | I-291 |
| Piulle, W. | I-253 |
| Potokar, R.W. | III-417 |
| Prem, A. | III-21 |
| Presser, A.M. | IV-26 |
| Pyle, B.E. | II-66 |
| Raemhild, G.A. | II-349 |
| Reardon, F.X. | III-102 |
| Rimberg, D.B. | II-262 |
| Rinaldi, G.M. | IV-95 |
| Rinard, G. | II-283, II-295 |
| Rubow, L.N. | IV-83 |

AUTHOR INDEX (cont.)


| AUTHOR NAME | PAGE |
|---|---|
| Rugg, D. | II-273 |
| Samuel, E.A. | II-149 |
| Schliesser, S.P. | II-252 |
| Semrau, K.T. | III-43 |
| Shilling, N.Z. | II-230 |
| Smith, W.B. | I-96 |
| Snaddon, R.W.L. | IV-74 |
| Sparks, L.E. | II-314, II-326 |
| Spawn, P.D. | IV-335 |
| Starke, J. | III-428 |
| Stevens, N.J. | I-313 |
| Sullivan, K.M. | II-141 |
| Tatsch, C.E. | IV-353 |
| Teller, A.J. | III-393 |
| Thompson, C.R. | II-415 |
| Urone, P. | IV-275 |
| VanOsdell, D.W. | I-35 |
| Viner, A.S. | IV-168 |
| Wakabayashi, A. | III-332 |
| Wang, H.H. | IV-36 |
| Wang, J.C.F. | IV-373 |
| Wegrzyn, J. | IV-46 |
| Weyers, L.L. | I-226 |
| Wilks, W.H. | IV-15 |

AUTHOR INDEX (cont.)


| AUTHOR NAME | PAGE |
|---|---|
| Williamson, A.D. | IV-297 |
| Yamamoto, T. | II-87 |
| Yung, S. | IV-1, IV-155 |
| Zarfoss, J.R. | II-208 |


☆USGPO: 1982 — 559-092/0432